

Kristaps Leškovskis

**ANNELĒTU AZIDOPYRIMIDĪNU ENERĢĒTISKAIS
PROFILS UN REAKCIJAS AR NUKLEOFĪLIEM**

Promocijas darbs

**ENERGETIC PROFILE OF ANNULATED AZIDOPYRIMIDINES
AND THEIR REACTIONS WITH NUCLEOPHILES**

Doctoral Thesis



RĪGAS TEHNISKĀ UNIVERSITĀTE

Dabaszinātņu un tehnoloģiju fakultāte
Ķīmijas un ķīmijas tehnoloģijas institūts

RIGA TECHNICAL UNIVERSITY

Faculty of Natural Sciences and Technology
Institute of Chemistry and Chemical Technology

Kristaps LEŠKOVSKIS

Doktora studiju programmas “Ķīmija, materiālzinātne un tehnoloģijas” doktorants
Doctoral Student of the Study Program “Chemistry, Materials Science and Engineering”

**ANNEĻĒTU AZIDOPIRIMIDĪNU
ENERĢĒTISKAIS PROFILS UN REAKCIJAS
AR NUKLEOFĪLIEM**

Promocijas darbs

**ENERGETIC PROFILE OF ANNULATED
AZIDOPYRIMIDINES AND THEIR REACTIONS
WITH NUCLEOPHILES**

Doctoral Thesis

Zinātniskie vadītāji / Scientific supervisors

Dr. chem. MĀRIS TURKS

Dr. chem. IRINA NOVOSJOLOVA

RTU Izdevniecība / RTU Press

Rīga 2024 / Riga 2024

Leškovskis K. Annelētu azidopirimidīnu enerģētiskais profils un reakcijas ar nukleofiliem. Promocijas darbs. Rīga: RTU Izdevniecība, 2024. 229 lpp.

Leškovskis, K. Energetic Profile of Annulated Azidopyrimidines and their Reactions with Nucleophiles. Doctoral Thesis. Riga: RTU Press, 2024. – 229 p.

Publicēts saskaņā ar RTU promocijas padomes “P-01” 2024. gada 18. marta lēmumu, protokols Nr. 59.

Published in accordance with the decision of the RTU Promotion Council “P-01” of 18 March 2024, No. 59.

Vāka attēla autors – Kristaps Leškovskis
Cover image by Kristaps Leškovskis

PATEICĪBAS

Promocijas darbs izstrādāts, pateicoties Latvijas Zinātnes padomes projekta Nr. LZP-2020/1-0348, Eiropas Sociālā fonda projekta Nr. 8.2.2.0/20/I/008 “Rīgas Tehniskās universitātes un Banku augstskolas doktorantu un akadēmiskā personāla stiprināšana stratēģiskās specializācijas jomās”, Rīgas Tehniskās universitātes Doktorantūras grantu programmas un Baltijas-Vācijas augstskolu biroju projekta “Enerģētisko azidopurīnu un to analoģu dizains un izpēte” finansiālam atbalstam.

ACKNOWLEDGMENTS

The Thesis was developed with the financial support from the Latvian Council of Science grant No. LZP-2020/1-0348, ESF project No. 8.2.2.0/20/I/008 “Strengthening of PhD students and academic personnel of Riga Technical University and BA School of Business and Finance in the strategic fields of specialization”, Riga Technical University's Doctoral Grant program, and The Baltic-German University Liaison Office project “Development of energetic azido purines and their congeners” financial support.

PROMOCIJAS DARBS IZVIRZĪTS ZINĀTNES DOKTORA GRĀDA IEGŪŠANAI RĪGAS TEHNISKAJĀ UNIVERSITĀTĒ

Promocijas darbs zinātnes doktora (*Ph. D.*) grāda iegūšanai tiek publiski aizstāvēts 2024. gada 4. jūnijā plkst. 14 Rīgas Tehniskās universitātes Dabaszinātņu un tehnoloģiju fakultātē, Rīgā, Paula Valdena ielā 3, 272. auditorijā.

OFICIĀLIE RECENZENTI

Vadošais pētnieks *Dr. chem.* Mārtiņš Katkevičs,
Latvijas Organiskās sintēzes institūts, Latvija

Profesors *Dr. habil. chem.* Sigitas Tumkevičius,
Viļņas Universitāte, Lietuva

Profesors *Ph. D. José I. Borrell Bilbao*,
Ramona Lullas Universitāte (*University Ramon Llull*), Spānija

APSTIPRINĀJUMS

Apstiprinu, ka esmu izstrādājis šo promocijas darbu, kas iesniegts izskatīšanai Rīgas Tehniskajā universitātē zinātnes doktora (*Ph. D.*) grāda iegūšanai. Promocijas darbs zinātniskā grāda iegūšanai nav iesniegts nevienā citā universitātē.

Kristaps Leškovskis

(paraksts)

Datums

Promocijas darbs sagatavots kā tematiski vienotu zinātnisko publikāciju kopa ar kopsavilkumu latviešu un angļu valodā. Promocijas darbs apkopo trīs zinātniskos oriģinālrakstus, vienu apskatrakstu un vienu sagatavotu manuskriptu. Publikācijas zinātniskajos žurnālos rakstītas angļu valodā, to kopējais apjoms, ieskaitot pielikumus, ir 180 lpp. Publikācijas manuskripts ir uzrakstīts angļu valodā, tā apjoms, ieskaitot pielikumus, ir 52 lpp.

SATURS

PATEICĪBAS.....	3
PROMOCIJAS DARBA VISPĀRĒJS RAKSTUROJUMS	7
Tēmas aktualitāte	7
Pētījuma mērķis un uzdevumi	9
Zinātniskā novitāte un galvenie rezultāti	9
Darba struktūra un apjoms	11
Darba aprobācija un publikācijas.....	11
Darba drošības informācija	12
PROMOCIJAS DARBA GALVENIE REZULTĀTI	13
1. Azīda-tetrazola līdzsvars un tā pielietojums sintētiskajā metodoloģijā	13
1.1. Azīda-tetrazola līdzsvars purīna sistēmā un pirimidīna cikla atvēršana.....	18
1.2. Azīda-tetrazola līdzsvara un S _N Ar reakciju pētījumi pirido[2,3- <i>d</i>]pirimidīna heterociklā	25
1.3. Azīda-tetrazola līdzsvara un S _N Ar reakciju pētījumi pirido[3,2- <i>d</i>]pirimidīna heterociklā	29
2. Poliazidopirimidīnu sintēze un fizikālo īpašību pētījumi.....	36
SECINĀJUMI	41
LITERATŪRAS SARAKSTS	82

1. Pielikums: Leškovskis, K.; Zaķis, J.; Novosjolova, I.; Turks, M. Applications of Purine Ring Opening in the Synthesis of Imidazole, Pyrimidine, and New Purine Derivatives. *Eur. J. Org. Chem.* **2021**, 2021, 5027-5052. doi:10.1002/ejoc.202100755
2. Pielikums: Zaķis, J. M.; Leškovskis, K.; Ozols, K.; Kapilinskis, Z.; Kumar, D.; Mishnev, A.; Žalubovskis, R.; Supuran, C. T.; Abdoli, M.; Bonardi, A.; Novosjolova, I.; Turks, M. Diazidopurine Ring Opening – Synthesis of Tetrazolyimidazole Derivatives. *Manuskripts iesniegts Journal of Organic Chemistry*.
3. Pielikums: Leškovskis, K.; Novosjolova, I.; Turks, M. Structural Study of Azide-Tetrazole Equilibrium in Pyrido[2,3-*d*]Pyrimidines. *J. Mol. Struct.*, **2022**, 1269, 133784. doi:10.1016/j.molstruc.2022.133784
4. Pielikums: Leškovskis, K.; Mišņovs, A.; Novosjolova, I.; Turks, M. S_NAr Reactions of 2,4-Diazidopyrido[3,2-*d*]pyrimidine and Azide-Tetrazole Equilibrium Studies of the Obtained 5-Substituted Tetrazolo[1,5-*a*]pyrido[2,3-*e*]pyrimidines. *Molecules* **2022**, 27, 7675-7675. doi:10.3390/molecules27227675

5. Pielikums: Leškovskis, K.; Mišņovs, A.; Novosjolova, I.; Krumm, B.; Klapötke, T.; Turks, M. 2,4,6,8-Tetraazidopyrimido[5,4-*d*]pyrimidine: a Novel Energetic Binary Compound. *Cryst. Eng. Comm.* **2023**, *25*, 3866-3869. doi:10.1039/D3CE00563A
6. Pielikums: Annelētu diazidopirimidīnu drošības profils. *Nepublicētie rezultāti.*
7. Pielikums: 2,4,6,8-Tetraazidopirido[5,4-*d*]pirimidīna solvātu sintēze. *Nepublicētie rezultāti.*

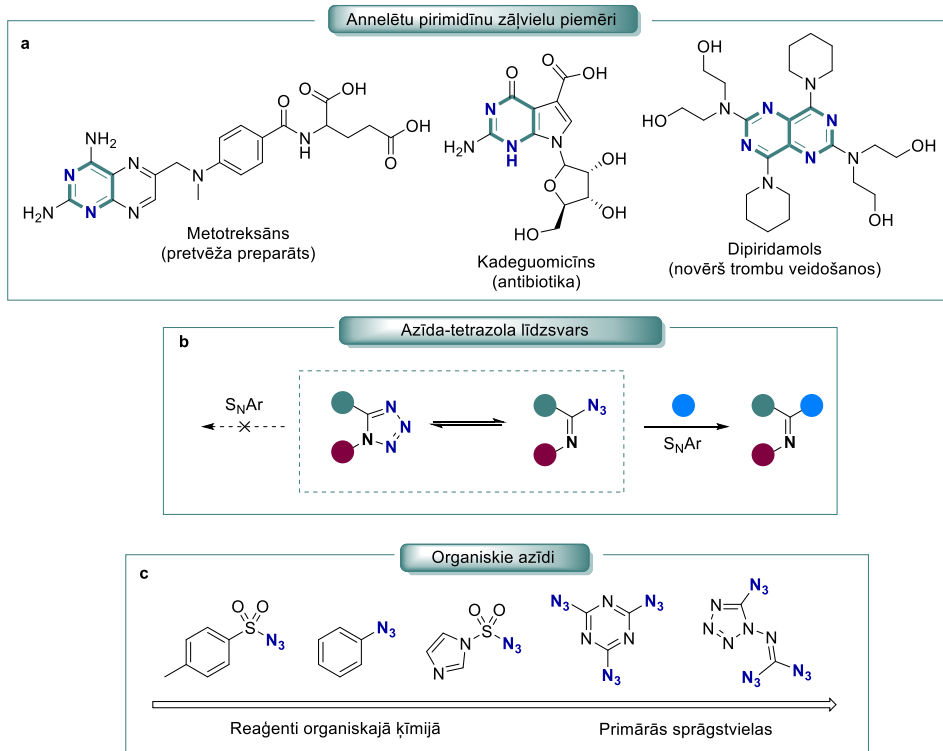
PROMOCIJAS DARBA VISPĀRĒJS RAKSTUROJUMS

Tēmas aktualitāte

Annelēti pirimidīni ir medicīnas ķīmijā privilģētās heterocikliskās struktūras ar daudzveidīgu bioloģisko aktivitāšu profilu atkarībā no pamatcikla uzbūves un aizvietotāju rakstura. Tas saistīts ar annelēto pirimidīnu strukturālo līdzību gan dzīvo organismu šūnu ģenētiskās informācijas nesējiem, gan signālmolekulām, gan arī koenzīmiem. Purīna heterocikls ir dzīvajos organismos visplašāk pārstāvētais annelēto pirimidīnu pārstāvis, jo ietilpst nukleīnskābju sastāvā. Turklāt adenoziņa trifosfāts ir šūnu enerģiju nesošā molekula, un citi adenoziņa atvasinājumi darbojas kā kardiovaskulārās sistēmas signālmolekulas. Tādēļ annelēto pirimidīnu fragmenti ar labiem rezultātiem tiek izmantoti pretvīrusu, pretvēža, kā arī sirds un citu slimību zāļvielu izstrādē (1. a shēma).^{1,2} Biomimētisku struktūru modificēšana un pilnveidošana medicīnas ķīmijā ir labi zināma stratēģija zāļvielu izveidē. Tādēļ jaunu³ sintēzes metožu izstrāde, kas dod iespēju radīt gan jaunus molekulāros skeletus, gan modificēt esošos strukturālos būvblokus, ir nozīmīga inovāciju komponente medicīnas ķīmijā.³ Daudziem no annelētajiem pirimidīniem, ieskaitot purīnu atvasinājumus, ir novērojama luminescence, kas paver to lietojuma iespējas bioorganiskajā un analītiskajā ķīmijā kā sensoriem un materiālzinātnē kā *OLED* (organiskās gaismu emitējošās diodes) materiāliem.⁴⁻⁶ Arī šajā lietojuma sfērā jaunu sintēzes metožu attīstība dod iespēju uzlabot nepieciešamās vielu fizikālās īpašības.

Heterociklisko savienojumu aizvietotāju modificēšanā dominē tādas metodes kā nukleofīlās (hetero)aromātiskās aizvietošanas reakcijas (S_NAr), kā arī pārejas metālu katalizēti C-C un C-heteroatoms saišu veidošanas procesi, lietojot šķērssametīnāšanas^{7,8} un C-H saišu aktivēšanas^{8,9} reakcijas. Daudzos ķīmiskās modifikācijas procesos tiek izmantotas tradicionālās halogēnu aizejošās grupas, kā arī aktivēti *O*- un *S*-aizvietotāji, piemēram, TfO-, TsO-, RS-, RSO₂-.¹⁰ Krietni retāk aprakstītas *N*-centrētas aizejošās grupas, kas ietver imīdus, amīdus, imidazolus un 1,2,4-triazolus, kā arī promocijas darba autora zinātniskās grupas ieteiktos 1,2,3-triazolus.¹¹⁻¹³ Šajā kontekstā azidogrupas heterocikliskajos savienojumos ir raksturojamas kā *N*-centrēti pseidohalogenīdu tipa aizvietotāji – tās var piedalīties S_NAr reakcijās, dodot azīdjonu (pseidohalogenīds) kā aizejošo grupu, kas ir zināmas, tomēr maz pētītas, reakcijas.^{12,14,15} Svarīgi, ka azidogrupas novietošana blakus heterocikliskā slāpekļa atomam (α -pozīcijā) dod azidoazometīna struktūras fragmentu, kam ir raksturīgs azīda-tetrazola tautomērais līdzsvars (1. b shēma).¹⁶⁻¹⁹ Tika izteikta hipotēze, ka, lietojot azidogrupas kā aizejošās grupas heterociklu S_NAr reakcijās, ar azīda-tetrazola līdzsvaru iespējams modulēt reakcijas spēju heterociklos. Reakcijas spējas modulācija paver iespēju dizainēt jaunas reakcijas un ietekmēt zināmu pārvērtību reģioselektivitāti, jo īpaši, ja molekulā ir vairāki azidoaizvietotāji.

Promocijas darbā autors un zinātniskā grupa fokusējās uz azidoheterociklu preparatīvo sintētisko metožu izstrādi divos virzienos: 1) purīnu ķīmisko transformāciju attīstība ar mērķi radīt jaunas reakcijas labi zināmā un ļoti plaši lietotā vielu klasē; 2) piridopirimidīnu funkcionalizēšana, jo šī vielu klase ir krietni mazāk pētīta, salīdzinot ar citiem annelētajiem pirimidīniem.



1. shēma. Izvēlētas annēlētu pirimidīnu zālvielas un azīdu īpašības.

Turklāt, veicot pētījumus ar vielām, kam ir augsts slāpekļa saturs, radās loģiska nepieciešamība noteikt savienojumu enerģētisko profilu (1. c shēma). Azidogrupas ievadīšana organiskajos savienojumos palielina sistēmas termodinamisko enerģiju par ~ 355 kJ/mol, tādēļ savienojumi ar vairākām azidogrupām veido materiālus ar augstu enerģijas blīvumu.^{20, 21} Azīdi ir jutīgi pret ārēju triecienu un siltumu, un sadaloties veido N_2 gāzi un izdala lielu siltuma daudzumu. Tādēļ organiskie azīdi ir potenciāli sprāgstoši savienojumi un azidoizvietotāju kā eksplozoforu funkcionālo grupu bieži izmanto augsta blīvuma enerģētisko savienojumu ķīmijā.²² Īpaši enerģētiski piesātināti ir smago metālu azīdi un mazmolekulārie organiskie azīdi ar augstu slāpekļa masas bilanci (> 50 %). Augstās triecienjutības dēļ mazmolekulāros azīdus izmanto primāro sprāgstvielu dizainā. Enerģētiskā profila noteikšana promocijas darbā apskatītajiem azidoheterocikliem ļauj pamatot izstrādāto sintētisko metožu drošu lietojumu. Iegūtās zināšanas palīdzēja attīstīt jauna binārā enerģētiskā savienojuma dizainēšanu, mērķtiecīgi lietojot annēlētu pirimidīnu molekulāro skeletu un tajā ievadot maksimālo azidogrupu skaitu. Šeit jāuzsver, ka bināru enerģētisko C_xN_y savienojumu dizains un sintēze patlaban piedzīvo renesansi,^{23–25} kas saistīta ar vidi nepiesārņojošu detonatoru izstrādi, apzināti izvairoties no smago metālu savienojumu lietojuma.^{26, 27}

Apvienojot interesi par annēlētu pirimidīnu reaģētspējas izpēti un azīda-tetrazola līdzsvara ietekmi uz reakciju gaitu, ir izstrādātas vairākas jaunas preparatīvas metodes purīnu un piridopirimidīnu ķīmijā, kā arī noteikti azīda-tetrazola līdzsvara fizikālķīmiskie raksturlielumi šajās vielu klasēs. Pētītajiem azidoheterocikliem ir noteikts to enerģētiskais profils, lai gūtu pārliecību par sintētisko metožu drošumu. Iegūtās zināšanas ļāva izstrādāt jaunu enerģētisko

savienojumu, apzināti pārkāpjot robežu starp tradicionālo sintētisko organisko ķīmiju un sprāgstvielu ķīmiju.

Pētījuma mērķis un uzdevumi

Promocijas darba mērķis ir jaunu sintētisko metodoloģiju izstrāde annelētu azidopirimidīnu funkcionalizēšanai, izmantojot azīda-tetrazola līdzsvaru reģioselektivitātes inducēšanai un azīda funkcionālās grupas daudzpusīgās ķīmiskās īpašības. Ņemot vērā iespējamās enerģētiskās īpašības vielām ar augstu slāpekļa saturu, otrs darba mērķis ir eksperimentāli noteikt šo vielu enerģētisko profilu un/vai lietojumu primāro sprāgstvielu izstrādē.

Mērķa izpildei tika noteikti vairāki uzdevumi:

- S_NAr reakciju reģioselektivitātes izpēte annelētu pirimidīnu – purīna, pirido[2,3-*d*]pirimidīna un pirido[3,2-*d*]pirimidīna, diazidoatvasinājumos;
- sintēzes metožu izstrāde S_NAr aizvietošanai annelētajos diazidopirimidīnos;
- sintēzes metožu izstrāde 2,6-diazidopurīnu pirimidīna gredzena atvēršanai;
- reaģētspējas pārbaude selektīvi aizvietoto annelēto azidopirimidīnu tālākai azidogrupas funkcionalizēšanai;
- enerģētiskā profila fizikālo rādītāju noteikšana darbā pētitajiem annelētajiem azidopirimidīniem un vismaz viena jauna tipa savienojuma dizainēšana šajā grupā, kas atbilstu binārajai C_xN_y enerģētisko savienojumu klasei ar augstu slāpekļa saturu.

Zinātniskā novitāte un galvenie rezultāti

No iespējamā annelēto azidopirimidīnu klāsta šajā promocijas darbā apskatīti:

- 2,4-diazidopirido[2,3-*d*]pirimidīni un 2,4-diazidopirido[3,2-*d*]pirimidīni kā jauna tipa struktūras, kam izpētīta reakcijas spēja;
- purīni, kam atklātas jauna tipa cikla atvēršanas reakcijas, kas dod tetrazolimidazolu ar aizvietotu sānu ķēdi;
- pirimidopirimidīns, uz kā bāzes dizainēts binārais enerģētiskais savienojums C_6N_{16} un annelēti diazidopirimidīni, kam noteikts to enerģētiskais profils.

2,4-Diazidopirido[2,3-*d*]pirimidīni un 2,4-diazidopirido[3,2-*d*]pirimidīni

Promocijas darbā pirmo reizi izpētīta 2,4-diazidopirido[2,3-*d*]pirimidīna un 2,4-diazidopirido[3,2-*d*]pirimidīna iegūšana un to azīda-tetrazola līdzsvāri. Atklāts, ka šie savienojumi šķīdumos raksturojas ar sarežģītu līdzsvaru, kurā iespējamās līdz pat četrām tautomērajām formām 2,4-diazidopirido[2,3-*d*]pirimidīnā un līdz pat septiņām tautomērajām formām 2,4-diazidopirido[3,2-*d*]pirimidīnā. Vienīgais šķīdinātājs, kura polārā daba un ūdeņraža saišu tīkls nodrošina tautomērā līdzsvāra pilnīgu novirzīšanu uz diazidoformu, ir trifluoretiķskābe. Savukārt kristāliskajā fāzē abos gadījumos ir novērotas tikai monotetrazola formas, kas no C(2)-azīda grupas veido jaunas annelētas tricikliskas struktūras: pirido[3,2-*e*]tetrazolo[1,5-*a*]pirimidīns un pirido[2,3-*e*]tetrazolo[1,5-*a*]pirimidīns.

Abās heterocikliskajās sistēmās nukleofilās aromātiskās aizvietošanas reakcijas ar *N*-, *O*- un *S*-nukleofiliem notiek selektīvi pie piridopirimidīna C(4), dodot C(5)-aizvietotus pirido[3,2-*e* un 2,3-*e*]tetrazolo[1,5-*a*]pirimidīnus, ko atkarībā no aizvietotāju prioritātes var

dēvēt arī par aizvietotiem tetrazolo[1,5-*a*]pirido[3,2-*e* un 2,3-*e*]pirimidīniem. Šie savienojumi šķīdumos pastāv galvenokārt tetrazola formā, tomēr sistēmās ir novērojams azīda-tetrazola līdzsvars. C(5)-Aizvietotu pirido[2,3-*e*]tetrazolo[1,5-*a*]pirimidīnu gadījumā tautomērā līdzsvara ΔG_{298} vērtības ir robežās no $-3,33$ kJ/mol līdz $-7,52$ kJ/mol, bet pirido[3,2-*e*]tetrazolo[1,5-*a*]pirimidīnu gadījumā ΔG_{298} ir $-3,02$ līdz kJ/mol $-5,70$ kJ/mol. Iegūtie annelētie tetrazola atvasinājumi ir funkcionalizējami vara katalizētā azīda-alkīna 1,3-dipolārā ciklopievienošanas (CuAAC) reakcijās par attiecīgajiem triazolīem, pateicoties azīda-tetrazola līdzsvaram šajās sistēmās. Līdzsvara pētījumos tika novērots, ka: 1) sistēmās ar elektronu donoriem aizvietotajiem līdzsvars ir stiprāk novirzīts uz tetrazola pusi; 2) palielinot šķīdinātāja polaritāti, tetrazola tautomēra koncentrācija palielinās; 3) šķīdumus sildot, palielinās azīda tautomēra koncentrācija. Šie novērojumi jaunajās heterocikliskajās sistēmās labi korelē ar literatūrā aprakstītām azīda-tetrazola līdzsvara procesa īpašībām.

Izstrādātā sintēzes metode, kurā kā izejvielas lieto 2,4-dihlorpiridopirimidīnus, tos pārvēršot par diazīdiem, pēc tam selektīvi aizvietojot ar *N*-, *O*- un *S*-nukleofiliem, darbojas efektīvāk nekā sākotnēja selektīva mono- S_NAr reakcija pie C(4) ar sekojošu azīda ievadīšanu pie C(2). Tas skaidrojams ar faktu, ka autora zinātniskās grupas piedāvātajā gadījumā annelētā tetrazola tautomērā forma gan nodrošina selektivitāti, gan veicina vispārējo S_NAr reakcijas spēju tetrazola elektronus atvelkošo īpašību dēļ. Savukārt klasiskajā pieejā, sākotnēji ievadot heteronukleofilu, kas kļūst par elektronodonoru aizvietotāju, tas aprūtinā nākamo S_NAr reakcijas soli.

2,6-Diazidopurīnu pirimidīna gredzena atvēršana

Aromātisko nukleofīlo aizvietošanu N(9)-aizvietotos 2,6-diazidopurīnos iespējams veikt reģioselektīvi C(2) vai C(6) pozīcijā, izvēloties piemērotu šķīdinātāju un reaģentu sistēmu. Tika atklāts, ka purīna atvasinājumiem, kam raksturīga annelētā tetrazola veidošanās pie C(6), iespējams pievienot papildus nukleofilu pie C(2). Tā rezultātā rodas Maizenhaimera komplekss, kas sabrūk ar pirimidīna cikla atvēršanos, jo tetrazols izrādās labāka aizejošā grupa nekā ienākošais *N*-, *O*- vai *S*-nukleofils. Arī šajā gadījumā azīda-tetrazola līdzsvars ne vien inducē reģioselektivitāti, bet arī aktivē purīna heterociklisko sistēmu nukleofīla uzbrukumam. Izmantojot šo divpakāpju sintēzes metodi, iegūstami augsti funkcionalizēti iminoimidazoliltetrazoli, kas aizvietoti ar dažādiem heteronukleofiliem. Tika parādīts, ka imidazoliltetrazolu alkilēšanas-ciklizācijas reakcijā iegūstami tetrazolodiazepīni, kas ir formāla tetrazolopurīna homologēšana, paplašinot tā heterociklisko sistēmu par vienu oglekļa atomu.

Enerģētiskais profils un jauns binārais savienojums

Visiem darbā pētītajiem azidoheterocikliem to enerģētiskais profils ir noteikts sadarbībā ar profesora Tomasa Klapetkes (*Thomas M. Klapötke*) grupu no Mīnhenes Ludviga Maksimiliāna universitātes. Dizainēts un iegūts jauns enerģētisks binārais C_6N_{16} savienojums – 2,4,6,8-tetraazidopirimido[5,4-*d*]pirimidīns. Šis tetraazīds šķīdumos pastāv azīda-tetrazola līdzsvarā un cietajā fāzē kristalizējas kā monotetrazola tautomērs. Pateicoties augstajai slāpekļa bilancei (75%), šim savienojumam piemīt primāro sprāgstvielu īpašības un tas detonējas vieglas berzes vai trieciena iedarbībā. Šis atklājums paver iespēju Latvijā uzsākt un attīstīt plašākus primāro sprāgstvielu (detonatoru materiālu) pētījumus.

Darba struktūra un apjoms

Promocijas darbs sagatavots kā tematiski vienotu zinātnisko publikāciju kopa, kas apkopo pētījumus par azidogrupas izmantošanu sintētiskajā metodoloģijā – reģioselektivitātes un reaģētspējas inducēšanai anelētos pirimidīnos un materiālzinātnē – jaunu primāro sprāgstvielu izstrādē. Promocijas darbā apkopotas četras publikācijas *SCI* žurnālos un viens raksta manuskripts.

Darba aprobācija un publikācijas

Promocijas darba galvenie rezultāti publicēti trīs zinātniskajos oriģinālrakstos, kā arī sagatavots viens oriģinālpētījuma raksta manuskripts. Promocijas darba izstrādes laikā sagatavots viens apskatraksts. Pētījumu rezultāti prezentēti deviņās zinātniskajās konferencēs.

Zinātniskās publikācijas

1. Zaķis, J. M.; **Leškovskis, K.**; Ozols, K.; Kapilinskis, Z.; Kumar, D.; Mishnev, A.; Žalubovskis, R.; Supuran, C. T.; Abdoli, M.; Bonardi, A.; Novosjolova, I.; Turks, M. Diazidopurine Ring Opening – Synthesis of Tetrazolyimidazole Derivatives. *Manuskripts iesniegts Journal of Organic Chemistry*.
2. **Leškovskis, K.**; Mišņovs, A.; Novosjolova, I.; Krumm, B.; Klapötke, T.; Turks, M. 2,4,6,8-Tetraazidopyrimido[5,4-*d*]pyrimidine: a Novel Energetic Binary Compound. *Cryst. Eng. Comm.* **2023**, *25*, 3866-3869. doi:10.1039/D3CE00563A.
3. **Leškovskis, K.**; Novosjolova, I.; Turks, M. Structural Study of Azide-Tetrazole Equilibrium in Pyrido[2,3-*d*]Pyrimidines. *J. Mol. Struct.*, **2022**, *1269*, 133784. doi:10.1016/j.molstruc.2022.133784.
4. **Leškovskis, K.**; Mišņovs, A.; Novosjolova, I.; Turks, M. S_NAr Reactions of 2,4-Diazidopyrido[3,2-*d*]pyrimidine and Azide-Tetrazole Equilibrium Studies of the Obtained 5-Substituted Tetrazolo[1,5-*a*]pyrido[2,3-*e*]pyrimidines. *Molecules* **2022**, *27*, 7675-7675. doi:10.3390/molecules27227675.
5. **Leškovskis, K.**; Zaķis, J.; Novosjolova, I.; Turks, M. Applications of Purine Ring Opening in the Synthesis of Imidazole, Pyrimidine, and New Purine Derivatives. *Eur. J. Org. Chem.* **2021**, *2021*, 5027-5052. doi:10.1002/ejoc.202100755.

Pētījumu rezultāti prezentēti deviņās konferencēs.

1. **Leškovskis, K.**, Novosjolova, I., Turks, M. Synthesis and physical properties of 2,6,8-triazidopurine and 2,4,6,8-tetraazidopyrimido[5,4-*d*]pyrimidine. No: *13th Paul Walden Symposium: Program and abstracts*, Latvija, Rīga, 14.-15. septembris, 2023. Rīga: 2023, 48. lpp.
2. **Leškovskis, K.**, Novosjolova, I., Turks, M. Azide-Tetrazole Equilibrium Driven Reactions of Fused Diazido Pyrimidines and Characterization of Tautomerism Therein. No: *International Symposium on Synthesis and Catalysis 2023: Book of Abstracts*, Portugāle, Evora, 5.–8. septembris, 2023. Evora: 2023, 211. lpp.
3. **Leškovskis, K.**; Novosjolova, I.; Turks, M. Azide-Tetrazole Equilibrium in Pyrido[3,2-*d*]pyrimidines. No: *Latvijas Universitātes 81. zinātniskā konference*

- ĶĪMIJAS sekcija: Book of Abstracts*, Latvija, Rīga, 17. marts, 2023. Rīga: 2023, 5. lpp.
4. **Leškovskis, K.**; Novosjolova, I.; Turks, M. Azidoazomethine-Tetrazole Tautomerism in Pyrimidines. No: *Balticum Organicum Syntheticum 2022: Program and Abstract Book*, Lietuva, Vilnius, 3.–6. jūlijs, 2022. Vilnius: 2022, 109. lpp.
 5. **Leškovskis, K.**; Novosjolova, I.; Turks, M. Synthesis of Tetrazole Fused Pyrido-Pyrimidines. No: *2nd Drug Discovery Conference: Abstract Book*, Latvija, Rīga, 22.–24. septembris, 2022. Rīga: 2022, 61. lpp.
 6. **Leškovskis, K.**; Turks, M.; Novosjolova, I. Azido-Azomethine – Tetrazole Tautomerism in Pyridopyrimidines. No: *ORCHEM22: Abstract Book*, Vācija, Minstere, 5.–7. septembris, 2022. Minstere: 2022, 115. lpp.
 7. **Leškovskis, K.** Aromatic Substitution of Azido-Pyridopyrimidines and Study of Their Azide Tetrazole Equilibrium. No: *The 27th Croatian Meeting of Chemists and Chemical Engineers: Book of Abstracts*, Horvātija, Veli Lošinj, 5.–8. oktobris, 2021. Veli Lošinj: 2021, 123. lpp.
 8. **Leškovskis, K.** Azide-Tetrazole Equilibrium Study in 2,4-Diazidopyrido[2,3-*d*]pyrimidine. No: *Rīga Technical University 62nd International Scientific Conference “Material Science and Applied Chemistry”*: Program and Abstracts, Latvija, Rīga, 22. oktobris, 2021. Rīga: 2021, 32. lpp.
 9. **Leškovskis, K.** S_NAr Regioselectivity and Azide-Tetrazole Equilibrium Study in Pyrido[2,3-*d*]pyrimidine. No: *12th Paul Walden Symposium on Organic Chemistry: Program and Abstract Book*, Latvija, Rīga, 28.–29. oktobris, 2021. Rīga: 2021, 34. lpp.

Darba drošības informācija

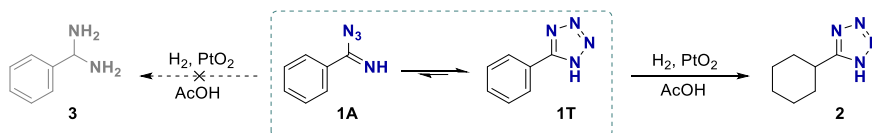
UZMANĪBU! Heteroaromātiskie azidosavienojumi ar slāpekļa saturu $\geq 50\%$ var būt spēcīgi enerģētiskie materiāli ar augstu jutību pret triecieniem un berzi. Sintezējot un strādājot ar vairākiem no aprakstītajiem azidoheterocikliem, ir jāievēro atbilstoši drošības pasākumi, kas ietver, bet neaprobežojas ar: drošības brillēm; sejas aizsargu; ausu aizbāžņiem; *Kevlar* cimdiem; drošības aizslietni; iezemētu laboratorijas aprīkojumu un apaviem.

PROMOCIJAS DARBA GALVENIE REZULTĀTI

1. Azīda-tetrazola līdzsvars un tā lietojums sintētiskajā metodoloģijā

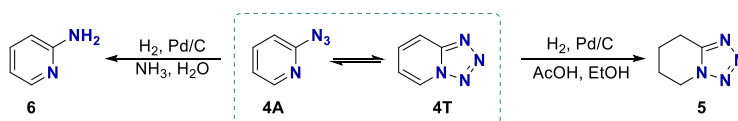
Heterocikli ar azidoazometīna struktūru ir unikāli ar iespējamo azīda-tetrazola līdzsvaru šķīdumos.^{28,29} Azīda-tetrazola līdzsvars ir valences tautomērisms, kas noris, azīdam savienojoties ar blakus esošu imīna fragmentu 1,5-dipolārā ciklizācijas reakcijā. Azīda-tetrazola līdzsvars ir dinamisks, un to ietekmē aizvietotāju stereoelektroniskie efekti, šķīdinātāja polaritāte, temperatūra un vides pH.^{30–32}

Izolēts tetrazola gredzens ir par ~ 40 kJ/mol stabilāks nekā azīda tautomērs, pateicoties 6 π -elektronu aromātiskajai sistēmai,³³ tādēļ tautomērais līdzsvars izolētā tetrazola sistēmā parasti nav novērojams. Tāpēc azīda funkcionālās grupas transformācijas šādām sistēmām nav iespējamas. Piemēram, 5-feniltetrazola (**1T**) reducēšana ar H₂ uz platīna katalizatora notiek ar selektīvu benzola aromātiskā gredzena reducēšanu un tetrazola funkcionālā grupa paliek neskarta (2. shēma).³⁴



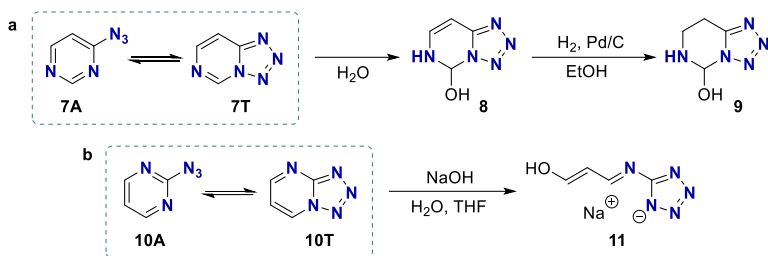
2. shēma. Feniltetrazola reducēšana.

Savukārt annelētās azidoazometīna sistēmās pastāv dinamisks azīda-tetrazola līdzsvars, ko iespējams novērot arī ar dažādām spektroskopiskajām metodēm (IS, UV, KMR). Reakcijas šādās sistēmās var notikt gan ar tetrazola formu – reaģē annelētā sistēma vai kāda cita tai piesaistīta funkcionālā grupa, gan ar azīda formu – reducēšana, ciklopievienošana vai nitrēnu reakcijas. Piemēram, 2-azidopiridīnu **4A** iespējams selektīvi reducēt līdz tetrahidropiridotetrazolam (**5**) vai 2-aminopiridīnam (**6**), mainot šķīdinātāju un vides pH (3. shēma).³⁵



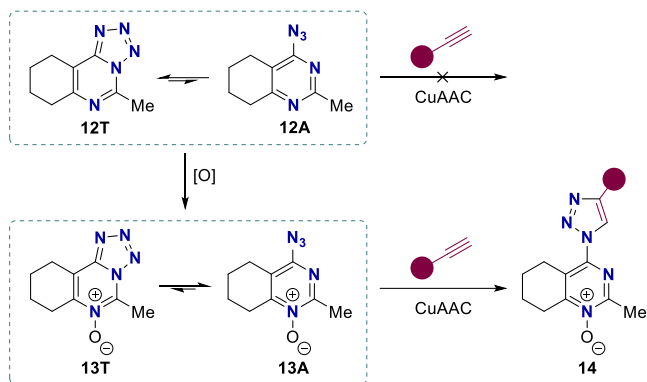
3. shēma. 2-Azidopiridīna reducēšana.

Pateicoties elektronus atvelkošās grupas īpašībām, annelētās tetrazola sistēmas ir reaģētspējīgākas nukleofilu pievienošanā, salīdzinot ar to azidoanalogiem. Piemēram, 4-azidopirimidīna **7** sistēma tautomerizējoties reaģē ar ūdeni jau normālos apstākļos bez skābes vai bāzes piedevām, veidojot hemiaminālu **8**. To iespējams viegli reducēt ar H₂ Pd/C katalizatora klātienē, iegūstot annelētās sistēmas reducēšanas produktu **9** ar saglabātu tetrazola funkcionālo grupu (4. a shēma).³⁶ Tetrazolo[1,5-*a*]pirimidīnu **10T** bāziskos apstākļos iespējams atvērt, veidojot tetrazola sāli **11** (4. b shēma).³⁷



4. shēma. Azidopirimidīnu funkcionalizēšana.

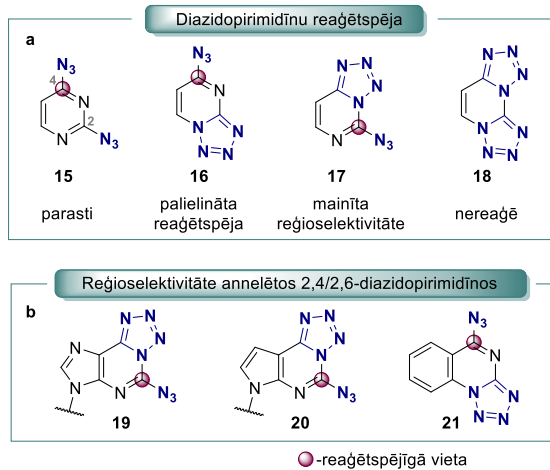
Azīda-tetrazola līdzsvaru stipri ietekmē annelētajā sistēmā esošo aizvietotāju elektroniskie efekti. Mainot sistēmas kopējo elektronu blīvumu, iespējams pilnīgi apgriezt tautomēro līdzsvaru. Piemēram, ar tetrazolu annelētā pirimidīna sistēmā **12**, oksidējot pirimidīnu par *N*-oksīdu, tetrazols **13T** tautomerizējas par azīdu **13A**, ko iespējams funkcionalizēt azīdam raksturīgajā CuAAC reakcijā (5. shēma).³⁸



5. shēma. Elektronisko efektu virzīta annelēta tetrazolo[1,5-*c*]pirimidīna funkcionalizēšana.

Heterocikliskajās sistēmās ar divām azidoazometīna grupām paveras iespēja veikt reģioselektīvas transformācijas, veicot apzinātu šķīdinātāja izvēli un temperatūras kontroli (1. a att.). Nukleofilu pievienošana pirimidīnos ar divām identiskām aizejošajām grupām parasti noris aktīvākajā C(4) vietā (1. att., **15**). Savukārt, mainoties līdzsvaram, pievienošanās var: 1) pātrināties (1. att., **16**), pateicoties tetrazola elektronus atvelkošajām īpašībām, kas stabilizē Maizenhaimera (*Meisenheimer*) kompleksa intermediātus vai 2) notikt ar mainītu reģioselektivitāti (1. att., **17**), sistēmā veidojoties tetrazolam, kas nevar stāties S_NAr reakcijā, vai 3) nenotikt vispār (1. att., **18**).

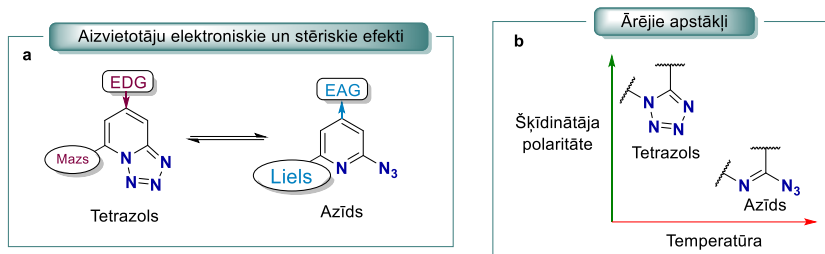
Annelētu 2,4-diazidopirimidīnu sērijā ir zināms, ka 2,6-diazidopurīnos **19**³⁹ un 2,6-diazidodeazapurīnos **20**⁴⁰ aizvietošanās noris C(2) pozīcijā ar mainītu reģioselektivitāti, ko sekmē annelētais tetrazola fragments, savukārt ar 2,4-diazidohinazolīnu **21**¹⁴ reģioselektivitātes maiņa nenotiek un reaģētspējīgāka ir C(4) pozīcija.



1. att. Azīda-tetrazola līdzsvars un reaģētspēja anelētos 2,4/2,6-diazidopirimidīnos.

Literatūrā ir labi zināms, ka aizvietotājiem heterocikliskajā sistēmā ir vitāla loma uz azīda-tetrazola tautomēro līdzsvaru (2. att.). Elektronu donorie aizvietotāji virza līdzsvaru uz tetrazola formas pusi, stabilizējot tetrazola tautomēru, kamēr elektronu akceptorie aizvietotāji – azīda formu.^{32, 41, 42} Galvenie līdzsvaru ietekmējošie ārējie faktori ir: šķīdinātāja polaritāte (polārāki šķīdinātāji stabilizē tetrazola sistēmas dipola momentu); temperatūra (augstākās temperatūrās veidojas termodinamiski izdevīgākā – azīda forma); heterocikliskās sistēmas protonēšana (elektroniem nabadzīgā sistēmā veidojas azīda tautomērs).²⁸ Biežāk izmantotie šķīdinātāji tautomerizācijas procesa pētījumiem ir DMSO, TFA un CHCl_3 . Šajos šķīdinātājos parasti iespējams novērot azīda-tetrazola sistēmas līdzsvara galējības: DMSO – tetrazols (augstās polaritātes dēļ); TFA – azīds (sistēma tiek protonēta vai veidots izteikts ūdeņraža saišu tīkls); CHCl_3 – tautomēru maisījums.^{36, 43, 44}

Azīda-tetrazola tautomērismu iespējams pierādīt ar tādām metodēm kā UV un IS spektroskopija.⁴⁵ Atsevišķos specifiskos gadījumos to var veikt ar plānslāņa hromatogrāfiju³⁵ un kušanas punkta noteikšanu.⁴⁴ Savukārt ar ^{15}N KMR iespējams analizēt slāpekļa atomus, lai arī magnētiski aktīvā ^{15}N kodola dabīgā koncentrācija savienojumos ir ~ 0,36 % un ^{15}N kodola žiromagnētiskā jutība ir ievērojami zemāka kā citiem kodoliem. Šo iemeslu dēļ ^{15}N KMR pētījumi substrātiem ar dabīgo slāpekļa izotopu sadalījumu ir apgrūtināti. Tomēr azīda-tetrazola līdzsvars savienojumos ar azīda-tetrazola fragmentam netālu esošiem protoniem ir ļoti labi novērojams un viegli kvantificējams ar ^1H KMR. Pēc signālu integrēšanas iegūst tautomēro formu attiecību, kas raksturojama ar līdzsvara konstanti $K_{\text{līdzsv.}}$.^{37, 46, 47} Uzņemot ^1H KMR spektrus dažādās temperatūrās, iespējams raksturot līdzsvara procesu ar termodinamiskajiem parametriem (Gibsa brīvā enerģija, entalpija un entropija).^{31, 48, 49}



2. att. Azīda-tetrazola līdzsvaru ietekmējošie faktori.

Jebkurš dinamiskā līdzsvara process ķīmijā tiek raksturots ar līdzsvara konstanti $K_{\text{līdzsv.}}$, kas ir apgriezeniskas ķīmiskās pārvērtības ātruma koeficientu attiecība sistēmai, kurā iestājies ķīmiskais līdzsvars. Tātad līdzsvara konstanti (1.1. vienādojums) var izteikt kā divu komponentu koncentrāciju attiecību līdzsvara stāvoklī, ko iespējams viegli noteikt ar ^1H KMR spektroskopiju pēc signālu integrālās attiecības.

$$K_{\text{līdzsv.}} = \frac{[T]}{[A]}, \quad (1.1.)$$

kur $K_{\text{līdzsv.}}$ – līdzsvara konstante;

T – tetrazola tautomēra koncentrācijas integrālā vērtība;

A – azīda tautomēra koncentrācijas integrālā vērtība.

Līdzsvarā esošas sistēmas var raksturot ar tautomerizācijas procesa termodinamiskajiem parametriem – Gibbsa brīvo enerģiju, entalpiju un entropiju. Gibbsa brīvā enerģija nosaka līdzsvara virzienu konkrētajos apstākļos un procesa termodinamisko iespējamību. Savukārt entalpija raksturo absolūto sistēmas stabilitāti neatkarīgi no ārējiem apstākļiem (augstāka vērtība – stabilāka sistēma). Izmantojot Gibbsa-Helmholca (*Gibbs-Helmholtz*) vienādojumu (1.2. vienādojums), iespējams aprēķināt Gibbsa brīvo enerģiju tautomerizācijas procesam.

$$\Delta G = -RT \ln K_{\text{līdzsv.}}, \quad (1.2.)$$

kur ΔG – Gibbsa brīvā enerģija tautomerizācijai, J/mol;

R – universālā gāzu konstante, J/(mol·K);

T – temperatūra, K;

$K_{\text{līdzsv.}}$ – līdzsvara konstante.

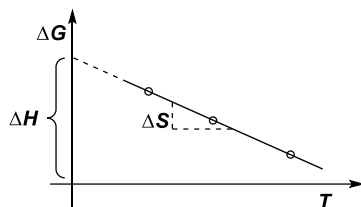
Tautomerizācijas procesa entalpiju un entropiju nosaka grafiski, attēlojot Gibbsa brīvo enerģiju pret temperatūru, un aprēķina pēc Gibbsa brīvās enerģijas vienādojuma (1.3. vienādojums), kur y ass vērtība absolūtās nulles temperatūrā (0 K) ir sistēmas entalpija, taisnes slīpums – sistēmas entropija (3. att.).

$$\Delta G = \Delta H - T\Delta S, \quad (1.3.)$$

kur ΔG – Gibbsa brīvā enerģija tautomerizācijai, J/mol;

ΔH – tautomerizācijas entalpija, J/mol;

ΔS – tautomerizācijas entropija, J/(mol·K).



3. att. Gibbsa brīvās enerģijas vienādojuma grafiskais attēlojums.

Dinamiskā līdzsvara procesā, lai gan iestājies līdzsvars, visu laiku pastāv apgriezeniska reakcija $A \rightleftharpoons B$, kas raksturojama kā divas reakcijas $A \xrightarrow{k_B} B$ un $B \xrightarrow{k_A} A$ ar ātruma konstantēm (k_A un k_B), kas ir savstarpēji proporcionālas un izsaka līdzsvara konstanti (1.4. vienādojums). Kinētiskās konstantes ļauj aprēķināt līdzsvara iestāšanās ātrumu, ko raksturo ar reakcijas puslaiku $\tau_{1/2}$.

$$K_{\text{līdzsv}} = \frac{k_B}{k_A}, \quad (1.4.)$$

kur $K_{\text{līdzsv}}$ – līdzsvara konstante;

k_B – tiešās reakcijas ātruma konstante (s^{-1});

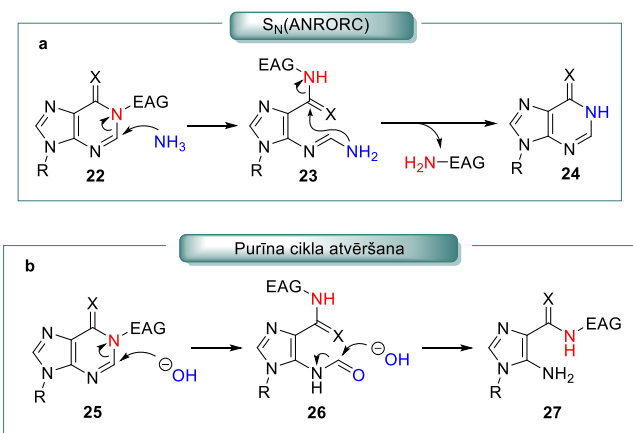
k_A – apgrieztās reakcijas ātruma konstante (s^{-1}).

Dinamiskā procesa ātruma mērīšanai ar KMR izmanto ķīmiskās apmaiņas spektroskopijas eksperimentu (*EXSY*), kurā mēra magnetizācijas pārnesei protonam tautomerizējoties no vienas formas otrā.⁵⁰ Azīda-tetrazola līdzsvara kinētisko konstanšu noteikšana ir svarīga līdzsvara raksturošanai. Piemēram, lēnas tautomerizācijas gadījumā līdzsvara pētījumu veikšanai nepieciešams ilgstošs laika periods līdzsvara stāvokļa sasniegšanai sistēmā.^{42, 51} Kinētiskās konstantes nosaka reaģētspējas ātrumu reakcijās, kad reaģē viens izvēlēts tautomērs.

1.1. Azīda-tetrazola līdzsvars purīna sistēmā un pirimidīna cikla atvēršana

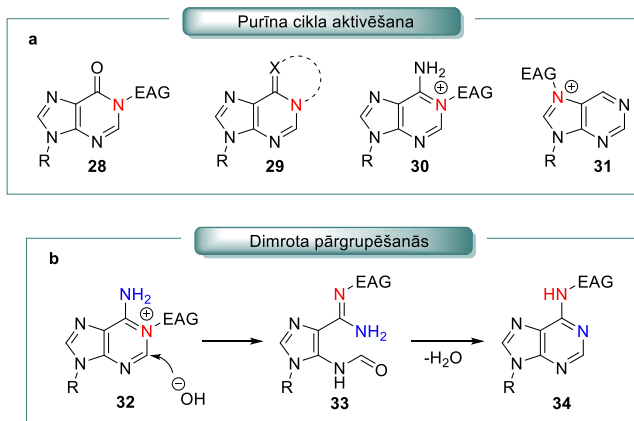
Purīns ir dabā plaši sastopams slāpekļa heterocikls, kura atvasinājumi – adenīns un guanīns – ietilpst DNS sastāvā. Tāpēc liela daļa pretvīrusu un pretvēža preparātu ir veidoti uz purīna un nukleozīdu fragmentu līdzības principa.

Purīns ir stabila heterocikliskā sistēma, pateicoties tās konjugētās π -elektronu sistēmas aromātiskumam. Tomēr elektronus atvelkošu funkcionālo grupu ievadīšana uz purīna cikla slāpekļiem padara sistēmu elektrofilāku un veicina nukleofilu pievienošanu. *N*-nukleofilu pievienošana aktivētiem purīniem rezultējas ar formālu N(1) grupas un slāpekļa atoma aizvietošanu tandēmā pirimidīna cikla atvēršanas un saslēgšanas reakcijā pēc $S_N(\text{ANRORC})$ mehānisma (6. a shēma). Savukārt sārma pievienošana šādām sistēmām parasti rezultējas ar C(2) oglekļa fragmenta izšķelšanu bez pirimidīna ciklizācijas (6. b shēma).⁵² Šāda purīna cikla atvēršana ir vienkārša sintētiskā stratēģija augsti funkcionalizētu imidazolu un pirimidīnu, kas ir bieži izmantoti farmakofori medicīnas ķīmijā, pateicoties to līdzībai ar bioloģiskajās sistēmās sastopamajiem nukleozīdiem, iegūšanai.^{53, 54}



6. shēma. Purīna pirimidīna cikla atvēršana.

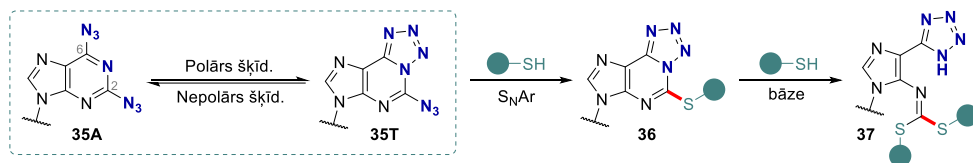
Pastāv četri iespējamie purīna sistēmas aktivēšanas mehānismi (7. shēma). Pirmkārt, hipoksantīni ir reaģētspējīgāki, pateicoties esošajai karbonilgrupai, un elektronus atvelkošās grupas ievadīšana N(1) pozīcijā ļauj atvērt hipoksantīnus ar dažādiem nukleofiliem jau istabas temperatūrā. Otrkārt, anelētos purīnos N(1) pozīcija ir daļa no atsevišķas konjugētās sistēmas, kas to padara par aizejošo grupu. Treškārt, elektronus atvelkošās grupas ievadīšana N(1) pozīcijā purīnos un adenīnos padara to par izcilu aizejošo grupu. Aktivētā adenīna sistēmā parasti notiek Dimrota (*Dimroth*) pārgrupēšanās.⁵⁵⁻⁵⁸ Visbeidzot, elektronu akceptorās grupas ievadīšana N(7) pozīcijā destabilizē imidazola ciklu un tā atvēršana notiek gandrīz jebkādos apstākļos.



7. shēma. Purīna cikla aktivēšanas mehānismi.

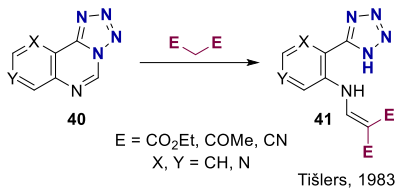
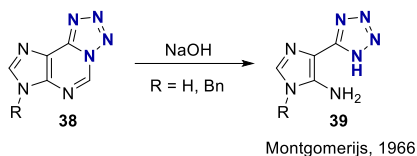
Detalizētāka informācija par purīnu aktivēšanas veidiem un atvēršanu – apskatrakstā 1. pielikumā.

Balstoties iepriekšējos pētījumos 9-aizvietotu 2,6-diazidopurīnu ķīmijā, ir zināms, ka, pateicoties azīda-tetrazola līdzsvaram, nukleofilā aromātiskā aizvietošanās šādās sistēmās notiek C(2) pozīcijā (8. shēma).^{5, 39, 59, 60} Šāda C(6) pozīcijas aizsargāšana nukleofila uzbrukumu veicina arī S_NAr procesu atlikušajā heterocikliskajā sistēmā, pateicoties tās elektronu atvelkošajām īpašībām. Kristera Ozola maģistra darbā aprakstītajos pētījumos, izmēģinot tālāku otra nukleofila pievienošanu 2,6-diazidopurīnam, tika novērots, ka iegūtais savienojums nebija sagaidāmais 2,6-diaizvietošanās produkts.⁶¹ Produkta analīze parādīja, ka tas satur divus pievienotos tiola nukleofilus un tetrazola fragmentu, kas atbilda purīna cikla atvēršanas produktam **37**.



8. shēma. K. Ozola novērtā S_NAr aizvietošana 2,6-diazidopurīnos un cikla atvēršana.⁶¹

Analizējot literatūras datus par pirimidīnu atvēršanu, tika noskaidrots, ka šāda tetrazolopirimidīna cikla atvēršana ir veikta divos piemēros. Pirmkārt, pievienojot stipru bāzi, demonstrējis Montgomerijs (*Montgomery*).⁴³ Otrkārt, ciklu atvēršanu ar oglekļa nukleofiliem, tiem saglabājoties produkta struktūrā, veicis Tišlers (*Tišler*)^{62,63} (9. shēma). Tādēļ šajā promocijas darbā tika izstrādāta metode purīna cikla atvēršanai ar dažādiem nukleofiliem, apvienojot reģioselektīvu 2,6-diazidopurīna aizvietošanu ar tandēmu pirimidīna cikla atvēršanu.

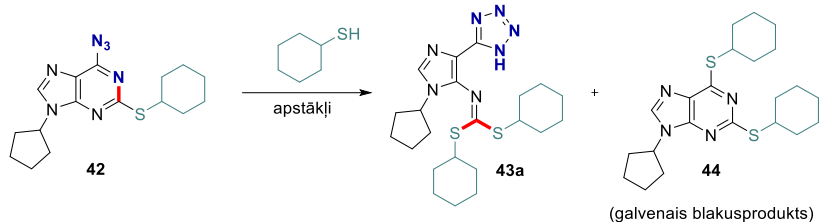


9. shēma. Tetrazolopirimidīnu cikla atvēršana.

Uzsākot pētījumu par 2,6-diazidopurīnu ciklu atvēršanu, vispirms tika veikta reakcijas apstākļu optimizācija tiola nukleofīla gadījumā (1.1. tab.), par substrātu izvēloties C(2) aizvietotu 6-azidopurīnu **42**, jo apstākļi reģioselektīvai 2,6-diazidopurīna aizvietošanai ar tioliem ir zināmi no K. Ozola maģistra darba. Savukārt cikla atvēršanas apstākļu optimizēšanai ar spirtu tika izvēlēts neaizvietots 2,6-diazidopurīns **45a** (1.2. tab.).

Cikla atvēršanā ar tioliem tika secināts: 1) nepolāros šķīdinātājos (toluols) aizvietošana notiek C(2) un C(6) pozīcijās, jo pastāv diazīda forma, tādēļ atvēršanai nepieciešams polārs šķīdinātājs DMF; 2) cikla atvēršanai nepieciešama stipra nenukleofīla bāze NaH, jo, izmantojot vājākas bāzes (DBU (1,8-diazabicyklo[5.4.0]undec-7-ēns), K₂CO₃), notiek aizvietošana C(2) un C(6) pozīcijās; 3) pazemināta temperatūra mazina blakusproduktu veidošanos, jo palielinās tetrazola koncentrācija un stabilizējas Maizenhaimera komplekss.

Optimizējot purīna cikla atvēršanas reakcijas apstākļus ar spirtiem, tika novērotas atšķirīgas tendences, salīdzinot ar tioliem. Piemērotākais šķīdinātājs bija toluols, kas deva augstāko selektivitāti cikla atvēršanas reakcijai. Šis novērojums ir pretējs purīnu atvēršanas apstākļiem ar tiola nukleofīliem un vispārīgajam konceptam, ka polāri šķīdinātāji stabilizē veidojošos Maizenhaimera intermediātu. Piemērotākā bāze arī šajā gadījumā izrādījās NaH, tomēr interesanti, ka līdzīgi rezultāti tika iegūti, izmantojot DBU, kas tiolu gadījumā nebija spējīgs veikt cikla atvēršanu. Arī temperatūras pazemināšana īpaši neietekmēja reakcijas iznākumu, lai gan temperatūras palielināšana pat nedaudz uzlaboja cikla atvēršanas reakcijas iznākumu un selektivitāti.

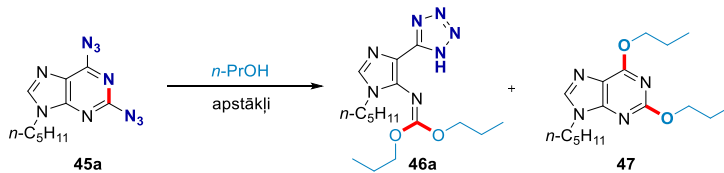
Reakcijas apstākļu optimizācija purīna **42** cikla atvēršanai ar tiolu

Nr.	Šķīdinātājs	Bāze (ekviv.)	<i>T</i> (°C)	Iznākums 43a (%) ^a	Izejviela 42 (%) ^a
1	DMF	NaH (1,5)	i. t.	55	12
2	DMF	KOtBu (1,5)	i. t.	62	4
3	DMF	DBU (1,5)	i. t.	0	55
4	toluols	NaH (1,5)	i. t.	5	76
5	toluols	KOtBu (1,5)	i. t.	4	68
6	MeCN	NaH (1,5)	i. t.	8	76
7	MeCN	KOtBu (1,5)	i. t.	50	20
8	THF	NaH (1,5)	i. t.	43	40
9	THF	KOtBu (1,5)	i. t.	36	30
10	<i>i</i> -PrOH	KOtBu (1,5)	i. t.	34	24
11	DMSO	KOtBu (1,5)	i. t.	64	2
12	NMP	NaH (1,5)	i. t.	39	21
13	DMF	NaH (0,9)	i. t.	44	32
14	DMF	KOtBu (2,5)	i. t.	54	7
15	DMF	NaH (1,5)	0	68	5
16	DMF	KOtBu (1,5)	0	64	8

a – iznākums noteikts ar kvantitatīvo ¹H KMR metodi reakcijas maisījumā, izmantojot 1,2,3-trimetoksibenzolu kā iekšējo standartu.

Šo atšķirīgo tendenci iespējams skaidrot ar reakcijas mehānisma maiņu atkarībā no nukleofila. Tiolāts kā labāks nukleofils pievienojas purīna sistēmai un veido Maizenhaimera kompleksu. Savukārt spirtu gadījumā reakcija notiek saskaņotā S_NAr procesā bez Maizenhaimera kompleksa veidošanās.⁶⁴⁻⁶⁶ Šāds mehānisms izskaidrotu reakcijas norisi nepolārā šķīdinātājā un relatīvi vājākas bāzes DBU spēju veikt cikla atvēršanu.

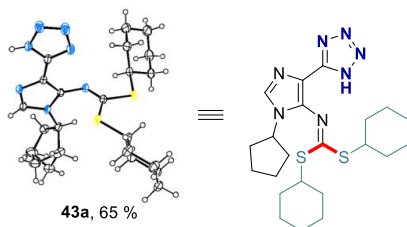
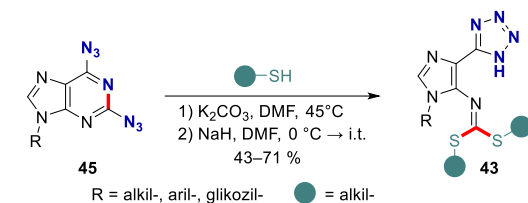
Reakcijas apstākļu optimizācija purīna **45a** cikla atvēršanai ar spirtu



Nr.	Šķīdinātājs	Bāze (ekviv.) ^b	<i>T</i> (°C)	Iznākums 46a (%) ^a	Iznākums 47 (%) ^a
1	DMF	NaH (3)	i. t.	38	21
2	MeCN	NaH (3)	i. t.	0	0
3	THF	NaH (3)	i. t.	36	33
4	<i>n</i> -PrOH	NaH (3)	i. t.	50	42
5	toluols	NaH (3)	i. t.	47	22
6	NMP	NaH (3)	i. t.	38	30
7	diglīms	NaH (3)	i. t.	44	16
8	toluols	K ₂ CO ₃ (3)	i. t.	0	0
10	toluols	KotBu (3)	i. t.	5	45
11	toluols	KOH (3)	i. t.	13	2
12	toluols	<i>n</i> -BuLi (3)	i. t.	7	4
13	toluols	NaH (3)	0	49	16
14	toluols	NaH (3)	50	55	13
15	toluols	NaH (5) ^c	i. t.	0	0
16	toluols	NaH (3)^d	i. t.	66	11
17	DMF	NaH (3) ^d	i. t.	21	42
18	DMF	DBU (3) ^d	i. t.	36	1
19	toluols	DBU (3) ^d	i. t.	49	1

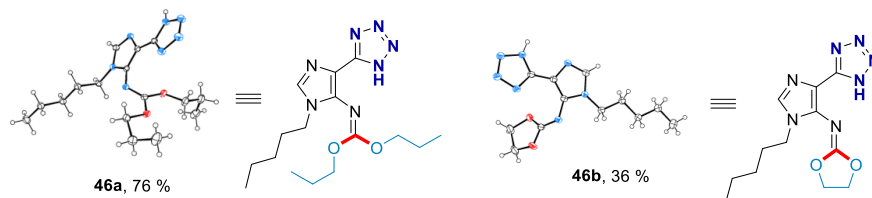
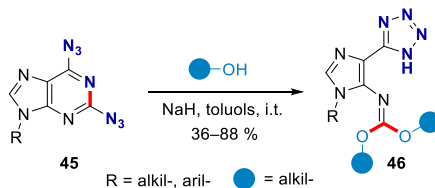
a – iznākums noteikts ar kvantitatīvo ¹H KMR metodi reakcijas maisījumā, izmantojot 1,2,3-trimetoksibenzolu kā iekšējo standartu; b – alkoksīds pievienots divās porcijās; c – alkoksīds pievienots vienā porcijā; d – alkoksīds pievienots pa pilienam.

Izmantojot optimizētos reakciju apstākļus, sadarbojoties ar laboratorijas kolēģiem (sk. raksta autoru sarakstu), izpētīts substrātu klāsts diazidopurīnu cikla atvēršanai ar tioliem (10. shēma). Purīna N(9) pozīcijas aizvietotājs praktiski neietekmēja reakciju iznākus, izņemot ribozilatvasinājumiem daļējas acetāta aizsarggrupu šķelšanās dēļ. Reakcijas noritēja veiksmīgi gan ar pirmējiem, gan otrējiem tioliem. Jāatzīmē, ka purīna cikla atvēršana ar aromātiskajiem tioliem nav iespējama konkrētajos apstākļos, visticamāk, tāpēc, ka ariltiolāts ir labāka aizejošā grupa nekā tetrazola anjons.



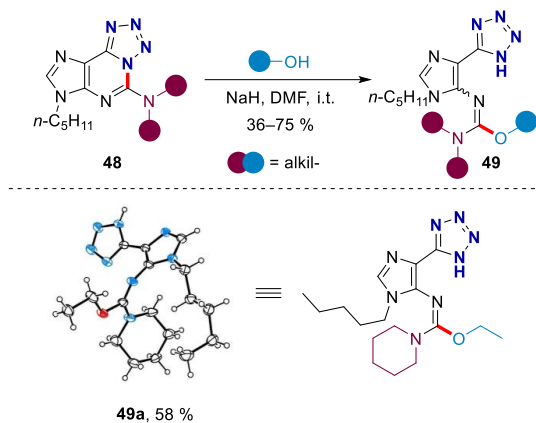
10. shēma. Diazidopurīna **45** atvēršana ar tioliem.

Izmantojot piemeklētos reakcijas apstākļus *O*-nukleofilu gadījumā (NaH/toluols), tika demonstrēts substrātu klāsts purīna cikla atvēršanai ar dažādiem spirtiem (11. shēma). Jāuzsver, ka izdevās iegūt ciklisko pievienošanās produktu **46b**, izmantojot etilēnglikolu kā nukleofilu. Arī šajā gadījumā purīna cikla atvēršana ar aromātiskiem (fenols) un stēriski lieliem (*t*-BuOH, adamantanols) spirtu nukleofīliem nav iespējama.



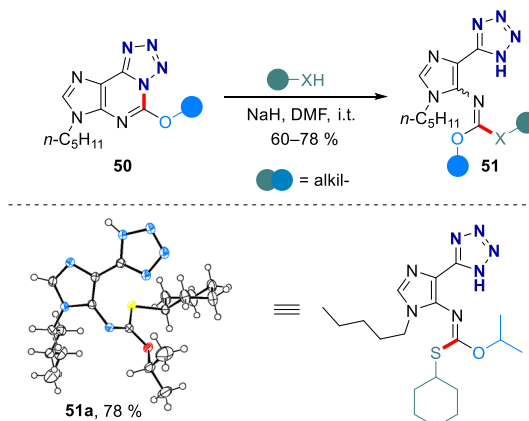
11. shēma. Diazidopurīna **45** cikla atvēršana ar spirtiem.

Purīna cikla atvēršana ar amīnu nukleofīliem izrādījās neiespējama. Tomēr, pakļaujot purīnus **48** ar aminoizvietotajiem C(2) pozīcijā cikla atvēršanas apstākļiem ar pirmējiem un otrējiem spirtiem, tika iegūti karbamimidāti **49** (12. shēma). Aromātisku (fenols) un stēriski lielu (*t*-BuOH) spirtu pievienošana nebija efektīva. Šajā gadījumā – reakcijā ar fenolu, tika iegūts hidrolīzes produkts ar 62 % iznākumu, kas arī bija galvenais blakusprodukts šī tipa reakcijās.



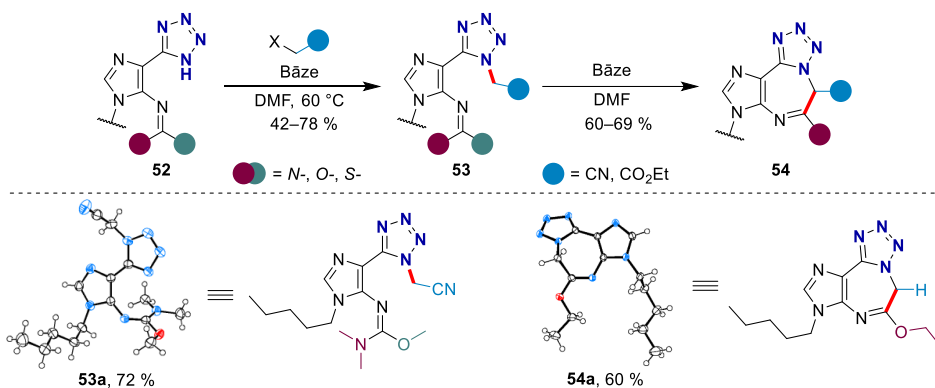
12. shēma. Tetrazoloaminopurīnu **48** cikla atvēršana ar spirtiem.

Līdzīgi tika iegūti arī alkoksiaizvietotu tetrazolopurīnu **50** cikla atvēršanas produkti **51** ar pirmējo un otrējo spirtu vai tiolu pievienošanu (13. shēma). Produktu stereoselektivitāti nebija iespējams noteikt ar KMR spektroskopiju, taču izdevās iegūt savienojuma **51a** monokristālu, kas parādīja Z-dubultsaites ģeometriju produktā.



13. shēma. Tetrazoloalkoksipurīnu **50** atvēršana ar alkoksīdiem un tioliem.

Izstrādātās metodes funkcionalitātes demonstrēšanai iegūtie cikla atvēršanas produkti **52** tika alkilēti un tālāk bāziskos apstākļos ciklizēti par diazepīna atvasinājumiem **54** (14. shēma), tādējādi veicot formālu purīna pirimidīna cikla paplašināšanu par vienu oglekļa atomu.

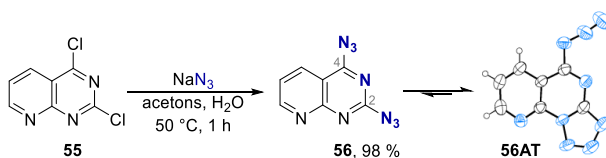


14. shēma. Annelētu tetrazolodiazepīnu **54** sintēze.

Šīs nodaļas pētījumi plašāk aprakstīti oriģinālpublikācijas manuskriptā 2. pielikumā.

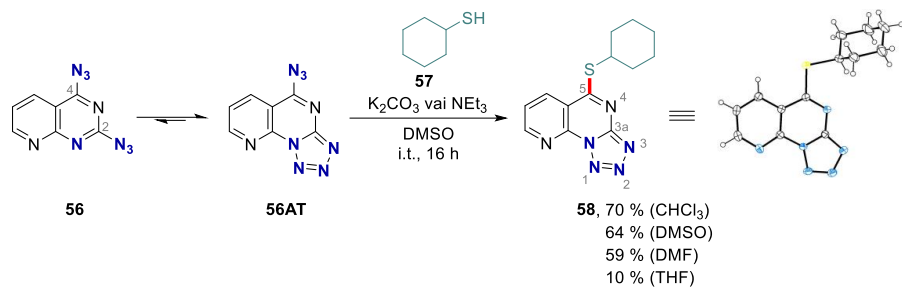
1.2. Azīda-tetrazola līdzsvara un S_NAr reakciju pētījumi pirido[2,3-*d*]pirimidīna heterociklā

Šī pētījuma daļa tika sākta ar galvenās izejvielas – 2,4-diazidopirido[2,3-*d*]pirimidīna **56** (*diazīds*) – sintēzi no dihlorīda **55** S_NAr reakcijā ar NaN_3 (15. shēma). Ar nosaukumu *diazīds* promocijas darbā ir apzīmētas formālās *diazīda* struktūras, jo šīs sistēmas eksistē kā vairāku azīda-tetrazola tautomēru maisījums. Stabilākais tautomērs 2,4-diazidopirimidīnu sistēmās parasti ir tetrazolo[1,5-*a*]pirimidīna formā.^{14, 44, 67, 68} Ar rentgenstruktūranalīzi tika noskaidrots, ka arī 2,4-diazidopirido[2,3-*d*]pirimidīna heterocikliskā sistēma kristāliskajā fāzē pastāv kā 5-azidopirido[3,2-*e*]tetrazolo[1,5-*a*]pirimidīns (**56AT**). Šīs tautomērās formas S_NAr reakcijas rezultētos ar nukleofilu pievienošanu C(4) pozīcijā, kas ir sagaidāms pirimidīna sistēmām ar diviem identiskiem C(2) un C(4) pozīcijas aizvietotājiem.

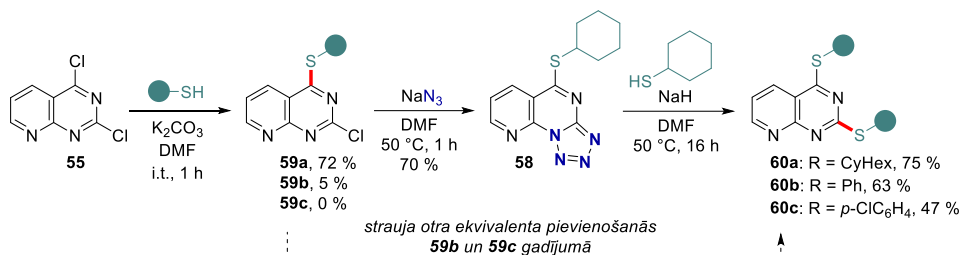


15. shēma. *Diazīda* **56** sintēze.

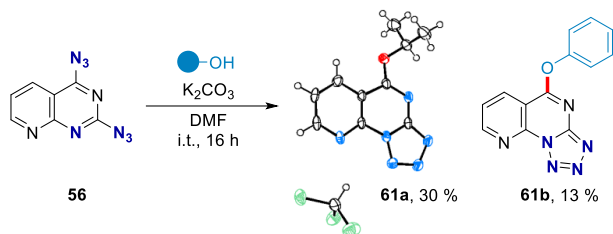
Tālāk tika izpētīts azīda-tetrazola līdzsvars, lai noteiktu iespējamo C(2) vai C(4) reģioselektivitāti S_NAr reakcijās ar *diazīdu* **56**. S_NAr reakciju pētījumi tika sākti ar cikloheksāntiols pievienošanu *diazīdam* **56** dažādas polaritātes šķīdinātājos: $CHCl_3$, THF, DMF un DMSO. Visos gadījumos pievienošanās noritēja C(4) pozīcijā, kas liecināja par tautomērās formas **56AT** pārkumu un augstāku reaģētspēju neatkarīgi no šķīdinātāja polaritātes (16. shēma). Aromātisko tiolu pievienošana nebija veiksmīga, un reakcijā tika atgūta izejviela.



Kā kontroles eksperiments tika veikta cikloheksāntiola un secīgu nātrija azīda pievienošana dihlorīdam **55** (17. shēma). Arī šajā reakciju sekvencē tika iegūts produkts **58** ar tādu pašu C(4) reģioselektivitāti kā aizvietojot *diazīdu* **56** ar tiolu. Taču, salīdzinot abas sintētiskās stratēģijas, jāsecina, ka *diazīda* sintēzes ceļš (16. shēma) ir vienkāršāks ar vieglāku produktu attīrīšanu un augstāku kopējo iznākumu. Pievienojot aromātisko tiolu (tiofenolu) dihlorīdam **55**, mono aizvietošanās produktus **59b** un **59c** praktiski nebija iespējams izdalīt no reakcijas maisījuma, jo reakcijas maisījumā strauji veidojās diaizvietotie produkti **60b** un **60c**.

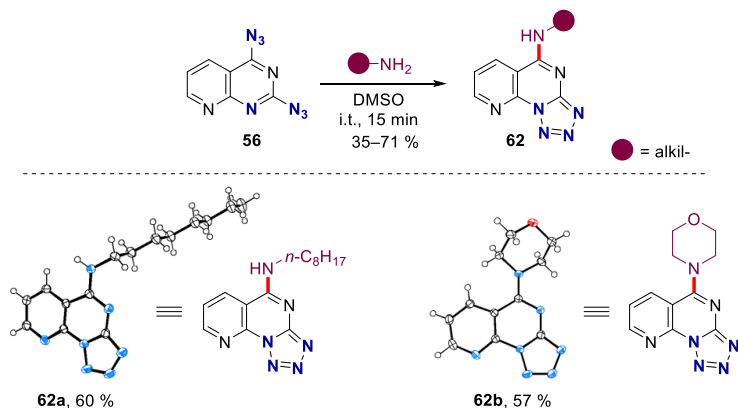


Tālāk tika veiktas S_NAr reakcijas ar *O*-nukleofiliem, kurās tika iegūti produkti ar zemiem iznākumiem hidroksīda pievienošanās (hidrolīzes) un citu blakusproduktu veidošanās dēļ (18. shēma). Jāatzīmē, ka šajā gadījumā iegūts aromātiskā nukleofila – fenola, pievienošanās produkts **61b**.



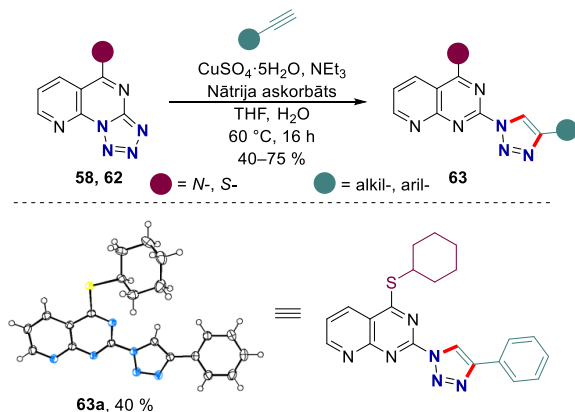
N-nukleofilu pievienošana *diazīdam* **56** noritēja salīdzinoši ātri, un amīnu S_NAr aizvietošanās produkti **62** tika iegūti ar labiem iznākumiem (19. shēma). Hidrazīna, hidroksilamīna un anilīna pievienošanas gadījumos tika novērota neidentificējamu produktu

maisījumu veidošanās. Iegūtie pirido[2,3-*d*]pirimidīna aminoatvasinājumi **62** uzrādīja zemu šķīdību lielākajā daļā organisko šķīdinātāju.



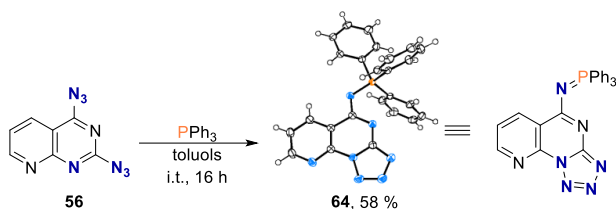
19. shēma. Diazīda **56** S_NAr aizvietošana ar *N*-nukleofiliem.

Lai demonstrētu aizvietoto produktu lietojumu un azīda-tetrazola līdzsvara esamību, savienojuma **62** reaģētspēja tika pārbaudīta CuAAC reakcijā. Izmantojot katalītisko sistēmu CuSO₄·5H₂O/nātrija askorbāts/NEt₃, tika iegūti triazoli **63** (20. shēma). Ņemot vērā tetrazola tautomēra pārākumu savienojumiem **62** šķīdumos un cietajā fāzē, azīda tautomēru funkcionalizēšana liecina par līdzsvara esamību, kas patstāvīgi atjauno zemākās koncentrācijas reaģējošā tautomēra – azīda, daudzumu sistēmā.



20. shēma. 2-(1,2,3-Triazolil)pirido[2,3-*d*]pirimidīnu **63** sintēze.

Diazīda **56** azīda-tetrazola tautomērisma raksturs tika demonstrēts arī Štaudingera (*Staudinger*) reakcijā ar trifenilfosfīnu (21. shēma). Interesanti, ka reakcijā izdalīts iminofosforāns **64**, kas parasti ir nestabils Štaudingera reakcijas starpprodukts.



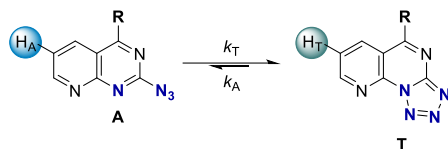
21. shēma. Iminofosforāna **64** sintēze Štaudingera reakcijā.

No iegūtajiem tetrazolo[1,5-*a*]pirido[3,2-*e*]pirimidīna atvasinājumiem līdzsvars CDCl_3 šķīdumos tika novērots merkaptoatvasinājumam **58** un alkoksiatvasinājumiem **61a** un **61b**. Aminogrupa kā elektrondonora aizvietotājs spēja pilnīgi nobīdīt līdzsvaru tetrazola formas virzienā. Arī polārajā $\text{DMSO-}d_6$ šķīdumā līdzsvars tika nobīdīts galēji tetrazola formas virzienā un azīda forma nebija novērojama, arī palielinot šķīduma temperatūru.

Tautomerizācijas procesa termodinamisko parametru vērtības dotas 1.3. tabulā. Iegūtās līdzsvara procesa entalpijas produktiem **61a**, **58** un **61b** ir attiecīgi $-23,19$ kJ/mol, $-21,30$ kJ/mol un $-17,02$ kJ/mol. Tā kā entalpija raksturo tetrazola sistēmas stabilitāti³¹ un elektrondonorie aizvietotāji stabilizē tetrazola formu, eksperimentāli iegūtās entalpiju vērtības secībā *Oi-Pr* **61a** > *Sc-Hex* **58** > *Oph* **61b** labi korelē ar literatūrā zināmo teoriju.

1.3. tabula

Līdzsvara konstantes un tautomerizācijas termodinamiskās vērtības aizvietotiem tetrazolo[1,5-*a*]pirido[3,2-*e*]pirimidīniem **58**, **61a** un **61b** CDCl_3 šķīdumā^a



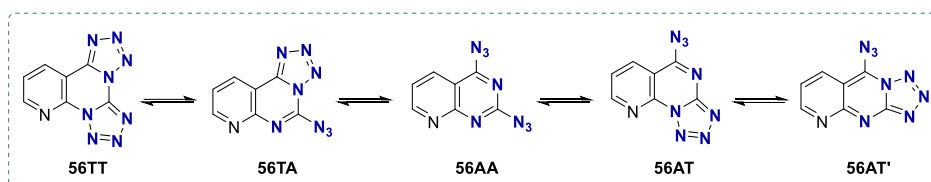
Savienojums	R	T (K)	$K_{\text{līdzsv}}^b$	ΔG_{298} (kJ/mol)	ΔH (kJ/mol)	ΔS (J/mol·K)
58		298	5,21	$-4,08 \pm 0,15$	$-21,30 \pm 0,78$	$-57,71 \pm 2,10$
		313	3,48			
		323	2,68			
61a		298	9,99	$-5,70 \pm 0,27$	$-23,19 \pm 1,09$	$-58,70 \pm 2,76$
		313	6,30			
		323	4,85			
61b		298	3,39	$-3,02 \pm 0,65$	$-17,02 \pm 3,69$	$-46,93 \pm 10,16$
		313	2,48			
		323	1,99			

a – A: azīda forma, T: tetrazola forma; b – $K_{\text{līdzsv}} = [T]/[A]$, izteikts kā ^1H KMR signāla integrāļu attiecība.

Diazīda tautomērais līdzsvars izrādījās pārāk sarežģīts termodinamisko parametru noteikšanai, jo sistēmā vienlaikus pastāv četras tautomērās formas. *Diazīdam* **56** ir piecas teorētiski iespējamās tautomērās struktūras: diazīds **56AA**, bis-tetrazols **56TT**, lineārs azidotetrazols **56AT'** un divi azidotetrazoli **56AT** un **56TA** (22. shēma). Pētot līdzsvaru ar ^1H KMR spektroskopiju, gandrīz visos organiskajos šķīdinātājos tika novērotas četras tautomērās formas un D_2SO_4 šķīdumā – viena forma. Provizoriskajos *diazīda* tautomēro formu DFT aprēķinos tika atklāts, ka lineārajai tetrazola formai **56AT'** ir par 60–75 kJ/mol augstāka

rašanās enerģija, salīdzinot ar pārējām struktūrām. Balstoties uz aprēķināto augsto enerģētisko barjeru, tika postulēts, ka ^1H KMR pētījumos lineāro formu **56AT'** nenovēro. Polārākos šķīdinātājos – DMSO- d_6 , MeCN, MeNO $_2$ un MeOD- d_4 – vājākos laukos esošie signāli (tetrazola tautomērā forma) tika novēroti pārākumā, bet mazāk polārajos (CDCl $_3$, MTBE, C $_6$ D $_6$) – stiprākos laukos esošo signālu (azīda tautomērā forma) intensitātes pieaug. Paaugstinot šķīdinātāju temperatūru, tika novērota stiprākos laukos esošo signālu (azīda forma) intensitātes palielināšanās. Šie signālu intensitātes maiņas novērojumi polaritātes un temperatūras ietekmē atbilst literatūras datiem – tetrazola forma ir pārākumā zemās temperatūrās un polāros šķīdinātājos, bet paaugstināta temperatūra un nepolāri šķīdinātāji veicina azīda formas veidošanos.

No šajā nodaļā pētītajiem savienojumiem vienīgi *diazīdam* **56** izdevās novērot signālu apmaiņas spektroskopijas eksperimentā (*EXSY*), kas pierādīja dinamiskā līdzsvara eksistenci šajā sistēmā.

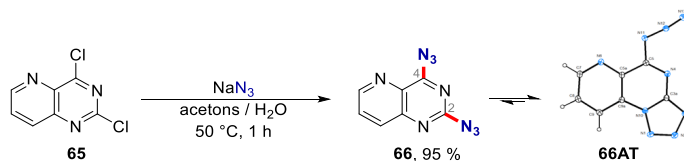


22. shēma. *Diazīda* **56** tautomērās struktūras.

Šīs apakšnodaļas pētījumi plašāk aprakstīti oriģinālpublikācijā 3. pielikumā.

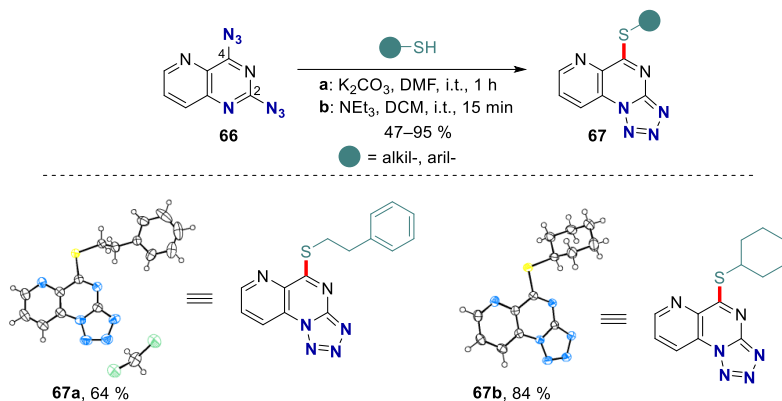
1.3. Azīda-tetrazola līdzsvara un $\text{S}_{\text{N}}\text{Ar}$ reakciju pētījumi pirido[3,2-*d*]pirimidīna heterociklā

Vispirms dihlorīda **65** $\text{S}_{\text{N}}\text{Ar}$ reakcijā ar NaN_3 tika iegūts 2,4-diazidopirido[3,2-*d*]pirimidīns **66** (23. shēma). Ar rentgenstruktūranalīzi tika noskaidrots, ka arī 2,4-diazidopirido[3,2-*d*]pirimidīna heterocikliskā sistēma kristāliskajā fāzē pastāv kā 5-azidopirido[2,3-*e*]tetrazolo[1,5-*a*]pirimidīns (**66AT**).



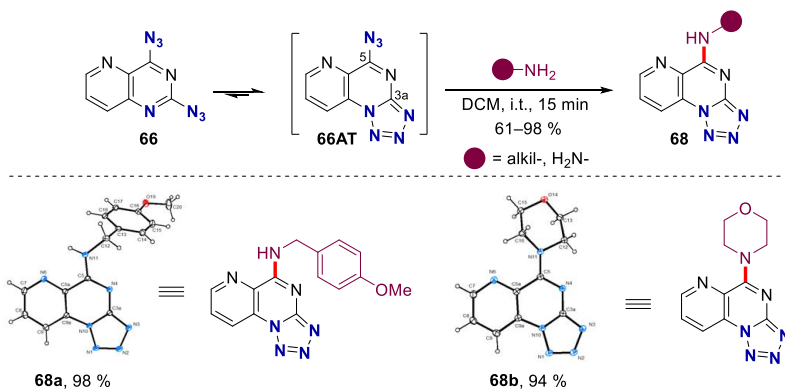
23. shēma. 2,4-Diazidopirido[3,2-*d*]pirimidīna (**66**) sintēze.

Vispirms pirido[3,2-*d*]pirimidīna $\text{S}_{\text{N}}\text{Ar}$ aizvietošanai tika izmēģināta $\text{K}_2\text{CO}_3/\text{DMF}$ reaģentu sistēma (24. shēma). Arī šajā gadījumā tika iegūti C(4) reģioselektivitātes aizvietošanās produkti **67**. Mainot reaģentu sistēmu uz mazāk polāru šķīdinātāju – metilēnchlorīdu – un bāzi uz trietilamīnu (apstākļi **b**), tika iegūts tās pašas C(4) reģioselektivitātes produkts **67**.



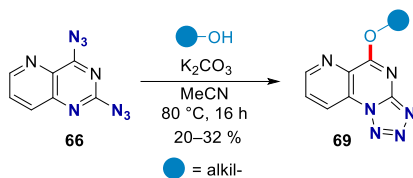
24. shēma. 2,4-Diazidopirido[3,2-*d*]pirimidīna (**66**) S_NAr aizvietošana ar tioliem.

Tālāk tika izmēģināta S_NAr reakcija ar *N*-nukleofiliem (25. shēma). DMSO vidē *p*-metoksibenzilamīna pievienošanas reakcijā tika iegūts produkts **68a** ar 49 % iznākumu bez papildu bāzes pievienošanas. Tika nolemts veikt šķīdinātāja polaritātes ietekmes izpēti uz reģioselektivitāti ar mērķi iegūt C(2) aizvietošanās produktu. Veicot reakciju dažādas polaritātes šķīdinātājos – benzols, toluols, DCM, CHCl₃, MeCN un EtOH, vienmēr tika iegūts C(4) aizvietošanās produkts **68a**. Tas norāda, ka 5-azidotetrazolo[1,5-*a*]pirido[2,3-*e*]pirimidīna (**66AT**) tautomērs ir reaģētspējīgāks tautomērs ar lielāko koncentrāciju šķīdumā neatkarīgi no izvēlētā šķīdinātāja polaritātes. Augstākais C(4) aizvietošanas iznākums tika iegūts DCM šķīdumā, tādēļ tas tika izmantots arī turpmākajos pētījumos. Reakcijās ar pirmējiem un otrējiem amīniem tika iegūti produkti ar labiem iznākumiem, un veiksmīgas bija arī amonjaka un hidrazīna pievienošanas reakcijas. Aizvietošana ar aromātisku amīnu – anizidīnu – nebija veiksmīga, un reakcijā tika atgūta izejviela.



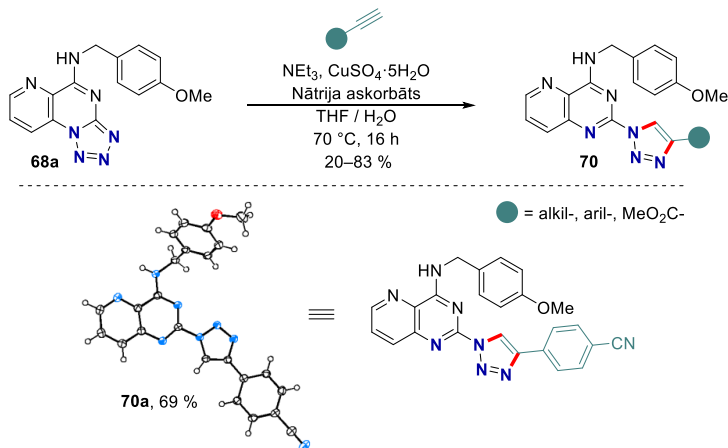
25. shēma. 2,4-Diazidopirido[3,2-*d*]pirimidīna (**66**) S_NAr aizvietošana ar amīniem.

Veicot S_NAr reakcijas ar *O*-nukleofiliem, tika novērota blakusproduktu veidošanās, un spirtu adukti **69** tika iegūti ar zemiem iznākumiem (26. shēma). Līdzīgi kā *N*-nukleofilu gadījumā, arī aril-*O*-nukleofili neuzrādīja reakcijas spēju.



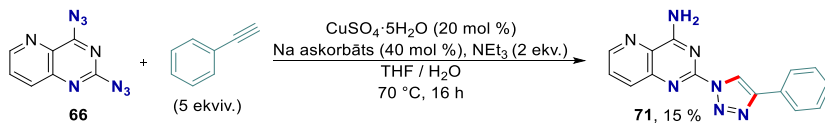
26. shēma. 2,4-Diazidopirido[3,2-*d*]pirimidīna (**66**) S_NAr aizvietošana ar alkohsiem.

Iegūto produktu tālākais lietojums veiksmīgi tika parādīts CuAAC reakcijā (27. shēma). Ņemot vērā tetrazola tautomēra pārkumu produktu **67–69** šķīdumu sistēmās (1.4. tab.) un cietajā fāzē, azīda tautomēru funkcionalizēšana liecina par līdzsvaru, kas patstāvīgi atjauno reaģējošā tautomēra – azīda – daudzumu sistēmā.



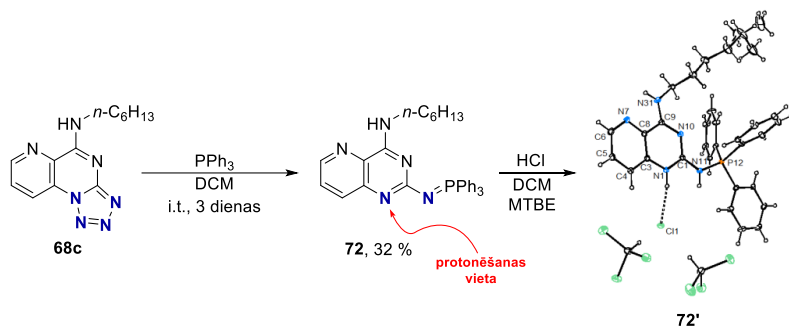
27. shēma. 2-Triazolilpirido[3,2-*d*]pirimidīnu **70** sintēze.

Bistriazola sintēze no *diazīda* **66** nebija veiksmīga daudzu blakusproduktu veidošanās dēļ. Galvenā komponente ar 15 % iznākumu reakcijas maisījumā bija daļēji reducētais CuAAC reakcijas produkts **71** (28. shēma). Literatūrā ir zināms, ka CuSO₄·5H₂O/nātrija askorbāta sistēma var reducēt azidoheterociklus līdz konkrētajam amīnam, kas arī novērots šajā gadījumā.⁶⁹



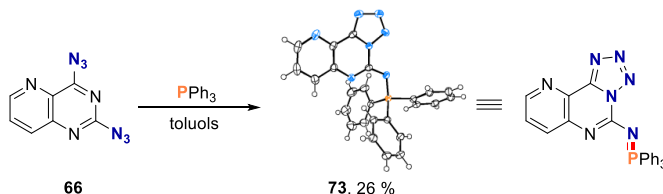
28. shēma. 2,4-Diazidopirido[3,2-*d*]pirimidīna (**66**) CuAAC reakcija ar tandēmu azīda reducēšanu.

Iegūto produktu **68c** izdevās funkcionalizēt arī Štaudingera reakcijā ar trifenilfosfīnu (29. shēma). Iegūtais iminofosforāns uzrādīja bāziskas īpašības un viegli protonējās heterocikla N(1) pozīcijā, veidojot sāli **72'**, kas tika pierādīts šķīdumā un cietā fāzē ar rentgenstruktūranalīzi. Savienojums **72** ir strukturāli līdzīgs fosfazīniem, kas ir nejoniskas superbāzes.^{70, 71}



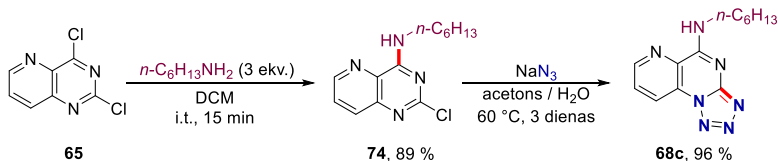
29. shēma. Iminofosforāna **72** un tā HCl sāls **72'** sintēze.

Štaudingera (*Staudinger*) reakcijā ar trifenilfosfīnu izdevās iegūt apgrieztās C(2) reģioselektivitātes produktu **73** (30. shēma), tā struktūra tika pierādīta rentgenstruktūranalizē. Šīs reakcijas reģioselektivitāte vēl nav izskaidrota, un pētījumi turpinās. Tomēr apgrieztās reģioselektivitātes produkts pierāda azīda-tetrazola līdzsvara virzītas selektīvas transformācijas iespējamību pirido[3,2-*d*]pirimidīna sistēmā.



30. shēma. Apgrieztās reģioselektivitātes Štaudingera reakcija.

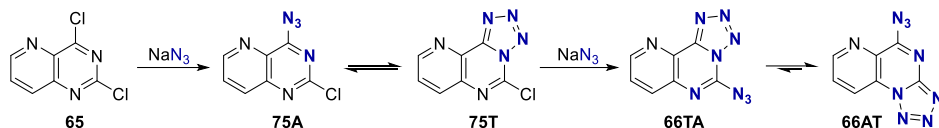
Tika veikti kontroleksperimenti, mainot reaģentu pievienošanas secību, lai pārliecinātos par C(4) augstāku reaģētspēju (salīdzinot ar C(2)) pirido[3,2-*d*]pirimidīna heterocikla sistēmā (31. shēma). Vispirms pievienojot amīnu un tad nātrija azīdu, tika iegūts identisks produkts **68c** kā *diazīda* **66** S_NAr reakcijā ar amīnu. Tomēr jānorāda, ka azīda pievienošanās C(2) pozīcijā noritēja trīs dienas paaugstinātā temperatūrā, līdz tika sasniegta pilnīga izejvielas konversija. Līdzīgā literatūras piemērā hlora aizvietošana 4-amino-2-hlorpirido[3,2-*d*]pirimidīnā ar nātrija azīdu nebija iespējama arī veicinošos apstākļos, reakciju veicot pie EtOH viršanas temperatūras.⁷² Lai arī produkta **74** veidošanās notiek selektīvi bez 2,4-diaminoprodukta veidošanās, aminogrupas elektrondonora efekts savienojumā **74** samazina vai pat aptur tālāku S_NAr reakciju norisi sistēmā.



31. shēma. Savienojuma **68c** sintēze mainītā reaģentu pievienošanas secībā.

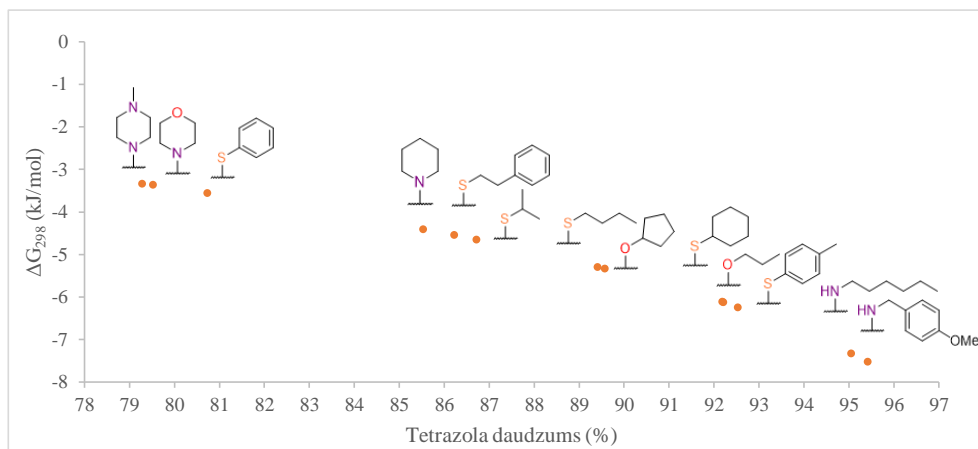
Interesanti, ka, veidojoties *diazīdam* **66**, azīda pievienošanās noris visnotaļ ātri (30 min) un istabas temperatūrā. Šis novērojums ļauj postulēt hipotēzi par tetrazola tautomēra veidošanos pēc pirmās azīda grupas pievienošanās C(4) pozīcijā (32. shēma). Veidojoties intermediātam

75T, tetrazols kā elektronus atvelkošā grupa veicina otrā azīda pievienošanos C(2) pozīcijā un tālāk notiek tautomerizācija uz stabilāko *diazīda* tautomēru **66AT**.



32. shēma. Hipotētiskais *diazīda* **66** veidošanās reakcijas mehānisms.

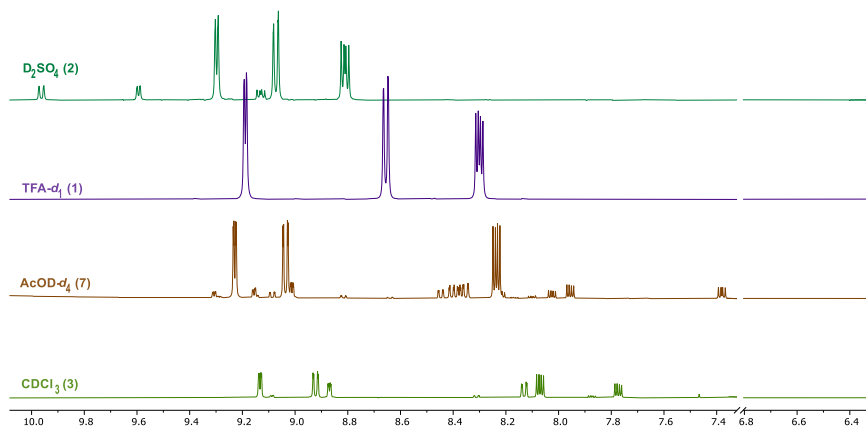
Tālākā darba gaitā tika veikta līdzsvara pētīšana ar ^1H KMR metodi tetrazoliem **67–69** dažādos šķīdumos un temperatūrās. Aprēķinātās azīda-tetrazola tautomerizācijas termodinamisko parametru – Gibbsa brīvā enerģija, entalpija un entropija – vērtības apkopotas 1.4. tabulā. Visiem iegūtajiem savienojumiem līdzsvars DMSO- d_6 šķīdumā ir pilnīgi novirzīts tetrazola tautomēra virzienā. Savukārt nepolārākā šķīdinātājā – CDCl_3 tika novērots azīda tautomērs un azīda-tetrazola līdzsvars. Palielinot šķīduma temperatūru, līdzsvars tika novirzīts uz azīda tautomēra veidošanos. Entalpijas vērtības tetrazola formai, kas aprēķinātas, izmantojot Gibbsa brīvās enerģijas vienādojumu (1.3. vienādojums), apstiprina tetrazolu kā enerģētiski izdevīgāko tautomēro formu dotajos eksperimentālajos apstākļos. Tetrazola tautomēra pārsvaru normālos apstākļos ($25\text{ }^\circ\text{C}$) tautomerizācijas procesam šķīdumos kvantitatīvi raksturo aprēķinātās Gibbsa brīvās enerģijas negatīvās vērtības. *p*-Metoksibenzilamino- un heksilamino aizvietoto produktu Gibbsa brīvās enerģijas bija vislielākās (1.4. tab., **68a** un **68c**), tādējādi līdzsvars tika vairāk novirzīts tetrazola virzienā. Spirtu aizvietoto produktu tautomerizācijas Gibbsa brīvās enerģijas vērtības (1.4. tab., **69a** un **69b**) ir augstākas nekā tiolu **67** analogiem. Zemākās tautomerizācijas Gibbsa brīvās enerģijas vērtības aprēķinātas otrējo amīnu aizvietotiem produktiem. Ņemot vērā šos datus (1.4. tab.), var secināt, ka elektrondonorie aizvietotāji – *N*-nukleofili > *O*-nukleofili > *S*-nukleofili – virza līdzsvaru uz tetrazola veidošanās pusi un otrējo amīnu telpiskie traucējumi nivelē tetrazola veidošanās procesu (4. att.).



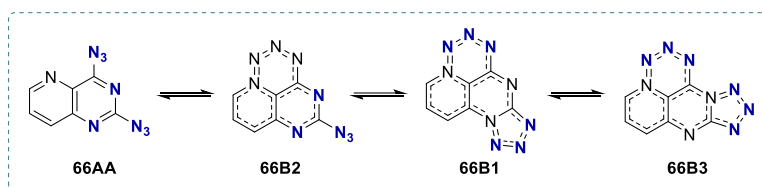
4. att. Tautomerizācijas Gibbsa brīvās enerģijas salīdzinājums tetrazoliem **67–69**.

Pētījumā tika apskatīts arī *diazīda* **66** tautomērais līdzsvars ar ^1H KMR spektroskopiju dažādos šķīdinātājos (5. att.). 2,4-Diazidopirido[3,2-*d*]pirimidīna augstākas kārtas tautomērais

līdzsvars bija pārāk sarežģīts, lai precīzi identificētu tautomēru formām raksturīgos signālus. Atkarībā no šķīdinātāja būtiski mainījās tautomēru signālu attiecība un tautomēro formu skaits šķīdumā. Palielinoties šķīdinātāja polaritātei, palielinās arī vājākos laukos esošo signālu intensitātes – līdzsvars tika virzīts uz tetrazola tautomēra veidošanās pusi. Šie novērojumi korelē ar literatūrā minētām azīda-tetrazola tautomērisma īpašībām. Vairumā gadījumu novērotas trīs līdz četras tautomērās formas. Trifluoretiķskābes šķīdumā novērota viena tautomērā forma, D₂SO₄ šķīdumā – divas tautomērās formas. Ļoti iespējams, ka skābajā vidē pirimidīna heterocikls tiek protonēts un pirimidīnija sistēmā līdzsvars tiek pilnībā novirzīts azīda formas virzienā. Visinteresantākā aina tika novērota AcOD-d₄ šķīdumā, kur pastāvēja septiņas tautomērās formas, kas liecina par kādas no betaīna formas esamību šķīdumā (6. att.).



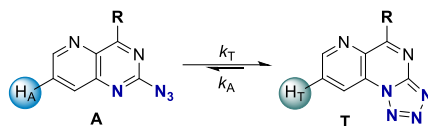
5. att. *Diazīda 66* ¹H KMR spektri dažādos šķīdinātājos (iekavās norādīts novēroto tautomēru skaits).



6. att. *Diazīda 66* iespējamās betaīna tautomēru struktūras.

Šīs apakšnodaļas pētījumi plašāk aprakstīti oriģinālpublikācijā 4. pielikumā.

Līdzsvara konstantes un tautomerizācijas termodinamiskās vērtības aizvietotiem tetrazolo[1,5-*a*]pirido[2,3-*e*]pirimidīniem **67–69** CDCl₃ šķīdumā^a



Savienojums	R	T (K)	$K_{\text{ līdzsv. }}^b$	ΔG_{298} (kJ/mol)	ΔH_{298} (kJ/mol)	ΔS_{298} (J/mol·K)
67a		298	8,44	-5,29 ± 0,11	-32,11 ± 1,94	-90,14 ± 6,24
		313	4,32			
		323	3,11			
67b		298	6,26	-4,54 ± 0,02	-23,63 ± 0,38	-64,08 ± 1,21
		313	3,92			
		323	2,99			
67c		298	12,39	-6,24 ± 0,02	-30,53 ± 0,34	-81,69 ± 1,11
		313	6,37			
		323	4,81			
67d		298	6,53	-4,65 ± 0,03	-20,14 ± 0,61	-51,96 ± 1,95
		313	4,49			
		323	3,47			
67e		298	4,19	-3,55 ± 0,28	-31,75 ± 4,90	-94,33 ± 15,74
		313	2,57			
		323	1,53			
67f		298	15,08	-6,11 ± 0,12	-42,05 ± 2,13	-120,72 ± 6,83
		313	4,96			
		323	3,30			
68a		298	20,83	-7,52 ± 0,22	-21,91 ± 3,91	-48,05 ± 12,53
		313	15,05			
		323	10,39			
68b		298	3,89	-3,36 ± 0,02	-22,65 ± 0,32	-64,71 ± 1,03
		313	2,53			
		323	1,91			
68c		298	19,20	-7,32 ± 0,03	-20,35 ± 0,56	-43,74 ± 1,78
		313	12,77			
		323	10,19			
68d		298	5,92	-4,40 ± 0,07	-24,52 ± 1,31	-67,42 ± 4,20
		313	3,81			
		323	2,74			
68e		298	3,83	-3,33 ± 0,01	-19,92 ± 0,25	-55,69 ± 0,79
		313	2,59			
		323	2,06			
69a		298	8,59	-5,33 ± 0,17	-48,02 ± 2,95	-143,27 ± 9,49
		313	3,36			
		323	1,92			
69b		298	11,84	-6,12 ± 0,16	-31,55 ± 2,75	-85,50 ± 8,83
		313	6,00			
		323	4,45			

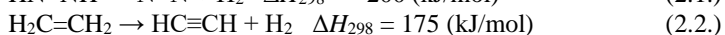
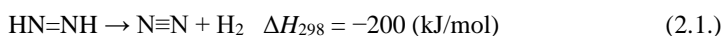
a – A: azīda forma, T: tetrazola forma; b – $K_{\text{līdzsv.}} = [T]/[A]$, izteikts kā ¹H KMR signāla integrāļu attiecība.

2. Poliazidopirimidīnu sintēze un fizikālo īpašību pētījumi

Azīda funkcionālā grupa organiskās ķīmijas speciālistam parasti asociējas ar bīstamību, jo, strādājot ar azīda grupu saturošiem mazmolekulāriem savienojumiem, pastāv sprādzienbīstamības risks. Lai gan organiskajā sintēzē tas ir nevēlams blakusefekts, enerģētisko materiālu (sprāgstvielu) izpētē detonācijas spēja un jutība pret ārējo impulsu ir svarīgas fizikālās īpašības.

Sprāgstvielas tiek izmantotas gan militārajā sfērā, gan civilajā inženierijā – ieroču munīcija, kalnrūpniecība, ceļu būve, ēku nojaukšana, gaisa spilveni u.c. Sprāgstvielas pēc to jutības un veiktspējas iedala divās kategorijās – primārās (iniciējošās) un sekundārās (brizantās) sprāgstvielas. Primārās sprāgstvielas bieži vien ir poliazidosavienojumi, kas ir jutīgi un detonējas pie nelielas ārējas enerģijas pievades – berzes, trieciena, siltuma vai elektriskā lādiņa izlādes formā. Primārās sprāgstvielas parasti nav brizantas un paredzētas izmantošanai detonatoros sekundāro sprāgstvielu iniciēšanai. Sekundārās sprāgstvielas ir daudz spēcīgākas un stabilākas par primārajām. To detonēšanai nepieciešams detonācijas vilnis, ko panāk ar detonatoriem. Sekundārās sprāgstvielas bieži vien ir bāzētas uz polinitroorganiskajiem savienojumiem un augsto enerģiju iegūst eksotermiskā, iekšmolekulārā oksidēšanās-reducēšanās procesā, kurā izdalās liels daudzums gāzveida produktu – CO₂, CO un N₂.^{73, 74}

Mūsdienīga tendence enerģētisko materiālu dizainā ir heterociklu funkcionalizēšana ar eksplozoforām grupām. Slāpekļa heterocikliskie savienojumi – tetrazols, triazols, furazāns, triazīns un tetraziņš – ir piemēroti būvbloki enerģētisko materiālu dizainam, pateicoties to lielai rašanās entalpijai no enerģētiski bagātajām N-N un C-N saitēm⁷⁵ un to augstajai termālajai stabilitātei.⁷⁶ N-N saites organiskajos savienojumos ir enerģētiski bagātas, jo to sadalīšanās rezultātā rodas slāpekļis (N₂), kura trīskāršā N≡N saite ir īpaši stabila. Salīdzinot ar analogu C≡C saiti, kuras veidošanās no divkāršās C=C saites ir endotermiska (pozitīva rašanās entalpija) (2.1. vienādojums), slāpekļa trīskāršās saites veidošanās process ir eksotermisks (negatīva rašanās entalpija) (2.2. vienādojums) un par ~ 375 kJ/mol termodinamiski izdevīgāks.⁷⁷

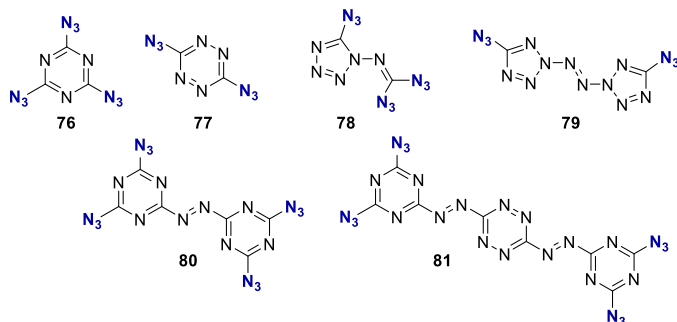


Binārie C_xN_y savienojumi ar augstu slāpekļa bilanci ir relatīvi jauna enerģētisko savienojumu klase. To dizains balstās uz slāpekli bagātiem heterocikliem, kas savstarpēji saistīti ar azo- vai diazotiltiņiem un satur vairākas azidogrupas. Bināro enerģētisko savienojumu enerģija nerodas oksidēšanās-reducēšanās procesā, bet no neparasti augstās rašanās entalpijas, kas skaidrojama ar lielo C-N un N=N saišu daudzumu un enerģētiskajām azido grupām.^{23, 24, 78–81} Ar slāpekli bagātiem enerģētiskajiem savienojumiem nereti ir augstāks vielas blīvums un labāka termiskā stabilitāte, salīdzinot ar klasiskajām polinitrosprāgstvielām. Jāuzsver, ka galvenais sadalīšanās produkts no šādiem slāpekli saturošiem savienojumiem ir nekaitīga N₂ gāze, kas ir svarīgs aspekts videi un cilvēkam nekaitīgu sprāgstvielu izstrādei un integrācijai industrijā.⁸²

Aktīva vides aizsardzība, saglabāšana un atjaunošana ir pagājušā gadsimta industrializācijas procesa sekas, to risināšana ir svarīgs uzdevums ilgtspējīgai nākotnei. Tādēļ modernajā industrijas un zinātnes attīstībā liela nozīme ir vidi saudzējošiem procesiem, tehnoloģijām un

materiāliem. Biežāk izmantotās primārās sprāgstvielas detonatoros ir svina azīds un svina stīfnāts, kas atstāj nelabvēlīgu ietekmi uz cilvēka veselību un apkārtējo vidi, tāpēc jaunu sprāgstvielu izstrādē aizvien nozīmīgāks kļūst vides nekaitīguma faktors.^{26, 27}

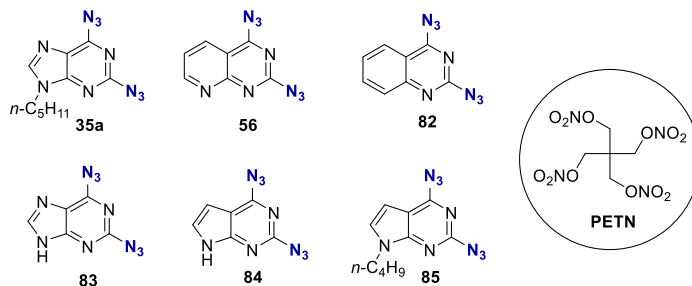
Līdz šim jaunatklāto bināro enerģētisko savienojumu klāstā (7. att.) nav materiālu, kas atbilstu noteiktajiem mūsdienīgu sprāgstvielu parametriem – augsta veiktspēja, zema triecienjutība, termālā un ķīmiskā stabilitāte, zema toksicitāte un mērogojama sintēze no lētām izejvielām.^{74, 83} Nereti binārajām enerģētiskajām savienojumiem ir zema sublimācijas temperatūra (**76**, **77**), pārlietu augsta jutība (**78**, **79**) vai sarežģīta sintēze un nepietiekama termālā stabilitāte (**80**, **81**).^{23, 24, 78–81}



7. att. Literatūrā zināmie slāpekļa bagāti binārie enerģētiskie savienojumi.

Promocijas darba izstrādes laikā, sadarbojoties ar profesora Tomasa Klapetkes grupu no Ludviga-Maksimiliāna universitātes Minhenē, tika nolemts pārbaudīt izmantoto azidoheterociklu enerģētisko profilu (2.1. tab.). Tika noskaidrots, ka darbā izmantotie diazīdi ir relatīvi stabili, kā to parāda trieciena un berzes jutības un sadalīšanās temperatūras. Purīna un tā atvasinājumi ar N(9) alkilaizvietotājiem uzrādīja labu stabilitāti, un savienojumu sadalīšanos ar triecienu vai berzi praktiski nav iespējams panākt. Pirimidīni bez alkilaizvietotājiem uzrādīja paaugstinātu trieciena un berzes jutību, un, pieliekot lielāku spēku, iespējams panākt to sadalīšanos. Toties 2,6-diazidopurīna (**83**) (120 N un 1 J), 2,6-diazidodeazapurīna (**84**) (80 N un 1 J) un 2,4-diazido-8-azahinazolīna (**56**) (40 N un 2 J) berzes un trieciena jutība līdzinās pentaeritrola tetranitrātam (PETN) (3 J un 60 N), kas ir etalons primāro sprāgstvielu jutības sliekšnim.⁸⁴ Tātad savienojumi **83**, **84** un **56** ietilpst primāro sprāgstvielu kategorijā, un darbs ar tiem lielos daudzumos ir bīstams.

Annelētu diazidopirimidīnu fizikālie un enerģētiskie parametri

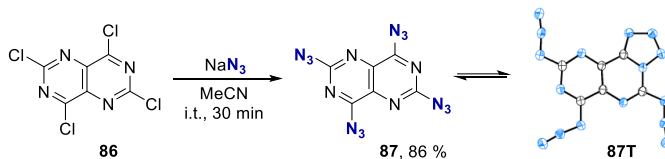


Savienojums	N bilance (%)	Berzes jutība (N)	Triecienu jutība (J)	ESI ^a (mJ)	k. p. (°C)	T _{sad.} ^b
35a	51	> 360	20	> 480	58	159
56	59	40	2	> 480	171	175
82	53	288	2	> 480	126	172
83	69	120	<1	> 480	sadalās	166
84	63	80	<1	> 480	sadalās	168
85	49	> 360	20	> 480	85	155
PETN ⁸⁵	18	60	3	60	143	179

a – elektrostātiskās izlādes jutība; b – sadalīšanās temperatūra.

Tālāk tika attīstīta ideja par vairāku azīda funkcionālo grupu ievadīšanu pirimidīnā, lai tam piešķirtu detonācijas īpašības. Darba gaitā autora zinātniskā grupa iedomājās par annelēta dipirimidīna – pirimido[5,4-*d*]pirimidīna poliazidēšanu, kurā, ievadot četras azīda funkcionālās grupas, iegūtu bināro savienojumu C₆N₁₆. Šis iegūtais produkts līdzinātos 1,3,5-triazidotriazīnam, bet būtu ar augstāku sublimācijas siltumietilpību un labāku termisko stabilitāti, kas ir triazidotriazīna iztrūkstošās īpašības.⁸⁶

No komerciāli pieejamā 2,4,6,8-tetrahlōrpirimido[5,4-*d*]pirimidīna S_NAr reakcijā ar NaN₃ izdevās iegūt tetraazīdu **87** (33. shēma). Monokristāla rentgendifrakcijas analīzē tika iegūta kristāla struktūra ar vienu tetrazola fragmentu, kas liecina par šī tautomēra preferenci cietā fāzē.



33. shēma. 2,4,6,8-Tetraazidopirimido[5,4-*d*]pirimidīna **87** sintēze.

Sadarbībā ar profesora Klapetkes grupu ir noteiktas vielas fizikālās īpašības un aprēķināti detonācijas veiktspējas parametri šim savienojumam, kas apkopoti 2.2. tabulā. Tetraazīds **87** izrādījās ārkārtīgi jutīgs uz ārējo impulsu, uzrādot < 1 J triecienu un 1 N lielu berzes jutību, kas ir līdzvērtīgi parametriem, ko uzrāda komerciālā primārā sprāgstviela Pb(N₃)₂. Diferenciāli termiskajā analīzē netika novērots vielas kušanas punkts, bet gan tikai strauja eksotermiska

sadalīšanās pie 155 °C. Karstās virsmas testā tetraazīds **87** sadalījās ar uzliesmojumu, un karstās adatas testā notika detonācija. Detonācija šajā testā ir pozitīvs rezultāts un norāda, ka šim savienojumam ir potenciāls kļūt par primāro sprāgstvielu. Tomēr, veicot divus sekundārās sprāgstvielas *PETN* iniciēšanas testus ar tetraazīdu **87**, sekundārās sprāgstvielas detonācija nenotika.

Izmantojot *EXPLO5* programmatūru, tika aprēķināts tetraazīda **87** detonācijas frontes spiediens – 20,8 GPa un detonācijas ātrums – 7477 m/s. Tetraazīda **87** detonācijas parametri ir salīdzināmi ar citu bināro savienojumu – 1,3,5-triazidotriazīns (TAT) un 3,6-bis-(2-(4,6-diazido-1,3,5-triazīn-2-il)-diazēnil)-1,2,4,5-tetrazīns (BDTDI), detonācijas īpašībām (2.2. tab.). Tomēr, salīdzinot ar $\text{Pb}(\text{N}_3)_2$, tetraazīdam **87** ir zemāks detonācijas spiediens, kas izskaidro pagaidām nepietiekamo veiktspēju sekundārās sprāgstvielas iniciēšanas testā.

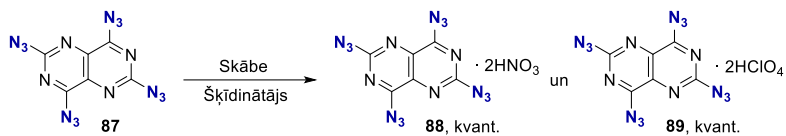
2.2. tabula

2,4,6,8-Tetraazidopirimido[5,4-*d*]pirimidīna (**87**) un citu bināro savienojumu un primārās sprāgstvielas – $\text{Pb}(\text{N}_3)_2$ – fizikālie un enerģētiskie parametri

Mēritie parametri	87	TAT ⁷⁸	BDTDI ²³	$\text{Pb}(\text{N}_3)_2$
Trieciena jutība (J)	< 1	1,5	5	2,5–4
Berzes jutība (N)	1	<5	29	0,1–1
Elektrostatiskās izlādes jutība (mJ)	13	360	174	< 5
ρ (g/cm ³)	1,703 ^a	1,707	1,763	4,8
<i>N</i> bilance (%)	75,7	82,4	79,13	28,9
Ω (%) ^b	–64,8	–47,0	–55,7	–11,0
<i>T</i> _{kuš.} (°C)	sadalās	94	sadalās	190
<i>T</i> _{sadalīšanās} (°C)	155	187	189	315
Aprēķinātie parametri^d				
$\Delta H_{\text{veidošanās}}$ (kJ/kg)	5095	5159	6130	1546
<i>T</i> _{detonācijas} (K)	3787	3536	4740	3401
<i>P</i> _{Cl} (GPa) ^c	20,8	22,6	29,4	33,8
<i>V</i> _{detonācijas} (m/s)	7477	7866	8602	5920

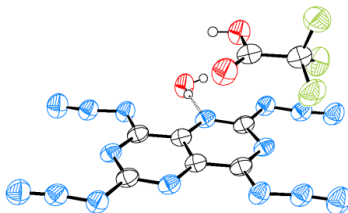
a – rentgenstaru difrakcijas analīzē iegūtais teorētiskais blīvums, kas pārrēķināts uz 298 K, izmantojot $\rho_{298} = \rho r / (1 + \alpha_v(298 - T))$ vienādojumu, kur $\alpha_v = 0,00015$ un *T* – monokristāla analīzes temperatūra; b – skābekļa bilance aprēķināta pret CO₂ ($\Omega_{\text{CO}_2} = (n\text{O} - 2x\text{C} - y\text{H}/2)(1600/\text{molmasa})$); c – detonācijas spiediens Čapmana-Žugē (*Chapman-Jouguet*) punktā; d – aprēķini veikti, izmantojot *Gaussian16* un *EXPLO5 (V7.01.01)* programmatūru.

Pētījumu turpinājumā tika veikta arī tetraazīda sāļu sintēze, izmantojot oksidējošās skābes (34. shēma). Ir zināms, ka sāļu veidošana ievērojami uzlabo savienojumu fizikālo un termisko stabilitāti, turklāt oksidējošo skābju izmantošana palielina skābekļa bilanci un detonācijas veiktspēju.^{74, 87, 88} Sintezētie nitrāta **88** un perhlorāta **89** sāļi fiziskās stabilitātes testos uzrādīja ievērojami labāku stabilitāti (1 → 2 J triecienjutība un 1 → 40 N berzes jutība). Savukārt sekundārās sprāgstvielas iniciācijas testos, izmantojot tetraazīda perhlorāta (**89**) detonatoru, pagaidām nav izdevies panākt detonāciju.



34. shēma. Tetraazīda sāļu **88** un **89** sintēze.

Pēc ilgstošiem tetraazīda sāļu **88** un **89** kristalizācijas mēģinājumiem tika iegūts monokristāls no trifluoretiķskābes šķīduma, kas kristalizējies nevis kā tetraazīda sāls, bet gan trifluoretiķskābes solvāts ar ūdens molekulas tiltiņu (8. att.).

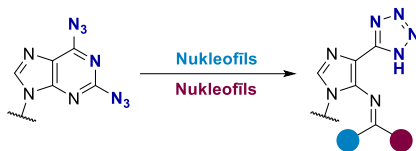


8. att. Rentgenstruktūranalizē iegūta tetraazīda **87** trifluoretiķskābes un ūdens solvāta molekulārā struktūra.

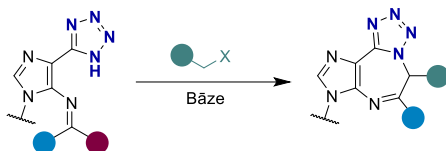
Šīs apakšnodaļas pētījumi plašāk aprakstīti oriģinālpublikācijā 5. pielikumā un nublicētajos rezultātos 6. un 7. pielikumā.

SECINĀJUMI

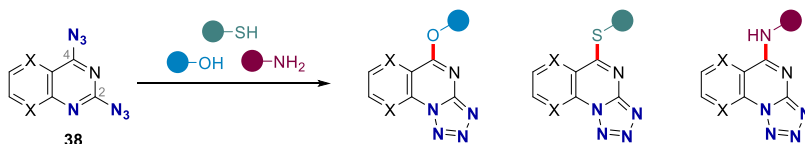
1. Nukleofilo aromātisko aizvietošanos 2,6-diazidopurīnos, pateicoties azīda-tetrazola līdzsvaram, iespējams veikt ar C(2) selektivitāti. Nākamā nukleofila pievienošana šīm sistēmām atkārtoti notiek C(2) pozīcijā, veidojot Maizenhaimera kompleksa intermediātu, kam seko purīna cikla atvēršana. Šī jaunā sintētiskā metode dod pieeju tetrazolimidazoliem ar augsti funkcionalizētu sānu ķēdi.



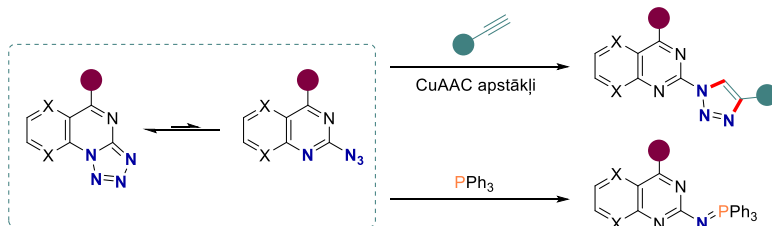
2. Reciklizējot tetrazolimidazolus, kas iegūti purīna cikla atvēršanas rezultātā, var iegūt tricikliskus imidazo[4,5-*f*]tetrazolo[1,5-*d*][1,4]diazepīnus, formāli paplašinot purīna pirimidīna ciklu par vienu oglekļa atomu.



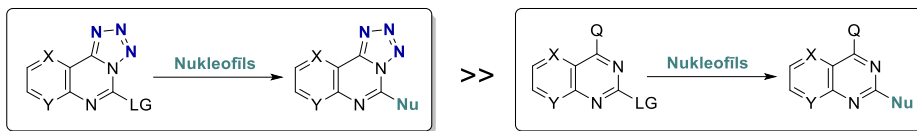
3. Nukleofilā aromātiskā aizvietošanās 2,4-diazidopiridopirimidīnos noris C(4) pozīcijā. Izstrādātās sintētiskās metodes C-5 aizvietotu tetrazolopiridopirimidīnu iegūšanai ir efektīvākas par konvencionālajām sintēzes stratēģijām.



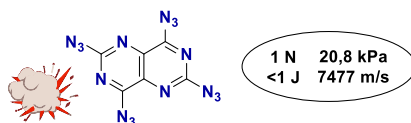
4. Iegūtie C-5 aizvietotie tetrazolopiridopirimidīni šķīdumos pastāv galvenokārt tetrazola formā, tomēr ir funkcionalizējami azīdiem raksturīgajās reakcijās, pateicoties azīda-tetrazola tautomēraim līdzsvaram.



5. Tetrazola funkcionālās grupas elektronus atvelkošās īpašības veicina S_NAr reakciju norisi anelētu pirimidīnu sistēmās, un tajās aizvietošanas reakcijas noris ātrāk nekā alternatīvi aizvietotos anelētos pirimidīnos.



6. 2,4,6,8-Tetraazidopirimido[5,4-*d*]pirimidīns (C_6N_{16}) ir jauns binārais enerģētiskais savienojums. Tas ir jutīgs pret berzi un triecienu un sadalās ar detonāciju. Šim struktūras dizainam ir liels nākotnes potenciāls enerģētisko materiālu izpētē un attīstībā, pateicoties augstajam slāpekļa saturam, labām funkcionalizēšanas iespējām un vieglai pieejamībai.



DOCTORAL THESIS PROPOSED TO RIGA TECHNICAL UNIVERSITY FOR THE PROMOTION TO THE SCIENTIFIC DEGREE OF DOCTOR OF SCIENCE

To be granted the scientific degree of Doctor of Science (Ph. D.), the present Doctoral Thesis has been submitted for defense at the open meeting of RTU Promotion Council on 4 June 2024 at 14.00 at the Faculty of Natural Sciences and Technology of Riga Technical University, 3 Paula Valdena Street, Room 272.

OFFICIAL REVIEWERS

Senior Researcher Dr. chem. Mārtiņš Katkevičs
Latvian Institute of Organic Synthesis, Latvia

Professor Dr. habil. Sigitas Tumkevičius
Vilnius University, Lithuania

Professor PhD José I. Borrell Bilbao
University Ramon Llull, Barcelona, Spain

DECLARATION OF ACADEMIC INTEGRITY

I hereby declare that the Doctoral Thesis submitted for review to Riga Technical University for promotion to the scientific degree of Doctor of Science (Ph. D.) is my own. I confirm that this Doctoral Thesis has not been submitted to any other university for promotion to a scientific degree.

Kristaps Leškovskis

(signature)

Date

The Doctoral Thesis has been prepared as a collection of thematically related scientific publications complemented by summaries in Latvian and English. The Doctoral Thesis unites three original scientific publications, one review article and one original manuscript for publication. The scientific publications have been written in English, with a total volume of 180 pages, including supplementary data. The manuscript for publication has been written in English, and its volume is 52 pages, including supplementary data.

CONTENTS

ACKNOWLEDGMENTS	3
GENERAL OVERVIEW OF THE THESIS	46
Introduction	46
Aims and Objectives	48
Scientific Novelty and Main Results	48
Structure and Volume of the Thesis	50
Publications and Approbation of the Thesis	50
Safety Statement	51
MAIN RESULTS OF THE THESIS	52
1. Azide-Tetrazole Equilibrium and its Application in Synthetic Methodology	52
1.1. Azide-Tetrazole Equilibrium in the Purine System and the Ring-Opening of its Pyrimidine Cycle	57
1.2. Azide-Tetrazole Equilibrium Studies and S _N Ar Reactions in the Pyrido[2,3- <i>d</i>]pyrimidine Heterocycle	64
1.3. Azide-Tetrazole Equilibrium Studies and S _N Ar Reactions in the Pyrido[3,2- <i>d</i>]pyrimidine Heterocycle	68
2. Synthesis and Physical Properties of Polyazidopyrimidines	75
CONCLUSIONS	80
REFERENCES	82
Appendix 1: Leškovskis, K.; Zaķis, J.; Novosjolova, I.; Turks, M. Applications of Purine Ring Opening in the Synthesis of Imidazole, Pyrimidine, and New Purine Derivatives. <i>Eur. J. Org. Chem.</i> 2021 , 2021, 5027-5052. doi:10.1002/ejoc.202100755	
Appendix 2: Zaķis, J. M.; Leškovskis, K.; Ozols, K.; Kapilinskis, Z.; Kumar, D.; Mishnev, A.; Ņalubovskis, R.; Supuran, C. T.; Abdoli, M.; Bonardi, A.; Novosjolova, I.; Turks, M. Diazidopurine Ring Opening – Synthesis of Tetrazolylimidazole Derivatives. <i>Manuskripts iesniegts Journal of Organic Chemistry</i> .	
Appendix 3: Leškovskis, K.; Novosjolova, I.; Turks, M. Structural Study of Azide-Tetrazole Equilibrium in Pyrido[2,3- <i>d</i>]Pyrimidines. <i>J. Mol. Struct.</i> , 2022 , 1269, 133784. doi:10.1016/j.molstruc.2022.133784	
Appendix 4: Leškovskis, K.; Mišņovs, A.; Novosjolova, I.; Turks, M. S _N Ar Reactions of 2,4-Diazidopyrido[3,2- <i>d</i>]pyrimidine and Azide-Tetrazole Equilibrium Studies of the Obtained 5-Substituted Tetrazolo[1,5- <i>a</i>]pyrido[2,3- <i>e</i>]pyrimidines. <i>Molecules</i> 2022 , 27, 7675-7675. doi:10.3390/molecules27227675	

- Appendix 5: Leškovskis, K.; Mišņovs, A.; Novosjolova, I.; Krumm, B.; Klapötke, T.; Turks, M. 2,4,6,8-Tetraazidopyrimido[5,4-*d*]pyrimidine: a Novel Energetic Binary Compound. *Cryst. Eng. Comm.* **2023**, *25*, 3866-3869. doi:10.1039/D3CE00563A
- Appendix 6: Safety Profile of Fused Diazidopyrimidines. *Unpublished results.*
- Appendix 7: Synthesis of 2,4,6,8-tetraazidopyrido[5,4-*d*]pyrimidine solvates. *Unpublished results.*

GENERAL OVERVIEW OF THE THESIS

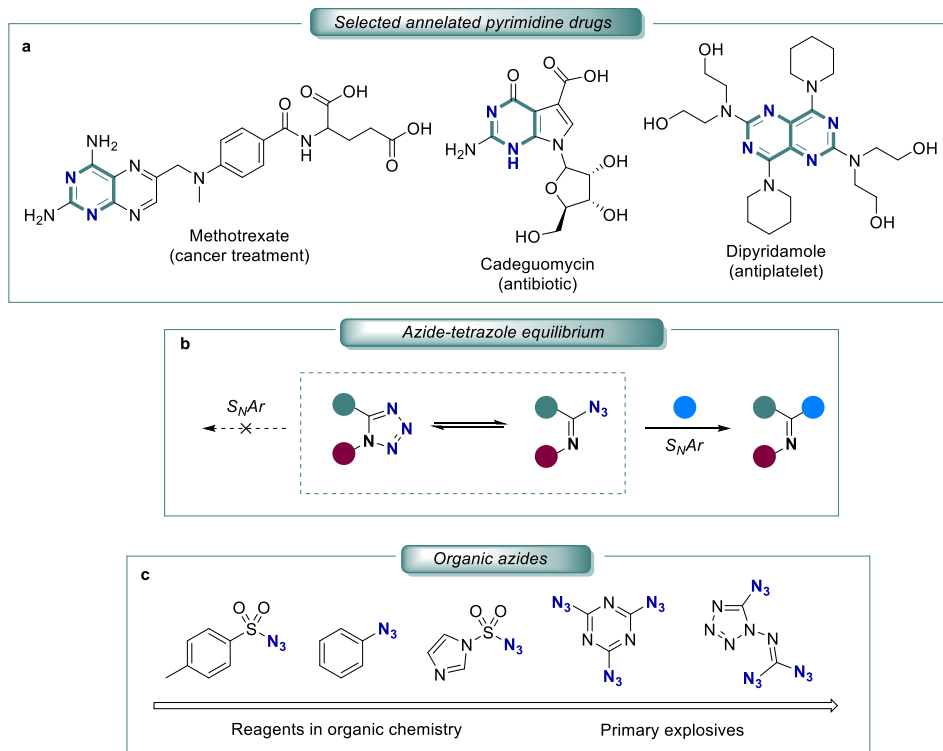
Introduction

Annulated pyrimidines are privileged heterocyclic structures in medicinal chemistry with a diverse profile of biological activities depending on the main ring's structure and the substituents' nature. This is related to the structural similarity of the annulated pyrimidines to the carriers of genetic information in cells of living organisms, signal molecules, and coenzymes. The purine heterocycle is part of nucleic acids and is the most widely represented member of annulated pyrimidines in living organisms. In addition, adenosine triphosphate is an energy-carrying molecule in cells, and other adenosine derivatives act as signaling molecules in the cardiovascular system. Therefore, fragments of annulated pyrimidines are used in the development of anti-viral and anti-cancer drugs, as well cardiovascular drugs and preparations with good results (Scheme 1, a).^{1,2} The modification and improvement of such biomimetic structures in medicinal chemistry is a well-known strategy for the development of new drugs. In this aspect, the development of new³ synthesis methods, which make it possible to create new building blocks and perform skeletal editing in new ways, is a vital innovation component in medicinal chemistry.³ Many of the annulated pyrimidines, including purine derivatives, exhibit luminescence, which opens up the possibilities of their application in bioorganic and analytical chemistry as sensors and in materials science as OLED materials.⁴⁻⁶ Also, in this field of application, developing new synthesis methods allows for improvement of substance's necessary physical properties.

The development of heterocyclic compound chemistry methods for modifying heterocyclic substituents is dominated by methods such as nucleophilic (hetero)aromatic substitution reactions (S_NAr), as well as transition metal-catalyzed C-C and C-heteroatom bond formation processes using cross-coupling^{7,8} and C-H activation^{8,9} reactions. Many of these processes use traditional halogen leaving groups or activated *O*- and *S*-substituents such as TfO-, TsO-, RS-, and RSO₂-.¹⁰ Scarcely described are *N*-centered leaving groups, which include imides, amides, imidazolyl- and 1,2,4-triazolyl substituents, and also 1,2,3-triazolyl moieties in purine derivatives recommended by our scientific group.¹¹⁻¹³ In this context, azido groups in heterocyclic compounds can be characterized as *N*-centered pseudohalide type substituents – i.e. they can participate in S_NAr reactions by giving an azide ion (pseudohalide) as a leaving group. Although reactions of this type are known, they have been little studied.^{12, 14, 15} Importantly, the placement of the azido group adjacent to the heterocyclic nitrogen atom (in the α -position) gives the azidoazomethine structural fragment which can undergo characteristic azide-tetrazole tautomeric equilibrium (Scheme 1, b).¹⁶⁻¹⁹ We proposed hypothesis that when using azido groups as leaving groups in heterocycle S_NAr reactions, their reactivity can be modulated by steering the azide-tetrazole equilibrium. This opens up the possibility of designing new reactions and affecting the regioselectivity of certain transformations, especially when the molecule contains several azido substituents.

Within the Thesis, we focused on the development of preparative synthetic methods of azidoheterocycles in two directions: 1) the development of purine chemistry methods with the aim of creating new methods in a well-known and widely used class of substances;

2) modification of pyridopyrimidines, because this class of substances has been less studied compared to other annulated pyrimidines.



Scheme 1. Properties of selected drugs and azides of annulated pyrimidines.

Additionally, while conducting research with substances with a high nitrogen content, there came a logical obligation to determine the energy profile of the compounds (Scheme 1, c).^{20, 21} Introduction of azido group in organic compounds increases the thermodynamic energy of the system by ~ 355 kJ/mol, hence, compounds with multiple azido groups are high energy density materials.^{20, 21} Azides are sensitive to external impact and heat, and upon decomposition, they form N_2 gas and release a large amount of heat. Therefore, organic azides are potentially explosive compounds, and the azido substituent as an explosophore functional group is often used in the chemistry of high-density energetic materials.²³ Heavy metal azides and low-molecular organic azides with a high nitrogen mass balance (> 50 %) are particularly energetically rich. Low molecular weight azides are used in the design of primary explosives due to their high impact sensitivity. Determination of the energetic profile of the azidoheterocycles used in the Thesis verifies the safety of the developed synthetic methods. This knowledge further led to the design of a new binary energetic compound by targeting the molecular skeleton of annulated pyrimidines and introducing the maximum number of azido groups into it. It should be emphasized here that the design and synthesis of binary energetic C_xN_y compounds is currently undergoing a renaissance^{23–25} associated with the search for environmentally friendly detonators, deliberately avoiding the use of heavy metal compounds.^{26, 27}

Combining interest of the reactivity of annulated pyrimidines and the effect of the azide-tetrazole equilibrium on the course of reactions, several new preparative methods in the chemistry of purines and pyridopyrimidines have been developed, as well as the physicochemical parameters of the azide-tetrazole equilibrium in these classes of substances have been determined. The energetic profile of azidoheterocycles used herein have been determined to gain confidence in the level of safety while working with them. The gained knowledge made it possible to develop a new energetic compound, deliberately crossing the line between traditional synthetic organic chemistry and chemistry of explosives.

Aims and Objectives

The aim of the Thesis is the development of new synthetic methodologies for the functionalization of annulated azido pyrimidines, using the azide-tetrazole equilibrium for regioselectivity induction and the versatile chemical properties of the azide functional group. Taking into account the possible energetic properties of substances with high nitrogen content, the second aim of the work is to experimentally determine the energetic profile and/or application of these substances in the development of primary explosives.

To fulfill the goal, several tasks were set:

- to investigate regioselectivity of S_NAr reactions in diazido derivatives of annulated pyrimidines – purine, pyrido[2,3-*d*]pyrimidine and pyrido[3,2-*d*]pyrimidine;
- to develop synthesis methods for S_NAr reactions in annulated diazidopyrimidines;
- to develop pyrimidine ring-opening methods of 2,6-diazidopurines;
- to explore further functionalization of the azido group of selectively substituted annulated azidopyrimidines;
- to determine the energetic profile of the used annulated azido pyrimidines and to design at least one new compound in this group that would correspond to the binary C_xN_y class of energetic compounds with high nitrogen content.

Scientific Novelty and Main Results

From the possible list of annulated azidopyrimidines, this Thesis examines:

- 2,4-diazidopyrido[2,3-*d*]pyrimidines and 2,4-diazidopyrido[3,2-*d*]pyrimidines as novel structures whose reactivity has been investigated;
- purines, for which a new type of ring-opening reactions that give tetrazolyimidazoles with a substituted side chain has been discovered;
- a new type of energetic binary compound C_6N_{16} based on pyrimidopyrimidine and the energetic profile of the more commonly used annulated diazidopyrimidines

2,4-Diazidopyrido[2,3-*d*]pyrimidines and 2,4-diazidopyrido[3,2-*d*]pyrimidines

In the Thesis, the synthesis of 2,4-diazidopyrido[2,3-*d*]pyrimidine and 2,4-diazidopyrido[3,2-*d*]pyrimidine and their azide-tetrazole equilibria were investigated for the first time. These compounds were found to exhibit a complex equilibrium in solutions in which up to four tautomeric forms are possible for 2,4-diazidopyrido[2,3-*d*]pyrimidine and up to seven tautomeric forms for 2,4-diazidopyrido[3,2-*d*]pyrimidine. Trifluoroacetic acid is the

only solvent whose polar nature and hydrogen bonding ensures a complete shift of the tautomeric equilibrium to the diazido form. On the other hand, in the crystalline phase, only monotetrazole tautomers from the C(2)-azide group are formed in both cases, and new annulated tricyclic structures – pyrido[3,2-*e*]tetrazolo[1,5-*a*]pyrimidine and pyrido[2,3-*e*]tetrazolo[1,5-*a*]pyrimidine are present.

In both heterocyclic systems, nucleophilic aromatic substitution reactions with *N*-, *O*-, and *S*-nucleophiles proceed selectively at C(4) of pyridopyrimidine to give C(5)-substituted pyrido[3,2-*e* and 2,3-*e*]tetrazolo[1,5-*a*]pyrimidines. These compounds exist mainly in the tetrazole form in solutions; however, the azide-tetrazole equilibrium is observed. In the case of C(5)-substituted pyrido[2,3-*e*]tetrazolo[1,5-*a*]pyrimidines, the free Gibbs energy values of tautomerization (ΔG_{298}) are in the range from -3.33 kJ/mol to -7.52 kJ/mol, while for pyrido[3,2-*e*]tetrazolo[1,5-*a*]pyrimidines, ΔG_{298} are -3.02 kJ/mol to -5.70 kJ/mol. Due to the azide-tetrazole equilibrium in these systems, the resulting annulated tetrazole derivatives are functionalizable in copper-catalyzed azide-alkyne 1,3-dipolar cycloaddition (CuAAC) reactions to the corresponding triazoles. In the equilibrium studies, we observed that 1) in systems with electron-donating substituents, the equilibrium is strongly shifted towards tetrazole; 2) by increasing the polarity of the solvent, the tetrazole tautomer concentration increases; 3) heating the solutions increases the concentration of the azide tautomer. These observations in the new heterocyclic systems correlate well with the properties of the azide-tetrazole equilibrium process described in the literature.

The developed synthetic method using 2,4-dichloropyridopyrimidines as starting materials, converting them to diazides and then selectively substituting them with *N*-, *O*-, and *S*-nucleophiles works more efficiently than the initial selective mono- S_NAr reaction at C(4) followed by the introduction of azide at C(2). This can be explained by the fact that in our procedure, the annulated tetrazole provides both selectivity and contributes to the overall S_NAr reactivity due to the electron-withdrawing properties of the tetrazole. Compared to the classical approach, the initial introduction of a heteronucleophile introduces an electron-donor substituent that makes the next step of the S_NAr reaction difficult.

Ring opening of the pyrimidine ring of 2,6-diazidopurines

Aromatic nucleophilic substitution in N(9)-substituted 2,6-diazidopurines can be performed regioselectively at the C(2) or C(6) position by choosing a suitable solvent and reagent system. We found that for purine derivatives, which have tendency for the formation of annulated tetrazole at C(6), it is possible to add an additional nucleophile at C(2). This results in a Meisenheimer complex that collapses with the opening of pyrimidine due to the tetrazole being a better leaving group than the incoming *N*-, *O*-, or *S*-nucleophile. Also, in this case, the azide-tetrazole equilibrium induces regioselectivity and activates the purine heterocyclic system for nucleophilic attack. Applying this two-step synthesis method, highly functionalized iminoimidazolyltetrazoles substituted with various heteronucleophiles can be obtained. We showed that tetrazolodiazepines are obtained by the alkylation-cyclization reaction of imidazolyltetrazoles, which is a formal homologation of tetrazolopurine as the expansion of the heterocyclic system by one carbon is achieved.

Energetic profile and new binary compound

The energetic profile of azidoheterocycles used in the research has been determined in collaboration with the group of Professor Thomas M. Klapötke at the Ludwig Maximilian University of Munich. A new energetic binary C₆N₁₆ compound – 2,4,6,8-tetraazidopyrimido[5,4-*d*]pyrimidine has been designed and obtained. This tetraazide exists in azide-tetrazole equilibrium in solutions and crystallizes in the solid phase as the monotetrazole tautomer. Due to its high nitrogen balance (75 %), this compound has the properties of a primary explosive and detonates under the influence of light friction or impact. This discovery opens up opportunities to begin more extensive studies of primary explosives (detonator materials) in Latvia.

Structure and Volume of the Thesis

The Doctoral Thesis has been prepared as a collection of thematically related scientific publications dedicated to the use of the azido group in synthetic methodology – inducing regioselectivity and reactivity in annulated pyrimidines and in materials science, specifically the development of new primary explosives. The Thesis includes four publications in SCI journals and one article manuscript.

Publications and Approbation of the Thesis

The results of the Thesis have been reported in three scientific original articles and one prepared manuscript. One review article has been published. The results have been presented in 9 conferences.

Scientific publications

1. Zaķis, J. M.; **Leškovskis, K.**; Ozols, K.; Kapilinskis, Z.; Kumar, D.; Mishnev, A.; Žalubovskis, R.; Supuran, C. T.; Abdoli, M.; Bonardi, A.; Novosjolova, I.; Turks, M. Diazidopurine Ring Opening – Synthesis of Tetrazolyimidazole Derivatives. *Manuscript is submitted in the Journal of Organic Chemistry.*
2. **Leškovskis, K.**; Mišņovs, A.; Novosjolova, I.; Krumm, B.; Klapötke, T.; Turks, M. 2,4,6,8-Tetraazidopyrimido[5,4-*d*]pyrimidine: a Novel Energetic Binary Compound. *Cryst. Eng. Comm.* **2023**, *25*, 3866–3869. doi:10.1039/D3CE00563A
3. **Leškovskis, K.**; Novosjolova, I.; Turks, M. Structural Study of Azide-Tetrazole Equilibrium in Pyrido[2,3-*d*]pyrimidines. *J. Mol. Struct.*, **2022**, *1269*, 133784. doi:10.1016/j.molstruc.2022.133784
4. **Leškovskis, K.**; Mišņovs, A.; Novosjolova, I.; Turks, M. S_NAr Reactions of 2,4-Diazidopyrido[3,2-*d*]pyrimidine and Azide-Tetrazole Equilibrium Studies of the Obtained 5-Substituted Tetrazolo[1,5-*a*]pyrido[2,3-*e*]pyrimidines. *Molecules* **2022**, *27*, 7675–7675. doi:10.3390/molecules27227675
5. **Leškovskis, K.**; Zaķis, J.; Novosjolova, I.; Turks, M. Applications of Purine Ring Opening in the Synthesis of Imidazole, Pyrimidine, and New Purine Derivatives. *Eur. J. Org. Chem.* **2021**, *2021*, 5027-5052. doi:10.1002/ejoc.202100755

The results of the Thesis have been presented at the following conferences

1. **Leškovskis, K.**; Novosjolova, I.; Turks, M. Synthesis and physical properties of 2,6,8-triazidopurine and 2,4,6,8-tetraazidopyrimido[5,4-*d*]pyrimidine. In: *13th Paul Walden Symposium: Program and abstracts*, Riga, Latvia, September 14–15, 2023. Riga: 2023, p. 48.
2. **Leškovskis, K.**; Novosjolova, I.; Turks, M. Azide-Tetrazole Equilibrium Driven Reactions of Fused Diazido Pyrimidines and Characterization of Tautomerism Therein. In: *International Symposium on Synthesis and Catalysis 2023: Book of Abstracts*, Evora, Portugal, September 5–8, 2023. Evora: 2023, p. 211.
3. **Leškovskis, K.**; Novosjolova, I.; Turks, M. Azide-Tetrazole Equilibrium in Pyrido[3,2-*d*]pyrimidines. In: *82nd International Scientific Conference of the University of Latvia: Section of Organic Chemistry Book of Abstracts*, Riga, Latvia, March 7, 2023. Riga: 2023, p. 5.
4. **Leškovskis, K.**; Novosjolova, I.; Turks, M. Azidoazomethine-Tetrazole Tautomerism in Pyrimidines. In: *Balticum Organicum Syntheticum 2022: Program and Abstract Book*, Vilnius, Lithuania, July 3–6, 2022. Vilnius: 2022, p. 109.
5. **Leškovskis, K.**; Novosjolova, I.; Turks, M. Synthesis of Tetrazole Fused Pyrido-Pyrimidines. In: *2nd Drug Discovery Conference: Abstract Book*, Riga, Latvia, September 22–24, 2022. Riga: 2022, p. 61.
6. **Leškovskis, K.**; Turks, M.; Novosjolova, I. Azido-Azomethine – Tetrazole Tautomerism in Pyridopyrimidines. In: *ORCHEM22: Abstract Book*, Munster, Germany, September 5–7, 2022. Munster: 2022, p. 115.
7. **Leškovskis, K.** Aromatic Substitution of Azido-Pyridopyrimidines and Study of Their Azide Tetrazole Equilibrium. In: *The 27th Croatian Meeting of Chemists and Chemical Engineers: Book of Abstracts*, Veli Lošinj, Croatia, October 5–8, 2021. Veli Lošinj: 2021, p. 123.
8. **Leškovskis, K.** Azide-Tetrazole Equilibrium Study in 2,4-Diazidopyrido[2,3-*d*]pyrimidine. In: *Riga Technical University 62nd International Scientific Conference “Material Science and Applied Chemistry”:* *Program and Abstracts*, Riga, Latvia, October 22, 2021. Riga: 2021, p. 32.
9. **Leškovskis, K.** S_NAr Regioselectivity and Azide-Tetrazole Equilibrium Study in Pyrido[2,3-*d*]pyrimidine. In: *12th Paul Walden Symposium on Organic Chemistry: Program and Abstract Book*, Riga, Latvia, October 28–29, 2021. Riga: 2021, p. 34.

Safety Statement

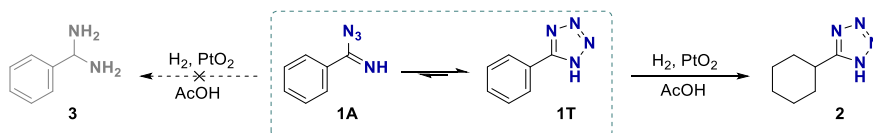
CAUTION! Heteroaromatic azidocompounds with nitrogen content $\geq 50\%$ can be powerful energetic materials with high sensitivities towards shock and friction. Therefore, proper security precautions must be applied while synthesizing and handling several of the described azidoheterocycles. The security precautions include but are not limited to safety goggles, face shield, ear plugs, *Kevlar* gloves, lab safety shield, earthed laboratory equipment and shoes.

MAIN RESULTS OF THE THESIS

1. Azide-Tetrazole Equilibrium and its Application in Synthetic Methodology

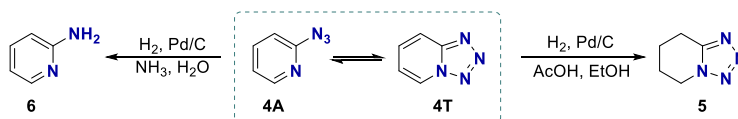
Heterocycles with the azidoazomethine structure are unique due to their possible azide-tetrazole equilibrium in solutions.^{28, 29} The azide-tetrazole equilibrium is a valence tautomerism that occurs when an azide adds to an adjacent imine moiety in a 1,5-dipolar cyclization reaction. The azide-tetrazole equilibrium is dynamic and is affected by the stereoelectronic effects of the substituents, solvent polarity, temperature, and pH of the solution.^{30–32}

An isolated tetrazole ring is ~ 40 kJ/mol more stable than the azide tautomer due to the 6π -electron aromatic system.³³ Thus, tautomeric equilibrium is not usually observed in an isolated tetrazole system. Consequently, transformations of the azide functional group are impossible for such systems. For example, 5-phenyltetrazole (**1T**) reduction with H_2 on a platinum catalyst occurs with selective reduction of the benzene aromatic ring, and the tetrazole functional group remains unreduced (Scheme 2).³⁴



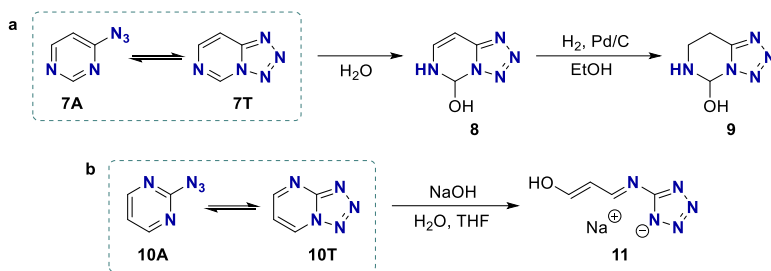
Scheme 2. Reduction of phenyltetrazole.

However, in annulated azidoazomethine systems, a dynamic azide-tetrazole equilibrium is present and can be observed with various spectroscopic methods (IR, UV, NMR). Reactions in such systems can occur with both tetrazole and azide tautomers. The latter can undergo reduction, cycloaddition, or nitrene reactions. For example, 2-azidopyridine (**4A**) can be selectively reduced to tetrahydropyridotetrazole (**5**) or 2-aminopyridine (**6**) by changing the reaction solvent and pH of the solution (Scheme 3).³⁵



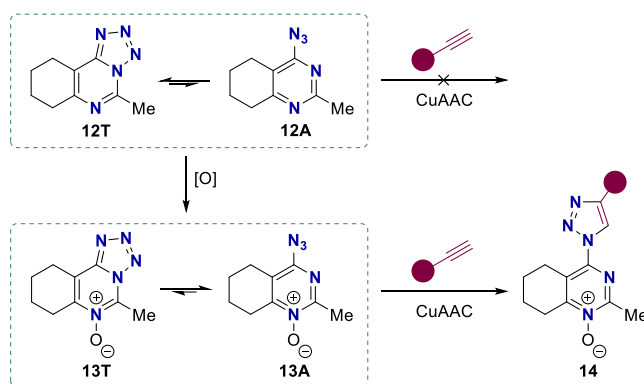
Scheme 3. Reduction of 2-azidopyridine.

Fused tetrazole systems are more reactive towards nucleophile addition than their azido analogs due to the electron-withdrawing properties of the tetrazole functional group. For example, the 4-azidopyrimidine system **7** undergoes tautomerization and reacts with water readily under normal conditions without acid or base additives, forming hemiaminal **8**. The reduction of formed hemiaminal with H_2 in the presence of a Pd/C catalyst yields the annulated system reduction product **9** with a preserved tetrazole functional group (Scheme 4 a).³⁶ Tetrazolo[1,5-*a*]pyrimidine **10T** can be opened under basic conditions to form tetrazolate salt **11** (Scheme 4 b).³⁷



Scheme 4. Functionalization of azidopyrimidines.

The electronic effects of the substituents present in the system strongly influence the azide-tetrazole equilibrium. Changing the total electron density in the system makes it possible to reverse the tautomeric equilibrium completely. For example, upon oxidation of tetrazolo annulated pyrimidine **12** to *N*-oxide, the formed tetrazole **13T** tautomerizes to azide **13A**, which can be functionalized in the azide-characteristic CuAAC reaction (Scheme 5).³⁸



Scheme 5. Electronic effects guided functionalization of annulated tetrazolo[1,5-*c*]pyrimidine.

In heterocyclic systems with two azidoazomethine groups, the opportunity to perform regioselective transformations opens up by carefully choosing the solvent and controlling the temperature (Fig. 1 a). Nucleophilic addition in pyrimidines with two identical leaving groups usually occurs at the most active C(4) site (Fig. 1, **15**). However, when the equilibrium shifts, the addition can: 1) accelerate (Fig. 1, **16**) due to the electron-withdrawing properties of the tetrazole, which stabilizes the intermediates of the Meisenheimer complex, or 2) occur with changed regioselectivity (Fig. 1, **17**), due to the formation of tetrazole in the system, which cannot enter the S_NAr reaction, or 3) not occur at all (Fig. 1, **18**).

In series of annulated 2,4-diazidopyrimidines, it is known that in 2,6-diazidopurines **19**³⁹ and 2,6-diazidodeazapurines **20**⁴⁰ the substitution proceeds with altered regioselectivity at the C(2) position facilitated by the annulated tetrazole fragment. Meanwhile, regioselectivity in 2,4-diazidoquinazolines **21**¹⁴ does not change, yet the C(4) position becomes more reactive.

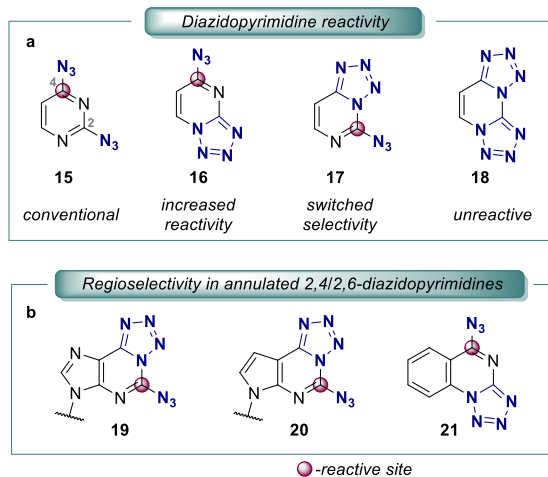


Fig. 1. Azide-tetrazole equilibrium and reactivity in 2,4/2,6-diazidopyrimidines.

It is well known in the literature that the substituents in the heterocyclic system play a vital role on the azide-tetrazole tautomeric equilibrium (Fig. 2). Electron-donating substituents shift the equilibrium towards the tetrazole tautomer by stabilizing the tetrazole tautomer, while electron-accepting substituents favor the azide tautomer.^{32, 41, 42} The main external factors affecting the equilibrium are solvent polarity (more polar solvents stabilize the dipole moment of the tetrazole system), temperature (at higher temperatures, the more thermodynamically stable azide tautomer is formed), and protonation of the heterocyclic system (azide tautomer is formed in an electron-poor system).²⁸ The most commonly used solvents for studies of the tautomerization process are DMSO, TFA, and CHCl_3 . In these solvents, it is usually possible to observe the extremes of the azide-tetrazole equilibrium: tetrazole in DMSO (due to high polarity), azide in TFA (the system is protonated or a distinct network of hydrogen bonds is formed), and a mixture of tautomers in CHCl_3 .^{36, 43, 44}

Azide-tetrazole tautomerism can be detected by methods such as UV and IR spectroscopy.⁴⁵ In certain cases, it can be performed with thin-layer chromatography³⁵ and melting point analysis.⁴⁴ With ^{15}N NMR, it is possible to analyze nitrogen atoms. However, the natural abundance of the magnetically active ^{15}N nucleus is $\sim 0.36\%$, and the gyromagnetic sensitivity of the ^{15}N nucleus is significantly lower than for other nuclei. Therefore, ^{15}N NMR on substrates with natural isotopic nitrogen distributions is difficult. However, the azide-tetrazole equilibrium in compounds with protons close to the azide-tetrazole fragment is very well observed and easily quantified by ^1H NMR. The ratio of tautomers is obtained by signal integration and characterized by the equilibrium constant K_{eq} .^{37, 46, 47} It is further possible to characterize the equilibrium process with thermodynamic parameters (Gibbs free energy, enthalpy, and entropy) by obtaining ^1H NMR spectra at different temperatures.^{31, 48, 49}

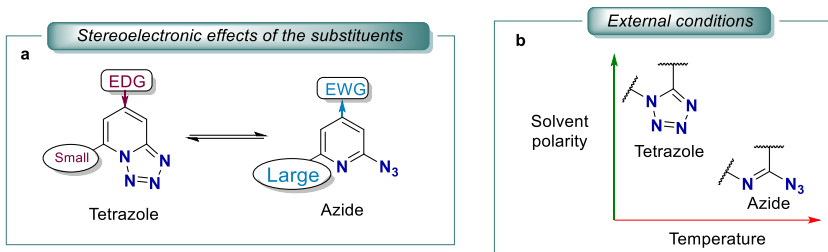


Fig. 2. Factors influencing the azide-tetrazole equilibrium.

A dynamic equilibrium process in chemistry is characterized by the equilibrium constant K_{eq} , the ratio of the reaction rate constants of a reversible chemical transformation for a system where chemical equilibrium has been reached. Hence, the equilibrium constant (1.1) can be expressed as the ratio of the concentrations of two components in an equilibrium state, which can be easily determined by ^1H NMR spectroscopy by the integral ratio of the signals.

$$K_{(eq.)} = [T]/[A], \quad (1.1)$$

where

K_{eq} – equilibrium constant;

T – integral value of tetrazole tautomer;

A – integral value of azide tautomer.

Systems in equilibrium can be characterized by the thermodynamic parameters of the tautomerization process – Gibbs free energy, enthalpy, and entropy. The Gibbs free energy characterizes the direction of equilibrium under the given conditions and the thermodynamic feasibility of the process. Enthalpy, on the other hand, describes the absolute stability of the system regardless of external conditions (higher value – more stable system). The Gibbs free energy for the tautomerization process is calculated with the Gibbs-Helmholtz Equation (1.2).

$$\Delta G = -RT \ln(K_{(eq.)}), \quad (1.2)$$

where

ΔG – Gibbs free energy of tautomerization, J/mol;

R – universal gas constant, J/(mol·K);

T – temperature, K;

K_{eq} – equilibrium constant.

Enthalpy and entropy of the tautomerization process are determined by graphically representing the Gibbs free energy against temperature and calculated according to the Gibbs free energy Equation (1.3), where the value of the y-axis at zero Kelvin temperature is the enthalpy of the system, and the slope is the entropy of the system (Fig. 3).

$$\Delta G = \Delta H - T\Delta S, \quad (1.3)$$

where

ΔG – Gibbs free energy of tautomerization, J/mol;

ΔH – enthalpy of tautomerization, J/mol;
 ΔS – entropy of tautomerization, J/(mol·K).

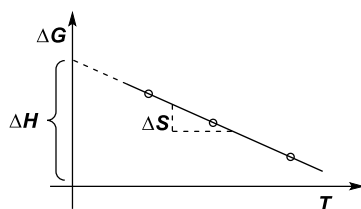


Fig. 3. Graphical representation of the Gibbs free energy equation.

Although an equilibrium is reached in a dynamic process, there is a reversible reaction $A \rightleftharpoons B$ still occurring, which can be characterized as two separate reactions $A \xrightarrow{k_B} B$ and $B \xrightarrow{k_A} A$ with rate constants (k_A un k_B). These constants are mutually proportional and express the equilibrium constant K_{eq} (1.4). Reaction rate kinetic constants allow the calculation of the equilibration time, which is characterized by the reaction half-time $\tau_{1/2}$.

$$K_{(eq.)} = k_B/k_A, \quad (1.4)$$

where

K_{eq} – equilibrium constant;

k_B – reaction rate constant (s^{-1});

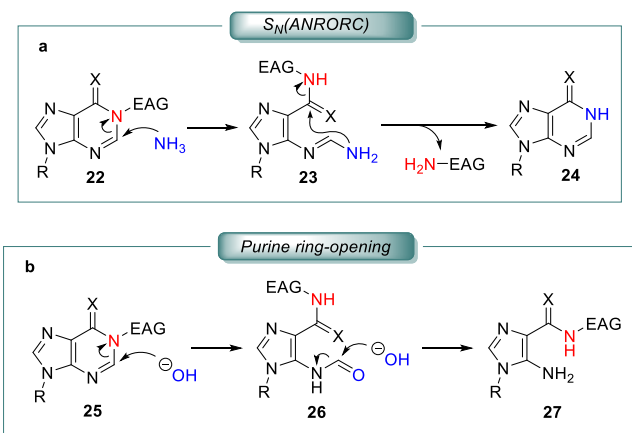
k_A – reverse reaction rate constant (s^{-1}).

Measuring the rate of the dynamic process is performed with an NMR chemical exchange spectroscopy experiment (EXSY) in which the transfer of magnetization during proton tautomerization from one tautomer to another is measured.⁵⁰ Determination of the kinetic constants of the azide-tetrazole tautomerization is essential for the characterization of the equilibrium. For example, to perform equilibrium studies in a case of slow tautomerization, a long period of time is required until an equilibrium state is reached in the system.^{42,51} Also, the rate of reactivity in reactions where one selected tautomer reacts can be determined.

1.1. Azide-Tetrazole Equilibrium in the Purine System and the Ring-Opening of its Pyrimidine Cycle

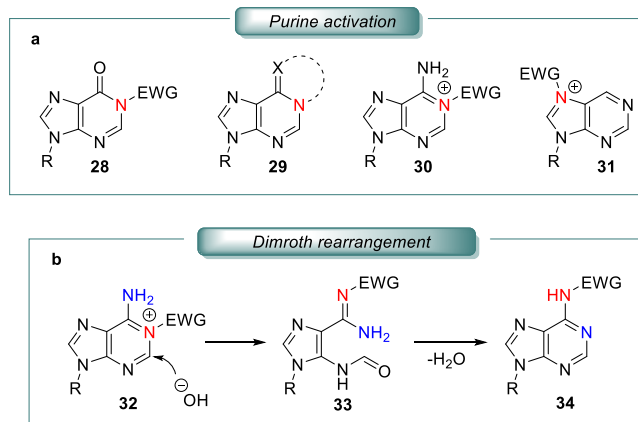
Purine is a nitrogen heterocycle widely found in nature, whose derivatives – adenine and guanine – are part of DNA. Therefore, many antiviral and anticancer drugs are based on purine and nucleoside fragments.

Purine is a stable heterocyclic system due to its conjugated aromatic π -electron system. However, introduction of an electron-withdrawing functional groups onto the nitrogens of the purine ring makes the system more electrophilic and favors the addition of nucleophiles. The addition of *N*-nucleophiles to N(1) activated purines results in a formal replacement of the N(1) group and the nitrogen atom in a tandem pyrimidine ring opening and closing reaction by the S_N (ANRORC) mechanism (Scheme 6 a). On the other hand, the addition of hydroxide to such systems usually results in cleavage of the C(2) carbon fragment without pyrimidine re-cyclization (Scheme 6 b).⁵² Such purine ring opening is a simple synthetic strategy to obtain highly functionalized imidazoles and pyrimidines, which are frequently used pharmacophores in medicinal chemistry due to their similarity to nucleosides found in biological systems.^{53, 54}



Scheme 6. Ring-opening of pyrimidine cycle in purines.

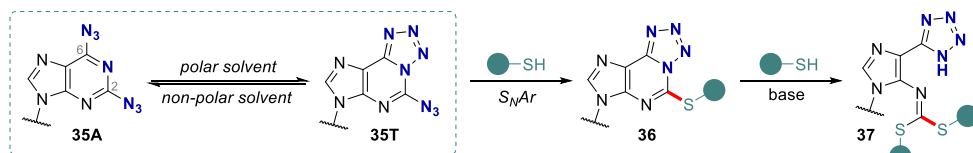
There are four possible activation mechanisms for the purine system (Scheme 7). First, hypoxanthines are more reactive due to the carbonyl group, and the introduction of an electron-withdrawing group at the N(1) position allows the opening of hypoxanthines with various nucleophiles readily at room temperature. Second, the N(1) position in annulated purines is part of a separate conjugated system, making it a leaving group. Third, the introduction of an electron-withdrawing group at the N(1) position in purines and adenines makes it an excellent leaving group. In activated adenine systems, Dimroth rearrangement usually takes place.^{55–58} Finally, the introduction of an electron-withdrawing group at the N(7) position destabilizes the imidazole ring, and its opening occurs almost instantly.



Scheme 7. Purine activation mechanisms.

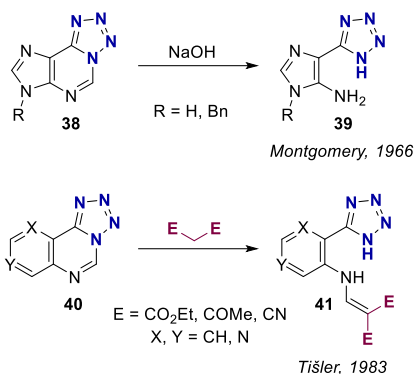
For details on the types of activation and opening of purines, see the review article in Appendix 1.

Based on the previous studies in the chemistry of 9-substituted 2,6-diazidopurines, nucleophilic aromatic substitution in such systems is known to occur at the C(2) position due to the C(6) azide tautomerization into a tetrazole (Scheme 8).^{5, 39, 59, 60} Such protection of C(6) site against nucleophile attack promotes the S_NAr process in the remaining heterocyclic system due to its electron-withdrawing properties. Kristers Ozols, in his Master's Thesis, explored the addition of two nucleophiles to 2,6-diazidopurine and observed that the resulting compound was not the expected 2,6-disubstitution product.⁶¹ Analysis of the product showed that it contains two added thiols as nucleophiles and the tetrazole fragment corresponding to the purine ring-opening product **37**.



Scheme 8. S_NAr substitution and ring-opening in 2,6-diazidopurines observed by K. Ozols.⁶¹

Literature review revealed two hits on the ring-opening of tetrazole annulated pyrimidines. First, one example of purine ring-opening with a hydroxide was demonstrated by Montgomery.⁴³ Second, a fused pyrimidine ring-opening with carbon nucleophiles, which enter in the product structure, by Tišler^{62,63} (Scheme 9). Therefore, in the Thesis, a method was developed of purine ring-opening with different nucleophiles, combining the regioselective 2,6-diazidopurine substitution and tandem pyrimidine ring-opening reaction.



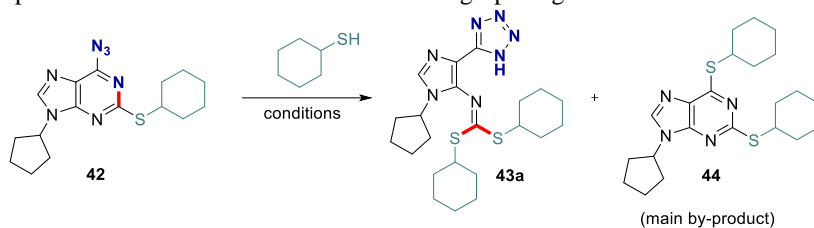
Scheme 9. Ring-opening of tetrazolopyrimidines.

The research began on the ring-opening of 2,6-diazidopyrimidines with optimization of reaction conditions in the case of thiol nucleophiles (Table 1.1). The C(2)-substituted 6-azidopyrimidine **42** was chosen as the substrate because the optimal conditions for regioselective substitution of 2,6-diazidopyrimidine with thiols are known from K. Ozols' Master's Thesis. Next, unsubstituted 2,6-diazidopyrimidine **45a** was chosen for optimization of reaction conditions in the case of alkoxynucleophiles (Table 1.2).

In the ring-opening reaction with thiols, it was concluded: 1) in non-polar solvents (toluene), the substitution takes place both at the C(2) and C(6) positions because of diazide tautomer – hence, a polar solvent (DMF) is needed for the ring-opening; 2) the ring-opening requires a strong non-nucleophilic base (NaH), because weaker bases (DBU (1,8-diazabicyclo[5.4.0]undec-7-ene), K_2CO_3) promote substitution at both C(2) and C(6) positions; 3) lower temperature reduces the formation of side products due to increased concentration of tetrazole and stabilization of the Meisenheimer complex intermediate.

Different trends were observed in the optimization of reaction conditions for purine ring-opening with alcohols compared to thiols. In this case, the most suitable reaction solvent was toluene, which gave the highest selectivity for the ring-opening reaction. This observation is contrary to the ring-opening with thiols and also to the general concept that polar solvents stabilize the forming Meisenheimer intermediate. The most suitable base, also in this case, was NaH. However, similar results were obtained using DBU, which was incapable of ring-opening in the case of thiols. Also, a decrease in the reaction temperature had an insignificant effect on the yield. Although, an increase in the reaction temperature even slightly improved the yield and selectivity of the ring-opening reaction.

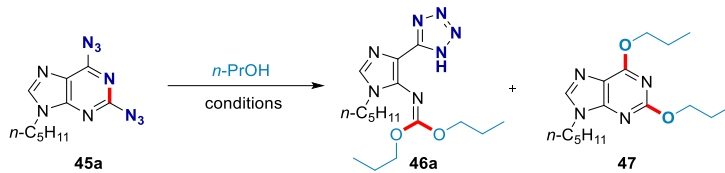
Table 1.1

Optimization of Reaction Conditions for Ring-opening of Purine **42** with a Thiol

No.	solvent	base (eq.)	<i>T</i> (°C)	yield 43a (%) ^a	starting material 42 (%) ^a
1	DMF	NaH (1.5)	r.t.	55	12
2	DMF	KorBu (1.5)	r.t.	62	4
3	DMF	DBU (1.5)	r.t.	0	55
4	toluene	NaH (1.5)	r.t.	5	76
5	toluene	KorBu (1.5)	r.t.	4	68
6	MeCN	NaH (1.5)	r.t.	8	76
7	MeCN	KorBu (1.5)	r.t.	50	20
8	THF	NaH (1.5)	r.t.	43	40
9	THF	KorBu (1.5)	r.t.	36	30
10	<i>i</i> -PrOH	KorBu (1.5)	r.t.	34	24
11	DMSO	KorBu (1.5)	r.t.	64	2
12	NMP	NaH (1.5)	r.t.	39	21
13	DMF	NaH (0.9)	r.t.	44	32
14	DMF	KorBu (2.5)	r.t.	54	7
15	DMF	NaH (1.5)	0	68	5
16	DMF	KorBu (1.5)	0	64	8

^a – yield was determined by quantitative ¹H NMR in the crude reaction mixture using 1,2,3-trimethoxybenzene as an internal standard.

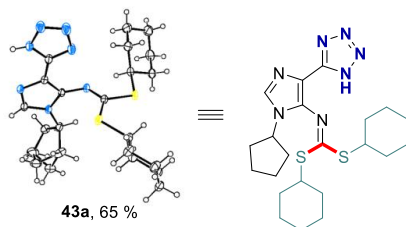
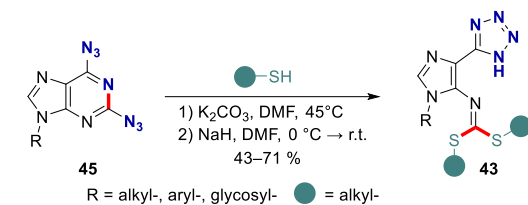
This contradictory trend might be explained by the change of the reaction mechanism depending on the nucleophile used. In the case of thiols, the reaction proceeds through a Meisenheimer complex, as the thiolate is a superior nucleophile. However, in the case of alcohols, the reaction presumably does not occur through the formation of a Meisenheimer complex but rather in a concerted S_NAr process.^{64–66} Such a mechanism would explain the course of reaction in a non-polar solvent and the ability of the relatively weak base (DBU) to carry out ring-opening.

Optimization of Reaction Conditions for the Ring opening of Purine **45a** with Propanol⁶⁴⁻⁶⁶

No.	Solvent	base (eq.) ^b	<i>T</i> (°C)	yield 46a (%) ^a	yield 47 (%) ^a
1	DMF	NaH (3)	r.t.	38	21
2	MeCN	NaH (3)	r.t.	0	0
3	THF	NaH (3)	r.t.	36	33
4	<i>n</i> -PrOH	NaH (3)	r.t.	50	42
5	toluene	NaH (3)	r.t.	47	22
6	NMP	NaH (3)	r.t.	38	30
7	diglyme	NaH (3)	r.t.	44	16
8	toluene	K ₂ CO ₃ (3)	r.t.	0	0
10	toluene	KotBu (3)	r.t.	5	45
11	toluene	KOH (3)	r.t.	13	2
12	toluene	<i>n</i> -BuLi (3)	r.t.	7	4
13	toluene	NaH (3)	0	49	16
14	toluene	NaH (3)	50	55	13
15	toluene	NaH (5) ^c	r.t.	0	0
16	toluene	NaH (3)^d	r.t.	66	11
17	DMF	NaH (3) ^d	r.t.	21	42
18	DMF	DBU (3) ^d	r.t.	36	1
19	toluene	DBU (3) ^d	r.t.	49	1

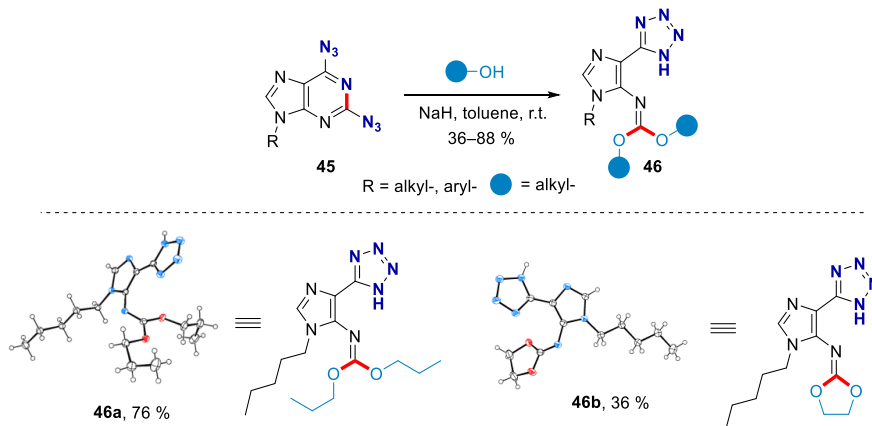
a – yield was determined by quantitative ¹H NMR in the crude reaction mixture, using 1,2,3-trimethoxybenzene as an internal standard; b – alkoxide was added in two portions; c – alkoxide was added in one portion; d – alkoxide was added dropwise.

In cooperation with laboratory colleagues (see the list of authors), a range of substrates for diazidopurine ring-opening with thiols were screened by applying the optimized reaction conditions (Scheme 10). The substituent at the N(9) position of the purine practically did not affect the yield, except for the ribosyl derivatives due to partial deprotection of the acetate protecting groups. The reactions proceeded smoothly with both primary and secondary thiols. It should be noted that purine ring-opening with aromatic thiols is not possible under the given conditions, most likely because the arylthiolate is a better leaving group than the tetrazole anion.



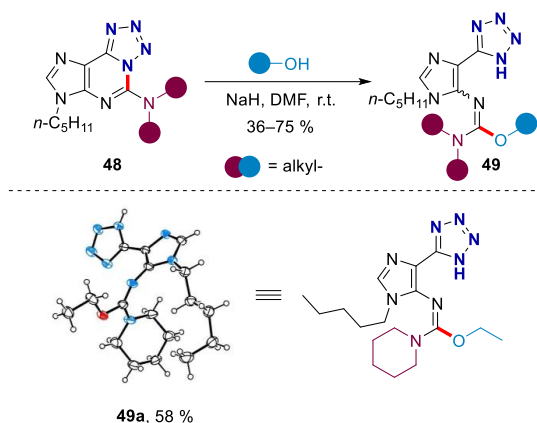
Scheme 10. Ring-opening of diazidopurine **45** with thiols.

Next, applying the optimal reaction conditions (NaH/toluene), a range of substrates was demonstrated for purine ring-opening with various alcohols (Scheme 11). It should be emphasized that the cyclic addition product **46b** was obtained using ethylene glycol as a nucleophile. Also, in this case, the addition of aromatic (phenol) and sterically large (*t*-BuOH, adamantanol) alcohols is not possible.



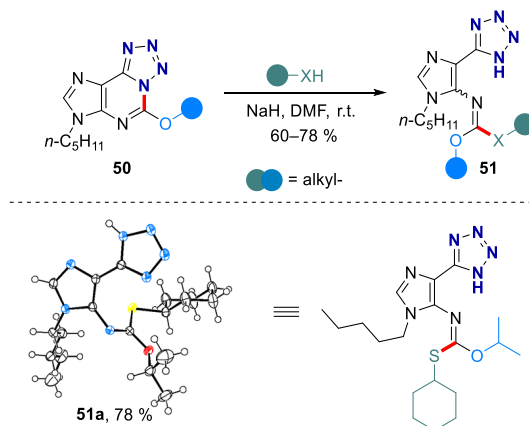
Scheme 11. Ring-opening of diazidopurine **45** with alcohols.

Purine ring-opening by the addition of amine nucleophile turned out to be impossible. However, subjecting purines **48** with amino substituents at the C(2) position to ring-opening conditions with primary and secondary alcohols yielded carbamimidates **49** (Scheme 12). Again, the addition of aromatic (phenol) and sterically large (*t*-BuOH) alcohols was not feasible. In this case, the hydrolysis product was obtained with a yield of 62 % in the reaction with phenol, which was also the main by-product.



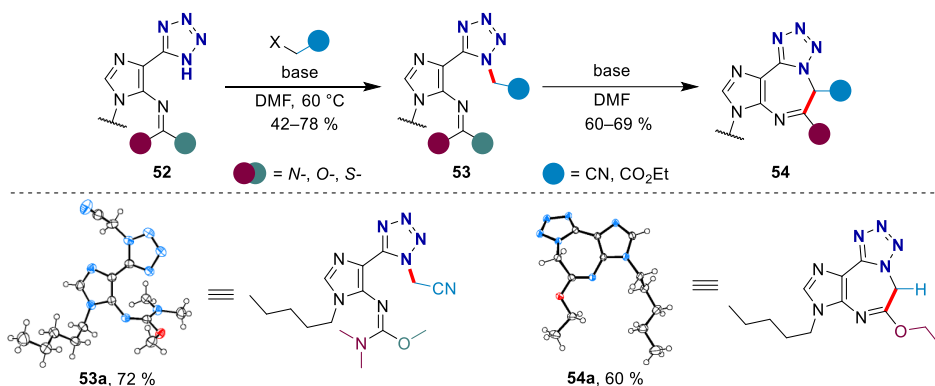
Scheme 12. Ring-opening of tetrazoloaminopurines **48** with alcohols.

Similarly, ring-opening products **51** of alkoxy-substituted tetrazolopurines **50** were obtained by adding primary and secondary alcohols and thiols (Scheme 13). The stereoselectivity of the products could not be determined by NMR spectroscopy, but a single crystal of compound **51a** was obtained, which showed the Z-double bond geometry in the product.



Scheme 13. Ring-opening of tetrazoloalkoxy purines **50** with alkoxides and thiols.

To demonstrate the utility of the ring-opened compounds, their cyclization into diazepine derivatives **54** was developed by the alkylation of the products **52** followed by cyclization in basic conditions (Scheme 14). Thus a formal enlargement of the pyrimidine ring of purine by one carbon was achieved.

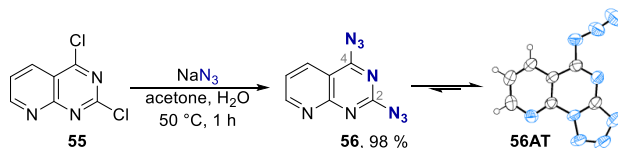


Scheme 14. Synthesis of annulated tetrazolidiazepines **54**.

For a more detailed description of the research in this chapter, see the original publication in Appendix 2.

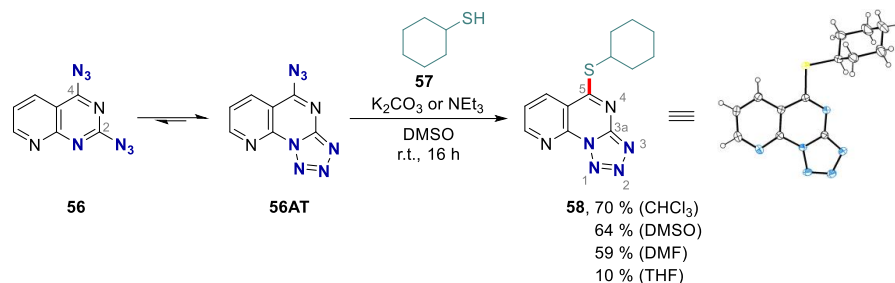
1.2. Azide-Tetrazole Equilibrium Studies and S_NAr Reactions in the Pyrido[2,3-*d*]pyrimidine Heterocycle

This subproject was started with the synthesis of the substrate of interest – 2,4-diazidopyrido[2,3-*d*]pyrimidine **56** (*diazide*) from dichloride **55** in S_NAr reaction with NaN_3 (Scheme 15). The name *diazide* in the Thesis refers to the formal *diazide* structures, as these systems exist as a mixture of several azide and tetrazole tautomers. The most stable tautomer in 2,4-diazidopyrimidine systems is usually in the form of tetrazolo[1,5-*a*]pyrimidine.^{14, 44, 67, 68} With the X-ray structural analysis, it was found that also the heterocyclic system of 2,4-diazidopyrido[2,3-*d*]pyrimidine in the crystalline phase exists as 5-azidopyrido[3,2-*e*]tetrazolo[1,5-*a*]pyrimidine (**56AT**). Reactions of this tautomer in S_NAr reactions would result in nucleophilic addition at the C(4) position, which is expected for pyrimidine systems with two identical substituents at the C(2) and C(4) positions.



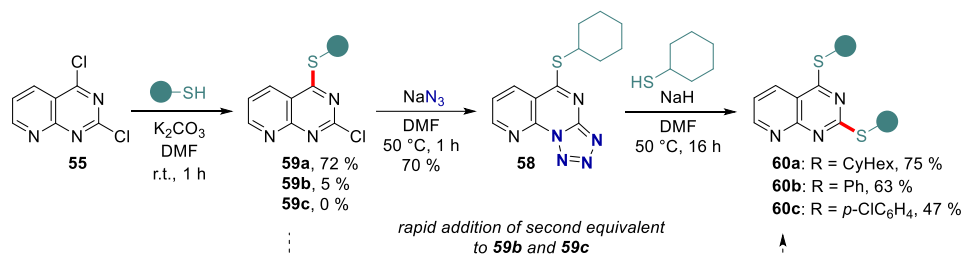
Scheme 15. Synthesis of *diazide* **56**.

Next, the azide-tetrazole equilibrium was explored to determine the possible C(2) or C(4) regioselectivity in S_NAr reactions with *diazide* **56**. The studies of S_NAr reactions started by adding cyclohexanethiol to *diazide* **56** in solvents of different polarities: $CHCl_3$, THF, DMF, and DMSO. In all cases, the nucleophile addition occurred at the C(4) position, indicating the higher reactivity of the tautomeric form **56AT** regardless of solvent polarity (Scheme 16). The addition of aromatic thiols was unsuccessful, as the starting materials were recovered unreacted.



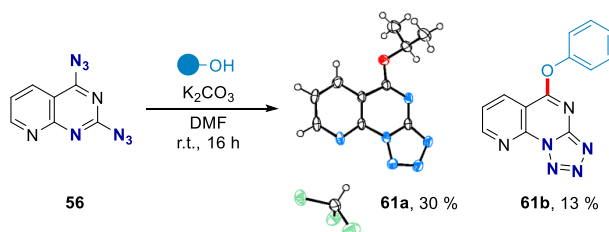
Scheme 16. Diazide **56** S_NAr reaction with cyclohexanethiol.

As control experiments, cyclohexanethiol was added to the dichloride **55**, followed by the addition of sodium azide (Scheme 17). In this reaction sequence, product **58** was obtained with the same C(4) regioselectivity as when reacting diazide **56** with a thiol. Nevertheless, comparing the two synthetic strategies, it should be noted that the diazide synthesis route (Scheme 16) is simpler, with easier product purification and higher overall yield. The mono-substitution products **59b** and **59c** were practically impossible to isolate from the reaction mixture upon the addition of an aromatic thiol (thiophenol) to the dichloride **55**, as the di-substitution products **60b** and **60c** formed rapidly in the reaction mixture.



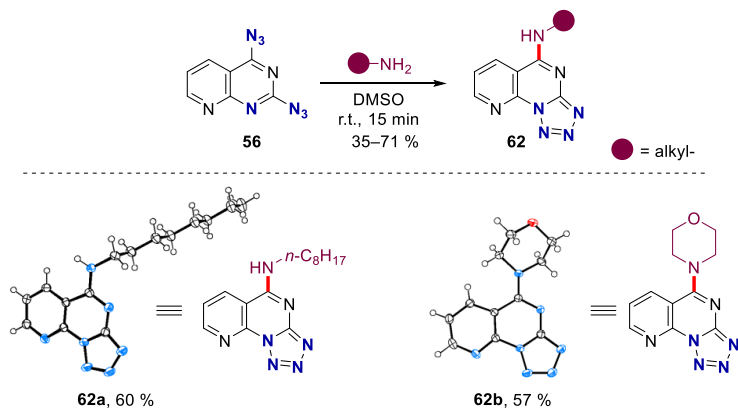
Scheme 17. Nucleophilic aromatic substitution in 2,4-dichloropyrido[2,3-*d*]pyrimidine (**55**).

Next, S_NAr reactions with *O*-nucleophiles were performed. Herein, products with low yields were obtained due to hydroxide addition (hydrolysis) and the formation of other side products (Scheme 18). It should be noted that the addition of aromatic alcohol – phenol – was successful, and product **61b** was obtained, albeit with a low yield.



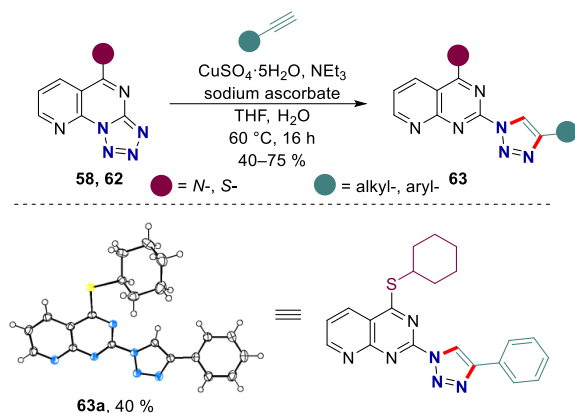
Scheme 18. S_NAr substitution in diazide **56** with *O*-nucleophiles.

The addition of *N*-nucleophiles to diazide **56** proceeded relatively quickly and the amine S_NAr substitution products **62** were obtained in good yields (Scheme 19). The formation of unidentifiable product mixtures was observed when hydrazine, hydroxylamine, and aniline were added. The resulting pyrido[2,3-*d*]pyrimidine amino derivatives **62** showed low solubility in most organic solvents.



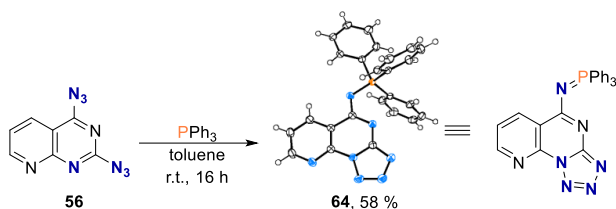
Scheme 19. S_NAr substitution in *diazide* **56** with *N*-nucleophiles.

Further reactivity of compound **62** was tested in CuAAC to demonstrate the utility of the substituted products and the presence of azide-tetrazole equilibrium. Triazoles **63** were successfully obtained using a $\text{CuSO}_4 \cdot 5\text{H}_2\text{O}$ /sodium ascorbate/ NEt_3 catalytic system (Scheme 20). Considering the tetrazole tautomer of compounds **62** being the major one, the achieved azide functionalization indicates the presence of an equilibrium that provides sufficient azide reacting concentration in the system.



Scheme 20. Synthesis of 2-(1,2,3-triazolyl)pyrido[2,3-*d*]pyrimidine **63**.

The azide-tetrazole equilibrium of *diazide* **56** was also demonstrated in the Staudinger reaction with triphenylphosphine (Scheme 21). Iminophosphorane **64** was isolated from this reaction, which is usually an unstable Staudinger reaction intermediate.



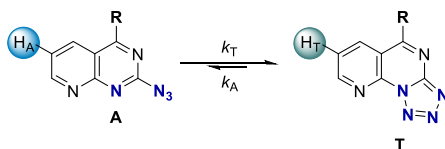
Scheme 21. Synthesis of iminophosphorane **64** in the Staudinger reaction.

From the obtained tetrazolo[1,5-*a*]pyrido[3,2-*e*]pyrimidine derivatives, the equilibrium in CDCl₃ solutions was observed for mercapto- and alkoxyderivatives **58**, **61a**, **61b**. The amino group, as an electron-donating substituent, was able to shift the equilibrium towards the tetrazole tautomer completely. Also, in the polar DMSO-*d*₆ medium, the equilibrium shifted towards the tetrazole tautomer, and the azide tautomer was not observed even at elevated temperatures.

Thermodynamic values of the tautomerization process are given in Table 1.3. The obtained equilibrium process enthalpies for products **61a**, **58**, and **61b** are -23.19 kJ/mol, -21.30 kJ/mol, and -17.02 kJ/mol, respectively. Since the enthalpy represents the absolute stability of the tetrazole system³¹ and the electron-donating substituents stabilize the tetrazole tautomer, the experimentally obtained enthalpy values in the order *Oi*-Pr (**61a**) > *Sc*-Hex (**58**) > *O*Ph (**61b**) correlate well with the theory in literature.

Table 1.3

Equilibrium Constants and Thermodynamic Values of Tautomerization of Tetrazolo[1,5-*a*]pyrido[3,2-*e*]pyrimidines **58**, **61a** and **61b** in CDCl₃ Solution^a



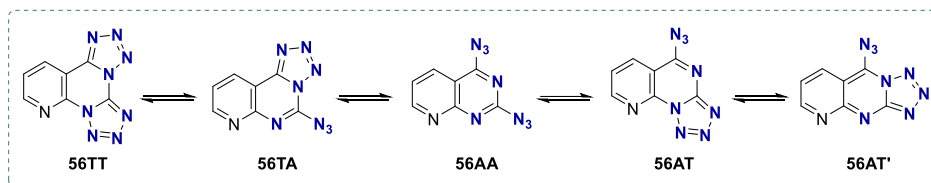
Compound	R	T (K)	K_{eq}^b	ΔG_{298} (kJ/mol)	ΔH (kJ/mol)	ΔS (J/mol·K)
58		298	5.21	-4.08 ± 0.15	-21.30 ± 0.78	-57.71 ± 2.10
		313	3.48			
		323	2.68			
61a		298	9.99	-5.70 ± 0.27	-23.19 ± 1.09	-58.70 ± 2.76
		313	6.30			
		323	4.85			
61b		298	3.39	-3.02 ± 0.65	-17.02 ± 3.69	-46.93 ± 10.16
		313	2.48			
		323	1.99			

a – A: azide tautomer; T: tetrazole tautomer; b – $K_{eq} = [T]/[A]$, expressed as the ratio of ¹H NMR signal integrals.

Four tautomeric forms for the diazide **56** in CDCl₃ solution existed simultaneously, and the equilibrium was too complicated to determine thermodynamic parameters. The diazide **56** has five theoretically possible tautomeric structures: diazide **56AA**, bis-tetrazole **56TT**, linear azidotetrazole **56AT'**, and two angular azidotetrazoles **56AT** and **56TA** (Scheme 22).

While studying the *diazide* **56** equilibrium with ^1H NMR spectroscopy, four tautomeric forms were observed in almost all organic solvents and one tautomeric form in D_2SO_4 solution. In preliminary DFT calculations of *diazide* tautomeric forms, it was found that the linear tetrazole form **56AT'** has a 60–75 kJ higher formation energy than the other structures. Therefore, it was postulated that the linear form **56AT'** was not observed in ^1H NMR studies based on the high energy barrier. The signals at weaker fields (tetrazole tautomeric form) were dominant in polar solvents – $\text{DMSO-}d_6$, MeCN, MeNO_2 , and $\text{MeOD-}d_4$, and the intensities of signals at stronger fields (azide tautomeric form) increased in less polar solvents (CDCl_3 , MTBE, C_6D_6). An increase was observed in signal intensities at stronger fields (azide form) with increasing the temperature of solutions. These observations of polarity and temperature changes agree with the data in literature. Tetrazole tautomers predominate at lower temperatures and in polar solvents. Meanwhile, elevated temperatures and non-polar solvents favor the formation of azido tautomers.

From all the compounds studied in this chapter, only for *diazide* **56**, was obtained a cross-peak signal in the exchange spectroscopy experiment (EXSY), which proved the existence of dynamic equilibrium in this system.

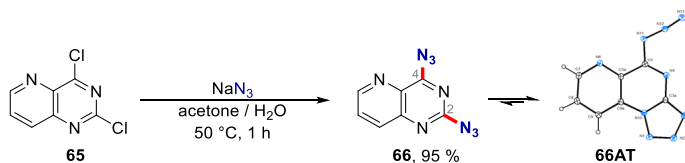


Scheme 22. Tautomeric structures of *diazide* **56**.

For a more detailed description of the research in this chapter, see the original publication in Appendix 3.

1.3. Azide-Tetrazole Equilibrium Studies and $\text{S}_{\text{N}}\text{Ar}$ Reactions in the Pyrido[3,2-*d*]pyrimidine Heterocycle

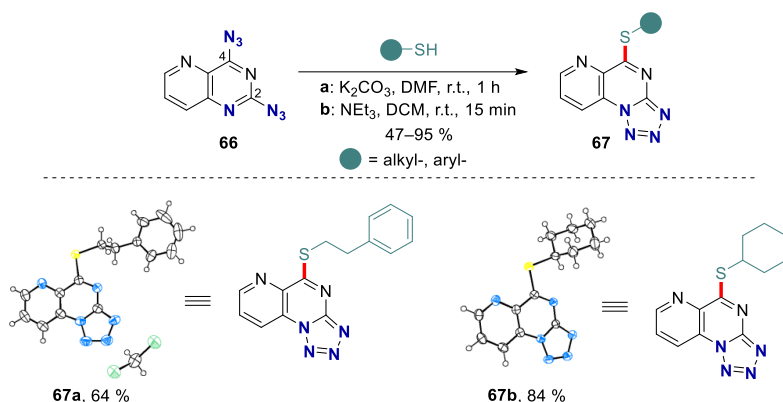
This subproject was started with the synthesis of 2,4-diazidopyrido[3,2-*d*]pyrimidine (*diazide*) from dichloride **65** in $\text{S}_{\text{N}}\text{Ar}$ reaction with NaN_3 (Scheme 23). With X-ray structural analysis it was found that the 2,4-diazidopyrido[3,2-*d*]pyrimidine heterocyclic system in the crystalline phase exists as 5-azidopyrido[2,3-*e*]tetrazolo[1,5-*a*]pyrimidine (**66AT**).



Scheme 23. Synthesis of 2,4-diazidopyrido[3,2-*d*]pyrimidine (**66**).

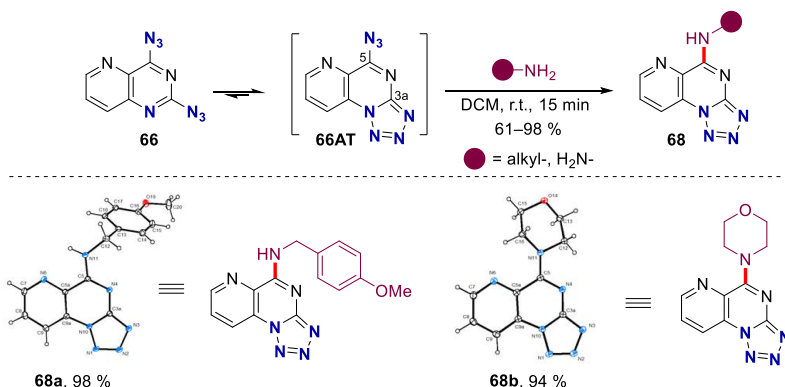
The $\text{S}_{\text{N}}\text{Ar}$ studies on *diazide* **66** began using thiols and the $\text{K}_2\text{CO}_3/\text{DMF}$ reagent system (Scheme 24). Herein, the products of type **67** were also obtained with selective substitution occurring at the C(4) position. Changing the reagent system, solvent to the less polar methylene

chloride and the base to triethylamine (condition b) yielded the product **67** with the same C(4) selectivity.



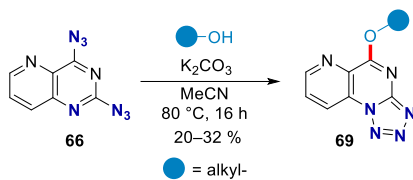
Scheme 24. $S_N\text{Ar}$ substitution of 2,4-diazidopyrido[3,2-*d*]pyrimidine (**66**) with thiols.

Next, the $S_N\text{Ar}$ substitution of *diazide* **66** with *N*-nucleophiles was tried (Scheme 25). Addition of *p*-methoxybenzylamine in DMSO gave product **68a** in 49 % yield in the absence of an additional base. At this point, the effect of solvent polarity on regioselectivity was investigated, which probably would give a rise to the C(2) substitution product. However, full C(4) substrate selectivity was proved for the substitution of **68a** in all investigated solvents: benzene, toluene, DCM, CHCl_3 , MeCN, and EtOH. This indicates that the 5-azidotetrazolo[1,5-*a*]pyrido[2,3-*e*]pyrimidine tautomer (**66AT**) is the most reactive regardless of the chosen solvent. The highest yield was obtained in DCM solution, therefore it was used throughout this study. Reactions with different primary and secondary amines gave products **68** in excellent yields. Also, the addition of ammonia and hydrazine were successful. Substitution with aromatic amine (anisidine) was unsuccessful, and the starting material remained unreacted.



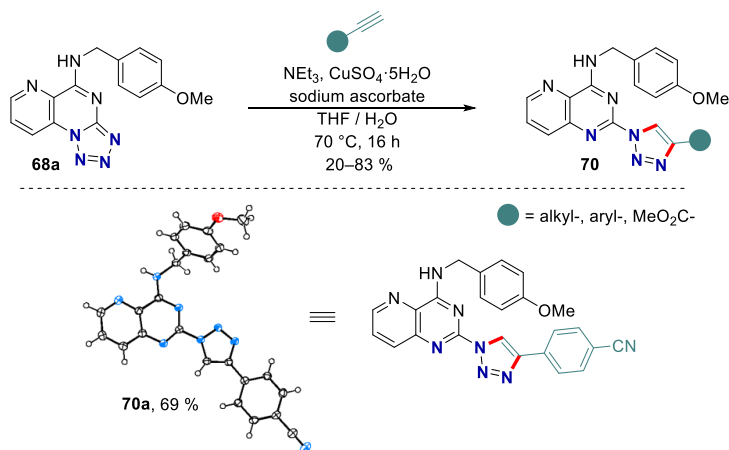
Scheme 25. $S_N\text{Ar}$ substitution of 2,4-diazidopyrido[3,2-*d*]pyrimidine (**66**) with amines.

The formation of alkoxy adducts **69** with *O*-nucleophiles occurred with formation of side-products, and the yields were low (Scheme 26). Also, aromatic *O*-nucleophiles showed no reactivity, similar to aromatic *N*-nucleophiles.



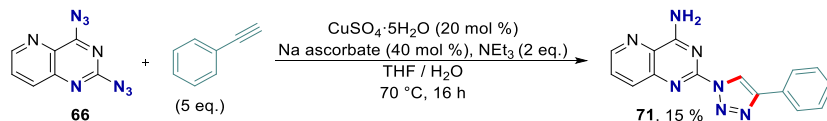
Scheme 26. $\text{S}_{\text{N}}\text{Ar}$ substitution of 2,4-diazidopyrido[3,2-*d*]pyrimidine (**66**) with alkoxides.

Further application of the obtained products in the CuAAC reaction was successfully demonstrated (Scheme 27). Taking into account the majority of the tetrazole tautomer present in compound **67–69** solutions (Table 1.4) and in the solid phase, the functionalization of azide tautomers indicates the presence of a sufficient equilibrium that restores the lower concentration reactive azide tautomer in the system.



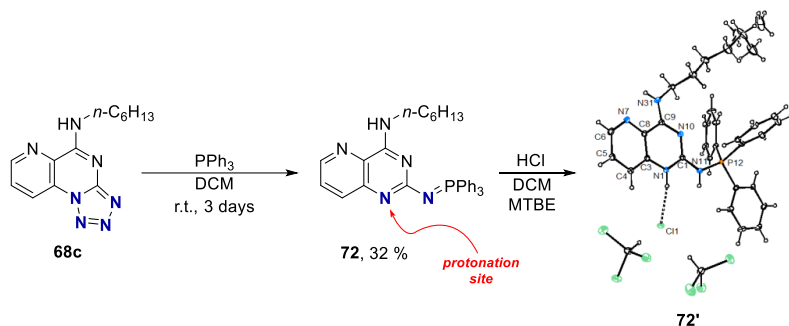
Scheme 27. Synthesis of 2-triazolylpyrido[3,2-*d*]pyrimidine **70**.

The synthesis of bistriazole from *diazide* **66** was unsuccessful due to the formation of side products. The major product in the reaction was the partially reduced CuAAC reaction product **71** in 15 % yield (Scheme 28). It is known that the $\text{CuSO}_4 \cdot 5\text{H}_2\text{O}$ /sodium ascorbate system can reduce azido heterocycles to amines, which was also observed in this case.⁶⁹



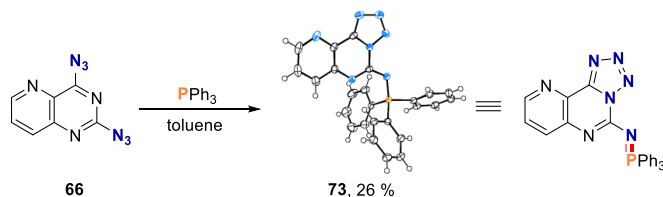
Scheme 28. CuAAC reaction of 2,4-diazidopyrido[3,2-*d*]pyrimidine (**66**) with tandem reduction of C(4) azide.

Product **68c** was also functionalized in the Staudinger reaction with triphenylphosphine (Scheme 29). The resulting iminophosphorane showed basic properties and readily protonated at the heterocycle's N(1) position to form salt **72'**, which was proved in solution and solid phase by X-ray structural analysis. Compound **72** is structurally similar to phosphazines, which are nonionic superbases.^{70, 71}



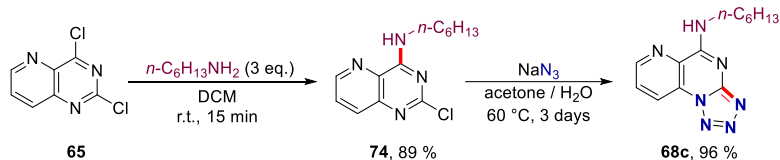
Scheme 29. Synthesis of iminophosphorane **72** and its HCl salt **72'**.

The Staudinger reaction of *diazide* **66** with triphenylphosphine yielded the switched C(2) regioselectivity product **73**, the structure of which was proved by X-ray analysis (Scheme 30). An explanation for the regioselectivity of this reaction needs to be clarified, and research is ongoing. However, the synthesis of a switched regioselectivity product demonstrates the feasibility of azide-tetrazole equilibrium-directed selective transformation in the pyrido[3,2-*d*]pyrimidine system.



Scheme 30. Switched regioselectivity Staudinger reaction.

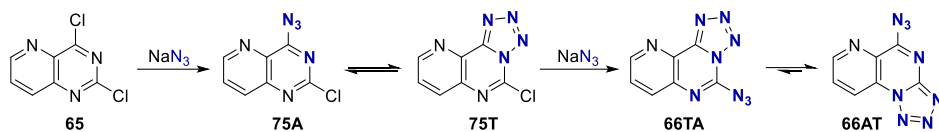
To confirm the higher reactivity of C(4) position (compared to C(2)) in the pyrido[3,2-*d*]pyrimidine heterocycle system, additional control experiments were performed. The order of addition of reagents was changed (Scheme 31). The addition of amine, followed by sodium azide, gave an identical product (**68c**) as the S_NAr reaction of *diazide* **66** with amine. However, it should be noted that the azide addition at the C(2) position proceeded for three days at elevated temperature until full conversion was achieved. In a similar literature example, the substitution of chlorine in 4-amino-2-chloropyrido[3,2-*d*]pyrimidine with sodium azide was not possible even under forced conditions.⁷² The electron-donating effect of the amino group in compound **74** reduces or even stops further S_NAr reactions in the system, and the formation of product **74** occurs selectively without the 2,4-diamino product.



Scheme 31. Conventional synthesis of **68c**.

Interestingly, the formation of *diazide* **66** proceeds rather quickly (30 min) and at room temperature. This observation leads to the hypothesis that tetrazole tautomer is formed after the

addition of the first azide group at the C(4) position (Scheme 32). In the intermediate **75T**, the tetrazole as an electron-withdrawing group promotes the addition of the second azide at the C(2) position, and tautomerization to the most stable *diazide* system yields **66AT**.



Scheme 32. Proposed mechanism of *diazide* **66** formation

Further studies focused on the equilibrium of tetrazoles **67–69** with ^1H NMR in solutions at different temperatures. The calculated thermodynamic parameter values – Gibbs free energy, enthalpy and entropy, of azide-tetrazole tautomerization are given in Table 1.4. The equilibrium in the DMSO- d_6 solution for all compounds is entirely shifted towards the tetrazole tautomer. However, the azide tautomer and azide-tetrazole equilibrium were observed in CDCl_3 as less polar solvent. Increasing the temperature of solutions shifts the equilibrium towards the azide tautomer. The calculated negative enthalpy values for the tetrazole tautomer confirm it as the energetically favorable tautomer at the given experimental conditions. The major tetrazole tautomer under normal conditions (25 °C) for tautomerization in solutions is quantitatively characterized by the calculated Gibbs free energy negative values. Gibbs free energy values of the *p*-methoxybenzylamino- and hexylamino-substituted products were the highest (Table 1.4, **68a** and **68c**), and the equilibrium is shifted more towards the tetrazole. Gibbs free energy values of tautomerization for alkoxy-substituted products (Table 1.4, **69a** and **69b**) are higher than their thiol analogs **67**. The lowest tautomerization Gibbs free energy values were calculated for secondary amine substituted products. From these data (Table 1.4), it can be concluded that the electron-donating substituents – *N*-nucleophiles > *O*-nucleophiles > *S*-nucleophiles, shift the equilibrium towards tetrazole and the steric effects of secondary amines suppress the tetrazole formation (Fig. 4).

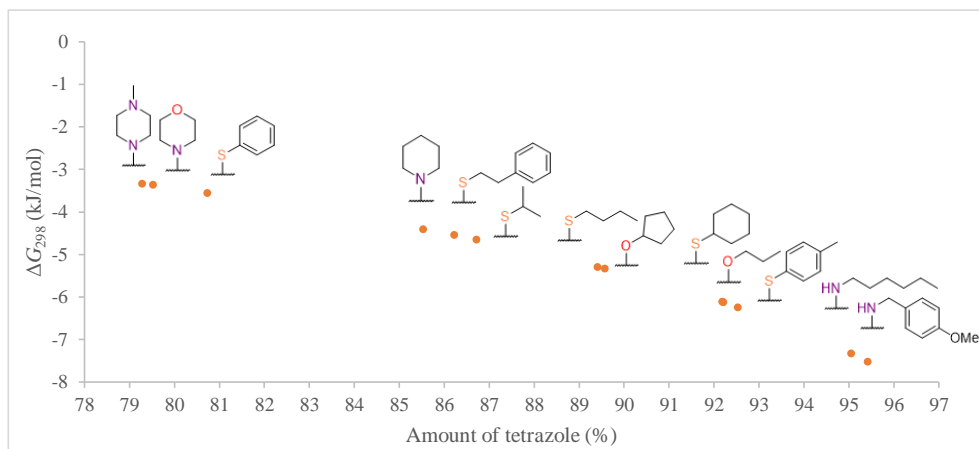


Fig. 4. Gibbs free energies of tautomerization for tetrazoles **67–69**.

Finally, the tautomeric equilibrium of *diazide* **66** was examined by ^1H NMR spectroscopy in different solvents (Figure 5). The high-order tautomeric equilibrium of

2,4-diazidopyrido[3,2-*d*]pyrimidine was too complex for unambiguous identification of tautomers. The ratio of tautomers and the number of tautomeric forms in the solution changed significantly depending on the solvent. The intensities of the signals at weaker fields increased as solvent polarity increased – the equilibrium shifts towards the tetrazole tautomer. These observations correlate with the properties of azide-tetrazole tautomerism reported in the literature. In most cases, three to four tautomeric forms are observed. One tautomeric form was observed in a deuterated trifluoroacetic acid solution, and two in a D₂SO₄ solution. The pyrimidine heterocycle is likely protonated in an acidic medium, and the equilibrium is completely shifted towards the azide form. The most interesting case was the AcOD-*d*₄ solution, where 7 tautomeric forms were observed, indicating the presence of one betaine form in the solution (Fig. 6).

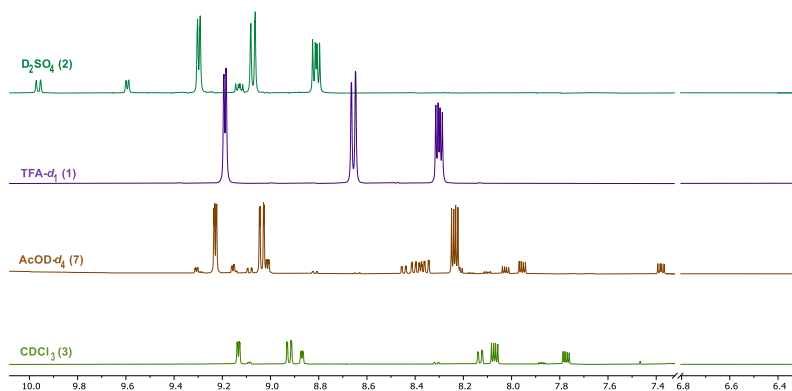


Fig. 5. ¹H NMR spectra of *diazide 66* in different solvents (the number of tautomers observed is given in brackets).

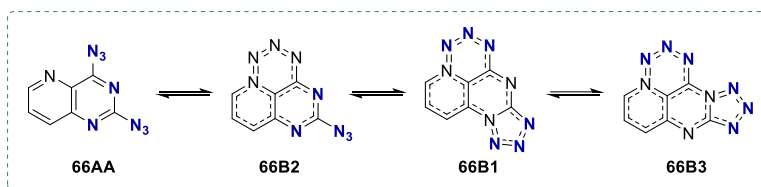
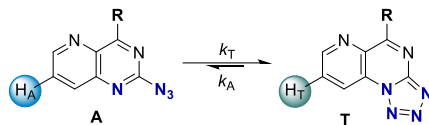


Fig. 6. Possible betaine tautomeric structures of *diazide 66*.

For a more detailed description of the research in this chapter, see the original publication in Appendix 4.

Table 1.4

Equilibrium Constants and Thermodynamic Values of Tautomerization of Tetrazolo[1,5-*a*]pyrido[2,3-*e*]pyrimidines **67–69** in CDCl₃ Solution^a



Compound	R	T (K)	K_{eq}^b	ΔG_{298} (kJ/mol)	ΔH_{298} (kJ/mol)	ΔS_{298} (J/mol·K)
67a		298	8.44			
		313	4.32	-5.29 ± 0.11	-32.11 ± 1.94	-90.14 ± 6.24
		323	3.11			
67b		298	6.26			
		313	3.92	-4.54 ± 0.02	-23.63 ± 0.38	-64.08 ± 1.21
		323	2.99			
67c		298	12.39			
		313	6.37	-6.24 ± 0.02	-30.53 ± 0.34	-81.69 ± 1.11
		323	4.81			
67d		298	6.53			
		313	4.49	-4.65 ± 0.03	-20.14 ± 0.61	-51.96 ± 1.95
		323	3.47			
67e		298	4.19			
		313	2.57	-3.55 ± 0.28	-31.75 ± 4.90	-94.33 ± 15.74
		323	1.53			
67f		298	15.08			
		313	4.96	-6.11 ± 0.12	-42.05 ± 2.13	-120.72 ± 6.83
		323	3.30			
68a		298	20.83			
		313	15.05	-7.52 ± 0.22	-21.91 ± 3.91	-48.05 ± 12.53
		323	10.39			
68b		298	3.89			
		313	2.53	-3.36 ± 0.02	-22.65 ± 0.32	-64.71 ± 1.03
		323	1.91			
68c		298	19.20			
		313	12.77	-7.32 ± 0.03	-20.35 ± 0.56	-43.74 ± 1.78
		323	10.19			
68d		298	5.92			
		313	3.81	-4.40 ± 0.07	-24.52 ± 1.31	-67.42 ± 4.20
		323	2.74			
68e		298	3.83			
		313	2.59	-3.33 ± 0.01	-19.92 ± 0.25	-55.69 ± 0.79
		323	2.06			
69a		298	8.59			
		313	3.36	-5.33 ± 0.17	-48.02 ± 2.95	-143.27 ± 9.49
		323	1.92			
69b		298	11.84			
		313	6.00	-6.12 ± 0.16	-31.55 ± 2.75	-85.50 ± 8.83
		323	4.45			

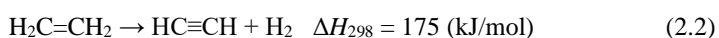
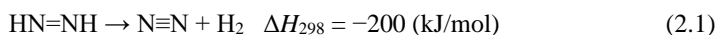
a – A: azide tautomer; T: tetrazole tautomer; b – $K_{eq} = [T]/[A]$, expressed as a ratio of ¹H NMR signal integrals.

2. Synthesis and Physical Properties of Polyazidopyrimidines

As there is a risk of explosion when working with small molecular compounds containing the azide groups, the azido functional group is usually associated with danger to the standard organic chemist. However, in the study of energetic materials (explosives), detonation ability and sensitivity to external impulses are essential physical properties.

Explosives are used in military and civil engineering applications such as weapon ammunition, mining, road construction, building demolition, airbags, etc. Explosives are divided into two categories based on their sensitivity and performance: primary (initiating) and secondary (high-performance) explosives. Primary explosives are often sensitive polyazido compounds that detonate upon a relatively small external energy input in friction, impact, heat, or an electrical discharge. Primary explosives generally have low brisance and are intended for use in detonators to initiate a secondary explosive. Secondary explosives are much stronger and more stable than primary explosives. Their detonation requires a detonation wave, which is generated by detonators. Secondary explosives are often based on polynitroorganic compounds, and their high energy comes from an exothermic intramolecular oxidation-reduction process in which a large amount of gaseous products – CO₂, CO, and N₂ are released.^{73, 74}

A modern trend in the design of novel energetic materials is the functionalization of heterocycles with explosophoric functional groups. Nitrogen heterocyclic compounds: tetrazole, triazole, furazan, triazine, and tetrazine are suitable building blocks for the design of energetic materials due to their high enthalpy of formation from energy-rich N-N and C-N bonds⁷⁵ and high thermal stability.⁷⁶ N-N bonds in organic compounds are energetically rich, as their decomposition results in elemental nitrogen (N₂), whose triple N≡N bond is particularly stable. The process of nitrogen triple bond formation is exothermic (negative enthalpy of formation) (2.2) and by ~ 375 kJ/mol thermodynamically more favorable as compared to the analogous C≡C bond formation from the C=C double bond which is endothermic (positive enthalpy of formation) (2.1).⁷⁷



Binary C_xN_y compounds with high nitrogen balance are a relatively new class of energetic compounds. Their design is based on nitrogen-rich heterocycles interconnected by azo- or diazobridges and functionalized with several azido groups. The energy of binary energetic compounds comes from the unusually high enthalpy of formation rather than from oxidation-reduction processes, which can be explained by a large amount of C-N and N=N bonds and energetic azido groups.^{23, 24, 78-81} Nitrogen-rich energetic materials often have a higher density and better thermal stability than classic polynitroexplosives. It should be emphasized that the main decomposition product of such nitrogen-containing compounds is N₂ gas, an important aspect for developing and integrating environmentally and human-safe explosives.⁸² Active protection, preservation, and restoration of the environment is a consequence of the industrialization process of the last century and is the basis for a sustainable future. Therefore, environmentally friendly processes, technologies, and materials are significant in modern industry and science. The most frequently used primary explosives in

detonators are lead azide and lead styphnate, which have an adverse effect on human health and the environment. So, the factor of environmental safety becomes more important in the development of new explosives.^{26, 27}

So far, there are no materials among the wide range of newly discovered binary energetic compounds that meet the requirements of modern explosives: high performance, low impact sensitivity, thermal and chemical stability, low toxicity, and scalable synthesis from inexpensive raw materials (Fig. 7).^{74, 83} Often, binary energetic compounds have issues such as low sublimation temperatures (**76**, **77**), excessively high sensitivity (**78**, **79**), complex synthesis, and insufficient thermal stability (**80**, **81**).^{23, 24, 78–81}

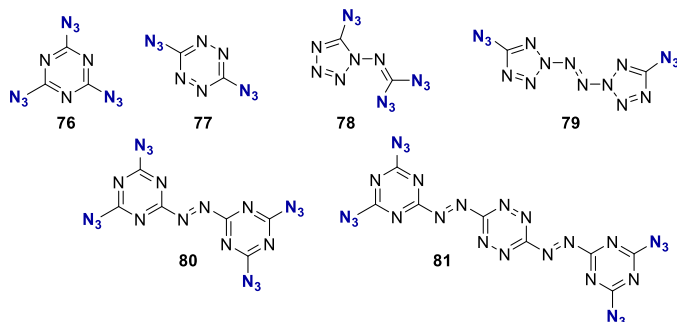
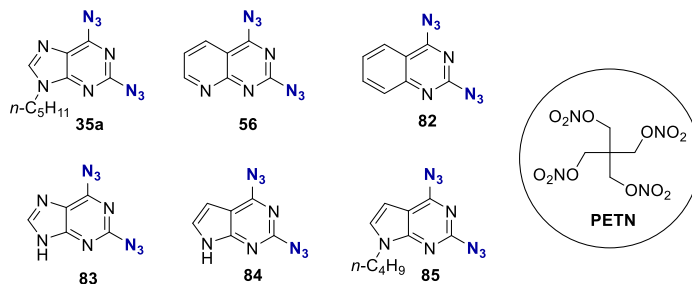


Fig. 7. Known nitrogen-rich binary energetic compounds.

During the Doctoral Thesis work, the energetic profile of the azidoheterocycles was determined in collaboration with Professor Tomas Klapötke's group at the Ludwig-Maximilians University in Munich (Table 2.1). It was found that the diazides used in the research are relatively stable, as shown by impact and friction sensitivities and decomposition temperatures. Purines and their derivatives with N(9) alkyl substituents showed good stability, and their decomposition by impact or friction is practically impossible. Pyrimidines without alkyl substituents showed increased sensitivity to impact and friction, and it is possible to achieve their decomposition by applying force. However, the friction and shock sensitivities of 2,6-diazidopurine (**83**) (120 N and 1 J), 2,6-diazido-7-deazapurine (**84**) (80 N and 1 J) and 2,4-diazido-8-azaquinazoline (**56**) (40 N and 2 J) are similar to pentaerythritol tetranitrate (PETN) (3 J and 60 N), which is the benchmark for the sensitivity threshold of primary explosives.⁸⁴ So, compounds **83**, **84**, and **56** are categorized as primary explosives, and working with them in large quantities is dangerous.

Physical and Energetic Parameters of Fused Diazidopyrimidines

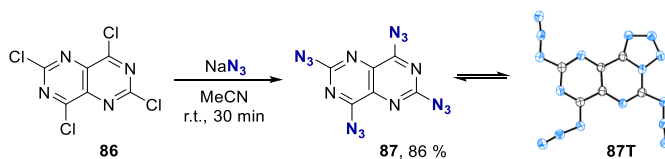


Compound	N balance (%)	Friction sensitivity (N)	Impact sensitivity (J)	ESD ^a (mJ)	m.p. (°C)	T _{dec.} ^b
35a	51	> 360	20	> 480	58	159
56	59	40	2	> 480	171	175
82	53	288	2	> 480	126	172
83	69	120	<1	> 480	decomposes	166
84	63	80	< 1	> 480	decomposes	168
85	49	> 360	20	> 480	85	155
PETN ⁸⁵	18	60	3	60	143	179

a – electrostatic discharge sensitivity; b – decomposition temperature.

Further, the idea of introducing several azide functional groups into a pyrimidine derivative was developed to give it explosive properties. Polyazidation of annulated dipyrimidine – pyrimido[5,4-*d*]pyrimidine was considered, from which the binary compound C₆N₁₆ would be obtained by introducing four azide functional groups. This binary compound would resemble 1,3,5-triazidotriazine but with properties that triazidotriazine lacks – a higher heat of sublimation and better thermal stability.⁸⁶

From the commercially available 2,4,6,8-tetrachloropyrimido[5,4-*d*]pyrimidine in an S_NAr reaction with NaN₃, tetraazide **87** was obtained (Scheme 33). Single-crystal X-ray analysis revealed a crystal structure with one tetrazole fragment, indicating the preference of this tautomer in the solid state.



Scheme 33. Synthesis of 2,4,6,8-tetraazidopyrimido[5,4-*d*]pyrimidine **87**.

In collaboration with Professor Klapötke's group the physical properties were determined and detonation performance for this compound was calculated (Table 2.2). The tetraazide **87** turned out to be extremely sensitive to physical force. It exhibits an impact sensitivity of < 1 J and friction sensitivity of < 1 N, which is equivalent to a commercially used primary

explosive – $\text{Pb}(\text{N}_3)_2$. Differential thermal analysis showed no melting point but only a rapid exothermic decomposition at 155 °C. The tetraazide **87** decomposed by a flash in the hot plate test, and a detonation occurred in the hot needle test. In this test, detonation is a positive indicator of the potential of a primary explosive. However, two runs of secondary explosive initiation tests of PETN with tetraazide **87** were unsuccessful so far.

The explosion performance of the tetraazide **87** was calculated using the EXPLO5 software. The tetraazide has a detonation front pressure of 20.8 GPa and a detonation speed of 7477 m/s. Hence, the detonation parameters of tetraazide **87** are comparable to other binary compounds: 1,3,5-triazidotriazine (TAT) and 3,6-bis-(2-(4,6-diazo-1,3,5-triazin-2-yl)-diazenyl)-1,2,4,5-tetrazine (BDTDI) (Table 2.2). However, compared to primary explosive – $\text{Pb}(\text{N}_3)_2$, the tetraazide **87** has lower detonation pressure, which explains the lack of performance in the secondary explosive initiation test.

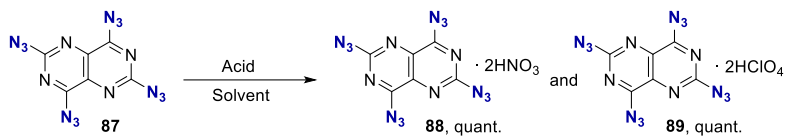
Table 2.2

Physical and Energetic Parameters of 2,4,6,8-tetraazidopyrimido[5,4-*d*]pyrimidine (**87**) and other Binary Compounds and $\text{Pb}(\text{N}_3)_2$

Measured values	87	TAT ⁷⁸	BDTDI ²³	$\text{Pb}(\text{N}_3)_2$
Impact sensitivity (J)	< 1	1.5	5	2.5–4
Friction sensitivity (N)	1	< 5	29	0.1–1
Electrostatic discharge sensitivity (mJ)	13	360	174	<5
ρ (g/cm ³)	1.703 ^a	1.707	1.763	4.8
<i>N</i> balance (%)	75.7	82.4	79.13	28.9
Ω (%) ^b	–64.8	–47.0	–55.7	–11.0
T_{melting} (°C)	decomposes	94	decomposes	190
$T_{\text{decomposition}}$ (°C)	155	187	189	315
Calculated values^d				
$\Delta H_{\text{formation}}$ (kJ/kg)	5095	5159	6130	1546
$T_{\text{detonation}}$ (K)	3787	3536	4740	3401
P_{CJ} (GPa) ^c	20.8	22.6	29.4	33.8
$V_{\text{detonation}}$ (m/s)	7477	7866	8602	5920

a – from X-ray diffraction analysis recalculated to 298 K using $\rho_{298} = \rho T / (1 + \alpha_V(298 - T))$ equation, where $\alpha_V = 0.00015$ and T = crystal analysis temperature; b – oxygen balance with respect to CO_2 ($\Omega_{\text{CO}_2} = (n\text{O} - 2x\text{C} - y\text{H}/2)(1600/\text{FW})$); c – detonation pressure at the Chapman–Jouguet point; d – calculated using Gaussian16 and EXPLO5 (V7.01.01).

Later, the focus was on synthesizing tetraazide salts with oxidizing acids (Scheme 34). It is well known that salt formation significantly improves the physical/thermal stability, and oxidizing acids increase the oxygen balance and detonation performance.^{74, 87, 88} The synthesized nitrate **88** and perchlorate **89** salts showed significantly better results in physical stability tests (1 → 2 J impact sensitivity and 1 → 40 N friction sensitivity). However, the secondary explosive initiation tests using the tetraazide perchlorate (**89**) detonator have been unsuccessful.



Scheme 34. Synthesis of tetraazide salts **88** and **89**.

After numerous attempts of tetraazide salt **88** and **89** crystallizations, a suitable monocystal was obtained for XRD analysis from a trifluoroacetic acid solution. Unfortunately, it crystallized not as a salt but as a trifluoroacetic acid solvate with a water molecule bridge (Fig. 8).

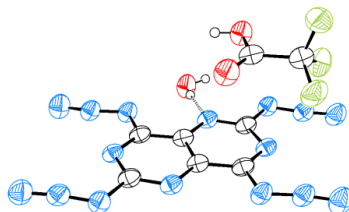
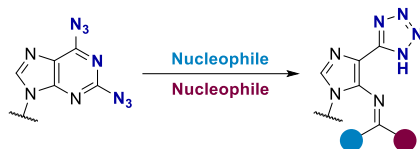


Fig. 8. X-ray molecular structure of tetraazide **87** trifluoroacetic acid and water solvate.

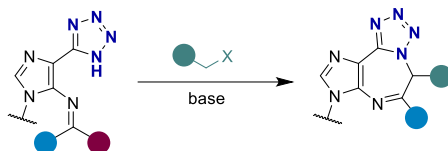
For a more detailed description of the research in this chapter, see the original publication in Appendix 5 and unpublished results in Appendixes 6 and 7.

CONCLUSIONS

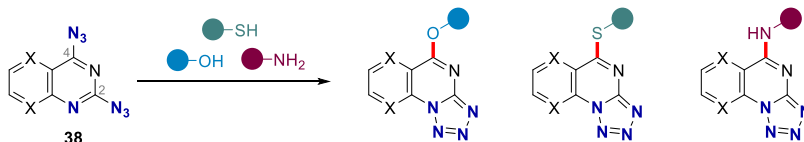
1. Nucleophilic aromatic substitution in 2,6-diazidopurines can be done regioselectively at the C(2) position due to azide-tetrazole equilibrium. Subsequent nucleophile addition to these systems occurs again at the C(2) position, forming a Meisenheimer complex intermediate, following a purine ring-opening. This new synthetic method gives access to tetrazolylimidazoles with a highly functionalized side chain.



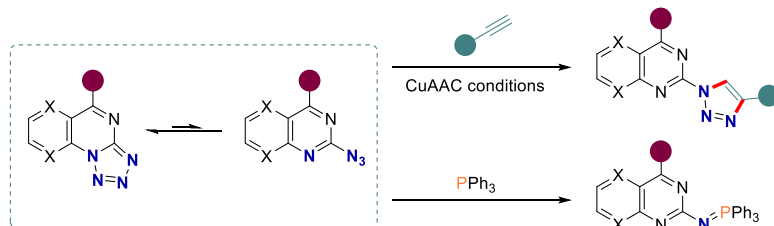
2. Cyclization of tetrazolylimidazoles obtained from purine ring-opening yield tricyclic imidazo[4,5-f]tetrazolo[1,5-d][1,4]diazepines, formally expanding the purine pyrimidine ring by one carbon atom.



3. Nucleophilic aromatic substitution in 2,4-diazidopyridopyrimidines takes place at the C(4) position. The developed synthetic methods for obtaining C-5 substituted tetrazolopyridopyrimidines are more efficient than conventional synthetic strategies.



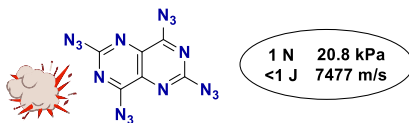
4. The resulting C-5 substituted tetrazolopyridopyrimidines exist mainly in tetrazole tautomeric form in solutions. Still, they are readily functionalized in CuAAC and Staudinger reactions as azides due to the present azide-tetrazole tautomeric equilibrium.



5. The electron-withdrawing properties of the tetrazole functional group promote S_NAr reactions in the fused pyrimidine systems, and substitution reactions proceed faster than in alternatively substituted pyrimidine analogs.



6. 2,4,6,8-Tetraazidopyrimido[5,4-*d*]pyrimidine (C₆N₁₆) is a new binary energetic compound. It is highly sensitive to friction and impact and decomposes by detonation. This structural design has great future potential in energetic materials research and development due to its high nitrogen content, good functionalization capabilities, and availability.



LITERATŪRAS SARAKSTS / REFERENCES

- (1) Mohana Roopan, S.; Sompalle, R. *Synth. Commun.* **2016**, *46*, 645–672.
- (2) De Coen, L. M.; Heugebaert, T. S. A.; García, D.; Stevens, C. V. *Chem. Rev.* **2016**, *116*, 80–139.
- (3) Voight, E. A.; Greszler, S. N.; Kym, P. R. *ACS Med. Chem. Lett.* **2021**, *12*, 1365–1373.
- (4) Li, P.; Xiang, Y.; Gong, S.; Lee, W.-K.; Huang, Y.-H.; Wang, C.-Y.; Yang, C.; Wu, C.-C. *J. Mater. Chem. C* **2021**, *9*, 12633–12641.
- (5) Sebris, A.; Novosjolova, I.; Traskovskis, K.; Kokars, V.; Tetervenoka, N.; Vembris, A.; Turks, M. *ACS Omega* **2022**, *7*, 5242–5253.
- (6) Li, B.; Li, Z.; Guo, F.; Song, J.; Jiang, X.; Wang, Y.; Gao, S.; Wang, J.; Pang, X.; Zhao, L.; Zhang, Y. *ACS Appl. Mater. Interfaces* **2020**, *12*, 14233–14243.
- (7) Seregin, I. V.; Gevorgyan, V. *Chem. Soc. Rev.* **2007**, *36*, 1173.
- (8) Campeau, L.-C.; Hazari, N. *Organometallics* **2019**, *38*, 3–35.
- (9) Zhao, B.; Prabagar, B.; Shi, Z. *Chem* **2021**, *7*, 2585–2634.
- (10) Bunnett, J. F.; Zahler, R. E. *Chem. Rev.* **1951**, *49*, 273–412.
- (11) Kriķis, K.-Ē.; Novosjolova, I.; Mishnev, A.; Turks, M. *Beilstein J. Org. Chem.* **2021**, *17*, 193–202.
- (12) Bucevicius, J.; Turks, M.; Tumkevicius, S. *Synlett* **2018**, *29*, 525–529.
- (13) De Vargas, E. B.; De Rossi, R. H. *J. Org. Chem.* **1984**, *49*, 3978–3983.
- (14) Jeminejs, A.; Goliškina, S. M.; Novosjolova, I.; Stepanovs, D.; Bizdēna, Ē.; Turks, M. *Synthesis* **2021**, *53*, 1543–1556.
- (15) Sirakanyan, S. N.; Spinelli, D.; Geronikaki, A.; Hovakimyan, A. A.; Noravyan, A. S. *Tetrahedron* **2014**, *70*, 8648–8656.
- (16) Bräse Stefan, K. B. *Organic Azides: Syntheses and Applications*; John Wiley & Sons, 2009.
- (17) Scriven, E. F. V.; Turnbull, K. *Chem. Rev.* **1988**, *88*, 297–368.
- (18) Song, X.-R.; Qiu, Y.-F.; Liu, X.-Y.; Liang, Y.-M. *Org. Biomol. Chem.* **2016**, *14*, 11317–11331.
- (19) Bräse, S.; Gil, C.; Knepper, K.; Zimmermann, V. *Angew. Chem., Int. Ed.* **2005**, *44*, 5188–5240.
- (20) Keicher, T.; Löbbecke, S. Lab-Scale Synthesis of Azido Compounds: Safety Measures and Analysis. *Organic Azides*; John Wiley & Sons, 2009; pp. 1–27.
- (21) Tang, Y.; Shreeve, J. M. *Chem. Eur. Journal.* **2015**, *21*, 7285–7291.
- (22) Agrawal, J. P.; Hodgson, R. D. *Organic Chemistry of Explosives*; John Wiley & Sons, 2006.
- (23) Chen, D.; Yang, H.; Yi, Z.; Xiong, H.; Zhang, L.; Zhu, S.; Cheng, G. *Angew. Chem., Int. Ed.* **2018**, *57*, 2081–2084.
- (24) Benz, M.; Klapötke, T. M.; Stierstorfer, J.; Voggenreiter, M. *J. Am. Chem. Soc.* **2022**, *144*, 6143–6147.
- (25) Zhang, H.; Cai, J.; Li, Z.; Lai, Q.; Yin, P.; Pang, S. *ACS Appl. Mater. Interfaces* **2024**, *16*, 4628–4636.

- (26) Huynh, M. H. V.; Hiskey, M. A.; Meyer, T. J.; Wetzler, M. *Proc. Natl. Acad. Sci.* **2006**, *103*, 5409–5412.
- (27) Tariq, Q.; Manzoor, S.; Tariq, M.; Cao, W.; Dong, W.; Arshad, F.; Zhang, J. *ChemistrySelect* **2022**, *7*, e202200017.
- (28) Tišler, M. *Synthesis* **1973**, *3*, 123–136.
- (29) Ostrovskii, V. A.; Popova, E. A.; Trifonov, R. E. Developments in Tetrazole Chemistry (2009–16). *Advances in Heterocyclic Chemistry*; Academic Press, 2017; 1–62.
- (30) Guillou, S.; Jacob, G.; Terrier, F.; Goumont, R. *Tetrahedron* **2009**, *65*, 8891–8895.
- (31) Cmoch, P.; Korczak, H.; Stefaniak, L.; Webb, G. A. *J. Phys. Org. Chem.* **1999**, *12*, 470–478.
- (32) Thomann, A.; Zapp, J.; Hutter, M.; Empting, M.; Hartmann, R. W. *Org. Biomol. Chem.* **2015**, *13*, 10620–10630.
- (33) McEwan, W. S.; Rigg, M. W. *J. Am. Chem. Soc.* **1951**, *73*, 4725–4727.
- (34) Elpern, B.; Nachod, F. C. *J. Am. Chem. Soc.* **1950**, *72*, 3379–3382.
- (35) Boyer, J. H.; Miller, E. J. *J. Am. Chem. Soc.* **1959**, *81*, 4671–4673.
- (36) Temple, C.; McKee, R. L.; Montgomery, J. A. *J. Org. Chem.* **1965**, *30*, 829–834.
- (37) Temple, C.; Montgomery, J. A. *J. Org. Chem.* **1965**, *30*, 826–829.
- (38) Nazarova, A. A.; Sedenkova, K. N.; Vasilenko, D. A.; Grishin, Y. K.; Kuznetsova, T. S.; Averina, E. B. *Mendeleev Commun.* **2020**, *30*, 714–716.
- (39) Novosjolova, I.; Bizdēna, Ē.; Turks, M. *Tetrahedron Lett.* **2013**, *54*, 6557–6561.
- (40) Bucevicius, J.; Turks, M.; Tumkevicius, S. *Synlett* **2018**, *29*, 525–529.
- (41) Sebris, A.; Turks, M. *Chem. Heterocycl. Compd.* **2019**, *55*, 1041–1043.
- (42) Nikolaenkova, E. B.; Aleksandrova, N. V.; Mamatyuk, V. I.; Krivopalov, V. P. *Rus. Chem. Bull.* **2018**, *67*, 893–901.
- (43) Temple, C.; Kussner, C. L.; Montgomery, J. A. *J. Org. Chem.* **1966**, *31*, 2210–2215.
- (44) Wentrup, C. *Tetrahedron* **1970**, *26*, 4969–4983.
- (45) Boyer, J.; Hyde, H. *J. Org. Chem.* **1960**, *25*, 458–459.
- (46) Temple, C.; Thorpe, M. C.; Coburn, W. C.; Montgomery, J. A. *J. Org. Chem.* **1966**, *31*, 935–938.
- (47) Temple, Carroll.; Montgomery, J. A. *J. Am. Chem. Soc.* **1964**, *86*, 2946–2948.
- (48) Cmoch, P.; Wiench, J. W.; Stefaniak, L.; Webb, G. A. *J. Mol. Struct.* **1999**, *510*, 165–178.
- (49) Sirakanyan, S. N.; Spinelli, D.; Geronikaki, A.; Kartsev, V. G.; Panosyan, H. A.; Ayvazyan, A. G.; Tamazyan, R. A.; Frenna, V.; Hovakimyan, A. A. *Tetrahedron* **2016**, *72*, 1919–1927.
- (50) Bain, A. D. *Prog. Nucl. Magn. Reson. Spectrosc.* **2003**, *43*, 63–103.
- (51) Aleksandrova, N. V.; Nikolaenkova, E. B.; Gatilov, Yu. V.; Polovyanenko, D. N.; Mamatyuk, V. I.; Krivopalov, V. P. *Rus. Chem. Bull.* **2022**, *71*, 1266–1272.
- (52) Kochetkov, N. K.; Budovskii, E. I. Reactions Involving the Cleavage or Rearrangement of Heterocyclic Rings of Nucleic Acid Bases and Their Derivatives. *Organic Chemistry of Nucleic Acids*; Springer, 1972; 381–423.

- (53) Guinan, M.; Benckendorff, C.; Smith, M.; Miller, G. J. *Molecules* **2020**, *25*, 2050.
- (54) Seley-Radtke, K. L.; Yates, M. K. *Antiviral Res.* **2018**, *154*, 66–86.
- (55) Van der Plas, H. C. S_N (ANRORC) Reactions in Azines, Containing an “Outside” Leaving Group. *Advances in Heterocyclic Chemistry*; Academic Press, 1999; 9–86.
- (56) Van der Plas, H. C. S_N (ANRORC) Reactions in Azaheterocycles Containing an “Inside” Leaving Group. *Advances in Heterocyclic Chemistry*; Academic Press, 1999; 87–151.
- (57) Van der Plas, H. C. Degenerate Ring Transformations Involving Side-Chain Participation. *Advances in Heterocyclic Chemistry*; Academic Press, 1999; 153–221.
- (58) Ashry, E. S. H. E.; Kilany, Y. E.; Rashed, N.; Assafir, H. Dimroth Rearrangement: Translocation of Heteroatoms in Heterocyclic Rings and Its Role in Ring Transformations of Heterocycles. *Advances in Heterocyclic Chemistry*; Academic Press, 1999; 79–165.
- (59) Novosjolova, I.; Bizdēna, Ē.; Turks, M. *Phosphorus Sulfur Silicon Relat. Elem.* **2015**, *190*, 1236–1241.
- (60) Šišūļins, A.; Bucevičius, J.; Tseng, Y.-T.; Novosjolova, I.; Traskovskis, K.; Bizdēna, Ē.; Chang, H.-T.; Tumkevičius, S.; Turks, M. *Beilstein J. Org. Chem.* **2019**, *15*, 474–489.
- (61) Ozols, K. Nukleofilās heteroaromātiskās aizvietošanas pētījumi purīna ciklā. *Maģistra darbs*. RTU: Rīga 2017.
- (62) Petrič, A.; Tišler, M.; Stanovnik, B. *Monatsh. Chem.* **1983**, *114*, 615–624.
- (63) Petrič, A.; Tišler, M.; Stanovnik, B. *Monatsh. Chem.* **1985**, *116*, 1309–1319.
- (64) Kwan, E. E.; Zeng, Y.; Besser, H. A.; Jacobsen, E. N. *Nat. Chem.* **2018**, *10*, 917–923.
- (65) Neumann, C. N.; Hooker, J. M.; Ritter, T. *Nature* **2016**, *534*, 369–373.
- (66) Rohrbach, S.; Smith, A. J.; Pang, J. H.; Poole, D. L.; Tuttle, T.; Chiba, S.; Murphy, J. A. *Angew. Chem., Int. Ed.* **2019**, *58*, 16368–16388.
- (67) Jeminejs, A.; Novosjolova, I.; Bizdēna, Ē.; Turks, M. *Org. Biomol. Chem.* **2021**, *19*, 7706–7723.
- (68) Manzoor, S.; Yang, J.; Tariq, Q.; Mei, H.; Yang, Z.; Hu, Y.; Cao, W.; Sinditskii, V. P.; Zhang, J. *ChemistrySelect* **2020**, *5*, 5414–5421.
- (69) Ozols, K.; Cīrule, D.; Novosjolova, I.; Stepanovs, D.; Liepinsh, E.; Bizdēna, Ē.; Turks, M. *Tetrahedron Lett.* **2016**, *57*, 1174–1178.
- (70) Weitkamp, R. F.; Neumann, B.; Stammler, H.; Hoge, B. *Chem. Eur. J.* **2021**, *27*, 10807–10825.
- (71) Saame, J.; Rodima, T.; Tshepelevitsh, S.; Kütt, A.; Kaljurand, I.; Haljasorg, T.; Koppel, I. A.; Leito, I. *J. Org. Chem.* **2016**, *81*, 7349–7361.
- (72) Boyomi, S. M.; Ismaiel, A.-K. M.; Eisa, H. M.; El-Kerdawy, M. M. *Arch. Pharm. Res.* **1989**, *12*, 8–11.
- (73) Agrawal, J. P.; Hodgson, R. D. *Organic Chemistry of Explosives*; John Wiley & Sons, 2006.
- (74) Gao, H.; Shreeve, J. M. *Chem. Rev.* **2011**, *111*, 7377–7436.
- (75) Xue, H.; Gao, Y.; Twamley, B.; Shreeve, J. M. *Chem. Mater.* **2005**, *17*, 191–198.
- (76) Parisi, E.; Landi, A.; Fusco, S.; Manfredi, C.; Peluso, A.; Wahler, S.; Klapötke, T. M.; Centore, R. *Inorg. Chem.* **2021**, *60*, 16213–16222.
- (77) Borden, W. T. *J. Phys. Chem. A* **2017**, *121*, 1140–1144.

- (78) Huynh, M. H. V.; Hiskey, M. A.; Hartline, E. L.; Montoya, D. P.; Gilardi, R. *Angew. Chem., Int. Ed.* **2004**, *43*, 4924–4928.
- (79) Huynh, M. H. V.; Hiskey, M. A.; Chavez, D. E.; Naud, D. L.; Gilardi, R. D. *J. Am. Chem. Soc.* **2005**, *127*, 12537–12543.
- (80) Klapötke, T. M.; Martin, F. A.; Stierstorfer, J. *Angew. Chem., Int. Ed.* **2011**, *50*, 4227–4229.
- (81) Miller, D. R.; Swenson, D. C.; Gillan, E. G. *J. Am. Chem. Soc.* **2004**, *126*, 5372–5373.
- (82) Herweyer, D.; Brusso, J. L.; Murugesu, M. *New J. Chem.* **2021**, *45*, 10150–10159.
- (83) Badgular, D. M.; Talawar, M. B.; Asthana, S. N.; Mahulikar, P. P. *J. Hazard. Mater.* **2008**, *151*, 289–305.
- (84) Klapötke, T. M. *Chemistry of High-Energy Materials*; De Gruyter, 2022.
- (85) Klapötke, T. M. *Energetic Materials Encyclopedia*; De Gruyter, 2018.
- (86) Korsunskiy, B. L.; Nedel'ko, V. V.; Zakharov, V. V.; Chukanov, N. V.; Chervonnyi, A. D.; Larikova, T. S.; Chapyshev, S. V. *Propellants, Explos., Pyrotech.* **2017**, *42*, 123–125.
- (87) Gálvez-Ruiz, J. C.; Holl, G.; Karaghiosoff, K.; Klapötke, T. M.; Löhnwitz, K.; Mayer, P.; Nöth, H.; Polborn, K.; Rohbogner, C. J.; Suter, M.; Weigand, J. J. *Inorg. Chem.* **2005**, *44*, 4237–4253.
- (88) Klapötke, T. M.; Miró Sabaté, C. *Eur. J. Inorg. Chem.* **2008**, *2008*, 5350–5366.

Pielikumi / Appendices

Leškovskis, K.; Zaķis, J.; Novosjolova, I.; Turks, M.

**Applications of Purine Ring Opening in the Synthesis of Imidazole,
Pyrimidine, and New Purine Derivatives**

Eur. J. Org. Chem. **2021**, 2021, 5027-5052

doi:10.1002/ejoc.202100755

Pārpublicēts ar *John Wiley and Sons* atļauju.

Copyright © 2024 Copyright Clearance Center, Inc. All Rights Reserved.

Reprinted with the permission from John Wiley and Sons.

Copyright © 2024 Copyright Clearance Center, Inc. All Rights Reserved.

Applications of Purine Ring Opening in the Synthesis of Imidazole, Pyrimidine, and New Purine Derivatives

Kristaps Leškovskis,^[a] Jānis Miķelis Zaķis,^[a] Irina Novosjolova,^{*,[a]} and Māris Turks^{*,[a]}

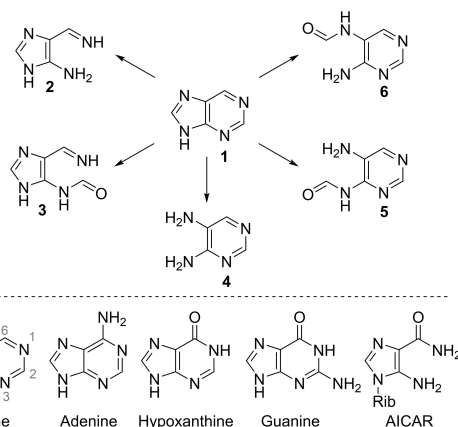
Purines, which are regarded as relatively stable heterocyclic systems, can be opened at both pyrimidine and imidazole rings. Purine ring opening also serves as a tool for the preparation of ring-modified purines through rearrangement/recyclization mechanisms. The obtained imidazole, pyrimidine, and purine derivatives are privileged molecular scaffolds in medicinal and agricultural chemistry. Purine ring-opening approach is a useful alternative for their synthesis, which competes well with *de*

novo approach or modification of a conserved heterocyclic core. The substitution patterns and groups that activate purines towards ring opening are reviewed. Moreover, mechanistic studies using labelled substrates, which are leading to rearranged purine derivatives are covered. Furthermore, an insight into imidazole ring opening upon exposure of purine system to DNA damaging agents is provided.

1. Introduction

Purine and its derived nucleobases – adenine and guanine are ubiquitous scaffolds in biological chemistry. A great number of purine derivatives have been developed as antivirals,^[1] drugs against autoimmune diseases,^[2] and anti-cancer^[3] agents. Hence, modifications of substituents and the purine ring system itself are continuously explored in order to discover different isosteres with improved activity.^[4–8] Imidazoles, pyrimidines, and their fused analogues are recognized as ring-opened purine isosteres with broad applications in modern medicinal chemistry.^[9–12] Purine ring opening with hydroxide is a simple method that provides access to substituted imidazoles and pyrimidines. The first exploration of this chemistry was performed in the late 1950s and 1960s, and was reviewed by Kochetkov in 1972.^[13] The discovery of 5-aminoimidazole-4-carboxamide-1- β -D-ribofuranoside (AICAR) also known as Adenosine, and its simple synthesis from inosine *via* pyrimidine ring opening in the 1990s gave the title transformations a second breath. Furthermore, ring-opened products of purines have been demonstrated as useful intermediates for the synthesis of variously substituted and/or fused purine analogs *via* recyclization. Recently, the synthesis of homopurine alkaloids mainly by diazepine ring construction from 5-aminoimidazole-4-carboxamide (AICA) derivatives was reviewed.^[14]

In this review, we will focus on imidazole and pyrimidine synthesis from purines *via* ring opening and the applications of such ring-opened products over the past half century (from 1970 to 2020) (Scheme 1).



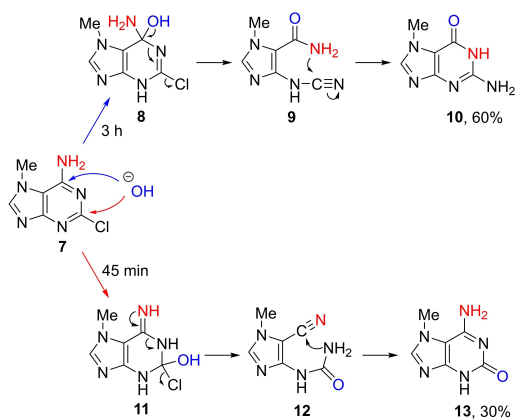
Scheme 1. Purine ring opening pathways.

2. Ring opening of the pyrimidine moiety in purines

Most of the pyrimidine ring opening reactions of purines are mediated by nucleophile addition to the electrophilic C-2 position of purine. Often, the C-2 carbon of ring opening product is subsequently eliminated by a second nucleophile attack, producing imidazoles. Ring opening can be forced with strong nucleophiles, whereas the introduction of an EWG in ring system facilitates the ring opening by making the C-2 site more electrophilic.

The first reported example of a purine ring opening reaction was the reaction of 2-chloro-7-methyladenine **7** with hydroxide.^[15] Initially, the expected S_NAr product **13** was not observed, and only its regioisomer **10** was formed (Scheme 2).

[a] K. Leškovskis, J. M. Zaķis, Dr. I. Novosjolova, Prof. Dr. M. Turks
Institute of Technology of Organic Chemistry, Faculty of Materials Science
and Applied Chemistry, Riga Technical University
P. Valdena Str. 3, Riga LV-1048, Latvia
E-mail: irina.novosjolova@rtu.lv
maris.turks@rtu.lv
https://www.rtu.lv/lv/mlkf



Scheme 2. Pyrimidine ring opening-closing sequence in adenine derivatives.

The formation of **10** was explained through a reaction sequence involving pyrimidine ring opening and subsequent closure, although the proposed intermediate **9** has never been isolated. In a separate investigation analyzing the same reaction before its completion, a new intermediate – nitrile **12** was isolated.^[3] Part of the starting material was transformed along this pathway, resulting in product **13**, which was generated through

a nucleophilic displacement $S_N(\text{ANRORC})$ mechanism instead of the initially expected $S_N\text{Ar}$ type mechanism.

In another experiment, cyanoimidazoles **16a–b** were isolated by Gundersen's group upon lithiation of 2-amino-6-chloropurine **14**.^[17] Deprotonation of aminopurine with 5 equivalents of LDA gave the dilithiated intermediate **15** that underwent ring opening to (4-cyanoimidazol-5-yl)cyanamides **16a–b** in high yields. As a proof of concept, when leaving group at C-6 was absent or the C-2 amine functionality was protected, only C-8 substitution took place (Scheme 3).

In a classic $S_N\text{Ar}$ reaction, a nucleophile attacks the carbon atom that bears the leaving group, and very often a Meisenheimer intermediate is formed. In the $S_N(\text{ANRORC})$ mechanism, the nucleophile attack occurs across the heterocyclic system – at the *ortho*-position relative to the leaving group. $S_N(\text{ANRORC})$ reactions can be represented by a nucleophile (NH_3) addition to pyrimidine **17** and the subsequent expulsion of leaving group, initially forming the ring-opened intermediate **18**. Then the ring closure *via* amine addition to cyano group takes place and product **19** is formed (Scheme 4). If a strong EWG is present at the pyrimidine nitrogen atom (**22**), the nitrogen itself becomes an inner leaving group upon the addition of a nucleophile at the *ortho*-position, followed by a ring opening to the intermediate **24** and subsequent ring closure to pyrimidine (**25**). The $S_N(\text{ANRORC})$ reaction is applicable to almost any nitrogen heterocycle and has been thoroughly reviewed by van der Plas^[18–20] and Ashry.^[21]

If nitrogen nucleophiles are used, the $S_N(\text{ANRORC})$ mechanism can be combined with the Dimroth rearrangement,^[13,22] in



Kristaps Leškovskis was born in 1995 and graduated from Riga Technical University (RTU), Latvia in 2020 with Master's degree in Chemical Technology. His Master's Thesis under supervision of Professor Māris Turks dealt with generation and reactions of carbenium ion intermediates in liquid sulfur dioxide. Mr. Leškovskis currently pursues his PhD studies under supervision of Irina Novosjolova and Māris Turks. His doctoral research project is focused on novel transformations of fused pyrimidines.



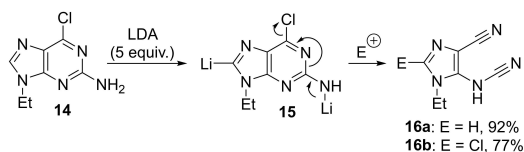
In 2020, Jānis M. Zaķis graduated with distinction from RTU with Master's degree in Chemical Technology. His Master's Thesis under supervision of Professor Irina Novosjolova and Māris Turks dealt with nucleophilic aromatic substitutions in purines and their ring opening reactions. Mr. Zaķis currently pursues his PhD studies as a part of the CHAIR collaboration project lead by Dr. Joanna Wencel-Delord (Strasbourg University, France) and Dr. Tomas Smejkal (Syngenta, Switzerland). His current research now focuses on transition metal catalyzed C–H borylation reactions.



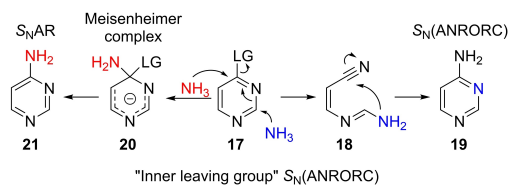
Irina Novosjolova studied Chemical Technology at RTU and obtained her Master's degree with distinction in 2011. In 2015, she obtained her doctoral degree in organic chemistry from RTU under the supervision of Professors Māris Turks and Ērika Bizdēna. Subsequently, Dr. Novosjolova spent two years as Postdoctoral Research Associate at Binghamton University (Binghamton, NY, USA) under the supervision of Professor Ēriks Rozners. Currently she is Senior Researcher and Docent at RTU Faculty of Materials Science and Applied Chemistry and her research interests deal with chemistry and materials science of fused pyrimidines.



In 2005, Māris Turks obtained his doctoral degree from the Swiss Federal Institute of Technology, Lausanne under the guidance of Professor Pierre Vogel. He pursued his postdoctoral research (2006) at Stanford University with Professor Barry M. Trost. In 2007, he accepted an academic position at the RTU Faculty of Materials Science and Applied Chemistry, where he is currently Full Professor. Since 2018, Māris Turks also serves as Dean of the Faculty at RTU. Prof. Turks' research interests involve applications of liquid sulfur dioxide in organic synthesis and chemistry of triterpenoids, functionalized heterocycles, organosilicon compounds, carbohydrates and nucleosides.



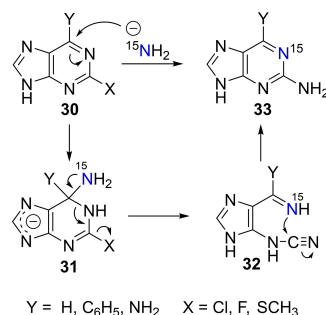
Scheme 3. 2-Amino-6-chloropurine 14 ring opening with LDA.



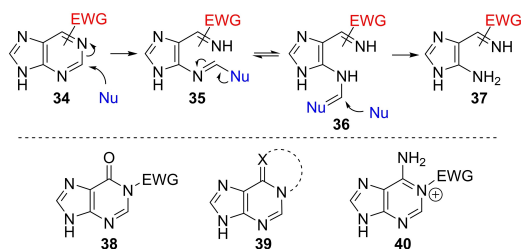
Scheme 4. $S_N(ANRORC)$ and Dimroth rearrangement mechanisms.

which the incoming nucleophile and the initial ring nitrogen have swapped their positions. Following this approach, amide-induced amination mechanisms of purines have also been investigated by numerous groups with ^{15}N isotope labelling to establish the ring opening-closing cascades in purine rearrangements. The aminolysis of 2-halo- or thiopurines with ^{15}N labelled KNH_2/NH_3 led to an incorporation of ^{15}N into the purine ring *N*-1 position, thus proving the $S_N(ANRORC)$ mechanism.^[15,23] However, no ring opening was observed in 6-chloro- and 6-methylthiopurine reactions with ^{15}N labelled KNH_2/NH_3 . The reaction of 2,6-dichloropurine (30: $\text{Y}=\text{X}=\text{Cl}$) with KNH_2/NH_3 at first yielded 6-amino-2-chloropurine (30: $\text{Y}=\text{NH}_2$; $\text{X}=\text{Cl}$) through a regular $S_N\text{Ar}$ process. Next, amide attacked the C-6 position and cleaved the purine ring to 4-iminoimidazol-5-yl-cyanamide (32: $\text{Y}=\text{NH}_2$) which could afterwards cyclize back to 2,6-diaminopurine (33: $\text{Y}=\text{NH}_2$) (Scheme 5).^[15,24]

There are three purine activation mechanisms that will be discussed in the following chapters (Scheme 6). First, hypoxanthines 38 are generally more prone to ring opening due to the presence of a carbonyl group in the ring system. With further EWG introduction at the *N*-1 atom, hypoxanthines could be opened with various nucleophiles at ambient or slightly elevated temperatures. Second, in fused purines 39 the *N*-1 site, being a part of another conjugated system, became a good leaving group. Finally, EWG introduction at the *N*-1 location in purines/adenines 40 made it an excellent leaving group.



Scheme 5. Amination of substituted purines containing leaving group at the C-2 position.



Scheme 6. Pyrimidine ring opening mechanism.

2.1. Ring opening of hypoxanthine derivatives

Since the discovery of AICAR, numerous groups have extensively synthesized AICAR analogues and developed different synthetic procedures for pyrimidine ring opening in purines. AICAR is an AMP-activated protein kinase (AMPK) activator that functions as a metabolic modulator capable of switching off cell anabolism and turning on catabolism, thus supplying energy by increased glucose uptake and fatty acid oxidation.^[25,26] AICAR has been administered in cases of myocardial ischemia,^[27] for the prevention of post-reperfusion infarct^[28] and reperfusion injury after coronary artery by-pass surgery (CABG).^[29] although some studies disprove its effectiveness.^[30] Nevertheless, AICAR has been widely studied for potential applications^[31] against diabetes,^[32] leukemia,^[33] and in the role of an antiviral drug.

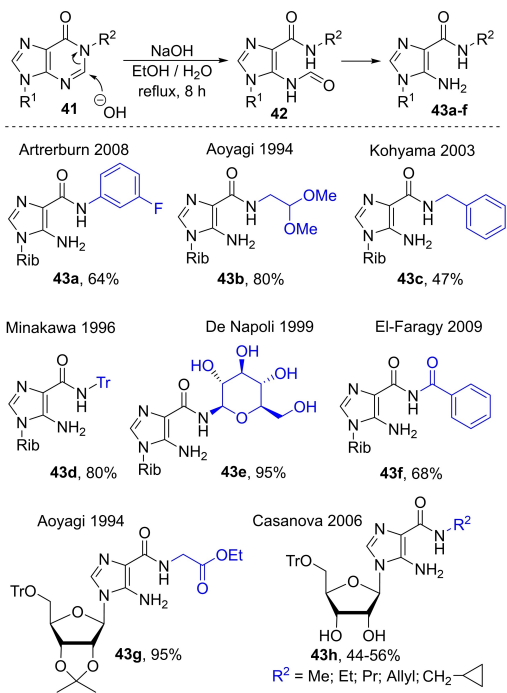
Inosine has been a frequent target of ring opening studies as a readily available AICAR precursor. Inosine is generally more reactive than purine or adenine derivatives due to the carbonyl group making C-2 position more electrophilic. Direct ring opening of purines with hydroxides requires strongly basic media and prolonged reflux. In order to avoid the need for harsh conditions, inosine can be activated by *N*-1 alkylation, thus making the C-2 position more electrophilic and providing a better leaving group. Moreover, ring opening of non-activated purines may also lead to imidazole ring opening (see Chapter 2. Imidazole ring opening).

Thus, hydroxide initiates ring opening by an attack at the C-2 position, breaking the N-1–C-2 bond and generating the formyl adduct **42** (Scheme 7). Since the formyl group is base labile, in most cases it is hydrolyzed to aminoimidazolecarboxamides **43**. Nevertheless, under appropriately mild conditions the formyl intermediates **42** can be isolated. A straightforward

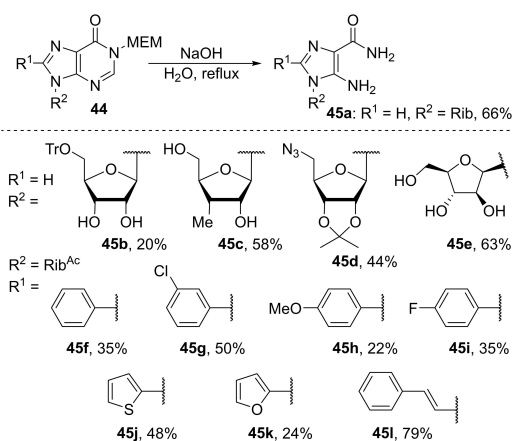
method for ring opening is refluxing of inosine **41** with NaOH in EtOH. Various AICAR analogues **43 a–f** have been obtained in such manner, bearing aryl (**43 a**),^[34] alkyl (**43 b,g,h**),^[35–37] benzyl (**43 c–d**),^[38,39] benzoyl (**43 f**),^[40] and glucosyl (**43 e**)^[41] substituents at the amide nitrogen.

In 2003, Yamamoto found that N-1-alkyloxymethylene substituted inosines **44** also underwent ring opening, but in that case the alkyloxymethylene group was also cleaved under the same conditions as the ring opening occurred (Scheme 8).^[39] Thus, AICAR (**45 a**) can be prepared in good yields from inosine in 4 steps, using MEM as activating group. In the initial step, inosine was O-acylated for selective MEM group introduction and then deacylated with NH₃/MeOH prior to ring opening for better solubility in water. Similarly, the acid labile 5-O-trityl-**45 b**,^[36] 3-deoxy-3-C-methyl-**45 c**,^[42] 5-azido-5-deoxy-2,3-O-isopropylidene-**45 d**,^[43] protected inosines and arabinosyl hypoxanthine (**45 e**)^[44] – could be transformed to AICAR analogues. The Yamamoto group also demonstrated a synthesis of 2-aryl-AICARs **45 f–i**. It is interesting to note that the Suzuki cross-coupling of 8-bromo-N-MEM inosine **44** did not proceed, thus the coupling of 8-bromo-inosine was performed prior to the introduction of N-1-MEM group, followed by ring opening.^[45]

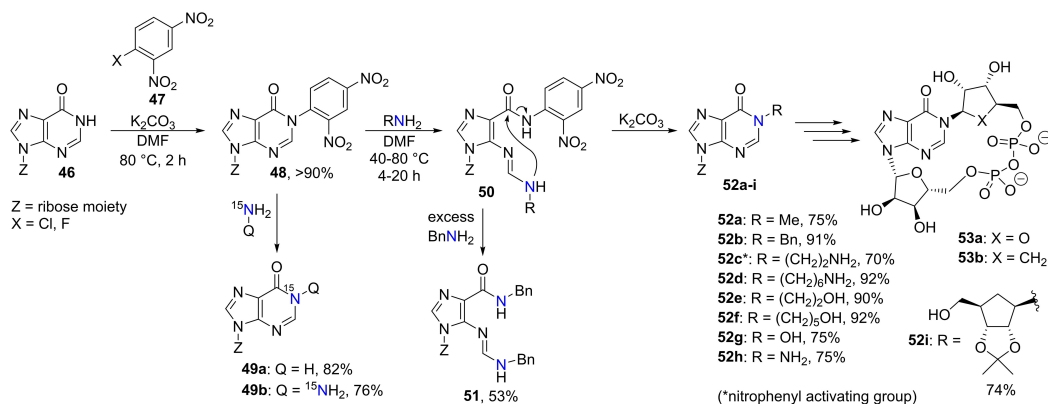
Piccialli's initial studies of inosine (**46**) activation at the C-2 position with electron-withdrawing substituents at N-1 for the synthesis of ¹⁵N-labelled inosines **49 a–b** set a stage not only for isotope labelling, but also for a general approach of N-1 substitution via ANRORC type mechanism (Scheme 9).^[46] ANRORC enables the use of nucleophilic amines for addition of substituents at the N-1 position, with higher yields than alkylation or Dimroth rearrangement. Although initially discovered using the example of 1-(inos-6-yl)-inosine,^[47] the choice of strongly activating nitrophenyl- and 2,4-dinitrophenyl- groups (DNP) is more appealing due to the easy introduction of such groups and the mild reaction conditions. Other strong electron-withdrawing groups, such as nitrophenyl, nitro,^[48] and sulfonyl^[49,50] also facilitated ring opening. First, inosine **46** was activated via arylation with 4-halo nitrobenzenes **47**, for example, the Sanger's reagent in DMF in the presence of a mild base (K₂CO₃). Further, nucleophilic attack at the C-2 atom of derivative **48** promoted ring cleavage to intermediate **50** and the addition of a mild base (K₂CO₃) induced cyclization to new inosine derivatives **52 a–g** with amine incorporated at the N-1 position. In some cases, the addition of a base was not necessary. In this manner, alkylamines, hydroxylamine and hydrazine were added to inosines in good yields.^[51–57] Substitution of DNP group in the intermediate product of ring opening step may occur faster than ring closure if an excess of amine is used, as in the dibenzylamine substituted imidazole **51**.^[48] Substituted inosines **52 a–i** can be further converted to N-substituted AICAR analogues with NaOH (Scheme 7). The method has been demonstrated for the synthesis of cyclic inosine diphosphate riboses **53 a** (cIDPR) and cyclic inosine diphosphate carbocyclic riboses **53 b** (cIDPCr) used as cyclic adenosine diphosphate ribose (cADPR) analogues – Ca²⁺ secondary messengers synthesized in biological systems from NAD⁺ by ADP ribosyl cyclase. Usually, cIDPCRs are obtained by



Scheme 7. Hydroxide mediated pyrimidine ring opening of inosines.



Scheme 8. Hydroxide mediated AICAR synthesis.



Scheme 9. The substitution of inosine *N*-1 position with amines via ANRORC rearrangement.

direct *N*-alkylation of inosine or from AICAR in lengthy syntheses and poor yields.^[58-64]

In order to obtain a product of type **55** by an alkylation method, a stereoinversion at carbosugar **54** should be planned (Scheme 10).

However, the stereocenter of carbocyclic ribosylamine **56** remains unchanged in the S_N (ANRORC) reaction leading to the product **57**.

The example with ethylenediamine in Scheme 9 is particularly interesting due to the possibility of different products forming depending on the *N*-1 substituent. In the case of nitrophenyl group, S_N (ANRORC) type rearrangement gives the *N*-1-(2-aminoethyl) product **52c**. However, in the case of DNP group, selective C-2 and DNP cleavage takes place to yield the AICA derivatives **61** (Scheme 11).^[51] The mechanism can be evidently explained by diamine attack at the C-2 position of hypoxanthine **58**, cyclization of **59** to the tetrahydroimidazole adduct **60**, followed by elimination of dihydroimidazole and DNP to yield the ring opening product **61** (AICA).^[65,66] In such way, DNCB together with EDA provides an easy access to

different AICA derivatives: tris-*O*-TBS **62a**,^[67] 5-deoxy-5-fluoro **62b**,^[68] 5-*O*-TBS-2,3-isopropylidene **62c**,^[69] ¹³C₅ labelled **62d**,^[70] 2-deoxy **62e**^[51] and **62f**,^[71] thio-**62g** and seleno-**62h**^[72] riboside and the open-chain ribose **62i**^[56] analogues from simple inosines.

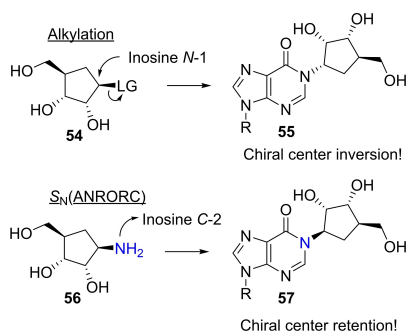
Selective C-2 cleavage can be achieved without removal of dinitrophenyl group from compound **61s** when THF is selected as reaction solvent instead of the commonly used DMF.^[73]

In 2009, a small library of benzyl/thiophenyl-AICA derivatives **61j-r** were synthesized as potential Hsp90 inhibitors. Inosine ring opening with Piccilli's DNP (i) and MEM C-2 (ii) activating methods was used as the key step to obtain AICA scaffold.^[74]

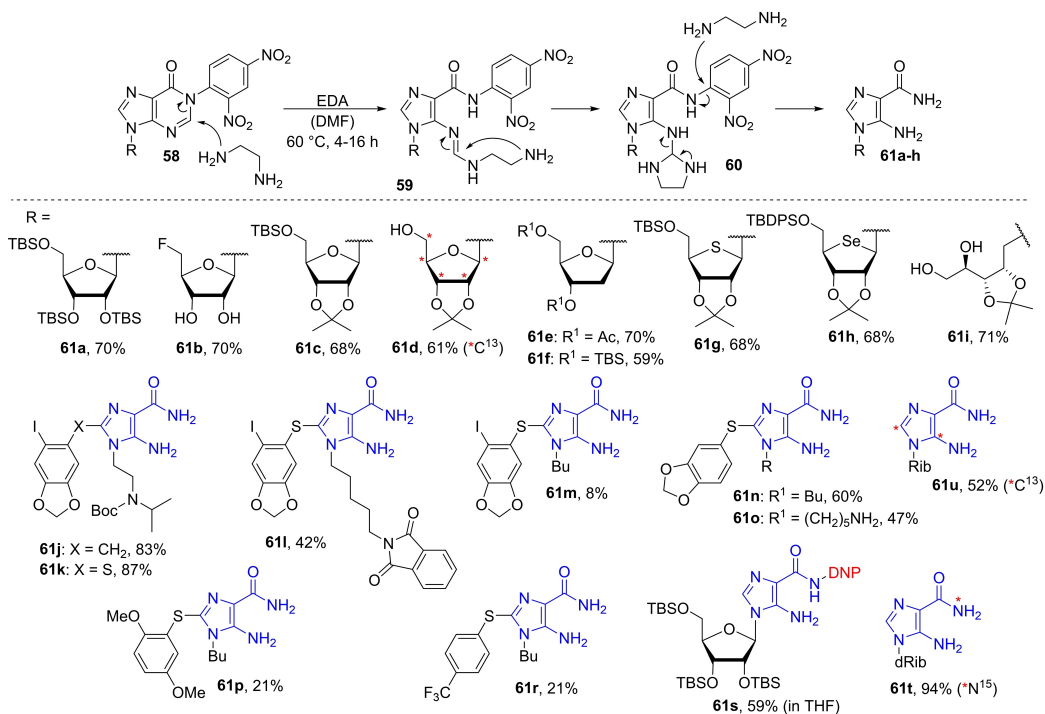
This method originated in 1995 when Piccilli demonstrated ring opening of ¹⁵N-1 labelled inosine **49a** with ethylenediamine to obtain ¹⁵N-labelled AICA **61t**. For simplification and overall cost reduction, the labelled ammonia was generated *in situ* using 1.1 equivalents of ¹⁵NH₄Cl/KOH system.^[46,75] Furthermore, treatment with *N*-acylisothiocyanate gave ¹⁵N-1 labelled 2'-deoxyguanosine in 89% yield.^[46,75]

Kan's group obtained doubly ¹³C-labelled AICAR (**61u**) via S_N (ANRORC), since direct condensation of aminoimidazolecarboxamide with penta-*O*-acetylribose was not selective and gave a mixture of products. In order to overcome this problem, the authors synthesized doubly ¹³C-labelled inosine by glycosylation of labelled hypoxanthine with penta-*O*-acetylribose. Further, S_N Ar with DNCB gave activated DNP inosine and EDA mediated ring opening produced doubly ¹³C-labelled AICAR (**61u**).^[76]

Piccilli's group also designed a solid phase method for the synthesis of AICAR derivatives by selective anchoring of inosine 5'-OH group to solid support. The DNP inosines **62** were bound to monomethoxytrityl chloride (MMTC) linker in the presence of DMAP in pyridine to form **63** in quantitative yields. While EDA mediated ring cleavage, yielding the resin-bound AICAR **66**, various amines could be added to inosine in ANRORC rearrangement to form *N*-1 substituted inosines **64a**. The inosines bound at the 5' position were also suitable for



Scheme 10. The alkylation and S_N (ANRORC) reaction at the *N*-1 position of inosine.



Scheme 11. Hypoxanthine ring opening with ethylenediamine.

modifications of the ribosyl 2' and 3'-OH groups, for example, through periodate-induced oxidative cleavage of C-2'-C-3' bond in **64a**, followed by reduction with NaBH_4 to diol, which led to the open-chain ribosyl analogues **64b**. Refluxing of N-1 substituted inosines in alcoholic NaOH solution formed the AICAR analogues **67a-b**. The treatment of solid supports with 2% TFA in DCM yielded inosines **65g-h**, as well as AICAR and its derivatives **68a-b** in excellent yields after simple workup (Scheme 12).^[54,77-80]

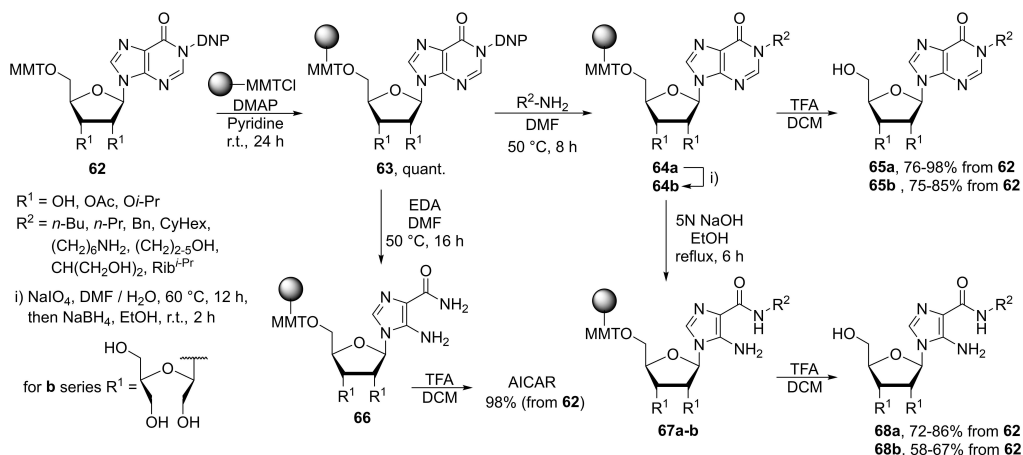
Another ring opening method for substrates on solid support involves anchoring of ribose through a 2',3'-O-*p*-hydroxybenzylidene motif to MMT linker. 5'-O-TBDPS protected inosine (**73**) was first condensed with *p*-hydroxymethylbenzaldehyde dimethylacetal and bound to solid support via a MMTCl linker to form the key intermediate **70**. The 2',3'-bound inosines were suitable for modifications at the 5'-position of the ribosyl group. In this case, phosphorylation with phosphoramidite and the subsequent introduction of DNP group formed the inosine monophosphates **71**. Similarly to the previous example, the treatment of **71** with EDA led to pyrimidine ring opening, while the other amines added to the N-1 position via ANRORC rearrangement, forming **72**. The latter inosine derivatives were opened by refluxing in alcoholic NaOH solution. Finally, all acid-labile groups: MMT, acetal, TMS, and cyanoethyl were cleaved with 2% TFA in DCM, providing inosine **73** and AICAR mono-

phosphate (ZMP) analogues **74** in good yields (Scheme 13).^[65,79,81,82]

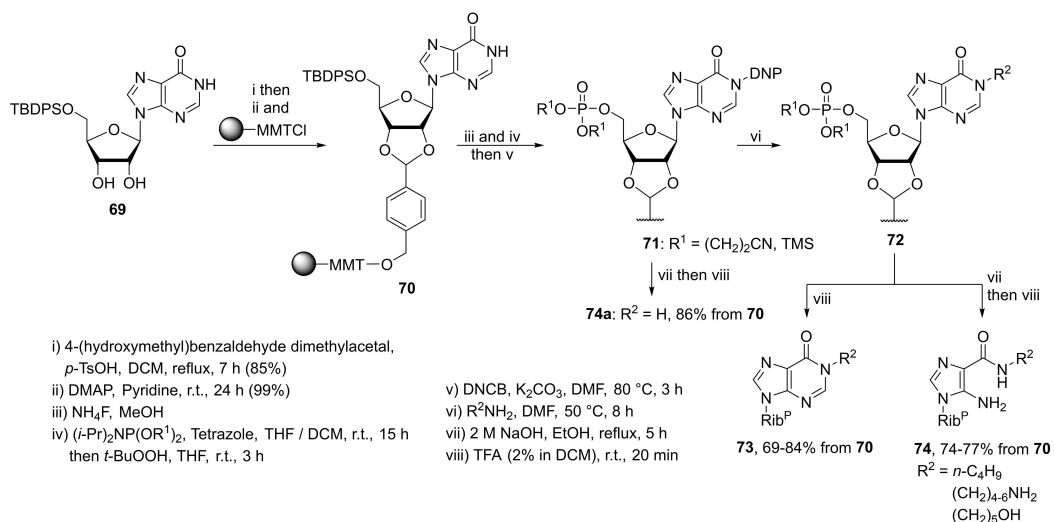
Various sulfonyl substituents (Ms, Tf, Ts, Ns, *p*Ns, DNs, pentafluorobenzenesulfonyl, mesitylenesulfonyl) have been investigated as potential EWG for N-1 substitution in S_N1 (ANRORC) by Ariza.^[50] The formation of adenosine **78** was observed when 2,4-dinitrobenzenesulfonyl group (DNs) was used. With ^{15}N and ^{18}O labelling, the authors presented a plausible reaction mechanism. After the initial ring opening induced by amine nucleophile, the amide oxygen attacked the *ipso* position of DNs and **77** was formed with a release of SO_2 . NMR analysis of **75** confirmed the selectivity of sulfonylation at the N-1 atom, with no rearrangement occurring prior to ring opening. Then, similarly to previous ANRORC reactions, the amine added to carboximidate, thus closing the pyrimidine ring to yield the adenosine **78** along with an equimolar amount of ^{18}O -labelled dinitrophenol (**79**) (Scheme 14).^[83]

2.2. Ring opening of fused purines

Fused [1,6]-purine adducts **80** often possess fluorescent properties and some of them can enter biological pathways. These fused purines are generally stable, although pyrimidine ring can open under the aforementioned ring opening conditions,



Scheme 12. Ring opening of *N*-9-solid phase bound inosine derivatives.



Scheme 13. Ring opening of 2',3'-solid phase bound inosine derivatives.

yielding imidazolyl derivatives **84–92** due to the pronounced intramolecular leaving group capability of this annulated heterocycle (Scheme 15). The reactivity and synthesis of fused purines has been previously reviewed by Rybar in 2005.^[84]

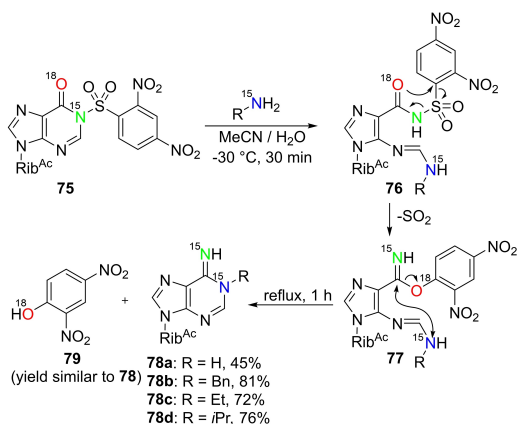
When triazine adducts are treated with methanolic ammonia, a cleavage at pyrimidine C-2 atom takes place, resulting in imidazolyltriazine **84**.^[85]

Pyrimidinopurines can undergo condensation of the third cycle with chlorotretic esters during prolonged refluxing in ethanol, cleaving the original purine moiety to imidazoloxopyrimidines **85a** in 30% yield and **85b** in 90% yield. The

conversion for **85a** can be increased to 71% with the addition of methanolic ammonia.^[86,87] It should be noted that triethylammonium bicarbonate (TEAB) as a mild base can be used to achieve selective ring scission to **86** with a retention of formyl group.^[88]

The exposure of oxadiazolone purine adducts to mildly acidic media yielded purine cleavage products at the C-2 atom - imidazolylloxadiazoles **87a–b**.^[89]

Hydroxide can also initiate such ring opening, for example, prolonged heating of tetrahydropyrimidine adenosine adduct with NaOH promoted the cleavage of pyrimidine moiety to



Scheme 14. Synthesis of *N*-1-alkyladenosines from activated inosine **75**.

imidazolyltetrahydropyrimidine **88**, although the yields were low due to further ring cleavage reactions.^[90] Also, annulated

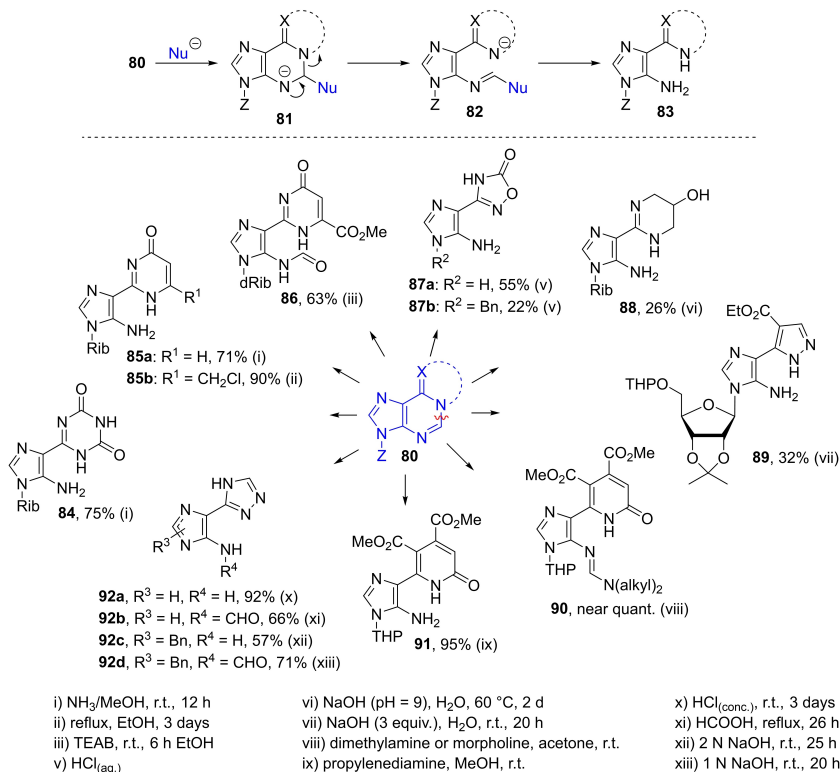
pyrazole purine adducts in alkaline media gave analogous imidazolylpyrazole products **89**.^[91]

Electron-deficient pyrido[1,6]purine adducts reacted with amines (dimethylamine, morpholine) and yielded imidazolylaminoimines **90** in nearly quantitative yields. When propylenediamine was used, the concomitant imine cleavage resulted in free imidazolylamino product **91**.^[66]

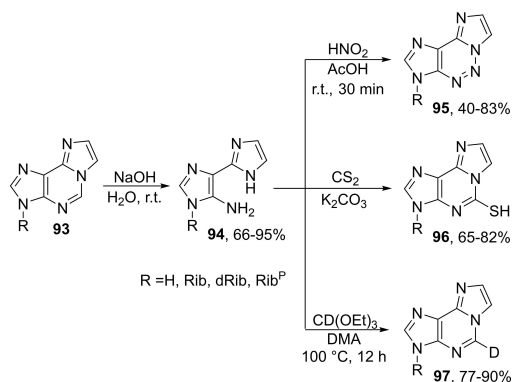
Fused 1,2,4-triazolopurines can be opened either in basic or acidic media to give imidazolyltriazoles **92a–d**. Similarly to the previous example, excessively acidic (concentrated HCl) or basic (2 N NaOH) reaction media led to ring opening with further formyl group cleavage to **92a** and **92c**, while under mild conditions (in this case, HCOOH or 1 N NaOH) formamido ($R^4 = \text{CHO}$) products **92b** and **92d** were obtained.^[92]

Imidazo[1,6]purines **93** readily underwent pyrimidine ring cleavage in alkaline media at room temperature, giving diimidazoles **94**^[93,94] in 66–95% yields. The ring opening products could be further transformed into imidazotriazines **95**,^[95,96] 2-thioimidazopurines **96**^[97,98] or 2-deuteroimidazopurines **97**^[99,100] (Scheme 16).

It is known that 6-azidopurines **98** in solution phase form equilibrium with annulated tetrazolopurines **99**^[101,102] from which the latter tautomer can be viewed a strong EWG and a



Scheme 15. Ring opening of annulated purines **80**.

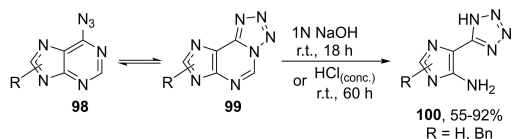


Scheme 16. Pyrimidine ring cleavage of 1, *N*⁶-ethenoadenosines (imidazo[2,1-*f*]purines).

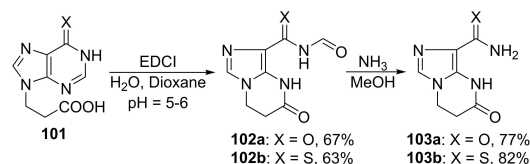
good leaving group, thus making the C-2 position susceptible to S_NAr reactions or, in this case, pyrimidine ring opening. 6-Azidopurines are readily opened in basic or strongly acidic media to yield imidazolyltetrazoles **100** in good yields (Scheme 17).^[103]

Intramolecular condensation of (thio)hypoxanthylpropanoic acid (**101**) led to the formation of a new 6-membered cycle along the purine *N*-3-*N*-9 nitrogen atoms, with concomitant pyrimidine C-2 cleavage that produced compounds **102a–b**. The formyl group of latter can be readily removed with NH₃/MeOH (Scheme 18).^[104]

Rangaathan *et al.* have demonstrated the assembly of imidazole **112** on the basis of parent imidazole template. Similar to the ATP-Imidazole cycle involved in the biosynthesis of imidazoles, the target imidazole was built on recyclable (5-aminoimidazol-4-yl)carboxamide **104** carrier molecule. Initially, the carboxamide **104** was condensed with formamide (**105**) to hypoxanthine **106**, followed by a selective alkylation at the *N*-1



Scheme 17. 6-Azidopurine ring opening.



Scheme 18. Ring opening by intramolecular *N*-3 acylation.

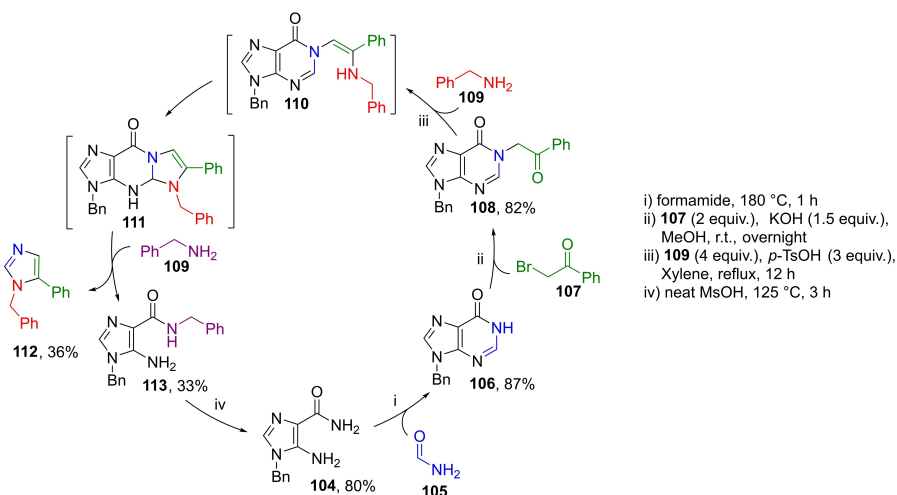
position with phenacyl bromide (**107**) to **108**. Further condensation with benzylamine (**109**) gave the intermediate **110**, which formed an unstable tricyclic hypoxanthine adduct **111**. Second benzylamine attack on hypoxanthine C-6 promoted ring cleavage and the formation of imidazole **112**. The parent imidazole **104** was then regenerated from amide **113** by using methanesulphonic acid (Scheme 19).^[105,106]

In 1975, Leonard found that *N*-3-benzyladenine (**114**) upon treatment with steam in autoclave at 120 °C formed a new adduct with high cytokinin activity.^[107] It is well known that a wide range of *N*⁶-substituted adenines are classified as cytokinins – plant growth hormones. It was established that *N*-3-benzyladenine had rearranged to *N*⁶-benzyladenine that was responsible for the observed cytokinin activity. Further investigation by isotope labelling (¹⁵N-1, ¹⁵N-9, and ¹⁵N⁶) proved this transformation to be more than a simple dealkylation/alkylation sequence (**114**→**115a**), since the labelled isotope at *N*⁶ had become a ring nitrogen in the product **115b–c** (i.e., *N*-3 or *N*-9) (Scheme 20). Since sole ring-openings of pyrimidine C-2-*N*-3 and imidazole *N*-7-*C*-8 cannot lead to adenines other than the starting material, these pathways are not discussed. Pyrimidine *N*-1-*C*-2 ring opening (pathway A) leads to the well-known Dimroth rearrangement product **117**, while imidazole C-8-*N*-9 ring opening (pathway B) led to the imidazole **119a**. Thus, a single ring opening/closing sequence of *N*-3-benzyladenine alone cannot yield *N*⁶-benzyladenine. In order to form *N*⁶-benzyladenine, two sequential (pathway B) or concerted (pathways C–F) ring opening and closing steps must occur. Hence, further Dimroth rearrangement of the previously discussed C-8-*N*-9 ring opening (pathway B) product **119a** would give *N*⁶-benzyladenine **115c**. Concomitant ring openings of both imidazole and pyrimidine (pathways C–F) were expected to yield the diformamido intermediates **120**, **122**, **123**, and **124**. In these open-chain intermediates, rotation along C-4-*C*-5 and C-5-*C*-6 bonds could occur, enabling cyclization with distant nitrogen atoms. Thus, pathways B, D, E, and F led to the formation of *N*⁶-benzyladenine (**115b**) and (**115c**), where *N*-3 became *N*⁶ nitrogen with attached benzyl group.

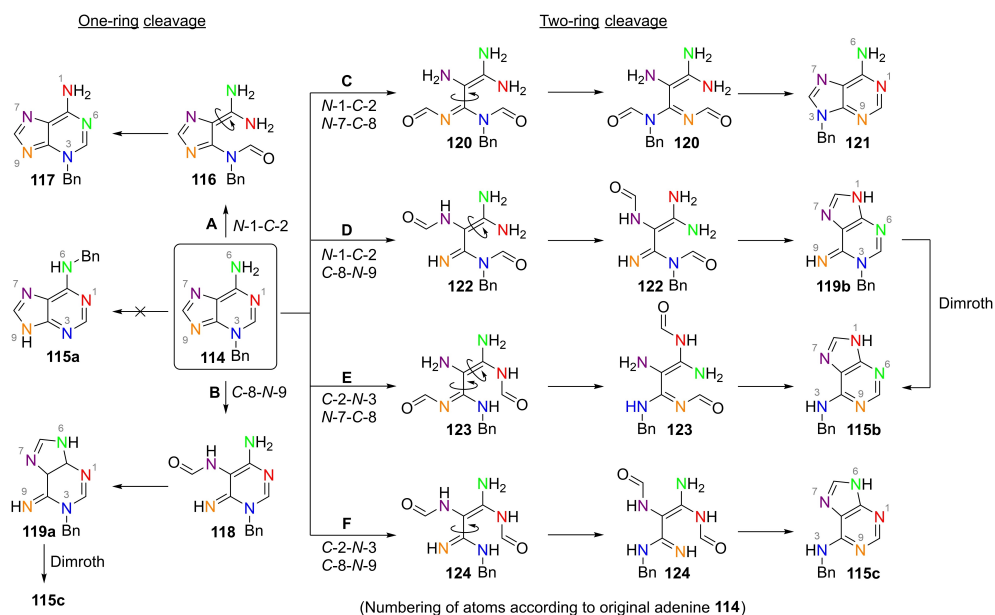
2.3. Ring opening of *N*-1-quaternized purines

The oxidation of adenines to *N*-oxides **126** makes pyrimidine ring electrophilic and prone to opening. Upon reflux in aqueous alkali, adenosine C-2 was cleaved to yield the unstable hydroxyamidine **127**. Further cyclisation with carbon disulfide provided 2-thioadenosines **128**. Thus, a three-step method for installation of C-2 thiol functionality in adenosines was designed (Scheme 21).^[108–112]

A modified approach was demonstrated by the alkylation of *N*-oxides to obtain **130**, which conferred stability to open-chain products. The Fujii group extensively studied the synthesis and cleavage of numerous purine *N*-oxides. In particular, they focused on the synthesis of 3,9-dialkyladenosines **135**. Direct alkylation of purines usually follows the order: *N*-9 > *N*-7 ≧ *N*-1 > *N*-3, with the *N*-3 unsubstituted alkylated derivative usually being the minor product. For adenines, the order is *N*-3 > *N*-9 ≧



Scheme 19. Synthesis of imidazole derivative **112** on the basis of parent imidazole carrier.

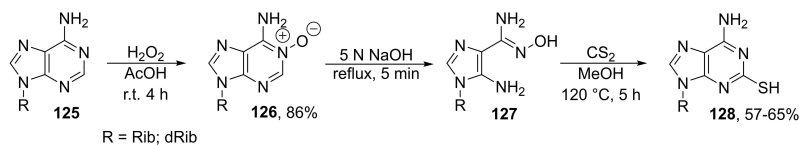


Scheme 20. Rearrangement pathways of 3-benzyladenine (**114**) to *N*⁶-benzyladenines **115a–c** in aqueous medium.

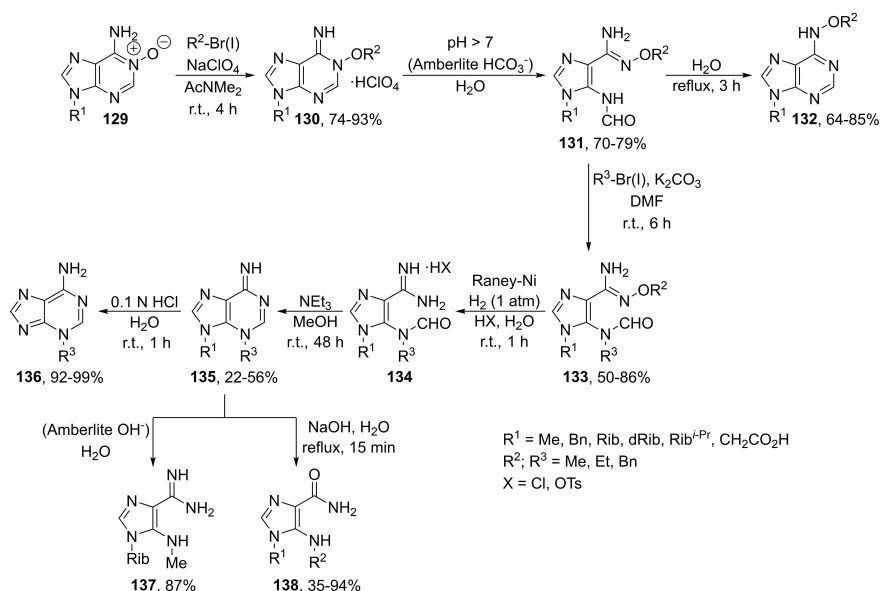
N-1 > *N*-7 (in non-basic medium at pH=7). However, the second alkylation of *N*-9 in substituted adenines changes the order to *N*-1 > *N*-7 > *N*-3.^[7] Selective *N*-3 alkylation has been observed only when steric hindrance at *N*⁶ diminished the possibility of alkylation at *N*-1, as in *N*⁶-alkylated adenines.^[113,114] It is apparent that a concise route to **135** is not feasible via a

simple alkylation procedure. Therefore, Fujii with coworkers presented a ring cleavage-alkylation-ring closure methodology as a unique synthetic approach to 3-alkyl- and 3,9-dialkyladenosines (Scheme 22).

The alkylation of *N*-oxide **129** with benzyl bromide yielded 1-alkoxyadenosines **130**. The latter were easily cleaved under



Scheme 21. Ring opening of adenosine *N*-oxide.



Scheme 22. The alkylation and ring opening of adenine *N*-oxide.

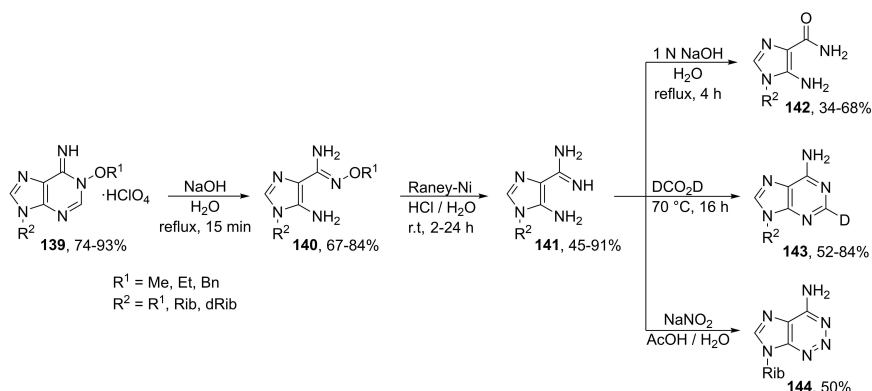
mild hydrolytic conditions: a simple treatment with water or the addition of basic Amberlite (HCO₃⁻) resin allowed to obtain oxamidines **131** that could be heated at reflux in neutral (pH = 7) water to obtain the Dimroth rearrangement products - *N*⁶-alkoxy adenines **132**.^[115,116] The 5-aminogroup of **131** was alkylated in the presence of base (K₂CO₃) in DMF medium at room temperature, providing **133**. Next, catalytic hydrogenolysis with an excess of Raney-Ni/H₂ in acidic (HCl, TsOH) aqueous solution cleaved the *N*-O bond and formed **134** in a low yield. Cyclization was subsequently accomplished with NEt₃/MeOH and yielded 3,9-dialkylated adeninoses **135**.^[117] However, the imidazole group of the latter product functioned as a leaving group, therefore slightly acidic media gave the hydrolysis products **136** by glycosidic bond cleavage. On the other hand, in weakly basic medium, the second ring cleavage could occur, yielding 5-*N*-methylaminoimidazolyl-4-carboxamidine **137**. In strongly alkaline medium,^[118] amidine hydrolysis of open-chain products gave carboxamides **138**.^[119,120,121,122,123]

When the *N*-oxide alkylation product **139** was refluxed in the presence of hydroxide, pyrimidine ring opened and the formyl group was cleaved, giving compound **140**. Subsequent

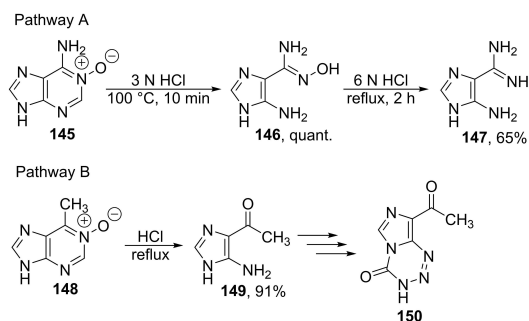
reduction with Raney-Ni/H₂ gave 5-aminoimidazole-4-carboximidines **141**, which were hydrolyzed to carboxamides **142** using NaOH.^[124] Carboximidines **141** could be transformed back to adenosines in the presence of orthoformate or formic acid in order to obtain deuterated adenosines **143**.^[125] The amino group of **141** readily underwent diazotization with NaNO₂ and the diazonium salt further cyclized into 2-azaadenosine (**144**) (Scheme 23).^[126] The latter cyclization is applicable to many purine derivatives and has been reviewed by Seela.^[127]

Also, acidic hydrolysis of adenosine *N*-oxides yielded imidazolyl- cleavage products **146** (Scheme 24A), although high temperatures and strongly acidic media were required.^[128] For example, the hydrolysis of 6-methylpurine *N*-oxide (**148**) under acidic conditions gave the C-2 fission product 1-(5-aminoimidazol-4-yl)-ethan-1-one (**149**) in 91% yield (Scheme 24B).^[129,130] The latter substrate can be used as a precursor to imidazotetrazines **150** - potential anti-cancer drugs for the treatment of glioblastoma.^[131]

S-Nucleophiles have been rarely used for purine ring opening reactions in comparison to *O*- and *N*-nucleophiles. The treatment of *O*-acylated adenosine *N*-oxides **151** with thiophe-



Scheme 23. The synthesis of aminocarboxamides from adenine *N*-oxides and their further applications.

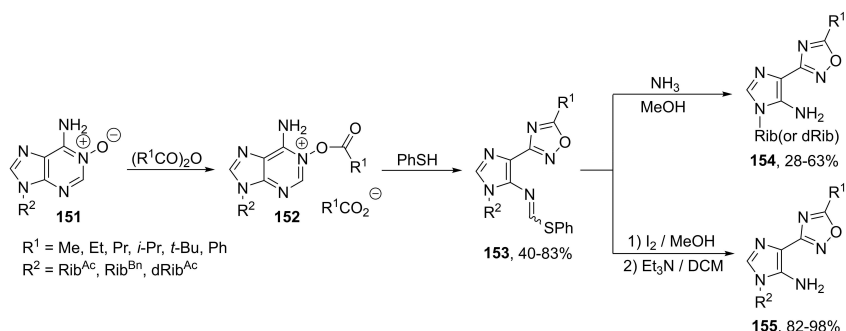


Scheme 24. Ring opening of purine *N*-oxides in acidic medium.

not allowed to obtain 5-amino-4-oxadiazolylimidazoles **154** and **155**.^[132] Without thiol, such *N*-oxides can be opened with acetic anhydride at elevated temperatures (140 °C). The reaction mechanism was revealed by the evident attack by acetate as nucleophile at the C-2 position, which led to pyrimidine ring

opening and subsequent hydrolysis of the acetate.^[133] Exploiting thiol as a good nucleophile accelerated the reaction rate under much milder conditions and allowed the acyl group to participate in the formation of oxadiazole cycle (Scheme 25).

When Grignard reagents are added to pyridine type *N*-oxides, addition occurs at the α -carbon, with cleavage of the adjacent bond yielding dienoximes.^[134,135] This is contrary to purines, where addition occurs at the C-6 position with high regioselectivity and retention of the cyclic system. Addition of Grignard reagents to purine *N*-oxide **156** proceeds at the C-6 position. Furthermore, ring opening of fused pyrimidine does not happen, thus *N*-1-hydroxy-6-alkyldihydropurines **158** are formed instead of the open-chain dienoximes **157**. Products **158** slowly dehydrate to 6-substituted purines **159**, but the addition of pyridine transforms **158** to the *N*-oxides **160**. Contrary to the first addition, the second addition of a Grignard reagent occurs at the C-2 position, accompanied by *N*-C-2 bond scission and leading to imidazole derivatives **162** instead of **161**. Intermediates **162** are unstable and slowly decompose to the 2,6-disubstituted purines **163**. This process can be

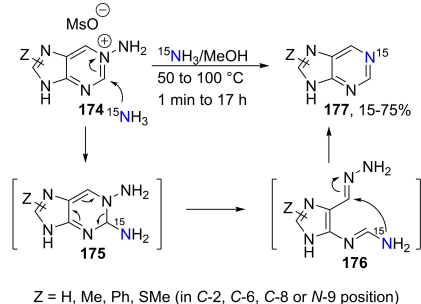


Scheme 25. Thiophen mediated ring opening of purine *N*-oxide.

accelerated with $\text{Ac}_2\text{O}/\text{Py}$.^[136] If peroxide is added, the ring expansion products **164** are obtained in high yields (Scheme 26).^[137]

1,3-Cycloaddition between dimethyl acetylenedicarboxylate (**166**) and nebularine *N*-1-oxide **165** led to both purine ring opening (path A) and ring expansion (path B) of the pyrimidine ring, producing a mixture of products **170** and **173**. Initially, dipolar cycloaddition product isoxazoline **167** was formed and the *N*-1–*O* bond could either cleave (path A) or rearrange to aziridine **171** (path B). In path A, the unstable α -ketoester fragment was lost by attack of any nucleophile. If MeOH was added, the pyrimidine ring of **169** was cleaved via attack by methanol molecule at the *C*-2 position, yielding imidazole derivative **170**. In path B, a second rearrangement gave the 7-membered ring expansion product **172** that lost its α -ketoester fragment, forming diazepine **173**. If other dienophiles (3-phenyl-2-propenenitrile, diphenylacetylene, dimethylmaleate, dimethylfumarate or *N*-methylmaleimide) were used, either no product formation was observed or cleavage of the isoxazoline *N*-1–*O* bond gave stable *C*-6 substituted nucleoside analogues of **168** (Scheme 27).^[138]

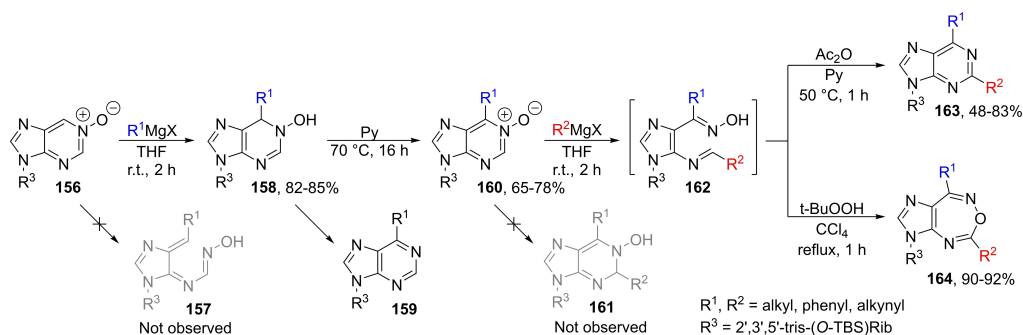
Similarly to *N*-oxides, *N*-aminopurinium mesylates **174** that can be synthesized by a reaction of purine with *O*-mesitylene-sulfonylhydroxylamine (MsONH_2) are also prone to ring opening. Thus, the addition of ^{15}N -labelled ammonia to the *C*-2



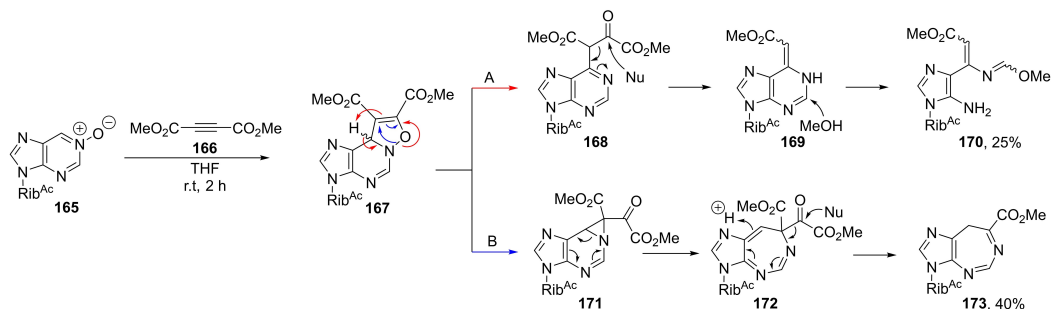
Scheme 28. Synthesis of ^{15}N -labelled purines via *N*-aminopurinium salts.

position of purine with concomitant ring opening yielded **176**, which cyclized to the ^{15}N -1-labelled purines **177** (Scheme 28).^[139]

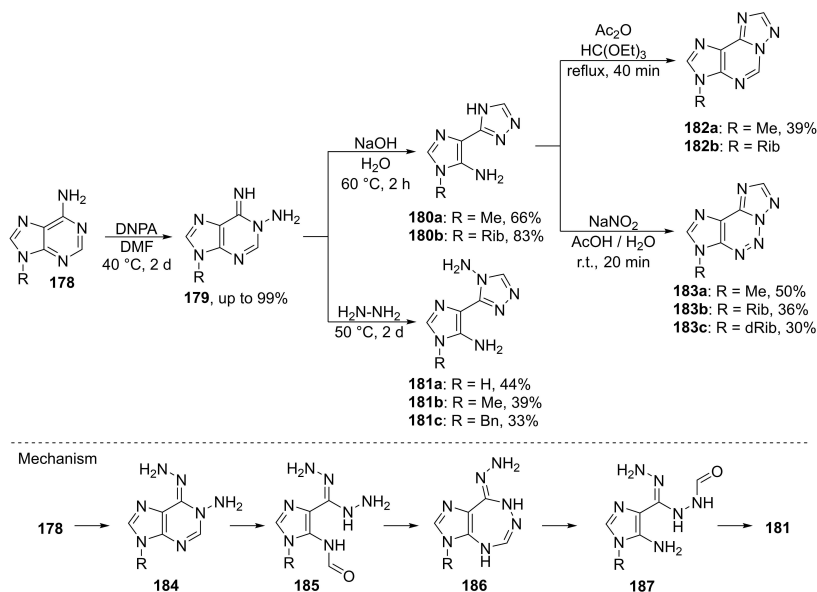
Electrophilic amination of adenines **178** with DNPA produced 1-aminoadenines **179** that displayed similar properties to *N*-oxides (Scheme 29). For instance, the ring opening in strongly alkaline media was accompanied by further cyclization to triazoles **180 a–b**.^[140,141] When the latter reaction was carried out in neat $\text{NH}_2\text{-NH}_2\cdot\text{H}_2\text{O}$, 4-aminotriazoles **181 a–c** were obtained.



Scheme 26. Addition of Grignard reagent to purine *N*-oxides.



Scheme 27. 1,3-Dipolar cycloaddition to nebularine *N*-oxide.



Scheme 29. Ring opening of *N*-1-aminoadenines.

If methanol was used as solvent, alkali-mediated Dimroth rearrangement occurred instead. As for the reaction mechanisms, the authors envisioned that hydrazine initially participated in a S_NAr reaction and after the ring opening the formyl group of **185** cyclized with a distant amine group to the seven-membered **186**. A second ring opening gave **187** that condensed to triazole **181**.^[142] Amination of guanines with DNPA gave *N*-7 aminoguanines that were hydrolyzed to 8-oxoguanines and did not undergo ring opening.^[143,144]

Acylation of adenosine leads to product mixtures of N^6 -, *N*-7-, and *N*-1-acylated products where regioselectivity is highly dependent on the reaction medium, the acylating reagent, and the nature of base. In most cases, N^6 -, N^6 -, 5'-*O*-triacylated adenosine **189** is the major product (Scheme 30). However, Anzai found that the formation of cyclonucleosides **190** was favored in DCM medium. Furthermore, when NEt_3 was employed as base, the formation of ring opening product – cyanoimidazole **191** was observed.^[145] As suggested by authors, the formation of ring opening product (cyanoimidazole **196**) could be explained by *N*-1 and *N*-3 benzylation of the initial adenosine **192** to **194**, followed by nucleophile addition to the C-2 and *N*-1–C-2 position and elimination from **195**.^[146] The ring opening product was not observed when pyridine was used instead of triethylamine, thus supporting the proposed mechanism, since NEt_3 is more nucleophilic than pyridine ($N(\text{NEt}_3)_{\text{DCM}} = 17.3$ and $N(\text{Py})_{\text{DCM}} = 12.9$ according to Mayr's nucleophilicity parameters^[147,148]).

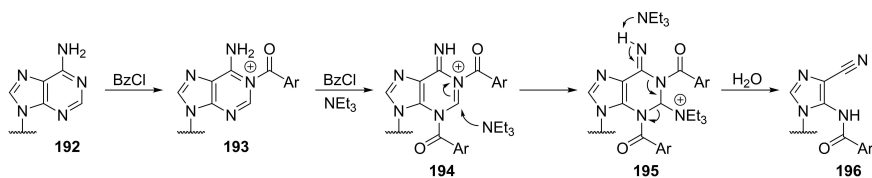
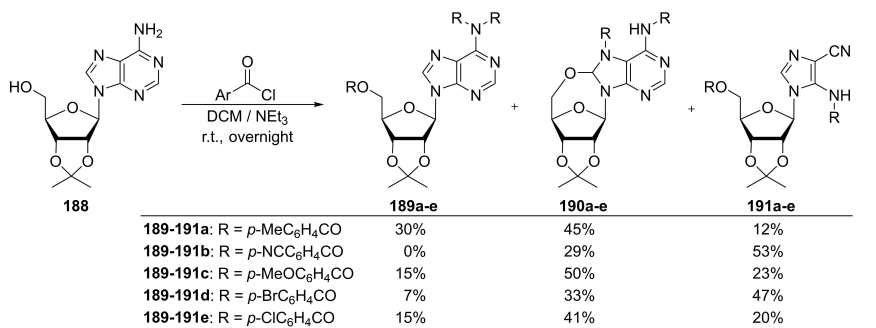
Thermal cyclization of 5'-*O*-tosyl-ribosylpurine derivatives gave the respective 3,5'-anhydro-ribosylpurine adducts. In the case of 5'-*O*-tosyl-2',3'-isopropylideneinosine (**197**), the cycliza-

tion product **198** was obtained as tosylate salt in a good yield, but the free base **199** was unstable in aqueous medium and the addition of water to C-2 in **200** mediated pyrimidine ring opening to formamide **203** (Scheme 31A).^[149] The oxidative cleavage of ribose diol **204** with periodate gave the unstable dialdehyde **205**. Further reduction with NaBH_4 caused hydrolytic pyrimidine ring opening to **206** (Scheme 31B).^[150]

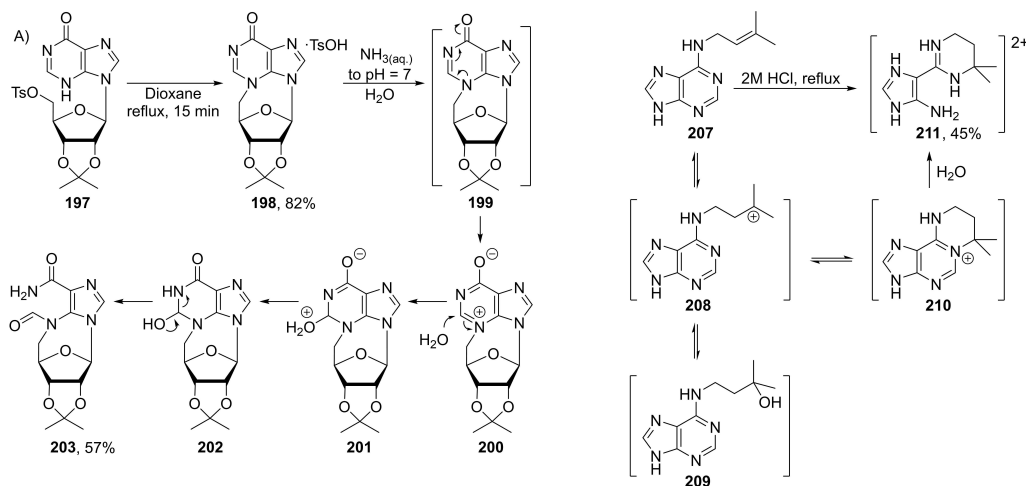
The cyclization of N^6 -isopentyladenosine (**207**) to annulated tetrahydropyrimidinium intermediate **210** was observed in acidic medium (1 M HCl). Further acidification (2 M HCl) and heating at reflux led to ring opening in the pyrimidine moiety, accompanied by formyl group cleavage that gave imidazolyltetrahydropyrimidine (**211**). As elucidated by the authors, the first step involved protonation of isopentenyl group to cation **208** that persisted in equilibrium with hydrated tertiary alcohol **209**. Cycloisomerization to **210** and opening of the activated pyrimidine moiety yielded the ring-opened product **211** (Scheme 32).^[151]

Guanosine deamination product - oxanine (**215**) formed *via* transnitrosation from *N*-nitrosoindole-3-acetonitrile **216**, a plant growth hormone present in various vegetables, notably Chinese cabbage. The reaction was initiated by nitrosation of guanosine (**212**) that produced the diazonium salt **213**. Loss of molecular nitrogen promoted the cleavage of *N*-1–C-6 bond, followed by hydrolysis and cyclization to oxanosine (**215**) (Scheme 33).^[152–154]

6-Azidopurine **217** underwent photocatalytic degradation under UV irradiation *via* the formation of nitrene intermediate **218**, followed by rearrangement to the seven-membered cyclic carbodiimide **219** and hydrolysis to triazepinone **220** (Scheme 34A).^[155,156] Also, 2-azidopurines have been shown to



Scheme 30. Ring opening via purine benzylation.

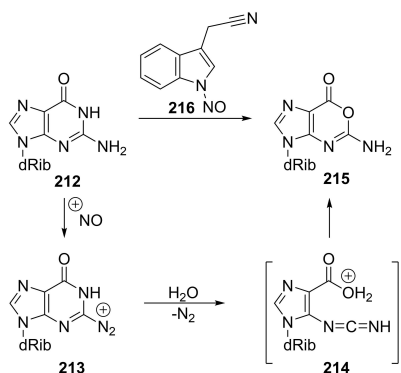


Scheme 32. Tetrahydropyrimidine synthesis by ring opening.

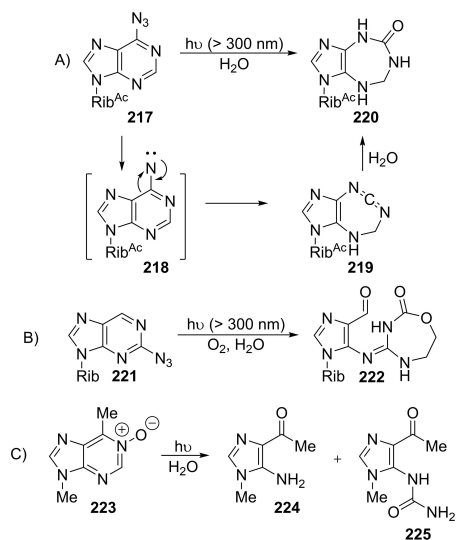
pyrimidine ring cleavage at C-2 to aminoacetylimidazoles **224** and **225** (Scheme 34C).^[158]

Scheme 31. Oxidative (A) and thermal (B) opening of cyclic inosine.

undergo photocatalytic degradation in aerobic media, yielding seven-membered oxadiazepane **222** (Scheme 34B).^[157] Purine *N*-oxides, on the contrary, upon irradiation undergo slow



Scheme 33. Nitrosation of guanosine.

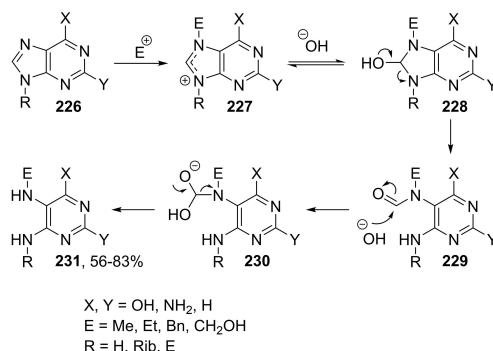


Scheme 34. Photocatalytic purine degradation pathways.

3. Ring opening of the imidazole moiety in purines

3.1. Ring opening reactions induced by O-nucleophiles

Alkylation of 9-substituted purine derivatives proceeds at *N*-7 and gives dialkylated imidazolium salts **227**. Such imidazolium intermediates are highly electron deficient and are prone to nucleophile attack at the C-8 position, as well as undergo imidazole ring cleavage when mixed with hydroxide. The imidazole ring opening in purines occurs with cleavage between C-8 and N-7 or N-9 that gives formamidopyrimidines (FAPY) **229** (Scheme 35).^[159] Similar opening reactions have been carried out using OH radicals.^[160,161] The formyl group of

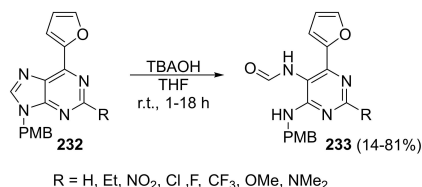


Scheme 35. Imidazole ring opening mechanism.

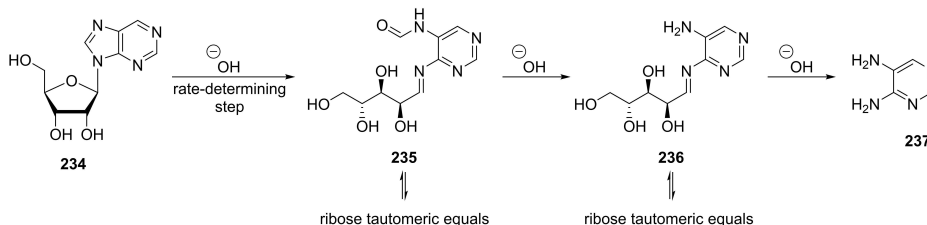
FAPY adducts can be located on either pyrimidine *N*⁵, *N*⁶ or exist as a mixture of both, as proven by ¹⁵N labelling.^[162] The position of formyl group is solely dependent on the reaction conditions, but since the formyl group is highly base labile it is often cleaved under the present ring opening conditions to 4,5-diaminopyrimidines **231**. Bases like group I metal hydroxides,^[159,163] diluted (~14%) aqueous ammonia^[164] or Na₂CO₃ can be used.^[122] Under such conditions, nucleosides can be also easily transformed to pyrimidine derivatives without disruption of the sugar moiety.

While studying *anti*-mycobacterial pyrimidine analogues, Gundersen's group synthesized various FAPYs **233** from 6-furanyl-9-*para*-methoxybenzylpurines via imidazole ring opening reaction of purines with tetrabutylammonium hydroxide (TBAOH) (Scheme 36).^[165,166] In their study, substrates with electron withdrawing groups (R=NO₂, F, CF₃) at C-2 readily participated in ring opening and gave products in high yields. As expected, non-activated (R=OMe, NMe₂) substrates required prolonged reaction times and their yields were significantly lower.

Lönnberg *et al.* have investigated purine ribonucleoside degradation mechanism and kinetics with ¹⁴C isotope labelled position 8 of the substrate, using various NaOH concentrations and temperatures. Mechanistic studies of the hydrolysis of ribosylpurine (**234**) showed that imidazole was initially cleaved to FAPY **235** and deformylation occurred, followed by hydrolysis of the ribosyl group to 4,5-diaminopyrimidine (**237**) (Scheme 37). It was found that the hydroxide ion attack on C-8



Scheme 36. TBAOH mediated imidazole ring opening.



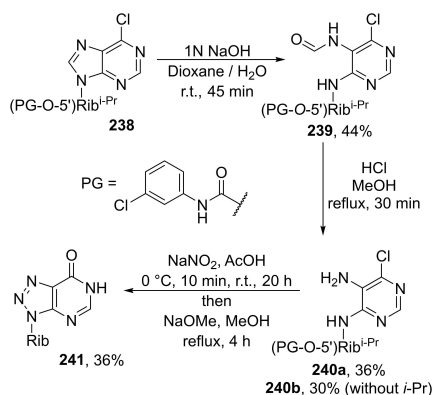
Scheme 37. Purine ribonucleoside degradation.

was the rate determining step.^[167] Similar research has been performed on *N*²-alkylated *P*¹,*P*³-diguanosine triphosphates.^[168]

It is well known that halopurines readily undergo S_NAr reactions with various nucleophiles. The substitution pattern and reactivity is highly dependent on: 1) the basicity of nucleophile, and 2) the substituents present in the purine system.^[4,5] Thus, in some cases imidazole ring opening requires milder conditions than those of halogen displacement. Such an example is the ring opening of 5'-*O*-protected 6-chloronebularine **238** with 1 N NaOH, which takes place already at room temperature (Scheme 38). The formyl group of FAPY **239** formed by imidazole ring opening can be cleaved under acidic (HCl) or basic (NH₃) conditions, but the latter option also hydrolyzes the *N*²-glycosidic bond, therefore acidic hydrolysis is preferred.

Under acidic conditions without 5'-*O*-carbamoyl protecting group, ribose tautomerizes to pyranose. Furthermore, 4,5-diaminopyrimidines **240 a–b** can be transformed to 8-azapurines by diazotation. The formed triazole moiety renders C-6 position highly reactive towards nucleophilic addition and the chlorine substituent is readily hydrolyzed to yield 8-azanebularine **241**.^[169]

The alkylation of *O*⁶-methylguanine with excess MeI (5 eq) generated activated guaninium species and led to imidazole ring opening. Initially, the *N*-9 methyl adduct **243** was formed

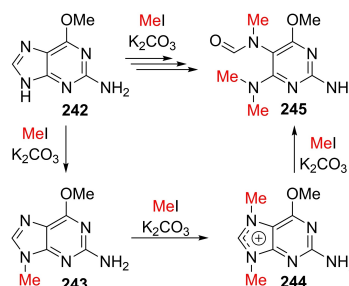


Scheme 38. 8-Azapurine synthesis via imidazole ring opening.

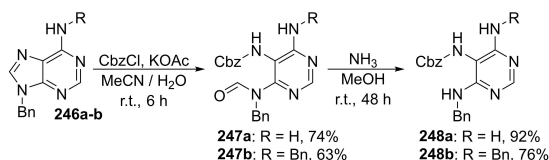
and further alkylation gave trimethylguaninium intermediate **244** that underwent ring opening by hydroxide attack on C-8 position and the final methylation produced tetramethylated FAPY **245** (Scheme 39).^[170]

The alkylation and acylation of unsubstituted adenine usually occur at the *N*⁶ and *N*-9 positions. Carbamoyl groups, on the contrary, add to the *N*-7 nitrogen atom and activate the imidazole ring toward nucleophilic attack. As depicted in the following schemes, chloroformates in a weakly alkaline medium (KOAc, NaHCO₃) reacted at the *N*-7 nitrogen with concomitant ring opening of imidazole. For example, the addition of Cbz-Cl to 9-benzyladenines **246 a–b** yielded **247 a–b** in good yields. Like previously, formyl group was easily cleaved in methanolic ammonia to obtain the substituted triaminopyrimidines **248 a–b** (Scheme 40).^[171]

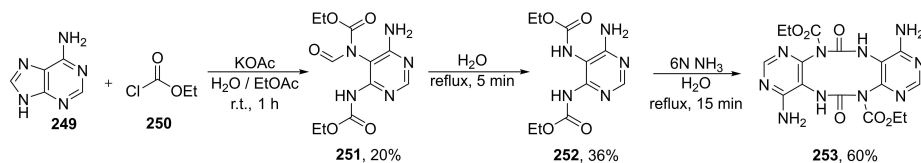
When adenine (**249**) was treated with ethyl chloroformate (**250**), quaternization occurred at *N*-7, facilitating imidazole ring opening between C-8 and *N*-9 to give FAPY **251**. The formyl group of this product was labile and could be easily removed



Scheme 39. Methylation of *O*⁶-methyl guanosine.



Scheme 40. Triaminopyrimidine synthesis from adenine.



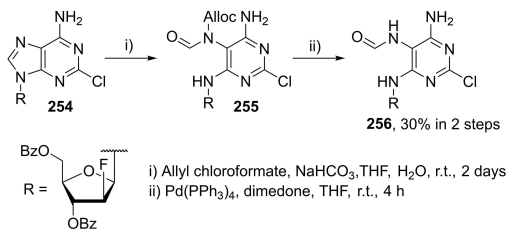
Scheme 41. Acetylation of adenine with ethyl chloroformate.

by refluxing in water to obtain **252**. Further treatment with aqueous ammonia gave the dimerization product **253** (Scheme 41).^[172]

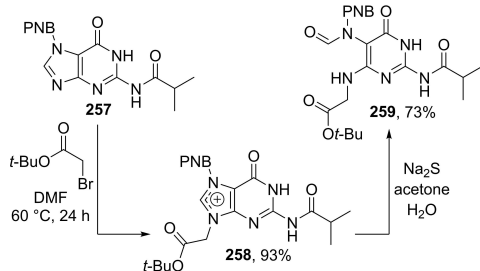
In a study of clofarabine degradation, Cantrell and co-workers designed a new adenosine ring opening mediated by chloroformate and bicarbonate, which yielded the Alloc-protected FAPY **255**. A selective cleavage of Alloc-protecting group with Pd⁰ subsequently produced FAPY **256** in 30% yield calculated from adenine **254** (Scheme 42).^[173]

Sodium sulfide is known to be used for the removal of PNB group, but in the case of imidazolium **258** hydroxyl mediated ring opening occurred instead of protecting group removal and the PNB protected FAPY **259** was obtained (Scheme 43).^[174]

FAPY fragments are also found in natural products, for example, agelasines **260a–c** are bioactive purine derivatives with terpene side chain found in marine sponges of genus *Agelas*. They are associated with antimicrobial bioactivity and cytotoxic effects in cells. Similarly, agelasins can be converted



Scheme 42. Allylchloroformate mediated imidazole ring opening.

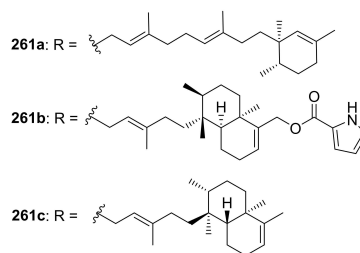
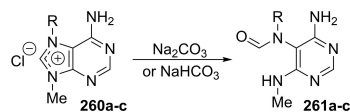


Scheme 43. Na₂S mediated imidazole ring cleavage.

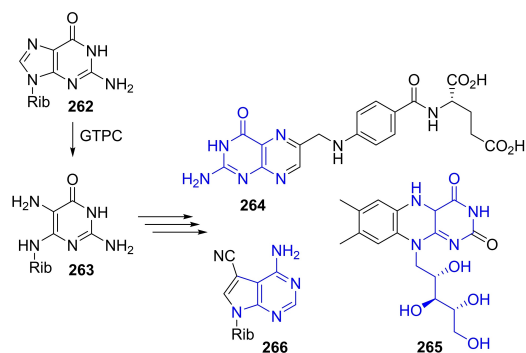
to axistatins **261a–c** by treatment with mild base (e.g., Na₂CO₃, NaHCO₃) (Scheme 44).^[175–180]

Imidazole ring opening is important in biosynthesis, as the first step in the synthesis of various annulated pyrimidines. Guanosine triphosphate cyclohydrolase (GTPC) enzymes catalyze the release of formate from imidazole ring of guanosine (**262**), leading to the formation of 4,5-diaminopyrimidine **263**^[181] that can react with dicarbonyl compounds, producing a pyrazine cycle. The new heterocycle can undergo side chain modifications to yield pteridine natural products like folic acid (**264**) and riboflavin (**265**)^[182–185,164] or 7-deazapurine natural products like toycamycin (**266**) (Scheme 45).^[186,187]

DNA-reactive carcinogens are any chemicals that form covalent DNA adducts. These substances are alkylating agents by nature or become such after metabolic processing, usually by cytochrome P450 mediated oxidation. Nucleobase modifications interfere with base pairing and affect cell replication, oncogene activation, inactivation of gene suppressors or inhibit apoptosis, which may lead to neoplastic cell development.^[188] Reviews by K. Gates,^[189] N. Tretyakova,^[190] N. Jena,^[191] and M. Dizdaroglu^[192] thoroughly describe DNA damage pathways, including the repair and formation of FAPY adducts. Therefore, only an overall insight in this topic is given in our review. Imidazole ring opening of adenosine and guanosine is one of the main mutation pathways in DNA strands. Therefore, many groups focus on the discovery of such DNA lesions and the



Scheme 44. Conversion of agelasines to axistatins.



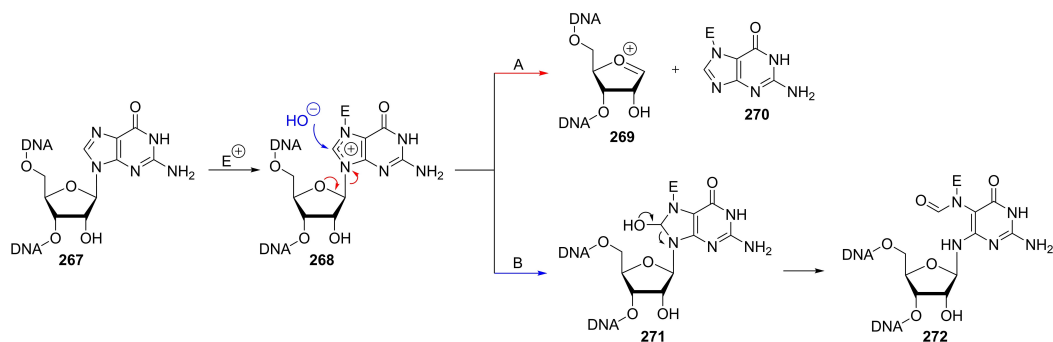
Scheme 45. Imidazole ring opening in biosynthesis.

development of methods for better detection of these changes.^[193,194]

Alkylation of deoxyguanosine in the DNA strand with most carcinogenic agents occurs primary at the *N*-7 position, yielding *N*-7 and *N*-9 disubstituted purinium adducts **268**. The activated deoxyguanosine adducts are either cleaved at the glycosidic bond (pathway A) to form abasic DNA site **269** and guanosine **270** or imidazolium ring opening yields FAPY **272** (pathway B) (Scheme 46).

In the latter manner, many carcinogens like butadiene (active carcinogenic metabolites: epoxybutadiene and diepoxybutadiene),^[195,196] aflatoxin B₁,^[197–199] dimethyl sulphate,^[200] glycidamide,^[201] and anti-cancer agents (mitomycin,^[202] nitrogen mustard^[203]) form FAPY adducts (Figure 1), which interfere with base pairing and cell development. Furthermore, Rizzo *et al.* have developed method for incorporation of nitrogen mustard FAPY adducts in DNA through solid phase synthesis.^[204]

Both UV and γ -radiation are known to cause mutations of DNA bases and may lead to deleterious cellular effects. The mutation mainly occurs through photooxidation at nucleoside C-8 position to give 8-hydroxy-7,8-dihydro-7-yl radical **274**



Scheme 46. Molecular mechanism for DNA-reactive carcinogenic reagents.

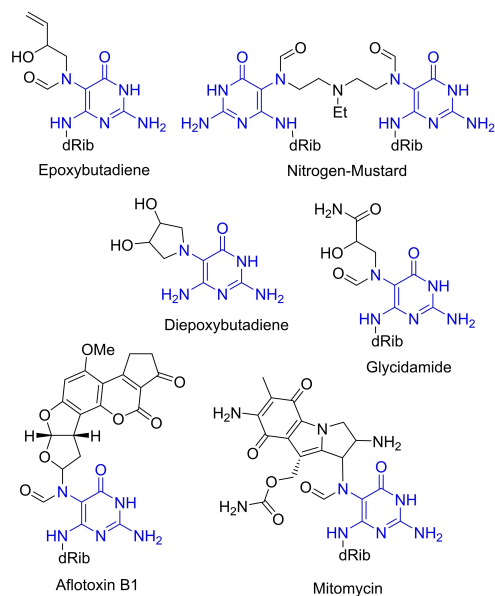
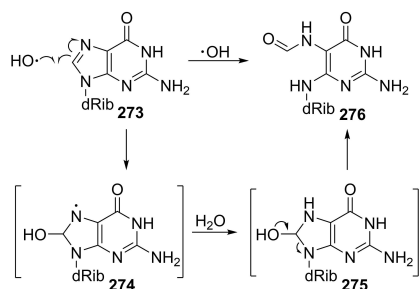


Figure 1. FAPY adducts of various carcinogens and anti-cancer agents.

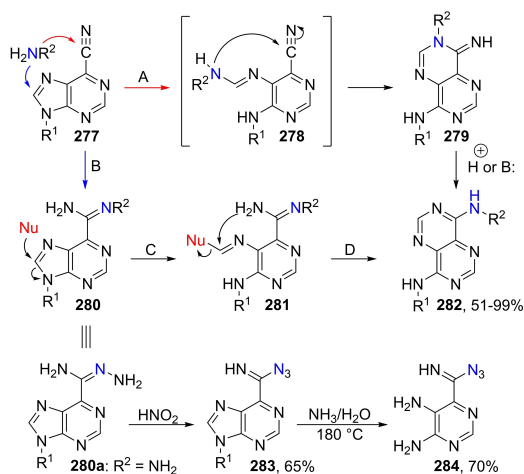
which abstracts hydrogen to form 8-hydroxy-7,8-dihydro-nucleoside **275**. Due to instability, the ring cleavage of the imidazole occurs to give FAPY **276** (Scheme 47).^[194,205–208]

3.2. *N*-Nucleophile induced ring opening reactions

6-Cyanopurine **277** reactions with different *N*-nucleophiles lead to the formation of pyrimido[5,4-*d*]pyrimidines **279** and **282** (Scheme 48).^[209–215] Depending on the *N*-nucleophile, addition occurs at C-8 (pathway A) or the cyano group at C-6 (pathway B). A mixture of products **279**, **280** and **282** is usually obtained, however, the conditions can be optimized for nearly selective



Scheme 47. Imidazole ring opening of deoxyguanosine in the presence of hydroxyl radicals.



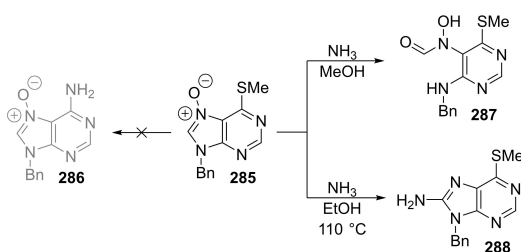
Scheme 48. 6-Cyanopurine ring opening with *N*-nucleophiles.

formation of the desired product. Treatment of 6-cyanopurine **277** with methanolic ammonia (R²=H) did not lead to the addition to the cyano moiety but instead resulted in the formation of pyrimidopyrimidine **279** that rapidly underwent a Dimroth rearrangement to the more stable derivative **282**.^[212,215] Similarly, in reactions with formamide,^[210] methylamine,^[213] hydrazide,^[214] benzyloxyamine,^[211] and hydrazine, ethanolamine, aniline, piperidine^[212] the products **279** could be obtained in good yields. The proposed reaction mechanism consists of nucleophilic attack at C-8 forming the opened ring intermediate **278**. Intramolecular amine addition to the cyano group yielded the product **279**.^[215] The substituent electronic effects at purine *N*-9 position for both EWG and EDG had little to no impact on the reaction pathway or on the obtained

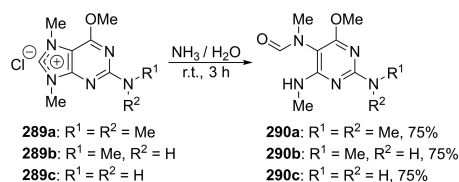
yield.^[212] Upon heating of **279** with acid (H₂SO₄, TFA) or base (DBU), a Dimroth rearrangement can occur to yield amino-pyrimidines **282**, although it can take up to 15 days.^[209] As alternative, *N*-nucleophiles can be added to the C-6 cyanogroup to form aminoimidates **280** (pathway B). The addition of sulphuric acid in catalytic amount directed the nucleophilic addition to C-6-cyanogroup over an attack on C-8. Further addition of a suitable nucleophile (e.g., piperidine) promoted ring cleavage at C-8 to **281** which then cycloisomerized to pyrimidopyrimidine **282** in a good yield.^[209] Also, aminohydrazone **280a** can be transformed to carbimidoylazide **283** via diazotation. The latter can be thermally cleaved in aqueous ammonia, producing diaminopyrimidine **284**.^[216] Similar pyrimido-pyrimidines have been obtained from purin-6-ylpyridinium chlorides in aqueous solutions using an analogous photo-induced hydrolytic imidazole ring opening and cycloisomerization sequence.^[217,218] There has also been research on formamide use for purine nucleoside degradation in DNA sequencing.^[210]

Similarly to *N*-1-oxides, 6-methylthiopurine-*N*-7-oxide (**285**) also does not undergo S_NAr reaction at C-6 to yield **286**. Instead, ring opening occurs to form FAPY **287** with formyl group located at the 5-amino nitrogen. In contrast to this, ammonia in hot ethanolic solution under pressure added to the C-8 position, giving **288** (Scheme 49).^[219,220]

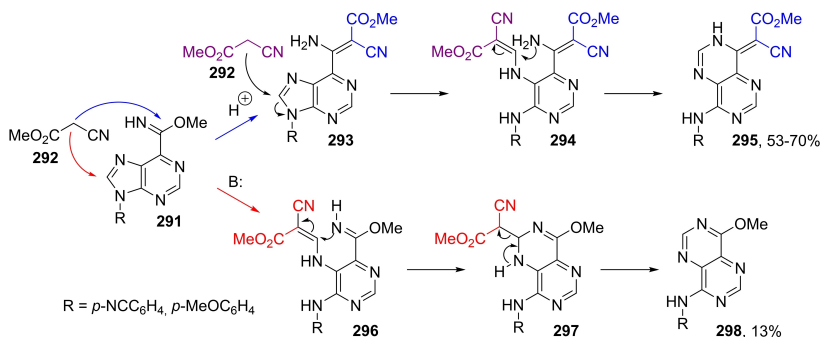
Heteroamines A–H are found in plant *Heterostemma brownii* used in folk medicine for the treatment of tumors. Heteroamines A–C **289a–c** can be readily obtained from guanine^[221] or 2-amino-6-chloropurine^[222] and, due to the activated imidazolium ring, can be converted to heteroamines F–H **290a–c** via ring opening with dilute aqueous ammonia (Scheme 50).^[223]



Scheme 49. Ring opening of 6-thiomethylpurine-*N*-oxide **285**.



Scheme 50. Imidazole ring opening in heteroamines A–C.



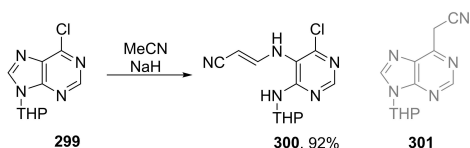
Scheme 51. Purine imidate reactions with methyl cyanoacetate.

3.3. C-Nucleophile induced ring opening reactions

The imidate functional group is prone to nucleophilic substitution in reactions with C-nucleophiles, leading to enamines. Also, nucleophilic attack may proceed at the C-8 position when reaction mixtures are heated at reflux for a prolonged time. Aryl-purine imidates **291** reacted with methyl cyanoacetate (**292**) in such a manner and imidazole ring opening formed pyrimido-pyrimidines **295** and **298**. The reaction of imidate **291** with methyl cyanoacetate **292** under mild acidic catalysis (pyridinium acetate) initially gave 6-enaminopurines **293** in good yields. When the mixture was refluxed for multiple days, further attack by cyanoacetate mediated imidazole ring opening to **294**, followed by cycloisomerization and elimination to pyrimido-pyrimidylidene **295**. When acid catalysis was replaced with base catalysis (DMAP), imidate substitution did not occur, but cyanoacetate **292** directly attacked the C-8 position instead to give diaminopyrimidine **296**, followed by imidate-mediated cycloisomerization and elimination to methoxy-pyrimido-pyrimidine **298** (Scheme 51).^[224]

When adding acetonitrile anion to 9-tetrahydropyryl-6-chloropurine (**299**), the nucleophile attacked the C-8 position, resulting in the ring opening product **300** in 92% yield. The formation of S_NAr product **301** was not observed (Scheme 52).^[225]

When the standard Reissert reaction^[226,227] conditions were employed for purines **302**, N-7 benzylation occurred and cyanide added to the imidazolium ring, cleaving the bond between N-7 and C-8 atoms and forming 5-amino-4-formamidopyrimidine **303** in 23% yield. Furthermore, under basic



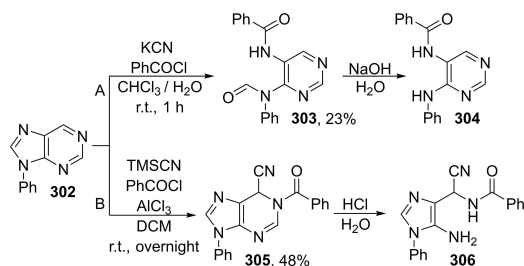
Scheme 52. Purine ring opening with acetonitrile anion.

conditions formamide was cleaved and diaminopyrimidine **304** was formed (Scheme 53A). Addition of a Lewis acid directed the benzylation to N-1 position and the Reissert reaction product -1-benzoyl-6-cyano-1,6-dihydro-9-phenyl-9H-purine (**305**) was obtained. Upon acidic treatment, the Reissert product underwent pyrimidine ring cleavage, producing imidazole **306** (Scheme 53B).^[228]

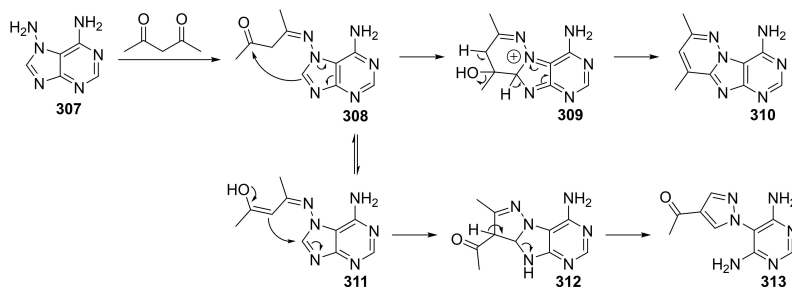
The reaction of 7-aminoadenine (**307**) with 2,4-pentanedione yielded mainly the tricyclic pyridazinopurine **310** accompanied by pyrazolopyrimidine **313** as a minor product. At first, the N-7 imine adduct **308** was formed, which underwent cyclization to yield **309** and further elimination that provided the aromatic pyridazinopurine **310**. However, ketone **308** was able to enolize to **311** and cyclization became possible, giving **312**. Further elimination gave aromatized pyrazole system and imidazole ring cleavage led to pyrazolopyrimidine **313** (Scheme 54).^[229]

3.4. Acid-induced opening of imidazole moiety in purines

Martinez *et al.* have designed a new aminopyrimidine type ligand **317** by arylating adenine (**314**) at the N-7 position with 2-chloropyrimidine (**315**) in the presence of a base (NaH, CS_2CO_3 or K_2CO_3), followed by Brønsted acid catalyzed imidazole ring cleavage that yielded ligand **317** after neutralization. Likewise,

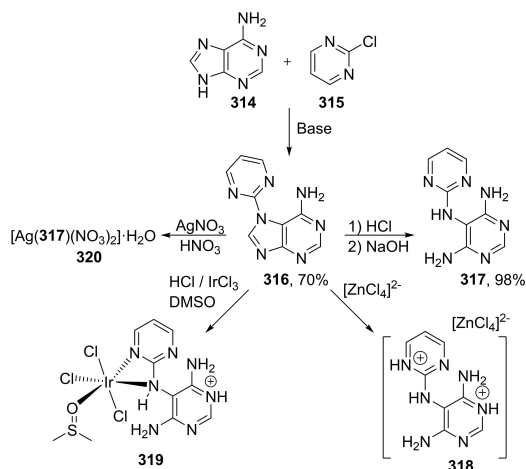


Scheme 53. The Reissert reaction of purines.

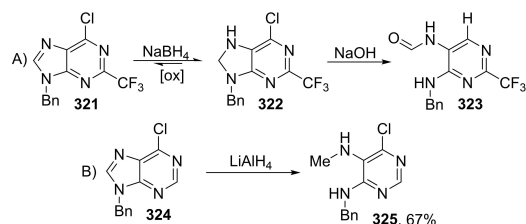


Scheme 54. Proposed reaction mechanism for pyrazolopyrimidine 313 formation.

transition metal can be added after acidic cleavage of C-8 position to yield metal-ligand complexes 318–320 (Scheme 55).^[230]



Scheme 55. Synthesis of ligand 317 from adenine and its application in complex formation.



Scheme 56. Reductive cleavage of the imidazole moiety in purine derivative.

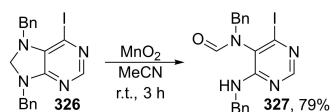
3.5. Imidazole ring opening of purines induced by redox reagents

The treatment of purines with NaBH₄ gave rise to the unstable 7,8-dihydropurine 322 that easily re-oxidized back to purine 321 in the presence of air oxygen. When a strong base was added to the reduced dihydropurine 322, dehydrochlorination occurred at first, followed by ring opening that yielded the FAPY product 323 (Scheme 56A).^[231] When a stronger reducing agent like LiAlH₄ was used, the intermediate aminal was first reduced to yield 4,5-diaminopyrimidine 325 (Scheme 56B).^[232]

During purine oxidation at the C-8 position, optimization studies were performed by the Tobrman group using MnO₂ in acetonitrile. Ring opening of the purine analog 326 was observed, providing access to FAPY 327 in 79% yield (Scheme 57).^[233]

4. Summary

Purines as a type of imidazopyrimidines can serve as useful starting materials for the synthesis of imidazole and pyrimidine derivatives, if one of the fused rings is cleaved. Readily available substrates (e.g., adenine, hypoxanthine, guanine and their derivatives) can be transformed *via* ring opening reactions, and thus provide a convenient synthetic methodology for obtaining numerous heterocyclic compounds that are important to the fields of medicinal and agricultural chemistry. Due to the stability of the aromatic system subject to cleavage, activation of the purine system by appropriate substituents and/or elevated temperatures is needed. Also sufficiently nucleophilic reagents must be used to overcome the energy barrier. If these prerequisites are met, purine derivatives can be preparatively



Scheme 57. Oxidative cleavage of imidazole ring in purine analogs.

transformed into 5-aminoimidazole-4-carboxamide derivatives, imidazolyl-substituted pyrimidines, azoles, triazines, and pyridines. The aforementioned structures are not always easy to prepare by cross-coupling reactions and purine ring opening offers an orthogonal strategy in synthetic planning. On the other hand, fused imidazo-heterocycles can be prepared by purine ring opening – recyclization sequence. When the imidazole ring is cleaved, various recyclization techniques can be applied to the obtained diamino- or triamino-pyrimidine derivatives to obtain the respective fused pyrimidines. Last but not least, imidazole ring opening of purines has biological importance and its reproduction in the lab provides mechanistic insights that help to understand several important biochemical pathways.

Abbreviations

AICA	5-aminoimidazole-4-carboxamide
AICAR	5-aminoimidazole-4-carboxamide-1- β -D-ribofuranoside
Alloc	allyloxycarbonyl
ANRORC	addition of nucleophile, ring opening, and ring closure
Cbz	benzyloxycarbonyl
DCM	dichloromethane
DMAP	<i>N,N</i> -dimethylaminopyridine
DNCB	2,4-dinitrochlorobenzene, DNP-2,4-dinitrophenyl-
DNPA	dinitrophenoxamine
EWG	electron-withdrawing group
EDA	ethylenediamine
FAPY	formamidopyrimidines
Rib	β -D-ribofuranosyl
Rib ^{Ac}	2',3',5'-tri- <i>O</i> -acetyl- β -D-ribofuranosyl
Rib ^{1-Pr}	2',3'- <i>O</i> - <i>iso</i> -propylidene- β -D-ribofuranosyl
Rib ^P	5'- <i>O</i> -phosphoryl- β -D-ribofuranosyl
MEM	methoxymethylene
Ns	2-nitrophenylsulfonyl
PNB	<i>p</i> -nitrobenzyl
<i>p</i> Ns	4-nitrophenylsulfonyl
DNs	2,4-dinitrobenzenesulfonyl
Ms	methanesulfonyl
TBDPS	<i>t</i> -butyldiphenylsilyl
TBS	<i>t</i> -butyldimethylsilyl
Tf	trifluoromethanesulfonyl
TFA	trifluoroacetic acid
TMS	trimethylsilyl
Ts	toluenesulfonyl

Acknowledgements

The authors would like to thank the Latvian Council of Science for grant LZP-2020/1-0348 that provided financial support. K.L. thanks Riga Technical University for the doctoral student research grant No. 34-14A00-DOK.0KTI/20.

Conflict of Interest

The authors declare no conflict of interest.

Keywords: Fused ring systems · Imidazoles · Nucleobases · Nucleophilic addition · Ring opening

- V. Gogineni, R. F. Schinazi, M. T. Hamann, *Chem. Rev.* **2015**, *115*, 9655–9706.
- J. D. Clark, M. E. Flanagan, J.-B. Telliez, *J. Med. Chem.* **2014**, *57*, 5023–5038.
- W. B. Parker, *Chem. Rev.* **2009**, *109*, 2880–2893.
- G. Shaw, in *Compr. Heterocycl. Chem.*, Elsevier, **1984**, pp. 499–605.
- I. Collins, J. J. Caldwell, in *Compr. Heterocycl. Chem. III*, Elsevier, **2008**, pp. 525–597.
- J. Décout, in *Ref. Modul. Chem. Mol. Sci. Chem. Eng.*, Elsevier, **2020**, pp. 1–81.
- J. H. Lister, *Chemistry of Heterocyclic Compounds*, John Wiley & Sons, Inc., Hoboken, NJ, USA, **1971**.
- G. Shaw, in *Compr. Heterocycl. Chem. II*, Elsevier, **1996**, pp. 397–429.
- V. Sharma, N. Chitranshi, A. K. Agarwal, *Int. J. Med. Chem.* **2014**, *2014*, 202784.
- J. Zhang, X.-M. Peng, G. L. V. Damu, R.-X. Geng, C.-H. Zhou, *Med. Res. Rev.* **2014**, *34*, 340–437.
- A. Verma, S. Joshi, D. Singh, *J. Chem.* **2013**, *2013*, 1–12.
- S. Kumar, B. Narasimhan, *Chem. Cent. J.* **2018**, *12*, 38.
- N. K. Kochetkov, E. I. Budovskii, in *Org. Chem. Nucleic Acids*, Springer US, Boston, MA, **1972**, pp. 381–423.
- S. Daley, G. A. Cordell, *Nat. Prod. Commun.* **2020**, *15*, 1–14.
- H. C. Van Der Plas, *Tetrahedron* **1985**, *41*, 237–281.
- S. Elliott, *J. Org. Chem.* **1962**, *27*, 883–885.
- T. R. Mahajan, L. L. Gundersen, *Tetrahedron Lett.* **2015**, *56*, 5899–5902.
- H. C. Van der Plas, *Adv. Heterocycl. Chem.* **1999**, *74*, 9–86.
- H. C. Van der Plas, *Adv. Heterocycl. Chem.* **1999**, *74*, 87–151.
- H. C. Van der Plas, *Adv. Heterocycl. Chem.* **1999**, *74*, 153–221.
- E. S. H. E. Ashry, Y. E. Kilany, N. Rashed, H. Assafir, in *Adv. Heterocycl. Chem.*, **1999**, pp. 79–165.
- V. A. Mamedov, N. A. Zhukova, M. S. Kadyrova, *Chem. Heterocycl. Compd.* **2021**, *57*, 342–368.
- N. J. Kos, H. C. van der Plas, *J. Org. Chem.* **1980**, *45*, 2942–2945.
- N. J. Kos, H. C. van der Plas, *J. Org. Chem.* **1983**, *48*, 1207–1210.
- G. F. Merrill, E. J. Kurth, D. G. Hardie, W. W. Winder, *Am. J. Physiol. Endocrinol. Metab.* **1997**, *273*, E1107–E1112.
- J. F. P. Wojtaszewski, S. B. Jorgensen, Y. Hellsten, D. G. Hardie, E. A. Richter, *Diabetes* **2002**, *51*, 284–292.
- M. Galiñanes, K. M. Mullane, D. Bullough, D. J. Hearse, *Circulation* **1992**, *86*, 598–608.
- D. T. Mangano, Y. Miao, I. C. Tudor, C. Dietzel, *J. Am. Coll. Cardiol.* **2006**, *48*, 206–214.
- D. T. Mangano, *JAMA* **1997**, *277*, 325–332.
- M. F. Newman, T. B. Ferguson, J. A. White, G. Ambrosio, J. Koglin, N. A. Nussmeier, R. G. Pearl, B. Pitt, A. S. Wechsler, R. D. Weisel, T. L. Reece, A. Lira, R. A. Harrington, *Surv. Anesthesiol.* **2013**, *57*, 59.
- B. G. Drew, B. A. Kingwell, *Expert Opin. Pharmacother.* **2008**, *9*, 2137–2144.
- E. S. Buhl, N. Jessen, R. Pold, T. Ledet, A. Flyvbjerg, S. B. Pedersen, O. Pedersen, O. Schmitz, S. Lund, *Diabetes* **2002**, *51*, 2199–2206.
- B. N. Cronstein, B. A. Kamen, *J. Pediatr.* **2007**, *29*, 805–807.
- J. B. Arterburn, C. B. Jonsson, W. B. Parker, *Azole Nucleosides and Use as Inhibitors of RNA and DNA Viral Polymerases*, **2008**, WO 2008/067002.
- M. Aoyagi, N. Minakawa, A. Matsuda, *Nucleosides Nucleotides* **1994**, *13*, 1535–1549.
- E. Casanova, A. I. Hernández, E. M. Priego, S. Liekens, M. J. Camarasa, J. Balzarini, M. J. Pérez-Pérez, *J. Med. Chem.* **2006**, *49*, 5562–5570.
- T. Fujii, T. Saito, H. Hisata, K. Shinbo, *Chem. Pharm. Bull.* **1990**, *38*, 3326–3330.
- N. Minakawa, Y. Sasabuchi, A. Kiyosue, N. Kojima, A. Matsuda, *Chem. Pharm. Bull.* **1996**, *44*, 288–295.
- N. Kohyama, Y. Yamamoto, *Synthesis* **2003**, *17*, 2639–2642.
- A. El-Faragy, A. Ghoneim, *Curr. Org. Chem.* **2009**, *13*, 1842–1847.

- [41] L. De Napoli, G. Di Fabio, A. Messere, D. Montesarchio, G. Piccialli, M. Varra, *J. Chem. Soc. Perkin Trans. 1* **1999**, 3489–3493.
- [42] M. Aljarah, S. Couturier, C. Mathé, C. Périgaud, *Bioorg. Med. Chem.* **2008**, *16*, 7436–7442.
- [43] A. Bracci, G. Colombo, F. Ronchetti, F. Compostella, *Eur. J. Org. Chem.* **2009**, *2009*, 5913–5919.
- [44] S. Stairs, M. W. Pownner, *Synlett* **2017**, *28*, 2650–2654.
- [45] N. Kohyama, T. Katashima, Y. Yamamoto, *Synthesis* **2004**, *17*, 2799–2804.
- [46] B. Catalanotti, L. De Napoli, A. Galeone, L. Mayol, G. Oliviero, G. Piccialli, M. Varra, *Eur. J. Org. Chem.* **1999**, *1999*, 2235–2239.
- [47] L. De Napoli, A. Messere, D. Montesarchio, G. Piccialli, C. Santacroce, M. Varra, *J. Chem. Soc. Perkin Trans. 1* **1994**, *1994*, 923–925.
- [48] X. Ariza, V. Bou, J. Vilarrasa, *J. Am. Chem. Soc.* **1995**, *117*, 3665–3673.
- [49] M. Terrazas, X. Ariza, J. Vilarrasa, *Org. Lett.* **2005**, *7*, 2477–2479.
- [50] M. Terrazas, X. Ariza, J. Vilarrasa, *Tetrahedron Lett.* **2005**, *46*, 5127–5130.
- [51] L. De Napoli, A. Messere, D. Montesarchio, G. Piccialli, M. Varra, *J. Chem. Soc. Perkin Trans. 1* **1997**, *1997*, 2079–2082.
- [52] A. Galeone, L. Mayol, G. Oliviero, G. Piccialli, M. Varra, *Eur. J. Org. Chem.* **2002**, *2002*, 4234–4238.
- [53] R. Narukulla, *Nucleic Acids Res.* **2005**, *33*, 1767–1778.
- [54] G. Oliviero, J. Amato, N. Borbone, S. D'Errico, G. Piccialli, L. Mayol, *Tetrahedron Lett.* **2007**, *48*, 397–400.
- [55] E. S. Carlson, P. Upadhyaya, P. W. Villalta, B. Ma, S. S. Hecht, *Chem. Res. Toxicol.* **2018**, *31*, 358–370.
- [56] S. D'Errico, G. Oliviero, N. Borbone, J. Amato, V. Piccialli, M. Varra, L. Mayol, G. Piccialli, *Molecules* **2013**, *18*, 9420–9431.
- [57] M. Kubota, A. Ono, *Tetrahedron Lett.* **2004**, *45*, 1187–1190.
- [58] M. Fukuoka, S. Shuto, N. Minakawa, Y. Ueno, A. Matsuda, *J. Org. Chem.* **2000**, *65*, 5238–5248.
- [59] S. Shuto, M. Fukuoka, H. Abe, A. Matsuda, *Nucleosides Nucleotides* **2001**, *20*, 461–470.
- [60] T. Kudoh, T. Murayama, M. Hashii, H. Higashida, T. Sakurai, C. Maechling, B. Spiess, K. Weber, A. H. Guse, B. V. L. Potter, M. Arisawa, A. Matsuda, S. Shuto, *Tetrahedron* **2008**, *64*, 9754–9765.
- [61] H. Wu, Z. Yang, L. Zhang, L. Zhang, *New J. Chem.* **2010**, *34*, 956.
- [62] A. Mahal, S. D'Errico, N. Borbone, B. Pinto, A. Secondo, V. Costantino, V. Tedeschi, G. Oliviero, V. Piccialli, G. Piccialli, *Beilstein J. Org. Chem.* **2015**, *11*, 2689–2695.
- [63] S. D'Errico, E. Basso, A. P. Falanga, M. Marzano, T. Pozzan, V. Piccialli, G. Piccialli, G. Oliviero, N. Borbone, *Mar. Drugs* **2019**, *17*, 476.
- [64] S. Shuto, A. Matsuda, *Curr. Med. Chem.* **2004**, *11*, 827–845.
- [65] G. Oliviero, S. D'Errico, N. Borbone, J. Amato, V. Piccialli, G. Piccialli, M. Luciano, *Eur. J. Org. Chem.* **2010**, *2010*, 1517–1524.
- [66] W. M. Odijk, G.-J. Koomen, *J. Chem. Soc. Perkin Trans. 2* **1987**, *1987*, 733.
- [67] M. D. Erlacher, K. Lang, B. Wotzel, R. Rieder, R. Micura, N. Polacek, *J. Am. Chem. Soc.* **2006**, *128*, 4453–4459.
- [68] S. D'Errico, G. Oliviero, N. Borbone, J. Amato, D. D'Alonzo, V. Piccialli, L. Mayol, G. Piccialli, *Molecules* **2012**, *17*, 13036–13044.
- [69] C. C. Streeter, Q. Lin, S. M. Firestine, *Biochemistry* **2019**, *58*, 2260–2268.
- [70] A. K. Zarkin, P. D. Elkins, A. Gilbert, T. L. Jester, H. H. Seltzman, *J. Labelled Compd. Radiopharm.* **2018**, *61*, 820–825.
- [71] N. B. Karalkar, K. Khare, R. Molt, S. A. Benner, *Nucleosides Nucleotides* **2017**, *36*, 256–274.
- [72] Y. Okano, N. Saito-Tarashima, M. Kurosawa, A. Iwabu, M. Ota, T. Watanabe, F. Kato, T. Hishiki, M. Fujimuro, N. Minakawa, *Bioorg. Med. Chem.* **2019**, *27*, 2181–2186.
- [73] K. Ikeuchi, R. Fujii, S. Sugiyama, T. Asakawa, M. Inai, Y. Hamashima, J. H. Choi, T. Suzuki, H. Kawagishi, T. Kan, *Org. Biomol. Chem.* **2014**, *12*, 3813–3815.
- [74] M. Martinell Pedemonte, I. Navarro Munoz, M. Soler Lopez, D. Mormeño Julian, M. Rosol, A. LLeBaria Soldevila, J. Aymami Bofarull, *New Compounds as Hsp90 Inhibitors*, **2009**, WO2009/007399.
- [75] L. De Napoli, A. Messere, D. Montesarchio, G. Piccialli, *J. Org. Chem.* **1995**, *60*, 2251–2253.
- [76] H. Ouchi, T. Asakawa, K. Ikeuchi, M. Inai, J. H. Choi, H. Kawagishi, T. Kan, *Tetrahedron Lett.* **2018**, *59*, 3516–3518.
- [77] G. Oliviero, J. Amato, S. D'Errico, N. Borbone, G. Piccialli, L. Mayol, *Nucleosides Nucleotides* **2007**, *26*, 1649–1652.
- [78] G. Oliviero, J. Amato, N. Borbone, S. D'Errico, G. Piccialli, E. Bucci, V. Piccialli, L. Mayol, *Tetrahedron* **2008**, *64*, 6475–6481.
- [79] S. D'Errico, G. Oliviero, N. Borbone, V. Piccialli, G. Piccialli, *Curr. Protoc. Nucleic Acid Chem.* **2015**, *63*, 1.35.1–1.35.24.
- [80] S. D'Errico, G. Oliviero, V. Piccialli, J. Amato, N. Borbone, V. D'Attri, F. D'Alessio, R. Di Noto, F. Ruffo, F. Salvatore, G. Piccialli, *Bioorg. Med. Chem. Lett.* **2011**, *21*, 5835–5838.
- [81] O. Scudiero, E. Nigro, M. L. Monaco, G. Oliviero, R. Polito, N. Borbone, S. D'Errico, L. Mayol, A. Daniele, G. Piccialli, *J. Enzyme Inhib. Med. Chem.* **2016**, *31*, 748–753.
- [82] G. Oliviero, S. D'Errico, N. Borbone, J. Amato, V. Piccialli, M. Varra, G. Piccialli, L. Mayol, *Tetrahedron* **2010**, *66*, 1931–1936.
- [83] M. Terrazas, X. Ariza, J. Farrás, J. Vilarrasa, *Chem. Commun.* **2005**, 3968–3970.
- [84] A. Rybár, in *Adv. Heterocycl. Chem.*, **2005**, pp. 175–229.
- [85] S. Kumar, N. J. Leonard, *J. Org. Chem.* **1988**, *53*, 3959–3967.
- [86] P. Roques, J. Y. Le Gall, M. Olomucki, L. Lacombe, *J. Org. Chem.* **1992**, *57*, 1579–1585.
- [87] M. Olomucki, J. Y. Le Gall, P. Rocruet, F. Blois, S. Colinart, *Nucleosides Nucleotides* **1985**, *4*, 161–163.
- [88] D. G. I. Petra, R. F. De Boer, G. J. Koomen, N. J. Meeuwenoord, E. Kuyt-Yeheskiely, G. A. Van Der Marel, J. H. Van Boom, *Recl. Trav. Chim. Pays-Bas* **1996**, *115*, 99–102.
- [89] J. P. Devlin, *Can. J. Chem.* **1976**, *54*, 2804–2806.
- [90] P. Sund, L. Kronberg, *Nucleosides Nucleotides* **2008**, *27*, 1215–1226.
- [91] N. Hamamichi, T. Miyasaka, *J. Org. Chem.* **1994**, *59*, 1525–1531.
- [92] C. Temple, C. K. Lussner, J. A. Montgomery, *J. Org. Chem.* **1965**, *30*, 3601–3603.
- [93] T. Karskela, H. Lönnberg, *J. Org. Chem.* **2009**, *74*, 9446–9451.
- [94] P. Rabinsson, A. Baurand, J. P. Cazenave, C. Gachet, M. Retat, B. Spiess, J. J. Bourguignon, *J. Med. Chem.* **2002**, *45*, 962–972.
- [95] K. F. Yip, K. C. Tsou, *Tetrahedron Lett.* **1973**, *14*, 3087–3090.
- [96] F. Seela, H. Rosemeyer, E. Schweinberger, D. Heindl, F. Bergman, *2-Azapurine Compounds and Their Use*, **2001**, WO2001016149.
- [97] J. R. Jefferson, G. A. Jamieson, J. B. Hunt, *J. Med. Chem.* **1987**, *30*, 2013–2016.
- [98] D. Flaherty, P. Balse, K. Li, B. M. Moore, M. B. Doughty, *Nucleosides Nucleotides* **1995**, *14*, 65–76.
- [99] P. Chirakul, J. R. Litzler, S. T. Sigurdsson, *Nucleosides Nucleotides* **2001**, *20*, 1903–1913.
- [100] M. Sako, T. Hayashi, K. Hirota, Y. Maki, *Chem. Pharm. Bull.* **1992**, *40*, 1656–1658.
- [101] J. N. M. Zakiş, K. Ozols, I. Novosjolova, R. Vīlškerstis, A. Mishnev, M. R. Turks, *J. Org. Chem.* **2020**, *85*, 4753–4771.
- [102] A. Sebris, M. Turks, *Chem. Heterocycl. Compd.* **2019**, *55*, 1041–1043.
- [103] C. Temple, C. K. Lussner, J. A. Montgomery, *J. Org. Chem.* **1966**, *31*, 2210–2215.
- [104] H. Rosemeyer, F. Seela, *Chem. Informationsdienst* **1986**, *17*, 131–132.
- [105] D. Ranganathan, F. Farooqui, D. Bhattacharyya, S. Mehrotra, K. Kesavan, *Tetrahedron* **1986**, *42*, 4481–4492.
- [106] D. Ranganathan, R. Rathi, S. Sharma, *J. Org. Chem.* **1990**, *55*, 4006–4010.
- [107] N. J. Leonard, T. R. Henderson, *J. Am. Chem. Soc.* **1975**, *97*, 4990–4999.
- [108] S. Bhattarai, J. Pippel, E. Scaletti, R. Idris, M. Freundlieb, G. Rolshoven, C. Renn, S. Y. Lee, A. Abdelrahman, H. Zimmermann, A. El-Tayeb, C. E. Müller, N. Sträter, *J. Med. Chem.* **2020**, *63*, 2941–2957.
- [109] D. Lee, C. Switzer, *Nucleosides Nucleotides* **2015**, *34*, 424–432.
- [110] K. Kido, H. Inoue, E. Ohtsuka, *Nucleic Acids Res.* **1992**, *20*, 1339–1344.
- [111] S. Costanzi, C. Lamberti, F. R. Portino, R. Volpini, S. Vittori, G. Cristalli, *Nucleosides Nucleotides* **2005**, *24*, 415–418.
- [112] K. Kikugawa, H. Suehiro, M. Ichino, *J. Med. Chem.* **1973**, *16*, 1381–1388.
- [113] T. Fujii, T. Saito, M. Shigeji, J. Chikazawa, *Tetrahedron Lett.* **1991**, *32*, 97–100.
- [114] T. Itaya, K. Ogawa, H. Matsumoto, T. Watanabe, *Chem. Pharm. Bull.* **1980**, *28*, 2522–2527.
- [115] T. Itaya, F. Tanaka, T. Fujii, *Tetrahedron* **1972**, *28*, 535–547.
- [116] T. Fujii, C. C. Wu, T. Itaya, S. Moro, T. Saito, *Chem. Pharm. Bull.* **1973**, *21*, 1676–1682.
- [117] T. Fujii, T. Saito, T. Nakasaka, *Chem. Pharm. Bull.* **1989**, *37*, 3243–3246.
- [118] T. Itaya, K. Ogawa, H. Matsumoto, T. Watanabe, *Chem. Pharm. Bull.* **1980**, *28*, 2819–2824.
- [119] T. Fujii, T. Saito, T. Nakasaka, *Chem. Pharm. Bull.* **1989**, *37*, 2601–2609.
- [120] T. Fujii, T. Itaya, T. Saito, K. Mohri, M. Kawanishi, T. Nakasaka, *Chem. Pharm. Bull.* **1989**, *37*, 1504–1513.
- [121] T. Fujii, T. Saito, Y. Kumazawa, *Chem. Pharm. Bull.* **1990**, *38*, 1392–1395.
- [122] T. Saito, I. Inaoue, T. Fujii, *Chem. Pharm. Bull.* **1990**, *38*, 1536–1547.
- [123] T. Itaya, T. Kanai, M. Shimada, T. Nishikawa, Y. Takada, Y. Hozumi, S. Mori, T. Saito, T. Fujii, *Chem. Pharm. Bull.* **1997**, *45*, 1601–1607.

- [124] T. Fujii, T. Itaya, T. Saito, M. Kawanishi, *Chem. Pharm. Bull.* **1978**, *26*, 1929–1936.
- [125] T. Fujii, T. Saito, K. Kizu, H. Hayashibara, Y. Kumazawa, S. Nakajima, *Heterocycles* **1986**, *24*, 2449–2454.
- [126] R. Storer, G. Gosselin, D. Dukhan, F. Leroy, C. J. Marshall, *Purine Nucleoside Analogues for Treating Flaviviridae Including Hepatitis C*, **2005**, WO2005/009418.
- [127] S. Budow, F. Seela, *Chem. Biodiversity* **2010**, *7*, 2145–2190.
- [128] M. A. Stevens, G. B. Brown, *J. Am. Chem. Soc.* **1958**, *80*, 2759–2762.
- [129] R. L. Svec, L. Furiassi, C. G. Skibinski, T. M. Fan, G. J. Riggins, P. J. Hergenrother, *ACS Chem. Biol.* **2018**, *13*, 3206–3216.
- [130] M. A. Stevens, A. Giner-Sorolla, H. W. Smith, G. B. Brown, *J. Org. Chem.* **1962**, *27*, 567–572.
- [131] P. J. Hergenrother, T. M. Fan, R. L. Svec, *Imidazotetrazine Compounds*, **2020**, WO 2020/033880.
- [132] I. Nowak, J. F. Cannon, M. J. Robins, *Org. Lett.* **2006**, *8*, 4565–4568.
- [133] G. B. Brown, in *Prog. Nucl. Acid Res. Mol. Biol.*, **1968**, pp. 209–255.
- [134] H. Andersson, X. Wang, M. Björklund, R. Olsson, F. Almqvist, *Tetrahedron Lett.* **2007**, *48*, 6941–6944.
- [135] H. Andersson, F. Almqvist, R. Olsson, *Org. Lett.* **2007**, *9*, 1335–1337.
- [136] S. D'Errico, G. Oliviero, N. Borbone, V. Piccialli, V. D'Atri, L. Mayol, G. Piccialli, *Eur. J. Org. Chem.* **2013**, *2013*, 6948–6954.
- [137] S. D'Errico, G. Oliviero, J. Amato, N. Borbone, V. Cerullo, A. Hemminki, V. Piccialli, S. Zaccaria, L. Mayol, G. Piccialli, *Chem. Commun.* **2012**, *48*, 9310.
- [138] S. D'Errico, V. Piccialli, G. Oliviero, N. Borbone, J. Amato, V. D'Atri, G. Piccialli, *Tetrahedron* **2011**, *67*, 6138–6144.
- [139] N. J. Kos, H. Jongejan, H. C. van der Plas, *Tetrahedron* **1987**, *43*, 4841–4848.
- [140] S. Asano, K. Itano, *Nucleosides Nucleotides* **1994**, *13*, 1453–1465.
- [141] G. F. Huang, M. Maeda, T. Okamoto, Y. Kawazoe, *Tetrahedron* **1975**, *31*, 1363–1367.
- [142] S. Asano, K. Itano, K. Kohda, Y. Yamagata, *J. Heterocycl. Chem.* **1996**, *33*, 1115–1121.
- [143] T. Kaiya, M. Ohta, K. Kohda, *Tetrahedron* **1993**, *49*, 8795–8804.
- [144] K. Kohda, M. Yasuda, H. Ukai, K. Baba, Y. Yamagata, Y. Kawazoe, *Tetrahedron* **1989**, *45*, 6367–6374.
- [145] K. Anzai, J. Uzawa, *Can. J. Chem.* **1986**, *64*, 2109–2114.
- [146] K. Anzai, J. Uzawa, *J. Org. Chem.* **1984**, *49*, 5076–5080.
- [147] J. Ammer, M. Baidya, S. Kobayashi, H. Mayr, *J. Phys. Org. Chem.* **2010**, *23*, 1029–1035.
- [148] F. Brotzel, B. Kempf, T. Singer, H. Zipse, H. Mayr, *Chem. A Eur. J.* **2007**, *13*, 336–345.
- [149] J. T. Witkowsiu, G. P. Kreishman, M. P. Schweizer, R. K. Robins, *J. Org. Chem.* **1973**, *38*, 180–182.
- [150] G. S. Chen, C. S. Chen, T. C. Chien, J. Y. Yeh, C. C. Kuo, R. S. Talekar, J. W. Chern, *Nucleosides Nucleotides* **2004**, *23*, 347–359.
- [151] Z. Trávníek, R. Novotná, J. Marek, I. Popa, M. Ipl, *Org. Biomol. Chem.* **2011**, *9*, 5703–5713.
- [152] L. T. Lucas, D. Gatehouse, D. E. G. Shuker, *J. Biol. Chem.* **1999**, *274*, 18319–18326.
- [153] L. T. Lucas, D. Gatehouse, G. D. D. Jones, D. E. G. Shuker, *Chem. Res. Toxicol.* **2001**, *14*, 158–164.
- [154] T. Suzuki, H. Ide, M. Yamada, N. Endo, K. Kanaori, K. Tajima, T. Morii, K. Makino, *Nucleic Acids Res.* **2000**, *28*, 544–551.
- [155] K. Komodziński, J. Nowak, J. Lepczyńska, J. Milecki, B. Skalski, *Tetrahedron Lett.* **2012**, *53*, 2316–2318.
- [156] K. Komodziński, J. Lepczyńska, Z. Gdaniec, L. Bartolotti, B. Delley, S. Franzen, B. Skalski, *Photochem. Photobiol. Sci.* **2014**, *13*, 563–573.
- [157] K. Komodziński, Z. Gdaniec, B. Skalski, *Nucleosides Nucleotides* **2015**, *34*, 235–245.
- [158] L. Lam, J. C. Parham, *J. Am. Chem. Soc.* **1975**, *97*, 2839–2844.
- [159] C. J. Chetsang, C. Makaroff, *Chem.-Biol. Interact.* **1982**, *41*, 235–249.
- [160] A. J. S. C. Vieira, S. Steenken, *J. Phys. Chem.* **1991**, *95*, 9340–9346.
- [161] A. J. S. C. Vieira, S. Steenken, *J. Am. Chem. Soc.* **1990**, *112*, 6986–6994.
- [162] W. G. Humphreys, F. P. Guengerich, *Chem. Res. Toxicol.* **1991**, *4*, 632–636.
- [163] P. Brookes, P. D. Lawley, *J. Chem. Soc.* **1961**, *1961*, 3923–3928.
- [164] L. B. Townsend, R. K. Robins, *J. Am. Chem. Soc.* **1963**, *85*, 242–243.
- [165] M. Brændvang, C. Charnock, L. Gundersen, *Bioorg. Med. Chem. Lett.* **2009**, *19*, 3297–3299.
- [166] M. L. Read, M. Brændvang, P. O. Miranda, L.-L. Gundersen, *Bioorg. Med. Chem.* **2010**, *18*, 3885–3897.
- [167] H. Lönnberg, P. Lehtikoinen, *J. Org. Chem.* **1984**, *49*, 4964–4969.
- [168] E. Darzynkiewicz, J. Stepinski, S. M. Tahara, R. Stolarski, I. Ekiel, D. Haber, K. Neuvonen, P. Lehtikoinen, I. Labadi, H. Lönnberg, *Nucleosides Nucleotides* **1990**, *9*, 599–618.
- [169] J. A. Montgomery, H. J. Thomas, *J. Org. Chem.* **1971**, *36*, 1962–1967.
- [170] K. Kohda, K. Baba, Y. Kawazoe, *Tetrahedron Lett.* **1987**, *28*, 6285–6288.
- [171] J. Altman, D. Ben-Ishai, *J. Heterocycl. Chem.* **1968**, *5*, 679–682.
- [172] K. Dyer, G. E. C. Emmett, D. M. Nye, D. B. Smith, *J. Heterocycl. Chem.* **1973**, *10*, 1043–1046.
- [173] W. R. Cantrell, D. Lovett, T. Engles, B. Anderson, W. E. Bauta, P. C. Wolstenholme-Hogg, *Nucleosides Nucleotides* **2008**, *27*, 901–913.
- [174] G. Ferenc, P. Forgó, Z. Kele, L. Kovács, *Collect. Czech. Chem. Commun.* **2005**, *70*, 85–102.
- [175] R. J. Capon, D. J. Faulkner, *J. Am. Chem. Soc.* **1984**, *106*, 1819–1822.
- [176] H. Wu, H. Nakamura, J. Kobayashi, M. Kobayashi, Y. Ohizumi, Y. Hirata, *Bull. Chem. Soc. Jpn.* **1986**, *59*, 2495–2504.
- [177] E. Cullen, J. P. Devlin, *Can. J. Chem.* **1975**, *53*, 1690–1691.
- [178] K. Ishida, M. Ishibashi, H. Shigemori, T. Sasaki, J. Kobayashi, *Chem. Pharm. Bull.* **1992**, *40*, 766–767.
- [179] G. R. Pettit, Y. Tang, Q. Zhang, G. T. Bourne, C. A. Arm, J. E. Leet, J. C. Knight, R. K. Pettit, J.-C. Chapuis, D. L. Doubek, F. J. Ward, C. Weber, J. N. A. Hooper, *J. Nat. Prod.* **2013**, *76*, 420–424.
- [180] B. Paulsen, K. A. Fredriksen, D. Petersen, L. Maes, A. Matheussen, A.-O. Naemi, A. A. Scheie, R. Simm, R. Ma, B. Wan, S. Franzblau, L.-L. Gundersen, *Bioorg. Med. Chem.* **2019**, *27*, 620–629.
- [181] L. L. Grochowski, H. Xu, K. Leung, R. H. White, *Biochemistry* **2007**, *46*, 6658–6667.
- [182] B. S. Mankodi, D. V. Rege, *Arch. Mikrobiol.* **1966**, *53*, 208–217.
- [183] F. Foor, G. M. Brown, *J. Biol. Chem.* **1975**, *250*, 3545–3551.
- [184] A. Bacher, S. Eberhardt, M. Fischer, K. Kis, G. Richter, *Annu. Rev. Nutr.* **2000**, *20*, 153–167.
- [185] T. Shiota, M. P. Palumbo, L. Tsai, *J. Biol. Chem.* **1967**, *242*, 1961–1969.
- [186] R. M. McCarty, V. Bandarian, *Bioorg. Chem.* **2012**, *43*, 15–25.
- [187] V. Bandarian, C. L. Drennan, *Curr. Opin. Struct. Biol.* **2015**, *35*, 116–124.
- [188] G. M. Williams, M. J. Iatropoulos, J. H. Weisburger, *Exp. Toxicol. Pathol.* **1996**, *48*, 101–111.
- [189] K. S. Gates, *Chem. Res. Toxicol.* **2009**, *22*, 1747–1760.
- [190] S. S. Pujari, N. Tretyakova, *Chem. Res. Toxicol.* **2017**, *30*, 434–452.
- [191] N. R. Jena, P. C. Mishra, *Free Radical Biol. Med.* **2012**, *53*, 81–94.
- [192] M. Dizdaroglu, G. Kirkali, P. Jaruga, *Free Radical Biol. Med.* **2008**, *45*, 1610–1621.
- [193] T. Barbara, *J. Biochem. Mol. Biol.* **2003**, *36*, 12–19.
- [194] M. M. Greenberg, *Acc. Chem. Res.* **2012**, *45*, 588–597.
- [195] X.-Y. Zhang, A. A. Elfarra, *Chem. Res. Toxicol.* **2004**, *17*, 521–528.
- [196] A. S. Groehler, D. Najjar, S. S. Pujari, D. Sangaraju, N. Y. Tretyakova, *Chem. Res. Toxicol.* **2018**, *31*, 885–897.
- [197] M. P. Stone, S. Gopalakrishnan, T. M. Harris, *J. Am. Chem. Soc.* **1989**, *111*, 7232–7239.
- [198] K. L. Brown, J. Z. Deng, R. S. Iyer, L. G. Iyer, M. W. Voehler, M. P. Stone, C. M. Harris, T. M. Harris, *J. Am. Chem. Soc.* **2006**, *128*, 15188–15199.
- [199] M. E. Smela, M. L. Hamm, P. T. Henderson, C. M. Harris, T. M. Harris, J. M. Essigmann, *Proc. Nat. Acad. Sci.* **2002**, *99*, 6655–6660.
- [200] K. Hemminki, K. Peltonen, P. Vodicka, *Chem.-Biol. Interact.* **1989**, *70*, 289–303.
- [201] S. H. Hansen, A. J. Pawlowicz, L. Kronberg, K. B. Gützkow, A. K. Olsen, G. Brunborg, *Mutagenesis* **2018**, *33*, 31–39.
- [202] M. Tomasz, R. Lipman, G. Verdine, K. Nakanishi, *J. Am. Chem. Soc.* **1985**, *107*, 6120–6121.
- [203] F. Gruppi, L. Hejazi, P. P. Christov, S. Krishnamachari, R. J. Turesky, C. J. Rizzo, *Chem. Res. Toxicol.* **2015**, *28*, 1850–1860.
- [204] P. P. Christov, K.-J. Son, C. J. Rizzo, *Chem. Res. Toxicol.* **2014**, *27*, 1610–1618.
- [205] C. E. Crespo-Hernández, R. Arce, *J. Photochem. Photobiol. B* **2004**, *73*, 167–175.
- [206] S. Frelon, T. Douki, J. Cadet, *Free Radical Res.* **2002**, *36*, 499–508.
- [207] A. J. S. C. Vieira, J. P. Telo, R. M. B. Dias, *Methods Enzymol.* **1999**, *300*, 194–201.
- [208] M. Berger, J. Cadet, *Z. Naturforsch. B* **1985**, *40*, 1519–1531.
- [209] A. Rocha, A. H. Bacelar, J. Fernandes, M. F. Proença, M. A. Carvalho, *Synlett* **2014**, *25*, 343–348.
- [210] R. Saladino, E. Mincione, C. Crestini, R. Negri, E. Di Mauro, G. Costanzo, *J. Am. Chem. Soc.* **1996**, *118*, 5615–5619.
- [211] A. Ribeiro, M. A. Carvalho, M. F. Proença, *Eur. J. Org. Chem.* **2009**, *2009*, 4867–4872.
- [212] M. A. Carvalho, S. Esperança, T. Esteves, M. F. Proença, *Eur. J. Org. Chem.* **2007**, *2007*, 1324–1331.

- [213] A. Al-Azmi, B. L. Booth, R. A. Carpenter, A. Carvalho, E. Marrelec, R. G. Pritchard, M. F. J. R. P. Proença, *J. Chem. Soc. Perkin Trans. 1* **2001**, 20, 2532–2537.
- [214] A. H. Bacelar, M. A. Carvalho, M. F. Proença, *Eur. J. Med. Chem.* **2010**, 45, 3234–3239.
- [215] H. M. Berman, R. J. Rousseau, R. W. Mancuso, G. P. Kreishman, R. K. Robins, *Tetrahedron Lett.* **1973**, 14, 3099–3101.
- [216] A. Giner-Sorolla, I. Zimmerman, A. Bendich, *J. Am. Chem. Soc.* **1959**, 81, 2515–2521.
- [217] B. Skalski, R. P. Steer, R. E. Verrall, *J. Am. Chem. Soc.* **1991**, 113, 1756–1762.
- [218] J. Nowak, B. Skalski, Z. Gdaniec, J. Milecki, *Tetrahedron Lett.* **2009**, 50, 1671–1673.
- [219] T. Fujii, K. Ogawa, T. Itaya, T. Date, J. Inagaki, F. Nohara, *Chem. Pharm. Bull.* **1995**, 43, 408–413.
- [220] K. Ogawa, T. Itaya, T. Fujii, *Heterocycles* **1994**, 38, 1225–1228.
- [221] E. Jakobsen, L. L. Gundersen, *Heterocycles* **2000**, 53, 935–940.
- [222] H. Roggen, C. Charnock, L. L. Gundersen, *Tetrahedron* **2009**, 65, 5199–5203.
- [223] Y. L. Lin, R. L. Huang, C. M. Chang, Y. H. Kuo, *J. Nat. Prod.* **1997**, 60, 982–985.
- [224] M. A. Carvalho, M. E. A. Zaki, Y. Álvares, M. F. Proença, B. L. Booth, *Org. Biomol. Chem.* **2004**, 2, 2340–2345.
- [225] W. M. Odijk, G. J. Koomen, *Tetrahedron* **1985**, 41, 1893–1904.
- [226] W. E. McEwen, R. L. Cobb, *Chem. Rev.* **1955**, 55, 511–549.
- [227] J. A. Bull, J. J. Mousseau, G. Pelletier, A. B. Charette, *Chem. Rev.* **2012**, 112, 2642–2713.
- [228] T. Higashino, A. Miyashita, S. Sato, T. Katori, *Chem. Pharm. Bull.* **1987**, 35, 4803–4812.
- [229] T. Kaiya, T. Saga, Y. Yamagata, K. Kohda, *Bioorg. Med. Chem. Lett.* **1998**, 8, 2197–2202.
- [230] D. Martínez, A. Pérez, S. Cañellas, I. Silió, A. Lancho, A. García-Raso, J. J. Fiol, A. Terrón, M. Barceló-Oliver, J. Ortega-Castro, E. Molins, A. Frontera, *J. Inorg. Biochem.* **2019**, 203, 110879.
- [231] J. L. Kelley, J. A. Linn, *J. Org. Chem.* **1986**, 51, 5435–5436.
- [232] V. Kotek, N. Chudíková, T. Tobrman, D. Dvořák, *Org. Lett.* **2010**, 12, 5724–5727.
- [233] T. Tobrman, D. Dvořák, *Synthesis* **2014**, 46, 660–668.

Manuscript received: June 26, 2021
Revised manuscript received: August 9, 2021
Accepted manuscript online: August 10, 2021

Zaķis, J. M.; Leškovskis, K.; Ozols, K.; Kapilinskis, Z.; Kumar, D.; Mishnev, A.; Žalubovskis, R.; Supuran, C. T.; Abdoli, M.; Bonardi, A.; Novosjolova, I.; Turks, M.

Diazidopurine Ring Opening – Synthesis of Tetrazolyimidazole Derivatives

Manuskripts iesniegts Journal of Organic Chemistry

Manuscript submitted to Journal of Organic Chemistry

Diazidopurine Ring Opening – Synthesis of Tetrazolylimidazole Derivatives

Jānis Miķelis Zaķis¹, Kristaps Leškovskis¹, Kristers Ozols¹, Zigfrīds Kapilinskis¹, Dinesh Kumar¹, Anatoly Mishnev², Raivis Žalubovskis^{1,2}, Claudiu T. Supuran³, Morteza Abdoli², Alessandro Bonardi³, Irina Novosjolova^{1*}, Māris Turks^{1*}

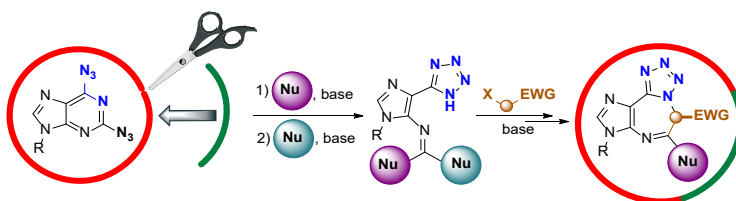
¹ Institute of Chemistry and Chemical Technology, Faculty of Natural Sciences and Technology, Riga Technical University, P. Valdena Str. 3, Riga, LV 1048, Latvia

² Latvian Institute of Organic Synthesis, Aizkraukles Str. 21, Riga, LV-1006, Latvia

³ NEUROFARBA Department, Sezione di Scienze Farmaceutiche, University of Florence, Via Ugo Schiff 6, Sesto Fiorentino, 50019 Florence, Italy

* Correspondence: Irina.Novosjolova@rtu.lv, Maris.Turks@rtu.lv

ABSTRACT: A protocol for the synthesis of tetrazolylimidazole derivatives by introducing two heteroatom nucleophiles at the purine C2 position has been developed. 9-Substituted 2,6-diazidopurines undergo S_NAr reaction with heteroatom nucleophiles at their C2 due to azide-tetrazole tautomeric equilibrium. The obtained 6-azido-2-heteroatom-substituted purine derivatives are susceptible to yet another nucleophile attack at C2, which leads to various tetrazolylimidazoles as ring-opening products. The latter contains an amine side chain, which is highly decorated in the form of carbonimidate, carbamimidate, or their thio analogs. The product yields are in the range of 36–88%. The tetrazole moiety of the ring-opening compounds can be *N*-alkylated and further used in cyclization providing fused 1,4-diazepines (50-62% yields), thus demonstrating a useful purine ring expansion protocol.



INTRODUCTION

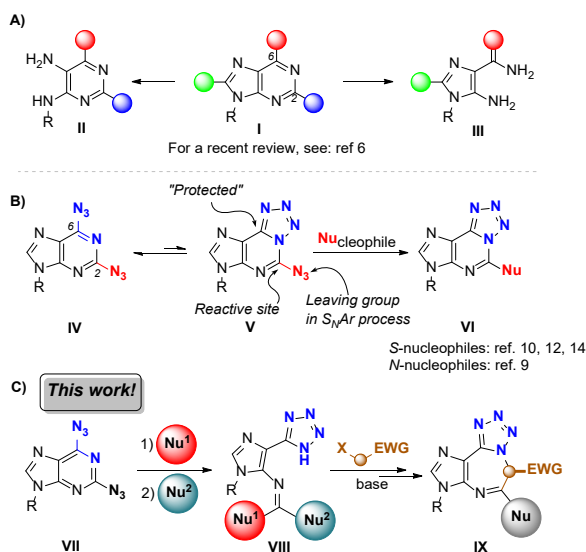
(Het)Aryl-(Het)Aryl structural unit is a well-established motif in medicinal chemistry and materials science. In most of the cases, it is achieved by transition metal-catalyzed cross-coupling reactions. However, cross-coupling of two nitrogen-rich heterocycles still remains a

challenging task due to unwanted coordination with the catalyst and due to the instability of several heterocyclic organometallic(metalloid) coupling partners.¹⁻⁵

In this context, purine ring-opening offers an alternative approach, leading either to substituted imidazoles or pyrimidines depending on the ring-opening site (Scheme 1, A).^{6,7} To construct a new heterobiaryl in the traditional setup one would need to transform the cleaved purine ring depending on the functional handles. Yet, if one would be able to combine azide-tetrazole equilibrium⁸ with purine ring-opening, then a single reaction would provide tetrazolylimidazole derivatives. Indeed, we⁹⁻¹² and others¹³ have observed that 2,6-diazidopurines are capable to undergo azide-tetrazole equilibrium (for example, **IV** ↔ **V** in Scheme 1, B). This in turn can lead to unusual C2-selectivity for purine S_NAr reactions,^{10-12,14} even if for 2,6-disubstituted substrate, which contains two identical leaving groups, the C6-position is more susceptible towards nucleophile attack.^{10,12,15-23} During our previous research on C2-selective S_NAr reactions of 2,6-diazidopurine scaffold we have sometimes encountered non-purine side products, especially if strong bases were used to facilitate the nucleophilic substitution process. Structure elucidation of all products and careful process design allowed us to create regio- and chemoselective C2-substitution of 2,6-diazidopurine derivatives (**IV** ↔ **V** → **VI**, Scheme 1, B).¹⁴ This reactivity can be extended to the controlled next nucleophile attack at the C2-position in compounds of type **VI**, which would result in the purine ring-opening (**VII** → **VIII**, Scheme 1, C). Hence, we report here the developed protocol for the synthesis of tetrazolylimidazole derivatives **VIII** bearing highly functionalized carbonimidate and carbamimidate side chains, including their thio-variations. We have also developed a ring-closing procedure of product **VIII** that results in novel tricyclic imidazo[4,5-*f*]tetrazolo[1,5-*d*][1,4]diazepines **IX** (Scheme 1, C).

To the best of our knowledge, there are only a scarce few reports on mono-azido pyrimidine ring-opening resulting in tetrazolyl systems^{13,24,25}, but our approach demonstrates the synthetic potential of simple purine starting materials in the synthesis of tetrazolylimidazoles with broad substrate scope and many variations on exocyclic nitrogen substitution pattern. The latter also permits ring closure due to the existing N=C functionality, which can be considered a form of skeletal editing of the original purine core.²⁶⁻³⁷ It should be mentioned that such tetrazolylimidazoles of type **VIII** can be considered as tetrazole isosteres³⁸⁻⁴⁰ of acadesine and AICAR (5-aminoimidazole-4-carboxamide ribonucleotide) that are adenosine regulating agents and known as “Exercise in a Pill”.^{41,42} The newly developed ring-opening-closing strategy could help facilitate new drug discovery, especially since the formed 1,4-diazepines

structures play a prominent role in medicinal chemistry.^{43–49} Additionally, imidazodiazepines, which are represented by natural product azepinomycin,^{50,51} belong to the class of homopurine alkaloids or ring-expanded (“fat”) purines^{52–54} that are known as guanase (EC 3.5.4.3) inhibitors.^{55–58}



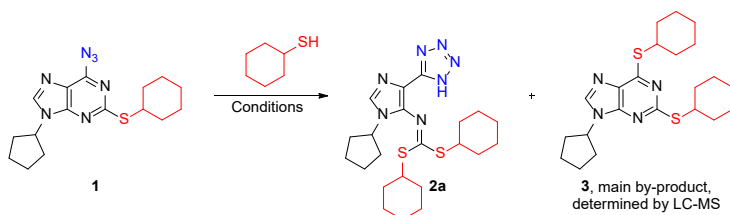
Scheme 1. Pyrimidine ring transformations in purines

RESULTS AND DISCUSSION

At the outset of the method development, we established the optimized conditions for the title reaction (Table 1). Starting material **1** was obtained by our previously reported method,^{10,12,14,59} which includes C2-selective S_NAr reaction of the corresponding thiol with 2,6-diazidopurine derivative. Cyclohexanethiol was chosen as a reactant to avoid possible E/Z-isomers for the expected carbonimidodithioate moiety of the product. Weaker bases (e.g. K_2CO_3) or those formally providing protic equilibrium conditions (DBU, entry 3, Table 1) gave either very low conversion of the starting material or resulted in unwanted C6-addition product **3**. Next, stronger bases were tested, and the ring-opening product **2a** formed in moderate 55–62% yields (entries 1 and 2, Table 1). At this point, different solvents were screened with 1.5–1.6 equivalents of base (NaH or KOtBu, entries 4–11, Table 1). In these experiments, DMF appeared to be the superior solvent. Variation of the amount of base either way also did not increase the yield (entries 12–13, Table 1). Finally, the impact of temperature on reaction yield was tested (entries 14–15, Table 1), and the best qNMR yield of 68% for product **2a** was

achieved at 0 °C. It is known that lowering the temperature shifts the equilibrium towards the tetrazole tautomer,^{60–63} which correlates with our results. Since DMF was also the most suitable solvent for the synthesis of starting material **1**¹⁴ purine ring-opening step can be nicely combined with the initial S_NAr substitution in a one-pot reaction with a stepwise addition of different bases.

Table 1. Optimization of reaction conditions for ring-opening of compound **1** with cyclohexanethiol

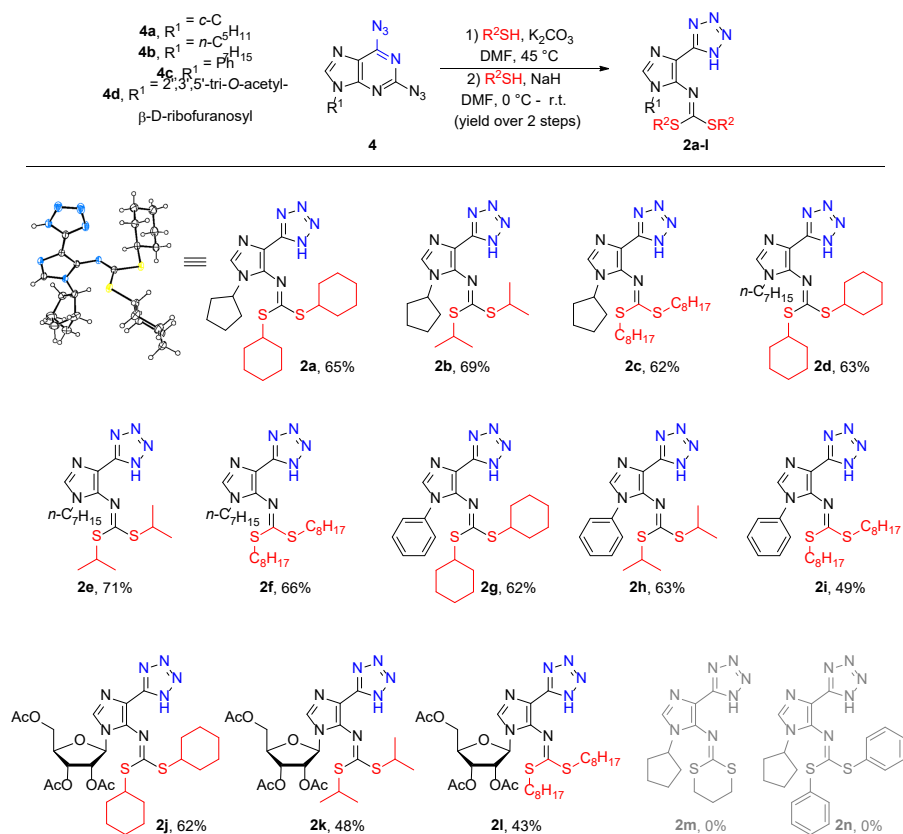


entry	solvent	base (eq)	temp (°C)	2a yield (%)*	Starting material 1 (%)*
1	DMF	NaH (1.5)	r.t.	55	12
2	DMF	KOtBu (1.5)	r.t.	62	4
3	DMF	DBU (1.5)	0	0	55
4	toluene	KOtBu (1.6)	r.t.	4	68
5	MeCN	NaH (1.5)	r.t.	8	76
6	MeCN	KOtBu (1.6)	r.t.	50	20
7	THF	NaH (1.5)	r.t.	43	40
8	THF	KOtBu (1.6)	r.t.	36	30
9	<i>i</i> -PrOH	KOtBu (1.6)	r.t.	34	24
10	DMSO	KOtBu (1.6)	r.t.	64	2
11	NMP	NaH (1.5)	r.t.	39	21
12	DMF	NaH (0.9)	r.t.	44	32
13	DMF	KOtBu (2.5)	r.t.	54	7
14	DMF	NaH (1.5)	0	68	5
15	DMF	KOtBu (1.6)	0	64	8

* qNMR yield of a crude reaction mixture using 1,2,3-trimethoxybenzene as an internal standard

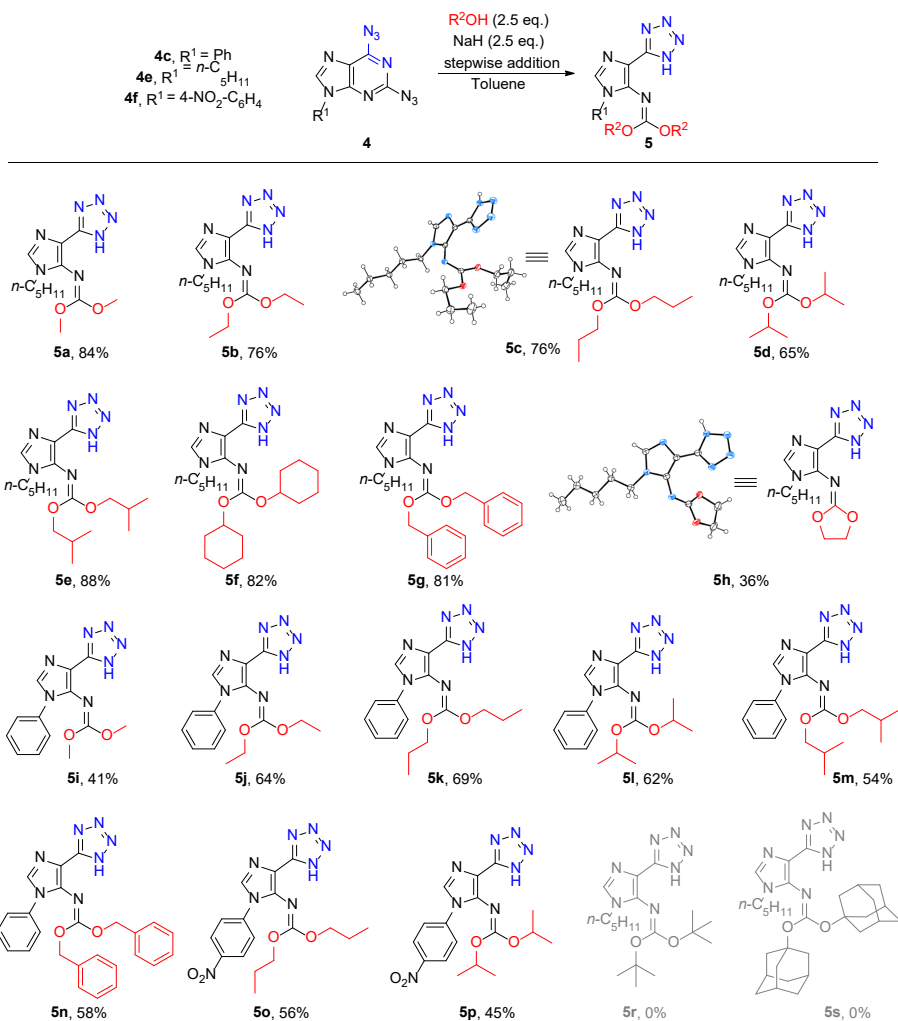
Having found the optimal reaction conditions, we examined the scope of the diazidopurine ring-opening reaction with thiolates (Scheme 2). Purines with *N*-9 alkyl, aryl, and ribosyl substituents provided the desired products in up to 71% yield. We have also demonstrated that

the ester protecting groups can be maintained for nucleoside analogs if controlled amounts of thiol and base are used (products **2j-l**). Reactions proceeded smoothly with both primary and secondary thiols. However, the synthesis of cyclized product **2m** with dithiane was unsuccessful under the explored reaction conditions. Also, aromatic thiols were unreactive towards ring-opening (envisaged compound **2n**), most probably due to the better-leaving group capacity of the thiophenolate ion. The main competing reaction in all cases was the formation of a 2,6-disubstituted product, which was separated from the main product by column chromatography.



Scheme 2. Scope of 2,6-diazidopurine **4a-d** ring-opening with thiolates; synthesis of starting materials **4b**⁹ and **4d**¹⁸ are previously reported. Crystallographic data for **2a** have been deposited with the Cambridge Crystallographic Data Center as a supplementary publication No. CCDC-2284095.

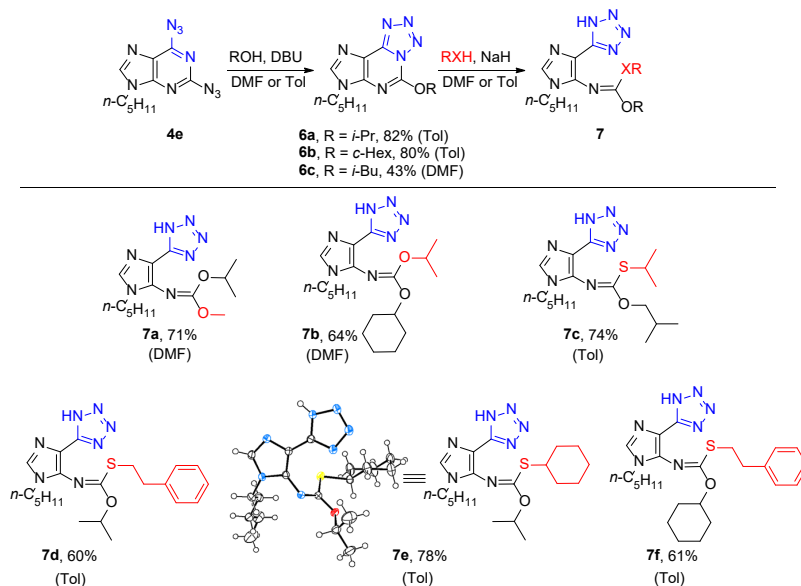
Afterwards, we focused our attention on the purine ring-opening with alkoxides in a symmetrical fashion, by adding at least two equivalents of the same alcohol in a step-wise process. This time toluene turned out to be the optimal choice of solvent for the one-pot stepwise addition of *O*-nucleophiles to 2,6-diazidopurines (screening of reaction conditions is described in ESI Table S1). It is interesting to note that conditions, that worked well for thiol nucleophiles (NaH / DMF, Scheme 2), gave mostly S_NAr product at C6 instead of the expected ring-opening. As alkoxides required a “special treatment”, we briefly reexamined also bases, but NaH still outperformed any other reagent. We were surprised to find out that KO^tBu in toluene displayed decent 9:1 selectivity towards C-6 substitution products. Finally, we found that a dropwise addition of the nucleophile was crucial for achieving higher selectivity towards C-2 substitution and further ring-opening. Then, the optimal conditions (NaH in toluene) were implemented to explore the substrate scope of the diazidopurine ring-opening with alkoxides (Scheme 3). Many primary and secondary alcohols were suitable for the reaction, and corresponding products (**5a–g**) were obtained in good yields. Furthermore, we obtained the cyclized ring-opening product **5h** using ethylene glycol. Purines bearing phenyl group at the *N*-9 position were also successfully transformed into ring-opening products (**5i–p**), although the yields were lower. At this point of method development, the reaction scope is limited only to aliphatic alcohols. Also, reactions with sterically demanding alcohols, such as adamantanol and *t*-butanol, were unfruitful. The lower-end yields are due to poor regioselectivity and hydrolysis of the ring-opening products to the respective carbamates.



Scheme 3. Scope of ring-opening of 2,6-diazidopurines **4c,e,f** with alkoxides; synthesis of starting material **4e**⁹ is previously reported. Crystallographic data for **5c** and **5h** have been deposited with the Cambridge Crystallographic Data Center as supplementary publications No. CCDC-2280801 and CCDC-2280803, respectively.

Next, we wanted to see if we can access bifunctional ring-opening products containing thio and alkoxy units. The initial attempts starting from 5-alkylthio-7-alkyl-7*H*-tetrazolo[5,1-*i*]purine were unsuccessful so instead we sought if we can access the bifunctional ring products from 5-alkoxy-7-pentyl-7*H*-tetrazolo[5,1-*i*]purine **6a-c** (tetrazole tautomers of 6-azido-2-alkoxy-purines) (Scheme 4).

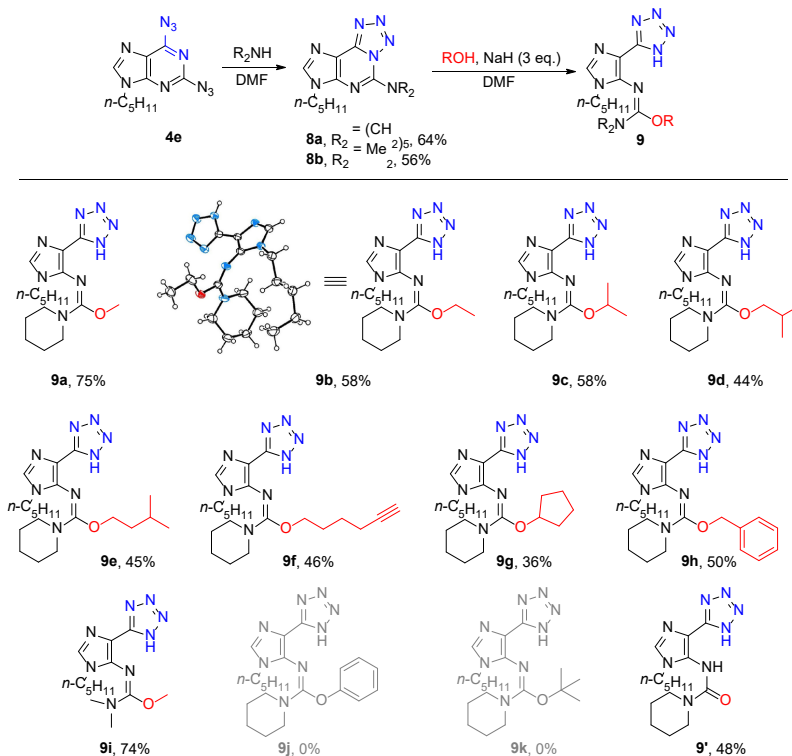
We soon realized that this transformation required some solvent fine-tuning. On some occasions previously found ring-opening conditions (NaH/DMF) gave satisfactory yields (products **7a,b**), but others required toluene as a solvent to reach similar yields. Also, the first S_NAr process (**4e** → **6a-c**) with alkoxide nucleophiles proceeded better in toluene. With this adjustment done, we were able to isolate purine ring-opening products by adding sequentially secondary and primary alcohol (**7a**), two different secondary alcohols (**7b**), and alcohol-first / thiol-second (**7c-f**). Both primary (phenylethanethiol) and secondary (*i*-PrSH, *c*-HexSH) alkanethiols can be used. Based on the obtained X-ray results we propose that a more electronegative group is located *anti* to imidazole ring (compounds **7e** and **9b**, Schemes 4 and 5, respectively). In the case of alkoxides, we compared the Taft inductive σ^* constants for alkoxy substituents ($\sigma^*(\text{OMe}) = 1.79$; $\sigma^*(\text{OiPr}) = 1.61$; $\sigma^*(\text{OcHex}) = 1.88$)⁶⁴⁻⁶⁶ and propose that product **7a** is with *Z* and product **7b** with *E* configuration (Scheme 4).



Scheme 4. Synthesis of 6-azido-2-alkoxy-purines **6a-c** and their ring-opening with alkoxides and thiolates; synthesis of starting material **4e**⁹ is previously reported. Crystallographic data for **7e** have been deposited with the Cambridge Crystallographic Data Center as a supplementary publication No. CCDC-2280805.

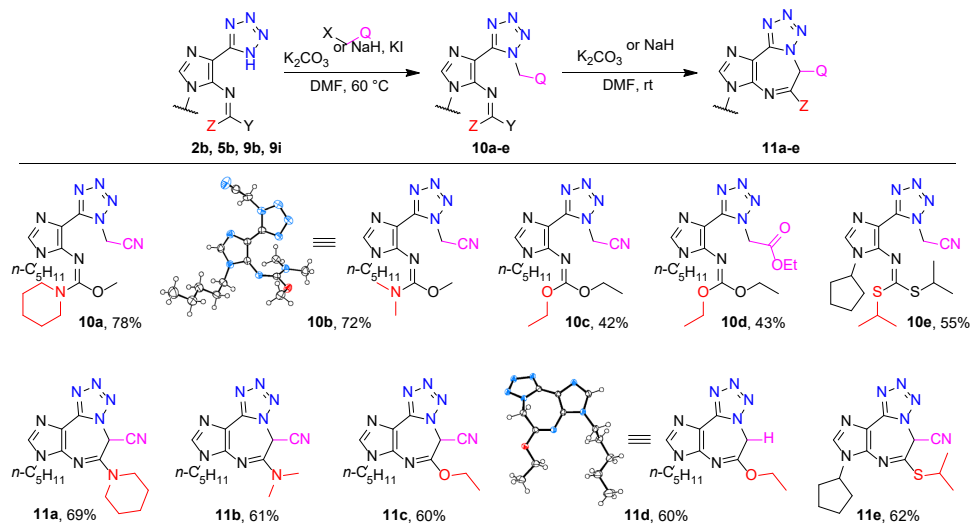
Next, we set out to explore the use of nitrogen nucleophiles for the ring-opening transformation. The S_NAr reactions of 2,6-diazidopurine **4e** with piperidine and dimethylamine proceed

smoothly in DMF without any other base additive similar to our previous reports (Scheme 5).^{9,11} It appeared that compounds of type **8a,b** were unreactive towards the second *N*-nucleophile, including their deprotonated versions. Fortunately, compounds **8a,b** were reactive towards alkoxides as *O*-nucleophiles, and expected carbamimidates **9a-i** were obtained (Scheme 5). A brief condition screening was accomplished (Table S2, see ESI), and again the NaH/DMF system proved to be the most effective one. Both primary and secondary alcohols gave the desired products, and the reaction with the least sterically hindered pair of substituents (such as Me₂N- and MeO-) provided the best outcome as demonstrated by product **9i**, which was obtained in 74% yield. However, phenol/phenoxide was unreactive in this reaction and the reaction with *tert*-butanol yielded a hydrolysis product – carboxamide **9'**, which was also the main by-product in other reactions within this scope, if piperidinyl-substituted starting material **8a** was used.



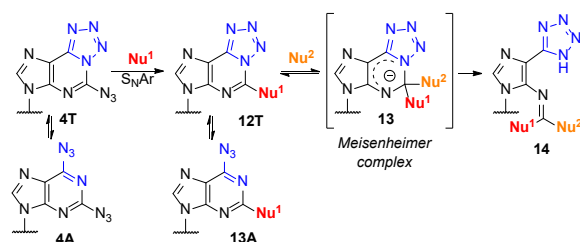
Scheme 5. Ring-opening of 2-amino-6-azido-purines (better represented as their tetrazole tautomer) **8** with alkoxides. Crystallographic data for **9b** have been deposited with the Cambridge Crystallographic Data Center as a supplementary publication No. CCDC-2284093.

After establishing the synthetic methodology for the purine ring-opening we were intrigued about the possibility to recycle these products and to obtain fused 1,4-diazepine structures as homopurine analogs. For this reason, we performed tetrazole *N*-alkylation either with 2-chloroacetonitrile or ethyl bromoacetate, which yielded intermediates **10a-e** (Scheme 6). The acidic methylene group could then be used to create an internal *C*-nucleophile, which would attack carbamimidate, carbonimidate, or carbonimidodithioate functionality and form the C-C bond. Implementation of this concept provided a fully substituted fused 1,4-diazepine core in products **11**, with the only exception being compound **11d** *en route* to which ester hydrolysis and decarboxylation occurred in the reaction mixture. There are some reports on purine ring expansion to imidazodiazepines,^{55–58,67–69} yet these approaches use standard AICAR intermediate. In these literature reports 5-amino group of 5-aminoimidazole-4-carboxamide moiety is reacted with C₂ synthon followed by cyclization upon reaction with 4-carboxamide group. Our approach requires only additional C₁-fragment for ring closure as the original purine carbon atom residing in carbonimidate, carbamimidate and carbonimidodithioate functionality is also used for the ring closure. Moreover, this is the first report on the formation of tricyclic imidazo[4,5-*f*]tetrazolo[1,5-*d*][1,4]diazepine core.



Scheme 6. Synthesis of tetrazole fused diazepines **11** using leaving group activity row RS>RO>RN in ring closing reactions. Crystallographic data for **10b** and **11d** have been deposited with the Cambridge Crystallographic Data Center as supplementary publications No. CCDC-2284094 and CCDC-2280807, respectively.

The proposed mechanism of the purine ring-opening reaction is depicted in Scheme 7. We propose that the transformation sequence is initiated by azide-tetrazole equilibrium directed regioselective S_NAr reaction leading to substitution product **12**. This is followed by the attack of a second nucleophile and the formation of Meisenheimer complex **13**. Evidently, the tetrazole moiety is the best leaving group in the intermediate **13** and thus the ring-opening occurs. The proposed Meisenheimer complex in this situation is very likely highly stabilized due to the electron-withdrawing properties of the fused tetrazole ring as shown in similar cases studied by us recently.⁷⁰



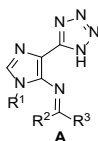
Scheme 7. Proposed mechanism for 2,6-diazidopurine ring-opening with nucleophiles.

With several dozens of novel tetrazolylimidazoles in hand, we decided to test conceptually their prospective application in medicinal chemistry. Imidazoles and tetrazoles belong to the group of azoles that are well-established as ligands for metal coordination.^{71–76} On the other hand, among the enzymes that are regarded as drug targets, a prominent group is metalloenzymes, and within this group, zinc enzymes constitute the largest number.^{77,78} Thus, we have chosen human carbonic anhydrases (CAs, EC 4.2.1.1) as representative zinc enzymes and have tested the inhibitory capacity of selected purine ring-opening products against the isoforms CA I, II, IV, and IX (**Table 2**). Both ubiquitous cytosolic CA I and CA II being off-targets^{79,80} were not inhibited by the studied compounds.

The membrane-associated isozyme hCA IV^{81–83} was moderately inhibited with K_I s being in the low micromolar range. The compounds studied can be divided into two groups with $K_I < 3 \mu\text{M}$ and less active compounds with $K_I > 3 \mu\text{M}$. Compounds belonging to the most active group (**2d**, **2l**, **5g**, **5k**, **5o**, **7d**, and **7e**) inhibited CA IV with K_I s values in the range from 2.38 μM to 2.93 μM , where the most active compound was **7d**. The less active compounds (**2a**, **2g**, **5b**, **7b**, **9a**, **9f**, **9h**, and **9i**) inhibited CA IV with K_I values in the range from 3.01 to 4.98 μM .

Cancer associated CA IX isoform^{79,80} was inhibited in the micromolar range by most of the inhibitors. Compounds **2a**, **2d**, **2g**, and **7e** showed weaker inhibition with K_i values in the range from 2.96 to 5.76 μM . The rest of the compounds can be divided into two groups, where less active compounds (**2l**, **9h**, **7d**, and **9i**) inhibited CA IX with K_i s in the range from 0.47 to 0.79 μM . The most active inhibitors (**5b**, **5g**, **5k**, **5o**, **7b**, **9a**, and **9f**) are several times more active having K_i s values below 0.25 μM and ranging from 0.14 to 0.25 μM . Even though the latter compounds are an order weaker inhibitors if compared to nonselective acetazolamide (**AAZ**), they exhibit notable selectivity towards CA IX over CA I and CA II, and good selectivity over CA IV. For instance, the most active inhibitor **5k** having $K_i = 0.14 \mu\text{M}$ shows selectivity CA IV/CA IX = 21.

Table 2. Inhibition data of human CA isoforms CA I, II, IV and IX with compounds **A** and the standard sulfonamide inhibitor acetazolamide (**AAZ**) by a stopped-flow CO_2 hydrase assay.⁸⁴



Comp.	R ¹	R ²	R ³	K _i (μM) ^a			
				hCA I	hCA II	hCA IV	hCA IX
2a	<i>c</i> -C ₃ H ₉ -	<i>c</i> -C ₆ H ₁₁ -S-	<i>c</i> -C ₆ H ₁₁ -S-	>100	>100	3.48	0.58
2d	<i>n</i> -C ₇ H ₁₅ -	<i>c</i> -C ₆ H ₁₁ -S-	<i>c</i> -C ₆ H ₁₁ -S-	>100	>100	2.55	0.39
2g	C ₆ H ₅ -	<i>c</i> -C ₆ H ₁₁ -S-	<i>c</i> -C ₆ H ₁₁ -S-	>100	>100	3.89	0.30
2l	<i>Tris</i> -OAc-Rib	<i>n</i> -C ₈ H ₁₇ -S-	<i>n</i> -C ₈ H ₁₇ -S-	>100	>100	2.93	0.48
5b	<i>n</i> -C ₅ H ₁₁ -	CH ₃ CH ₂ O-	CH ₃ CH ₂ O-	>100	>100	4.02	0.18
5g	<i>n</i> -C ₅ H ₁₁ -	C ₆ H ₅ CH ₂ O-	C ₆ H ₅ CH ₂ O-	>100	>100	2.47	0.23
5k	C ₆ H ₅ -	CH ₃ (CH ₂) ₂ O-	CH ₃ (CH ₂) ₂ O-	>100	>100	2.91	0.14
5o	4-NO ₂ -C ₆ H ₄ -	CH ₃ (CH ₂) ₂ O-	CH ₃ (CH ₂) ₂ O-	>100	>100	2.67	0.25
7b	<i>n</i> -C ₅ H ₁₁ -	<i>c</i> -C ₆ H ₁₁ -O-	(CH ₃) ₂ CHO-	>100	>100	3.10	0.16
7d	<i>n</i> -C ₅ H ₁₁ -	(CH ₃) ₂ CHO-	C ₆ H ₅ CH ₂ CH ₂ -S-	>100	>100	2.38	0.47
7e	<i>n</i> -C ₅ H ₁₁ -	(CH ₃) ₂ CHO-	<i>c</i> -C ₆ H ₁₁ -S-	>100	>100	2.54	0.51
9a	<i>n</i> -C ₅ H ₁₁ -	(CH ₂) ₅ N-	CH ₃ O-	>100	>100	4.21	0.20
9f	<i>n</i> -C ₅ H ₁₁ -	(CH ₂) ₅ N-	HC≡C(CH ₂) ₄ O-	>100	>100	3.69	0.21
9h	<i>n</i> -C ₅ H ₁₁ -	(CH ₂) ₅ N-	C ₆ H ₅ CH ₂ O-	>100	>100	4.52	0.62
9i	<i>n</i> -C ₅ H ₁₁ -	(CH ₃) ₂ N-	CH ₃ O-	>100	>100	4.98	0.79
AAZ	-	-	-	0.25	0.013	0.074	0.025

^a Mean from 3 different assays, by a stopped-flow technique (errors were in the range of ± 5 -10 % of the reported values).

In summary, we have developed a practical synthetic method, which provides divergent heteroatom-containing tetrazolylimidazoles *via* a ring-opening reaction of diazidopurines. The

preparative procedure employs widely available purines as substrates and uses common nucleophilic reagents. The intrinsic azide-tetrazole equilibrium of azidopurine substrates acts as a driving force for this transformation. Firstly, the tetrazole tautomer at the C-6 position blocks the S_NAr process at C-6 and activates the system towards nucleophile attack at C-2. Secondly, the fused tetrazole acts as an electron-withdrawing moiety and internal leaving group, thus enhancing the ring-opening of the pyrimidine cycle. The library of tetrazolyimidazoles bearing carbonimidodithioate (16 examples, 43–78%), carbonimidate (18 examples, 36–88%), and carbimidate (10 examples, 36–75%) side chains is obtained. The obtained ring-opening products are easily converted into tricyclic imidazo[4,5-*f*]tetrazolo[1,5-*d*][1,4]diazepines that represent a novel class of ring-expanded homopurines. This is a useful addition to the toolbox of purine skeletal editing, which sets a way for synthesis of novel diazepine analogs to well-known CNS drugs. Last but not least, the developed heteroatom-rich ring-opening products were found to be active as metalloenzyme inhibitors. A potent inhibitory activity of these compounds against cancer associated human carbonic anhydrase IX isoform was discovered. To the best of our knowledge, variously substituted tetrazolyimidazoles are new chemotype in the realm of carbonic anhydrases inhibitors, thus giving a solid ground for further investigations in terms of medicinal chemistry.

EXPERIMENTAL SECTION

General information

Reagents purchased from *Alfa Aesar*, *Acros Organics*, and *Sigma Aldrich* were used as received. All solvents were distilled before use. DMF, NMP, and DMSO were distilled from CaH₂ under reduced pressure. THF and toluene were distilled from Na under an Ar atmosphere. Upasil 60 silica gel (40–63 μm, 60 Å) was used for column chromatography. Chromatography was monitored by TLC (*E. Merck Kieselgel 60 F₂₅₄*) and visualized with UV light. HPLC analysis was performed using an *Agilent Technologies 1200 Series* system equipped with *Agilent G1315C DAD* (λ = 190–400 nm) and an *X-Bridge C18* column, 4.6 × 150 mm, particle size 3.5 μm, with a flow rate of 1 mL/min, using 0.1% TFA/H₂O and MeCN for the mobile phase. The IR spectra were recorded in KBr or hexachlorobutadiene (4000–2000 cm⁻¹) and paraffin oil (2000–450 cm⁻¹) with a *Perkin-Elmer Spectrum 100 BX* FTIR spectrometer. High-resolution mass (HRMS) (electrospray ionization (ESI)) was recorded with an *Agilent 1290 Infinity* series ultra-high pressure liquid chromatography connected to an *Agilent 6230* time-of-flight (TOF) mass spectrometer or (atmospheric pressure chemical ionization (APCI)) on a *7TsolariX XR*

(Bruker Daltonik GmbH) Fourier transform ion cyclotron resonance mass spectrometer equipped with an APCI source. Single-crystal diffraction data were collected on an *XtaLAB Synergy-S Dualflex* diffractometer (Rigaku Corporation, Tokyo, Japan) equipped with a *HyPix6000* detector and micro-focus sealed X-ray tube (Rigaku, Tokyo, Japan) using Cu K α radiation ($\lambda = 1.54184 \text{ \AA}$). Single crystals were fixed with oil in a nylon loop of a magnetic *CryoCap* and set on a goniometer head. The samples were cooled down to 150 K, and ω -scans were performed with a step size of 0.5° . Data collection and reduction were performed with *CrysAlisPro* 1.171.40.35a software (Oxford Diffraction Ltd., Abingdon, UK). The structure solution and refinement were performed with SHELXT⁸⁵ and SHELXL⁸⁶ software, which are part of the *CrysAlisPro* and *Olex2* suites. The H atoms were positioned geometrically and treated as riding on their parent C or N atoms. Molecular graphics were prepared using *ORTEP3* for Windows⁸⁷ and *Mercury*⁸⁸. The *PLATON*⁸⁹ tool was used for the geometrical calculations. ¹H and ¹³C NMR spectra were recorded on *Bruker Avance 300* and *Bruker Avance 500* spectrometers (Bruker Nordic AB, Solna, Sweden). Chemical shifts (δ) were reported in ppm, and coupling constants (J) in Hz. Residual solvent peaks (¹H) or (¹³C) were used as the reference (for ¹H-NMR: CDCl₃ $\delta = 7.26$ ppm, DMSO-*d*₆ $\delta = 2.50$ ppm, MeOD-*d*₄ $\delta = 3.31$ ppm, and for ¹³C-NMR: CDCl₃ $\delta = 77.16$ ppm, DMSO-*d*₆ $\delta = 39.52$ ppm, MeOD-*d*₄ $\delta = 49.1$ ppm). Multiplicities are reported as s (singlet), d (doublet), t (triplet), q (quartet), and m (multiplet). An applied photophysics stopped-flow instrument has been used for assaying the CA-catalysed CO₂ hydration activity. Phenol red (at a concentration of 0.2 mM) was used as an indicator, working at the absorbance maximum of 557 nm, with 20 mM Hepes (pH 7.5) as a buffer and 20 mM Na₂SO₄ (for maintaining constant the ionic strength), following the initial rates of the CA-catalysed CO₂ hydration reaction for a period of 10 – 100 s. The CO₂ concentrations ranged from 1.7 to 17 mM for the determination of the kinetic parameters and inhibition constants. For each inhibitor, at least six traces of the initial 5 – 10% of the reaction have been used for determining the initial velocity. The uncatalyzed rates were determined in the same manner and subtracted from the total observed rates. Stock solutions of inhibitor (0.1 mM) were prepared in distilled-deionized water, and dilutions up to 0.01 nM were done thereafter with the assay buffer. Inhibitor and enzyme solutions were preincubated together for 15 min at room temperature before assay to allow for the formation of the E-I complex. The inhibition constants were obtained by nonlinear least-squares methods using PRISM 3 and the Cheng-Prusoff equation, as reported earlier,^{90–94} and represent the mean from at least three different

determinations. All CA isoforms were recombinant ones obtained in-house as reported earlier.^{95–100}

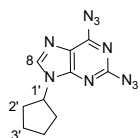
Synthesis methods and characterization of obtained compounds

Diazides **4b**, **4d**, and **4e** were prepared according to the literature procedures.^{9,18}

General procedure for the synthesis of diazidopurines **4a**, **4c** and **4f** (see ESI Scheme S1)

To a round bottom flask, 2,6-dichloropurine (1.0 eq.) and NaN_3 (4.0 eq.) were added, dissolved in acetone/water mixture (10:1 ratio), and stirred at 50 °C overnight. After reaction completion (monitored by HPLC), the reaction was cooled to r.t., and the solvent evaporated under reduced pressure. Water (40 mL) was added to the mixture and extracted with DCM (3×20 mL). The combined organic phase was washed with saturated NaCl solution (2×10 mL), dried over anhydrous Na_2SO_4 , filtered, and evaporated under reduced pressure to yield the product.

2,6-Diazido-9-cyclopentyl-9H-purine (**4a**)

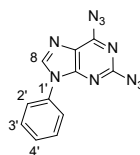


Prepared according to general procedure using 2,6-dichloro-9-cyclopentyl-9H-purine (2.01 g, 7.82 mmol, 1.0 eq.), NaN_3 (2.04 g, 31.4 mmol, 4.0 eq.) and acetone/water (30:3 mL). Yield: 2.03 g, 96%. Colourless solid, $R_f = 0.57$

(Tol/MeCN = 3:1). IR ν (cm^{-1}): 2962, 2880, 2133, 2122, 1608, 1569, 1356, 1224,

997, 788. $^1\text{H-NMR}$ (500 MHz, CDCl_3) δ (ppm): 7.93 (s, 1H, H-C(8)), 4.88 (quintet, 1H, $^3J = 7.0$ Hz, 1×H-C(1')), 2.34–2.24 (m, 2H, (-CH₂-)), 2.02–1.90 (m, 4H, 2×(-CH₂-)), 1.86–1.75 (m, 2H, (-CH₂-)). $^{13}\text{C}\{^1\text{H}\}\text{NMR}$ (126 MHz, CDCl_3) δ (ppm): 155.7, 154.0, 153.7, 142.1, 121.8, 56.5, 32.7, 24.1. HRMS (ESI): calculated for [$\text{C}_{10}\text{H}_{10}\text{N}_{10} + \text{H}^+$] 271.1163, found 271.1138.

2,6-Diazido-9-phenyl-9H-purine (**4c**)

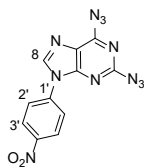


Prepared according to general procedure using 2,6-dichloro-9-phenyl-9H-purine¹⁰¹ (1.20 g, 4.52 mmol, 1.0 eq.), NaN_3 (1.18 g, 18.08 mmol, 4.0 eq.) and acetone/water (40:4 mL). Yield: 1.22 g, 97%. Colourless solid, $R_f = 0.63$

(Tol/MeCN = 3:1). IR ν (cm^{-1}): 2941, 2853, 2135, 2125, 1612, 1515, 1400,

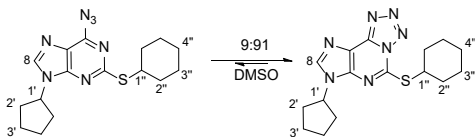
1353, 1267, 1181, 1042. $^1\text{H-NMR}$ (500 MHz, CDCl_3) δ (ppm): 8.18 (s, 1H, H-C(8)), 7.68 (d, 2H, $^3J = 7.8$ Hz, 2×H-C(2')), 7.58 (t, 2H, $^3J = 7.6$ Hz, 2×H-C(3')), 7.48 (t, 1H, $^3J = 7.6$ Hz, H-C(4')). $^{13}\text{C}\{^1\text{H}\}\text{NMR}$ (126 MHz, CDCl_3) δ (ppm): 156.8, 154.5, 153.6, 142.6, 134.2, 130.1, 128.8, 123.4, 121.9. HRMS (ESI): calculated for [$\text{C}_{11}\text{H}_6\text{N}_{10} + \text{H}^+$] 279.0850, found 279.0873.

2,6-Diazido-9-(4-nitrophenyl)-9H-purine (**4f**)



Prepared according to general procedure using 2,6-dichloro-9-(4-nitrophenyl)-9H-purine¹⁰¹ (1.00 g, 3.22 mmol, 1.0 eq.), NaN₃ (0.84 g, 12.9 mmol, 4.0 eq.) and acetone/water (30:3 mL). Yield: 1.00 g, 96%. Colourless solid, R_f = 0.50 (Tol/MeCN = 3:1 + 0.5% AcOH). IR ν (cm⁻¹): 3102, 2132, 1589, 1569, 1507, 1349, 1269, 1163, 1110. ¹H-NMR (500 MHz, CDCl₃) δ (ppm): 8.46 (d, 2H, ³J = 9.2 Hz, 2×H-C(2')), 8.28 (s, 1H, H-C(8)), 8.01 (d, 2H, ³J = 9.2 Hz, 2×H-C(3')). ¹³C{¹H}NMR (126 MHz, CDCl₃) δ (ppm): 157.4, 155.1, 153.4, 147.0, 141.3, 139.4, 125.7, 123.2, 122.1. HRMS (ESI): calculated for [C₁₁H₅N₁₁O₂ + H⁺] 324.0700, found 324.0705.

6-Azido-2-(cyclohexylthio)-9-cyclopentyl-9H-purine (1)



Cyclohexanethiol (0.50 mL, ρ = 0.95 g/cm³, 4.09 mmol, 1.1 eq.) was added to a suspension of K₂CO₃ (660 mg, 4.78 mmol, 1.3 eq.) in DMF (10 mL) and stirred at 20 °C for 20 min.

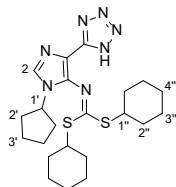
Next, 9-cyclopentyl-2,6-diaza-9H-purine (4a) (1.00 g, 3.63 mmol, 1.0 eq.) in DMF (10 mL) was added, and the reaction mixture was stirred at 45 °C temperature for 16 h (monitored by HPLC). Toluene (150 mL) was added to the reaction mixture, and the resulting solution was washed with H₂O (20 mL), followed by an aqueous 13% NaCl solution (10 mL). The aqueous layers were combined and back-extracted with toluene (3×4 mL). The combined organic phase was washed with saturated NaCl solution (2×8 mL), dried over anhydrous Na₂SO₄, filtered, and evaporated under vacuum. Crude mixture purified by silica gel column chromatography (Tol/MeCN, 0%→20%). Yield: 1.04 g, 82%. Colourless solid, R_f = 0.34 (Tol/MeCN = 3:1). IR ν (cm⁻¹): 3089, 2939, 2924, 2854, 1628, 1490, 1448, 1361, 1218, 1042, 934. ¹H-NMR (500 MHz, DMSO-*d*₆) δ (ppm): 8.53 (s, 1H, H-C(8)), 5.02 (quintet, 1H, ³J = 7.7 Hz, H-C(1')), 4.08 (tt, 1H, ³J = 10.4 Hz, ³J = 3.6 Hz, H-C(1'')), 2.30–2.12 (m, 6H, 3×(-CH₂-)), 1.98–1.89 (m, 2H, (-CH₂-)), 1.83–1.61 (m, 7H, 3×(-CH₂-), (H_a-CH)), 1.54–1.44 (m, 2H, (-CH₂-)), 1.41–1.34 (m, 1H, (H_b-CH)). ¹³C{¹H}NMR (126 MHz, DMSO-*d*₆) δ (ppm): 145.5, 145.0, 142.8, 142.0, 117.8, 57.2, 44.7, 31.9, 31.8, 25.5, 25.0, 24.0. HRMS (ESI): calculated for [C₁₆H₂₁N₇S + H⁺] 344.1652, found 344.1677.

General procedure for the synthesis of tetrazolyl-imidazolyl-carbonimidodithioates 2a-i

Thiol (1.1 eq.) was added to a suspension of K₂CO₃ (1.5 eq.) in DMF (5 mL) and stirred at 20 °C for 20 min. Next, 2,6-diaza-9H-purine derivative 4 (1.0 eq.) in DMF (5 mL) was added, and the reaction mixture was stirred at 45 °C overnight (monitored by HPLC). After complete conversion of the starting material was achieved, the reaction mixture was cooled to 0 °C.

Separately second portion of thiol (1.2 eq.) was added to a suspension of NaH (1.2 eq.) (57–63% suspension in mineral oil) in DMF (4 mL) and stirred at 20 °C for 20 min. The resulting mixture was added to the cooled purine solution, and the combined mixture was stirred at 0 °C for 1 h, then at 20 °C for 30 min. If starting material was still present (monitored by HPLC), additional thiol (0.2 eq.) and NaH (0.3 eq.) were added. The reaction was quenched with AcOH (0.75 mL) and diluted with toluene (200 mL). The mixture was washed with H₂O (1×20 mL) and aqueous 13% NaCl solution (2×10 mL). To the combined aqueous layer AcOH (0.25 mL) was added and back-extracted with toluene (3×8 mL). The combined organic phase was washed with saturated NaCl solution (2×10 mL), dried over anhydrous Na₂SO₄, filtered, and evaporated under vacuum. The crude reaction mixture was purified by silica gel column chromatography.

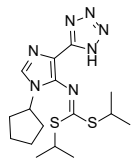
Dicyclohexyl (1-cyclopentyl-4-(1*H*-tetrazol-5-yl)-1*H*-imidazol-5-yl)carbonimidodithioate (2a)



Prepared according to general procedure using cyclohexanethiol (2×0.25 mL, $\rho = 0.95 \text{ g/cm}^3$, 2.04 mmol, 1.1 eq.), K₂CO₃ (380 mg, 2.75 mmol, 1.5 eq.), 2,6-diazidopurine **4a** (500 mg, 1.85 mmol, 1.0 eq.) and NaH (53 mg, 2.21 mmol, 1.2 eq.). Column chromatography gradient: Tol/MeCN

0%→20% (+0.5% AcOH). Yield: 560 mg, 65%. Colourless solid, $R_f = 0.27$ (Tol/MeCN = 3:1 (+0.5% AcOH)). IR ν (cm⁻¹): 2974, 2929, 2852, 1616, 1582, 1447, 1261, 1199, 1070, 981, 958. ¹H-NMR (300 MHz, CDCl₃, 50 °C) δ (ppm): 7.95 (s, 1H, H-C(2)), 4.37 (quintet, 1H, ³*J* = 6.8 Hz, H-C(1')), 3.84 (brs, 2H, 2×H-C(*c*-Hex)), 2.27–2.04 (m, 6H, 3×(-CH₂-)), 2.02–1.85 (m, 4H, 2×(-CH₂-)), 1.85–1.65 (m, 6H, 3×(-CH₂-)), 1.65–1.20 (m, 12H, 6×(-CH₂-)). ¹³C{¹H}NMR (126 MHz, CDCl₃, 50 °C) δ (ppm): 175.0, 149.8, 139.1, 133.0, 111.3, 57.0, 46.2, 33.6, 33.1, 26.1, 25.7, 24.1. HRMS (ESI): calculated for [C₂₂H₃₃N₇S₂ + H⁺] 460.2312, found 460.2290.

Diisopropyl (1-cyclopentyl-4-(1*H*-tetrazol-5-yl)-1*H*-imidazol-5-yl)carbonimidodithioate (2b)

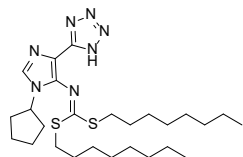


Prepared according to general procedure using *i*-propanethiol (2×0.18 mL, $\rho = 0.82 \text{ g/cm}^3$, 2×1.94 mmol, 2×1.1 eq.), K₂CO₃ (380 mg, 2.75 mmol, 1.5 eq.), 2,6-diazidopurine **4a** (500 mg, 1.85 mmol, 1.0 eq.) and NaH (53 mg, 2.21 mmol, 1.2 eq.). Column chromatography gradient: Tol/MeCN

0%→10% (+0.5% AcOH). Yield: 482 mg, 69%. Colourless solid, $R_f = 0.28$ (Tol/MeCN = 3:1 (+0.5% AcOH)). IR ν (cm⁻¹): 2965, 2922, 2868, 1607, 1563, 1451, 1359, 1156, 1070, 986, 946, 831. ¹H-NMR (500 MHz, CDCl₃, 50 °C) δ (ppm): 7.97 (s, 1H, H-C(2)), 4.38 (quintet, 1H, ³*J* = 7.0 Hz, H-

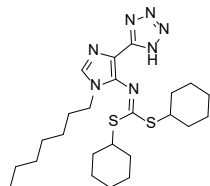
C(1'), 4.00 (brs, 2H, 2×H-C(1'')), 2.25–2.15 (m, 2H, (-CH₂-)), 2.01–1.88 (m, 4H, 2×(-CH₂-)), 1.81–1.70 (m, 2H, (-CH₂-)), 1.41 (brs, 12H, 4×(H₃C-(2'')). ¹³C{¹H}NMR (126 MHz, CDCl₃, 50 °C) δ (ppm): 175.4, 149.8, 139.1, 133.2, 111.4, 56.9, 38.5, 33.1, 24.2, 23.6. HRMS (ESI): calculated for [C₁₆H₂₅N₇S₂ + H⁺] 490.2781, found 490.2784.

Diocetyl (1-cyclopentyl-4-(1H-tetrazol-5-yl)-1H-imidazol-5-yl)carbonimidodithioate (2c)



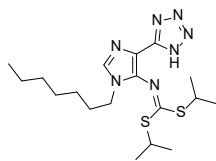
Prepared according to general procedure using *n*-octanethiol (2×0.36 mL, ρ = 0.84 g/cm³, 2×2.07 mmol, 2×1.1 eq.), K₂CO₃ (380 mg, 2.75 mmol, 1.5 eq.), 2,6-diazidopurine **4a** (500 mg, 1.85 mmol, 1.0 eq.) and NaH (53 mg, 2.21 mmol, 1.2 eq.). Column chromatography gradient: Tol/MeCN 0%→14% (+0.5% AcOH). Yield: 600 mg, 62%. Colourless solid, R_f = 0.27 (Tol/MeCN = 3:1 (+0.5 % AcOH)). IR ν (cm⁻¹): 2959, 2925, 2853, 1616, 1569, 1452, 1201, 1071, 985, 960, 817. ¹H-NMR (500 MHz, CDCl₃, 50 °C) δ (ppm): 7.97 (s, 1H, H-C(2)), 4.37 (quintet, 1H, ³J = 6.9 Hz, H-C(1')), 3.19 (brs, 4H, 2×H₂-C(1'')), 2.24–2.15 (m, 2H, (-CH₂-)), 2.00–1.87 (m, 4H, 2×(-CH₂-)), 1.81–1.65 (m, 6H, 3×(-CH₂-)), 1.43–1.34 (m, 4H, 2×(-CH₂-)), 1.34–1.22 (m, 16H, 8×(-CH₂-)), 0.87 (t, 6H, ³J = 6.9 Hz, 2×H₃-C(8'')). ¹³C{¹H}NMR (126 MHz, CDCl₃, 50 °C) δ (ppm): 176.2, 149.8, 139.0, 133.2, 111.5, 57.0, 33.1, 33.0, 31.9, 29.3, 29.2, 29.2, 29.0, 24.2, 22.7, 14.1. HRMS (ESI): calculated for [C₂₆H₄₅N₇S₂ + H⁺] 520.3251, found 520.3246.

Dicyclohexyl (1-heptyl-4-(1H-tetrazol-5-yl)-1H-imidazol-5-yl)carbonimidodithioate (2d)



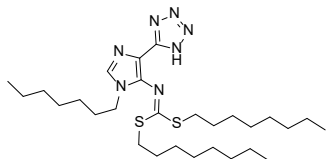
Prepared according to general procedure cyclohexanethiol (2×0.22 mL, ρ = 0.95 g/cm³, 2×1.80 mmol, 2×1.1 eq.), K₂CO₃ (320 mg, 2.32 mmol, 1.4 eq.), 2,6-diazidopurine **4b** (500 mg, 1.67 mmol, 1.0 eq.) and NaH (47 mg, 1.96 mmol, 1.2 eq.). Column chromatography gradient: Tol/MeCN 0%→10% (+0.5% AcOH). Yield: 512 mg, 63%. Colourless solid, R_f = 0.27 (Tol/MeCN = 3:1 (+0.5 % AcOH)). ¹H-NMR (500 MHz, CDCl₃, 50 °C) δ (ppm): 7.93 (s, 1H, H-C(2)), 3.93–3.74 (m, 4H, 2×H-C(1'')), H₂-C(1'), 2.30–2.04 (m, 4H, 2×(-CH₂-)), 1.85–1.67 (m, 6H, 3×(-CH₂-)), 1.65–1.55 (m, 2H, (-CH₂-)), 1.54–1.20 (m, 18H, 9×(-CH₂-)), 0.88 (t, 3H, ³J = 6.8 Hz, H₃C(7')). ¹³C{¹H}NMR (126 MHz, CDCl₃) δ (ppm): 174.9, 149.8, 138.8, 135.4, 111.4, 45.9, 45.1, 33.4, 31.7, 30.3, 28.9, 26.7, 26.1, 25.7, 22.7, 14.2. HRMS (ESI): calculated for [C₂₄H₃₉N₇S₂ + H⁺] 490.2781, found 490.2764.

Diisopropyl (1-heptyl-4-(1H-tetrazol-5-yl)-1H-imidazol-5-yl)carbonimidodithioate (2e)



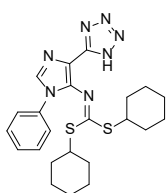
Prepared according to general procedure using *i*-propanethiol (2×0.17 mL, $\rho = 0.82 \text{ g/cm}^3$, 2×1.83 mmol, 2×1.1 eq.), K_2CO_3 (320 mg, 2.32 mmol, 1.4 eq.), 2,6-diazidopurine derivative **4b** (500 mg, 1.67 mmol, 1.0 eq.) and NaH (47 mg, 1.96 mmol, 1.2 eq.). Column chromatography gradient: Tol/MeCN 0%→10% (+0.5% AcOH). Yield: 483 mg, 71%. Colourless solid, $R_f = 0.26$ (Tol/MeCN = 3:1 (+0.5 % AcOH)). IR ν (cm^{-1}): 2964, 2922, 2864, 1611, 1563, 1501, 1367, 1250, 1174, 1075, 981, 948. $^1\text{H-NMR}$ (500 MHz, CDCl_3 , 50 °C) δ (ppm): 7.94 (s, 1H, H-C(2)), 4.00 (brs, 2H, 2×H-C(1'')), 3.84 (t, 2H, $^3J = 7.3 \text{ Hz}$, $\text{H}_2\text{-C}(1')$), 1.81 (quintet, 2H, $^3J = 7.1 \text{ Hz}$, $\text{H}_2\text{-C}(2')$), 1.54–1.22 (m, 20H, 4×(-CH₂-), 4×H₃C-(2'')), 0.88 (t, 3H, $^3J = 6.8 \text{ Hz}$, H₃C-(7')). $^{13}\text{C}\{^1\text{H}\}\text{NMR}$ (126 MHz, CDCl_3 , 50 °C) δ (ppm): 175.5, 149.8, 138.9, 135.4, 111.4, 45.2, 38.5, 31.7, 30.3, 28.9, 26.7, 23.5, 22.7, 14.1. HRMS (ESI): calculated for [$\text{C}_{18}\text{H}_{31}\text{N}_7\text{S}_2 + \text{H}^+$] 410.2155, found 410.2171.

Diocyl (1-heptyl-4-(1H-tetrazol-5-yl)-1H-imidazol-5-yl)carbonimidodithioate (2f)



Prepared according to general procedure using *n*-octanethiol (2×0.32 mL, $\rho = 0.84 \text{ g/cm}^3$, 2×1.84 mmol, 2×1.1 eq.), K_2CO_3 (320 mg, 2.32 mmol, 1.4 eq.), 2,6-diazidopurine **4b** (500 mg, 1.67 mmol, 1.0 eq.) and NaH (47 mg, 1.96 mmol, 1.2 eq.). Column chromatography gradient: Tol/MeCN 0%→14% (+0.5% AcOH). Yield: 600 mg, 66%. Colourless solid, $R_f = 0.34$ (Tol/MeCN = 3:1 (+0.5 % AcOH)). IR ν (cm^{-1}): 2957, 2923, 2854, 1610, 1563, 1513, 1377, 1237, 1073, 980, 950. $^1\text{H-NMR}$ (500 MHz, CDCl_3 , 50 °C) δ (ppm): 7.94 (s, 1H, H-C(2)), 3.84 (t, 2H, $^3J = 7.2 \text{ Hz}$, $\text{H}_2\text{-C}(1')$), 3.18 (m, 4H, 2×H₂-C(1'')), 1.86–1.76 (m, 2H, (-CH₂-)), 1.71 (brs, 4H, 2×(-CH₂-)), 1.44–1.20 (m, 28H, 14×(-CH₂-)), 0.92–0.83 (m, 9H, 3×(H₃C-)). $^{13}\text{C}\{^1\text{H}\}\text{NMR}$ (126 MHz, CDCl_3 , 50 °C) δ (ppm): 176.4, 149.8, 138.8, 135.3, 111.4, 45.2, 33.0, 31.9, 31.8, 30.3, 29.3, 29.3, 29.2, 29.0, 28.9, 26.7, 22.8, 22.7, 14.1, 14.1. HRMS (ESI): calculated for [$\text{C}_{28}\text{H}_{51}\text{N}_7\text{S}_2 + \text{H}^+$] 550.3720, found 550.3743.

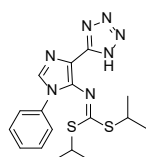
Dicyclohexyl (1-phenyl-4-(1H-tetrazol-5-yl)-1H-imidazol-5-yl)carbonimidodithioate (2g)



Prepared according to general procedure using cyclohexanethiol (2×0.24 mL, $\rho = 0.95 \text{ g/cm}^3$, 2×1.96 mmol, 2×1.1 eq.), K_2CO_3 (360 mg, 2.61 mmol, 1.5 eq.), 2,6-diazidopurine **4c** (500 mg, 1.80 mmol, 1.0 eq.) and NaH (52 mg, 2.18 mmol, 1.2 eq.). Column chromatography gradient: Tol/MeCN 0%→8.5% (+0.5% AcOH). Yield: 525 mg, 62%. Colourless solid, $R_f = 0.34$ (Tol/MeCN = 3:1 (+0.5 % AcOH)). IR ν (cm^{-1}): 2972, 2928, 2854, 1615, 1562, 1501, 1270, 1198, 1077, 961, 953. $^1\text{H-NMR}$ (500 MHz, CDCl_3 , 50 °C) δ (ppm): 8.14 (s, 1H, H-C(2)), 7.53–

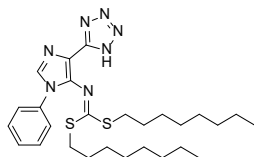
7.42 (m, 5H, 5×H-C(Ph)), 3.73 (brs, 2H, 2×H-C(1'')), 2.03–1.93 (m, 4H, 2×(-CH₂-)), 1.71–1.61 (m, 4H, 2×(-CH₂-)), 1.58–1.50 (m, 2H, (-CH₂-)), 1.40–1.17 (m, 10H, 5×(-CH₂-)). ¹³C{¹H}NMR (126 MHz, CDCl₃, 50 °C) δ (ppm): 175.5, 149.7, 139.1, 135.5, 135.0, 129.6, 129.0, 125.4, 112.0, 46.2, 33.4, 26.0, 25.7. HRMS (ESI): calculated for [C₂₃H₂₉N₇S₂ + H⁺] 468.1999, found 468.2015.

Diisopropyl (1-phenyl-4-(1H-tetrazol-5-yl)-1H-imidazol-5-yl)carbonimidodithioate (2h)



Prepared according to general procedure using *i*-propanethiol (2×0.18 mL, ρ = 0.82 g/cm³, 2×1.94 mmol, 2×1.1 eq.), K₂CO₃ (360 mg, 2.61 mmol, 1.5 eq.), 2,6-diazidopurine **4c** (500 mg, 1.80 mmol, 1.0 eq.) and NaH (52 mg, 2.18 mmol, 1.2 eq.). Column chromatography gradient: Tol/MeCN 0%→8% (+0.5% AcOH). Yield: 440 mg, 63%. Colourless solid, R_f = 0.30 (Tol/MeCN = 3:1 (+0.5 % AcOH)). IR ν (cm⁻¹): 3119, 2967, 2927, 1620, 1568, 1498, 1194, 1081, 959, 948, 775, 692. ¹H-NMR (500 MHz, CDCl₃, 50 °C) δ (ppm): 8.14 (s, 1H, H-C(2)), 7.54–7.43 (m, 5H, 5×H-C(Ph)), 3.90 (brs, 2H, 2×H-C(1'')), 1.31 (d, 12H, ³J = 6.8 Hz, 4×H₃C-(2'')). ¹³C{¹H}NMR (126 MHz, CDCl₃, 50 °C) δ (ppm): 176.1, 149.6, 139.1, 135.4, 134.9, 129.7, 129.1, 125.3, 111.9, 38.6, 23.4. HRMS (ESI): calculated for [C₁₇H₂₁N₇S₂ + H⁺] 388.1373, found 388.1372.

Diocetyl (1-phenyl-4-(1H-tetrazol-5-yl)-1H-imidazol-5-yl)carbonimidodithioate (2i)



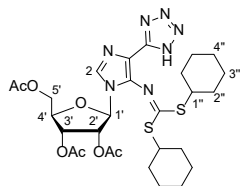
Prepared according to general procedure using *n*-octanethiol (2×0.34 mL, ρ = 0.84 g/cm³, 2×1.95 mmol, 2×1.1 eq.), K₂CO₃ (360 mg, 2.61 mmol, 1.5 eq.), 2,6-diazidopurine **4c** (500 mg, 1.80 mmol, 1.0 eq.) and NaH (52 mg, 2.18 mmol, 1.2 eq.). Column chromatography gradient: Tol/MeCN 0%→4% (+0.5% AcOH). Yield: 465 mg, 49%. Colourless solid, R_f = 0.33 (Tol/MeCN = 3:1 (+0.5 % AcOH)). IR ν (cm⁻¹): 2921, 2851, 1611, 1565, 1499, 1382, 1191, 1078, 961, 778, 694. ¹H-NMR (500 MHz, CDCl₃) δ (ppm): 8.18 (s, 1H, H-C(2)), 7.55–7.41 (m, 5H, 5×H-C(Ph)), 3.08 (t, 4H, ³J = 7.2 Hz, 2×H₂-C(1'')), 1.57 (quintet, 4H, ³J = 7.2 Hz, 2×H₂-C(2'')), 1.33–1.17 (m, 20H, 10×(-CH₂-)), 0.86 (t, 6H, ³J = 7.2 Hz, 2×H₃C-(8'')). ¹³C{¹H}NMR (126 MHz, CDCl₃) δ (ppm): 176.9, 149.6, 138.8, 135.5, 134.7, 129.7, 129.0, 125.0, 111.9, 32.8, 31.9, 29.2, 29.1, 29.0, 28.9, 22.8, 14.2. HRMS (ESI): calculated for [C₂₇H₄₁N₇S₂ + H⁺] 528.2938, found 528.2935.

General procedure for the synthesis of ribofuranosyl-tetrazolyl-imidazolyl-carbonimidodithioates 2j-l

Thiol (1.05 eq.) was added to a suspension of K₂CO₃ (1.5 eq.) in DMF (5 mL) and stirred at 20 °C for 20 min. Next, 2,6-diazidopurine **4d** (1.0 eq.) in DMF (5 mL) was added, and the

reaction mixture was stirred at 40 °C overnight. After full conversion of the starting material was achieved (monitored by HPLC), the reaction mixture was cooled to 0 °C. Separately second portion of thiol (1.05 eq.) was added to a suspension of NaH (1.3 eq.) in DMF (4 mL) and stirred at 20 °C for 20 min. The resulting mixture was added to the cooled purine solution, and the combined mixture was stirred at 0 °C for 1 h, then at 20 °C for 30 min. If starting material was still present (monitored by HPLC), additional thiol (0.2 eq.) and NaH (0.3 eq.) were added. The reaction was quenched with AcOH (0.75 mL) and diluted with toluene (200 mL). The mixture was washed with H₂O (1×20 mL) and then with aqueous 13% NaCl solution (2×10 mL). To the combined aqueous layer AcOH (0.25 mL) was added and back-extracted with toluene (3×10 mL). The combined organic phase was washed with saturated NaCl solution (2×10 mL), dried over anhydrous Na₂SO₄, filtered, and evaporated under vacuum. The crude reaction mixture was purified by silica gel column chromatography.

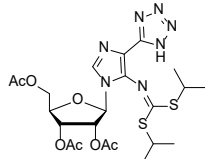
Dicyclohexyl (1-(2',3',5'-tri-*O*-acetyl-β-D-ribofuranosyl)-4-(1*H*-tetrazol-5-yl)-1*H*-imidazol-5-yl)carbonimidodithioate (2j)



Prepared according to general procedure using cyclohexanethiol (2×0.20 mL, $\rho = 0.95 \text{ g/cm}^3$, 1.14 mmol, 1.05 eq.), K₂CO₃ (220 mg, 1.59 mmol, 1.5 eq.), 2,6-diazidopurine **4d** (500 mg, 1.09 mmol, 1.0 eq.) and NaH (33 mg, 1.38 mmol, 1.3 eq.). Column chromatography gradient: Tol/MeCN 0%→25% (+0.5% AcOH). Yield: 440 mg, 62%.

Colourless solid, $R_f = 0.25$ (Tol/MeCN = 3:1 (+0.5% AcOH)). IR ν (cm⁻¹): 2930, 2853, 1749, 1615, 1562, 1448, 1370, 1222, 1070, 948, 952. ¹H-NMR (300 MHz, CDCl₃, 50 °C) δ (ppm): 8.16 (s, 1H, H-C(2)), 5.77 (d, 1H, ³J_{1'-2'} = 5.0 Hz, H-C(1')), 5.63 (t, 1H, ³J_{1'-2'} = ³J_{2'-3'} = 5.0 Hz, H-C(2')), 5.43–5.39 (m, 1H, H-C(3')), 4.38 (s, 3H, H-C(4'), H₂-C(5')), 3.95–3.73 (m, 2H, 2×H₂-C(1')), 3.08, 2.10, 2.10 (s, 9H, 3×H₃-C(Ac)), 2.19–2.05 (m, 4H, 2×(-CH₂-)), 1.76–1.67 (m, 4H, 2×(-CH₂-)), 1.62–1.54 (m, 2H, (-CH₂-)), 1.51–1.35 (m, 8H, 4×(-CH₂-)), 1.31–1.23 (m, 2H, (-CH₂-)). ¹³C{¹H}NMR (126 MHz, CDCl₃, 50 °C) δ (ppm): 177.6, 170.6, 169.3, 169.0, 149.4, 138.4, 133.6, 111.5, 87.1, 80.2, 70.3, 62.9, 46.5, 33.5 (2C), 26.1, 26.0, 25.7, 20.9 (2C), 20.5, 20.5. HRMS (ESI): calculated for [C₂₈H₃₉N₇O₇S₂ + H⁺] 650.2425, found 650.2402.

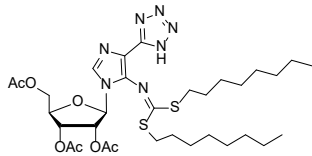
Diisopropyl (1-(2',3',5'-tri-*O*-acetyl-β-D-ribofuranosyl)-4-(1*H*-tetrazol-5-yl)-1*H*-imidazol-5-yl)carbonimidodithioate (2k)



Prepared according to general procedure using *i*-propanethiol (2×0.10 mL, $\rho = 0.82 \text{ g/cm}^3$, 2×1.09 mmol, 2×1.0 eq.), K_2CO_3 (220 mg, 1.59 mmol, 1.5 eq.), 2,6-diazidopurine **4d** (500 mg, 1.09 mmol, 1.0 eq.) and NaH (33 mg, 1.38 mmol, 1.3 eq.). Column chromatography gradient: Tol/MeCN 4%→20% (+0.5% AcOH). Yield: 299 mg, 48%. Colourless

solid, $R_f = 0.24$ (Tol/MeCN = 3:2 (+0.5 % AcOH)). IR ν (cm^{-1}): 2972, 2929, 2868, 1748, 1615, 1562, 1368, 1221, 1054, 985, 950. $^1\text{H-NMR}$ (500 MHz, CDCl_3 , 50 °C) δ (ppm): 8.16 (s, 1H, H-C(2)), 5.78 (d, 1H, $^3J_{1'2'} = 5.0 \text{ Hz}$, H-C(1')), 5.63 (t, 1H, $^3J_{1'2'} = ^3J_{2'3'} = 5.0 \text{ Hz}$, H-C(2')), 5.41 (t, 1H, $^3J_{2'3'} = 5.0 \text{ Hz}$, $^3J_{3'4'} = 5.0 \text{ Hz}$, H-C(3')), 4.39 (brs, 3H, H-C(4'), H₂-C(5')), 4.00 (brs, 2H, H-C(1'')), 2.22, 2.10, 2.10 (3s, 9H, 3×H₃-C(2',3',5'-Ac)), 1.47–1.36 (m, 12H, 4×H₃C-(2'')). $^{13}\text{C}\{^1\text{H}\}\text{NMR}$ (126 MHz, CDCl_3 , 50 °C) δ (ppm): 177.9, 170.6, 169.3, 169.0, 149.4, 138.2, 133.6, 111.6, 87.1, 80.2, 74.4, 70.2, 62.9, 38.8, 23.5, 20.9, 20.5, 20.4. HRMS (ESI): calculated for $[\text{C}_{22}\text{H}_{31}\text{N}_7\text{O}_7\text{S}_2 + \text{H}^+]$ 570.1799, found 570.1797.

Diocetyl (1-(2',3',5'-tri-*O*-acetyl- β -D-ribofuranosyl)-4-(1*H*-tetrazol-5-yl)-1*H*-imidazol-5-yl) carbonimidodithioate (2l)



Prepared according to general procedure using *n*-octanethiol (2×0.20 mL, $\rho = 0.84 \text{ g/cm}^3$, 2×1.15 mmol, 2×1.05 eq.), K_2CO_3 (220 mg, 1.59 mmol, 1.5 eq.), 2,6-diazidopurine **4d** (500 mg, 1.09 mmol, 1.0 eq.) and NaH (33 mg, 1.38 mmol, 1.3 eq.).

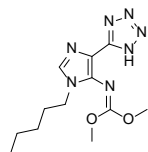
Column chromatography gradient: Tol/MeCN 2.5%→12% (+0.5% AcOH). Yield: 329 mg, 43%. Colourless solid, $R_f = 0.35$ (Tol/MeCN = 3:1 (+0.5 % AcOH)). IR ν (cm^{-1}): 2928, 2854, 1746, 1744, 1615, 1559, 1368, 1229, 1210, 1069, 989. $^1\text{H-NMR}$ (300 MHz, $\text{DMSO-}d_6$, 50 °C) δ (ppm): 8.05 (s, 1H, H-C(2)), 5.75 (d, 1H, $^3J_{1'2'} = 5.5 \text{ Hz}$, H-C(1')), 5.66 (t, 1H, $^3J_{1'2'} = ^3J_{2'3'} = 5.5 \text{ Hz}$, H-C(2')), 5.56 (t, 1H, $^3J_{2'3'} = ^3J_{3'4'} = 5.5 \text{ Hz}$, H-C(3')), 4.37–4.19 (m, 3H, H-C(4'), H₂-C(5')), 3.20–3.00 (m, 4H, 2×H₂-C(1'')), 2.09, 2.06, 2.05 (3s, 9H, 3×H₃-C(2',3',5'-Ac)), 1.70–1.54 (m, 4H, 2×(-CH₂-)), 1.36–1.17 (m, 20H, 10×(-CH₂-)), 0.84 (t, 6H, $^3J = 6.7 \text{ Hz}$, 2×H₃C-(8'')). $^{13}\text{C}\{^1\text{H}\}\text{NMR}$ (126 MHz, $\text{DMSO-}d_6$) δ (ppm): 174.8, 170.0, 169.3, 169.1, 149.7, 136.8, 134.6, 111.9, 85.8, 79.0, 72.5, 69.7, 63.1, 31.9, 31.2, 28.6, 28.5, 28.3, 28.0, 22.0, 20.5, 20.3, 20.2, 13.9. HRMS (ESI): calculated for $[\text{C}_{32}\text{H}_{51}\text{N}_7\text{O}_7\text{S}_2 + \text{H}^+]$ 710.3364, found 710.3342.

General procedure for the synthesis of tetrazolyl-imidazolyl-carbonimidates 5a-p

To a 25 mL round bottom flask methanol (1 eq.) was added to a suspension of NaH (57–63% suspension in mineral oil) (1 eq.) in toluene and stirred at r.t. for 10 min. Then 2,6-diazidopurine **4** (1.0 eq.) was added, and 30 minutes later, another portion of NaH (1 eq.) and methanol (1 eq.)

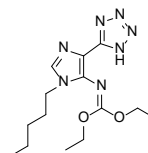
were added and stirred for another 30 min. The final portion of NaH (0.5 eq.) and methanol (0.5 eq.) were added, and the reaction mixture was stirred for an extra 30 min. After reaction completion (monitored by HPLC), the reaction was quenched by addition of a 10% acetic acid-ice mixture (10 mL). The aqueous phase was extracted with DCM (3×10 mL). The combined organic phase was washed with saturated NaCl solution (2×10 mL), dried over anhydrous Na₂SO₄, filtered, and evaporated under vacuum. The crude reaction mixture was purified by silica gel column chromatography.

Dimethyl (1-pentyl-4-(1*H*-tetrazol-5-yl)-1*H*-imidazol-5-yl)carbonimidate (5a)



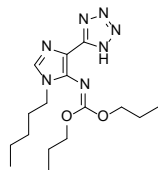
Prepared according to general procedure using 2,6-diazidopurine **4e** (100 mg, 0.37 mmol, 1.0 eq.), methanol (37 μ L, ρ = 0.79 g/mL, 0.92 mmol, 2.5 eq. in 3 portions) and NaH (60% suspension in mineral oil) (37 mg, 0.92 mmol, 2.5 eq. in 3 portions) in toluene (2 mL). Column chromatography gradient: DCM/MeCN 0%→50% (+0.5% AcOH). Yield: 90 mg, 84%. Colourless solid, R_f = 0.30 (DCM/MeCN = 7/3 (+0.5 % AcOH)). IR (KBr) ν (cm⁻¹): 3128, 2955, 2924, 2853, 1644, 1609, 1316, 1073, 1015. ¹H-NMR (300 MHz, CDCl₃, 50 °C) δ (ppm): 7.86 (s, 1H, H-C(2)), 3.96 (brs, 6H, 2×(-CH₃)), 3.91 (t, 2H, ³ J = 6.6 Hz, (-CH₂-)), 1.80 (quintet, 2H, ³ J = 7.2 Hz, (-CH₂-)), 1.31 – 1.25 (m, 4H, 2×(-CH₂-)), 0.90 (t, 3H, ³ J = 7.2 Hz, (-CH₃)). ¹³C{¹H}NMR (75 MHz, CDCl₃, 50 °C) δ (ppm): 161.8, 155.8, 153.6, 142.0, 118.9, 54.6, 44.2, 29.7, 28.8, 22.2, 14.0. HRMS (ESI): calculated for [C₁₂H₁₉N₇O₂ + H⁺] 294.1673, found 294.1653.

Diethyl (1-pentyl-4-(1*H*-tetrazol-5-yl)-1*H*-imidazol-5-yl)carbonimidate (5b)



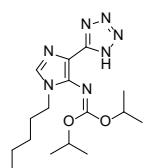
Prepared according to general procedure using 2,6-diazidopurine **4e** (100 mg, 0.37 mmol, 1.0 eq.), ethanol (54 μ L, ρ = 0.79 g/mL, 0.92 mmol, 2.5 eq. in 3 portions), and NaH (60% suspension in mineral oil) (37 mg, 0.92 mmol, 2.5 eq. in 3 portions) in toluene (2 mL). Column chromatography gradient: DCM/MeCN 0%→50% (+0.5% AcOH). Yield: 89 mg, 76%. Colourless solid, R_f = 0.30 (DCM/MeCN = 7/3 (+0.5 % AcOH)). IR (KBr) ν (cm⁻¹): 2957, 2928, 2866, 1641, 1613, 1301, 1064, 1028. ¹H-NMR (300 MHz, CDCl₃, 50 °C) δ (ppm): 7.83 (s, 1H, H-C(2)), 4.42 – 4.33 (m, 4H, 2×(-CH₂-)), 3.89 (t, 2H, ³ J = 7.2 Hz, (-CH₂-)), 1.81 (quintet, 2H, ³ J = 7.2 Hz, (-CH₂-)), 1.42 – 1.12 (m, 10H, 2×(-CH₂-), 2×(-CH₃)), 0.91 (t, 3H, ³ J = 7.2 Hz, (-CH₃)). ¹³C{¹H}NMR (75 MHz, CDCl₃, 50 °C) δ (ppm): 155.6, 150.6, 138.3, 134.1, 112.1, 65.7, 44.5, 30.0, 28.8, 22.3, 14.4, 13.9. HRMS (ESI): calculated for [C₁₄H₂₃N₇O₂ + H⁺] 322.1986, found 322.1994.

Dipropyl (1-pentyl-4-(1*H*-tetrazol-5-yl)-1*H*-imidazol-5-yl)carbonimidate (5c)



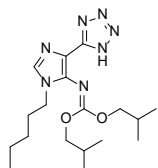
Prepared according to general procedure using 2,6-diazidopurine **4e** (100 mg, 0.37 mmol, 1.0 eq.), *n*-propanol (69 μ L, ρ = 0.80 g/mL, 0.92 mmol, 2.5 eq. in 3 portions) and NaH (60% suspension in mineral oil) (37 mg, 0.92 mmol, 2.5 eq. in 3 portions) in toluene (2 mL). Column chromatography gradient: DCM/MeCN 0% \rightarrow 30% (+0.5 % AcOH). Yield: 97 mg, 76%. Colourless solid, R_f = 0.40 (DCM/MeCN = 7/3 (+0.5 % AcOH)). IR (KBr) ν (cm^{-1}): 2952, 2933, 2872, 1634, 1610, 1300, 1073. $^1\text{H-NMR}$ (300 MHz, CDCl_3 , 50 $^\circ\text{C}$) δ (ppm): 7.82 (s, 1H, H-C(2)), 4.28 (brs, 4H, $2\times(-\text{CH}_2-)$), 3.89 (t, 2H, 3J = 7.2 Hz, $(-\text{CH}_2-)$), 1.81 (quintet, 2H, 3J = 7.2 Hz, $(-\text{CH}_2-)$), 1.64 (brs, 4H, $2\times(-\text{CH}_2-)$), 1.42 – 1.27 (m, 4H, $2\times(-\text{CH}_2-)$), 0.91 (t, 3H, 3J = 7.2 Hz, $(-\text{CH}_3)$), 0.87 (brs, 6H, $2\times(-\text{CH}_3)$). $^{13}\text{C}\{^1\text{H}\}\text{NMR}$ (75 MHz, CDCl_3) δ (ppm): 155.8, 150.6, 138.4, 134.1, 112.1, 71.2, 44.4, 30.0, 28.8, 22.3, 22.2, 13.9, 10.2. HRMS (ESI): calculated for $[\text{C}_{16}\text{H}_{27}\text{N}_7\text{O}_2 + \text{Na}^+]$ 350.2299, found 350.2274.

Diisopropyl (1-pentyl-4-(1H-tetrazol-5-yl)-1H-imidazol-5-yl)carbonimidate (**5d**)



Prepared according to general procedure using 2,6-diazidopurine **4e** (100 mg, 0.37 mmol, 1.0 eq.), isopropanol (70 μ L, ρ = 0.79 g/mL, 0.92 mmol, 2.5 eq. in 3 portions) and NaH (60% suspension in mineral oil) (37 mg, 0.92 mmol, 2.5 eq. in 3 portions) in toluene (2 mL). Column chromatography gradient: Tol/MeCN 0% \rightarrow 10% (+0.5 % AcOH). Yield: 83 mg, 65%. Colourless solid, R_f = 0.35 (Tol/MeCN = 7/3 (+0.5 % AcOH)). IR (KBr) ν (cm^{-1}): 3110, 2956, 2931, 2860, 1635, 1608, 1301, 1100, 1059. $^1\text{H-NMR}$ (300 MHz, CDCl_3 , 50 $^\circ\text{C}$) δ (ppm): 7.82 (s, 1H, H-C(2)), 5.21 – 5.00 (m, 2H, $2\times(-\text{CH}-)$), 3.88 (t, 2H, 3J = 7.2 Hz, $(-\text{CH}_2-)$), 1.81 (quintet, 2H, 3J = 7.2 Hz, $(-\text{CH}_2-)$), 1.43 – 1.31 (m, 4H, $2\times(-\text{CH}_2-)$), 1.28 (d, 12H, 3J = 5.5 Hz, $4\times(-\text{CH}_3)$), 0.91 (t, 3H, 3J = 7.2 Hz, $(-\text{CH}_3)$). $^{13}\text{C}\{^1\text{H}\}\text{NMR}$ (75 MHz, CDCl_3) δ (ppm): 154.6, 150.6, 138.6, 133.9, 112.1, 73.7, 44.5, 30.0, 28.8, 22.3, 22.2, 13.9. HRMS (ESI): calculated for $[\text{C}_{16}\text{H}_{27}\text{N}_7\text{O}_2 + \text{Na}^+]$ 350.2299, found 350.2298.

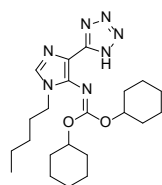
Diisobutyl (1-pentyl-4-(1H-tetrazol-5-yl)-1H-imidazol-5-yl)carbonimidate (**5e**)



Prepared according to general procedure using 2,6-diazidopurine **4e** (100 mg, 0.37 mmol, 1.0 eq.), isobutanol (85 μ L, ρ = 0.80 g/mL, 0.92 mmol, 2.5 eq. in 3 portions) and NaH (60% suspension in mineral oil) (37 mg, 0.92 mmol, 2.5 eq. in 3 portions) in toluene (2 mL). Column chromatography gradient: Tol/MeCN 0% \rightarrow 6% (+0.5 % AcOH). Yield: 122 mg, 88%. Colourless solid, R_f = 0.38 (Tol/MeCN = 7/3 (+0.5 % AcOH)). IR (KBr) ν (cm^{-1}): 3091, 2960, 2932, 1635, 1610, 1316, 1070. $^1\text{H-NMR}$ (300 MHz, CDCl_3 , 50 $^\circ\text{C}$) δ (ppm): 7.82 (s, 1H, H-C(2)), 4.14 (d, 4H, 3J =

6.2 Hz, 2×(-CH₂-)), 3.92 (t, 2H, ³J = 7.2 Hz, (-CH₂-)), 2.05 – 1.90 (m, 2H, 2×(-CH-)), 1.84 (quintet, 2H, ³J = 7.2 Hz, (-CH₂-)), 1.45 – 1.31 (m, 4H, 2×(-CH₂-)), 0.91 (t, 3H, ³J = 6.2 Hz, (-CH₃)), 0.89 (d, 12H, ³J = 6.5 Hz, 4×(-CH₃)). ¹³C{¹H}NMR (75 MHz, CDCl₃, 50 °C) δ (ppm): 155.9, 150.6, 138.4, 134.0, 112.1, 75.6, 44.4, 30.1, 28.8, 28.0, 22.3, 19.0, 13.9. HRMS (ESI): calculated for [C₁₈H₃₁N₇O₂ + Na⁺] 378.2612, found 378.2615.

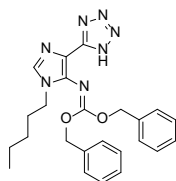
Dicyclohexyl (1-pentyl-4-(1H-tetrazol-5-yl)-1H-imidazol-5-yl)carbonimidate (5f)



Prepared according to general procedure using 2,6-diazidopurine **4e** (100 mg, 0.37 mmol, 1.0 eq.), cyclohexanol (96 μL, ρ = 0.96 g/mL, 0.92 mmol, 2.5 eq. in 3 portions), NaH (60% suspension in mineral oil) (37 mg, 0.92 mmol, 2.5 eq. in 3 portions) in toluene (2 mL). Column chromatography gradient: Tol/MeCN 0%→10% (+0.5 % AcOH). Yield: 127 mg, 82%. Colourless solid,

R_f = 0.35 (Tol/MeCN = 7/3 (+0.5 % AcOH)). IR (KBr) ν (cm⁻¹): 2935, 2857, 1631, 1608, 1296, 1068, 1014. ¹H-NMR (300 MHz, CDCl₃, 50 °C) δ (ppm): 7.80 (s, 1H, H-C(2)), 4.90 (brs, 2H, 2×(-CH-)), 3.88 (t, 2H, ³J = 7.2 Hz, (-CH₂-)), 1.90 (brs, 4H, 2×(-CH₂-)), 1.80 (quintet, 2H, ³J = 7.2 Hz, (-CH₂-)), 1.65 (brs, 4H, 2×(-CH₂-)), 1.56 – 1.18 (m, 16H, 8×(-CH₂-)), 0.91 (t, 3H, ³J = 7.2 Hz, (-CH₃)). ¹³C{¹H}NMR (75 MHz, CDCl₃) δ (ppm): 154.5, 150.6, 138.7, 133.9, 112.1, 78.3, 44.5, 31.8, 30.1, 28.8, 25.6, 23.7, 22.3, 13.9. HRMS (ESI): calculated for [C₂₂H₃₅N₇O₂ + H⁺] 430.2925, found 430.2915.

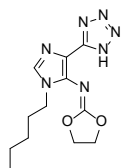
Dibenzyl (1-pentyl-4-(1H-tetrazol-5-yl)-1H-imidazol-5-yl)carbonimidate (5g)



Prepared according to general procedure using 2,6-diazidopurine **4e** (100 mg, 0.37 mmol, 1.0 eq.), benzyl alcohol (95 μL, ρ = 1.04 g/mL, 0.92 mmol, 2.5 eq. in 3 portions) and NaH (60% suspension in mineral oil) (37 mg, 0.92 mmol, 2.5 eq. in 3 portions) in toluene (2 mL). Column chromatography gradient: Tol/MeCN 0%→20% (+0.5 % AcOH). Yield:

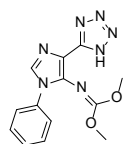
133 mg, 81 %. Colourless solid, R_f = 0.42 (Tol/MeCN = 7/3 (+0.5 % AcOH)). IR (KBr) ν (cm⁻¹): 2957, 2928, 2857, 1654, 1614, 1302, 1071, 1018. ¹H-NMR (300 MHz, CDCl₃) δ (ppm): 7.76 (s, 1H, H-C(2)), 7.39 – 7.27 (m, 10H, 10×H-C (Ar)), 5.40 (s, 4H, 2×(-CH₂-)), 3.78 (t, 2H, ³J = 7.2 Hz, (-CH₂-)), 1.70 (quintet, 2H, ³J = 7.2 Hz, (-CH₂-)), 1.39 – 1.14 (m, 4H, 2×(-CH₂-)), 0.88 (t, 3H, ³J = 7.2 Hz, (-CH₃)). ¹³C{¹H}NMR (75 MHz, CDCl₃, 50 °C) δ (ppm): 155.0, 150.6, 137.7, 135.5, 134.2, 128.6, 128.5, 128.3, 112.2, 71.5, 44.5, 30.0, 28.7, 22.3, 13.9. HRMS (ESI): calculated for [C₂₄H₂₇N₇O₂ + Na⁺] 446.2299, found 446.2300.

N-(1-Pentyl-4-(1H-tetrazol-5-yl)-1H-imidazol-5-yl)-1,3-dioxolan-2-imine (5h)



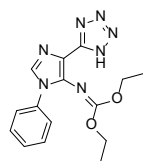
Prepared according to general procedure using 2,6-diazidopurine **4e** (100 mg, 0.37 mmol, 1.0 eq.), ethylene glycol (26 μL , $\rho = 1.11 \text{ g/mL}$, 0.46 mmol, 1.25 eq. in 3 portions) and NaH (60% suspension in mineral oil) (37 mg, 0.92 mmol, 2.5 eq. in 3 portions) in toluene (2 mL). Column chromatography gradient: DCM/MeCN 20% \rightarrow 30% (+0.5 % AcOH). Yield: 39 mg, 36%. Colourless solid, $R_f = 0.25$ (DCM/MeCN = 9/1 (+0.5 % AcOH)). IR (KBr) ν (cm^{-1}): 2956, 1677, 1609, 1229, 1205, 1058, 965. $^1\text{H-NMR}$ (300 MHz, CDCl_3) δ (ppm): 7.86 (s, 1H, H-C(2)), 4.66 (s, 4H, $2\times(-\text{CH}_2-)$), 3.96 (t, 2H, $^3J = 6.6 \text{ Hz}$, $(-\text{CH}_2-)$), 1.82 (quintet, 2H, $^3J = 7.2 \text{ Hz}$, $(-\text{CH}_2-)$), 1.42 – 1.29 (m, 4H, $2\times(-\text{CH}_2-)$), 0.89 (t, 3H, $^3J = 7.2 \text{ Hz}$, $(-\text{CH}_3)$). $^{13}\text{C}\{^1\text{H}\}\text{NMR}$ (75 MHz, CDCl_3) δ (ppm): 158.8, 150.3, 137.5, 134.4, 112.2, 66.8, 44.7, 30.0, 28.7, 22.3, 14.0. HRMS (ESI): calculated for $[\text{C}_{12}\text{H}_{17}\text{N}_7\text{O}_2 + \text{H}^+]$ 292.1516, found 292.1521.

Dimethyl (1-phenyl-4-(1H-tetrazol-5-yl)-1H-imidazol-5-yl)carbonimidate (**5i**)



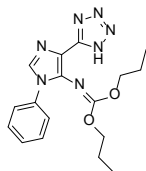
Prepared according to general procedure using 2,6-diazidopurine **4c** (100 mg, 0.36 mmol, 1.0 eq.), methanol (36 μL , $\rho = 0.79 \text{ g/mL}$, 0.90 mmol, 2.5 eq. in 3 portions) and NaH (60% suspension in mineral oil) (37 mg, 0.90 mmol, 2.5 eq. in 3 portions) in toluene (2 mL). Column chromatography gradient: DCM/MeCN 0% \rightarrow 16% (+0.5 % AcOH). Yield: 44 mg, 41%. Colourless solid, $R_f = 0.24$ (DCM/MeCN = 7/3 (+0.5 % AcOH)). IR (KBr) ν (cm^{-1}): 2658, 1649, 1616, 1506, 1314, 1076, 1013, 958. $^1\text{H-NMR}$ (300 MHz, CDCl_3 , 50 $^\circ\text{C}$) δ (ppm): 8.04 (s, 1H, H-C(2)), 7.60 – 7.39 (m, 5H, Ar), 3.88 (s, 6H, $2\times(-\text{CH}_3)$). $^{13}\text{C}\{^1\text{H}\}\text{NMR}$ (75 MHz, CDCl_3 , 50 $^\circ\text{C}$) δ (ppm): 156.5, 150.3, 138.1, 135.3, 134.4, 129.5, 128.7, 125.1, 112.8, 56.6. HRMS (ESI): calculated for $[\text{C}_{13}\text{H}_{13}\text{N}_7\text{O}_2 + \text{H}^+]$ 300.1203, found 300.1201.

Diethyl (1-phenyl-4-(1H-tetrazol-5-yl)-1H-imidazol-5-yl)carbonimidate (**5j**)



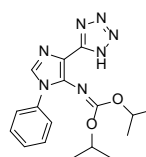
Prepared according to general procedure using 2,6-diazidopurine **4c** (100 mg, 0.36 mmol, 1.0 eq.), ethanol (52 μL , $\rho = 0.79 \text{ g/mL}$, 0.90 mmol, 2.5 eq. in 3 portions) and NaH (60% suspension in mineral oil) (37 mg, 0.90 mmol, 2.5 eq. in 3 portions) in toluene (2 mL). Column chromatography gradient: DCM/MeCN 0% \rightarrow 16% (+0.5 % AcOH). Yield: 75 mg, 64%. Colourless solid, $R_f = 0.28$ (DCM/MeCN = 7/3 (+0.5 % AcOH)). IR (KBr) ν (cm^{-1}): 2921, 1647, 1614, 1595, 1502, 1307, 1268, 1070. $^1\text{H-NMR}$ (300 MHz, CDCl_3 , 50 $^\circ\text{C}$) δ (ppm): 8.05 (s, 1H, H-C(2)), 7.55 – 7.41 (m, 5H, Ar), 4.31 (q, 4H, $^3J = 7.2 \text{ Hz}$, $(-\text{CH}_2-)$), 1.19 (t, 6H, $^3J = 7.2 \text{ Hz}$, $(-\text{CH}_3)$). $^{13}\text{C}\{^1\text{H}\}\text{NMR}$ (75 MHz, CDCl_3 , 50 $^\circ\text{C}$) δ (ppm): 155.4, 150.4, 138.4, 135.4, 134.4, 129.4, 128.5, 125.1, 112.9, 65.8, 14.3. HRMS (ESI): calculated for $[\text{C}_{15}\text{H}_{17}\text{N}_7\text{O}_2 + \text{H}^+]$ 328.1516, found 328.1518.

Dipropyl (1-phenyl-4-(1H-tetrazol-5-yl)-1H-imidazol-5-yl)carbonimidate (5k)



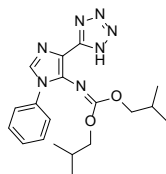
Prepared according to general procedure using 2,6-diazidopurine **4c** (100 mg, 0.36 mmol, 1.0 eq.), *n*-propanol (67 μ L, ρ = 0.80 g/mL, 0.90 mmol, 2.5 eq. in 3 portions) and NaH (60% suspension in mineral oil) (37 mg, 0.90 mmol, 2.5 eq. in 3 portions) in toluene (2 mL). Column chromatography gradient: DCM/MeCN 0% \rightarrow 16% (+0.5 % AcOH). Yield: 88 mg, 69%. Colourless solid, R_f = 0.37 (DCM/MeCN = 7/3 (+0.5 % AcOH)). IR (KBr) ν (cm^{-1}): 2968, 1647, 1614, 1504, 1291, 1195, 1071, 958. $^1\text{H-NMR}$ (300 MHz, CDCl_3 , 50 $^\circ\text{C}$) δ (ppm): 8.04 (s, 1H, H-C(2)), 7.56 – 7.41 (m, 5H, Ar), 4.22 (t, 4H, 3J = 7.2 Hz, (-CH₂-)), 1.60 (sextet, 4H, 3J = 7.2 Hz, (-CH₂)), 0.83 (t, 6H, 3J = 7.2 Hz, (-CH₃)). $^{13}\text{C}\{^1\text{H}\}$ NMR (75 MHz, CDCl_3 , 50 $^\circ\text{C}$) δ (ppm): 155.6, 150.4, 138.4, 135.4, 134.3, 129.4, 128.5, 125.1, 112.9, 71.3, 22.1, 10.1. HRMS (ESI): calculated for [$\text{C}_{17}\text{H}_{21}\text{N}_7\text{O}_2 + \text{H}^+$] 356.1829, found 356.1824.

Diisopropyl (1-phenyl-4-(1H-tetrazol-5-yl)-1H-imidazol-5-yl)carbonimidate (5l)



Prepared according to general procedure using 2,6-diazidopurine **4c** (100 mg, 0.36 mmol, 1.0 eq.), isopropanol (69 μ L, ρ = 0.79 g/mL, 0.90 mmol, 2.5 eq. in 3 portions) and NaH (60% suspension in mineral oil) (37 mg, 0.90 mmol, 2.5 eq. in 3 portions) in toluene (2 mL). Column chromatography gradient: DCM/MeCN 0% \rightarrow 10% (+0.5 % AcOH). Yield: 79 mg, 62%. Colourless solid, R_f = 0.30 (DCM/MeCN = 7/3 (+0.5 % AcOH)). IR (KBr) ν (cm^{-1}): 2923, 1635, 1608, 1596, 1503, 1390, 1296, 1098, 1064. $^1\text{H-NMR}$ (300 MHz, CDCl_3 , 50 $^\circ\text{C}$) δ (ppm): 8.01 (s, 1H, H-C(2)), 7.54 – 7.41 (m, 5H, Ar), 5.04 (septet, 2H, 3J = 5.5 Hz, 2 \times (-CH-)), 1.21 (d, 12H, 3J = 5.5 Hz, 4 \times (-CH₃)). $^{13}\text{C}\{^1\text{H}\}$ NMR (75 MHz, CDCl_3) δ (ppm): 154.4, 150.4, 138.6, 135.6, 134.3, 129.5, 128.6, 125.2, 112.9, 73.8, 22.0. HRMS (ESI): calculated for [$\text{C}_{17}\text{H}_{21}\text{N}_7\text{O}_2 + \text{H}^+$] 356.1829, found 356.1834.

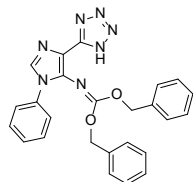
Diisobutyl (1-phenyl-4-(1H-tetrazol-5-yl)-1H-imidazol-5-yl)carbonimidate (5m)



Prepared according to general procedure using 2,6-diazidopurine **4c** (100 mg, 0.36 mmol, 1.0 eq.), isobutanol (83 μ L, ρ = 0.80 g/mL, 0.90 mmol, 2.5 eq. in 3 portions) and NaH (60% suspension in mineral oil) (37 mg, 0.90 mmol, 2.5 eq. in 3 portions) in toluene (2 mL). Column chromatography gradient: DCM/MeCN 0% \rightarrow 6% (+0.5 % AcOH). Yield: 75 mg, 54%. Colourless solid, R_f = 0.38 (Tol/MeCN = 7/3 (+0.5 % AcOH)). IR (KBr) ν (cm^{-1}): 2961, 1652, 1616, 1504, 1318, 1194, 1069, 1011. $^1\text{H-NMR}$ (300 MHz, CDCl_3 , 50 $^\circ\text{C}$) δ (ppm): 8.05 (s, 1H, H-C(2)), 7.57 – 7.39 (m, 5H, Ar), 4.05 (d, 4H, 3J = 6.2 Hz, 2 \times (-CH₂-)), 1.89 (nonet, 2H, 3J = 6.2 Hz, 2 \times (-CH-

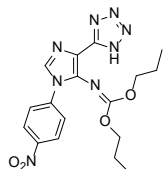
)), 0.82 (d, 12H, $^3J = 6.2$ Hz, $4 \times (-\text{CH}_3)$). $^{13}\text{C}\{^1\text{H}\}$ NMR (75 MHz, CDCl_3 , 50°C) δ (ppm): 155.8, 150.4, 138.5, 135.4, 134.3, 129.5, 128.6, 125.1, 112.9, 75.8, 27.9, 18.9. HRMS (ESI): calculated for $[\text{C}_{19}\text{H}_{25}\text{N}_7\text{O}_2 + \text{H}^+]$ 384.2142, found 384.2139.

Dibenzyl (1-pentyl-4-(1H-tetrazol-5-yl)-1H-imidazol-5-yl)carbonimidate (5n)



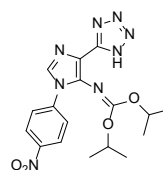
Prepared according to general procedure using 2,6-diazidopurine **4c** (100 mg, 0.36 mmol, 1.0 eq.), benzyl alcohol (93 μL , $\rho = 1.04$ g/mL, 0.90 mmol, 2.5 eq. in 3 portions) and NaH (60% suspension in mineral oil) (37 mg, 0.90 mmol, 2.5 eq. in 3 portions) in toluene (2 mL). Column chromatography gradient: DCM/MeCN 0% \rightarrow 5% (+0.5 % AcOH). Yield 94 mg, 58 %. Colourless solid, $R_f = 0.36$ (DCM/MeCN = 7/3 (+0.5 % AcOH)). IR (KBr) ν (cm^{-1}): 3033, 2959, 2659, 1644, 1613, 1505, 1299, 1194, 1067. ^1H -NMR (300 MHz, $\text{DMSO}-d_6$, 50°C) δ (ppm): 7.76 (s, 1H, H-C(2)), 7.48 – 7.39 (m, 5H, Ar), 7.33 – 7.09 (m, 10H, $2 \times \text{Ar}$), 5.28 (s, 4H, $2 \times (-\text{CH}_2-)$). $^{13}\text{C}\{^1\text{H}\}$ NMR (75 MHz, $\text{DMSO}-d_6$, 50°C) δ (ppm): 153.5, 150.5, 135.9, 134.9, 134.8, 134.1, 129.1, 128.1, 128.0, 127.7, 124.1, 113.1, 70.4. HRMS (ESI): calculated for $[\text{C}_{25}\text{H}_{21}\text{N}_7\text{O}_2 + \text{H}^+]$ 452.1829, found 452.1821.

Dipropyl (1-(4-nitrophenyl)-4-(1H-tetrazol-5-yl)-1H-imidazol-5-yl)carbonimidate (5o)



Prepared according to general procedure using 2,6-diazidopurine **4f** (100 mg, 0.31 mmol, 1.0 eq.), *n*-propanol (58 μL , $\rho = 0.80$ g/mL, 0.77 mmol, 2.5 eq. in 3 portions) and NaH (60% suspension in mineral oil) (32 mg, 0.77 mmol, 2.5 eq. in 3 portions) in toluene (2 mL). Column chromatography gradient: DCM/MeCN, 0% \rightarrow 16% (+0.5 % AcOH). Yield: 69 mg, 56%. Slightly yellow solid, $R_f = 0.31$ (DCM/MeCN = 7/3 (+0.5 % AcOH)). IR (KBr) ν (cm^{-1}): 2970, 1637, 1614, 1595, 1522, 1505, 1343, 1309, 1071. ^1H -NMR (300 MHz, CDCl_3 , 50°C) δ (ppm): 8.40 (d, 2H, $^3J = 8.8$ Hz, Ar), 8.12 (s, 1H, H-C(2)), 7.76 (d, 2H, $^3J = 8.8$ Hz, Ar), 4.26 (t, 4H, $^3J = 7.2$ Hz, $(-\text{CH}_2-)$), 1.62 (sextet, 4H, $^3J = 7.2$ Hz, $(-\text{CH}_2)$), 0.85 (t, 6H, $^3J = 7.2$ Hz, $(-\text{CH}_3)$). $^{13}\text{C}\{^1\text{H}\}$ NMR (75 MHz, CDCl_3 , 50°C) δ (ppm): 156.4, 150.1, 147.5, 140.5, 138.5, 133.7, 125.3, 125.1, 113.5, 71.8, 22.1, 10.2. HRMS (ESI): calculated for $[\text{C}_{17}\text{H}_{20}\text{N}_8\text{O}_4 + \text{H}^+]$ 401.1680, found 401.1661.

Diisopropyl (1-(4-nitrophenyl)-4-(1H-tetrazol-5-yl)-1H-imidazol-5-yl)carbonimidate (5p)



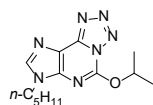
Prepared according to general procedure using 2,6-diazidopurine **4f** (100 mg, 0.31 mmol, 1.0 eq.), isopropanol (59 μL , $\rho = 0.79$ g/mL, 0.77 mmol, 2.5 eq. in 3 portions) and NaH (60% suspension in mineral oil) (32 mg, 0.77 mmol, 2.5 eq. in 3 portions) in toluene (2 mL). Column chromatography gradient: DCM/MeCN 0% \rightarrow 10% (+0.5 % AcOH). Yield: 56 mg, 45%. Slightly yellow

solid $R_f = 0.26$ (DCM/MeCN = 7/3 (+0.5 % AcOH)). IR (KBr) ν (cm^{-1}): 2990, 1607, 1595, 1523, 1504, 1342, 1302, 1098, 1062, 1005. $^1\text{H-NMR}$ (300 MHz, CDCl_3 , 50 °C) δ (ppm): 8.39 (d, 2H, $^3J = 8.8$ Hz, Ar), 8.11 (s, 1H, H-C(2)), 7.74 (d, 2H, $^3J = 8.8$ Hz, Ar), 5.08 (septet, 2H, $^3J = 5.6$ Hz, $2 \times (-\text{CH}-)$), 1.21 (d, 12H, $^3J = 5.6$ Hz, $4 \times (-\text{CH}_3)$). $^{13}\text{C}\{^1\text{H}\}$ NMR (75 MHz, CDCl_3) δ (ppm): 155.2, 150.1, 147.5, 140.6, 138.7, 133.7, 125.4, 125.1, 113.6, 74.4, 22.1. HRMS (ESI): calculated for $[\text{C}_{17}\text{H}_{20}\text{N}_8\text{O}_4 + \text{H}^+]$ 401.1680, found 401.1681.

General procedure for the synthesis 2-alkoxy-6-azidopurines 6a-c

In a 50 mL round bottom flask DBU (1.4 eq.) and 2,6-diazidopurine **4** (1.0 eq.) were dissolved in DMF or toluene under a nitrogen atmosphere. Isopropanol (1.4 eq.) was added, and the reaction mixture was stirred at r.t. overnight. The reaction was quenched by adding 10% AcOH solution in water (10 mL) and extracted with DCM (3×10 mL). The combined organic phase was washed with saturated NaCl solution (2×10 mL), dried over anhydrous Na_2SO_4 , filtered, and evaporated under vacuum. Additional washing with 5% $\text{LiCl}_{(\text{aq})}$ solution (2×10 mL) was performed if DMF was used as the solvent. The crude reaction mixture was purified by silica gel column chromatography.

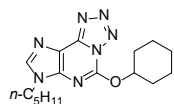
5-Isopropoxy-7-pentyl-7H-tetrazolo[5,1-*i*]purine (6a)



Prepared according to general procedure using 2,6-diazidopurine **4e** (100 mg, 0.37 mmol, 1.0 eq.), isopropanol (39 μL , $\rho = 0.79$ g/mL, 0.51 mmol, 1.4 eq.) and DBU (76 μL , $\rho = 1.03$ g/mL, 0.51 mmol, 1.4 eq.) in toluene (2 mL).

Column chromatography gradient: DCM/MeCN 0% \rightarrow 15%. Yield: 87 mg, 82%. Colourless solid, $R_f = 0.45$ (DCM/MeCN = 9/1). IR (KBr) ν (cm^{-1}): 2958, 1645, 1547, 1338, 1279, 1103, 1072. $^1\text{H-NMR}$ (500 MHz, CDCl_3) δ (ppm): 7.79 (s, 1H, H-C(8)), 5.35 (heptet, 1H, $^3J = 6.2$ Hz, $(-\text{CH}-)$), 4.13 (t, 2H, $^3J = 7.2$ Hz, $(-\text{CH}_2-)$), 1.86 (quintet, 2H, $^3J = 7.2$ Hz, $(-\text{CH}_2-)$), 1.43 (d, 6H, $^3J = 6.2$ Hz, $2 \times (-\text{CH}_3)$), 1.34 (quintet, 2H, $^3J = 7.2$ Hz, $(-\text{CH}_2-)$), 1.32 – 1.23 (m, 2H, $(-\text{CH}_2-)$), 0.88 (t, 3H, $^3J = 7.2$ Hz, $(-\text{CH}_3)$). $^{13}\text{C}\{^1\text{H}\}$ NMR (75 MHz, CDCl_3) δ (ppm): 160.8, 154.7, 153.7, 142.6, 120.0, 71.2, 44.0, 29.6, 28.8, 22.2, 22.0, 14.0. HRMS (ESI): calculated for $[\text{C}_{13}\text{H}_{19}\text{N}_7\text{O} + \text{Na}^+]$ 290.1724, found 290.1736.

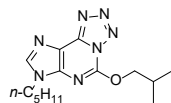
5-Cyclohexyloxy-7-pentyl-7H-tetrazolo[5,1-*i*]purine (6b)



Prepared according to general procedure using 2,6-diazidopurine **4e** (100 mg, 0.37 mmol, 1.0 eq.), cyclohexanol (51 μL , $\rho = 0.96$ g/mL, 0.51 mmol, 1.4 eq.) and DBU (76 μL , $\rho = 1.03$ g/mL, 0.51 mmol, 1.4 eq.) in toluene (2 mL). Column chromatography gradient: DCM/MeCN 0% \rightarrow 15%. Yield: 97 mg, 80%. Colourless solid, $R_f = 0.5$ (DCM/MeCN = 9/1). IR (KBr) ν (cm^{-1}): 2928, 1645, 1551,

1357, 1278, 1235, 1072, 1004. $^1\text{H-NMR}$ (500 MHz, CDCl_3) δ (ppm): 7.79 (s, 1H, H-C(8)), 5.03 (m, 1H, (-CH-)), 4.13 (t, 2H, $^3J = 7.2$ Hz, (-CH₂-)), 2.14 – 2.09 (m, 2H, 2×H-C(Cy)), 1.90 – 1.80 (m, 4H, 2×(-CH₂-)), 1.66 – 1.57 (m, 2H, (-CH₂-)), 1.47 – 1.25 (m, 8H, 4×(-CH₂-)), 0.88 (t, 3H, $^3J = 7.2$ Hz, (-CH₃)). $^{13}\text{C}\{^1\text{H}\}$ NMR (75 MHz, CDCl_3) δ (ppm): 160.8, 154.7, 153.6, 142.6, 120.0, 76.5, 43.9, 31.9, 29.6, 28.8, 25.6, 24.3, 22.2, 14.0. HRMS (ESI): calculated for $[\text{C}_{16}\text{H}_{23}\text{N}_7\text{O} + \text{H}^+]$ 330.2037, found 330.2034.

5- Isobutoxy-7-pentyl-7H-tetrazolo[5,1-*i*]purine (6c)

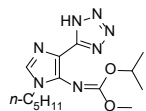


Prepared according to general procedure using 2,6-diazidopurine **4e** (200 mg, 0.73 mmol, 1.0 eq.), isobutanol (95 μL , $\rho = 0.80$ g/mL, 1.03 mmol, 1.4 eq.) and DBU (152 μL , $\rho = 1.03$ g/mL, 1.03 mmol, 1.4 eq.) in DMF (2 mL). Column chromatography gradient: DCM/MeCN 0%→8%. Yield: 95 mg, 43 %. Colourless solid, $R_f = 0.48$ (DCM/MeCN = 9/1). IR (KBr) ν (cm^{-1}): 2958, 2129, 1646, 1549, 1356, 1236, 1069. $^1\text{H-NMR}$ (500 MHz, CDCl_3) δ (ppm): 7.80 (s, 1H, H-C(8)), 4.19 (d, 2H, $^3J = 6.7$ Hz, (-CH₂-)), 4.14 (t, 2H, $^3J = 7.2$ Hz, (-CH₂-)), 2.18 (nonet, 1H, $^3J = 6.7$ Hz, (-CH-)), 1.87 (quintet, 2H, $^3J = 7.2$ Hz, (-CH₂-)), 1.32 – 1.25 (m, 4H, 2×(-CH₂-)), 1.05 (d, 6H, $^3J = 6.7$ Hz, 2×(-CH₃)), 0.89 (t, 3H, $^3J = 7.2$ Hz, (-CH₃)). $^{13}\text{C}\{^1\text{H}\}$ NMR (75 MHz, CDCl_3) δ (ppm): 161.3, 154.5, 153.4, 142.6, 120.1, 74.5, 43.8, 29.5, 28.7, 27.9, 22.1, 19.3, 13.8. HRMS (ESI): calculated for $[\text{C}_{14}\text{H}_{21}\text{N}_7\text{O} + \text{H}^+]$ 304.1880, found 304.1862.

General procedure for the synthesis of carbonimidates/carbonimidothioate **7a-f**

Desired alcohol or thiol was added to a suspension of NaH (57-63% suspension in mineral oil) in DMF and stirred at r.t. for 10 min. Then 2-alkoxy-6-azidopurine **6a** was added to the alcoholate suspension and stirred at r.t. for 30 min. After reaction completion (monitored by HPLC), the reaction was quenched with 10% AcOH solution (10 mL). The aqueous phase was extracted with DCM (3×10 mL). Combined organic phases were washed with saturated NaCl solution (3×10 mL), dried over anhydrous sodium sulfate, filtered, and evaporated under vacuum. The crude product was purified by silica gel column chromatography.

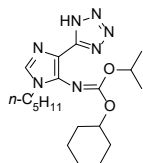
Isopropyl methyl (*Z*)-(1-pentyl-4-(1H-tetrazol-5-yl)-1H-imidazol-5-yl)carbonimidate (7a)



Prepared according to general procedure using 2-isopropoxy-6-azidopurine **6a** (50 mg, 0.17 mmol, 1.0 eq.), methanol (14 μL , $\rho = 0.79$ g/mL, 0.34 mmol, 2.0 eq.) and NaH (60% suspension in mineral oil) (14 mg, 0.34 mmol, 2.0 eq.) in DMF (1 mL). Column chromatography gradient: DCM/MeCN 0%→20% (+0.5% AcOH). Yield: 39 mg, 71 %. Colourless solid, $R_f = 0.25$ (DCM/MeCN = 8/2 (+0.5% AcOH)). IR (KBr) ν (cm^{-1}): 2953, 2928, 1638, 1613, 1440, 1363, 1309, 1068, 972. $^1\text{H-NMR}$ (500 MHz, CDCl_3) δ

(ppm): 7.81 (s, 1H, H-C(2)), 5.16 (heptet, 1H, $^3J = 5.8$ Hz, (-CH-)), 3.89 – 3.79 (m, 5H, (-CH₂-), (-CH₃)), 1.80 (quintet, 2H, $^3J = 7.2$ Hz, (-CH₂-)), 1.50 – 1.09 (m, 10H, 2×(-CH₂-), 2×(-CH₃)), 0.92 (t, 3H, $^3J = 7.2$ Hz, (-CH₃)). ¹³C{¹H}NMR (75 MHz, CDCl₃) δ (ppm): 155.5, 150.6, 138.3, 134.1, 112.1, 74.2, 56.1, 44.4, 30.0, 28.8, 22.2, 22.1, 13.9. HRMS (ESI): calculated for [C₁₄H₂₃N₇O₂ + H⁺] 322.1986, found 322.1978.

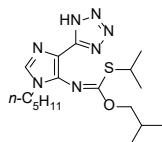
Cyclohexyl isopropyl (*E*)-(1-pentyl-4-(1*H*-tetrazol-5-yl)-1*H*-imidazol-5-yl)carbonimidate (7b)



Prepared according to general procedure using 2-cyclohexyloxy-6-azidopurine **6b** (75 mg, 0.23 mmol, 1.0 eq.), isopropanol (35 μL, $\rho = 0.79$ g/mL, 0.46 mmol, 2.0 eq.) and NaH (60% suspension in mineral oil) (18 mg, 0.46 mmol, 2.0 eq.) in DMF (2 mL). Column chromatography gradient: DCM/MeCN 0%→10%

(+0.5% AcOH). Yield: 56 mg, 64%. Colourless solid, $R_f = 0.50$ (DCM/MeCN = 8/2 (+0.5% AcOH)). IR (KBr) ν (cm⁻¹): 2959, 2935, 2858, 1631, 1609, 1359, 1298, 1064, 982. ¹H-NMR (500 MHz, CDCl₃) δ (ppm): 7.81 (s, 1H, H-C(2)), 5.21 – 5.01 (m, 1H, (-CH-)), 4.99 – 4.79 (br s, 1H, H-C(Cy)), 3.88 (t, 2H, $^3J = 7.2$ Hz, (-CH₂-)), 2.01 – 1.86 (m, 2H, H-C(Cy)), 1.80 (quintet, 2H, $^3J = 7.2$ Hz, (-CH₂-)), 1.74 – 1.60 (m, 2H, H-C(Cy)), 1.57 – 1.16 (m, 16H, 6×H-C(Cy), 2×(-CH₂-), 2×(-CH₃)), 0.91 (t, 3H, $^3J = 7.2$ Hz, (-CH₃)). ¹³C{¹H}NMR (75 MHz, CDCl₃) δ (ppm): 154.5, 150.6, 138.6, 134.0, 112.2, 78.2, 73.6, 44.5, 31.8, 30.0, 28.8, 25.5, 23.7, 22.3, 22.2, 13.9. HRMS (ESI): calculated for [C₁₉H₃₁N₇O₂ + H⁺] 390.2612, found 390.2598.

***O*-Isobutyl *S*-isopropyl (*Z*)-(1-pentyl-4-(1*H*-tetrazol-5-yl)-1*H*-imidazol-5-yl)carbonimidothioate (7c)**

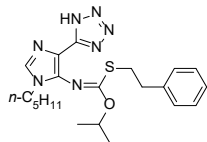


Prepared according to general procedure using 2-isobutoxy-6-azidopurine **6c** (100 mg, 0.33 mmol, 1.0 eq.), isopropylthiol (93 μL, $\rho = 0.82$ g/mL, 0.99 mmol, 3.0 eq.) and NaH (60% suspension in mineral oil) (40 mg, 0.99 mmol, 3.0 eq.) in toluene (2 mL). Column chromatography gradient: DCM/MeCN

0%→12% (+0.5% AcOH). Yield: 83 mg, 74%. Colourless solid, $R_f = 0.25$ (DCM/MeCN = 8/2 (+0.5% AcOH)). IR (KBr) ν (cm⁻¹): 2957, 2933, 2870, 1607, 1591, 1248, 1203, 1172, 1072. ¹H-NMR (500 MHz, CDCl₃) δ (ppm): 7.92 (s, 1H, H-C(2)), 4.36 (d, 2H, $^3J = 6.7$ Hz, (-CH₂-)), 3.84 (t, 2H, $^3J = 7.2$ Hz, (-CH₂-)), 3.75 (heptet, 1H, $^3J = 6.2$ Hz, (-CH-)), 2.21 (nonet, 1H, $^3J = 6.7$ Hz, (-CH-)), 1.80 (quintet, 2H, $^3J = 7.2$ Hz, (-CH₂-)), 1.41 – 1.31 (m, 4H, 2×(-CH₂-)), 1.28 (d, 6H, $^3J = 6.2$ Hz, 2×(-CH₃)), 1.08 (d, 6H, $^3J = 6.7$ Hz, 2×(-CH₃)), 0.91 (t, 3H, $^3J = 7.2$ Hz, (-CH₃)). ¹³C{¹H}NMR (75 MHz, CDCl₃) δ (ppm): 167.7, 149.8, 137.7, 135.1, 112.1, 76.5, 44.7, 36.9,

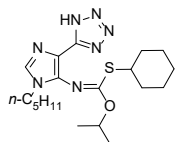
29.8, 28.7, 27.9, 23.7, 22.2, 19.3, 13.9. HRMS (ESI): calculated for [C₁₇H₂₉N₇OS + H⁺] 380.2227, found 380.2217.

***O*-isopropyl *S*-phenethyl (*Z*)-(1-pentyl-4-(1*H*-tetrazol-5-yl)-1*H*-imidazol-5-yl)carbonimido-thioate (7d)**



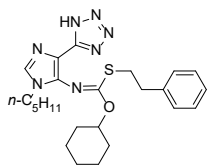
Prepared according to general procedure using 2-isopropoxy-6-azidopurine **6a** (50 mg, 0.17 mmol, 1.0 eq.), phenylethylthiol (70 μ L, ρ = 1.03 g/mL, 0.52 mmol, 3.0 eq.) and NaH (60% suspension in mineral oil) (20 mg, 0.52 mmol, 3.0 eq.) in toluene (2 mL). Column chromatography gradient: DCM/MeCN 0% \rightarrow 20% (+0.5% AcOH). Yield: 45 mg, 60 %. Colourless solid, R_f = 0.55 (DCM/MeCN = 8/2 (+0.5% AcOH)). IR (KBr) ν (cm⁻¹): 2952, 2926, 2854, 1600, 1457, 1196, 1164, 1094, 1071. ¹H-NMR (500 MHz, CDCl₃) δ (ppm): 7.89 (s, 1H, H-C(2)), 7.27 (t, 2H, Ar), 7.20 (t, 1H, Ar), 7.14 (t, 2H, Ar) 5.59 (heptet, 1H, ³*J* = 5.8 Hz, (-CH-)), 3.83 (t, 2H, ³*J* = 7.2 Hz, (-CH₂-)), 3.12 (t, 2H, ³*J* = 7.5 Hz, (-CH₂-)), 2.89 (t, 2H, ³*J* = 7.5 Hz, (-CH₂-)), 1.80 (quintet, 2H, ³*J* = 7.2 Hz, (-CH₂-)), 1.55 (d, 6H, ³*J* = 5.8 Hz, 2 \times (-CH₃)), 1.41 – 1.31 (m, 4H, 2 \times (-CH₂-)), 0.91 (t, 3H, ³*J* = 7.2 Hz, (-CH₃)). ¹³C{¹H}NMR (75 MHz, CDCl₃) δ (ppm): 166.7, 149.8, 139.9, 137.8, 135.0, 128.7, 128.7, 126.7, 112.0, 74.7, 44.9, 36.7, 32.6, 29.8, 28.8, 22.3, 22.1, 14.0. HRMS (ESI): calculated for [C₂₁H₂₉N₇OS + H⁺] 428.2227, found 428.2232.

***S*-Cyclohexyl *O*-isopropyl (*Z*)-(1-pentyl-4-(1*H*-tetrazol-5-yl)-1*H*-imidazol-5-yl)carbonimidothioate (7e)**



Prepared according to general procedure using 2-isopropoxy-6-azidopurine **6a** (50 mg, 0.17 mmol, 1.0 eq.), cyclohexylthiol (63 μ L, ρ = 0.85 g/mL, 0.52 mmol, 3.0 eq.) and NaH (20 mg, 0.52 mmol, 3.0 eq.) in toluene (2 mL). Column chromatography gradient: DCM/MeCN 0% \rightarrow 15% (+0.5% AcOH). Yield: 55 mg, 78%. Colourless solid, R_f = 0.60 (DCM/MeCN = 8/2 (+0.5% AcOH)). IR (KBr) ν (cm⁻¹): 2958, 2934, 2855, 1609, 1445, 1238, 1170, 1100, 1072. ¹H-NMR (500 MHz, CDCl₃) δ (ppm): 7.91 (s, 1H, H-C(2)), 5.60 – 5.51 (m, 1H, (-CH-)), 3.83 (t, 2H, ³*J* = 7.2 Hz, (-CH₂-)), 3.55 – 3.44 (m, 1H, H-C(Cy)), 2.01 – 1.88 (m, 2H, H-C(Cy)), 1.80 (quintet, 2H, ³*J* = 7.2 Hz, 2 \times (-CH₂-)), 1.70 – 1.59 (m, 2H, 2 \times H-C(Cy)), 1.55 (d, 6H, ³*J* = 5.8 Hz, 2 \times (-CH₃)), 1.40 – 1.13 (m, 10H, 2 \times (-CH₂-), 6 \times H-C(Cy)), 0.91 (t, 3H, ³*J* = 7.2 Hz, (-CH₃)). ¹³C{¹H}NMR (75 MHz, CDCl₃) δ (ppm): 166.9, 149.9, 138.0, 135.1, 112.1, 74.1, 44.8, 44.7, 33.5, 29.8, 28.7, 25.8, 25.5, 22.2, 21.9, 14.0. HRMS (ESI): calculated for [C₁₉H₃₁N₇OS + H⁺] 406.2384, found 406.2394.

***S*-cyclohexyl *O*-isopropyl (*Z*)-(1-pentyl-4-(1*H*-tetrazol-5-yl)-1*H*-imidazol-5-yl)carbonimido-thioate (7f)**

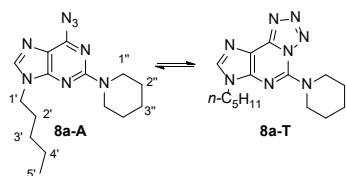


Prepared according to general procedure using 2-cyclohexyloxy-6-azidopurine **6b** (100 mg, 0.30 mmol, 1.0 eq.), phenylethylthiol (120 μ L, $\rho = 1.03$ g/mL, 0.91 mmol, 3.0 eq.) and NaH (34 mg, 0.91 mmol, 3.0 eq.) in toluene (2 mL). Column chromatography gradient: DCM/MeCN 0% \rightarrow 4% (+0.5% AcOH). Yield: 87 mg, 61%. Colourless solid, $R_f = 0.55$ (DCM/MeCN = 9/1 (+0.5% AcOH)). IR (KBr) ν (cm^{-1}): 2926, 2854, 1593, 1445, 1241, 1207, 1172, 1071, 986. $^1\text{H-NMR}$ (500 MHz, CDCl_3) δ (ppm): 7.91 (s, 1H, H-C(2)), 7.27 (t, 2H, Ar), 7.20 (t, 1H, Ar), 7.14 (t, 2H, Ar), 5.37 (m, 1H, (-CH-)), 3.83 (t, 2H, $^3J = 7.2$ Hz, (-CH₂-)), 3.13 (t, 2H, $^3J = 7.5$ Hz, (-CH₂-)), 2.91 (t, 2H, $^3J = 7.5$ Hz, (-CH₂-)), 2.26 – 2.15 (m, 2H, H-C(Cy)), 1.90 – 1.69 (m, 6H, 2 \times H-C(Cy), 2 \times (-CH₂-)), 1.67 – 1.56 (m, 1H, H-C(Cy)), 1.42 – 1.28 (m, 5H, 2 \times (-CH₂-), H-C(Cy)), 0.91 (t, 3H, $^3J = 7.2$ Hz, (-CH₃)). $^{13}\text{C}\{^1\text{H}\}$ NMR (75 MHz, CDCl_3) δ (ppm): 166.4, 149.9, 139.9, 137.8, 135.2, 128.6, 128.6, 126.6, 112.2, 79.1, 44.8, 36.7, 32.5, 31.6, 29.8, 28.7, 25.5, 23.8, 22.2, 14.0. HRMS (ESI): calculated for [$\text{C}_{24}\text{H}_{33}\text{N}_7\text{OS} + \text{H}^+$] 468.2540, found 468.2531.

General procedure for the synthesis of 2-amino-6-azidopurines **8a-b**

To a 100 mL round bottom flask charged with 2,6-diazidopurine **4e** (1.0 eq.) was added DMF and amine (3.0 eq.). The resulting mixture was stirred at r.t. overnight. After reaction completion (monitored by HPLC), the mixture was transferred to a separatory funnel, diluted with H₂O (40 mL), and extracted with EtOAc (3 \times 20 mL). The combined organic phase was washed with 5% LiCl_(aq) solution (2 \times 10 mL) and saturated NaCl solution (2 \times 10 mL), dried over anhydrous Na₂SO₄, filtered, and evaporated under vacuum. The crude reaction mixture was purified by silica gel column chromatography.

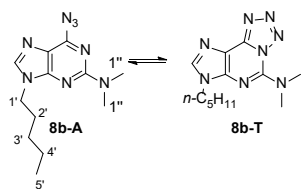
A mixture of 6-azido-9-pentyl-2-(piperidin-1-yl)-9H-purine (**8a-A**) and 7-pentyl-5-(piperidin-1-yl)-7H-tetrazolo[5,1-*i*]purine (**8a-T**)



Prepared according to general procedure using 2,6-**4e** (1.5 g, 5.51 mmol, 1.0 eq.) and piperidine (1.6 mL, $\rho = 0.862$ g/mL, 16.53 mmol, 3.0 eq.) in DMF (15 mL). Column chromatography gradient: DCM/MeCN 0% \rightarrow 14%. Yield: 1.10 g, 64%. Dark yellow solid, $R_f = 0.66$ (DCM/MeCN = 7:3). IR ν (cm^{-1}): 2927, 2850, 2117, 1614, 1557, 1531, 1244, 1221. Analyzed azido form. $^1\text{H-NMR}$ (500 MHz, CDCl_3) δ (ppm): 7.58 (s, 1H, H-C(8)), 4.03 (t, 2H, $^3J = 7.1$ Hz, H₂-C(1')), 3.85–3.77 (m, 4H, 2 \times H₂-C(1'')), 1.84 (quintet, 2H, $^3J = 7.4$ Hz, H₂-C(2')), 1.71–1.64 (m, 2H, H₂-C(3'')), 1.63–1.57 (m, 4H, 2 \times H₂-C(2'')), 1.39–1.33 (m, 2H, H₂-C(3')), 1.31–1.26 (m, 2H, H₂-C(4')), 0.88 (t, 3H, $^3J =$

7.2 Hz, H₃-C(5')). ¹³C{¹H}NMR (126 MHz, CDCl₃) δ (ppm): 158.6, 154.9, 152.6, 140.8, 117.1, 45.5, 43.4, 29.4, 28.8, 25.8, 25.0, 22.2, 14.0. HRMS (ESI): calculated for [C₁₅H₂₂N₈ + H⁺] 315.2040, found 315.2053.

A mixture of 6-azido-2-*N,N*-dimethylamino-9-pentyl-9*H*-purine and *N,N*-dimethyl-7-pentyl-7*H*-tetrazolo[5,1-*i*]purin-5-amine (8b-T)



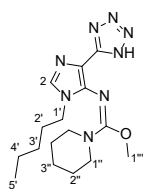
Prepared according to general procedure using 2,6-diazidopurine **4e** (2.0 g, 7.35 mmol, 1.0 eq.) and dimethylamine (20% solution in H₂O, 5.58 mL, ρ = 0.89 g/mL, 22.05 mmol, 3.0 eq.) in DMF (15 mL). Column chromatography gradient: DCM/MeCN 0% → 14%. Yield: 1.13 g, 56%. Brown solid, R_f =

0.62 (DCM/MeCN = 7:3). IR ν (cm⁻¹): 2959, 2928, 2859, 2116, 1621, 1572, 1548, 1392, 1258, 783. Analyzed azido form. ¹H-NMR (500 MHz, CDCl₃) δ (ppm): 7.58 (s, 1H, H-C(8)), 4.05 (t, 2H, ³J = 7.2 Hz, H₂-C(1')), 3.21 (s, 6H, 2×H₃-C(1'')), 1.85 (quintet, 2H, ³J = 7.3 Hz, H₂-C(2')), 1.39–1.27 (m, 4H, H₂-C(3'), H₂-C(4')), 0.89 (t, 3H, ³J = 7.2 Hz, H₃-C(5')). ¹³C{¹H}NMR (126 MHz, CDCl₃) δ (ppm): 159.2, 154.9, 152.4, 140.6, 117.0, 43.4, 37.4, 29.4, 28.8, 22.2, 14.0. HRMS (ESI): calculated for [C₁₂H₁₈N₈ + H⁺] 275.1727, found 275.1704.

General procedure for the synthesis of tetrazolyl-imidazolyl-carbimides 9a-i

Alcohol was added to a suspension of NaH (57-63% suspension in mineral oil) in DMF and stirred at r.t. for 1 h. Then 2-amino-6-azidopurine **8** was added to the alcoholate suspension and stirred at r.t. for 30 min. After reaction completion (monitored by HPLC), the reaction was quenched with 10% AcOH solution (10 mL). The aqueous phase was extracted with toluene (4×5 mL). The combined organic phase was washed with water (3×5 mL) and saturated NaCl solution (2×5 mL). The aqueous phase was back extracted with toluene (1×5 mL). Combined organic phases were dried over anhydrous sodium sulfate, filtered, and evaporated under vacuum. The crude product was purified by crystallization from Et₂O.

Methyl (*E*)-*N*-(1-pentyl-4-(1*H*-tetrazol-5-yl)-1*H*-imidazol-5-yl)piperidine-1-carbimide (9a)

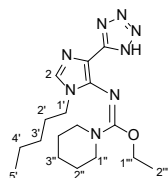


Prepared according to general procedure using 2-piperidinyl-6-azidopurine **8a** (300 mg, 0.95 mmol, 1.0 eq.), NaH (60% suspension in mineral oil) (114 mg, 2.86 mmol, 3.0 eq.) and methanol (116 μL, ρ = 0.79 g/mL, 2.86 mmol, 3.0 eq.) in DMF (3 mL). Yield: 247 mg, 75%. Colourless solid, R_f = 0.35 (DCM/MeCN = 7:3 (+1% AcOH)). IR ν (cm⁻¹): 2938, 2919, 2852, 1621, 1593,

1441, 1069, 948. ¹H-NMR (500 MHz, CDCl₃) δ (ppm): 7.78 (s, 1H, HC(2)), 3.89 (t, 2H, ³J =

7.4 Hz, H₂C(1'')), 3.87 (s, 3H, H₃C(1''')), 3.15 (br s, 4H, 2×H₂C(1'')), 1.82 (quintet, 2H, ³J = 7.3 Hz, H₂C(2'')), 1.41–1.35 (m, 10H, 5×H₂C), 0.91 (t, 3H, ³J = 6.8 Hz, H₃C(5')). ¹³C{¹H}NMR (126 MHz, CDCl₃) δ (ppm): 158.3, 150.7, 140.7, 133.4, 109.2, 56.0, 46.7, 44.2, 29.6, 28.9, 25.6, 24.2, 22.4, 14.0. HRMS (ESI): calculated for [C₁₆H₂₆N₈O + H⁺] 347.2302, found 347.2328.

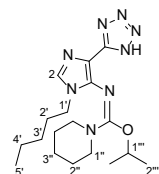
Ethyl (*E*)-*N*-(1-pentyl-4-(1*H*-tetrazol-5-yl)-1*H*-imidazol-5-yl)piperidine-1-carbimidate (9b)



Prepared according to general procedure using 2-piperidinyl-6-azidopurine **8a** (100 mg, 0.32 mmol, 1.0 eq.), NaH (60% suspension in mineral oil, 38 mg, 0.96 mmol, 3.0 eq.) and ethanol (75 μL, ρ = 0.79 g/mL, 1.28 mmol, 4.0 eq.) in DMF (1 mL). Yield: 67 mg, 58%. Colourless solid, R_f = 0.37 (DCM/MeCN = 7:3 (+1% AcOH)). IR ν (cm⁻¹): 2932, 2853, 2651, 1619,

1591, 1229, 1071. ¹H-NMR (500 MHz, CDCl₃) δ (ppm): 7.78 (s, 1H, HC(2)), 4.28 (q, 2H, ³J = 7.1 Hz, H₃C(1''')), 3.89 (t, 2H, ³J = 7.3 Hz, H₂C(1')), 3.17 (br s, 4H, 2×H₂C(1'')), 1.82 (quintet, 2H, ³J = 7.2 Hz, H₂C(2'')), 1.42–1.32 (m, 13H, (5×H₂C, H₃C(2'''))), 0.91 (t, 3H, ³J = 6.8 Hz, H₃C(5')). ¹³C{¹H}NMR (126 MHz, CDCl₃) δ (ppm): 157.9, 150.6, 140.7, 133.3, 109.1, 64.9, 46.6, 44.2, 29.6, 28.9, 25.6, 24.2, 22.4, 14.9, 14.0. HRMS (ESI): calculated for [C₁₇H₂₈N₈O + H⁺] 361.2459, found 361.2461.

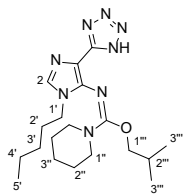
Isopropyl (*E*)-*N*-(1-pentyl-4-(1*H*-tetrazol-5-yl)-1*H*-imidazol-5-yl)piperidine-1-carbimidate (9c)



Prepared according to general procedure using 2-piperidinyl-6-azidopurine **8a** (100 mg, 0.32 mmol, 1.0 eq.), NaH (60% suspension in mineral oil) (115 mg, 2.88 mmol, 9.0 eq.), isopropanol (245 μL, ρ = 0.79 g/mL, 3.2 mmol, 10.0 eq.) in DMF (1 mL). Yield: 70 mg, 58%. Colourless solid, R_f = 0.32 (DCM/MeCN = 7:3 (+1% AcOH)). IR ν (cm⁻¹): 2931, 2854, 1582, 1540, 1420, 1369, 1253,

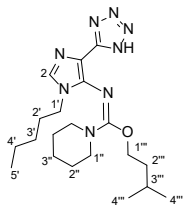
1069, 973, 920. ¹H-NMR (500 MHz, CDCl₃) δ (ppm): 7.76 (s, 1H, HC(2)), 5.03 (heptet, 1H, ³J = 6.2 Hz, HC(1''')), 3.88 (t, 2H, ³J = 7.0 Hz, H₂C(1')), 3.21–3.10 (m, 4H, 2×H₂C(1'')), 1.82 (quintet, 2H, ³J = 7.2 Hz, H₂C(2'')), 1.47–1.35 (m, 10H, 5×H₂C), 1.34 (d, 6H, ³J = 6.2 Hz, 2×H₃C(2''')), 0.91 (t, 3H, ³J = 6.8 Hz, H₃C(5')). ¹³C{¹H}NMR (126 MHz, CDCl₃) δ (ppm): 157.5, 150.7, 140.9, 133.4, 109.0, 72.2, 46.5, 44.1, 29.6, 28.9, 25.5, 24.3, 22.5, 22.4, 14.0. HRMS (ESI): calculated for [C₁₈H₃₀N₈O + H⁺] 375.2615, found 375.2612.

Isobutyl (*E*)-*N*-(1-pentyl-4-(1*H*-tetrazol-5-yl)-1*H*-imidazol-5-yl)piperidine-1-carbimidate (9d)



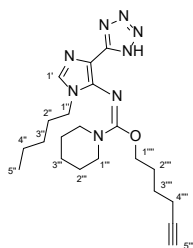
Prepared according to general procedure using 2-piperidinyl-6-azidopurine **8a** (100 mg, 0.32 mmol, 1.0 eq.), NaH (60% suspension in mineral oil) (38 mg, 0.96 mmol, 3.0 eq.) and isobutanol (119 μL , $\rho = 0.80 \text{ g/mL}$, 1.28 mmol, 4.0 eq.) in DMF (1 mL). Yield: 55 mg, 44%. Colourless solid, $R_f = 0.39$ (DCM/MeCN = 7:3 (+1% AcOH)). IR ν (cm^{-1}): 2930, 2853, 2661, 1616, 1591, 1422, 1253, 1229, 1073. $^1\text{H-NMR}$ (500 MHz, CDCl_3) δ (ppm): 7.76 (s, 1H, HC(2)), 3.98 (d, 2H, $^3J = 3.5 \text{ Hz}$, $\text{H}_2\text{C}(1''')$), 3.88 (t, 2H, $^3J = 6.4 \text{ Hz}$, $\text{H}_2\text{C}(1')$), 3.27–3.11 (m, 4H, $2 \times \text{H}_2\text{C}(1'')$), 2.06 (nonet, 1H, $^3J = 6.7 \text{ Hz}$, HC(2''')), 1.82 (quintet, 2H, $^3J = 7.2 \text{ Hz}$, $\text{H}_2\text{C}(2'')$), 1.46–1.35 (m, 10H, $5 \times \text{H}_2\text{C}$), 0.97 (d, 6H, $^3J = 6.7 \text{ Hz}$, $2 \times \text{H}_3\text{C}(3''')$), 0.91 (t, 3H, $^3J = 6.8 \text{ Hz}$, $\text{H}_3\text{C}(5')$). $^{13}\text{C}\{^1\text{H}\}\text{NMR}$ (126 MHz, CDCl_3) δ (ppm): 157.9, 150.6, 140.7, 133.3, 109.1, 75.2, 46.6, 44.1, 29.6, 28.9, 28.2, 25.6, 24.3, 22.4, 19.4, 14.1. HRMS (ESI): calculated for $[\text{C}_{19}\text{H}_{32}\text{N}_8\text{O} + \text{H}]^+$ 389.2772, found 389.2772.

Isopentyl (*E*)-*N*-(1-pentyl-4-(1*H*-tetrazol-5-yl)-1*H*-imidazol-5-yl)piperidine-1-carbimide (9e**)**



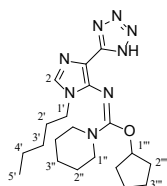
Prepared according to general procedure using 2-piperidinyl-6-azidopurine **8a** (100 mg, 0.32 mmol, 1.0 eq.), NaH (60% suspension in mineral oil) (51 mg, 1.28 mmol, 4.0 eq.) and isopentanol (174 μL , $\rho = 0.81 \text{ g/mL}$, 1.60 mmol, 5.0 eq.) in DMF (1 mL). Yield: 58 mg, 45%. Colourless solid, $R_f = 0.44$ (DCM/MeCN = 7:3 (+1% AcOH)). IR ν (cm^{-1}): 2928, 2849, 2360, 1614, 1592, 1366, 1073, 957, 534. $^1\text{H-NMR}$ (500 MHz, CDCl_3) δ (ppm): 7.75 (s, 1H, HC(2)), 4.23 (t, 2H, $^3J = 6.8 \text{ Hz}$, $\text{H}_2\text{C}(1''')$), 3.88 (t, 2H, $^3J = 7.2 \text{ Hz}$, $\text{H}_2\text{C}(1')$), 3.23–3.13 (m, 4H, $2 \times \text{H}_2\text{C}(1'')$), 1.82 (quintet, 2H, $^3J = 7.3 \text{ Hz}$, $\text{H}_2\text{C}(2'')$), 1.76 (nonet, 1H, $^3J = 6.6 \text{ Hz}$, HC(3''')), 1.61 (q, 2H, $^3J = 6.8 \text{ Hz}$, $\text{H}_2\text{C}(2''')$), 1.47–1.33 (m, 10H, $5 \times \text{H}_2\text{C}$), 0.92 (d, 6H, $^3J = 6.7 \text{ Hz}$, $2 \times \text{H}_3\text{C}(4''')$), 0.91–0.90 (m, 3H, $\text{H}_3\text{C}(5')$). $^{13}\text{C}\{^1\text{H}\}\text{NMR}$ (126 MHz, CDCl_3) δ (ppm): 157.9, 150.7, 140.7, 133.4, 109.2, 67.6, 46.6, 44.1, 38.0, 29.6, 28.9, 25.6, 25.2, 24.2, 22.7, 22.4, 14.0. HRMS (ESI): calculated for $[\text{C}_{20}\text{H}_{34}\text{N}_8\text{O} + \text{H}]^+$ 403.2928, found 403.2912.

Hex-5-yn-1-yl (*E*)-*N*-(1-pentyl-4-(1*H*-tetrazol-5-yl)-1*H*-imidazol-5-yl)piperidine-1-carbimide (9f**)**



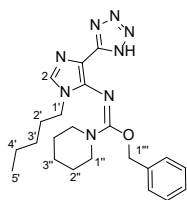
Prepared according to general procedure using 2-piperidinyl-6-azidopurine **8a** (200 mg, 0.64 mmol, 1.0 eq.), NaH (60% suspension in mineral oil) (76 mg, 1.91 mmol, 3.0 eq.) and 5-hexyn-1-ol (355 μL , $\rho = 0.88 \text{ g/mL}$, 3.18 mmol, 5.0 eq.) in DMF (2 mL). Yield: 122 mg, 46%. Red solid. $R_f = 0.56$ (DCM/MeCN = 7:3 (+1% AcOH)). IR ν (cm^{-1}): 2942, 1590, 1443, 1344, 1268, 1145, 1073, 974. $^1\text{H-NMR}$ (500 MHz, CDCl_3) δ (ppm): 7.77 (s, 1H, HC(1')), 4.25 (t, 2H, $\text{H}_2\text{C}(1''''')$), 3.88 (t, 2H, $\text{H}_2\text{C}(1''')$), 3.29–3.01 (m, 4H, $2 \times \text{H}_2\text{C}(1''')$), 2.31–2.21 (2 \times dt, 2H, $^2J = 7.0 \text{ Hz}$, $^3J = 2.6 \text{ Hz}$, $\text{H}_2\text{C}(2''''')$), 1.94 (t, 1H, $\text{H}_2\text{C}(5''''')$), 1.90–1.76 (m, 4H, $2 \times \text{H}_2\text{C}$), 1.67 (quintet, 2H, $^3J = 7.0 \text{ Hz}$, H_2C), 1.47–1.30 (m, 10H, $5 \times \text{H}_2\text{C}$), 0.91 (t, 3H, $^3J = 7.0 \text{ Hz}$, $\text{H}_3\text{C}(5')$). $^{13}\text{C}\{^1\text{H}\}\text{NMR}$ (126 MHz, CDCl_3) δ (ppm): 157.8, 150.7, 140.7, 133.4, 109.2, 84.3, 68.7, 68.3, 46.6, 44.2, 29.6, 28.9, 28.2, 25.5, 25.1, 24.2, 22.4, 18.2, 14.1. HRMS (ESI): calculated for $[\text{C}_{21}\text{H}_{33}\text{N}_8\text{O} + \text{H}]^+$ 413.2772, found 413.2761.

Cyclopentyl (*E*)-*N*-(1-pentyl-4-(1*H*-tetrazol-5-yl)-1*H*-imidazol-5-yl)piperidine-1-carbimidate (**9g**)



Prepared according to general procedure using 2-piperidinyl-6-azidopurine **8a** (100 mg, 0.32 mmol, 1.0 eq.), NaH (60% suspension in mineral oil) (51 mg, 1.28 mmol, 4.0 eq.) and cyclopentanol (145 μL , $\rho = 0.95 \text{ g/mL}$, 1.60 mmol, 5.0 eq.) in DMF (1 mL). Yield: 46 mg, 36%. Colourless solid, $R_f = 0.43$ (DCM/MeCN = 7:3 (+1% AcOH)). IR ν (cm^{-1}): 2928, 2853, 1586, 1421, 1253, 1070, 977, 753, 662. $^1\text{H-NMR}$ (500 MHz, CDCl_3) δ (ppm): 7.76 (s, 1H, HC(2)), 5.20 (quintet, 1H, $^3J = 5.1 \text{ Hz}$, HC(1''')), 3.88 (t, 2H, $^3J = 7.2 \text{ Hz}$, $\text{H}_2\text{C}(1')$), 3.23–3.08 (m, 4H, $2 \times \text{H}_2\text{C}(1'')$), 1.95–1.64 (m, 8H, $4 \times \text{H}_2\text{C}$), 1.62–1.50 (m, 2H, H_2C), 1.46–1.31 (m, 10H, $5 \times \text{H}_2\text{C}$), 0.91 (t, 3H, $^3J = 6.8 \text{ Hz}$, $\text{H}_3\text{C}(5')$). $^{13}\text{C}\{^1\text{H}\}\text{NMR}$ (126 MHz, CDCl_3) δ (ppm): 157.2, 150.7, 140.7, 133.4, 109.1, 81.3, 46.5, 44.2, 33.0, 29.6, 29.0, 25.6, 24.3, 24.0, 22.4, 14.1. HRMS (ESI): calculated for $[\text{C}_{20}\text{H}_{32}\text{N}_8\text{O} + \text{H}]^+$ 401.2772, found 401.2761; calculated for $[\text{C}_{20}\text{H}_{32}\text{N}_8\text{O} + \text{Na}]^+$ 423.2591, found 423.2556.

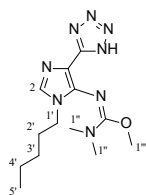
Benzyl (*E*)-*N*-(1-pentyl-4-(1*H*-tetrazol-5-yl)-1*H*-imidazol-5-yl)piperidine-1-carbimidate (**9h**)



Prepared according to general procedure using 2-piperidinyl-6-azidopurine **8a** (100 mg, 0.32 mmol, 1.0 eq.), NaH (60% suspension in mineral oil) (51 mg, 1.28 mmol, 4.0 eq.) and benzyl alcohol (167 μL , $\rho = 1.04 \text{ g/mL}$, 1.60 mmol, 5.0 eq.) in DMF (1 mL). Yield: 68 mg, 50%. Colourless solid, $R_f = 0.37$ (DCM/MeCN = 7:3 (+1% AcOH)). IR ν (cm^{-1}): 2930, 2848, 1616,

1593, 1446, 1273, 1076, 962, 879, 725, 691, 558. ¹H-NMR (500 MHz, CDCl₃) δ (ppm): 7.78 (s, 1H, HC(2)), 7.46 (d, 2H, ³J = 7.5 Hz, 2×HC(Ar)), 7.37 (t, 2H, ³J = 7.5 Hz, 2×HC(Ar)), 7.31 (t, 1H, ³J = 7.3 Hz, HC(Ar)), 5.31 (s, 2H, H₂C(1''')), 3.85 (t, 2H, ³J = 7.2 Hz, H₂C(1')), 3.26–3.14 (m, 4H, 2×H₂C(1'')), 1.79 (quintet, 2H, ³J = 7.3 Hz, H₂C(2')), 1.44–1.32 (m, 10H, 5×H₂C), 0.91 (t, 3H, ³J = 6.8 Hz, H₃C(5')). ¹³C{¹H}NMR (126 MHz, CDCl₃) δ (ppm): 157.5, 150.7, 140.5, 137.2, 133.5, 128.5, 128.1, 128.0, 109.4, 70.5, 46.7, 44.2, 29.6, 28.9, 25.6, 24.2, 22.4, 14.1. HRMS (ESI): calculated for [C₂₂H₃₀N₈O + H]⁺ 423.2615, found 423.2625.

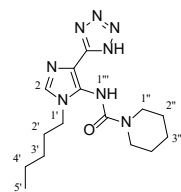
Methyl (*E*)-*N,N*-dimethyl-*N'*-(1-pentyl-4-(1*H*-tetrazol-5-yl)-1*H*-imidazol-5-yl)carbamimidate (9i)



Prepared according to general procedure using 2-dimethylamino-6-azidopurine **8b** (100 mg, 0.36 mmol, 1.0 eq.), NaH (60% suspension in mineral oil) (28 mg, 0.72 mmol, 2.0 eq.) and methanol (29 μL, ρ = 0.79 g/mL, 0.72 mmol, 2.0 eq.) in DMF (1 mL). Yield: 82 mg, 74%. Colourless solid, R_f = 0.23 (DCM/MeCN = 7:3 (+1% AcOH)). IR ν (cm⁻¹): 2931, 2863, 1644, 1598, 1487, 1360, 1214,

1051, 960, 873. ¹H-NMR (500 MHz, CDCl₃) δ (ppm): 7.77 (s, 1H, HC(2)), 3.90 (t, 2H, ³J = 7.3 Hz, H₂C(1')), 3.87 (s, 3H, H₃C(1''')), 2.72 (s, 6H, 2×H₃C(1'')), 1.84 (quintet, 2H, ³J = 7.2 Hz, H₂C(2')), 1.41–1.33 (m, 4H, H₂C(3'), H₂C(4')), 0.91 (t, 3H, ³J = 6.8 Hz, H₃C(5')). ¹³C{¹H}NMR (126 MHz, CDCl₃) δ (ppm): 158.5, 150.7, 140.2, 133.3, 109.8, 56.0, 44.1, 38.2, 29.6, 28.9, 22.3, 14.0. HRMS (ESI): calculated for [C₁₃H₂₂N₈O + H]⁺ 307.1989, found 307.1979.

***N*-(1-Pentyl-4-(1*H*-tetrazol-5-yl)-1*H*-imidazol-5-yl)piperidine-1-carboxamide (9')**



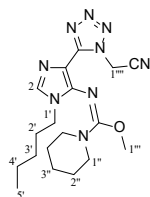
Prepared according to general procedure using 2-piperidinyl-6-azidopurine **8a** (100 mg, 0.32 mmol, 1.0 eq.) and potassium *tert*-butoxide (144 mg, 1.28 mmol, 4.0 eq.) in DMF (1 mL). Yield: 46 mg, 48%. Colourless solid, R_f = 0.60 (EtOH). IR ν (cm⁻¹): 3461, 3208, 2934, 2853, 1662, 1625, 1519, 1268, 1018, 965, 882, 657. ¹H-NMR (500 MHz, CDCl₃) δ (ppm): 7.91 (s, 1H,

HN(1''')), 7.82 (s, 1H, HC(2)), 4.11 (t, 2H, ³J = 7.4 Hz, H₂C(1')), 3.64–3.56 (m, 4H, 2×H₂C(1'')), 1.89 (quintet, 2H, ³J = 7.2 Hz, H₂C(2')), 1.74–1.67 (m, 6H, 3×H₂C), 1.43–1.29 (m, 4H, 2×H₂C), 0.92 (t, 3H, ³J = 6.9 Hz, H₃C(5')). ¹³C{¹H}NMR (126 MHz, CDCl₃) δ (ppm): 154.8, 149.9, 136.0, 132.1, 115.3, 46.9, 45.8, 29.2, 28.9, 25.9, 24.4, 22.3, 14.0. HRMS (ESI): calcd for [C₁₅H₂₄N₈O + H]⁺ 333.2146, found 333.2160.

General procedure for the synthesis of alkylated tetrazoles 10a-e

To a solution of tetrazolyl-imidazole derivative **2**, **5** or **9** in DMF K_2CO_3 or NaH (57–63% suspension in mineral oil), KI, 2-chloroacetonitrile or bromethylacetate were added and the reaction mixture was stirred at 60 °C for 3 h. After reaction completion (monitored by HPLC), the reaction was quenched with 10% AcOH solution (10 mL) and extracted with toluene (3×10 mL). The combined organic phase was washed with 5% $\text{LiCl}_{(\text{aq})}$ solution (2×10 mL), saturated NaCl solution (2×10 mL), dried over anhydrous Na_2SO_4 , filtered, and evaporated under vacuum. The crude product was purified by silica gel column chromatography.

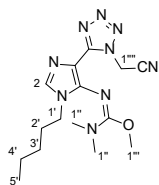
Methyl (*E*)-*N*-(4-(1-(cyanomethyl)-1*H*-tetrazol-5-yl)-1-pentyl-1*H*-imidazol-5-yl) piperidine-1-carbimide (10a**)**



Prepared according to general procedure using tetrazolyl-imidazole **9a** (380 mg, 1.1 mmol, 1.0 eq.), K_2CO_3 (760 mg, 5.5 mmol, 5.0 eq.), 2-chloroacetonitrile (521 μL , $\rho = 1.19 \text{ g/mL}$, 8.2 mmol, 7.5 eq.) and KI (73 mg, 0.44 mmol, 0.4 eq.) in DMF (4 ml). Column chromatography gradient: Toluene/MeCN 0% \rightarrow 12%. Yield: 332 mg, 78%. Colourless solid, $R_f = 0.92$

(DCM/MeCN = 7:3). IR ν (cm^{-1}): 2937, 2857, 1612, 1570, 1536, 1442, 1270, 1084, 948, 764, 658. $^1\text{H-NMR}$ (500 MHz, CDCl_3) δ (ppm): 7.29 (s, 1H, H-C(2)), 6.00 (s, 2H, $\text{H}_2\text{-C}(1''''')$), 3.83 (s, 3H, $\text{H}_3\text{-C}(1''''')$), 3.83 (t, 2H, $^3J = 7.3 \text{ Hz}$, $\text{H}_2\text{-C}(1''')$), 3.16–3.05 (m, 4H, $2\times\text{H}_2\text{-C}(1''')$), 1.78 (quintet, 2H, $^3J = 7.2 \text{ Hz}$, $\text{H}_2\text{-C}(2'')$), 1.46–1.33 (m, 10H, $2\times\text{H}_2\text{-C}(2'')$, $\text{H}_2\text{-C}(3'')$, $\text{H}_2\text{-C}(3')$, $\text{H}_2\text{-C}(4'')$), 0.92 (t, 3H, $^3J = 7.1 \text{ Hz}$, $\text{H}_3\text{-C}(5'')$). $^{13}\text{C}\{^1\text{H}\}\text{NMR}$ (126 MHz, CDCl_3) δ (ppm): 158.1, 149.4, 142.8, 133.0, 113.7, 109.0, 56.0, 46.7, 43.9, 36.4, 29.6, 28.9, 25.5, 24.1, 22.3, 14.0. HRMS (ESI): calculated for $[\text{C}_{18}\text{H}_{27}\text{N}_9\text{O} + \text{H}^+]$ 386.2411, found 386.2422.

Methyl (*E*)-*N*'-(4-(1-(cyanomethyl)-1*H*-tetrazol-5-yl)-1-pentyl-4,5-dihydro-1*H*-imidazol-5-yl)-*N,N*-dimethylcarbimide (10b**)**

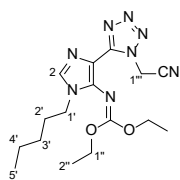


Prepared according to general procedure using tetrazolyl-imidazole derivative **9i** (400 mg, 1.31 mmol, 1.0 eq.), K_2CO_3 (906 mg, 6.55 mmol, 5 eq.), 2-chloroacetonitrile (495 μL , $\rho = 1.19 \text{ g/mL}$, 7.83 mmol, 6.0 eq.) and KI (86 mg, 0.52 mmol, 0.4 eq.) in DMF (6 mL). Conditions: 60 °C, 2 h. Column chromatography gradient: Toluene/MeCN 0% \rightarrow 9%. Yield: 325 mg, 72%.

Green solid, $R_f = 0.93$ (DCM/MeCN = 7:3). IR ν (cm^{-1}): 3119, 2952, 2592, 2250, 1625, 1574, 1541, 1425, 1218, 1054, 960, 771, 658. $^1\text{H-NMR}$ (500 MHz, CDCl_3) δ (ppm): 7.28 (s, 1H, H-C(2)), 6.00 (s, 2H, $\text{H}_2\text{-C}(1''''')$), 3.83 (s, 3H, $\text{H}_3\text{-C}(1''''')$), 3.83 (t, 2H, $^3J = 7.3 \text{ Hz}$, $\text{H}_2\text{-C}(1''')$), 2.68 (s, 6H, $2\times\text{H}_3\text{-C}(1''')$), 1.79 (quintet, 2H, $^3J = 7.3 \text{ Hz}$, $\text{H}_2\text{-C}(2'')$), 1.39–1.33 (m, 4H, $\text{H}_2\text{-C}(3'')$, $\text{H}_2\text{-C}(4'')$), 0.91 (t, 3H, $^3J = 7.0 \text{ Hz}$, $\text{H}_3\text{-C}(5'')$). $^{13}\text{C}\{^1\text{H}\}\text{NMR}$ (126 MHz, CDCl_3) δ (ppm):

158.4, 149.4, 142.3, 132.9, 113.8, 109.7, 56.0, 43.8, 38.1, 36.5, 29.5, 28.9, 22.3, 14.0. HRMS (ESI): calculated for $[C_{15}H_{23}N_9O + H^+]$ 346.2098, found 346.2101.

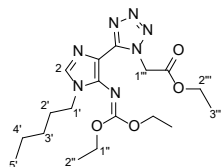
Diethyl (4-(1-(cyanomethyl)-1H-tetrazol-5-yl)-1-pentyl-1H-imidazol-5-yl)carbonimidate (10c)



Prepared according to general procedure using tetrazolyl-imidazole derivative **5b** (320 mg, 0.99 mmol, 1.0 equiv.), NaH (44 mg, 1.09 mmol, 1.1 equiv.), 2-chloroacetonitrile (125 μ L, $\rho = 1.19$ g/mL, 1.98 mmol, 2.0 equiv.), and KI (8 mg, 0.05 mmol, 0.05 eq.), DMF (5 mL). Conditions: 3 h at 60 $^{\circ}$ C.

Flash column chromatography (DCM/MeCN, 0% \rightarrow 12%). Yield 150 mg, 42%. Yellow oil. HPLC: $t_R = 5.88$ min, 98% purity. IR (KBr) ν (cm^{-1}): 2911, 2934, 2860, 1635, 1592, 1532, 1415, 1376, 1302, 1075, 1032. $^1\text{H-NMR}$ (500 MHz, CDCl_3) δ (ppm): 7.36 (s, 1H, H-C(2)), 6.00 (s, 2H, (-CH₂-)), 4.31 (br. s, 4H, (2 \times (-CH₂-))), 3.83 (t, 2H, $^3J = 7.2$ Hz, (-CH₂-)), 1.75 (quintet, 2H, $^3J = 7.2$ Hz, (-CH₂-)), 1.41–0.97 (m, 10H, 2 \times (-CH₂-), 2 \times (-CH₃)), 0.90 (t, 3H, $^3J = 7.0$ Hz, (-CH₃)). $^{13}\text{C}\{^1\text{H}\}$ NMR (75.5 MHz, CDCl_3) δ (ppm): 155.0, 149.5, 140.0, 133.7, 113.5, 111.5, 65.6, 44.1, 36.3, 30.0, 28.7, 22.3, 14.4, 14.0. HRMS (ESI): calculated $[C_{16}H_{24}N_8O_2 + H^+]$ 361.2022, found 361.2092.

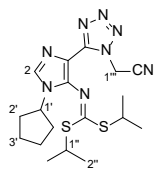
Ethyl 2-(5-(5-((diethoxymethylene)amino)-1-pentyl-1H-imidazol-4-yl)-1H-tetrazol-1-yl)acetate (10d)



Prepared according to general procedure using tetrazolyl-imidazole derivative **5b** (400 mg, 1.25 mmol, 1.0 eq.), K_2CO_3 (379 mg, 2.74 mmol, 2.20 eq.), and bromethylacetate (119 μ L, $\rho = 1.19$ g/mL, 1.88 mmol, 1.5 eq.) in DMF (4 mL). Column chromatography gradient: DCM/MeCN 0% \rightarrow 15%. Yield: 220 mg, 43%. Yellow oil, $R_f = 0.43$ (DCM/MeCN =

9:1). IR ν (cm^{-1}): 2933, 2871, 1754, 1643, 1592, 1375, 1303, 1210, 1069, 1027, 996. $^1\text{H NMR}$ (500 MHz, $\text{MeOD-}d_4$) δ (ppm) 7.50 (s, 1H, H-C(2)), 5.68 (s, 2H, H-C(1'')), 4.22–4.40 (m, 4H, 2 \times H₂-C(1'')), 4.20 (q, 2H, $^3J = 7.1$ Hz, H₂-C(2'')), 3.89 (t, 2H, $^3J = 7.0$ Hz, H₂-C(1')), 1.74 (quintet, 2H, $^3J = 7.1$ Hz, H₂-C(2')), 1.24–1.40 (m, 10H, H₂-C(3'), H₂-C(4'), 2 \times H₃-C(2'')), 1.22 (t, 3H, $^3J = 7.1$ Hz, H₃-C(3'')), 0.90 (t, 3H, $^3J = 7.0$ Hz, H₃-C(5')). $^{13}\text{C}\{^1\text{H}\}$ NMR (126 MHz, $\text{MeOD-}d_4$) δ (ppm) 168.2, 156.0, 151.7, 140.4, 135.4, 112.9, 66.6, 63.0, 50.6, 44.8, 31.0, 29.7, 23.2, 14.5, 14.3, 14.2. HRMS (ESI): calculated for $[C_{18}H_{29}N_7O_4 + H^+]$ 408.2354, found 408.2353.

Diisopropyl (4-(1-(cyanomethyl)-1H-tetrazol-5-yl)-1-cyclopentyl-1H-imidazol-5-yl)carbonimidodithioate (10e)

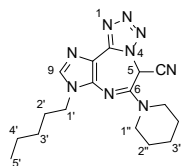


Prepared according to general procedure using tetrazolyl-imidazole derivative **2b** (50 mg, 0.13 mmol, 1.0 eq.), NaH (11 mg, 0.26 mmol, 2.0 eq.), 2-chloroacetonitrile (33 μ L, $\rho = 1.19$ g/mL, 0.53 mmol, 4 eq.) and KI (8 mg, 0.05 mmol, 0.05 eq.) in DMF (4 mL). Column chromatography gradient: DCM/MeCN 0% \rightarrow 7%. Yield: 30 mg, 55%. Colourless solid, $R_f = 0.73$ (DCM/MeCN = 9:1). IR ν (cm^{-1}): 2966, 2930, 2869, 1592, 1557, 1501, 1421, 1366, 1257, 1107, 986. ^1H NMR (500 MHz, CDCl_3) δ (ppm) 7.50 (s, 1H, H-C(2)), 5.95 (s, 2H, $\text{H}_2\text{-C}(1''')$), 4.32 (quintet, 1H, $^3J = 6.9$ Hz, H-C(1')), 3.70–4.20 (m, 2H, H-C(1'')), 2.11–2.21 (m, 2H,), 1.83–1.94 (m, 4H), 1.70–1.80 (m, 2H), 1.21–1.54 (m, 12H, H-C(2'')). $^{13}\text{C}\{^1\text{H}\}$ NMR (126 MHz, CDCl_3) δ (ppm) 174.8, 148.9, 140.7, 132.7, 113.4, 110.8, 56.6, 38.4, 36.3, 33.1, 24.1, 23.5. HRMS (ESI): calculated for $[\text{C}_{18}\text{H}_{26}\text{N}_8\text{S}_2 + \text{H}^+]$ 419.1795, found 419.1793.

General procedure for the synthesis of tetrazolodiazepines 11a-e

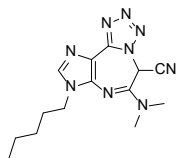
To a solution of tetrazolyl-imidazole derivative **10** in DMF K_2CO_3 (or NaH (57-63% suspension in mineral oil)) was added and the reaction mixture was stirred at rt for 24 h. After reaction completion (monitored by HPLC), the reaction was quenched with 10% AcOH solution (10 mL) and extracted with toluene (3×10 mL). The organic phase was washed with water (2×5 mL) and then with brine (2×5 mL), dried over anhydrous Na_2SO_4 , filtered, and evaporated under vacuum. The crude product was purified by silica gel column chromatography.

8-Pentyl-6-(piperidin-1-yl)-5,8-dihydroimidazo[4,5-f]tetrazolo[1,5-d][1,4]diazepine-5-carbonitrile (11a)



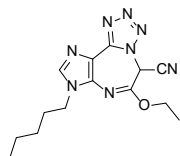
Prepared according to the general procedure using **10a** (400 mg, 1.04 mmol, 1.0 eq.) and K_2CO_3 (575 mg, 4.16 mmol, 4.0 eq.) in DMF (4 mL). Column chromatography gradient: DCM/MeCN 0% \rightarrow 15%. Yield: 255 mg, 69%. Brown solid, $R_f = 0.53$ (DCM/MeCN = 7:3). IR ν (cm^{-1}): 3375, 2952, 2923, 2853, 1676, 1612, 1572, 1442, 1197, 1019, 649. ^1H -NMR (500 MHz, CDCl_3) δ (ppm): 7.62 (s, 1H, H-C(9)), 7.45 (s, 1H, H-C(5)), 4.00 (ABqt, 2H, $\Delta\delta_{\text{AB}} = 0.07$, $J_{\text{AB}} = 13.8$ Hz, $^3J = 7.0$ Hz, $\text{H}_2\text{-C}(1')$), 3.82–3.71 (m, 4H, $2 \times \text{H}_2\text{-C}(1'')$), 1.84–1.67 (m, 8H, $\text{H}_2\text{-C}(2')$, $\text{H}_2\text{-C}(2'')$, $\text{H}_2\text{-C}(3'')$), 1.38–1.22 (m, 4H, $\text{H}_2\text{-C}(3')$, $\text{H}_2\text{-C}(4')$), 0.87 (t, 3H, $^3J = 7.0$ Hz, $\text{H}_3\text{-C}(5')$). $^{13}\text{C}\{^1\text{H}\}$ NMR (126 MHz, CDCl_3) δ (ppm): 149.9, 143.7, 139.7, 137.7, 111.1, 110.4, 49.1, 44.5, 44.1, 30.0, 28.7, 25.8, 24.2, 22.2, 14.0. HRMS (ESI): calculated for $[\text{C}_{17}\text{H}_{23}\text{N}_9 + \text{H}^+]$ 354.2149, found 354.2150.

6-(Dimethylamino)-8-pentyl-5,7a,8,10a-tetrahydroimidazo[4,5-f]tetrazolo[1,5-d][1,4]diazepine-5-carbonitrile (11b)



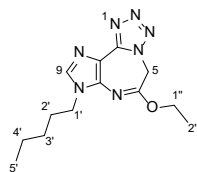
Prepared according to the general procedure using **10b** (220 mg, 0.64 mmol, 1.0 eq.) and K_2CO_3 (354 mg, 2.56 mmol, 4.0 eq.) in DMF (3 mL). Column chromatography gradient: DCM/MeCN 0% \rightarrow 7%. Yield: 122 mg, 61%. Brown solid, $R_f = 0.49$ (DCM/MeCN = 7:3). IR ν (cm^{-1}): 2930, 1616, 1577, 1403, 1276, 1156, 1064, 1003. 1H -NMR (500 MHz, $CDCl_3$) δ (ppm): 7.61 (s, 1H, H-C(9)), 7.44 (s, 1H, H-C(5)), 4.01 (ABqt, 2H, $\Delta\delta_{AB} = 0.08$, $J_{AB} = 13.7$ Hz, $^3J = 7.1$ Hz, H₂-C(1')), 3.65–3.07 (m, 6H, 2 \times H₃-C(1'')), 1.79 (quintet, 2H, $^3J = 6.8$ Hz, H₂-C(2')), 1.36–1.29 (m, 4H, H₂-C(3'), H₂-C(4')), 0.87 (t, 3H, $^3J = 7.0$ Hz, H₃-C(5')). $^{13}C\{^1H\}$ NMR (126 MHz, $CDCl_3$) δ (ppm): 150.0, 144.6, 139.8, 137.6, 110.7, 110.3, 44.7, 44.2, 40.2, 30.0, 28.7, 22.2, 14.0. HRMS (ESI): calculated for $[C_{14}H_{19}N_9 + H^+]$ 314.1836, found 314.1819.

6-Ethoxy-8-pentyl-5,8-dihydroimidazo[4,5-f]tetrazolo[1,5-d][1,4]diazepine-5-carbonitrile (**11c**)



Prepared according to the general procedure using **10c** (150 mg, 0.42 mmol, 1.0 eq.) and K_2CO_3 (230 mg, 1.66 mmol, 4.0 eq.) in DMF (2 mL). Column chromatography gradient: DCM/MeCN 0% \rightarrow 15%. Yield: 79 mg, 60%. Brown oil, $R_f = 0.54$ (DCM/MeCN = 9:1). IR ν (cm^{-1}): 2957, 2932, 2871, 1725, 1625, 1590, 1444, 1372, 1299, 1094, 957. 1H NMR (500 MHz, $CDCl_3$) δ (ppm) 7.72 (s, 1H, H-C(9)), 6.67 (s, 1H, H-C(5)), 4.47 (Abqq, 2H, $\Delta\delta_{AB} = 0.07$, $J_{AB} = 10.7$ Hz, $^3J = 7.2$ Hz, H₂-C(1'')), 4.06 (ABqt, 2H, $\Delta\delta_{AB} = 0.03$, $J_{AB} = 10.7$ Hz, $^3J = 7.2$ Hz, H₂-C(1')), 1.84 (quintet, 2H, $^3J = 7.2$ Hz, H₂-C(2')), 1.48 (t, 3H, $^3J = 7.1$ Hz, H₃-C(2'')), 1.28-1.39 (m, 4H, H₂-C(3'), H₂-C(4')), 0.90 (t, 3H, $^3J = 7.0$ Hz, H₃-C(5')). $^{13}C\{^1H\}$ NMR (126 MHz, $CDCl_3$) δ (ppm) 149.2, 148.9, 138.7, 135.1, 114.2, 109.5, 67.0, 49.6, 44.7, 30.2, 28.7, 22.2, 14.0, 13.9. HRMS (ESI): calculated for $[C_{14}H_{18}N_8O + H^+]$ 315.1676, found 315.1677.

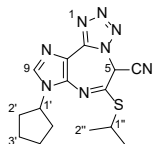
6-Ethoxy-8-pentyl-5,8-dihydroimidazo[4,5-f]tetrazolo[1,5-d][1,4]diazepine (**11d**)



Prepared according to general procedure using **10d** (200 mg, 0.49 mmol, 1.0 eq.) and NaH (24 mg, 0.59 mmol, 1.2 eq.) in DMF (3 mL). Column chromatography gradient: DCM/MeCN 0% \rightarrow 20%. Yield: 85 mg, 60%. White amorphous solid, $R_f = 0.60$ (DCM/MeCN = 4:1). IR ν (cm^{-1}): 2952, 2928, 2866, 1639, 1586, 1377, 1332, 1299, 1276, 1034, 987. 1H NMR (500 MHz, $CDCl_3$) δ (ppm) 7.61 (s, 1H, H-C(9)), 5.11 (s, 2H, H-C(5)), 4.37 (q, 2H, $^3J = 7.1$ Hz, H-C(1'')), 4.00 (t, 2H, $^3J = 7.1$ Hz, H-C(1')), 1.81 (quintet, 2H, $^3J = 7.1$ Hz, H-C(2')), 1.41 (t, 3H, $^3J = 7.1$ Hz, H-C(2'')), 1.28-1.39 (m, 4H, H-C(3'), H-C(4')), 0.90 (t, 3H, $^3J = 7.0$ Hz, H-C(5')). $^{13}C\{^1H\}$ NMR (126 MHz, $CDCl_3$) δ (ppm) 155.1, 149.9, 137.5, 136.6, 113.9, 65.2, 48.8,

44.4, 30.1, 28.8, 22.2, 14.0, 13.9. HRMS (ESI): calculated for [C₁₃H₁₉N₇O + H⁺] 290.1724, found 290.1724.

8-Cyclopentyl-6-(isopropylthio)-5,8-dihydroimidazo[4,5-f]tetrazolo[1,5-d][1,4]diazepine-5-carbonitrile (11e)



Prepared according to general procedure using **10e** (30 mg, 0.07 mmol, 1.0 eq.) and K₂CO₃ (39 mg, 0.29 mmol, 4.0 eq.) in DMF (0.5 mL). Column chromatography gradient: DCM/MeOH 0% → 5%. Yield: 15 mg, 62%.

Yellowish solid, R_f = 0.30 (DCM/MeCN = 9:1). IR ν (cm⁻¹): 2967, 2928, 2867, 1610, 1575, 1450, 1300, 1235, 1099, 1055, 1032. ¹H NMR (500 MHz, CDCl₃) δ (ppm) 7.78 (s, 1H, H-C(9)), 6.51 (s, 1H, H-C(5)), 4.72-4.80 (m, 1H, H-C(1')), 3.90 (heptet, 1H, ³J = 6.8 Hz, H-C(1')), 2.17-2.34 (m, 2H, 2×H-C(2')), 1.77-2.06 (m, 6H, 2×H₂-C(2'), 2×H₂-C(3')), 1.52 (d, 3H, ³J = 6.8 Hz, H_{3A}-C(2')), 1.43 (d, 3H, ³J = 6.8 Hz, H_{3B}-C(2')). ¹³C {¹H}NMR (126 MHz, CDCl₃) δ (ppm) 151.0, 149.1, 137.8, 136.9, 114.7, 109.7, 57.0, 51.5, 39.1, 33.4, 32.7, 23.9, 22.1, 22.0. HRMS (ESI): calculated for [C₁₅H₁₈N₈S + H⁺] 343.1448, found 343.1447.

ACKNOWLEDGMENTS

The authors thank the Latvian Council of Science grant LZP-2020/1-0348 for financial funding. K.L. thanks the European Social Fund within Project No. 8.2.2.0/20/I/008 “Strengthening of PhD students and academic personnel of Riga Technical University and BA School of Business and Finance in the strategic fields of specialization”. The authors thank *Dr. chem.* Kristīne Lazdoviča for IR analysis.

Data Availability Statement

Supporting information availability statement

ASSOCIATED CONTENT

The Supporting Information is available free of charge via the Internet at <http://pubs.acs.org>.

- Optimization of reaction conditions
- Synthesis of 2,6-diazidopurine derivatives **4**
- NMR spectra of synthesized compounds
- X-Ray Crystallography data
- Checkcif files for compounds **2a**, **5c**, **5h**, **7e**, **9b**, **10b**, **11d**
- Cif files for compounds **2a**, **5c**, **5h**, **7e**, **9b**, **10b**, **11d**

REFERENCES

- (1) Hansen, E. C.; Li, C.; Yang, S.; Pedro, D.; Weix, D. J. Coupling of Challenging Heteroaryl Halides with Alkyl Halides via Nickel-Catalyzed Cross-Electrophile Coupling. *J. Org. Chem.*, **2017**, *82* (14), 7085–7092. <https://doi.org/10.1021/acs.joc.7b01334>.
- (2) Santos, A.; Mortinho, A.; Marques, M. Metal-Catalyzed Cross-Coupling Reactions on Azaindole Synthesis and Functionalization. *Molecules*, **2018**, *23* (10), 2673. <https://doi.org/10.3390/molecules23102673>.
- (3) Ayogu, J. I.; Onoabedje, E. A. Recent Advances in Transition Metal-Catalysed Cross-Coupling of (Hetero)Aryl Halides and Analogues under Ligand-Free Conditions. *Catal. Sci. Technol.*, **2019**, *9* (19), 5233–5255. <https://doi.org/10.1039/C9CY01331H>.
- (4) Obydenov, D. L.; Simbirtseva, A. E.; Piksin, S. E.; Sosnovskikh, V. Y. 2,6-Dicyano-4-Pyrone as a Novel and Multifarious Building Block for the Synthesis of 2,6-Bis(Hetaryl)-4-Pyrones and 2,6-Bis(Hetaryl)-4-Pyridinols. *ACS Omega*, **2020**, *5* (51), 33406–33420. <https://doi.org/10.1021/acsomega.0c05357>.
- (5) Cook, X. A. F.; de Gombert, A.; McKnight, J.; Pantaine, L. R. E.; Willis, M. C. The 2-Pyridyl Problem: Challenging Nucleophiles in Cross-Coupling Arylations. *Angew. Chem. Int. Ed.*, **2021**, *60* (20), 11068–11091. <https://doi.org/10.1002/anie.202010631>.
- (6) Leškovskis, K.; Zaķis, J. M.; Novosjolova, I.; Turks, M. Applications of Purine Ring Opening in the Synthesis of Imidazole, Pyrimidine, and New Purine Derivatives. *Eur. J. Org. Chem.*, **2021**, *2021* (36), 5027–5052. <https://doi.org/10.1002/ejoc.202100755>.
- (7) Scheitl, C. P. M.; Okuda, T.; Adelman, J.; Höbartner, C. Ribozyme-Catalyzed Late-Stage Functionalization and Fluorogenic Labeling of RNA. *Angew. Chem.*, **2023**, *135* (31). <https://doi.org/10.1002/ange.202305463>.
- (8) Sebris, A.; Turks, M. Recent Investigations and Applications of Azidoazomethine-Tetrazole Tautomeric Equilibrium (Microreview). *Chem. Heterocycl. Compd. (N Y)*, **2019**, *55* (11), 1041–1043. <https://doi.org/10.1007/s10593-019-02574-7>.
- (9) Šišuljins, A.; Bucevičius, J.; Tseng, Y.-T.; Novosjolova, I.; Traskovskis, K.; Bizdēna, Ē.; Chang, H.-T.; Tumkevičius, S.; Turks, M. Synthesis and Fluorescent Properties of N(9)-Alkylated 2-Amino-6-Triazolylpurines and 7-Deazapurines. *Beilstein J. Org. Chem.*, **2019**, *15*, 474–489. <https://doi.org/10.3762/bjoc.15.41>.
- (10) Novosjolova, I.; Bizdēna, Ē.; Turks, M. Application of 2,6-Diazidopurine Derivatives in the Synthesis of Thiopurine Nucleosides. *Tetrahedron Lett.*, **2013**, *54* (48), 6557–6561. <https://doi.org/10.1016/j.tetlet.2013.09.095>.
- (11) Sebris, A.; Novosjolova, I.; Traskovskis, K.; Kokars, V.; Tetervenoka, N.; Vembris, A.; Turks, M. Photophysical and Electrical Properties of Highly Luminescent 2/6-Triazolyl-Substituted Push-Pull Purines. *ACS Omega*, **2022**, *7* (6), 5242–5253. <https://doi.org/10.1021/acsomega.1c06359>.

- (12) Novosjolova, I.; Bizdēna, Ē.; Turks, M. Synthesis of Novel 2- And 6-Alkyl/Arylthiopurine Derivatives. *Phosphorus Sulfur Silicon Relat. Elem.*, **2015**, *190* (8), 1236–1241. <https://doi.org/10.1080/10426507.2014.989435>.
- (13) Temple, C.; Kussner, C. L.; Montgomery, J. A. Studies on the Azidoazomethine—Tetrazole Equilibrium. V. 2- and 6-Azidopurines 1. *J. Org. Chem.*, **1966**, *31* (7), 2210–2215. <https://doi.org/10.1021/jo01345a031>.
- (14) Ozols, K.; Novosjolova, I.; Jeminejs, A.; Hopmann, K. H.; Morello, G. R.; Mishnev, A.; Stepanovs, D.; Cīrule, D.; Bizdēna, Ē.; Gaidai, O. V.; Gunchenko, P. A.; Fokin, A. A.; Turks, M. Azide – Tetrazole Tautomeric Equilibrium as Regioselectivity Switch for Purine C2-Selective S_NAr Reactions with Thiols. *J. Org. Chem.*, submitted on December 5, 2023, manuscript ID jo-2023-02787q.
- (15) Cīrule, D.; Novosjolova, I.; Spuris, A.; Mishnev, A.; Bizdēna, Ē.; Turks, M. Toward Unsymmetrical 2,6-Bistriazolylpurine Nucleosides. *Chem. Heterocycl. Compd. (NY)*, **2021**, *57* (3), 292–297. <https://doi.org/10.1007/s10593-021-02906-6>.
- (16) Cīrule, D.; Novosjolova, I.; Bizdēna, Ē.; Turks, M. 1,2,3-Triazoles as Leaving Groups: S_NAr Reactions of 2,6-Bistriazolylpurines with O- And C-Nucleophiles. *Beilstein J. Org. Chem.*, **2021**, *17*, 410–419. <https://doi.org/10.3762/BJOC.17.37>.
- (17) Kapilinskis, Z.; Novosjolova, I.; Bizdēna, Ē.; Turks, M. Synthesis of 2-Triazolylpurine Phosphonates. *Chem. Heterocycl. Compd. (NY)*, **2021**, *57* (1), 55–62. <https://doi.org/10.1007/s10593-021-02867-w>.
- (18) Kovaļovs, A.; Novosjolova, I.; Bizdena, E.; Bižane, I.; Skardziute, L.; Kazlauskas, K.; Jursenas, S.; Turks, M. 1,2,3-Triazoles as Leaving Groups in Purine Chemistry: A Three-Step Synthesis of N6-Substituted-2-triazolyl-adenine Nucleosides and Photophysical Properties Thereof. *Tetrahedron Lett.*, **2013**, *54* (8), 850–853. <https://doi.org/10.1016/j.tetlet.2012.11.095>.
- (19) Kriķis, K. E.; Novosjolova, I.; Mishnev, A.; Turks, M. 1,2,3-Triazoles as Leaving Groups in S_NAr-Arbuzov Reactions: Synthesis of C6-Phosphonated Purine Derivatives. *Beilstein J. Org. Chem.*, **2021**, *17*, 193–202. <https://doi.org/10.3762/BJOC.17.19>.
- (20) Sebris, A.; Traskovskis, K.; Novosjolova, I.; Turks, M. Synthesis and Photophysical Properties of 2-Azoyl-6-Piperidinylpurines. *Chem. Heterocycl. Compd. (NY)*, **2021**, *57* (5), 560–567. <https://doi.org/10.1007/s10593-021-02943-1>.
- (21) Cīrule, D.; Ozols, K.; Platnieks, O.; Bizdēna, Ē.; Māliņa, I.; Turks, M. Synthesis of Purine Nucleoside—Amino Acid Conjugates and Their Photophysical Properties. *Tetrahedron*, **2016**, *72* (29), 4177–4185. <https://doi.org/10.1016/j.tet.2016.05.043>.
- (22) Ozols, K.; Cīrule, D.; Novosjolova, I.; Stepanovs, D.; Liepinsh, E.; Bizdena, E.; Turks, M. Development of N6-Methyl-2-(1,2,3-Triazol-1-yl)-2'-deoxyadenosine as a Novel Fluorophore and Its Application in Nucleotide Synthesis. *Tetrahedron Lett.*, **2016**, *57* (10), 1174–1178. <https://doi.org/10.1016/j.tetlet.2016.02.003>.
- (23) Schinazi, R. F.; Sivets, G. G.; Detorio, M. A.; McBrayer, T. R.; Whitaker, T.; Coats, S. J.; Amblard, F. Synthesis and Antiviral Evaluation of 2',3'-Dideoxy-2',3'-difluoro-D-

- arabinofuranosyl 2,6-Disubstituted Purine Nucleosides. *Heterocycl. Comm.*, **2015**, *21* (5), 315–327. <https://doi.org/10.1515/hc-2015-0174>.
- (24) Petrič, A.; Tišler, M.; Stanovnik, B. Syntheses of Some Azolopyridopyrimidines. *Monatshefte für Chemie Chemical Monthly*, **1983**, *114* (5), 615–624. <https://doi.org/10.1007/BF00798617>.
- (25) Petrič, A.; Tišler, M.; Stanovnik, B. Ring-Opening Reactions of Triazolo- and Tetrazolo-Pyridopyrimidines or Quinazolines with Some Carbon Nucleophiles. *Monatshefte für Chemie Chemical Monthly*, **1985**, *116* (11), 1309–1319. <https://doi.org/10.1007/BF00811102>.
- (26) Woo, J.; Stein, C.; Christian, A. H.; Levin, M. D. Carbon-to-Nitrogen Single-Atom Transmutation of Azaarenes. *Nature*, **2023**, *623* (7985), 77–82. <https://doi.org/10.1038/s41586-023-06613-4>.
- (27) Jurczyk, J.; Woo, J.; Kim, S. F.; Dherange, B. D.; Sarpong, R.; Levin, M. D. Single-Atom Logic for Heterocycle Editing. *Nat. Synth.*, **2022**, *1* (5), 352–364. <https://doi.org/10.1038/s44160-022-00052-1>.
- (28) Mykura, R.; Sánchez-Bento, R.; Matador, E.; Duong, V. K.; Varela, A.; Angelini, L.; Carbajo, R. J.; Llaveria, J.; Ruffoni, A.; Leonori, D. Synthesis of Polysubstituted Azepanes by Dearomative Ring Expansion of Nitroarenes. *Nat. Chem.*, **2024**. <https://doi.org/10.1038/s41557-023-01429-1>.
- (29) Boudry, E.; Bourdreux, F.; Marrot, J.; Moreau, X.; Ghiazza, C. Dearomatization of Pyridines: Photochemical Skeletal Enlargement for the Synthesis of 1,2-Diazepines. *ChemRxiv* **2023**. DOI:10.26434/chemrxiv-2023-jjf8h. This content is a preprint and has not been peer-reviewed.
- (30) He, Y.; Wang, J.; Zhu, T.; Zheng, Z.; Wei, H. Nitrogen Atom Insertion into Arenols to Access Benzazepines. *Chem. Sci.*, **2024**. <https://doi.org/10.1039/D3SC05367A>.
- (31) Dherange, B. D.; Kelly, P. Q.; Liles, J. P.; Sigman, M. S.; Levin, M. D. Carbon Atom Insertion into Pyrroles and Indoles Promoted by Chlorodiazirines. *J. Am. Chem. Soc.*, **2021**, *143* (30), 11337–11344. <https://doi.org/10.1021/jacs.1c06287>.
- (32) Wang, J.; Lu, H.; He, Y.; Jing, C.; Wei, H. Cobalt-Catalyzed Nitrogen Atom Insertion in Arylcycloalkenes. *J. Am. Chem. Soc.* **2022**, *144* (49), 22433–22439. <https://doi.org/10.1021/jacs.2c10570>.
- (33) Bartholomew, G. L.; Carpaneto, F.; Sarpong, R. Skeletal Editing of Pyrimidines to Pyrazoles by Formal Carbon Deletion. *J. Am. Chem. Soc.*, **2022**, *144* (48), 22309–22315. <https://doi.org/10.1021/jacs.2c10746>.
- (34) Jurczyk, J.; Lux, M. C.; Adpressa, D.; Kim, S. F.; Lam, Y.; Yeung, C. S.; Sarpong, R. Photomediated Ring Contraction of Saturated Heterocycles. *Science*, **2021**, *373* (6558), 1004–1012. <https://doi.org/10.1126/science.abi7183>.
- (35) Cheng, Q.; Bhattacharya, D.; Haring, M.; Cao, H.; Mück-Lichtenfeld, C.; Studer, A. Skeletal Editing of Pyridines through Atom-Pair Swap from CN to CC. *Nat. Chem.*, **2024**. <https://doi.org/10.1038/s41557-023-01428-2>.

- (36) Liu, Z.; Sivaguru, P.; Ning, Y.; Wu, Y.; Bi, X. Skeletal Editing of (Hetero)Arenes Using Carbenes. *Chem. Eur. J.*, **2023**, *29* (42), e202301227. <https://doi.org/10.1002/chem.202301227>.
- (37) Joynson, B. W.; Ball, L. T. Skeletal Editing: Interconversion of Arenes and Heteroarenes. *Helv. Chim. Acta*, **2023**, *106* (3), e202200182. <https://doi.org/10.1002/hlca.202200182>.
- (38) Vondenhoff, G. H.; Gadakh, B.; Severinov, K.; Van Aerschot, A. Microcin C and Albomycin Analogues with Aryl-tetrazole Substituents as Nucleobase Isosters Are Selective Inhibitors of Bacterial Aminoacyl TRNA Synthetases but Lack Efficient Uptake. *ChemBioChem*, **2012**, *13* (13), 1959–1969. <https://doi.org/10.1002/cbic.201200174>.
- (39) Ornstein, P. L.; Arnold, M. B.; Allen, N. K.; Bleisch, T.; Borromeo, P. S.; Lugar, C. W.; Leander, J. D.; Lodge, D.; Schoepp, D. D. Structure–Activity Studies of 6-Substituted Decahydroisoquinoline-3-Carboxylic Acid AMPA Receptor Antagonists. 2. Effects of Distal Acid Bioisosteric Substitution, Absolute Stereochemical Preferences, and in Vivo Activity. *J. Med. Chem.*, **1996**, *39* (11), 2232–2244. <https://doi.org/10.1021/jm950913h>.
- (40) Martinez-Perez, J. A.; Iyengar, S.; Shannon, H. E.; Bleakman, D.; Alt, A.; Clawson, D. K.; Arnold, B. M.; Bell, M. G.; Bleisch, T. J.; Castaño, A. M.; Del Prado, M.; Dominguez, E.; Escribano, A. M.; Filla, S. A.; Ho, K. H.; Hudziak, K. J.; Jones, C. K.; Mateo, A.; Mathes, B. M.; Mattiuz, E. L.; Ogden, A. M. L.; Simmons, R. M. A.; Stack, D. R.; Stratford, R. E.; Winter, M. A.; Wu, Z.; Ornstein, P. L. GluK1 Antagonists from 6-(Tetrazolyl)Phenyl Decahydroisoquinoline Derivatives: In Vitro Profile and in Vivo Analgesic Efficacy. *Bioorg. Med. Chem. Lett.*, **2013**, *23* (23), 6463–6466. <https://doi.org/10.1016/j.bmcl.2013.09.045>.
- (41) Višnjić, D.; Lalić, H.; Dembitz, V.; Tomić, B.; Smoljo, T. Aicar, a Widely Used Ampk Activator with Important Ampk-Independent Effects: A Systematic Review. *Cells*, **2021**, *10* (5), 1095. <https://doi.org/10.3390/cells10051095>.
- (42) Narkar, V. A.; Downes, M.; Yu, R. T.; Emblar, E.; Wang, Y. X.; Banayo, E.; Mihaylova, M. M.; Nelson, M. C.; Zou, Y.; Juguilon, H.; Kang, H.; Shaw, R. J.; Evans, R. M. AMPK and PPAR δ Agonists are Exercise Mimetics. *Cell*, **2008**, *134* (3), 405–415. <https://doi.org/10.1016/j.cell.2008.06.051>.
- (43) Meyer, A. G.; Bissember, A. C.; Hyland, C. J. T.; Williams, C. C.; Szabo, M.; Wales, S. M.; Constable, G. E. O.; Olivier, W. J. Seven-Membered Rings; 2021; pp 565–614. <https://doi.org/10.1016/B978-0-323-89812-6.00016-X>.
- (44) Boa, A. N.; McPhillie, M. J. 1,4-Diazepines. In *Comprehensive Heterocyclic Chemistry IV*; Elsevier, 2022; pp 243–268. <https://doi.org/10.1016/B978-0-12-818655-8.00110-4>.
- (45) Belen'kii, L. I.; Gazieva, G. A.; Evdokimenkova, Y. B.; Soboleva, N. O. The Literature of Heterocyclic Chemistry, Part XIX, 2019; 2022; pp 225–295. <https://doi.org/10.1016/bs.aihch.2021.09.002>.
- (46) Adarve-Cardona, L.; Garay-Talero, A.; Gamba-Sánchez, D. Synthesis of Naturally Occurring Seven-Membered Nitrogen Heterocycles and Related Bioactive Compounds; 2023; pp 189–235. <https://doi.org/10.1016/B978-0-323-91253-2.00016-9>.

- (47) Rashid, M. A.; Ashraf, A.; Rehman, S. S.; Shahid, S. A.; Mahmood, A.; Faruq, M. 1,4-Diazepines: A Review on Synthesis, Reactions and Biological Significance. *Curr. Org. Synth.*, **2019**, *16* (5), 709–729. <https://doi.org/10.2174/1570179416666190703113807>.
- (48) Sakaine, G.; Ture, A.; Pedroni, J.; Smits, G. Isolation, Chemistry, and Biology of Pyrrolo[1,4]benzodiazepine Natural Products. *Med. Res. Rev.*, **2022**, *42* (1), 5–55. <https://doi.org/10.1002/med.21803>.
- (49) Batlle, E.; Lizano, E.; Viñas, M.; Dolors Pujol, M. 1,4-Benzodiazepines and New Derivatives: Description, Analysis, and Organic Synthesis. In *Medicinal Chemistry*; IntechOpen, 2019. <https://doi.org/10.5772/intechopen.79879>.
- (50) Coggins, A. J.; Tocher, D. A.; Powner, M. W. One-Step Protecting-Group-Free Synthesis of Azepinomycin in Water. *Org. Biomol. Chem.*, **2015**, *13* (11), 3378–3381. <https://doi.org/10.1039/C5OB00210A>.
- (51) Isshiki, K.; Takahashi, Y.; Iinuma, H.; Naganawa, H.; Umezawa, Y.; Takeuchi, T.; Umezawa, H.; Nishimura, S.; Okada, N.; Tatsuta, K. Synthesis of Azepinomycin and Its β -D-Ribofuranoside. *J. Antibiot. (Tokyo)*, **1987**, *40* (10), 1461–1463. <https://doi.org/10.7164/antibiotics.40.1461>.
- (52) Daley, S.; Cordell, G. A. Homopurine Alkaloids: A Brief Overview. *Nat. Prod. Commun.*, **2020**, *15* (4), 1934578X2091778. <https://doi.org/10.1177/1934578X20917787>.
- (53) Hosmane, R. S. Chapter 2: Ring-Expanded ('Fat') Purines and Their Nucleoside/Nucleotide Analogues as Broad-Spectrum Therapeutics; 2009; pp 35–68. [https://doi.org/10.1016/S0959-6380\(09\)70029-7](https://doi.org/10.1016/S0959-6380(09)70029-7).
- (54) Hosmane, R. Ring-Expanded Nucleosides as Broad-Spectrum Anticancer and Antiviral Agents. *Curr. Top Med. Chem.*, **2002**, *2* (10), 1093–1109. <https://doi.org/10.2174/1568026023393147>.
- (55) Tantravedi, S.; Chakraborty, S.; Shah, N. H.; Fishbein, J. C.; Hosmane, R. S. Analogs of Iso-Azepinomycin as Potential Transition-State Analog Inhibitors of Guanase: Synthesis, Biochemical Screening, and Structure–Activity Correlations of Various Selectively Substituted Imidazo[4,5-*e*][1,4]Diazepines. *Bioorg. Med. Chem.*, **2013**, *21* (17), 4893–4903. <https://doi.org/10.1016/j.bmc.2013.06.069>.
- (56) Chakraborty, S.; Shah, N. H.; Fishbein, J. C.; Hosmane, R. S. A Novel Transition State Analog Inhibitor of Guanase Based on Azepinomycin Ring Structure: Synthesis and Biochemical Assessment of Enzyme Inhibition. *Bioorg. Med. Chem. Lett.*, **2011**, *21* (2), 756–759. <https://doi.org/10.1016/j.bmcl.2010.11.109>.
- (57) Chakraborty, S.; Shah, N. H.; Fishbein, J. C.; Hosmane, R. S. Investigations into Specificity of Azepinomycin for Inhibition of Guanase: Discrimination between the Natural Heterocyclic Inhibitor and Its Synthetic Nucleoside Analogues. *Bioorg. Med. Chem. Lett.*, **2012**, *22* (23), 7214–7218. <https://doi.org/10.1016/j.bmcl.2012.09.053>.
- (58) Ujjinamatada, R. K.; Bhan, A.; Hosmane, R. S. Design of Inhibitors against Guanase: Synthesis and Biochemical Evaluation of Analogues of Azepinomycin. *Bioorg. Med. Chem. Lett.*, **2006**, *16* (21), 5551–5554. <https://doi.org/10.1016/j.bmcl.2006.08.033>.

- (59) Ozols, K. Study on Nucleophilic Heteroaromatic Substitution Reactions in Purine Ring, Master Thesis, Riga Technical University, Riga, **2017**.
- (60) Cmoch, P.; Korczak, H.; Stefaniak, L.; Webb, G. A. ^1H , ^{13}C And ^{15}N NMR and IR Studies of Halogen-Substituted Tetrazolo[1,5-*a*]Pyridines. *J. Phys. Org. Chem.*, **1999**, *12* (6), 470–478. [https://doi.org/10.1002/\(SICI\)1099-1395\(199906\)12:6<470::AID-POC151>3.0.CO;2-U](https://doi.org/10.1002/(SICI)1099-1395(199906)12:6<470::AID-POC151>3.0.CO;2-U).
- (61) Cmoch, P.; Wiench, J. W.; Stefaniak, L.; Webb, G. A. The Tetrazole–Azide Tautomerism of Some Nitrotetrazolo[1,5-*a*]Pyridines Studied by NMR, IR Spectroscopy and Molecular Orbital Calculations. *J. Mol. Struct.*, **1999**, *510* (1–3), 165–178. [https://doi.org/10.1016/S0022-2860\(99\)00075-7](https://doi.org/10.1016/S0022-2860(99)00075-7).
- (62) Leškovskis, K.; Mishnev, A.; Novosjolova, I.; Turks, M. Structural Study of Azide-Tetrazole Equilibrium in Pyrido[2,3-*d*]pyrimidines. *J. Mol. Struct.*, **2022**, *1269*, 133784. <https://doi.org/10.1016/j.molstruc.2022.133784>.
- (63) Leškovskis, K.; Mishnev, A.; Novosjolova, I.; Turks, M. $\text{S}_{\text{N}}\text{Ar}$ Reactions of 2,4-Diazidopyrido[3,2-*d*]pyrimidine and Azide-Tetrazole Equilibrium Studies of the Obtained 5-Substituted Tetrazolo[1,5-*a*]pyrido[2,3-*e*]pyrimidines. *Molecules*, **2022**, *27* (22). <https://doi.org/10.3390/molecules27227675>.
- (64) Hansch, Corwin.; Leo, A.; Taft, R. W. A Survey of Hammett Substituent Constants and Resonance and Field Parameters. *Chem. Rev.*, **1991**, *91* (2), 165–195. <https://doi.org/10.1021/cr00002a004>.
- (65) Cherkasov, A. R.; Galkin, V. I.; Cherkasov, R. A. The Problem of the Quantitative Evaluation of the Inductive Effect: Correlation Analysis. *Russ. Chem. Rev.*, **1996**, *65* (8), 641–656. <https://doi.org/10.1070/RC1996v065n08ABEH000227>.
- (66) Cherkasov, A. R.; Galkin, V. I.; Zueva, E. M.; Cherkasov, R. A. The Concept of Electronegativity. The Current State of the Problem. *Russ. Chem. Rev.*, **1998**, *67* (5), 375–392. <https://doi.org/10.1070/RC1998v067n05ABEH000383>.
- (67) Ivanov, É. I. Synthesis of Crown Containing Imidazo[4,5-*e*] and-[5,4-*e*][1,4]Diazepines. *Chem. Heterocycl. Compd. (NY)*, **1998**, *34* (6), 723–726. <https://doi.org/10.1007/BF02252284>.
- (68) Aoyagi, M.; Minakawa, N.; Matsuda, A. Nucleosides and Nucleotides. 130. The Synthesis of Imidazo[4, 5-*e*][1,4] Diazepine Nucleosides From N^1 -Substituted Inosines. *Nucleosides Nucleotides* **1994**, *13* (6–7), 1535–1549. <https://doi.org/10.1080/15257779408012169>.
- (69) Rajappan, V. P.; Hosmane, R. S. Pentafluorophenol: A Superior Reagent for Condensations in Heterocyclic Chemistry. *Synth. Commun.*, **1998**, *28* (4), 753–764. <https://doi.org/10.1080/00397919808005949>.
- (70) Zaķis, J. M.; Ozols, K.; Novosjolova, I.; Vilšķērstis, R.; Mishnev, A.; Turks, M. R. Sulfonyl Group Dance: A Tool for the Synthesis of 6-Azido-2-sulfonyl-purine Derivatives. *J. Org. Chem.*, **2020**, *85* (7), 4753–4771. <https://doi.org/10.1021/acs.joc.9b03518>.

- (71) Cortat, Y.; Zobi, F. Resurgence and Repurposing of Antifungal Azoles by Transition Metal Coordination for Drug Discovery. *Pharmaceutics*, **2023**, *15* (10), 2398. <https://doi.org/10.3390/pharmaceutics15102398>.
- (72) Kashyap, S.; Singh, R.; Singh, U. P. Inorganic and Organic Anion Sensing by Azole Family Members. *Coord. Chem. Rev.*, **2020**, *417*, 213369. <https://doi.org/10.1016/j.ccr.2020.213369>.
- (73) Wood, O. G.; Hawes, C. S. Fused Aza-Heterocyclic Ligands: Expanding the MOF Chemist's Toolbox. *CrystEngComm.*, **2022**, *24* (47), 8197–8207. <https://doi.org/10.1039/D2CE01475K>.
- (74) Verma, C.; Thakur, A.; Ganjoo, R.; Sharma, S.; Assad, H.; Kumar, A.; Quraishi, M. A.; Alfantazi, A. Coordination Bonding and Corrosion Inhibition Potential of Nitrogen-Rich Heterocycles: Azoles and Triazines as Specific Examples. *Coord. Chem. Rev.*, **2023**, *488*, 215177. <https://doi.org/10.1016/j.ccr.2023.215177>.
- (75) Kumar Bhaumik, P.; Ghosh, K.; Chattopadhyay, S. Synthetic Strategies, Crystal Structures and Biological Activities of Metal Complexes with the Members of Azole Family: A Review. *Polyhedron*, **2021**, *200*, 115093. <https://doi.org/10.1016/j.poly.2021.115093>.
- (76) Aromí, G.; Barrios, L. A.; Roubeau, O.; Gamez, P. Triazoles and Tetrazoles: Prime Ligands to Generate Remarkable Coordination Materials. *Coord. Chem. Rev.*, **2011**, *255* (5–6), 485–546. <https://doi.org/10.1016/j.ccr.2010.10.038>.
- (77) Thompson, M. W. Regulation of Zinc-Dependent Enzymes by Metal Carrier Proteins. *BioMetals*, **2022**, *35* (2), 187–213. <https://doi.org/10.1007/s10534-022-00373-w>.
- (78) Andreini, C.; Banci, L.; Bertini, I.; Rosato, A. Counting the Zinc-Proteins Encoded in the Human Genome. *J. Proteome Res.*, **2006**, *5* (1), 196–201. <https://doi.org/10.1021/pr050361j>.
- (79) Ivanova, J.; Nocentini, A.; Tārs, K.; Leitāns, J.; Dvinskis, E.; Kazaks, A.; Domračeva, I.; Supuran, C. T.; Žalubovskis, R. Atropo/Tropo Flexibility: A Tool for Design and Synthesis of Self-Adaptable Inhibitors of Carbonic Anhydrases and Their Antiproliferative Effect. *J. Med. Chem.*, **2023**, *66* (8), 5703–5718. <https://doi.org/10.1021/acs.jmedchem.3c00007>.
- (80) Grandāne, A.; Nocentini, A.; Domračeva, I.; Žalubovskis, R.; Supuran, C. T. Development of Oxathiino[6,5-*b*]pyridine 2,2-Dioxide Derivatives as Selective Inhibitors of Tumor-Related Carbonic Anhydrases IX and XII. *Eur. J. Med. Chem.*, **2020**, *200*, 112300. <https://doi.org/10.1016/j.ejmech.2020.112300>.
- (81) Angeli, A.; Kartsev, V.; Petrou, A.; Lichitsky, B.; Komogortsev, A.; Geronikaki, A.; Supuran, C. T. Substituted Furan Sulfonamides as Carbonic Anhydrase Inhibitors: Synthesis, Biological and in Silico Studies. *Bioorg. Chem.*, **2023**, *138*, 106621. <https://doi.org/10.1016/j.bioorg.2023.106621>.
- (82) Abdoli, M.; Supuran, C. T.; Žalubovskis, R. 2-((1*H*-Benzo[*d*]imidazol-2-yl)amino)benzo[*d*]thiazole-6-sulphonamides: A Class of Carbonic Anhydrase II and VII-

- Selective Inhibitors. *J. Enzyme Inhib. Med. Chem.*, **2023**, *38* (1). <https://doi.org/10.1080/14756366.2023.2174981>.
- (83) Cuffaro, D.; Di Leo, R.; Ciccone, L.; Nocentini, A.; Supuran, C. T.; Nuti, E.; Rossello, A. New Isoxazolidinyl-Based *N*-Alkylethanolamines as New Activators of Human Brain Carbonic Anhydrases. *J. Enzyme Inhib. Med. Chem.*, **2023**, *38* (1). <https://doi.org/10.1080/14756366.2022.2164574>.
- (84) Khalifah, R. G. The Carbon Dioxide Hydration Activity of Carbonic Anhydrase. I. Stop-Flow Kinetic Studies on the Native Human Isoenzymes B and C. *J. Biol. Chem.*, **1971**, *246* (8), 2561–2573.
- (85) Sheldrick, G. M. *SHELXT* – Integrated Space-Group and Crystal-Structure Determination. *Acta Crystallogr. A Found Adv.*, **2015**, *71* (1), 3–8. <https://doi.org/10.1107/S2053273314026370>.
- (86) Sheldrick, G. M. A Short History of *SHELX*. *Acta Crystallogr. A*, **2008**, *64* (1), 112–122. <https://doi.org/10.1107/S0108767307043930>.
- (87) Farrugia, L. J. *WinGX* and *ORTEP for Windows*: An Update. *J. Appl. Crystallogr.*, **2012**, *45* (4), 849–854. <https://doi.org/10.1107/S0021889812029111>.
- (88) Bruno, I. J.; Cole, J. C.; Edgington, P. R.; Kessler, M.; Macrae, C. F.; McCabe, P.; Pearson, J.; Taylor, R. New Software for Searching the Cambridge Structural Database and Visualizing Crystal Structures. *Acta Crystallogr. B*, **2002**, *58* (3), 389–397. <https://doi.org/10.1107/S0108768102003324>.
- (89) Spek, A. L. Single-Crystal Structure Validation with the Program *PLATON*. *J. Appl. Crystallogr.*, **2003**, *36* (1), 7–13. <https://doi.org/10.1107/S0021889802022112>.
- (90) Vermelho, A. B.; da Silva Cardoso, V.; Ricci Junior, E.; dos Santos, E. P.; Supuran, C. T. Nanoemulsions of Sulfonamide Carbonic Anhydrase Inhibitors Strongly Inhibit the Growth of *Trypanosoma Cruzi*. *J. Enzyme Inhib. Med. Chem.*, **2018**, *33* (1), 139–146. <https://doi.org/10.1080/14756366.2017.1405264>.
- (91) Nocentini, A.; Carta, F.; Tanc, M.; Selleri, S.; Supuran, C. T.; Bazzicalupi, C.; Gratteri, P. Deciphering the Mechanism of Human Carbonic Anhydrases Inhibition with Sulfocoumarins: Computational and Experimental Studies. *Chem. Eur. J.*, **2018**, *24* (31), 7840–7844. <https://doi.org/10.1002/chem.201800941>.
- (92) Pustenko, A.; Nocentini, A.; Gratteri, P.; Bonardi, A.; Vozny, I.; Žalubovskis, R.; Supuran, C. T. The Antibiotic Furagin and Its Derivatives Are Isoform-Selective Human Carbonic Anhydrase Inhibitors. *J. Enzyme Inhib. Med. Chem.*, **2020**, *35* (1), 1011–1020. <https://doi.org/10.1080/14756366.2020.1752201>.
- (93) Nocentini, A.; Bonardi, A.; Gratteri, P.; Cerra, B.; Gioiello, A.; Supuran, C. T. Steroids Interfere with Human Carbonic Anhydrase Activity by Using Alternative Binding Mechanisms. *J. Enzyme Inhib. Med. Chem.*, **2018**, *33* (1), 1453–1459. <https://doi.org/10.1080/14756366.2018.1512597>.

- (94) Chohan, Z. H.; Munawar, A.; Supuran, C. T. Transition Metal Ion Complexes of Schiff-Bases. Synthesis, Characterization and Antibacterial Properties. *Met. Based Drugs*, **2001**, *8* (3), 137–143. <https://doi.org/10.1155/MBD.2001.137>.
- (95) Ivanova, J.; Carta, F.; Vullo, D.; Leitans, J.; Kazaks, A.; Tars, K.; Žalubovskis, R.; Supuran, C. T. N-Substituted and Ring Opened Saccharin Derivatives Selectively Inhibit Transmembrane, Tumor-Associated Carbonic Anhydrases IX and XII. *Bioorg. Med. Chem.*, **2017**, *25* (13), 3583–3589. <https://doi.org/10.1016/j.bmc.2017.04.007>.
- (96) Briganti, F.; Pierattelli, R.; Scozzafava, A.; Supuran, C. Carbonic Anhydrase Inhibitors. Part 37. Novel Classes of Isozyme I and II Inhibitors and Their Mechanism of Action. Kinetic and Spectroscopic Investigations on Native and Cobalt-Substituted Enzymes. *Eur. J. Med. Chem.*, **1996**, *31* (12), 1001–1010. [https://doi.org/10.1016/S0223-5234\(97\)86179-X](https://doi.org/10.1016/S0223-5234(97)86179-X).
- (97) Pastorekova, S.; Casini, A.; Scozzafava, A.; Vullo, D.; Pastorek, J.; Supuran, C. T. Carbonic Anhydrase Inhibitors: The First Selective, Membrane-Impermeant Inhibitors Targeting the Tumor-Associated Isozyme IX. *Bioorg. Med. Chem. Lett.*, **2004**, *14* (4), 869–873. <https://doi.org/10.1016/j.bmcl.2003.12.029>.
- (98) Carta, F.; Supuran, C. T.; Scozzafava, A. Sulfonamides and Their Isosters as Carbonic Anhydrase Inhibitors. *Future Med. Chem.*, **2014**, *6* (10), 1149–1165. <https://doi.org/10.4155/fmc.14.68>.
- (99) Yıldırım, A.; Atmaca, U.; Keskin, A.; Topal, M.; Çelik, M.; Gülçin, İ.; Supuran, C. T. N-Acylsulfonamides Strongly Inhibit Human Carbonic Anhydrase Isoenzymes I and II. *Bioorg. Med. Chem.*, **2015**, *23* (10), 2598–2605. <https://doi.org/10.1016/j.bmc.2014.12.054>.
- (100) Innocenti, A.; Gülçin, I.; Scozzafava, A.; Supuran, C. T. Carbonic Anhydrase Inhibitors. Antioxidant Polyphenols Effectively Inhibit Mammalian Isoforms I–XV. *Bioorg. Med. Chem. Lett.*, **2010**, *20* (17), 5050–5053. <https://doi.org/10.1016/j.bmcl.2010.07.038>.
- (101) Niu, H. Y.; Xia, C.; Qu, G. R.; Zhang, Q.; Jiang, Y.; Mao, R. Z.; Li, D. Y.; Guo, H. M. CuBr Catalyzed C–N Cross Coupling Reaction of Purines and Diaryliodonium Salts to 9-Arylpurines. *Org. Biomol. Chem.*, **2011**, *9* (14), 5039–5042. <https://doi.org/10.1039/c1ob05333g>.

Leškovskis, K.; Novosjolova, I.; Turks, M.

**Structural Study of Azide-Tetrazole Equilibrium in
Pyrido[2,3-*d*]Pyrimidines**

J. Mol. Struct., **2022**, 1269, 133784

doi:10.1016/j.molstruc.2022.133784

Publikācija un tās pielikums pieejams bez maksas

[Elsevier mājaslapā](#)

The Publication and Supporting Information is available free of charge on the

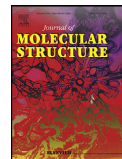
[Elsevier website](#)

Pārpublicēts ar *Elsevier* atļauju.

Copyright © 2022 Elsevier B.V. All rights reserved.

Reprinted with the permission from Elsevier.

Copyright © 2022 Elsevier B.V. All rights reserved.



Structural study of azide-tetrazole equilibrium in pyrido[2,3-*d*]pyrimidines

Kristaps Leškovskis^a, Anatoly Mishnev^b, Irina Novosjolova^{a,*}, Māris Turks^{a,*}

^a Institute of Technology of Organic Chemistry, Faculty of Materials Science and Applied Chemistry, Riga Technical University, P. Valdena Str. 3, Riga, LV 1048, Latvia

^b Latvian Institute of Organic Synthesis, Aizkraukles Str. 21, Riga, LV-1006, Latvia



ARTICLE INFO

Article history:

Received 13 June 2022

Revised 11 July 2022

Accepted 22 July 2022

Available online 24 July 2022

Keywords:

Azide

Tetrazole

S_NAr

Triazole

Pyrido[2,3-*d*]pyrimidine

Tautomeric equilibrium

ABSTRACT

C-5 Substituted pyrido[3,2-*e*]tetrazolo[1,5-*a*]pyrimidines were obtained by simple azidation of 2,4-dichloropyrido[2,3-*d*]pyrimidine followed by S_NAr reactions with S-, N- and O-nucleophiles. Their NMR and IR studies revealed that the mono-azido products undergo azide-tetrazole equilibrium, whereas 2,4-diazidopyrido[2,3-*d*]pyrimidine exists in four tautomeric forms in various solutions, and its solid phase tautomer was established by the X-ray analysis. In total, nine of the obtained products are fully characterized by their single crystal X-ray structures and seven of them revealed a novel annulated pyrido[3,2-*e*]tetrazolo[1,5-*a*]pyrimidine skeleton. Among the studied products the amino derivatives - 5-aminopyrido[3,2-*e*]tetrazolo[1,5-*a*]pyrimidines - exist mainly in their tetrazole form both in the solid phase and in the solutions. However, also the latter enter the tautomeric equilibrium and the liberated azido group is able to undergo copper(I)-catalyzed azide-alkyne cycloaddition (CuAAC) reaction and form the corresponding 1,2,3-triazole derivatives. Free Gibbs energies of the tautomerization of C-5 substituted cyclohexylmercapto-, isopropoxy- and phenoxy-pyrido[3,2-*e*]tetrazolo[1,5-*a*]pyrimidines were found to be -21.30, -23.19 and -17.02 kJ/mol, respectively.

© 2022 Elsevier B.V. All rights reserved.

1. Introduction

Fused pyrimidines are privileged heterocyclic pharmacophores found in many marketed drugs [1–3]. As such, they display future potential for more potent and efficient drug development [4–6]. Interest for pyrido[2,3-*d*]pyrimidine scaffold by medicinal chemists in new drug design increases in recent years [7–12]. Hence, new synthetic methods are continuously being developed to obtain more complex functionalized pyrimidines, including pyrido[2,3-*d*]pyrimidines [13–17]. In this context, azido-substituted heterocycles play a crucial role due to versatile reactivity patterns of azido group.

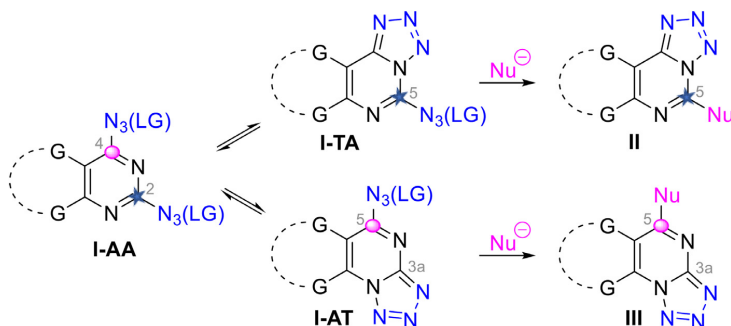
Heterocycles possessing azido-azomethine structural entity are particularly interesting by several aspects: 1) they undergo dynamic azide-tetrazole equilibrium in solution phase [18–20] and this has been reviewed [21–23]; 2) azido group as pseudohalide displays properties of a leaving group in the S_NAr reactions [24–30]; 3) rich chemistry of azido substituent offers further modification possibilities [31]. Additionally, from the synthetic chemistry point of view the azide-tetrazole ring-chain tautomerism

is known to modulate the S_NAr reactivity. In the case of fused azido-pyrimidines **I-AA**, which possesses two identical leaving groups at C-2 and C-4, a nucleophile would primarily react at C-4 (Scheme 1). If the tautomer **I-TA** prevails, the regioselectivity of the nucleophile attack will be changed to C-2 (equals to C-5 in tetrazolo-tautomer **I-TA**) and product **II** will be obtained. On the other hand, an equilibrium towards **I-AT** gives a matched case, which ensures reactivity at C-4 (equals to C-5 in tetrazolo-tautomer **I-AT**) and provides product **III**. Additionally, the electron-withdrawing character of the fused tetrazolopyrimidine system may significantly enhance the rate of the S_NAr reaction at the C- N_3 reactive center.

During the past decades several 2,4-diazido-pyrimidine derivatives and their fused analogs have been investigated. The published reports reveal that there are different tautomeric equilibria in structural classes **A-C** (Fig. 1). For example, 2,4-diazidopyrimidines **A** [19,20] and 2,4-diazidoquinazolines **C** [29] tend to enhance the classical reactivity at C-4 by tetrazole formation from the azido group at C-2. On the other hand, tetrazole from azido group at C-6 prevail in purines ($X = N$) [27,30,32] and 7-deazapurines ($X = CH$) **B** [25,28]. Intrigued by the underexplored yet privileged pyrido[2,3-*d*]pyrimidine scaffold, we decided to explore the structure and reactivity of its 2,4-diazido substituted form **D** and its S_NAr reaction products. To the best of our knowledge, the

* Corresponding authors.

E-mail addresses: Irina.Novosjolova@rtu.lv (I. Novosjolova), Maris.Turks@rtu.lv (M. Turks).



Scheme 1. S_NAr regioselectivity in fused azidopyrimidines; C-2 position of structure **I-AA** equals to C-5 in tetrazolo-tautomer **I-TA** and product **II**, C-4 position of structure **I-AA** equals to C-5 in tetrazolo-tautomer **I-AT** and product **III**.

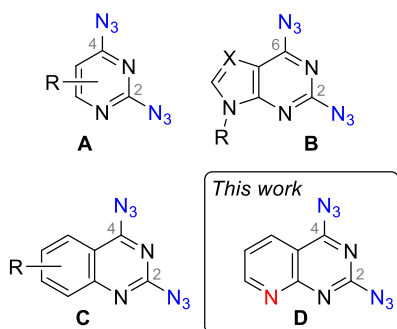


Fig. 1. 2,4-Diazo derivatives in pyrimidine class.

annulated scaffold of pyrido[3,2-*e*]tetrazolo[1,5-*a*]pyrimidines has been reported only once for 4-alkylated 6,8-dimethylpyrido[3,2-*e*]tetrazolo[1,5-*a*]pyrimidin-5(4*H*)-ones, which are potent anticancer and antidepressant agents [33].

Hence, we report here our findings on the reactivity pattern of 2,4-diazidopyrido[2,3-*d*]pyrimidine **D** with *O*-, *N*- and *S*-nucleophiles, which is accompanied by IR, NMR and single crystal X-ray studies of the substitution products.

2. Results and discussion

2.1. Synthesis

First, we obtained our key starting material 2,4-diazidopyrido[2,3-*d*]pyrimidine (**2**) with practically quantitative

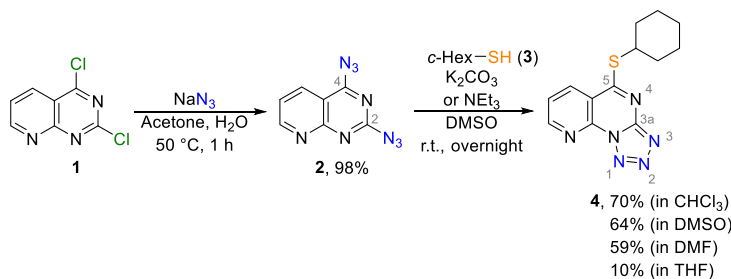
yield in a simple reaction of commercially available dichloride **1** with sodium azide (Scheme 2). Here and further the name *diazide* and structure **2** are used as formal simplification, as compound **2** does not exist in a pure diazide form, but rather as a mixture of azide-tetrazole tautomeric forms. We observed diazide **2** undergoing azide-tetrazole tautomerism in solutions by NMR. Addition of cyclohexanethiol (**3**) to diazide **2** in various solvents (DMSO, DMF, THF, $CHCl_3$) in basic medium (K_2CO_3 or NEt_3) proceeded at the C-4 position. The best yield (70%) of tetrazolo[1,5-*a*]pyrimidine **4** was obtained in $CHCl_3$.

For comparison, the addition of cyclohexanethiol as the first nucleophile and sodium azide as the second nucleophile yields 5-(cyclohexylthio)pyrido[3,2-*e*]tetrazolo[1,5-*a*]pyrimidine (**4**) in 50% yield over two steps (Scheme 3). The diazide route (Scheme 2) has a simpler workup and a higher total yield. Further addition of the second thiol equivalent to the intermediate **4** gave 2,4-dithiopyrido[2,3-*d*]pyrimidine **6a**.

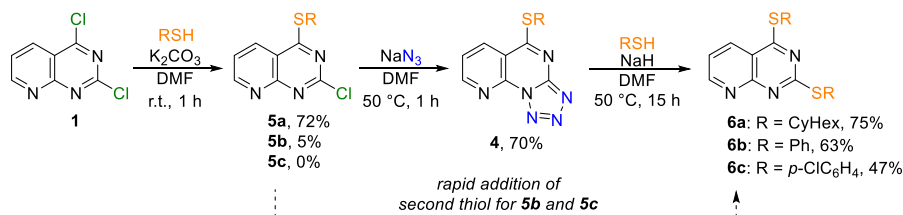
Arylthiols were unreactive towards azido group substitution in compound **2**, whereas dichloride **1** readily reacted with arylthiols to give disubstituted products **6b**, **6c**.

The S_NAr reaction of diazide **2** with *O*-nucleophiles in DMF proceeded in the presence of K_2CO_3 and tetrazolo[1,5-*a*]pyrimidines **7a-b** were obtained, however with low yields due to multiple byproduct formation (Scheme 4).

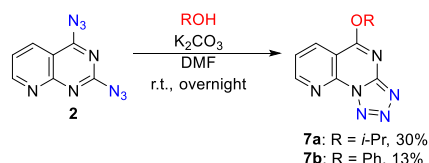
On the other hand, primary and secondary amines undergo a rapid S_NAr reaction with diazide **2** to give 5-aminopyrido[3,2-*e*]tetrazolo[1,5-*a*]pyrimidines **8** in good yields (Scheme 5). The addition of hydrazine, hydroxylamine or aniline gave mixtures of unidentified compounds. The obtained amino derivatives **8** had poor solubility in organic solvents. Especially pyrrolidine and morpholine adducts **8d-e** were particularly insoluble in common solvents (MeOH, DMSO, $CHCl_3$, H_2O , THF, MeCN, DCM, EtOAc, toluene, acetone, pyridine).



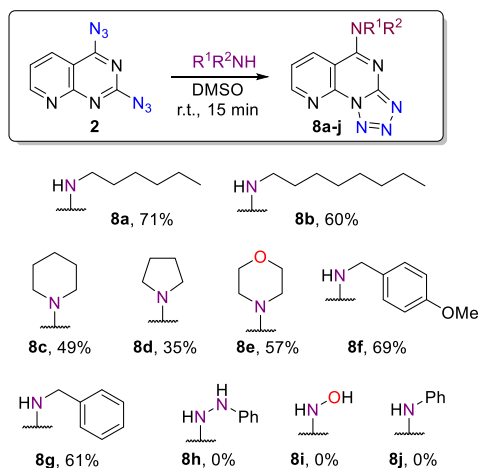
Scheme 2. Synthesis of 2,4-diazidopyrido[2,3-*d*]pyrimidine (**2**) and its regioselective substitution with cyclohexanethiol.



Scheme 3. Stepwise synthesis of pyrido[3,2-*e*]tetrazolo[1,5-*a*]pyrimidines **4** and 2,4-dithiopyrido[2,3-*d*]pyrimidines **6**.



Scheme 4. S_NAr substitution of diazide **2** with *O*-nucleophiles.



Scheme 5. Synthesis of 5-aminopyrido[3,2-*e*]tetrazolo[1,5-*a*]pyrimidines **8**.

It is interesting to note, that basic additives (e.g. K_2CO_3) led to a hydrolysis of azido groups, but the Lewis acid catalysts (e.g. $ZnCl_2$) [34] gave significantly lower yields of product **8**.

To showcase the azide-tetrazole tautomerism, we functionalized 5-aminotetrazolo[1,5-*a*]pyrimidine **8a** in a copper(I)-catalyzed azide-alkyne cycloaddition (CuAAC) reaction [35] to yield 1,2,3-triazole **10a**. Since the tetrazole is the major tautomer for **8a** both in a solid state and in solutions, this reaction demonstrates well the dynamic equilibrium to the minor tautomer, which is the reactive component in the CuAAC reaction. Initially, we screened conditions for the CuAAC reaction of model substrate **8a** with phenylacetylene (Table 1). Without catalyst no reaction occurred even at elevated temperatures, but at temperatures ≥ 120 °C substrate degradation was observed (Table 1, entry 1). When CuI was used as the catalyst, bisphenylacetylene formation was observed in the Glaser-type coupling (Table 1, entries 2–3) [36]. Finally, a compromise between suitable tautomeric equilibrium conditions and the preparative solubility of all reaction components was reached with $CuSO_4 \cdot 5H_2O$ /sodium ascorbate in THF/ H_2O (Table 1, entry 6).

Triazoles **10b** and **10c** were obtained in the further CuAAC reactions with *p*-tolyl and hexyl alkynes (Scheme 6). Next, 2-(1,2,3-triazolyl)-4-thiopyrido[2,3-*d*]pyrimidine **11** was successfully obtained in the CuAAC reaction using thio-derivative **4**.

Besides the reactivity pattern of systems containing different 2,4-substituents, we also explored additional reactivity of diazide **2**. Thus, we were able to isolate stable iminophosphorane **12** in the Staudinger reaction, when triphenylphosphine was reacted with diazide **2** (Scheme 7).

2.2. Single crystal X-ray analysis

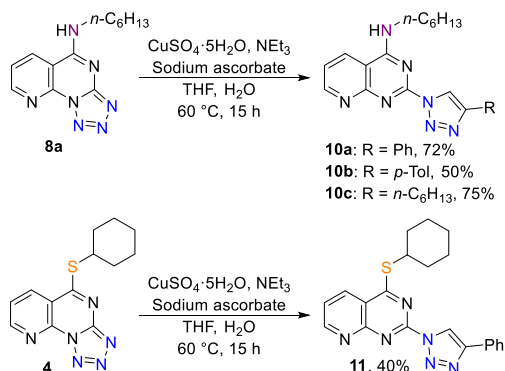
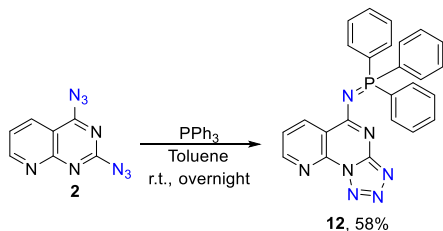
Most of the newly obtained pyrido[2,3-*d*]pyrimidine derivatives appeared to be highly crystalline substances. This allowed us to perform crystal structure studies of compounds **2**, **4**, **5b**, **7a**, **8b**, **8e**, **8g**, **11**, and **12** by single crystal X-ray analysis. Crystal data and refinement details for the studied crystals are presented in Table 2. ORTEP views (50% probability ellipsoids) of the molecules, packing of the molecules in the crystal and atom labeling schemes are shown in Table 3. The molecules **2** in the crystal are essentially

Table 1
Optimization of CuAAC reaction conditions.

Entry	Catalyst	Solvent	Temperature (°C)	Additive	Yield of 10a (%)
1	–	DMF	120	–	0
2	CuI	CH_2Cl_2	25	NEt_3	0
3	CuI	THF / H_2O	25	NEt_3	<5
4	$CuSO_4 \cdot 5H_2O$	<i>t</i> -BuOH / H_2O	60	Sodium ascorbate	10
5	$CuSO_4 \cdot 5H_2O$	DMF	80	Sodium ascorbate	23
6	$CuSO_4 \cdot 5H_2O$	THF / H_2O	60	NEt_3 , sodium ascorbate	72

Table 2
Crystal data and refinement details.

Compound	2	4	5b	7a	8b	8e	8g	11	12
Structural formula	C ₇ H ₃ N ₉	C ₁₃ H ₁₄ N ₆ S	C ₁₃ H ₈ ClN ₃ S	C ₁₁ H ₁₁ Cl ₃ N ₆ O	C ₁₅ H ₂₁ N ₇	C ₁₁ H ₁₁ N ₇ O	C ₄₂ H ₃₃ N ₂₁	C ₂₁ H ₂₀ N ₆ S	C ₂₅ H ₁₈ N ₇ P
Molar weight (g/mol)	213.18	286.36	273.73	349.61	299.39	257.27	277.30	388.49	447.43
Crystal system	Orthorhombic	Monoclinic	Monoclinic	Triclinic	Monoclinic	Monoclinic	Triclinic	Monoclinic	Monoclinic
Space group	<i>Pbc</i> ₂₁ / <i>c</i>	<i>P2</i> ₁ / <i>c</i>	<i>P2</i> ₁ / <i>c</i>	<i>P</i> -1	<i>P2</i> ₁ / <i>c</i>	<i>P2</i> ₁ / <i>c</i>	<i>P</i> -1	<i>P2</i> ₁ / <i>c</i>	<i>P2</i> ₁ / <i>c</i>
<i>Z</i>	8	4	4	2	4	4	6	4	4
<i>a</i> (Å)	8.8799 (3)	20.0785 (2)	5.4128 (1)	6.6752 (5)	20.9737 (5)	17.8729 (3)	11.1482 (2)	13.2199 (1)	9.3396 (1)
<i>b</i> (Å)	8.7781 (3)	9.0150 (1)	29.1050 (5)	8.8492 (5)	4.5734 (1)	8.9502 (2)	12.9283 (2)	12.2552 (1)	17.0598 (2)
<i>c</i> (Å)	22.7102 (9)	7.7468 (1)	7.6278 (1)	13.3964 (9)	15.9981 (5)	7.0113 (2)	14.9433 (2)	12.8190 (1)	13.5331 (1)
α (°)	90	90	90	77.473 (5)	90	90	113.804 (1)	90	90
β (°)	90	98.828 (1)	98.181 (1)	79.327 (6)	94.101 (2)	101.264 (2)	95.832 (1)	110.592 (1)	98.641 (1)
γ (°)	90	90	90	80.906 (5)	90	90	99.836 (1)	90	90
<i>V</i> (Å ³)	1770.23 (11)	1385.62 (3)	1189.45 (3)	753.37 (9)	1530.63 (7)	1099.97 (4)	1906.49 (5)	1944.15 (3)	2131.78 (4)
Calculated density (mg/m ³)	1.600	1.373	1.529	1.541	1.299	1.554	1.449	1.327	1.394
Absorption coefficient (mm ⁻¹)	0.99	2.07	4.34	5.59	0.67	0.91	0.78	1.63	1.38
θ -range for data collection (°)	3.9–75.5°	4.4–75.7°	3.0–76.3°	3.4–76.3°	2.8–76.4°	5.0–75.4°	3.3–76.5°	3.6–76.2°	4.2–76.4°
Index ranges	–9 to 11 –6 to 11 –27 to 28	–23 to 25 –11 to 10 –8 to 9	–5 to 6 –34 to 36 –9 to 9	–8 to 8 –11 to 7 –16 to 16	–26 to 26 –5 to 4 –20 to 19	–21 to 21 –11 to 5 –8 to 8	–14 to 13 –15 to 16 –14–18	–16 to 16 –15 to 15 –16 to 13	–11 to 9 –20 to 21 –17 to 16
Data collected	8736	13,130	11,237	11,328	16,290	5852	36,397	18,598	20,640
Unique reflections	1740	2760	2392	2974	3098	1984	7775	3923	4301
Unique reflections with <i>I</i> > 2 σ (<i>I</i>)	1464	2485	2184	2473	2794	1758	7002	3694	4021
Symmetry factor (<i>R</i> _{int})	0.048	0.034	0.034	0.058	0.039	0.031	0.034	0.027	0.030
Completeness to θ_{max}	93.8	99.5	96.2	92.7	99.9	92.4	99.9	96.5	96.1
<i>R</i> (000)	864	600	560	356	640	536	864	816	928
Parameters refined	145	181	164	193	202	173	569	254	299
Goodness of fit on <i>F</i> ²	1.06	1.066	1.06	1.11	1.14	0.958	1.05	1.07	1.07
Final <i>R</i> ₁ factor for <i>I</i> > 2 σ (<i>I</i>)	0.059	0.035	0.033	0.086	0.080	0.035	0.035	0.033	0.03
w <i>R</i> ₂ factor for all data	0.187	0.097	0.090	0.255	0.247	0.096	0.097	0.089	0.092
Largest diff. peak/hole (e/Å ³)	0.43–0.25	0.22–0.28	0.30–0.36	1.15–0.66	0.58–0.26	0.22–0.27	0.30–0.22	0.32–0.26	0.43–0.37
CCDC deposition number	2,151,125	2,129,256	2,129,262	2,129,264	2,129,257	2,129,258	2,129,261	2,129,263	2,129,265

**Scheme 6.** Synthesis of 2-(1,2,3-triazolyl)pyrido[2,3-d]pyrimidines **10** and **11**.**Scheme 7.** Synthesis of iminophospharane **12**.

planar. Atomic deviations from the least squares mean plane of the molecule do not exceed 0.05 Å. Azide group is turned in the direction opposite to the pyridine ring. The valence angle C5–N10–N11 is equal to 113.8(2)°. Azide group is not strictly linear, the va-

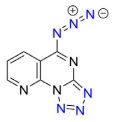
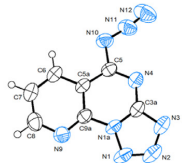
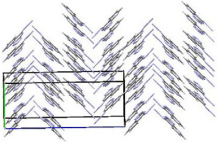
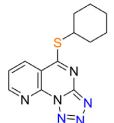
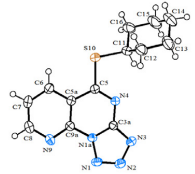
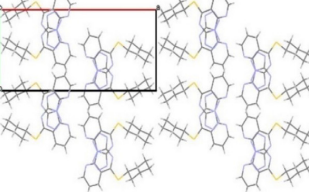
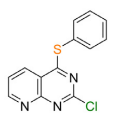
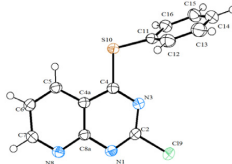
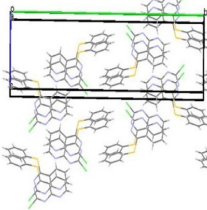
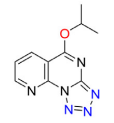
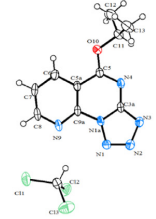
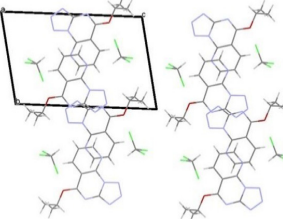

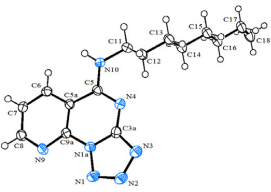
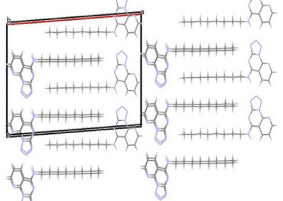
lence angle N10–N11–N12 is 171.6(2)°. The molecules are assembled in the layers stabilized by $\pi \cdots \pi$ stacking interactions. The stacks are characterized by pyridine/tetrazole fragment centroid distance of 3.869(2) Å and pyridine/pyridine centroid distance equals to 3.624(2) Å.

In the structure **4** the lone electron pairs of S10 atom are involved in the common conjugate system of the tricycle. The bond length C5–S10 = 1.736 (1) Å is shortened as compared to a standard single C–S bond [37]. Orientation of the cyclohexane cycle is described by the torsion angle \angle C5–S10–C11–C12 = –85.13 (12)°. Atom C11 is situated in the plane of the tricycle [torsion angle \angle C11–S10–C5–N4 = 1.54 (13)°]. The slope of the mean plane of cyclohexane to the plane of the tricycle is 56.65°. The packing contains layers formed by polar and nonpolar parts of the molecules perpendicular to *a*-axis of the unit cell. The tricyclic heterosystems are arranged in the stacks stabilized by $\pi \cdots \pi$ stacking interactions. The shortest distance between the atoms in the stacks is 3.199(1) Å (N3 \cdots C9a), while the minimal distance between the centroids in the adjacent tricycles is 3.628(2) Å.

The crystal structure **7a** is a chloroform solvate. The atom C11 is situated close to the average plane of the aromatic system [\angle N4–C5–O11–C11 = 1.47(1)°] and the lone electron pairs of O10 atom participate in the common conjugate system of the tricycle. This results in a shortening of bond length C5–O10 [1.3105(1) Å] as compared to the C–O single bond [37]. The polar and nonpolar parts of the molecules form layers perpendicular to *a*-axis of the unit cell. The layers of the tricyclic heterosystems consist of the stacks stabilized by $\pi \cdots \pi$ stacking interactions. The shortest distance between the centroids of the adjacent tricyclic heterosystems is 3.615(2) Å, while the shortest distance between the atoms in the stacks is 3.230(1) Å [C3a \cdots C3a].

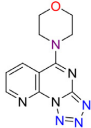
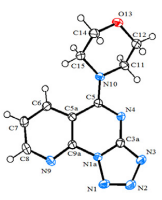
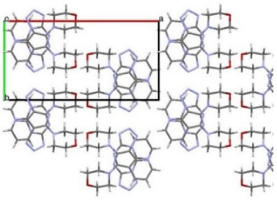
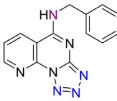
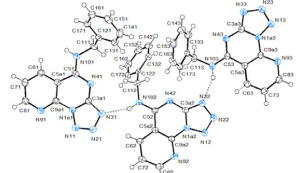
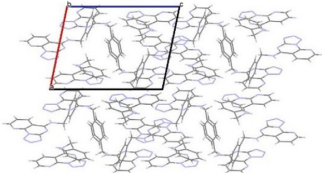
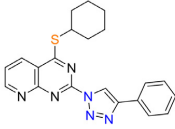
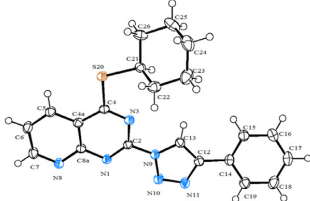
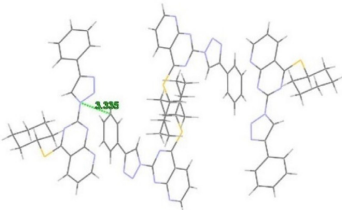
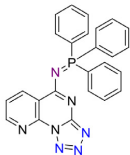
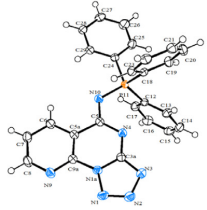
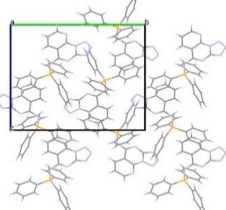
In the structure **8b** the atoms N10 and C11 are situated close to the average plane of the aromatic system and the lone electron pair of N10 atom participates in the common conjugate system of the tricycle. Therefore, bond length C5–N10, equal to 1.342(4) Å, is shortened as compared to the C–N single bond [37]. The

Table 3
ORTEP views (50% probability ellipsoids; ORTEP3 for Windows) [38], Mercury [39] drawings of crystal packing showing supramolecular features and atom labeling schemes for compounds **2**, **4**, **5b**, **7a**, **8b**, **8e**, **8g**, **11** and **12**.

Comp. Nr.	Formula	ORTEP	Crystal packing
2			
4			
5b			
7a			
8b			

(continued on next page)

Table 3 (continued)

8e			
8g			
11			
12			

orientation of the long aliphatic chain is defined by the torsion angle $\angle C5 - N10 - C11 - C12 = 82.75 (25)^\circ$. The polar and nonpolar parts of the molecules form layers perpendicular to \mathbf{a} -axis of the unit cell. The layers of the tricyclic heterosystems consist of the stacks stabilized by $\pi \cdots \pi$ interactions. The shortest distance between the centroids of the adjacent tricyclic heterosystems is $3.801(2) \text{ \AA}$, while the shortest distance between the atoms in the stacks is $3.421 \text{ \AA}(1)$ ($C8 \cdots C5a$). In the stacks the molecules are assembled in chains along axis \mathbf{c} of the unit cell by means of hydrogen bonds $N10-H14 \cdots N2$ ($x, 1/2 - y, -1/2 + z$) ($H \cdots N = 2.11 \text{ \AA}$, $N \cdots N = 2.941(1) \text{ \AA}$, $\angle N-H \cdots N = 158^\circ$).

In the crystal structure **8e** the morpholine cycle is oriented in such a way ($\angle N4-C5-N10-C11 = 12.53^\circ$) that the lone electron pair of the nitrogen atom N11 participates in a common conjugation in the heterocycle. As a result $C5-N10$ bond length is shortened to the value of $1.3491 (17) \text{ \AA}$. As in the previous structures, the molecules are assembled in the layers containing polar and nonpolar parts of the molecules. In the polar layers the tricyclic heterosystems form stacks stabilized by $\pi \cdots \pi$ interactions. The shortest distance between the centroids of the adjacent tricyclic heterosystems is

$3.473(2) \text{ \AA}$, while the shortest distance between the atoms in the stacks is $3.276(1) \text{ \AA}$ ($N9 \cdots C5a$).

Crystal structure **8g** contains three independent molecules in the asymmetric unit. The last digit in the atomic labels refer to the molecule number (Table 3). Geometry of the molecules is similar, but their conformations differ by the orientations of the phenyl rings. The torsion angles $C5-N10-C11-C12$ for the three molecules are $-101.87(1)^\circ$, $-87.17(1)^\circ$ and $84.58(1)^\circ$, respectively. In the unit cell the tricycles of all independent molecules are situated in one and the same plane. By means of their tricyclic fragments the molecules in the crystal are arranged into stacks. However, the layer structure is less pronounced. The stacks propagate along the \mathbf{a} axis of the unit cell. In its turn the stacks are cross-linked by the hydrogen bonds of the $N-H \cdots N$ type (Table 4).

In the crystal structure **11** the aromatic fragments in the molecule are not coplanar. Dihedral angles of the triazole fragment with the bicycle and the phenyl ring are 4.59° and 11.49° , respectively. The slope of the least squares mean plane of cyclohexane to the plane of the bicycle is 45.40° . There are no well-defined stacks in the structure. However, the bicyclic heterosystem has an overlap

Table 4
Hydrogen-bond geometry (Å,°) for **8 g** structure^a.

D–H...A	D–H	H...A	D–A	D–H...A
N101–H...N33 ^b	0.88	2.18	3.006(1)	157
N102–H...N31 ^c	0.88	2.09	2.911(1)	156
N103–H...N32	0.88	2.11	2.917(1)	153

^a PLATON tool [38] was used for geometrical calculations.^b Symmetry code x, –1 + y, z.^c Symmetry code 1–x, 1–y, 1–z.

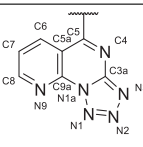
with the triazole fragment and the shortest intermolecular distance N8...C13 is 3.373(1) Å.

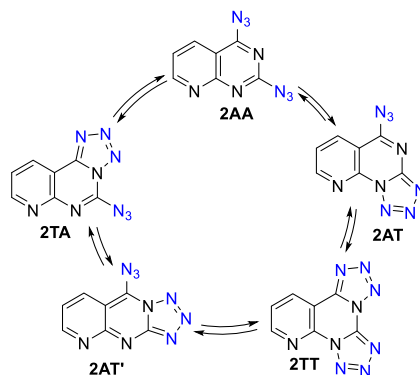
In the crystal structure **12** the torsion angle C4–C5–N10–P11 is –3.40(1)°, and the electron lone pair of the nitrogen atom is involved in conjugation of the whole aromatic heterosystem and C5–N10 bond is 1.337(2) Å long. The N10–P11 bond length [1.6142(1) Å] corresponds to a standard value [1.599(18) Å] of the N–P double bond [37]. The orientations of the phenyl rings with respect to the tricyclic heterosystem are described by torsion angles C5–N10–P11–C12/C18/C24, which are –59.23(1)°, 68.00(1)° and –176.25(1)°, respectively.

A comparison of crystal structure **5b** with **11** reveals some distinctions in molecular geometry. In compound **11** single bond S20–C21 is equal to 1.819(1) Å, whereas in compound **5b** a similar S10–C11 bond is shortened [1.773(2) Å] due to conjugation with the phenyl ring. In compound **11** torsion angle N3–C4–S10–C11 is –5.41(1)°, that facilitates conjugation of sulfur atom lone pairs with the bicyclic heterosystem and C4–S20 bond is 1.740(1) Å long. In the structure **5b** the analogous torsion angle is equal to –11.47(1)°, that reduces the conjugation. Therefore C4–S10 bond is slightly longer [1.756(2) Å]. There are two types of stacks in **5b** structure, and the first one is built from the bicyclic heterosystem with a pyridine/pyridine centroid distance 3.816(2) Å and the shortest interatomic distance in the stacks N1...C7 = 3.276(1) Å. The second type of stacks consists of phenyl rings. The centroid and the shortest interatomic distances in these stacks are 3.923(2) Å and 3.427(1) Å (C14...C15), respectively.

Search of the Cambridge Structure Database (CSD, version 5.42, November 2020) for synthesized tricyclic tetrazolopyridopyrimidine heterocyclic system did not reveal any hits and, thus, gave evidence that it was not studied by single crystal X-ray diffraction yet. For this reason, we list in Table 5 selected geometrical parameters of the studied compounds that shows changes in their values taking place in the process of azide-tetrazole transformation.

Table 5
Selected bond lengths and valence angles for studied crystal structures^a.

Moiety	Comp. Nr.	N1a–C3a /N1–C2	C3a–N4/C2–N3	N1a–C3a–N3/N1–C2–X ^b	N1a–C3a–N4/N1–C2–N3
	2	1.350(3)	1.358(3)	108.5(2)	124.8(2)
	4	1.3576(17)	1.3582(17)	108.61(12)	123.99(12)
	7a	1.359(6)	1.347(6)	107.2(4)	124.8(4)
	8b	1.370(4)	1.338(5)	107.2(3)	124.4(3)
	8e	1.3501(18)	1.3420(18)	108.32(12)	124.67(12)
	8 g-1	1.3589(14)	1.3476(14)	107.34(9)	124.97(10)
	8 g-2	1.3564(13)	1.3454(13)	107.38(9)	124.77(9)
	8 g-3	1.3596(14)	1.3473(14)	107.58(9)	124.46(10)
	12	1.3652(17)	1.3506(17)	107.62(12)	124.42(12)
	5b	1.296(2)	1.350(2)	115.40(12)	130.87(15)
	11	1.3003(15)	1.3526(15)	117.61(10)	130.75(11)

^a PLATON tool [40] was used for geometrical calculations.^b X = N9 (for **11**), X = Cl9 (for **5b**).**Fig. 2.** Possible tautomeric forms of diazide **2**.

3. NMR spectroscopy

3.1. Spectroscopic investigation of diazide **2**

There are five theoretically possible azide-tetrazole tautomeric forms for diazide **2**: diazide **2AA**, bis-tetrazole **2TT**, linear azidotetrazole **2AT*** and two angular azidotetrazoles **2AT** and **2TA** (Fig. 2). Indeed, ¹H NMR analysis of diazide **2** showed multiple sets of signals in CDCl₃ identifying azide-tetrazole equilibrium in solution (Fig. 3). We have identified four sets of signals for proton H–C(6) (atom numbering for all tautomers refers to diazide **2AA** for simplicity) that appear in the range from 7.4 ppm to 8.0 ppm and are the most distinguishable from the all other signals. Since we could not undeniably assign the NMR signals to correct tautomers, we labeled the signal pairs as α , β , γ and δ tautomers. Angular (bent) fused tetrazole ring systems in pyrimidines are favored over linear based on DFT calculations [41,42] and experimental reports [43]. However, on some occasions linear tetrazolotriazine structures have been unambiguously proved by X-ray and ¹⁵N-NMR analysis [44–46]. Our preliminary DFT calculations of diazidopyrido[2,3-*d*]pyrimidine **2** tautomers indicate that the linear **2AT*** structure is 14–18 kcal higher in base energy than others. Thus, we speculate that tautomeric form **2AT*** was not observed among 4 registered tautomers in the tested solutions.

With exchange spectroscopy (EXSY) [47] we have observed chemical exchange only between δ and γ tautomers by H–C(5) and

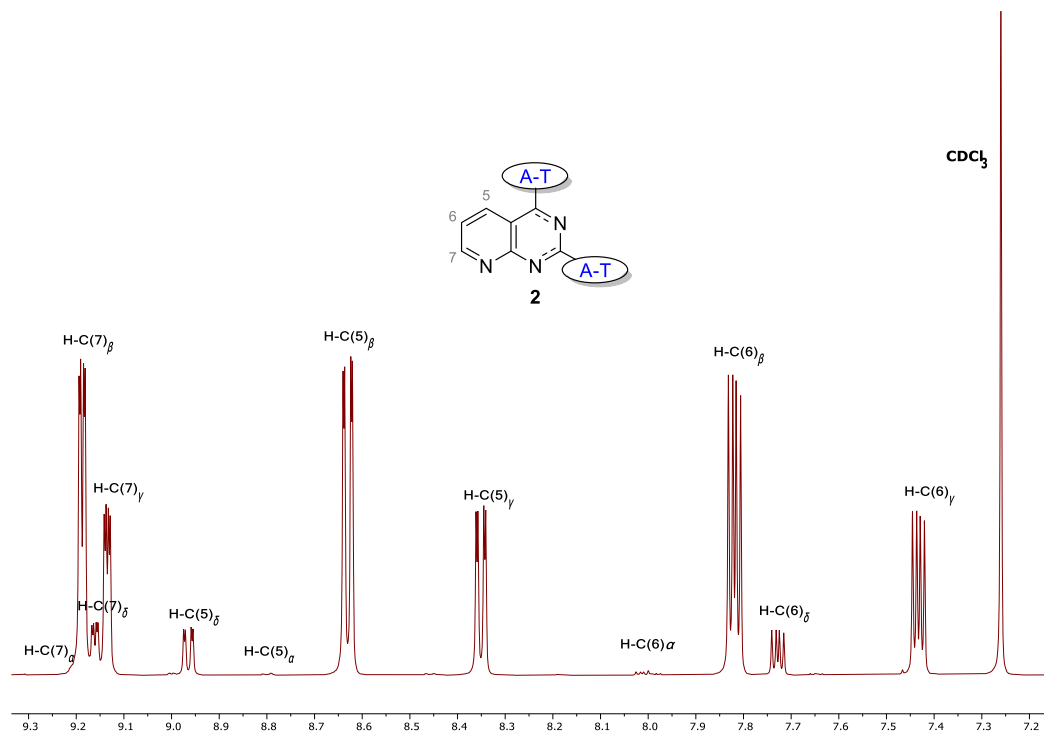


Fig. 3. ^1H NMR spectrum of diazide **2** in CDCl_3 .

H-C(6) protons at 7.44 / 7.73 ppm and 8.35 / 8.97 ppm (Figure S1). In the 1D selective excitation experiments (Figure S2) we were able to see slower exchange rate tautomerizations between other tautomers that were not visible in the 2D spectra.

The main factors influencing the tautomeric equilibrium are: solvent polarity (tetrazole form dominates in polar solvents), temperature (azide form is thermodynamically more stable and dominates at higher temperatures) and protonation of fused heterocycle (electron deficiency in the ring system favors the azide form) [21]. In various organic solvents the azide-tetrazole equilibrium varied greatly based on the solvent polarity and dielectric constant ϵ . In more polar solvents (DMSO- d_6 , MeCN, MeNO $_2$, MeOD- d_4) downfield α and β tautomers (tetrazole form) dominated and in non-polar solvents (CDCl_3 , MTBE, C_6D_6) upfield γ and δ tautomers (azide form) started to appear (Figure S3). Relative ratios of diazide **2** tautomers in different solvents are given in Table S1 and graphically depicted in Fig. 4. The results are in the agreement with other NMR studies of azide-tetrazole equilibrium and conform that the polar solvents favor the tetrazole tautomer, which appears further downfield compared to the azido tautomer [48–51].

During the NMR titration of CDCl_3 solution of diazide **2** with DMSO- d_6 the ^1H NMR signals shifted towards downfield tautomeric forms with significant decrease of δ tautomer and increase of α tautomer (Figure S4). The equilibrium constants for diazide **2** showed also temperature dependency. Elevating the temperature shifted the equilibrium towards azido tautomers γ and δ (Figure S5-S6). The relative ratios of tautomers are given in Figs. 5 and 6.

Thus, azide-tetrazole equilibrium in pyrido[2,3-*d*]pyrimidine system displays similar physical properties as in other azidopy-

rimidines [21]: 1) tetrazole tautomer is favored in polar solvents whereas azido form in nonpolar solvents; 2) tetrazole tautomer is the major component at lower temperatures, whereas the azide tautomer ratio increases at higher temperatures. Further NMR studies on structural assignment and detailed DFT calculations for diazide **2** will be reported elsewhere.

3.2. FT-IR spectroscopy

FT-IR analysis of diazide **2** showed four characteristic azido group ($\text{N}=\text{N}$) asymmetric stretching bands at 2104, 2165, 2221 and 2265 cm^{-1} and symmetric azido group stretching bands at 1303, 1322 and 1344 cm^{-1} (Figure S7) [52]. Phosphonimidate **12** showed one azido ($\text{N}=\text{N}$) stretching band at 2216 cm^{-1} (Figure S8). Other monoazido derivatives **4**, **7**, **8** did not show any azido group stretching bands. It can be concluded from the IR studies, that most of here described pyrido[3,2-*e*]tetrazolo[1,5-*a*]pyrimidines in the solid phase exist solely in their tetrazole form.

3.3. Exchange rate and free energy calculation for azide-tetrazole equilibrium of substituted pyrido[3,2-*e*]tetrazolo[1,5-*a*]pyrimidines

Substituents of the annulated systems play a major role in the azide-tetrazole equilibrium. The electron-donating groups shift the equilibrium towards the tetrazolo-form, whereas the electron withdrawing groups favor the azido-form [21,53,54]. In our study, we observed tautomeric equilibrium for compounds **4**, **7a**, **7b**, **8a** and **12**. Thus, amine substituent as the electron-donating group is powerful enough to strongly shift the equilibrium towards the tetrazole

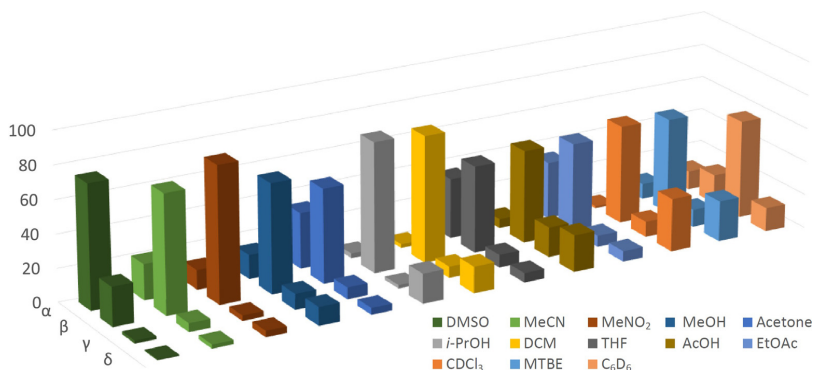


Fig. 4. Relative tautomeric ratios of diazide **2** in different solvents in descending order of solvent dielectric constants ϵ .

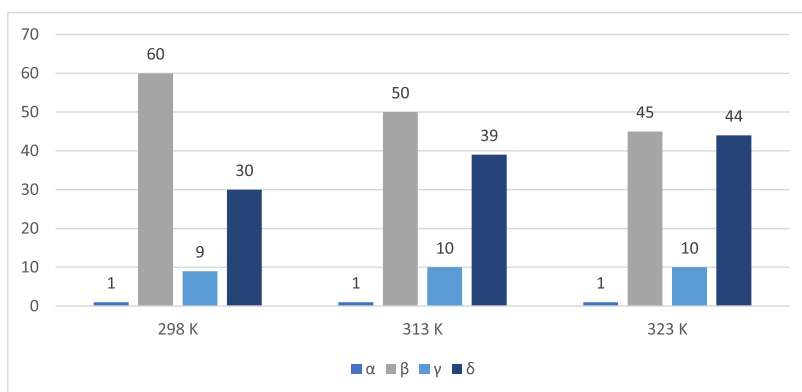


Fig. 5. Relative tautomer ratios of diazide **2** at different temperatures in CDCl_3 .

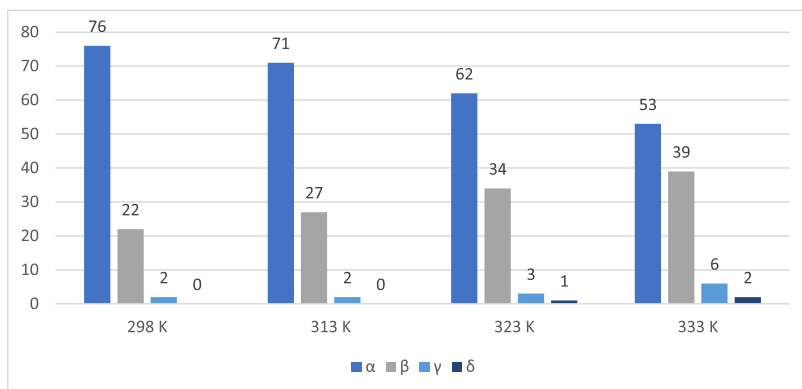
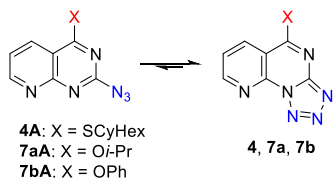


Fig. 6. Relative tautomer ratios of diazide **2** at different temperatures in $\text{DMSO}-d_6$.

form in 5-aminopyrido[3,2-*e*]tetrazolo[1,5-*a*]pyrimidines **8**. Tetrazole was the major tautomer in all obtained compounds, which is common for other similar fused tetrazolopyrimidines [24,29,55]. Regardless the fact that the previously described transformation **8a** \rightarrow **10a-b** logically involves a formation of the azido-tautomer at an equilibrium concentration, the concentration of the latter was too low to be determined by the NMR studies.

To calculate free energies for tautomerization ^1H NMR spectra were acquired at variable temperatures. For compounds **4**, **7a** and **7b** the equilibrium at elevated temperatures shifted towards azide form and equilibrium constant $K_{T/A}$ values decreased (Figures S9-S11). On the other hand, the change was negligible for hexylamino derivative **8a** ($K_{T/A} = 7.46$ in CDCl_3 at 298 K) and iminophosphorane **12** ($K_{T/A} = 2.57$ in CDCl_3 ; $K_{T/A} = 0.85$ in $\text{DMSO}-d_6$ at 298 K).

Table 6
Equilibrium constants $K_{T/A} = [\text{tetrazole}]/[\text{azide}]$ and thermodynamic heats of tautomerization for **4**, **7a** and **7b** in CDCl_3 .



Compound	T (K)	$K_{T/A}$	ΔG_{298} (kJ/mol)	ΔH (kJ/mol)	ΔS (J/mol·K)
4	298	5.21	-4.08 ± 0.15	-21.30 ± 0.78	-57.71 ± 2.10
	313	3.48			
	323	2.68			
7a	298	9.99	-5.70 ± 0.27	-23.19 ± 1.09	-58.70 ± 2.76
	313	6.30			
	323	4.85			
7b	298	3.39	-3.02 ± 0.65	-17.02 ± 3.69	-46.93 ± 10.16
	313	2.48			
	323	1.99			

The equilibrium constant for compound **12** in CDCl_3 was larger than in $\text{DMSO}-d_6$, which is opposed to the generally accepted concept that polar solvents favor the tetrazole form.

The Gibbs-Helmholtz equation $\Delta G = -RT \ln(K_{eq})$ was used to calculate Gibbs free energy of tautomerization. Enthalpy and entropy values were obtained by plotting the Gibbs free energy equation $\Delta G = \Delta H - T\Delta S$ (Figures S12–S14). Thermodynamic heats of tautomerization are given in Table 6. Very similar results were obtained by plotting the van't Hoff equation $\ln(K_{eq}) = -\frac{\Delta H}{RT} + \frac{\Delta S}{R}$ (see ESI). Errors were calculated using the mean square error method. The obtained enthalpy and entropy values are similar to those of fused tetrazoles: 5-trifluoromethyltetrazolo[1,5-*a*]pyrimidine ($\Delta H = 19.4$ kJ/mol; $\Delta S = 66$ J/mol) [54] and halotetrazolo[1,5-*a*]pyridines ($\Delta H = 10.6$ – 24.1 kJ/mol; $\Delta S = 50.6$ – 57.4 J/mol) [56]. The obtained enthalpy values for **7a**, **4** and **7b** are -23.19 , -21.30 and -17.02 kJ/mol, respectively. Enthalpy is the thermodynamic value for stability of tetrazole ring [56] and higher values mean lower tendency for the ring opening. Since the electron-donating substituents favor the tetrazole form, our enthalpy value order for substituents: *Or*-Pr > SCyHex > OPh, from experimental data correlate very well with the theoretical calculations.

4. Experimental

Reagents purchased from Alfa Aesar, Acros Organics, Merck - Sigma Aldrich were used as received. All solvents were distilled prior to use. THF and toluene were distilled from sodium metal under argon atmosphere. DMF, DMSO and sulfolane were distilled from CaH_2 under reduced pressure. Silica gel Upasil 60 (40–63 μm , 60 Å) was used for column chromatography. Reaction progress and flash chromatographic separation was monitored by TLC (E. Merck Kieselgel 60 F₂₅₄), visualized with UV light.

HPLC analysis was performed using an Agilent Technologies 1200 Series system equipped with an XBridge C-18 column, 4.6 × 150 mm, particle size 3.5 μm , with a flow rate of 1 mL/min, using 0.1% TFA/ H_2O and MeCN for the mobile phase. The wavelength of detection was 260 nm.

IR spectra were recorded in a KBr tablet with a Perkin–Elmer Spectrum BX FT-IR spectrometer (4000–450 cm^{-1}).

High-resolution mass (HRMS) (electrospray ionization (ESI)) were recorded with an Agilent 1290 Infinity series ultra-high pressure liquid chromatography connected to an Agilent 6230 time-of-flight mass spectrometer or (atmospheric pressure chemical ion-

ization (APCI)) on 7 T solarix XR (Bruker Daltonik GmbH) Fourier transform ion cyclotron resonance mass spectrometer equipped with an APCI source.

Single-crystal diffraction data were collected on an XtaLAB Synergy-S Dualflex diffractometer (Rigaku Corporation, Tokyo, Japan) equipped with a HyPix6000 detector and micro-focus sealed X-ray tube using $\text{Cu K}\alpha$ radiation ($\lambda = 1.54184$ Å). Single crystals were fixed with oil in a nylon loop of a magnetic CryoCap and set on a goniometer head. The samples were cooled down to 150 K, and ω -scans were performed with a step size of 0.5°. Data collection and reduction were performed with the CrysAlisPro 1.171.40.35a software (Oxford Diffraction Ltd., Abingdon, UK). Structure solution and refinement were performed with SHELXT [57] and SHELXL [58] software that are parts of the CrysAlisPro and Olex2 suites. The H atoms were positioned geometrically and treated as riding on their parent C or N atoms. Molecular graphics were prepared using ORTEP3 for Windows [38] and Mercury [39]. PLATON tool [40] was used for the geometrical calculations.

^1H NMR and ^{13}C NMR spectra were recorded on Bruker Avance 500 spectrometer. Chemical shifts (δ) reported in ppm and coupling constants (*J*) in Hz. Residual solvent peaks (^1H) or (^{13}C) were used as the reference (for ^1H NMR: CDCl_3 $\delta = 7.26$ ppm; $\text{DMSO}-d_6$ $\delta = 2.50$ ppm; $\text{AcOD}-d_4$ $\delta = 2.04$ ppm, pyridine-*d*₅ $\delta = 8.74$ ppm and for ^{13}C NMR: CDCl_3 $\delta = 77.16$ ppm, $\text{DMSO}-d_6$ $\delta = 39.52$ ppm, $\text{AcOD}-d_4$ $\delta = 20.00$ ppm, pyridine-*d*₅ $\delta = 150.45$ ppm). For ^{31}P -NMR spectra H_3PO_4 $\delta = 0.0$ ppm was added as external reference. Multiplicities are reported as s (singlet), d (doublet), t (triplet), q (quartet), quint (quintet), m (multiplet).

4.1. Synthetic procedures and product characterization

General procedure **A** - synthesis of 5-aminopyrido[3,2-*e*]tetrazolo[1,5-*a*]pyrimidines **8a-g**: substituted amine (1.407 mmol, 3 equiv.) was added to 2,4-diazidopyrido[2,3-*d*]pyrimidine (**2**) (0.469 mmol, 1 equiv.) in DMSO (1 mL) and stirred for 15 min at ambient temperature. Ice (10 mL) was added to the reaction mixture and it was vigorously shaken. The resulting suspension was filtered and washed with distilled water. The obtained crude mixture is then recrystallized from EtOH or pyridine to give the final product.

General procedure **B** - synthesis of **10a-c** and **11** in CuAAC reaction: sodium ascorbate (0.4 equiv.), $\text{CuSO}_4 \cdot 5\text{H}_2\text{O}$ (0.2 equiv.), NEt_3 (2 equiv.), pyrido[3,2-*e*]tetrazolo[1,5-*a*]pyrimidine (1 equiv.) and substituted acetylene (1.5 equiv.) were dissolved in a mixture of THF (1 mL) and H_2O (0.1 mL) and stirred at 60 °C overnight. The resulting mixture was filtered through silica gel and anhydrous Na_2SO_4 plug and evaporated under reduced pressure. The obtained crude product was purified by column chromatography.

4.2. 2,4-Diazidopyrido[2,3-*d*]pyrimidine (**2**)

To 2,4-dichloropyrido[2,3-*d*]pyrimidine (**1**) (200 mg, 1 mmol, 1 equiv.) and NaN_3 (260 mg, 4 mmol, 4 equiv.) acetone (1 mL) and water (0.1 mL) were added and the resulting reaction mixture was heated at 50 °C for 1 h. When the reaction was complete (monitored by HPLC), the reaction mixture was cooled to ambient temperature and the solvent was evaporated under reduced pressure. Water (10 mL) was added to the residue and the resulting mixture was extracted with dichloromethane (3 × 10 mL). The combined organic phases were washed with saturated aqueous NaCl solution (2 × 10 mL), then dried over anhydrous Na_2SO_4 , filtered and evaporated under reduced pressure. Product **2** was obtained as slightly yellow amorphous solid (208 mg, 98% yield). Product was further recrystallized from EtOH. Major tautomer: ^1H NMR (500 MHz, $\text{DMSO}-d_6$) δ 9.26 (dd, 1H, $^3J = 8.0$ Hz, $^4J = 1.5$ Hz, H-C(5)), 9.23 (dd, 1H, $^3J = 4.8$ Hz, $^4J = 1.5$ Hz, H-C(7)), 8.14 (dd, 1H, $^3J = 8.0$,

4.8 Hz, H-C(6)) ppm. ^{13}C NMR (126 MHz, DMSO- d_6) δ 154.4, 149.3, 145.1, 142.0, 135.9, 126.1, 107.7 ppm. **Minor tautomer:** ^1H NMR (500 MHz, DMSO- d_6) δ 9.24 (dd, 1H, $^3J = 4.8$ Hz, $^4J = 1.5$ Hz, H-C(7)), 8.71 (dd, 1H, $^3J = 8.0$ Hz, $^4J = 1.5$ Hz, H-C(5)), 7.98 (dd, 1H, $^3J = 8.0$, 4.8 Hz, H-C(6)) ppm. ^{13}C NMR (126 MHz, DMSO- d_6) δ 161.6, 156.6, 155.5, 142.0, 135.8, 125.1, 109.8 ppm. HRMS calcd. for $[\text{C}_7\text{H}_3\text{N}_9 + \text{H}^+]$ = 214.0584, found 214.0579.

4.3. 5-(Cyclohexylthio)pyrido[3,2-*e*]tetrazolo[1,5-*a*]pyrimidine (4)

Cyclohexanethiol (60 mg, 0.516 mmol, 1.1 equiv.) was added under argon atmosphere to a solution of 2,4-diazidopyrido[2,3-*d*]pyrimidine (**2**) (100 mg, 0.469 mmol, 1 equiv.) and NEt_3 (57 mg, 0.562 mmol, 1.2 equiv.) in CHCl_3 (1 mL). The resulting reaction mixture was stirred overnight at ambient temperature. Then it was evaporated under reduced pressure and the product was purified by column chromatography ($R_f = 0.50$ in 50% Hex/EtOAc) to obtain white amorphous solid (94 mg, 70% yield). ^1H NMR (500 MHz, DMSO- d_6) δ 9.15 (dd, 1H, $^3J = 4.6$ Hz, $^4J = 1.2$ Hz, H-C(8)), 8.79 (dd, 1H, $^3J = 8.2$ Hz, $^4J = 1.2$ Hz, H-C(6)), 7.92 (dd, 1H, $^3J = 8.2$ Hz, $^4J = 4.6$ Hz, H-C(7)), 4.20–4.27 (m, 1H, H-C(1')), 2.13–2.20 (m, 2H, 2 x H-CH), 1.73–1.81 (m, 2H, 2 x H-CH), 1.59–1.69 (m, 3H, 3 x H-CH), 1.49–1.59 (m, 2H, 2 x H-CH), 1.33–1.42 (m, 1H, H-CH) ppm. ^{13}C NMR (126 MHz, DMSO- d_6) δ 171.5, 155.7, 154.3, 142.2, 135.7, 124.9, 114.4, 43.7, 32.0, 25.4, 25.2 ppm. HRMS calcd. for $[\text{C}_{13}\text{H}_{14}\text{N}_6\text{S} + \text{H}^+]$ = 287.1073, found 287.1092.

5-(Cyclohexylthio)pyrido[3,2-*e*]tetrazolo[1,5-*a*]pyrimidine (4) and 2-azido-4-(cyclohexylthio)pyrido[2,3-*d*]pyrimidine (4A) observed in CDCl_3 solution as tautomer mixture in 86:14 ratio. **Azide:** ^1H NMR (500 MHz, CDCl_3) δ 9.08 (dd, 1H, $^3J = 4.6$ Hz, $^4J = 1.6$ Hz, H-C(7)), 8.37 (dd, 1H, $^3J = 8.2$ Hz, $^4J = 1.6$ Hz, H-C(5)), 7.39 (dd, 1H, $^3J = 8.2$, 4.6 Hz, H-C(6)), 4.16–4.23 (m, 1H, H-C(1')), 2.13–2.19 (m, 2H, 2 x H-CH), 1.78–1.87 (m, 2H, 2 x H-CH), 1.48–1.73 (m, 5H, 5 x H-CH), 1.34–1.43 (m, 1H, H-CH) ppm. **Tetrazole:** ^1H NMR (500 MHz, CDCl_3) δ 9.12 (dd, 1H, $^3J = 4.6$ Hz, $^4J = 1.6$ Hz, H-C(8)), 8.65 (dd, 1H, $^3J = 8.2$ Hz, $^4J = 1.6$ Hz, H-C(6)), 7.76 (dd, 1H, $^3J = 8.2$, 4.6 Hz, H-C(7)), 4.36–4.45 (m, 1H, H-C(1')), 2.19–2.27 (m, 2H, 2 x H-CH), 1.78–1.87 (m, 2H, 2 x H-CH), 1.48–1.73 (m, 5H, 5 x H-CH), 1.34–1.43 (m, 1H, H-CH) ppm.

4.4. 2-Chloro-4-(cyclohexylthio)pyrido[2,3-*d*]pyrimidine (5a)

Cyclohexanethiol (64 mg, 0.55 mmol, 1.1 equiv.) was added to 2,4-dichloropyrido[2,3-*d*]pyrimidine (**1**) (100 mg, 0.5 mmol, 1 equiv.) and K_2CO_3 (83 mg, 0.6 mmol, 1.2 equiv.) dissolved in DMF (1 mL) and the resulting reaction mixture was stirred at ambient temperature overnight. Water (10 mL) was added to the reaction mixture and it was extracted with toluene (3×10 mL). The combined organic phase was washed with saturated aqueous NaCl solution (2×10 mL), dried over anhydrous Na_2SO_4 , filtered and evaporated under reduced pressure. The crude product was purified by column chromatography ($R_f = 0.40$ in 50% Hex/EtOAc) to obtain yellowish amorphous solid (101 mg, 72% yield). ^1H NMR (500 MHz, CDCl_3) δ 9.15 (dd, 1H, $^3J = 4.3$ Hz, $^4J = 1.7$ Hz, H-C(7)), 8.41 (dd, 1H, $^3J = 8.3$ Hz, $^4J = 1.7$ Hz, H-C(5)), 7.49 (dd, 1H, $^3J = 8.3$, 4.3 Hz, H-C(6)), 4.20–4.28 (m, 1H, H-C(1')), 2.12–2.20 (m, 2H, 2 x H-CH), 1.48–1.84 (m, 8H, 8 x H-CH) ppm. ^{13}C NMR (126 MHz, CDCl_3) δ 176.7, 159.7, 158.2, 157.8, 133.6, 122.6, 117.4, 44.3, 32.7, 25.9, 25.7 ppm.

4.5. 2-Chloro-4-(phenylthio)pyrido[2,3-*d*]pyrimidine (5b)

Thiophenol (121 mg, 1.1 mmol, 1.1 equiv.) was added to 2,4-dichloropyrido[2,3-*d*]pyrimidine (**1**) (200 mg, 1 mmol, 1 equiv.) and K_2CO_3 (152 mg, 1.1 mmol, 1.1 equiv.) dissolved in DMF (1 mL)

and the resulting reaction mixture was stirred at ambient temperature overnight. Water (10 mL) was added to the reaction mixture and it was extracted with toluene (3×10 mL). The combined organic phase was washed with saturated aqueous NaCl solution (2×10 mL), dried over anhydrous Na_2SO_4 , filtered and evaporated under reduced pressure. The crude product was purified by column chromatography ($R_f = 0.45$ in 50% Hex/EtOAc) to obtain yellowish amorphous solid (13 mg, 5% yield). ^1H NMR (500 MHz, CDCl_3) δ 8.95 (d, 1H, $^3J = 3.4$ Hz, H-C(7)), 8.30 (d, 1H, $^3J = 8.3$ Hz, H-C(5)), 7.34–7.37 (m, 2H, 2 x H-C(Ar)), 7.32 (dd, 1H, $^3J = 8.3$, 3.4 Hz, H-C(6)), 7.22–7.27 (m, 3H, 3 x H-C(Ar)) ppm. ^{13}C NMR (126 MHz, CDCl_3) δ 176.1, 159.8, 158.6, 157.9, 135.6, 133.4, 130.5, 129.7, 125.5, 123.0, 116.7 ppm. HRMS calcd. for $[\text{C}_{13}\text{H}_8\text{ClN}_3\text{S} + \text{H}^+]$ = 274.0206, found 274.0228.

4.6. 2,4-Bis(cyclohexylthio)pyrido[2,3-*d*]pyrimidine (6a)

Cyclohexanethiol (63 mg, 0.538 mmol, 1.1 equiv.) was added under argon atmosphere to mixture of 5-(cyclohexylthio)pyrido[3,2-*e*]tetrazolo[1,5-*a*]pyrimidine (**4**) (140 mg, 0.489 mmol, 1 equiv.) and NaH (60% suspension in oil, 23 mg, 0.587 mmol, 1.2 equiv.) in DMF (1 mL). The obtained reaction mixture was stirred at 50°C overnight. Water (10 mL) was added to the reaction mixture and it was extracted with toluene (3×10 mL). The combined organic phase was washed with saturated aqueous NaCl solution (2×10 mL), dried over anhydrous Na_2SO_4 , filtered and evaporated under reduced pressure. The crude product was purified by column chromatography ($R_f = 0.65$ in 50% Hex/EtOAc) to obtain white amorphous solid (134 mg, 75% yield). ^1H NMR (500 MHz, CDCl_3) δ 9.02 (dd, 1H, $^3J = 4.4$ Hz, $^4J = 1.9$ Hz, H-C(7)), 8.30 (dd, 1H, $^3J = 8.1$ Hz, $^4J = 1.9$ Hz, H-C(5)), 7.32 (dd, 1H, $^3J = 8.1$, 4.4 Hz, H-C(6)), 4.13–4.20 (m, 1H, H-CH), 4.02–4.09 (m, 1H, H-CH), 2.11–2.23 (m, 4H, 4 x H-CH), 1.76–1.84 (m, 4H, 4 x H-CH), 1.48–1.63 (m, 10H, 10 x H-CH), 1.32–1.41 (m, 2H, 2 x H-CH) ppm. ^{13}C NMR (126 MHz, CDCl_3) δ 183.8, 172.7, 171.4, 157.2, 133.7, 120.9, 116.3, 43.6, 43.5, 33.2, 32.9, 26.1, 26.1, 25.9, 25.8 ppm. HRMS calcd. for $[\text{C}_{19}\text{H}_{25}\text{N}_3\text{S}_2 + \text{H}^+]$ = 360.1563, found 360.1553.

4.7. 2,4-Bis(phenylthio)pyrido[2,3-*d*]pyrimidine (6b)

Thiophenol (165 mg, 1.5 mmol, 3 equiv.) was added to a mixture of 2,4-dichloropyrido[2,3-*d*]pyrimidine (**1**) (100 mg, 0.5 mmol, 1 equiv.) and K_2CO_3 (207 mg, 1.5 mmol, 3 equiv.) in DMF (1 mL). The obtained reaction mixture was stirred at ambient temperature overnight. Water (10 mL) was added to the reaction mixture and it was extracted with EtOAc (3×10 mL). The combined organic phase was washed with saturated aqueous NaCl solution (2×10 mL), dried over anhydrous Na_2SO_4 , filtered and evaporated under reduced pressure. The crude product was purified by column chromatography ($R_f = 0.20$ in 50% Hex/EtOAc) to obtain yellow amorphous solid (110 mg, 63% yield). ^1H NMR (500 MHz, CDCl_3) δ 9.02 (d, 1H, $^3J = 4.2$ Hz, H-C(7)), 8.40 (d, 1H, $^3J = 8.0$ Hz, H-C(5)), 7.18–7.46 (m, 11H, H-C(6), 10 x H-C(Ar)) ppm. ^{13}C NMR (126 MHz, CDCl_3) δ 173.0, 171.6, 157.9, 157.2, 135.5, 135.0, 133.5, 130.0, 129.5, 129.2 (3xC), 126.0, 121.5, 115.9 ppm. HRMS calcd. for $[\text{C}_{19}\text{H}_{13}\text{N}_3\text{S}_2 + \text{H}^+]$ = 348.0629, found 348.0640.

4.8. 2,4-Bis((4-chlorophenyl)thio)pyrido[2,3-*d*]pyrimidine (6c)

p-Chlorothiophenol (217 mg, 1.5 mmol, 3 equiv.) was added to a mixture of 2,4-dichloropyrido[2,3-*d*]pyrimidine (**1**) (100 mg, 0.5 mmol, 1 equiv.) and K_2CO_3 (207 mg, 1.5 mmol, 3 equiv.) in DMF (1 mL). The obtained reaction mixture was stirred at ambient temperature overnight. Water (10 mL) was added to the reaction mixture and it was extracted with EtOAc (3×10 mL). The combined organic phase washed with saturated aqueous NaCl solution

(2 × 10 mL), dried over Na₂SO₄, filtered and evaporated under reduced pressure. The crude product was purified by column chromatography ($R_f = 0.30$ in 50% Hex/EtOAc) to obtain yellow amorphous solid (98 mg, 47% yield).

¹H NMR (500 MHz, CDCl₃) δ 9.02 (d, 1H, ³J = 4.4 Hz, H-C(7)), 8.35 (d, 1H, ³J = 8.1 Hz, H-C(5)), 7.35 (dd, 1H, ³J = 8.1, 4.4 Hz, H-C(6)), 7.16–7.30 (m, 8H, 8 × H-C(Ar)) ppm. ¹³C NMR (126 MHz, CDCl₃) δ 172.8, 171.1, 158.2, 157.2, 136.9, 136.7, 136.5, 135.7, 133.4, 129.7, 129.4, 127.6, 124.3, 121.8, 115.8 ppm. HRMS calcd. for [C₁₉H₁₁Cl₂N₃S₂ + H⁺] = 415.9850, found 415.9846.

4.9. 5-Isopropoxyprido[3,2-e]tetrazolo[1,5-a]pyrimidine (7a)

Isopropanol (31 mg, 0.516 mmol, 1.1 equiv.) was added to mixture of 2,4-diazidopyrido[2,3-d]pyrimidine (**2**) (100 mg, 0.469 mmol, 1 equiv.) and K₂CO₃ (78 mg, 0.563 mmol, 1.2 equiv.) in DMF (1 mL). The obtained reaction mixture was stirred at ambient temperature overnight. Water (10 mL) was added to the reaction mixture and it was extracted with toluene (3 × 10 mL). The combined organic phase was washed with saturated aqueous NaCl solution (2 × 10 mL), dried over Na₂SO₄, filtered and evaporated under reduced pressure. The crude product was purified by column chromatography ($R_f = 0.25$ in 50% Hex/EtOAc) to obtain yellowish amorphous solid (32 mg, 30% yield). ¹H NMR (500 MHz, DMSO-*d*₆) δ 9.13 (d, 1H, ³J = 4.4 Hz, H-C(8)), 8.71 (d, 1H, ³J = 7.9 Hz, H-C(6)), 7.92 (dd, 1H, ³J = 7.9, 4.2 Hz, H-C(7)), 5.66 (septet, 1H, ³J = 6.2 Hz, H-C(1')), 1.51 (d, 6H, ³J = 6.2 Hz, 2 × H₃-C(2')) ppm. ¹³C NMR (126 MHz, DMSO-*d*₆) δ 163.9, 155.3, 154.6, 144.4, 136.0, 124.6, 109.4, 72.9, 21.3 ppm. HRMS calcd. for [C₁₀H₁₀N₆O + H⁺] = 231.0994, found 231.1002.

2-Azido-4-isopropoxyprido[2,3-d]pyrimidine (7aA) and 5-isopropoxyprido[3,2-e]tetrazolo[1,5-a]pyrimidine (7aB) observed in CDCl₃ solution as tautomer mixture in 91:9 ratio. Azide: ¹H NMR (500 MHz, CDCl₃) δ 9.05 (d, 1H, ³J = 4.4 Hz, H-C(7)), 8.43 (d, 1H, ³J = 7.9 Hz, H-C(5)), 7.39 (dd, 1H, ³J = 7.9, 4.4 Hz, H-C(6)), 5.64 (septet, 1H, ³J = 6.2 Hz, H-C(1')), 1.48 (d, 6H, ³J = 6.2 Hz, 2 × H₃-C(2')) ppm. Tetrazole: ¹H NMR (500 MHz, CDCl₃) δ 9.11 (d, 1H, ³J = 4.4 Hz, H-C(8)), 8.68 (d, 1H, ³J = 7.9 Hz, H-C(6)), 7.76 (dd, 1H, ³J = 7.9, 4.4 Hz, H-C(7)), 5.82 (septet, 1H, ³J = 6.2 Hz, H-C(1')), 1.56 (d, 6H, ³J = 6.2 Hz, 2 × H₃-C(2')) ppm. ¹³C NMR (126 MHz, CDCl₃) δ 163.9, 155.7, 154.8, 144.8, 136.2, 124.3, 109.2, 74.2, 21.8 ppm.

4.10. 5-Phenoxyprido[3,2-e]tetrazolo[1,5-a]pyrimidine (7b)

Phenol (49 mg, 0.516 mmol, 1.1 equiv.) was added to a mixture of 2,4-diazidopyrido[2,3-d]pyrimidine (**2**) (100 mg, 0.469 mmol, 1 equiv.) and K₂CO₃ (78 mg, 0.563 mmol, 1.2 equiv.) in DMF (1 mL). The obtained reaction mixture was stirred at ambient temperature overnight. Water (10 mL) was added to the reaction mixture and it was extracted with toluene (3 × 10 mL). The combined organic phase was washed with saturated aqueous NaCl solution (2 × 10 mL), dried over Na₂SO₄, filtered and evaporated under reduced pressure. The crude product was purified by column chromatography ($R_f = 0.20$ in 50% Hex/EtOAc) and recrystallized from EtOH to obtain yellowish amorphous solid (16 mg, 13% yield). ¹H NMR (500 MHz, DMSO-*d*₆) δ 9.24 (d, 1H, ³J = 4.5 Hz, H-C(8)), 9.02 (d, 1H, ³J = 7.9 Hz, H-C(6)), 8.03 (dd, 1H, ³J = 7.9, 4.5 Hz, H-C(7)), 7.59 (t, 2H, ³J = 7.7 Hz, 2 × H-C(2')), 7.44 (t, 1H, ³J = 7.7 Hz, H-C(3')), 7.42 (d, 2H, ³J = 7.7 Hz, 2 × H-C(1')) ppm. ¹³C NMR (126 MHz, DMSO-*d*₆) δ 164.7, 155.9, 154.1, 151.7, 144.6, 136.3, 130.0, 126.6, 125.0, 121.8, 109.3 ppm. HRMS calcd. for [C₁₃H₈N₆O + H⁺] = 265.0838, found 265.0838.

2-Azido-4-phenoxyprido[2,3-d]pyrimidine (7bA) and 5-phenoxyprido[3,2-e]tetrazolo[1,5-a]pyrimidine (7bB) observed in CDCl₃ solution as tautomer mixture in 87:13 ratio. Azide: ¹H

NMR (500 MHz, CDCl₃) δ 9.16 (dd, 1H, ³J = 4.7 Hz, ⁴J = 2.0 Hz, H-C(7)), 8.66 (dd, 1H, ³J = 8.0 Hz, ⁴J = 2.0 Hz, H-C(5)), 7.52 (t, 2H, ³J = 7.5 Hz, 2 × H-C(2')), 7.48 (dd, 1H, ³J = 8.0, 4.7 Hz, H-C(6)), 7.39 (t, 1H, ³J = 7.5 Hz, H-C(3')), 7.32 (d, 2H, ³J = 7.5 Hz, 2 × H-C(1')) ppm. Tetrazole: ¹H NMR (500 MHz, CDCl₃) δ 9.21 (dd, 1H, ³J = 4.7 Hz, ⁴J = 2.0 Hz, H-C(8)), 8.91 (dd, 1H, ³J = 8.0 Hz, ⁴J = 2.0 Hz, H-C(6)), 7.89 (dd, 1H, ³J = 8.0, 4.7 Hz, H-C(7)), 7.52 (t, 2H, ³J = 7.5 Hz, 2 × H-C(2')), 7.39 (t, 1H, ³J = 7.5 Hz, H-C(3')), 7.32 (d, 2H, ³J = 7.5 Hz, 2 × H-C(1')) ppm.

4.11. N-Hexylpyrido[3,2-e]tetrazolo[1,5-a]pyrimidin-5-amine (8a)

According to the general procedure **A** white amorphous solid was obtained (91 mg, 71% yield). ¹H NMR (500 MHz, DMSO-*d*₆) δ 9.01 (d, 1H, ³J = 4.6 Hz, H-C(8)), 8.98 (t, 1H, ³J = 5.1 Hz, NH), 8.93 (d, 1H, ³J = 8.1 Hz, H-C(6)), 7.87 (dd, 1H, ³J = 8.1, 4.6 Hz, H-C(7)), 3.58 (dt, 2H, ³J = 7.2, 5.1 Hz, H₂-C(1')), 1.69 (quintet, 2H, ³J = 7.2 Hz, H₂-C(2')), 1.36–1.45 (m, 2H, H₂-C(3')), 1.27–1.35 (m, 4H, H₂-C(4'), H₂-C(5')), 0.87 (t, 3H, ³J = 6.6 Hz, H₃-C(6')) ppm. ¹³C NMR (126 MHz, DMSO-*d*₆) δ 157.7, 155.7, 154.0, 143.5, 134.7, 123.8, 108.6, 41.4, 31.0, 28.0, 26.2, 22.1, 13.9 ppm. HRMS calcd. for [C₁₃H₁₇N₇ + H⁺] = 272.1618, found 272.1621.

4.12. N-Octylpyrido[3,2-e]tetrazolo[1,5-a]pyrimidin-5-amine (8b)

According to the general procedure **A** white amorphous solid was obtained (84 mg, 60% yield). ¹H NMR (500 MHz, DMSO-*d*₆) δ 9.00 (d, 1H, ³J = 3.4 Hz, H-C(8)), 8.96 (dd, 1H, ³J = 8.0, 3.4 Hz, H-C(7)), 8.92 (d, 1H, ³J = 8.0 Hz, H-C(6)), 7.84–7.89 (m, 1H, NH), 3.53–3.60 (m, 2H, H₂-C(1')), 1.63–1.73 (m, 2H, H₂-C(2')), 1.18–1.43 (m, 10H, 5 × -CH₂-), 0.79–0.88 (m, 3H, H₃-C(8')) ppm. ¹³C NMR (126 MHz, DMSO-*d*₆) δ 157.6, 155.7, 154.0, 143.5, 134.7, 123.7, 108.5, 41.4, 31.2, 28.8, 28.6, 28.0, 26.6, 22.1, 13.9 ppm. HRMS calcd. for [C₁₅H₂₁N₇ + H⁺] = 300.1931, found 300.1934.

4.13. 5-(Piperidin-1-yl)pyrido[3,2-e]tetrazolo[1,5-a]pyrimidine (8c)

According to the general procedure **A** white amorphous solid was obtained (59 mg, 49% yield). ¹H NMR (500 MHz, DMSO-*d*₆) δ 9.00 (d, 1H, ³J = 4.6 Hz, H-C(8)), 8.60 (d, 1H, ³J = 7.9 Hz, H-C(6)), 7.80 (dd, 1H, ³J = 7.9, 4.6 Hz, H-C(7)), 3.75–3.81 (m, 4H, 2 × H₂-C(1')), 1.69–1.79 (m, 6H, 6 × H-CH) ppm. ¹³C NMR (126 MHz, DMSO-*d*₆) δ 162.4, 154.9, 153.8, 144.7, 137.9, 123.1, 109.1, 50.8, 25.3, 23.8 ppm. HRMS calcd. for [C₁₂H₁₃N₇ + H⁺] = 256.1305, found 242.1307.

2-Azido-4-(piperidin-1-yl)pyrido[2,3-d]pyrimidine (8cA) and 5-(piperidin-1-yl)pyrido[3,2-e]tetrazolo[1,5-a]pyrimidine (8cB) Tetrazole: ¹H NMR (500 MHz, CDCl₃) δ 8.96 (d, 1H, ³J = 4.6 Hz, H-C(8)), 8.40 (d, 1H, ³J = 8.2 Hz, H-C(6)), 7.66 (dd, 1H, ³J = 8.2, 4.6 Hz, H-C(7)), 3.74–3.91 (m, 4H, 2 × H₂-C(1')), 1.69–1.92 (m, 6H, 3 × -CH₂-) ppm. ¹³C NMR (126 MHz, CDCl₃) δ 162.5, 161.2, 154.3, 145.2, 137.2, 122.7, 109.0, 51.7, 25.9, 24.4 ppm. Azide: ¹H NMR (500 MHz, CDCl₃) δ 8.88 (d, 1H, ³J = 4.6 Hz, H-C(7)), 8.13 (d, 1H, ³J = 8.2 Hz, H-C(5)), 7.23 (dd, 1H, ³J = 8.2, 4.6 Hz, H-C(6)), 3.74–3.91 (m, 4H, 2 × H₂-C(1')), 1.69–1.92 (m, 6H, 3 × -CH₂-) ppm. ¹³C NMR (126 MHz, CDCl₃) δ 166.1, 161.8, 155.9, 155.2, 134.9, 118.9, 108.4, 50.9, 26.0, 24.4 ppm.

4.14. 2-Azido-4-(pyrrolidin-1-yl)pyrido[2,3-d]pyrimidine (8dA) and 5-(pyrrolidin-1-yl)pyrido[3,2-e]tetrazolo[1,5-a]pyrimidine (8d)

According to the general procedure **A** white amorphous solid was obtained (40 mg, 35% yield). ¹H NMR (500 MHz, acetic acid-*d*₄) δ 8.85–9.06 (m, 2H), 7.55–7.81 (m, 1H), 4.00–4.14 (m, 4H), 2.10–2.20 (m, 4H) ppm. ¹³C NMR could not be acquired due to low sample concentration caused by poor solubility and tautomerization. HRMS calcd. for [C₁₁H₁₂N₇ + H⁺] = 242.1149, found 242.1117.

4.15. 4-(Pyrido[3,2-*e*]tetrazolo[1,5-*a*]pyrimidin-5-yl)morpholine (8e)

According to the general procedure **A** white amorphous solid was obtained (69 mg, 57% yield). ^1H NMR (500 MHz, Pyr-*d*₅, 70 °C) δ 9.02–9.07 (m, 1H, H-C(8)), 8.54–8.60 (m, 1H, H-C(6)), 7.65–7.60 (m, 1H, H-C(7)), 3.89–3.96 (m, 8H, 4 x -CH₂-) ppm. ^{13}C NMR (126 MHz, Pyr-*d*₅, 70 °C) δ 163.4, 157.0, 156.4, 155.0, 146.3, 137.9, 109.9, 67.1, 51.5 ppm. HRMS calcd. for [C₁₁H₁₁N₇O + H⁺] = 258.1098, found 258.1092.

4.16. N-(4-Methoxybenzyl)pyrido[3,2-*e*]tetrazolo[1,5-*a*]pyrimidin-5-amine (8f)

According to the general procedure **A** white amorphous solid was obtained (100 mg, 69% yield). ^1H NMR (500 MHz, DMSO-*d*₆) δ 9.65 (s, 1H, NH), 8.87 (dd, 1H, $^3J = 4.7$ Hz, $^4J = 1.8$ Hz, H-C(8)), 8.71 (dd, 1H, $^3J = 7.8$ Hz, $^4J = 1.8$ Hz, H-C(6)), 7.46 (dd, 1H, $^3J = 7.8$, 4.7 Hz, H-C(7)), 7.42 (d, 2H, $^3J = 8.5$ Hz, 2 x H-C(1')), 6.88 (d, 2H, $^3J = 8.5$ Hz, 2 x H-C(2')), 4.76 (s, 2H, -CH₂-), 3.71 (s, 3H, H₃C-O) ppm. ^{13}C NMR (126 MHz, DMSO-*d*₆) δ 158.4, 155.2, 154.8, 150.1, 142.9, 133.3, 130.2, 128.9, 119.4, 113.6, 106.3, 55.0, 43.6 ppm. HRMS calcd. for [C₁₅H₁₃N₇ + H⁺] = 308.1254, found 242.1260.

4.17. N-Benzylpyrido[3,2-*e*]tetrazolo[1,5-*a*]pyrimidin-5-amine (8g)

According to the general procedure **A** white amorphous solid was obtained (78 mg, 61% yield). ^1H NMR (500 MHz, DMSO-*d*₆) δ 9.55 (s, 1H, NH), 9.02 (d, 1H, $^3J = 4.3$ Hz, H-C(8)), 8.98 (d, 1H, $^3J = 8.0$ Hz, H-C(6)), 7.88 (dd, 1H, $^3J = 8.0$, 4.3 Hz, H-C(7)), 7.43 (d, 2H, $^3J = 7.3$ Hz, 2 x H-C(1')), 7.34 (t, 2H, $^3J = 7.3$ Hz, 2 x H-C(2')), 7.26 (t, 1H, $^3J = 7.3$ Hz, H-C(3')), 4.85 (s, 2H, -CH₂-) ppm. ^{13}C NMR (126 MHz, DMSO-*d*₆) δ 157.9, 155.6, 154.1, 143.6, 138.1, 134.7, 128.4, 127.5, 127.1, 123.8, 108.6, 44.4 ppm. HRMS calcd. for [C₁₄H₁₁N₇ + H⁺] = 278.1149, found 242.1146.

4.18. N-Hexyl-2-(4-phenyl-1H-1,2,3-triazol-1-yl)pyrido[2,3-*d*]pyrimidin-4-amine (10a)

Product was obtained according to the general procedure **B**: sodium ascorbate (20 mg, 0.148 mmol, 0.4 equiv.), CuSO₄·5H₂O (18 mg, 0.074 mmol, 0.2 equiv.), NEt₃ (74 mg, 0.738 mmol, 2 equiv.), N-hexylpyrido[3,2-*e*]tetrazolo[1,5-*a*]pyrimidin-5-amine (**8a**) (100 mg, 0.369 mmol, 1 equiv.) and phenylacetylene (56 mg, 0.553 mmol, 1.5 equiv.); white amorphous solid was obtained (100 mg, 72% yield). ^1H NMR (500 MHz, DMSO-*d*₆) δ 9.33 (s, 1H, H-C(triazole)), 9.08 (t, 1H, $^3J = 5.2$ Hz, NH), 9.02 (d, 1H, $^3J = 4.4$ Hz, H-C(7)), 8.78 (d, 1H, $^3J = 8.1$ Hz, H-C(5)), 8.06 (d, 2H, $^3J = 7.6$ Hz, 2 x H-C(1'')), 7.57 (dd, 1H, $^3J = 8.1$, 4.4 Hz, H-C(6)), 7.49 (t, 2H, $^3J = 7.6$ Hz, 2 x H-C(2'')), 7.39 (t, 1H, $^3J = 7.6$ Hz, H-C(3'')), 7.70 (td, 2H, $^3J = 7.2$, 5.2 Hz, H₂-C(1')), 1.71 (quintet, 2H, $^3J = 3.7$ Hz, H₂-C(2')), 1.39 (quintet, 2H, $^3J = 7.2$ Hz, H₂-C(3')), 1.22–1.35 (m, 4H, H₂-C(4')), H₂-C(5')), 0.83 (t, 3H, $^3J = 7.0$ Hz, H₃-C(6')) ppm. ^{13}C NMR (126 MHz, DMSO-*d*₆) δ 162.3, 158.8, 156.3, 153.5, 146.4, 132.9, 130.1, 128.9, 128.3, 125.6, 121.4, 119.8, 109.3, 41.2, 31.0, 28.3, 26.2, 22.1, 13.9 ppm. ^1H NMR (500 MHz, CDCl₃) δ 9.04 (s, 1H, H-C(triazole)), 9.03 (d, 1H, $^3J = 4.4$ Hz, H-C(7)), 8.37 (d, 1H, $^3J = 8.2$ Hz, H-C(5)), 7.95 (d, 2H, $^3J = 7.6$ Hz, 2 x H-C(1'')), 7.47 (t, 2H, $^3J = 7.6$ Hz, 2 x H-C(2'')), 7.41 (dd, 1H, $^3J = 8.2$, 4.4 Hz, H-C(6)), 7.37 (t, 1H, $^3J = 7.6$ Hz, H-C(3'')), 6.77 (t, 1H, $^3J = 5.3$ Hz, NH), 3.83 (dt, 2H, $^3J = 7.3$, 5.3 Hz, H₂-C(1')), 1.74 (quintet, 2H, $^3J = 7.3$ Hz, H₂-C(2')), 1.40 (quintet, 2H, $^3J = 7.3$ Hz, H₂-C(3')), 1.23–1.33 (m, 4H, H₂-C(4')), H₂-C(5')), 0.85 (t, 3H, $^3J = 6.9$ Hz, H₃-C(6')) ppm. ^{13}C NMR (126 MHz, CDCl₃) δ 162.6, 159.4, 156.7, 154.2, 147.8, 131.4, 130.4, 129.1, 128.6, 126.1, 121.4, 119.2, 109.2, 42.4, 31.6, 29.2, 26.8, 22.7,

14.1 ppm. HRMS calcd. for [C₂₁H₂₃N₇ + H⁺] = 374.2093, found 374.2096.

4.19. N-Hexyl-2-(4-(*p*-tolyl)-1H-1,2,3-triazol-1-yl)pyrido[2,3-*d*]pyrimidin-4-amine (10b)

Product was obtained according to the general procedure **B**: sodium ascorbate (25 mg, 0.125 mmol, 0.4 equiv.), CuSO₄·5H₂O (16 mg, 0.063 mmol, 0.2 equiv.), NEt₃ (63 mg, 0.626 mmol, 2 equiv.), N-hexylpyrido[3,2-*e*]tetrazolo[1,5-*a*]pyrimidin-5-amine (**8a**) (85 mg, 0.313 mmol, 1 equiv.) and *p*-tolylacetylene (55 mg, 0.470 mmol, 1.5 equiv.); white amorphous solid was obtained (60 mg, 50% yield). ^1H NMR (500 MHz, CDCl₃) δ 9.04 (d, 1H, $^3J = 4.4$ Hz, H-C(7)), 9.00 (s, 1H, H-C(triazole)), 8.32 (d, 1H, $^3J = 8.1$ Hz, H-C(5)), 7.84 (d, 2H, $^3J = 8.0$ Hz, 2 x H-C(1'')), 7.41 (dd, 1H, $^3J = 8.1$, 4.4 Hz, H-C(6)), 7.28 (d, 2H, $^3J = 8.0$ Hz, 2 x H-C(2'')), 6.64 (t, 1H, $^3J = 6.7$ Hz, NH), 3.84 (dt, 2H, $^3J = 7.5$, 6.7 Hz, H₂-C(1')), 2.40 (s, 3H, H₃-C(3'')), 1.74 (quintet, 2H, $^3J = 7.5$ Hz, H₂-C(2')), 1.41 (quintet, 2H, $^3J = 7.3$ Hz, H₂-C(3')), 1.24–1.34 (m, 4H, H₂-C(4')), H₂-C(5')), 0.86 (t, 3H, $^3J = 6.9$ Hz, H₃-C(6')) ppm. ^{13}C NMR (126 MHz, CDCl₃) δ 162.6, 159.4, 156.7, 154.3, 147.9, 138.5, 131.3, 129.7, 127.5, 126.0, 121.4, 118.8, 109.1, 42.4, 31.6, 29.2, 26.8, 22.7, 21.5, 14.1 ppm. HRMS calcd. for [C₂₂H₂₅N₇ + H⁺] = 388.2250, found 388.2267.

4.20. N-Hexyl-2-(4-hexyl-1H-1,2,3-triazol-1-yl)pyrido[2,3-*d*]pyrimidin-4-amine (10c)

Product was obtained according to the general procedure **B**: sodium ascorbate (26 mg, 0.133 mmol, 0.4 equiv.), CuSO₄·5H₂O (17 mg, 0.066 mmol, 0.2 equiv.), NEt₃ (67 mg, 0.663 mmol, 2 equiv.), N-hexylpyrido[3,2-*e*]tetrazolo[1,5-*a*]pyrimidin-5-amine (**8a**) (90 mg, 0.332 mmol, 1 equiv.) and 1-octyne (55 mg, 0.498 mmol, 1.5 equiv.); white amorphous solid was obtained (95 mg, 75% yield). ^1H NMR (500 MHz, CDCl₃) δ 9.00 (d, 1H, $^3J = 4.4$ Hz, H-C(7)), 8.53 (s, 1H, H-C(triazole)), 8.42 (d, 1H, $^3J = 8.1$ Hz, H-C(5)), 7.38 (dd, 1H, $^3J = 8.1$, 4.4 Hz, H-C(6)), 6.96 (t, 1H, $^3J = 6.0$ Hz, NH), 3.78 (dt, 2H, $^3J = 7.4$, 6.0 Hz, H₂-C(1'')), 2.81 (t, 2H, $^3J = 7.6$ Hz, H₂-C(1'')), 1.73 (quintet, 2H, $^3J = 7.6$ Hz, H₂-C(2'')), 1.67 (quintet, 2H, $^3J = 7.4$ Hz, H₂-C(2'')), 1.20–1.41 (m, 12H, 6 x -CH₂-), 0.88 (t, 3H, $^3J = 6.6$ Hz, -CH₃), 0.83 (t, 3H, $^3J = 6.6$ Hz, -CH₃) ppm. ^{13}C NMR (126 MHz, CDCl₃) δ 162.6, 159.4, 156.6, 154.3, 148.7, 131.6, 121.3, 120.5, 109.2, 42.3, 31.7, 31.6, 29.3, 29.1, 29.0, 26.8, 25.8, 22.7, 22.6, 14.2, 14.1 ppm. HRMS calcd. for [C₂₁H₃₁N₇ + H⁺] = 382.2719, found 382.2745.

4.21. 4-(Cyclohexylthio)-2-(4-phenyl-1H-1,2,3-triazol-1-yl)pyrido[2,3-*d*]pyrimidine (11)

Product was obtained according to the general procedure **B**: sodium ascorbate (12 mg, 0.058 mmol, 0.4 equiv.), CuSO₄·5H₂O (7 mg, 0.029 mmol, 0.2 equiv.), NEt₃ (30 mg, 0.293 mmol, 2 equiv.), 5-(cyclohexylthio)pyrido[3,2-*e*]tetrazolo[1,5-*a*]pyrimidine (**4**) (42 mg, 0.147 mmol, 1 equiv.) and phenylacetylene (22 mg, 0.220 mmol, 1.5 equiv.); white amorphous solid was obtained (23 mg, 40% yield). ^1H NMR (500 MHz, CDCl₃) δ 9.21 (d, 1H, $^3J = 4.4$ Hz, H-C(7)), 9.07 (s, 1H, H-C(triazole)), 8.51 (d, 1H, $^3J = 8.2$ Hz, H-C(5)), 7.98 (d, 2H, $^3J = 7.6$ Hz, 2 x H-C(1'')), 7.54 (dd, 1H, $^3J = 8.2$, 4.4 Hz, H-C(6)), 7.49 (t, 2H, $^3J = 7.6$ Hz, 2 x H-C(2'')), 7.40 (t, 1H, $^3J = 7.6$ Hz, H-C(3'')), 4.46–4.53 (m, 1H, H-C(1')), 2.25–2.33 (m, 2H, 2 x H-CH), 1.81–1.89 (m, 2H, 2 x H-CH), 1.62–1.76 (m, 5H, 5 x H-CH), 1.36–1.47 (m, 1H, H-CH) ppm. ^{13}C NMR (126 MHz, CDCl₃) δ 178.1, 158.5, 157.4, 152.3, 148.1, 133.9, 130.2, 129.1, 128.8, 126.1, 122.6, 118.9, 118.3, 45.0, 32.7, 26.0, 25.8 ppm. HRMS calcd. for [C₂₁H₂₀N₆S + H⁺] = 389.1548, found 389.1523.

4.22. N-(Triphenylphosphorylidene)pyrido[3,2-e]tetrazolo[1,5-a]pyrimidine-5-amine (12) and N-(triphenylphosphorylidene)-2-azidopyrido[2,3-d]pyrimidin-4-yl-amine (12A)

Triphenylphosphine (308 mg, 1.173 mmol, 2.5 equiv.) and 2,4-diazidopyrido[2,3-d]pyrimidine (**2**) (100 mg, 0.469 mmol, 1 equiv.) were dissolved in toluene (1 mL) and the resulting reaction mixture was stirred at ambient temperature overnight. The reaction mixture was evaporated under reduced pressure and the crude product was purified by column chromatography ($R_f = 0.15$ in 50% Hex/EtOAc) to obtain white amorphous solid (185 mg, 58% yield). Products **12** provides tautomeric mixtures in $CDCl_3$ and $DMSO-d_6$ solutions in 72:28 and 46:54 ratios, respectively.

Azide: 1H NMR (500 MHz, $CDCl_3$) δ 8.80 (dd, 1H, $^3J = 4.7$ Hz, $^4J = 1.8$ Hz, H-C(7)), 8.68 (dd, 1H, $^3J = 8.0$ Hz, $^4J = 1.8$ Hz, H-C(5)), 8.01 (ddd, 6H, $^3J_{H-P} = 12.6$ Hz, $^3J = 8.0$ Hz, $^4J = 1.5$ Hz, 6 x H-C(2')), 7.59 (tdt, 3H, $^3J = 8.0$, 7.5 Hz, $^5J_{H-P} = 1.8$ Hz, 3 x H-C(4')), 7.53 (ddd, 6H, $^3J = 8.0$, 7.5 Hz, $^4J_{H-P} = 3.3$ Hz, 6 x H-C(3')), 7.22 (dd, 1H, $^3J = 8.0$, 4.7 Hz, H-C(6)) ppm. ^{13}C NMR (126 MHz, $CDCl_3$) δ 155.8 (2 x C), 154.7, 150.7, 133.7, 133.6 (d, $^2J_{C-P} = 10.4$ Hz), 133.1 (d, $^4J_{C-P} = 2.8$ Hz), 129.1 (d, $^3J_{C-P} = 12.7$ Hz), 126.4 (d, $^1J_{C-P} = 103.1$ Hz), 118.8, 107.2 ppm. ^{31}P NMR (202 MHz, $CDCl_3$) δ 21.8 ppm.

1H NMR (500 MHz, $DMSO-d_6$) δ 8.76 (dd, 1H, $^3J = 4.6$ Hz, $^4J = 2.0$ Hz, H-C(7)), 8.65 (dd, 1H, $^3J = 7.8$ Hz, $^4J = 2.0$ Hz, H-C(5)), 8.01 (ddd, 6H, $^3J_{H-P} = 12.6$ Hz, $^3J = 8.0$ Hz, $^4J = 1.5$ Hz, 6 x H-C(2')), 7.72 (tdt, 3H, $^3J = 8.0$, 7.5 Hz, $^5J_{H-P} = 1.8$ Hz, 3 x H-C(4')), 7.64 (ddd, 6H, $^3J = 8.0$, 7.5 Hz, $^4J_{H-P} = 3.3$ Hz, 6 x H-C(3')), 7.38 (dd, 1H, $^3J = 7.8$, 4.6 Hz, H-C(6)) ppm. ^{13}C NMR (126 MHz, $DMSO-d_6$) δ 155.2, 155.0, 154.4, 150.4 (d, $^2J = 1.6$ Hz), 133.2 (d, $^4J = 2.6$ Hz), 133.1 (d, $^2J = 10.6$ Hz), 133.1, 129.1 (d, $^3J = 12.4$ Hz), 126.1 (d, $^1J = 102.3$ Hz), 119.1, 106.4 ppm. ^{31}P NMR (202 MHz, $DMSO-d_6$) δ 21.4 ppm.

Tetrazole: 1H NMR (500 MHz, $CDCl_3$) δ 9.12 (dd, 1H, $^3J = 8.0$ Hz, $^4J = 1.8$ Hz, H-C(6)), 9.00 (dd, 1H, $^3J = 4.7$ Hz, $^4J = 1.8$ Hz, H-C(8)), 8.01 (ddd, 6H, $^3J_{H-P} = 12.6$ Hz, $^3J = 8.0$ Hz, $^4J = 1.5$ Hz, 6 x H-C(2')), 7.88 (dd, 1H, $^3J = 8.0$, 4.7 Hz, H-C(7)), 7.72 (tdt, 3H, $^3J = 8.0$, 7.5 Hz, $^5J_{H-P} = 1.8$ Hz, 3 x H-C(4')), 7.64 (ddd, 6H, $^3J = 8.0$, 7.5 Hz, $^4J_{H-P} = 3.3$ Hz, 6 x H-C(3')) ppm. ^{13}C NMR (126 MHz, $CDCl_3$) δ 165.2 (d, $^2J_{C-P} = 6.0$ Hz), 153.6, 147.3 (d, $^4J_{C-P} = 3.2$ Hz), 144.7 (d, $^4J_{C-P} = 3.2$ Hz), 138.4, 133.5 (d, $^2J_{C-P} = 10.1$ Hz), 132.9 (d, $^4J_{C-P} = 2.7$ Hz), 129.0 (d, $^3J_{C-P} = 12.5$ Hz), 126.8 (d, $^1J_{C-P} = 101.4$ Hz), 123.4, 114.7 (d, $^3J_{C-P} = 23.7$ Hz) ppm. ^{31}P NMR (202 MHz, $CDCl_3$) δ 21.6 ppm.

1H NMR (500 MHz, $DMSO-d_6$) δ 9.22 (dd, 1H, $^3J = 7.8$ Hz, $^4J = 2.0$ Hz, H-C(6)), 9.00 (dd, 1H, $^3J = 4.6$ Hz, $^4J = 2.0$ Hz, H-C(8)), 8.01 (ddd, 6H, $^3J_{H-P} = 12.6$ Hz, $^3J = 8.0$ Hz, $^4J = 1.5$ Hz, 6 x H-C(2')), 7.88 (dd, 1H, $^3J = 7.8$, 4.6 Hz, H-C(7)), 7.72 (tdt, 3H, $^3J = 8.0$, 7.5 Hz, $^5J_{H-P} = 1.8$ Hz, 3 x H-C(4')), 7.64 (ddd, 6H, $^3J = 8.0$, 7.5 Hz, $^4J_{H-P} = 3.3$ Hz, 6 x H-C(3')) ppm. ^{13}C NMR (126 MHz, $DMSO-d_6$) δ 164.9 (d, $^2J_{C-P} = 6.0$ Hz), 153.8, 146.9 (d, $^4J_{C-P} = 3.1$ Hz), 144.1 (d, $^4J_{C-P} = 3.1$ Hz), 138.4, 132.0 (d, $^4J = 2.6$ Hz), 132.0 (d, $^2J = 10.6$ Hz), 129.1 (d, $^3J = 12.4$ Hz), 126.5 (d, $^1J = 100.2$ Hz), 124.1, 114.3 (d, $^3J_{C-P} = 23.3$ Hz) ppm. ^{31}P NMR (202 MHz, $DMSO-d_6$) δ 20.5 ppm. HRMS calcd. for $[C_{25}H_{18}N_7P + H^+]$ = 448.1440, found 448.1466.

5. Conclusions

In summary, for the first time C-5 substituted pyrido[3,2-e]tetrazolo[1,5-a]pyrimidines were obtained in sequential S_NAr reactions of 2,4-dichloropyrido[2,3-d]pyrimidine with NaN_3 followed by various O-, S- and N- nucleophiles. Further application of C-5 substituted pyrido[3,2-e]tetrazolo[1,5-a]pyrimidines for synthesis of triazoles in CuAAC reaction was possible due to the azide-tetrazole tautomeric equilibrium of these compounds. To the best

of our knowledge, the annulated tricyclic pyrido[3,2-e]tetrazolo[1,5-a]pyrimidine heterocyclic skeleton was unambiguously characterized by single crystal X-ray diffraction for the first time. Also, azide-tetrazole equilibrium rate constants ($K_{T/A}$) and free Gibbs energies for the tautomeric equilibrium of pyrido[3,2-e]tetrazolo[1,5-a]pyrimidines were calculated using variable temperature NMR and the obtained numerical values were similar to those of other azidopyrimidines. A detailed NMR and DFT study of structurally rich tautomeric interplay of 2,4-diazidopyrido[2,3-d]pyrimidine is currently under progress and will be reported elsewhere.

Declaration of Competing Interest

The authors declare that they have no known competing financial interests or personal relationships that could have appeared to influence the work reported in the manuscript "Structural Study of Azide-Tetrazole Equilibrium in Pyrido[2,3-d]pyrimidines", which is submitted to the *Journal of Molecular Structure*.

CRediT authorship contribution statement

Kristaps Leškovskis: Investigation, Visualization, Writing – original draft, Funding acquisition. **Anatoly Mishnev:** Writing – original draft. **Irina Novosjolova:** Supervision, Conceptualization, Writing – review & editing, Funding acquisition. **Māris Turks:** Supervision, Conceptualization, Methodology, Writing – review & editing.

Data Availability

Data will be made available on request.

Acknowledgments

I.N. thanks the Latvian Council of Science grant LZP-2020/1-0348 and K.L. thanks the European Social Fund within the Project No 8.2.2.0/20/1/008 «Strengthening of PhD students and academic personnel of Riga Technical University and BA School of Business and Finance in the strategic fields of specialization» of the Specific Objective 8.2.2 «To Strengthen Academic Staff of Higher Education Institutions in Strategic Specialization Areas» of the Operational Programme «Growth and Employment».

Supplementary materials

Supplementary material associated with this article can be found, in the online version, at doi:10.1016/j.molstruc.2022.133784.

References

- [1] R. Kaur, P. Kaur, S. Sharma, G. Singh, S. Mehdiratta, P. Bedi, K. Nepali, Anti-cancer pyrimidines in diverse scaffolds: a review of patent literature, *Recent Pat Anticancer Drug Discov.* 10 (2014) 23–71, doi:10.2174/1574892809666140917104502.
- [2] S. Wang, X.-H. Yuan, S.-Q. Wang, W. Zhao, X.-B. Chen, B. Yu, FDA-approved pyrimidine-fused bicyclic heterocycles for cancer therapy: synthesis and clinical application, *Eur. J. Med. Chem.* 214 (2021) 113218, doi:10.1016/j.ejmech.2021.113218.
- [3] T.P. Selvam, K.R. James, P.V. Dniandev, S.K. Valzita, A mini review of pyrimidine and fused pyrimidine marketed drugs, *Res. Pharm.* 2 (2012) 1–9 <https://updatepublishing.com/journal/index.php/rip/article/view/271>. (accessed July 10, 2022).
- [4] K.R.A. Abdellatif, R.B. Bakr, Pyrimidine and fused pyrimidine derivatives as promising protein kinase inhibitors for cancer treatment, *Med. Chem. Res.* 30 (2021) 31–49, doi:10.1007/s00044-020-02656-8.
- [5] A. Mahapatra, T. Prasad, T. Sharma, Pyrimidine: a review on anticancer activity with key emphasis on SAR, *Future J. Pharmaceut. Sci.* 7 (2021) 123, doi:10.1186/s43094-021-00274-8.
- [6] S. Kumar, B. Narasimhan, Therapeutic potential of heterocyclic pyrimidine scaffolds, *Chem. Centr. J.* 12 (2018) 38, doi:10.1186/s13065-018-0406-5.

- [7] W.D. Hong, F. Benayoud, G.L. Nixon, L. Ford, K.L. Johnston, R.H. Clare, A. Cassidy, D.A.N. Cook, A. Sieu, M. Shiotani, P.J.H. Webborn, S. Kavanagh, G. Aljayoussi, E. Murphy, A. Steven, J. Archer, D. Struever, S.J. Frohberger, A. Ehrens, M.P. Hübner, A. Hoerauf, A.P. Roberts, A.T.M. Hubbard, E.W. Tate, R.A. Serwa, S.C. Leung, L. Qie, N.G. Berry, F. Gusovsky, J. Hemingway, J.D. Turner, M.J. Taylor, S.A. Ward, P.M. O'Neill, AWZ10665, a highly specific anti-Wolbachia drug candidate for a short-course treatment of filariasis, *Proc. Natl. Acad. Sci USA* 116 (2019) 1414–1419, doi:10.1073/pnas.1816585116.
- [8] K.E. Arnst, S. Banerjee, Y. Wang, H. Chen, Y. Li, L. Yang, W. Li, D.D. Miller, W. Li, X-ray Crystal Structure Guided Discovery and Antitumor Efficacy of Dihydroquinolinone as Potent Tubulin Polymerization Inhibitors, *ACS Chem. Biol.* 14 (2019) 2810–2821, doi:10.1021/acscmbio.9b00696.
- [9] S. Banerjee, K.E. Arnst, Y. Wang, G. Kumar, S. Deng, L. Yang, G. Li, J. Yang, S.W. White, W. Li, D.D. Miller, Heterocyclic-fused pyrimidines as novel tubulin polymerization inhibitors targeting the colchicine binding site: structural basis and antitumor efficacy, *J. Med. Chem.* 61 (2018) 1704–1718, doi:10.1021/acs.jmedchem.7b01858.
- [10] E.M. AbedelRehim, M. AbdEllatif, Synthesis of Some Novel Pyrido[2,3-d]pyrimidine and Pyrido[3,2-e][1,3,4]triazolo and Tetrazolo[1,5-c]pyrimidine derivatives as potential antimicrobial and anticancer agents, *J. Heterocycl. Chem.* 55 (2018) 419–430, doi:10.1002/hlct.3058.
- [11] T. Iwaki, T. Tanaka, K. Miyazaki, Y. Suzuki, Y. Okamura, A. Yamaki, M. Iwanami, N. Morozumi, M. Furuya, Y. Oyama, Discovery and in vivo effects of novel human natriuretic peptide receptor A (NPR-A) agonists with improved activity for rat NPR-A, *Bioorg. Med. Chem.* 25 (2017) 6680–6694, doi:10.1016/j.bmc.2017.11.006.
- [12] A.A.K. Al-Ashmary, F.A. Ragab, K.M. Elokely, M.M. Anwar, O. Perez-Leal, M.C. Rico, J. Gordon, E. Bichenko, G. Mateo, E.M.M. Kassem, G.H. Hegazy, M. Abou-Gharbia, W. Childers, Design, synthesis and SAR of new-di-substituted pyridopyrimidines as ATP-competitive dual PI3K/mTOR inhibitors, *Bioorg. Med. Chem. Lett.* 27 (2017) 3117–3122, doi:10.1016/j.bmcl.2017.05.044.
- [13] Z. Zhou, Y. Liu, Q. Ren, D. Yu, H. Lu, Synthesis, crystal structure and DFT study of a novel compound N-(4-(2,4-dimorpholinopyrido[2,3-d]pyrimidin-6-yl)phenyl)pyrrolidine-1-carboxamide, *J. Mol. Struct.* 1235 (2021) 130261, doi:10.1016/j.molstruc.2021.130261.
- [14] Y. Riadi, M. Geesi, Photochemical route for the synthesis of novel 2-mono-substituted pyrido[2,3-d]pyrimidines by palladium-catalyzed cross-coupling reactions, *Chem. Papers* 72 (2018) 697–701, doi:10.1007/s11696-017-0325-2.
- [15] G. Shen, M. Liu, J. Lu, T. Meng, Practical synthesis of Vistusertib (AZD2014), an ATP competitive mTOR inhibitor, *Tetrahedron Lett.* 60 (2019) 151333, doi:10.1016/j.tetlet.2019.151333.
- [16] Y. Riadi, S. Lazar, G. Guillaumet, Regioselective palladium-catalyzed Suzuki-Miyaura coupling reaction of 2,4,6-trihalogenopyrido[2,3-d]pyrimidines, *Comptes Rendus Chimie* 22 (2019) 294–298, doi:10.1016/j.crci.2019.01.006.
- [17] T.A. Clohessy, A. Roberts, E.S. Manas, V.K. Patel, N.A. Anderson, A.J.B. Watson, Chemoselective one-pot synthesis of functionalized amino-azaheterocycles enabled by coveare, *Org. Lett.* 19 (2017) 6368–6371, doi:10.1021/acs.orglett.7b03214.
- [18] S.L. Deev, T.S. Shestakova, Z.O. Shenkarev, A.S. Paramonov, I.A. Khalymbadza, O.S. Eltsov, V.N. Charushin, O.N. Chupakhin, ¹⁵N chemical shifts and J_N-couplings as diagnostic tools for determination of the azide-tetrazole equilibrium in tetrazolozines, *J. Org. Chem.* 87 (2022) 211–222, doi:10.1021/acs.joc.1c02225.
- [19] S. Manzoor, J.-Q. Yang, Q. Tariq, H.-Z. Mei, Z.-L. Yang, Y. Hu, W.-L. Cao, V.P. Sinditskii, J.-G. Zhang, Tetrazole and azido derivatives of pyrimidine: synthesis, mechanism, thermal behaviour & steering of azido-tetrazole equilibrium, *ChemistrySelect* 5 (2020) 5414–5421, doi:10.1002/slct.202001087.
- [20] N.V. Aleksandrova, E.B. Nikolaenkova, Yu.V. Gatilov, D.N. Polovyanenko, V.I. Mamatyuk, V.P. Krivopalov, Synthesis and study of azide-tetrazole tautomerism in 2-azido-6-phenylpyrimidin-4(3H)-one and 2-azido-4-chloro-6-phenylpyrimidine, *Russ. Chem. Bull.* 71 (2022) 1266–1272, doi:10.1007/s11172-022-3529-8.
- [21] A. Sebris, M. Turks, Recent investigations and applications of azidoazomethine-tetrazole tautomeric equilibrium, *Chem. Heterocycl. Comp.* 55 (2019) 1041–1043, doi:10.1007/s10593-019-02574-7.
- [22] V.A. Ostrovskii, E.A. Popova, R.E. Trifonov, Developments in tetrazole chemistry 2009–2016, *Adv. Heterocycl. Chem.* 123 (2017) 1–62, doi:10.1016/bs.aihch.2016.12.003.
- [23] M. Tišler, Some Aspects of Azido-Tetrazolo Isomerization, *Synthesis (Mass)* 1973 (1973) 123–136, doi:10.1055/s-1973-22145.
- [24] A. Jeminejs, S.M. Goliskina, I. Novosjolova, D. Stepanovs, Ē. Bizdēna, M. Turks, Application of azide-tetrazole tautomerism and arylsulfanyl group dance in the synthesis of thio-substituted tetrazolopyrimidines, *Synthesis (Mass)* 53 (2021) 1543–1556, doi:10.1055/s-0040-1706568.
- [25] J. Bucevičius, M. Turks, S. Tumkevičius, Easy access to isomeric 7-deazapurine-1,2,3-triazole conjugates via S_NAr and CuAAC reactions of 2,6-diazido-7-deazapurines, *Synlett* 29 (2018) 525–529, doi:10.1055/s-0036-1590942.
- [26] S.N. Sirakanyan, D. Spinelli, A. Geronikaki, A.A. Hovakimyan, A.S. Norayyan, New heterocyclic systems derived from pyridine: new substrates for the investigation of the azide/tetrazole equilibrium, *Tetrahedron* 70 (2014) 8648–8656, doi:10.1016/j.tet.2014.09.047.
- [27] A. Sebris, I. Novosjolova, K. Traskovskis, V. Kokars, N. Tetervenoka, A. Vembris, M. Turks, Photophysical and electrical properties of highly luminescent 2/6-triazolyl-substituted push-pull purines, *ACS Omega* 7 (6) (2022) 5242–5253, doi:10.1021/acsomega.1c06359.
- [28] A. Šišujins, J. Bucevičius, Y.-T. Tseng, I. Novosjolova, K. Traskovskis, Ē. Bizdēna, H.-T. Chang, S. Tumkevičius, M. Turks, Synthesis and fluorescent properties of N(9)-alkylated 2-amino-6-triazolopyrimidines and 7-deazapurines, *Beilstein J. Org. Chem.* 15 (2019) 474–489, doi:10.3762/bjoc.15.41.
- [29] A. Kalniņa, Ē. Bizdēna, G. Kiselovs, A. Mishnev, M. Turks, Structural proof of tetrazolo[1,5-*a*]quinoxaline derivatives and their application in the synthesis of 4-amino-2-(1,2,3-triazol-1-yl)quinoxalines, *Chem. Heterocycl. Comp.* 49 (2014) 1667–1673, doi:10.1007/s10593-014-1418-2.
- [30] I. Novosjolova, Ē. Bizdēna, M. Turks, Application of 2,6-diazidopyrimidine derivatives in the synthesis of thiopyrimidines, *Tetrahedron. Lett.* 54 (48) (2013) 6557–6561, doi:10.1016/j.tetlet.2013.09.095.
- [31] S. Bräse, K. Banert (Eds.), *Organic Azides: Syntheses and Applications*, John Wiley & Sons, 2010, doi:10.1002/9780470682517.
- [32] J.M. Zaķis, K. Ozols, I. Novosjolova, R. Vilšķērtis, A. Mishnev, M. Turks, Sulfonyl group dance: a tool for the synthesis of 6-Azido-2-sulfonylpyrimidine derivatives, *J. Org. Chem.* 85 (7) (2020) 4753–4771, doi:10.1021/acs.joc.9b03518.
- [33] H.-J. Zhang, S.-B. Wang, X. Wen, J.-Z. Li, Z.-S. Quan, Design, synthesis, and evaluation of the anticonvulsant and antidepressant activities of pyrido[2,3-d]pyrimidine derivatives, *Med. Chem. Res.* 25 (2016) 1287–1298, doi:10.1007/s00044-016-1559-1.
- [34] S. Abou-Shehada, M.C. Teasdale, S.D. Bull, C.E. Wade, J.M.J. Williams, Lewis acid activation of pyrimidines for nucleophilic aromatic substitution and conjugate addition, *ChemSusChem* 8 (2015) 1083–1087, doi:10.1002/cssc.201403154.
- [35] E. Haldón, M.C. Nicasio, P.J. Pérez, Copper-catalysed azide-alkyne cycloadditions (CuAAC): an update, *Org. Biomol. Chem.* 13 (2015) 9528–9550, doi:10.1039/c5ob01457c.
- [36] K.S. Sindhu, G. Anilkumar, Recent advances and applications of Glaser coupling employing greener protocols, *RSC Adv.* 4 (2014) 27867–27887, doi:10.1039/c4ra02416b.
- [37] F.H. Allen, D.G. Watson, L. Brammer, A.G. Orpen, R. Taylor, Typical interatomic distances: organic compounds, in: *International Tables for Crystallography*, International Union of Crystallography, Chester, England, 2006, pp. 790–811, doi:10.1107/97809555360260000621.
- [38] L.J. Farrugia, WinGX and ORTEP for Windows: an update, *J. Appl. Cryst.* 45 (2012) 849–854, doi:10.1107/S0021889812029111.
- [39] I.J. Bruno, J.C. Cole, P.R. Edgington, M. Kessler, C.F. Macrae, P. McCabe, J. Pearson, R. Taylor, Structural science new software for searching the Cambridge structural database and visualizing crystal structures, *Acta Cryst. Sect. B* 58 (2002) 389–397, doi:10.1107/S0108768102003324.
- [40] A.L. Spek, Single-crystal-structure validation with the program PLATON, *J. Appl. Cryst.* 36 (2003) 7–13, doi:10.1107/S0021889802022112.
- [41] I. Alkorta, F. Blanco, J. Elguero, R.M. Claramunt, The azido-tetrazole and diazo-1,2,3-triazole tautomerism in six-membered heteroaromatic rings and their relationships with aromaticity: azines and perimidine, *Tetrahedron* 66 (2010) 2863–2868, doi:10.1016/j.tet.2010.02.035.
- [42] A.N. Asaad, El S.H.El Ashry, A Theoretical Study on Intramolecular Cyclization of Azidobenzotriazine to Tetrazolobenzotriazines, *Z. Naturforsch. A* 51 (1996) 1012–1018, doi:10.1515/zna-1996-0907.
- [43] S.L. Deev, T.S. Shestakova, V.N. Charushin, O.N. Chupakhin, Synthesis and azido-tetrazole tautomerism of 3-azido-1,2,4-triazines, *Chem. Heterocycl. Comp.* 53 (2017) 963–975, doi:10.1007/s10593-017-2157-y.
- [44] Z. Karczmarzyk, M. Mojzych, A. Rykowski, Synthesis and structure of a novel mesomeric betaine 6,7-dimethyl-2H-pyrazolo[4,3-*e*]tetrazolo[4,5-*b*]1,2,4-triazine, *J. Mol. Struct.* 829 (2007) 22–28, doi:10.1016/j.molstruc.2006.06.003.
- [45] S.L. Deev, Z.O. Shenkarev, T.S. Shestakova, O.N. Chupakhin, V.L. Rusinov, A.S. Arseniev, Selective ¹⁵N-labeling and analysis of ¹³C-¹⁵N J couplings as an effective tool for studying the structure and azide-tetrazole equilibrium in a series of tetrazolo[1,5-*b*]1,2,4-triazines and tetrazolo[1,5-*a*]pyrimidines, *J. Org. Chem.* 75 (2010) 8487–8497, doi:10.1021/jo1017876.
- [46] M. Mojzych, Z. Karczmarzyk, A. Rykowski, Synthesis and structure of 7-methyl-5-phenyl-1H-pyrazolo[4,3-*e*]tetrazolo[4,5-*b*]1,2,4-triazine, *J. Chem. Cryst.* 35 (2005) 151–155, doi:10.1007/s10870-005-2805-4.
- [47] A.D. Bain, Chemical exchange in NMR, *Prog. Nucl. Magn. Reson. Spectrosc.* 43 (2003) 63–103, doi:10.1016/j.pnmrs.2003.08.001.
- [48] M.K. Lakshman, M.K. Singh, D. Parrish, R. Balachandran, B.W. Day, Azide/tetrazole equilibrium of C-6 azidopyrimidines and their ligation reactions with alkynes, *J. Org. Chem.* 75 (2010) 2461–2473, doi:10.1021/jo902342z.
- [49] E. Scapin, P.R.S. Salbego, C.R. Bender, A.R. Meyer, A.B. Pagliari, T. Orlando, G.C. Zimmer, C.P. Frizzo, H.G. Bonacorso, N. Zanatta, M.A.P. Martins, Synthesis, effect of substituents on the regiochemistry and equilibrium studies of tetrazolo[1,5-*a*]pyrimidine/2-azidopyrimidines, *Beilstein J. Org. Chem.* 13 (2017) 2396–2407, doi:10.3762/bjoc.13.237.
- [50] S.N. Sirakanyan, D. Spinelli, A. Geronikaki, V.G. Kartsev, H.A. Panosyan, A.G. Ayvazyan, R.A. Tamazyan, V. Frenna, A.A. Hovakimyan, The azide/tetrazole equilibrium: an investigation in the series of furo- and thieno[2,3-*e*]tetrazolo[3,2-*d*]pyrimidine derivatives, *Tetrahedron* 72 (2016) 1919–1927, doi:10.1016/j.tet.2016.02.048.
- [51] A.Y. Denisov, V.P. Krivopalov, V.I. Mamatyuk, V.P. Mamaev, Use of ¹³C-¹H coupling constants for the investigation of azide-tetrazole tautomerism in aromatic nitrogen heterocycles. Detection of ditetrazolo [1,5-*a* : 1',5'-*c*] pyrimidine, *Magn. Res. Chem.* 26 (1988) 42–46, doi:10.1002/mrc.1260260111.
- [52] C.N.R.Rao E.Lieber, T.S. Chao, C.W.W. Hoffman, Infrared Spectra of Organic Azides, *Anal. Chem.* 29 (1957) 916–918, doi:10.1021/ac60126a016.

- [53] A. Thomann, J. Zapp, M. Hutter, M. Empting, R.W. Hartmann, Steering the azido-tetrazole equilibrium of 4-azidopyrimidines via substituent variation-implications for drug design and azide-alkyne cycloadditions, *Org. Biomol. Chem.* 13 (2015) 10620–10630, doi:[10.1039/c5ob01006c](https://doi.org/10.1039/c5ob01006c).
- [54] E.B. Nikolaenkova, N.v Aleksandrova, V.I. Mamatyuk, V.P. Krivopalov, N.N. Vorozhtsov, Synthesis and study of the azide-tetrazole tautomerism in 2-azido-4-(trifluoromethyl)-6-R-pyrimidines (R=H, 4-ClC₆H₄), *Russ. Chem. Bull., Int. Ed.* 67 (2018) 893–901, doi:[10.1007/S11172-018-2154-Z](https://doi.org/10.1007/S11172-018-2154-Z).
- [55] A. Jeminejs, I. Novosjolova, Ē. Bizdēna, M. Turks, Nucleophile–nucleofuge duality of azide and arylthiolate groups in the synthesis of quinazoline and tetrazoloquinazoline derivatives, *Org. Biomol. Chem.* 19 (2021) 7706–7723, doi:[10.1039/D1OB01315G](https://doi.org/10.1039/D1OB01315G).
- [56] P. Cmoch, H. Korczak, L. Stefaniak, G.A. Webb, ¹H, ¹³C and ¹⁵N NMR and IR studies of halogen-substituted tetrazolo[1,5-*a*]pyridines, *J. Phys. Org. Chem.* 12 (1999) 470–478, doi:[10.1002/\(SICI\)1099-1395\(199906\)12:6<470::AID-POC151>3.0.CO;2-U](https://doi.org/10.1002/(SICI)1099-1395(199906)12:6<470::AID-POC151>3.0.CO;2-U).
- [57] G.M. Sheldrick, SHELXT - Integrated space-group and crystal-structure determination, *Acta Cryst. Sect. A* 71 (2015) 3–8, doi:[10.1107/S2053273314026370](https://doi.org/10.1107/S2053273314026370).
- [58] G.M. Sheldrick, A short history of SHELX, *Acta Cryst. Sect. A* 64 (2008) 112–122, doi:[10.1107/S0108767307043930](https://doi.org/10.1107/S0108767307043930).

Leškovskis, K.; Mišņovs, A.; Novosjolova, I.; Turks, M.

S_NAr Reactions of 2,4-Diazidopyrido[3,2-*d*]pyrimidine and Azide-Tetrazole Equilibrium Studies of the Obtained 5-Substituted Tetrazolo[1,5-*a*]pyrido[2,3-*e*]pyrimidines

Molecules **2022**, *27*, 7675-7675

doi:10.3390/molecules27227675

Publikācija un tās pielikums pieejams bez maksas

[MDPI mājaslapā](#)

The Publication and Supporting Information is available free of charge on the

[MDPI website](#)

Pārpublicēts ar *MDPI AG* atļauju.



Copyright Creative Commons CC BY 4.0

Reprinted with the permission from MDPI AG.

Copyright Creative Commons CC BY 4.0

Article

SNAr Reactions of 2,4-Diazidopyrido[3,2-*d*]pyrimidine and Azide-Tetrazole Equilibrium Studies of the Obtained 5-Substituted Tetrazolo[1,5-*a*]pyrido[2,3-*e*]pyrimidines

 Kristaps Leškovskis ¹, Anatoly Mishnev ², Irina Novosjolova ^{1,*}  and Māris Turks ^{1,*} 
¹ Institute of Technology of Organic Chemistry, Faculty of Materials Science and Applied Chemistry, Riga Technical University, P. Valdena str. 3, LV-1048 Riga, Latvia

² Latvian Institute of Organic Synthesis, Aizkraukles str. 21, LV-1006 Riga, Latvia

* Correspondence: irina.novosjolova@rtu.lv (I.N.); maris.turks@rtu.lv (M.T.)

Abstract: A straightforward method for the synthesis of 5-substituted tetrazolo[1,5-*a*]pyrido[2,3-*e*]pyrimidines from 2,4-diazidopyrido[3,2-*d*]pyrimidine in SNAr reactions with *N*-, *O*-, and *S*- nucleophiles has been developed. The various *N*- and *S*-substituted products were obtained with yields from 47% to 98%, but the substitution with *O*-nucleophiles gave lower yields (20–32%). Furthermore, the fused tetrazolo[1,5-*a*]pyrimidine derivatives can be regarded as 2-azidopyrimidines and functionalized in copper(I)-catalyzed azide-alkyne dipolar cycloaddition (CuAAC) and Staudinger reactions due to the presence of a sufficient concentration of the reactive azide tautomer in solution. In total, seven products were fully characterized by their single crystal X-ray studies, while five of them were representatives of the tetrazolo[1,5-*a*]pyrido[2,3-*e*]pyrimidine heterocyclic system. Equilibrium constants and thermodynamic values were determined using variable temperature ¹H NMR and are in agreement of favoring the tetrazole tautomeric form ($\Delta G_{298} = -3.33$ to -7.52 (kJ/mol), $\Delta H = -19.92$ to -48.02 (kJ/mol) and $\Delta S = -43.74$ to -143.27 (J/mol·K)). The key starting material 2,4-diazidopyrido[3,2-*d*]pyrimidine presents a high degree of tautomerization in different solvents.

Keywords: azide; tetrazole; SNAr; triazole; CuAAC chemistry; pyrido[3,2-*d*]pyrimidine; tautomeric equilibrium; X-ray structure determination



Citation: Leškovskis, K.; Mishnev, A.; Novosjolova, I.; Turks, M. SNAr Reactions of 2,4-Diazidopyrido[3,2-*d*]pyrimidine and Azide-Tetrazole Equilibrium Studies of the Obtained 5-Substituted Tetrazolo[1,5-*a*]pyrido[2,3-*e*]pyrimidines. *Molecules* **2022**, *27*, 7675. <https://doi.org/10.3390/molecules27227675>

Academic Editors: Bagrat A. Shainyan, Gilbert Kirsch, José C. González-Gómez and Antonio Massa

Received: 18 October 2022

Accepted: 4 November 2022

Published: 8 November 2022

Publisher's Note: MDPI stays neutral with regard to jurisdictional claims in published maps and institutional affiliations.



Copyright: © 2022 by the authors. Licensee MDPI, Basel, Switzerland. This article is an open access article distributed under the terms and conditions of the Creative Commons Attribution (CC BY) license (<https://creativecommons.org/licenses/by/4.0/>).

1. Introduction

Fused-pyrimidine heterocycles are privileged scaffolds that have attracted great interest due to their biological properties [1]. The modification and refinement of such scaffolds are a promising strategy for the development of novel drugs. Among them, pyrido[3,2-*d*]pyrimidine motif as a purine and pteridine analogue is a commonly used building block in drug discovery [2–7].

From the synthesis perspective, heterocycles with an azido-azomethine structural entity are interesting due to their intrinsic dynamic azide-tetrazole tautomeric equilibrium in the solution phase (Figure 1a) [8–15] alongside rich azide functional group chemistry [16].

The azide-tetrazole equilibrium greatly varies based on the substituent electronic effects, solvent polarity, and temperature [17–20]. This phenomenon raises the opportunity to selectively substitute one position of 2,4-diazidopyrimidines (Figure 1b). Conventionally, nucleophile attack on pyrimidines takes place at a more reactive C-4 position when two identical leaving groups are present (Figure 1b, I). However, as the equilibrium shifts, (1) the addition rate of nucleophiles can be enhanced (Figure 1b, II) by the electron withdrawing effect of the tetrazole moiety, which stabilizes the Meisenheimer complex intermediate; (2) the addition site can be switched (Figure 1b, III), since tetrazole cannot be substituted and the substitution takes place at the C-2 position; and (3) addition can be completely omitted (Figure 1b, IV). Indeed, SNAr reactions in 2,4-diazidopurines V [21–23] and deazapurines VI [24,25] take place at the C-2 position (Figure 1c). However, this is not the case with

quinazoline VII [26,27] and pyrido[2,3-*d*]pyrimidine VIII [28], where a conventional C-4 addition is observed.

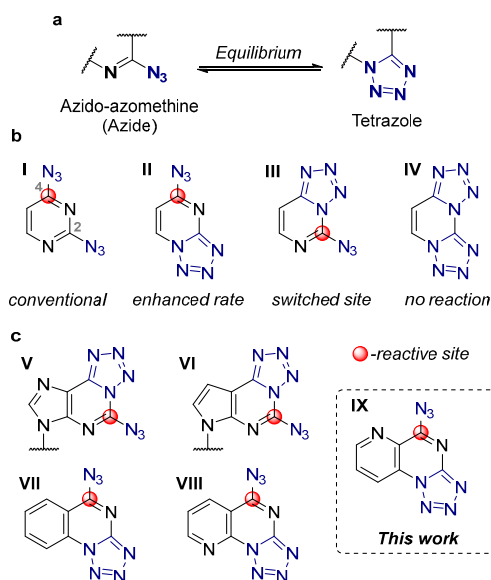


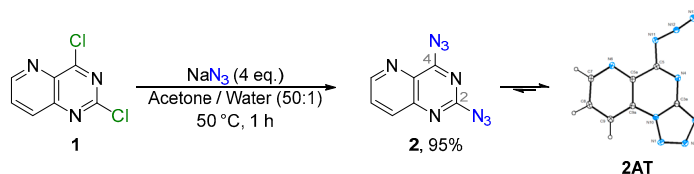
Figure 1. (a) Azide-tetrazole equilibrium; (b) reactivity of 2,4-diazidopyrimidines; (c) SNAr regioselectivity in fused 2,4-diazidopyrimidines.

To the best of our knowledge, only a handful of papers have mentioned tetrazolopyrido[2,3-*e*]pyrimidines [29–32], providing a vague idea of the azide-tetrazole tautomerism, and one paper describing the ring opening of tetrazolo[1,5-*c*]pyrido[2,3-*e*]pyrimidine with reactive C-nucleophiles [33]. Hence, in this paper, we report on the SNAr reactions of 2,4-diazidopyrido[3,2-*d*]pyrimidine IX for the first time, describe azide-tetrazole tautomerism in the obtained tetrazolo[1,5-*a*]pyrido[2,3-*e*]pyrimidines, further functionalize the remaining azide moiety, and provide insights into the azide-tetrazole tautomerism in 2,4-diazidopyrido[3,2-*d*]pyrimidine.

2. Results and Discussion

2.1. Synthesis

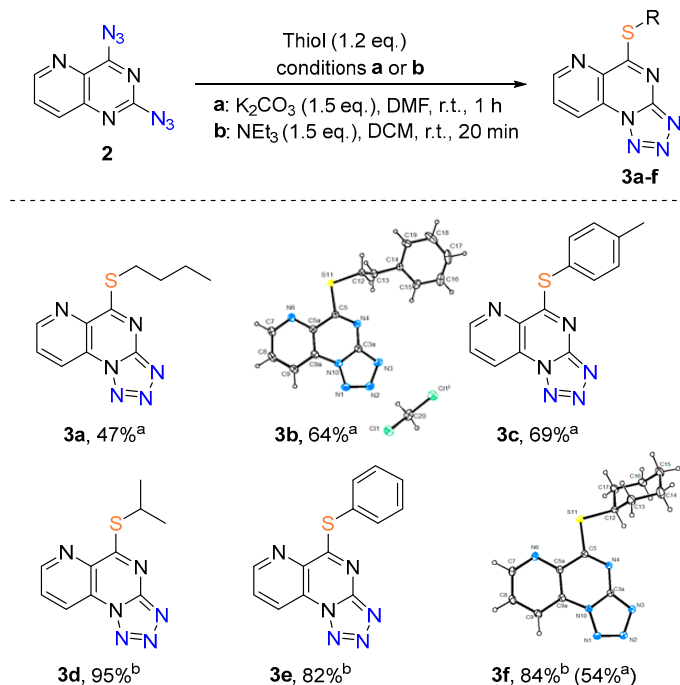
First, we acquired our key starting material, 2,4-diazidopyrido[3,2-*d*]pyrimidine **2**, in excellent yield from commercially available dichloride **1** with sodium azide (Scheme 1). Here and further, the name *diazide* and structure **2** are used as formal simplification, as it does not exist in pure diazide form, but rather as a mixture of azide-tetrazole tautomeric forms.



Scheme 1. Synthesis of 2,4-diazidopyrido[3,2-*d*]pyrimidine (**2**).

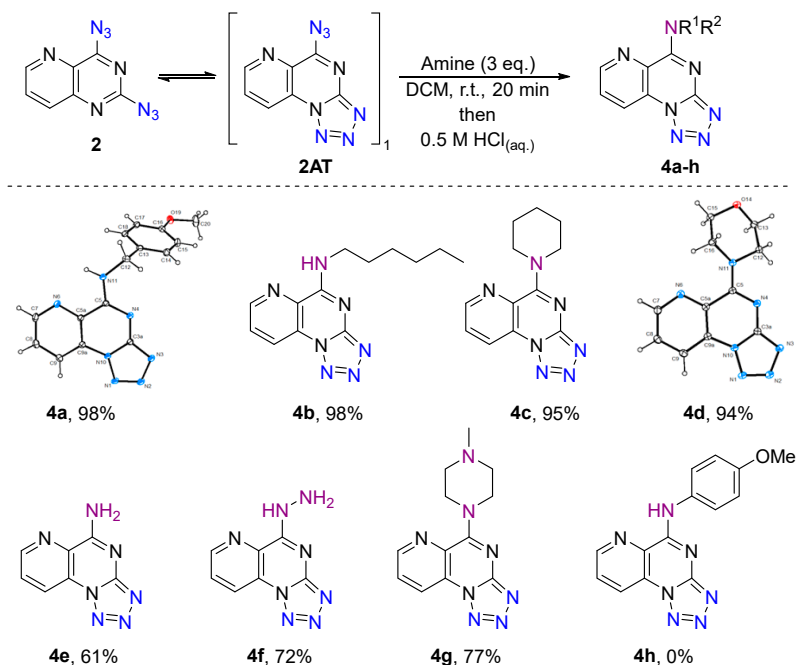
As the initial conditions for the substitution of *diazide* **2** with thiols, we chose the K_2CO_3 /DMF system (Scheme 2, conditions a). 5-Thiotetrazolo[1,5-*a*]pyrido[2,3-*e*]pyrimidines

3a–c,f were obtained in moderate yields with substitution proceeding at the expected C-4 position. These conditions were found to be most suitable in our previous work on pyrido[2,3-*d*]pyrimidines [28]. However, we discovered that the reaction could be undertaken in DCM using NEt₃ as a base (conditions **b**). In these conditions, the work-up was easier and products **3d–f** were obtained in higher yields.



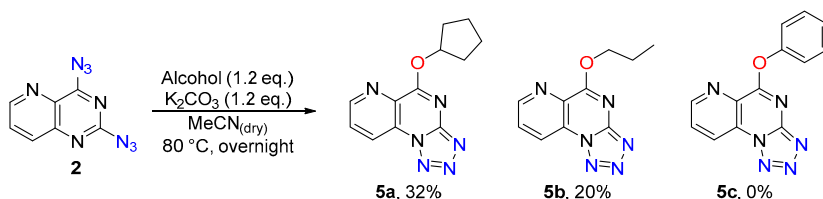
Scheme 2. SNAr reaction of *diazide 2* with thiols.

Next, we explored the SNAr reaction between *diazide 2* and the amines. As with the thiols, we adopted the previously used reaction conditions [28] and an addition of *p*-methoxybenzylamine to *diazide 2* in DMSO provided product **4a** in 49% yield without an additional base. At this point, we decided to investigate the solvent effect on tautomerization and thus manipulate the site of nucleophile attack. To do this, we carried out SNAr reactions of *diazide 2* with *p*-methoxybenzylamine in various solvents: toluene, benzene, DCM, EtOH, CHCl₃, DMSO, and MeCN. In all cases, the same product **4a** was obtained. This means that 5-azidotetrazolo[1,5-*a*]pyrimidine tautomer **2AT** is always predominant, despite the selected solvents. The highest yield with the easiest work-up procedure was obtained in DCM, and it was the solvent of choice in further research. To explore the scope of the reaction, we used optimized conditions for the synthesis of different amino derivatives **4a–g** in good yields (Scheme 3). Products bearing the benzylic **4a**, aliphatic primary **4b**, and secondary **4c**, **4d**, **4g** amine moieties were obtained. In addition, ammonia and hydrazine showed good reactivity and provided products **4h** and **4f**. However, substitution of *diazide 2* with aromatic amine (anisidine) to **4h** was unsuccessful and only the starting material was recovered after 3 days of stirring.



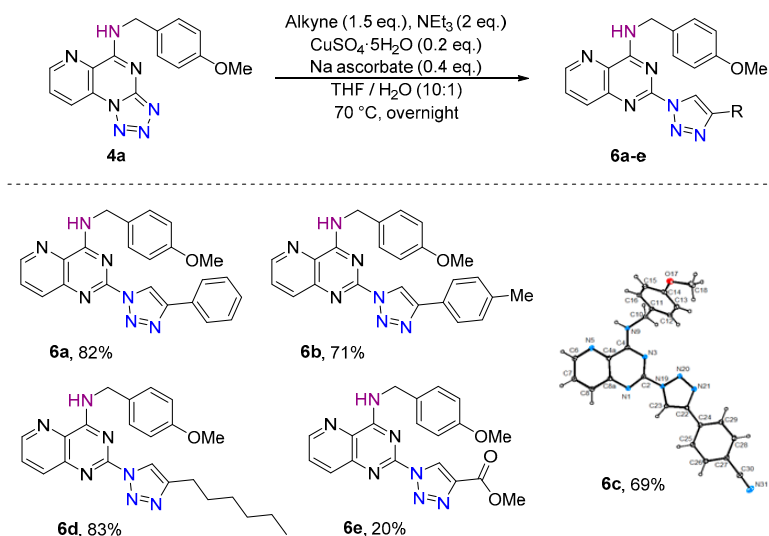
Scheme 3. SNAr reaction of *diazide 2* with amines.

Substitution of *diazide 2* with simple alcohols proceeded in the presence of a base (K_2CO_3) in dry MeCN, yielding products **5a** and **5b** (Scheme 4), although the products were obtained in low yields, mainly due to partial hydrolysis in the basic reaction medium as a side reaction. A complex mixture of unidentified products was obtained in the reaction of *diazide 2* with phenol, most probably due to further substitution reactions of the phenyloxy moiety as a leaving group.



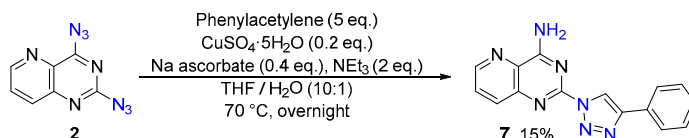
Scheme 4. SNAr reaction of *diazide 2* with alcohols.

Given that the compounds **2–5** persist in equilibrium between tetrazolo[1,5-*a*]pyrimidines and 2-azidopyrimidines, it should be possible to functionalize them as heterylazides [12,34] and tetrazoles [35]. Indeed, a series of 1,2,3-triazole-substituted pyrido[3,2-*d*]pyrimidines **6a–e** were obtained from tetrazolo[1,5-*a*]pyrido[2,3-*e*]pyrimidine **4a** in the copper(I)-catalyzed azide-alkyne cycloaddition (CuAAC) reaction (Scheme 5).



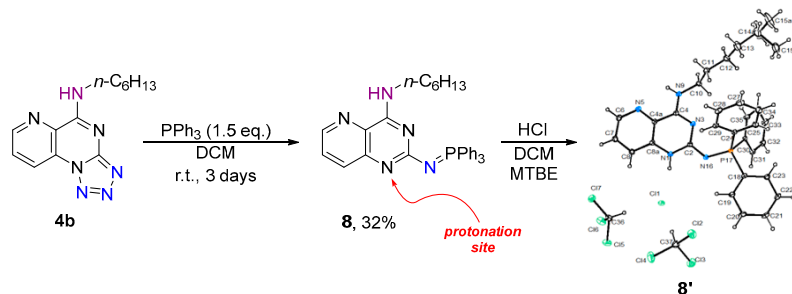
Scheme 5. Synthesis of 2-triazolylpyrido[3,2-d]pyrimidines 6a–e.

Synthesis of 2,4-bistriazole from diazide 2 was not successful due to the formation of multiple side products. The major component was found to be partially reduced 2-triazolylpyrido[3,2-d]pyrimidine 7 (Scheme 6). We [36–38] and others [39] have previously observed that azido groups can be selectively reduced to their respective amino derivatives by Cu(I), which is generated by the CuSO_4 /ascorbate system.



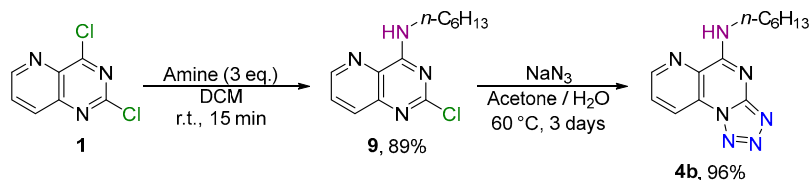
Scheme 6. Partial reduction of compound 2 during its CuAAC reaction.

Additionally, we were able to functionalize 5-aminotetrazolo[1,5-a]pyrimidine 4b in the Staudinger reaction to iminophosphorane 8 (Scheme 7). Interestingly, its NMR and single crystal X-ray analysis revealed a protonated form 8', which was obtained by the precipitation of compound 8 with anhydrous HCl in the DCM/MTBE system. The protonation occurred at the N(1) position of the molecule.



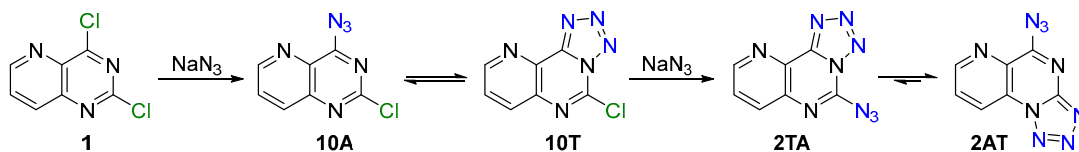
Scheme 7. Synthesis of iminophosphorane 8 and its HCl salt 8'.

To confirm that the C-4 position is the more reactive site in pyrido[3,2-*d*]pyrimidines with identical leaving groups in positions C-2 and C-4 (substrate **1**), we switched the order of nucleophile addition. Indeed, the addition of amine first to the 2,4-dichloropyrido[3,2-*d*]pyrimidine (**1**), followed by sodium azide, afforded the expected **4b** (Scheme 8). However, it should be mentioned that the addition rate of the second nucleophile—azide was rather slow. It took 3 days to achieve near complete conversion of intermediate **9**. Previously, Boyomi et al. [29] reported failed attempts of 4-amino and 4-benzyloxy substituted 2-chloropyrido[3,2-*d*]pyrimidine substitution with sodium azide in refluxed ethanol. Moreover, in our case, the amino product **9** was obtained in high yield without the formation of the diamino product. The electron-donating effect of the amino group slowed or even inhibited further S_NAr process.



Scheme 8. Conventional synthesis route for compound **4b**.

It is interesting to note that the addition of two azido groups in the synthesis of diazide **2** was relatively fast (<1 h). This suggests that the first azido group after the addition to C-4 tautomerizes to tetrazole **10T**, where tetrazole, as an electron-withdrawing group, makes the pyrimidine system more reactive toward a second nucleophilic addition, and the final 2,4-disubstituted system is formed (Scheme 9).



Scheme 9. Synthesis pathway of diazide **2**.

2.2. Single Crystal X-ray Analysis

Compounds **2**, **3b**, **3f**, **4a**, **4d**, **5a**, and the product **8** protonated form **8'** were obtained in crystalline form and their chemical structures were confirmed by single crystal X-ray analysis. Crystal data and refinement details for the studied crystals are presented in Table 1. Search of the Cambridge structure database (CSD, version 5.43, November 2021) for synthesized pyrido[2,3-*e*]tetrazolo[1,5-*a*]pyrimidine heterosystem did not reveal any hits and, thus, gave evidence that it had not been studied by single crystal X-ray diffraction yet. Below, we discuss the geometry of this new tricyclic heterosystem in detail. The pyrido[3,2-*d*]pyrimidine heterosystem search gave five hits [40–42]. Comparison of compound **6c** with structures from CSD showed that their geometry fit very well.

Table 1. Crystal data and refinement details of compounds **2**, **3b**, **3f**, **4a**, **4d**, **6a**, and **8'**.

Compound	2	3b	3f	4a	4d	6a	8'
Structural formula	C ₇ H ₃ N ₉	C ₃₁ H ₂₆ Cl ₂ N ₁₂ S ₂	C ₁₃ H ₁₄ N ₆ S	C ₁₅ H ₁₃ N ₇ O	C ₁₁ H ₁₁ N ₇ O	C ₂₄ H ₁₈ N ₈ O	C ₃₃ H ₃₅ Cl ₇ N ₅ P
Molar weight (g/mol)	213.18	701.66	286.36	307.32	257.27	434.46	780.78
Crystal system	Monoclinic	Monoclinic	Orthorhombic	Monoclinic	Triclinic	Triclinic	Triclinic
Space group	<i>P</i> 2 ₁ / <i>n</i>	<i>P</i> 2/ <i>n</i>	<i>Pbca</i>	<i>P</i> 2 ₁ / <i>c</i>	<i>P</i> -1	<i>P</i> -1	<i>P</i> -1
<i>a</i> (Å)	7.7018 (2)	9.5365 (2)	5.8380 (1)	13.9255 (3)	6.8386 (3)	8.0329 (5)	9.51807 (7)
<i>b</i> (Å)	4.9727 (1)	6.9099 (2)	15.1883 (2)	8.3800 (2)	8.7709 (5)	10.3423 (4)	12.55333 (10)
<i>c</i> (Å)	22.0045 (4)	24.5953 (4)	30.4815 (4)	13.3706 (3)	10.4546 (5)	13.5771 (4)	16.07767 (12)
α (°)	90.00	90.00	90.00	90.00	67.195 (5)	109.489 (3)	96.7786 (7)
β (°)	92.956 (2)	94.787 (2)	90.00	115.495 (3)	81.477 (4)	97.968 (3)	98.3660 (6)
γ (°)	90.00	90.00	90.00	90.00	71.424 (4)	100.796 (4)	98.8468 (6)
<i>V</i> (Å ³)	841.62 (3)	1615.08 (6)	2702.77(7)	1408.35 (6)	547.72 (5)	1019.59 (8)	1858.49 (2)
<i>Z</i>	4	2	8	4	2	2	2
<i>T</i> (K)	160(2)	150(2)	200(2)	150(2)	160(2)	150(2)	150(2)
Absorption coefficient (mm ⁻¹)	1.04	3.38	2.13	0.82	0.92	0.76	5.53
Calculated density (mg/m ³)	1.682	1.443	1.407	1.449	1.560	1.415	1.395
Data collected	7965	15480	24550	13282	9722	12025	35065
θ-range for data collection (°)	4.0–76.3	3.6–76.4	2.9–76.1	3.5–75.9	4.6–76.1	3.5–76.4	2.8–76.6
Unique reflections	1491	3180	2757	2735	2171	3983	7454
Symmetry factor (<i>R</i> _{int})	0.024	0.037	0.043	0.047	0.051	0.032	0.036
<i>R</i> _{sigma}	0.017	0.029	0.020	0.037	0.034	0.031	0.026
Final <i>R</i> ₁ factor for <i>I</i> > 2σ(<i>I</i>)	0.034	0.048	0.033	0.041	0.052	0.037	0.037
w <i>R</i> ₂ factor for all data	0.094	0.132	0.093	0.108	0.160	0.104	0.103
CCDC deposition number	2208559	2208560	2208556	2208558	2208557	2208561	2208562

In the crystal structure **2**, the tricyclic heterosystem was planar within $\pm 0.021(1)$ Å. Atoms N12 and N13 of the azide group deviated from this plane by $0.0736(9)$ Å and $0.1356(11)$ Å, respectively. Thus, the azide group is involved in a common conjugate system of the molecule, and the C5-N11 single bond, equal to $1.391(2)$ Å, was shortened when compared to a standard single C-N bond [43]. The azide group was not exactly linear and the valence angle N11-N12-N13 was $171.88(12)^\circ$.

The crystal structure **3b** was a dichloromethane solvate. Heterocyclic fragment of the molecule was strictly planar. Deviation of the S11 atom from this plane was $0.121(1)$ Å. The lone electron pairs of S11 atom were involved in the common conjugate system of the heterosystem, which resulted in shortening of the bond C5-S11 = $1.731(2)$ Å compared to a standard single C-S bond [43]. Aromatic fragments of the molecule, forming a dihedral angle of $5.15(9)^\circ$, were nearly parallel to each other.

In the crystal structure **3f**, some violation of the planarity of the heterocyclic system was observed. The dihedral angle between the tetrazolo-pyrimidine and pyridine fragments was $5.97(5)^\circ$. The C5-S11 bond ($1.745(1)$ Å) in the **3f** structure was longer than in **3b**. The least squares mean planes of tricyclic heterosystem and cyclohexane fragments formed a dihedral angle of $61.40(7)^\circ$.

In the crystal structure **4a**, the heterocyclic system was strictly planar (± 0.01 Å). Deviation of the N11 atom from this plane was $0.0358(11)$ Å and the lone electron pair of N11 atom participated in the common conjugate system of a tricycle. The dihedral angle between aromatic fragments of the molecule was $73.98(5)^\circ$. Orientation of the methoxy group was characterized by the torsion angle C20-O19-C16-C15 = $-6.8(2)^\circ$.

In the crystal structure **4d**, we again observed minor violation of the planarity of the heterocyclic system. The dihedral angle between the tetrazolo-pyrimidine and pyridine fragments was $3.39(7)^\circ$. The least squares mean planes of the heterocyclic system and morpholine fragment formed a dihedral angle of $19.71(7)^\circ$. The morpholine fragment assumed a chair conformation. Atoms N11 and O14 deviated from the plane formed by four carbon atoms by $0.6142(15)$ Å and $-0.6703(14)$ Å, respectively.

In the structure **6c**, the bicyclic heterosystem was sufficiently planar. The C4-N9 bond length was $1.3366(15)$ Å. Dihedral angles of the triazole fragment with mean planes of bicycle and adjacent phenyl ring were $4.38(6)^\circ$ and $11.16(7)^\circ$, respectively. The slope of the mean plane of the second phenyl fragment to the plane of the bicycle was $75.71(5)^\circ$. Orientation of the methoxy group was characterized by the torsion angle C18-O17-C14-C13 = $7.2(2)^\circ$.

Compound **8** was crystallized in the form of hydrochloride chloroform disolvate. In contrast to the previous structure **6a** in **8**, atom N1 became protonated and bond C2-N16 [$1.328(2)$ Å] assumed a double bond character. Least squares planes of pyridine and pyrimidine fragments in the heterosystem formed a dihedral angle of $3.87(8)^\circ$. Two atoms at the end of an aliphatic chain in the structure were disordered and assumed two positions with an occupancy ratio of 0.7:0.3.

Since the pyrido[2,3-*e*]tetrazolo[1,5-*a*]pyrimidine heterosystem has not been studied by single crystal X-ray diffraction until now, we present a comparison of the geometric parameters with the tetrazolo[1,5-*a*]pyrimidine fragment of the crystal structures deposited with CCDC. Table 2 lists the selected geometrical parameters of the studied compounds and data from the literature.

Table 2. The selected bond lengths for the studied crystal structures and data from the literature *.

	N1-N2	N1-N10	N2-N3	N3-C3a	C3a-N4	C3a-N10	N4-C5
2	1.301(1)	1.357(1)	1.357(1)	1.328(1)	1.356(1)	1.357(1)	1.304(1)
3b	1.308(3)	1.356(3)	1.364(3)	1.334(3)	1.354(3)	1.354(3)	1.308(3)
3f	1.306(2)	1.355(2)	1.358(2)	1.325(2)	1.359(2)	1.357(2)	1.308(2)
4a	1.298(2)	1.362(2)	1.359(2)	1.331(2)	1.354(2)	1.363(2)	1.324(2)
4d	1.301(2)	1.364(2)	1.348(2)	1.334(2)	1.341(2)	1.353(2)	1.329(2)
Ivajoh	1.304(2)	1.365(23)	1.350(2)	1.336(2)	1.343(2)	1.363(2)	1.324(2)
Pesvuh	1.305(2)	1.358(2)	1.347(2)	1.328(2)	1.350(2)	1.359(2)	1.303(2)
Pulsib	1.306(3)	1.369(3)	1.365(3)	1.330(3)	1.348(3)	1.368(3)	1.308(3)
Sowwik	1.307(7)	1.354(7)	1.367(8)	1.308(7)	1.369(8)	1.365(7)	1.315(8)
Uxazid	1.300(1)	1.351(1)	1.345(1)	1.326(1)	1.348(1)	1.363(1)	1.309(1)
Vendoh	1.289(4)	1.365(5)	1.343(4)	1.330(5)	1.343(4)	1.351(4)	1.316(4)

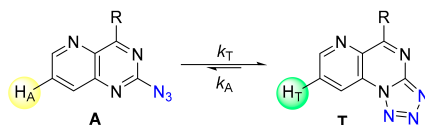
* Ivajoh [44], Pesvuh [45], Pulsib [46], Sowwik [47], Uxazid [48], Vendoh [49].

The analysis of Table 2 shows that, overall, the geometry of the tetrazolo[1,5-*a*]pyrimidine fragment in the studied compounds corresponded to the published data. The geometry of the tetrazole fragment was the most conservative and was practically the same in all structures. The most variable bonds of the heterocyclic system were C3a-N4 and N4-C5. Their length was related to the type of substituent in position 5.

2.3. Free Energy Calculation for Azide-Tetrazole Equilibrium of Substituted Tetrazolo[1,5-*a*]pyrido[2,3-*e*] Pyrimidines

The system in equilibrium can be quantitatively characterized by thermodynamic values—Gibbs free energy, enthalpy, and entropy. The Gibbs free energy describes the equilibrium at given state of conditions, while the enthalpy defines the absolute stability of the tetrazole system (a higher value means a higher stability of tetrazole).

The Gibbs–Helmholtz equation $\Delta G = -RT\ln(K_{eq})$ was used to calculate the Gibbs free energy of tautomerization [50]. ^1H NMR spectra of tetrazoles 3–5 were acquired in CDCl_3 at variable temperatures (see Supplementary Materials) to obtain equilibrium constants (K_{eq}) expressed as the integral ratio of tetrazole/azido tautomeric forms $K_{(eq)} = [\text{T}]/[\text{A}]$. Enthalpy and entropy values were obtained by plotting the Gibbs free energy equation $\Delta G = \Delta H - T\Delta S$ (see Supplementary Materials). The calculated thermodynamic values for the tautomerization of the obtained compounds are given in Table 3. Very similar results were also obtained by plotting the van't Hoff equation (see Supplementary Materials). Errors were calculated using the mean square error method.

Table 3. Equilibrium constant and thermodynamic heat of the tautomerization of substituted tetrazolo[1,5-*a*]pyrido[2,3-*e*]pyrimidines 3–5 in CDCl₃; (A) azide form, (T) tetrazole form.

Compound	R	T (K)	K _(eq) *	ΔG ₂₉₈ (kJ/mol)	ΔH ₂₉₈ (kJ/mol)	ΔS ₂₉₈ (J/mol·K)
3a		298	8.44	−5.29 ± 0.11	−32.11 ± 1.94	−90.14 ± 6.24
		313	4.32			
		323	3.11			
3b		298	6.26	−4.54 ± 0.02	−23.63 ± 0.38	−64.08 ± 1.21
		313	3.92			
		323	2.99			
3c		298	12.39	−6.24 ± 0.02	−30.53 ± 0.34	−81.69 ± 1.11
		313	6.37			
		323	4.81			
3d		298	6.53	−4.65 ± 0.03	−20.14 ± 0.61	−51.96 ± 1.95
		313	4.49			
		323	3.47			
3e		298	4.19	−3.55 ± 0.28	−31.75 ± 4.90	−94.33 ± 15.74
		313	2.57			
		323	1.53			
3f		298	15.08	−6.11 ± 0.12	−42.05 ± 2.13	−120.72 ± 6.83
		313	4.96			
		323	3.30			
4a		298	20.83	−7.52 ± 0.22	−21.91 ± 3.91	−48.05 ± 12.53
		313	15.05			
		323	10.39			
4b		298	19.20	−7.32 ± 0.03	−20.35 ± 0.56	−43.74 ± 1.78
		313	12.77			
		323	10.19			
4c		298	5.92	−4.40 ± 0.07	−24.52 ± 1.31	−67.42 ± 4.20
		313	3.81			
		323	2.74			
4d		298	3.89	−3.36 ± 0.02	−22.65 ± 0.32	−64.71 ± 1.03
		313	2.53			
		323	1.91			
4g		298	3.83	−3.33 ± 0.01	−19.92 ± 0.25	−55.69 ± 0.79
		313	2.59			
		323	2.06			
5a		298	8.59	−5.33 ± 0.17	−48.02 ± 2.95	−143.27 ± 9.49
		313	3.36			
		323	1.92			
5b		298	11.84	−6.12 ± 0.16	−31.55 ± 2.75	−85.50 ± 8.83
		313	6.00			
		323	4.45			

* Expressed as an integral an integral ratio of the tetrazole/azide tautomeric forms $K_{(eq)} = [T]/[A]$.

As previously mentioned, the azide-tetrazole equilibrium is influenced by the solvent polarity, temperature, substituent electronic effects, and sterics [8]. In our case, the equilibrium of tetrazolo[1,5-*a*]pyrido[2,3-*e*]pyrimidines 3–5 was fully shifted toward tetrazole in DMSO-*d*₆ and the azido tautomer was not observed in this solvent. On the other hand, the equilibrium in less polar CDCl₃ was notable and varied with different substituents.

As expected, the equilibrium shifted toward the azido tautomer at elevated temperatures. The calculated negative enthalpy values confirmed that the tetrazole is an energetically more stable form and the negative Gibbs free energy affirms that tetrazole in pyrido[3,2-*d*]pyrimidines 3–5 is a major tautomer present at 25 °C.

It is well-known that electron donating substituents stabilize the fused tetrazole ring, while electron withdrawing substituents favor the azido tautomer. In our case, the Gibbs free energy values of *p*-methoxybenzylamino- (4a) and hexylamino- (4b) products were the highest. Therefore, the equilibrium was strongly shifted toward the tetrazole tautomer (Figure 2). However, the Gibbs free energy values for products containing secondary amine moieties piperidine (4c), morpholine (4d), and *N*-methylpiperazine (4g) were significantly lower than those of primary amine moieties 4a and 4b. Additionally, alkoxy-substituted 5a and 5b were shifted toward the tetrazole tautomer and the Gibbs free energy values were higher than those of the thiols.

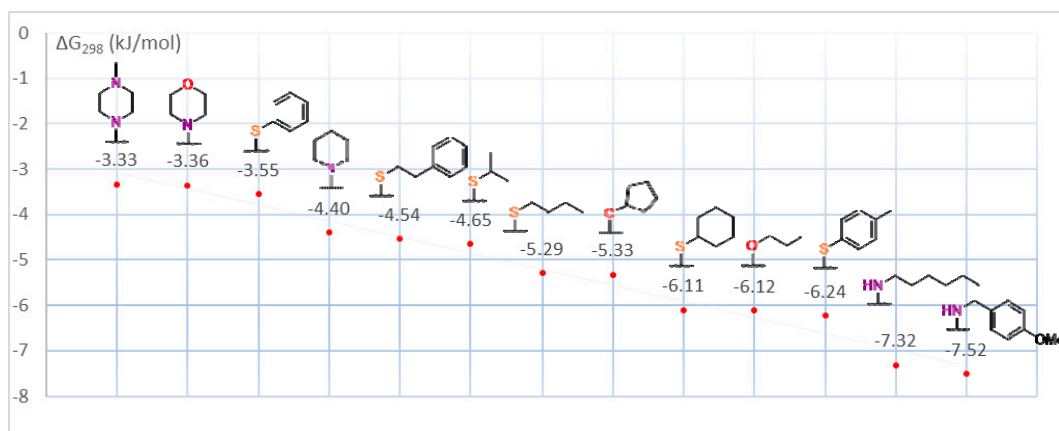


Figure 2. Composition of the Gibbs free energy of tautomerization for the substituted tetrazoles 3–5.

2.4. Tautomerism of Diazidopyrido[3,2-*d*]Pyrimidine

Finally, we looked at the tautomeric equilibrium of diazide 2. The $^1\text{H-NMR}$ spectra of diazide 2 in various solvents are shown in Figure 3. A different number of tautomeric forms were present depending on the solvent polarity. Tetrazole as the electron withdrawing moiety shifted signals downfield, while azido tautomer signals were more upfield. By going up in solvent polarity, the signals appeared more downfield and the ratio of the downfield/upfield signals increased. Thus, as in theory, the tetrazole tautomer becomes more dominant in polar solvents. At the present time, we are unable to undeniably provide the structural identity of each set of signals. For a thorough assignment of tautomeric forms, ^{15}N labeling is required.

In most cases, three to four tautomeric forms were observed. In TFA, only one tautomeric form was present and two tautomeric forms were observed in D_2SO_4 . It is most likely that these solvents shift the equilibrium to bistetrazole 2TT due to far-out polarity. However, the pyridine ring in such acidic conditions can be protonated, making the ring system extremely electron deficient and shifting the equilibrium toward diazide 2P. It is interesting to note that in $\text{AcOD-}d_4$, seven out of nine possible tautomeric forms were present. There are five possible tautomeric structures and three betaine structures for diazide 2 (Figure 4). To prove that these are indeed tautomeric forms, we acquired spectra after prolonged storage and redissolving the stored sample in a different solvent. To our delight, acquiring spectra after 7 days and 30 days of storage at 4 °C in acetic acid solution presented identical spectra to that of the freshly prepared sample (Figure 5). Furthermore,

evaporation of the acetic acid and redissolving the 30 day stored sample in CDCl_3 provided identical spectra to one obtained by dissolving *diazide 2* in CDCl_3 .

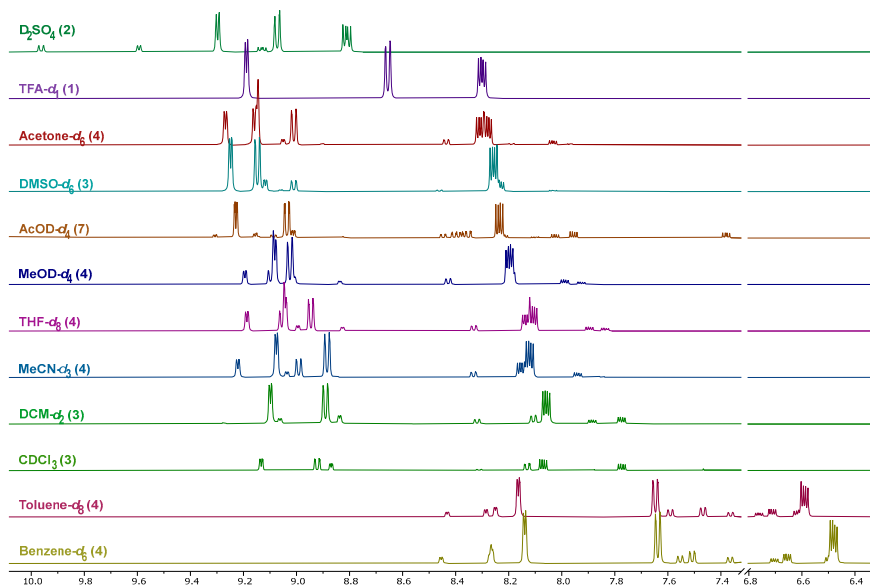
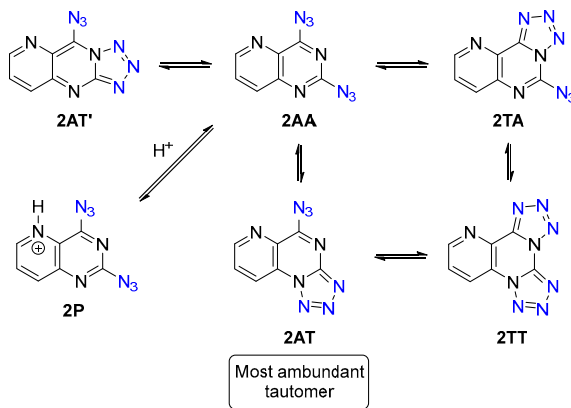


Figure 3. $^1\text{H-NMR}$ spectra of *diazide 2* in various solvents (number of the observed tautomers reported in parentheses).

Diazide 2 tautomeric structures



Theoretical *Betaine* structures of *diazide 2*

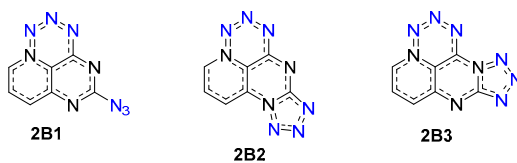


Figure 4. Tautomeric structures of *diazide 2*.

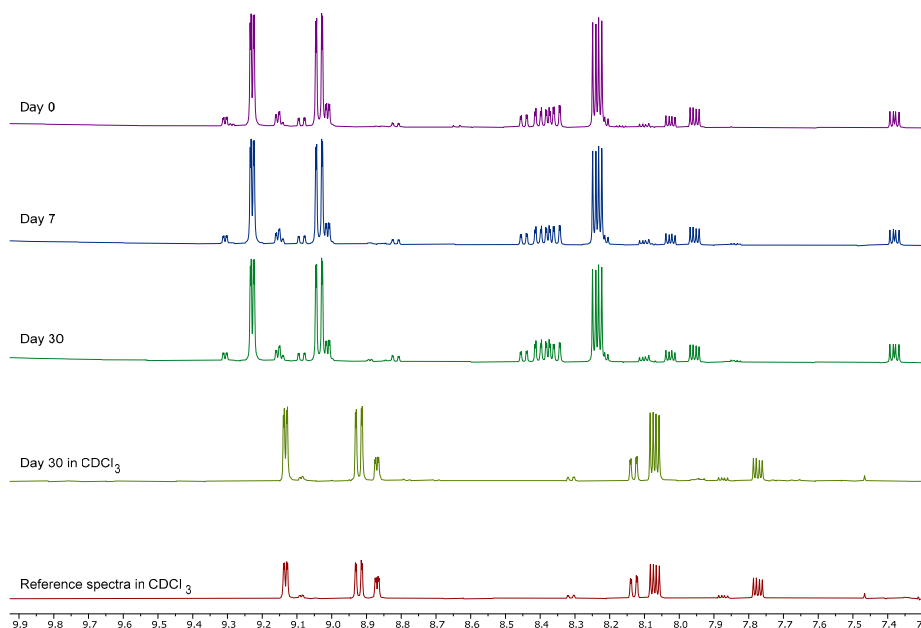


Figure 5. $^1\text{H-NMR}$ spectra of *diazide 2* in $\text{AcOD-}d_4$ and CDCl_3 .

3. Materials and Methods

3.1. General Information

Reagents purchased from Alfa Aesar, Acros Organics, Sigma Aldrich were used as received. All solvents were distilled prior to use. THF and toluene were distilled from Na under an Ar atmosphere. DMF and DMSO were distilled from CaH_2 under reduced pressure. For column chromatography, ROCC silica gel (40–60 μm , 60 Å) was used. Chromatography was monitored by TLC (E. Merck Kieselgel 60 F₂₅₄) and visualized with UV light.

HPLC analysis was performed using an Agilent Technologies 1200 Series system equipped with an X Bridge C-18 column, 4.6 \times 150 mm, particle size 3.5 μm , with a flow rate of 1 mL/min, using 0.1% TFA/ H_2O and MeCN for the mobile phase.

The IR spectra were recorded in KBr with a Perkin-Elmer Spectrum BX FTIR spectrometer (4000–450 cm^{-1}).

High-resolution mass (HRMS) (electrospray ionization (ESI)) was recorded with an Agilent 1290 Infinity series ultra-high pressure liquid chromatography connected to an Agilent 6230 time-of-flight mass spectrometer or (atmospheric pressure chemical ionization (APCI)) on a 7 T solariX XR (Bruker Daltonik GmbH) Fourier transform ion cyclotron resonance mass spectrometer equipped with an APCI source.

Single-crystal diffraction data were collected on an XtaLAB Synergy-S Dualflex diffractometer (Rigaku Corporation, Tokyo, Japan) equipped with a HyPix6000 detector and micro-focus sealed X-ray tube (Rigaku, Tokyo, Japan) using Cu K α radiation ($\lambda = 1.54184$ Å). Single crystals were fixed with oil in a nylon loop of a magnetic CryoCap and set on a goniometer head. The samples were cooled down to 150 K, and ω -scans were performed with a step size of 0.5°. Data collection and reduction were performed with CrysAlisPro 1.171.40.35a software (Oxford Diffraction Ltd., Abingdon, UK). The structure solution and refinement were performed with SHELXT [50] and SHELXL [51] software, which are part of the CrysAlisPro and Olex2 suites. The H atoms were positioned geometrically and treated as riding on their parent C or N atoms. Molecular graphics were prepared using

ORTEP3 for Windows [52] and Mercury [53]. The PLATON [54] tool was used for the geometrical calculations.

^1H and ^{13}C NMR spectra were recorded on a Bruker Avance 500 spectrometer (Bruker BioSpin GmbH, Rheinstetten, Germany). Chemical shifts (δ) were reported in ppm and coupling constants (J) in Hz. Residual solvent peaks (^1H) or (^{13}C) were used as the reference (for ^1H -NMR: CDCl_3 δ = 7.26 ppm, $\text{DMSO-}d_6$ δ = 2.50 ppm, $(\text{CD}_3)_2\text{CO}$ δ = 2.05 ppm, CD_3COOD δ = 2.04 ppm, C_6D_6 δ = 7.16 ppm, CD_2Cl_2 δ = 5.32 ppm, D_2SO_4 δ = 11.20 ppm, CD_3CN δ = 1.94 ppm, CD_3OD δ = 3.31 ppm, CF_3COOD δ = 11.50 ppm, $\text{THF-}d_8$ δ = 3.58 ppm, toluene- d_8 δ = 6.98 ppm and for ^{13}C -NMR: CDCl_3 δ = 77.16 ppm, $\text{DMSO-}d_6$ δ = 39.52 ppm). H_3PO_4 (85% aq.) δ = 0.00 ppm was used as the external standard for ^{31}P NMR. Multiplicities were reported as s (singlet), d (doublet), t (triplet), q (quartet), and m (multiplet).

3.2. Synthesis Methods and Product Characterization

General procedure A: A synthesis of 5-thiotetrazolo[1,5-*a*]pyrido[2,3-*e*]pyrimidines **3c-f**. Thiol (1.5 eq) was added to 2,4-diazidopyrido[3,2-*d*]pyrimidine (**2**) (1 eq) and triethylamine (1.2 eq) in DCM (1 mL) in a 10 mL glass vial and stirred for 15 min at ambient temperature. After the reaction completion (HPLC monitoring), the reaction mixture was filtered through a silica gel plug with 10% DCM/MeCN and evaporated under reduced pressure to yield the crude product.

General procedure B: A synthesis of 5-aminotetrazolo[1,5-*a*]pyrido[2,3-*e*]pyrimidines **4a-d**. An amine (3 eq) was added to 2,4-diazidopyrido[3,2-*d*]pyrimidine (**2**) (1 eq) in DCM (1 mL) in a 10 mL glass vial and stirred for 15 min at ambient temperature. After the reaction completion (HPLC monitoring), an additional DCM (5 mL) was added and the mixture was washed with 0.5 M $\text{HCl}_{(\text{aq})}$ solution (2×5 mL), followed by saturated $\text{NaCl}_{(\text{aq})}$ wash (2×5 mL). The organic phase was dried over anhydrous Na_2SO_4 , then filtered and evaporated to yield the product.

General procedure C: A synthesis of triazoles **6a-e**. Sodium ascorbate (0.4 eq), $\text{CuSO}_4 \cdot 5\text{H}_2\text{O}$ (0.2 eq), NEt_3 (2 eq), *N*-(4-methoxybenzyl)pyrido[2,3-*e*]tetrazolo[1,5-*a*]pyrimidin-5-amine (**4a**) (1 eq), and substituted acetylene (1.5 eq) were dissolved in THF (1 mL) and H_2O (0.1 mL) in a 10 mL glass vial and stirred at 60 °C overnight. The resulting mixture was filtered through silica gel and the Na_2SO_4 plug, evaporated under reduced pressure. Crude product was purified by column chromatography.

2,4-Diazidopyrido[3,2-*d*]pyrimidine (**2**):

2,4-Dichloropyrido[3,2-*d*]pyrimidine (**1**) (1 g, 5 mmol, 1 eq) and NaN_3 (1.6 g, 20 mmol, 4 eq) were weighed in a 50 mL round bottom flask. Acetone (10 mL) and water (1 mL) was added, and the mixture was stirred at 50 °C for 1 h. After the reaction completion (monitored by HPLC), the reaction mixture was cooled to room temperature and the solvent was evaporated under reduced pressure. Water (20 mL) was added to the mixture and extracted with dichloromethane (3×20 mL). Combined organic phases were washed with a saturated NaCl solution (2×10 mL) and dried over anhydrous Na_2SO_4 , filtered, and evaporated under reduced pressure. Product was obtained as a slightly yellow amorphous solid (1 g, 95%). The product can be recrystallized from EtOH to obtain yellowish crystals (m.p. 168 °C). A single crystal for X-ray analysis was obtained by slow evaporation from DCM/MeOH.

^1H NMR (500 MHz, CF_3COOD) δ 9.19 (dd, 1H, 3J = 4.7 Hz, 4J = 1.4 Hz, H-C(8)), 8.66 (dd, 1H, 3J = 8.8 Hz, 4J = 1.4 Hz, H-C(6)), 8.30 (dd, 1H, 3J = 8.8, 4.7 Hz, H-C(7)) ppm. ^{13}C NMR (125 MHz, CF_3COOD) δ 169.0, 160.6, 152.0, 143.2, 136.0, 135.6, 127.7 ppm.

Observed as a mixture of three tautomers in a 80:17:3 ratio in $\text{DMSO-}d_6$. First tautomer: ^1H NMR (500 MHz, $\text{DMSO-}d_6$) δ 9.25 (dd, 1H, 3J = 4.7 Hz, 4J = 1.5 Hz), 9.15 (dd, 1H, 3J = 8.6 Hz, 4J = 1.5 Hz), 8.26 (dd, 1H, 3J = 8.5, 4.5 Hz) ppm. Second tautomer: ^1H NMR (500 MHz, $\text{DMSO-}d_6$) δ 9.12 (dd, 1H, 3J = 4.5 Hz, 4J = 1.5 Hz), 9.01 (dd, 1H, 3J = 8.5 Hz, 4J = 1.5 Hz), 8.23 (dd, 1H, 3J = 8.5, 4.4 Hz) ppm. Third tautomer: ^1H NMR (500 MHz,

DMSO- d_6) δ 9.06 (dd, 1H, $^3J = 4.6$ Hz, $^4J = 1.6$ Hz), 8.46 (dd, 1H, $^3J = 8.4$ Hz, $^4J = 1.6$ Hz), 8.03 (dd, 1H, $^3J = 8.4$, 4.3 Hz) ppm.

Observed as a mixture of three tautomers in a 59:35:6 ratio in CDCl₃. First tautomer: ^1H NMR (500 MHz, CDCl₃) δ 9.13 (dd, 1H, $^3J = 4.5$ Hz, $^4J = 1.5$ Hz), 8.92 (dd, 1H, $^3J = 8.5$ Hz, $^4J = 1.5$ Hz), 8.07 (dd, 1H, $^3J = 8.5$, 4.5 Hz) ppm. Second tautomer: ^1H NMR (500 MHz, CDCl₃) δ 8.86 (dd, 1H, $^3J = 4.3$ Hz, $^4J = 1.5$ Hz), 8.12 (dd, 1H, $^3J = 8.5$ Hz, $^4J = 1.5$ Hz), 7.77 (dd, 1H, $^3J = 8.5$, 4.3 Hz) ppm. Third tautomer: ^1H NMR (500 MHz, CDCl₃) δ 9.08 (dd, 1H, $^3J = 4.4$ Hz, $^4J = 1.5$ Hz), 8.31 (dd, 1H, $^3J = 8.5$ Hz, $^4J = 1.5$ Hz), 7.87 (dd, 1H, $^3J = 8.5$, 4.4 Hz) ppm.

IR (KBr): 3074, 2377, 2225, 2164, 2144, 1598, 1539 cm⁻¹.

HRMS calculated for [C₇H₃N₉ + H⁺] = 214.0584, found 214.0584.

5-(Butylthio)pyrido[2,3-*e*]tetrazolo[1,5-*a*]pyrimidine (3a):

2,4-Diazidopyrido[3,2-*d*]pyrimidine (100 mg, 0.469 mmol, 1 eq) and K₂CO₃ (71 mg, 0.516 mmol, 1.1 eq) were added to a 10 mL round bottom flask, flushed with N₂, and capped with a septum. Through the septum, absolute DMF (1 mL) and buthanethiol (44 mg, $d = 0.84$ g/mL, $v = 52$ μ L, 0.493 mmol, 1.05 eq) were added and stirred for 1 h at room temperature. After the reaction completion (HPLC control), water (10 mL) was added and extracted with toluene (3 \times 10 mL). The combined organic phase was washed with 5% LiCl solution (2 \times 10 mL) and dried over anhydrous Na₂SO₄, filtered, and evaporated under reduced pressure to give the crude product. The crude product purification by silica gel column chromatography (DCM/MeOH, gradient 0 \rightarrow 2%) and crystallization from *n*-PrOH yielded yellow crystals (57 mg, 47%, $R_f = 0.50$ in 50% Hex/EtOAc, m.p. 136 $^{\circ}$ C).

^1H NMR (500 MHz, DMSO- d_6) δ 9.06 (dd, 1H, $^3J = 4.5$ Hz, $^4J = 1.4$ Hz, H-C(7)), 8.94 (dd, 1H, $^3J = 8.5$ Hz, $^4J = 1.4$ Hz, H-C(9)), 8.18 (dd, 1H, $^3J = 8.5$, 4.5 Hz, H-C(8)), 3.35 (t, 2H, $^3J = 7.4$ Hz, H₂-C(1')), 1.78 (quintet, 2H, $^3J = 7.4$ Hz, H₂-C(2')), 1.51 (sextet, 2H, $^3J = 7.4$ Hz, H₂-C(3')), 0.96 (t, 3H, $^3J = 7.4$ Hz, H₃-C(4')) ppm. ^{13}C NMR (125 MHz, DMSO- d_6) δ 174.3, 152.3, 150.3, 134.2, 130.1, 128.2, 124.9, 30.0, 29.0, 21.6, 13.5 ppm.

IR (KBr): 3067, 2963, 2932, 1592, 1526, 1504 cm⁻¹.

HRMS calculated for [C₁₁H₁₂N₆S + H⁺] = 261.0917, found 261.0922.

2-Azido-4-(butylthio)pyrido[3,2-*d*]pyrimidine (3aA) and 5-(butylthio)pyrido[2,3-*e*]tetrazolo[1,5-*a*]pyrimidine (3a): observed in CDCl₃ solution as a tautomer mixture in 11:89 ratio.

Azide: ^1H NMR (500 MHz, CDCl₃) δ 8.81 (dd, 1H, $^3J = 4.5$ Hz, $^4J = 1.5$ Hz, H-C(6)), 8.08 (dd, 1H, $^3J = 8.5$ Hz, $^4J = 1.5$ Hz, H-C(8)), 7.72 (dd, 1H, $^3J = 8.5$, 4.5 Hz, H-C(7)), 3.32 (t, 2H, $^3J = 7.4$ Hz, H₂-C(1')), 1.85 (quintet, 2H, $^3J = 7.4$ Hz, H₂-C(2')), 1.56 (sextet, 2H, $^3J = 7.4$ Hz, H₂-C(3')), 1.00 (t, 3H, $^3J = 7.4$ Hz, H₃-C(4')) ppm.

Tetrazole: ^1H NMR (500 MHz, CDCl₃) δ 9.06 (dd, 1H, $^3J = 4.5$ Hz, $^4J = 1.5$ Hz, H-C(7)), 8.85 (dd, 1H, $^3J = 8.5$ Hz, $^4J = 1.5$ Hz, H-C(9)), 7.99 (dd, 1H, $^3J = 8.5$, 4.5 Hz, H-C(8)), 3.46 (t, 2H, $^3J = 7.4$ Hz, H₂-C(1')), 1.85 (quintet, 2H, $^3J = 7.4$ Hz, H₂-C(2')), 1.56 (sextet, 2H, $^3J = 7.4$ Hz, H₂-C(3')), 1.00 (t, 3H, $^3J = 7.4$ Hz, H₃-C(4')) ppm.

5-(Phenethylthio)pyrido[2,3-*e*]tetrazolo[1,5-*a*]pyrimidine (3b):

2,4-Diazidopyrido[3,2-*d*]pyrimidine (100 mg, 0.469 mmol, 1 eq) and K₂CO₃ (71 mg, 0.516 mmol, 1.1 eq) were added to a 10 mL round bottom flask, flushed with N₂, and capped with a septum. Through the septum, absolute DMF (1 mL) and phenethanethiol (68 mg, $d = 1.03$ g/mL, $v = 66$ μ L, 0.493 mmol, 1.05 eq) were added and stirred for 1 h at room temperature. After the reaction completion (HPLC control), water (10 mL) was added and extracted with toluene (3 \times 10 mL). The combined organic phase was washed with 5% LiCl solution (2 \times 10 mL) and dried over anhydrous Na₂SO₄, filtered, and evaporated under reduced pressure to give the crude product. Crystallization from *n*-PrOH yielded yellow crystals (93 mg, 63%, m.p. 184 $^{\circ}$ C). A single crystal for X-ray analysis was obtained by slow evaporation from DCM/Hex.

^1H NMR (500 MHz, DMSO- d_6) δ 9.06 (dd, 1H, $^3J = 4.4$ Hz, $^4J = 1.3$ Hz, H-C(7)), 8.95 (dd, 1H, $^3J = 8.5$ Hz, $^4J = 1.3$ Hz, H-C(9)), 8.18 (dd, 1H, $^3J = 8.5$, 4.4 Hz, H-C(8)), 7.22–7.40 (m, 5H, 5 \times H-C(Ar)), 3.61 (t, 2H, $^3J = 7.5$ Hz, H₂-C(1')), 3.11 (t, 2H, $^3J = 7.5$ Hz, H₂-C(2'))

ppm. ^{13}C NMR (125 MHz, DMSO- d_6) δ 174.1, 152.3, 150.3, 139.9, 134.2, 130.2, 128.6, 128.5, 128.2, 126.5, 124.9, 33.6, 30.8 ppm.

IR (KBr): 3078, 1596, 1533, 1504 cm^{-1} .

HRMS calculated for $[\text{C}_{15}\text{H}_{12}\text{N}_6\text{S} + \text{H}^+]$ = 309.0917, found 309.0899.

2-Azido-4-(phenethylthio)pyrido[3,2-*d*]pyrimidine (**3bA**) and 5-(phenethylthio)pyrido[2,3-*e*]tetrazolo[1,5-*a*]pyrimidine (**3b**): observed in CDCl_3 solution as a tautomer mixture in 7:43 ratio.

Azide: ^1H NMR (500 MHz, CDCl_3) δ 8.81 (d, 1H, $^3J = 4.2$ Hz, H-C(6)), 8.09 (d, 1H, $^3J = 8.6$ Hz, H-C(8)), 7.72 (dd, 1H, $^3J = 8.6$, 4.2 Hz, H-C(7)), 7.22–7.37 (m, 5H, 5 \times H-C(Ar)), 3.59 (t, 2H, $^3J = 7.7$ Hz, H-C(1')), 3.12 (t, 2H, $^3J = 7.7$ Hz, H-C(2')) ppm.

Tetrazole: ^1H NMR (500 MHz, CDCl_3) δ 9.04 (d, 1H, $^3J = 4.5$ Hz, H-C(7)), 8.86 (d, 1H, $^3J = 8.5$ Hz, H-C(9)), 7.99 (dd, 1H, $^3J = 8.5$, 4.5 Hz, H-C(8)), 7.22–7.37 (m, 5H, 5 \times H-C(Ar)), 3.71 (t, 2H, $^3J = 7.6$ Hz, H-C(1')), 3.17 (t, 2H, $^3J = 7.6$ Hz, H-C(2')) ppm.

5-(*p*-Tolylthio)pyrido[2,3-*e*]tetrazolo[1,5-*a*]pyrimidine (**3c**):

Prepared according to procedure A using 2,4-diazidopyrido[3,2-*d*]pyrimidine (**2**) (50 mg, 0.235 mmol, 1 eq), *p*-thiocresol (35 mg, 0.282 mmol, 1.2 eq), and triethylamine (36 mg, $d = 0.73$ g/mL, $v = 49$ μL , 0.353 mmol, 1.5 eq). Crystallization from *n*-PrOH yielded yellow crystals (48 mg, 69%, m.p. 235 $^\circ\text{C}$).

^1H NMR (500 MHz, DMSO- d_6) δ 9.14 (dd, 1H, $^3J = 4.4$ Hz, $^4J = 1.5$ Hz, H-C(7)), 8.98 (dd, 1H, $^3J = 8.5$ Hz, $^4J = 1.5$ Hz, H-C(9)), 8.23 (dd, 1H, $^3J = 8.5$, 4.4 Hz, H-C(8)), 7.57 (d, 2H, $^3J = 8.0$ Hz, 2 \times H-C(1')), 7.41 (d, 2H, $^3J = 8.0$ Hz, 2 \times H-C(2')), 2.44 (s, 3H, H₃-C(3')) ppm. ^{13}C NMR (125 MHz, DMSO- d_6) δ 174.1, 152.3, 150.4, 140.2, 135.5, 133.7, 130.4 (2 \times C), 128.4, 125.0, 122.9, 21.0 ppm.

IR (KBr): 3082, 2919, 1592, 1540, 1504 cm^{-1} .

HRMS calculated for $[\text{C}_{14}\text{H}_{10}\text{N}_6\text{S} + \text{H}^+]$ = 295.0760, found 295.0787.

2-Azido-4-(*p*-tolylthio)pyrido[3,2-*d*]pyrimidine (**3cA**) and 5-(*p*-tolylthio)pyrido[2,3-*e*]tetrazolo[1,5-*a*]pyrimidine (**3c**): observed in CDCl_3 solution as a tautomer mixture in 1:9 ratio.

Azide: ^1H NMR (500 MHz, CDCl_3) δ 8.88 (dd, 1H, $^3J = 4.2$ Hz, $^4J = 1.5$ Hz, H-C(6)), 8.10 (dd, 1H, $^3J = 8.5$ Hz, $^4J = 1.5$ Hz, H-C(8)), 7.75 (dd, 1H, $^3J = 8.5$, 4.2 Hz, H-C(7)), 7.52 (d, 2H, $^3J = 8.0$ Hz, 2 \times H-C(1')), 7.30 (d, 2H, $^3J = 8.0$ Hz, 2 \times H-C(2')), 2.43 (s, 3H, H₃-C(3')) ppm.

Tetrazole: ^1H NMR (500 MHz, CDCl_3) δ 9.11 (dd, 1H, $^3J = 4.5$ Hz, $^4J = 1.5$ Hz, H-C(7)), 8.87 (dd, 1H, $^3J = 8.5$ Hz, $^4J = 1.5$ Hz, H-C(9)), 8.03 (dd, 1H, $^3J = 8.5$, 4.5 Hz, H-C(8)), 7.53 (d, 2H, $^3J = 8.0$ Hz, 2 \times H-C(1')), 7.33 (d, 2H, $^3J = 8.0$ Hz, 2 \times H-C(2')), 2.46 (s, 3H, H₃-C(3')) ppm.

5-(*Isopropylthio*)pyrido[2,3-*e*]tetrazolo[1,5-*a*]pyrimidine (**3d**):

Prepared according to procedure A using 2,4-diazidopyrido[3,2-*d*]pyrimidine (**2**) (50 mg, 0.235 mmol, 1 eq), isopropanethiol (22 mg, $d = 0.82$ g/mL, $v = 26$ μL , 0.282 mmol, 1.2 eq), and triethylamine (36 mg, $d = 0.73$ g/mL, $v = 49$ μL , 0.353 mmol, 1.5 eq). Yielded a yellow amorphous solid (55 mg, 95%). Crystallization from *n*-PrOH yielded yellowish crystals (m.p. 151 $^\circ\text{C}$).

^1H NMR (500 MHz, DMSO- d_6) δ 9.05 (dd, 1H, $^3J = 4.5$ Hz, $^4J = 1.4$ Hz, H-C(7)), 8.94 (dd, 1H, $^3J = 8.5$ Hz, $^4J = 1.4$ Hz, H-C(9)), 8.17 (dd, 1H, $^3J = 8.5$, 4.5 Hz, H-C(8)), 4.18 (heptet, 1H, $^3J = 6.9$ Hz, H-C(1')), 1.50 (d, 6H, $^3J = 6.9$ Hz, H-C(2')) ppm. ^{13}C NMR (125 MHz, DMSO- d_6) δ 174.0, 152.3, 150.2, 134.1, 130.1, 128.3, 124.9, 34.8, 22.2 ppm.

IR (KBr): 3063, 2968, 2952, 2926, 2865, 1598, 1527, 1505 cm^{-1} .

HRMS calculated for $[\text{C}_{10}\text{H}_{10}\text{N}_6\text{S} + \text{H}^+]$ = 247.0760, found 247.0769.

2-Azido-4-(*isopropylthio*)pyrido[3,2-*d*]pyrimidine (**3dA**) and 5-(*isopropylthio*)pyrido[2,3-*e*]tetrazolo[1,5-*a*]pyrimidine (**3d**): observed in CDCl_3 solution as a tautomer mixture in 13:87 ratio.

Azide: ^1H NMR (500 MHz, CDCl_3) δ 8.80 (dd, 1H, $^3J = 4.3$ Hz, $^4J = 1.6$ Hz, H-C(6)), 8.08 (dd, 1H, $^3J = 8.5$ Hz, $^4J = 1.6$ Hz, H-C(8)), 7.71 (dd, 1H, $^3J = 8.5$, 4.3 Hz, H-C(7)), 4.20 (heptet, 1H, $^3J = 6.9$ Hz, H-C(1')), 1.53 (d, 6H, $^3J = 6.9$ Hz, H-C(2')) ppm.

Tetrazole: ^1H NMR (500 MHz, CDCl_3) δ 9.04 (dd, 1H, $^3J = 4.6$ Hz, $^4J = 1.5$ Hz, H-C(7)), 8.85 (dd, 1H, $^3J = 8.5$ Hz, $^4J = 1.5$ Hz, H-C(9)), 7.98 (dd, 1H, $^3J = 8.5$, 4.6 Hz, H-C(8)), 4.38 (heptet, 1H, $^3J = 6.8$ Hz, H-C(1')), 1.57 (d, 6H, $^3J = 6.8$ Hz, H-C(2')) ppm.

5-(Phenylthio)pyrido[2,3-*e*]tetrazolo[1,5-*a*]pyrimidine (3e):

Prepared according to procedure A using 2,4-diazidopyrido[3,2-*d*]pyrimidine (2) (50 mg, 0.235 mmol, 1 eq), thiophenol (31 mg, 0.282 mmol, 1.2 eq) and triethylamine (36 mg, $d = 0.73$ g/mL, $v = 49$ μL , 0.353 mmol, 1.5 eq). Purification by silica gel column chromatography (DCM without gradient) yielded a yellowish amorphous solid (54 mg, 82%, Rf = 0.80 in 50% Hex/EtOAc).

^1H NMR (500 MHz, $\text{DMSO-}d_6$) δ 9.15 (dd, 1H, $^3J = 4.4$ Hz, $^4J = 1.4$ Hz, H-C(7)), 8.99 (dd, 1H, $^3J = 8.5$ Hz, $^4J = 1.4$ Hz, H-C(9)), 8.24 (dd, 1H, $^3J = 8.5$, 4.4 Hz, H-C(8)), 7.58–7.72 (m, 5H, 5 \times H-C(Ar)) ppm. ^{13}C NMR (125 MHz, $\text{DMSO-}d_6$) δ 173.8, 152.3, 150.5, 135.6, 133.7, 130.5, 130.3, 129.7, 128.4, 126.5, 125.0 ppm.

IR (KBr): 3085, 3064, 1592, 1542, 1533, 1506 cm^{-1} .

HRMS calculated for $[\text{C}_{13}\text{H}_8\text{N}_6\text{S} + \text{H}^+]$ = 281.0604, found 281.0630.

2-Azido-4-(phenylthio)pyrido[3,2-*d*]pyrimidine (3eA) and 5-(phenylthio)pyrido[2,3-*e*]tetrazolo[1,5-*a*]pyrimidine (3e): observed in CDCl_3 solution as a tautomer mixture in 19:81 ratio.

Azide: ^1H NMR (500 MHz, CDCl_3) δ 8.87 (dd, 1H, $^3J = 4.3$ Hz, $^4J = 1.6$ Hz, H-C(6)), 8.11 (dd, 1H, $^3J = 8.5$ Hz, $^4J = 1.6$ Hz, H-C(8)), 7.76 (dd, 1H, $^3J = 8.5$, 4.3 Hz, H-C(7)), 7.45–7.70 (m, 5H, 5 \times H-C(Ar)) ppm.

Tetrazole: ^1H NMR (500 MHz, CDCl_3) δ 9.12 (dd, 1H, $^3J = 4.4$ Hz, $^4J = 1.5$ Hz, H-C(7)), 8.88 (dd, 1H, $^3J = 8.5$ Hz, $^4J = 1.6$ Hz, H-C(9)), 8.04 (dd, 1H, $^3J = 8.5$, 4.4 Hz, H-C(8)), 7.45–7.70 (m, 5H, 5 \times H-C(Ar)) ppm.

5-(Cyclohexylthio)pyrido[2,3-*e*]tetrazolo[1,5-*a*]pyrimidine (3f):

Prepared according to procedure A using 2,4-diazidopyrido[3,2-*d*]pyrimidine (2) (50 mg, 0.235 mmol, 1 eq), cyclohexanethiol (33 mg, $d = 0.95$ g/mL, $v = 35$ μL , 0.282 mmol, 1.2 eq), and triethylamine (36 mg, $d = 0.73$ g/mL, $v = 49$ μL , 0.353 mmol, 1.5 eq). Yellow amorphous solid (56 mg, 84%). Crystallization from *n*-PrOH yielded yellowish crystals (m.p. 156 $^\circ\text{C}$). A single crystal for X-ray analysis was obtained by slow evaporation from DCM/Hex.

^1H NMR (500 MHz, $\text{DMSO-}d_6$) δ 9.04 (dd, 1H, $^3J = 4.5$ Hz, $^4J = 1.2$ Hz, H-C(7)), 8.93 (dd, 1H, $^3J = 8.5$ Hz, $^4J = 1.2$ Hz, H-C(9)), 8.17 (dd, 1H, $^3J = 8.5$, 4.5 Hz, H-C(8)), 4.05–4.12 (m, 1H, H-C(1')), 2.11–2.19 (m, 2H, 2 \times H-CH), 1.73–1.82 (m, 2H, 2 \times H-CH), 1.32–1.68 (m, 6H, 6 \times H-CH) ppm. ^{13}C NMR (125 MHz, $\text{DMSO-}d_6$) δ 173.7, 152.3, 150.2, 134.1, 130.2, 128.3, 124.9, 42.1, 31.8, 25.4, 25.2 ppm.

HRMS calculated for $[\text{C}_{13}\text{H}_{14}\text{N}_6\text{S} + \text{H}^+]$ = 287.1073, found 287.1074.

5-(Cyclohexylthio)pyrido[2,3-*e*]tetrazolo[1,5-*a*]pyrimidine (3f) and 2-azido-4-(cyclohexylthio)pyrido[3,2-*d*]pyrimidine (3fA): observed in CDCl_3 solution as a tautomer mixture in 2:23 ratio.

Azide: ^1H NMR (500 MHz, CDCl_3) δ 8.80 (dd, 1H, $^3J = 4.2$ Hz, $^4J = 1.5$ Hz, H-C(6)), 8.08 (dd, 1H, $^3J = 8.5$ Hz, $^4J = 1.5$ Hz, H-C(8)), 7.70 (dd, 1H, $^3J = 8.5$, 4.2 Hz, H-C(7)), 4.05–4.12 (m, 1H, H-C(1')), 1.34–2.26 (m, 10H, 5 \times $\text{H}_2\text{-C(c-Hex)}$) ppm.

Tetrazole: ^1H NMR (500 MHz, CDCl_3) δ 9.04 (dd, 1H, $^3J = 4.6$ Hz, $^4J = 1.5$ Hz, H-C(7)), 8.84 (dd, 1H, $^3J = 8.5$ Hz, $^4J = 1.5$ Hz, H-C(9)), 7.98 (dd, 1H, $^3J = 8.5$, 4.6 Hz, H-C(8)), 4.29 (tt, 1H, $^3J = 10.0$, 3.9 Hz, H-C(1')), 1.34–2.26 (m, 10H, 5 \times $\text{H}_2\text{-C(c-Hex)}$) ppm.

***N*-(4-Methoxybenzyl)pyrido[2,3-*e*]tetrazolo[1,5-*a*]pyrimidin-5-amine (4a):**

Prepared according to procedure B using 2,4-diazidopyrido[3,2-*d*]pyrimidine (2) (50 mg, 0.235 mmol, 1 eq) and *p*-methoxybenzylamine (97 mg, $d = 1.05$ g/mL, $v = 92$ μL , 0.705 mmol, 1 eq). White amorphous solid (71 mg, 98%). Further crystallization from *n*-PrOH yielded white crystals (m.p. 200 $^\circ\text{C}$). A single crystal for X-ray analysis was obtained by slow evaporation from DCM/Hex.

^1H NMR (500 MHz, $\text{DMSO-}d_6$) δ 9.58 (t, 1H, $^3J = 6.4$ Hz, H-N), 8.98 (dd, 1H, $^3J = 4.5$ Hz, $^4J = 1.4$ Hz (H-C(7)), 8.78 (dd, 1H, $^3J = 8.4$ Hz, $^4J = 1.4$ Hz, H-C(9)), 8.07 (dd, 1H, $^3J = 8.4$,

4.5 Hz, H-C(8)), 7.38 (d, 2H, $^3J = 8.6$ Hz, $2 \times$ H-C(2')), 6.88 (d, 2H, $^3J = 8.6$ Hz, $2 \times$ H-C(3')), 4.74 (d, 2H, $^3J = 6.4$ Hz, H₂-C(1')), 3.71 (s, 3H, H₃-C(4')) ppm. ^{13}C NMR (125 MHz, DMSO-*d*₆) δ 158.3, 157.0, 153.8, 149.2, 130.4, 129.3, 129.1 ($2 \times$ C), 129.0, 124.6, 113.7, 55.0, 43.2 ppm.

IR (KBr): 3235, 3080, 3004, 2930, 2832, 1615, 1538, 1517 cm^{-1} .

HRMS calculated for [C₁₅H₁₃N₇ + H⁺] = 308.1254, found 308.1224.

2-Azido-*N*-(4-methoxybenzyl)pyrido[3,2-*d*]pyrimidin-4-amine (**4aA**) and *N*-(4-methoxybenzyl)pyrido[2,3-*e*]tetrazolo[1,5-*a*]pyrimidin-5-amine (**4a**): observed in CDCl₃ solution as a tautomer mixture in 1:19 ratio.

Azide: ^1H NMR (500 MHz, CDCl₃) δ 8.54 (dd, 1H, $^3J = 4.3$ Hz, $^4J = 1.5$ Hz, H-C(6)), 7.94 (dd, 1H, $^3J = 8.4$ Hz, $^4J = 1.5$ Hz, H-C(8)), 7.77 (bs, 1H, H-N), 7.58 (dd, 1H, $^3J = 8.4$, 4.3 Hz, H-C(7)), 7.34 (d, 2H, $^3J = 8.6$ Hz, $2 \times$ H-C(2')), 6.91 (d, 2H, $^3J = 8.6$ Hz, $2 \times$ H-C(3')), 4.76 (d, 2H, $^3J = 5.8$ Hz, H₂-C(1')), 3.8 (s, 3H, H₃-C(4')) ppm.

Tetrazole: ^1H NMR (500 MHz, CDCl₃) δ 8.84 (dd, 1H, $^3J = 4.5$ Hz, $^4J = 1.4$ Hz, H-C(7)), 8.73 (dd, 1H, $^3J = 8.4$ Hz, $^4J = 1.4$ Hz, H-C(9)), 7.88 (dd, 1H, $^3J = 8.4$, 4.5 Hz, H-C(8)), 7.77 (bs, 1H, H-N), 7.39 (d, 2H, $^3J = 8.6$ Hz, $2 \times$ H-C(2')), 6.91 (d, 2H, $^3J = 8.6$ Hz, $2 \times$ H-C(3')), 4.89 (d, 2H, $^3J = 5.8$ Hz, H₂-C(1')), 3.81 (s, 3H, H₃-C(4')) ppm.

N-Hexylpyrido[2,3-*e*]tetrazolo[1,5-*a*]pyrimidin-5-amine (**4b**):

Prepared according to procedure B using 2,4-diazidopyrido[3,2-*d*]pyrimidine (**2**) (50 mg, 0.235 mmol, 1 eq) and hexylamine (71 mg, $d = 0.77$ g/mL, $v = 92$ μL , 0.705 mmol, 1 eq). White amorphous solid (64 mg, 98%). Further crystallization from *n*-PrOH yielded white crystals (m.p. 132 °C).

Alternative preparation from **9**: 2-Chloro-*N*-hexylpyrido[3,2-*d*]pyrimidin-4-amine (**9**) (50 mg, 0.189 mmol, 1 eq) and NaN₃ (25 mg, 0.378 mmol, 2 eq) were weighed in a 10 mL vial. Acetone (1 mL) and water (0.1 mL) was added, and the mixture was stirred at 60 °C for 3 days. After the reaction completion (monitored by HPLC), the reaction mixture was cooled to room temperature and the solvent was evaporated under reduced pressure. Water (10 mL) was added to the mixture and extracted with dichloromethane (3×10 mL). Combined organic phases were washed with saturated NaCl solution (2×5 mL) and dried over anhydrous Na₂SO₄, filtered, and evaporated under reduced pressure. Product was obtained as a white amorphous solid (49 mg, 96%).

^1H NMR (500 MHz, DMSO-*d*₆) δ 9.12 (t, 1H, $^3J = 6.7$ Hz, H-N), 8.96 (d, 1H, $^3J = 4.3$ Hz, H-C(7)), 8.76 (d, 1H, $^3J = 8.4$ Hz, H-C(9)), 8.05 (dd, 1H, $^3J = 8.4$, 4.3 Hz, H-C(8)), 3.59 (q, 2H, $^3J = 6.7$ Hz, H₂-C(1')), 1.69 (quintet, 2H, $^3J = 6.7$ Hz, H₂-C(2')), 1.24–1.42 (m, 6H, H₂-C(3'), H₂-C(4'), H₂-C(5')), 0.82–0.92 (m, 3H, H₃-C(6')) ppm. ^{13}C NMR (125 MHz, DMSO-*d*₆) δ 157.0, 153.9, 149.1, 129.2, 129.1, 129.0, 124.6, 40.6, 31.0, 28.1, 26.2, 22.1, 13.9 ppm.

IR (KBr): 3388, 3068, 2967, 2936, 2854, 1613, 1576, 1539, 1525 cm^{-1} .

HRMS calculated for [C₁₃H₁₇N₇ + H⁺] = 272.1624, found 272.1635.

2-Azido-*N*-hexylpyrido[3,2-*d*]pyrimidin-4-amine (**4bA**) and *N*-hexylpyrido[2,3-*e*]tetrazolo[1,5-*a*]pyrimidin-5-amine (**4b**): observed in CDCl₃ solution as a tautomer mixture in 1:19 ratio.

Azide: ^1H NMR (500 MHz, CDCl₃) δ 8.56 (d, 1H, $^3J = 4.6$ Hz, H-C(6)), 7.92 (d, 1H, $^3J = 8.5$ Hz, H-C(8)), 7.53–7.63 (m, 2H, H-N, H-C(7)), 3.61–3.67 (m, 2H, H₂-C(1')), 1.70–1.82 (m, 2H, H₂-C(2')), 1.28–1.50 (m, 6H, H₂-C(3'), H₂-C(4'), H₂-C(5')), 0.85–0.96 (m, 3H, H₃-C(6')) ppm.

Tetrazole: ^1H NMR (500 MHz, CDCl₃) δ 8.87 (d, 1H, $^3J = 4.6$ Hz, H-C(7)), 8.71 (d, 1H, $^3J = 8.4$ Hz, H-C(9)), 7.92 (dd, 1H, $^3J = 8.4$, 4.6 Hz, H-C(8)), 7.59 (bs, 1H, H-N), 3.77 (td, 2H, $^3J = 7.5$ Hz, 5.4 Hz, H₂-C(1')), 1.78 (quintet, 2H, $^3J = 7.5$ Hz, H₂-C(2')) 1.28–1.51 (m, 6H, H₂-C(3'), H₂-C(4'), H₂-C(5')), 0.90 (t, 3H, $^3J = 7.0$ Hz, H-C(6')) ppm.

5-(Piperidin-1-yl)pyrido[2,3-*e*]tetrazolo[1,5-*a*]pyrimidine (**4c**):

Prepared according to procedure B using 2,4-diazidopyrido[3,2-*d*]pyrimidine (**2**) (50 mg, 0.235 mmol, 1 eq) and piperidine (60 mg, $d = 0.86$ g/mL, $v = 70$ μL , 0.705 mmol, 1 eq).

White amorphous solid (58 mg, 95%). Further crystallization from *n*-PrOH yielded white crystals (m.p. 182 °C).

^1H NMR (500 MHz, DMSO- d_6) δ 8.98 (dd, 1H, $^3J = 4.4$ Hz, $^4J = 1.6$ Hz, H-C(7)), 8.79 (dd, 1H, $^3J = 8.5$ Hz, $^4J = 1.6$ Hz, H-C(9)), 8.03 (dd, 1H, $^3J = 8.5$, 4.4 Hz, H-C(8)), 4.10–4.60 (m, 4H, 4 \times H-CH), 1.65–1.75 (m, 6H, 6 \times H-CH) ppm. ^{13}C NMR (125 MHz, DMSO- d_6) δ 157.2, 152.8, 147.9, 130.9, 130.6, 128.3, 124.7, 49.2, 26.0, 24.1 ppm.

IR (KBr): 3049, 2938, 2849, 1605, 1587, 1538 cm^{-1} .

HRMS calculated for $[\text{C}_{12}\text{H}_{13}\text{N}_7 + \text{H}^+] = 256.1305$, found 256.1314.

2-Azido-4-(piperidin-1-yl)pyrido[3,2-*d*]pyrimidine (**4cA**) and 5-(piperidin-1-yl)pyrido[2,3-*e*]tetrazolo[1,5-*a*]pyrimidine (**4c**): observed in CDCl_3 solution as a tautomer mixture in 7:43 ratio.

Azide: ^1H NMR (500 MHz, CDCl_3) δ 8.58 (dd, 1H, $^3J = 4.1$ Hz, $^4J = 1.6$ Hz, H-C(6)), 7.92 (dd, 1H, $^3J = 8.5$ Hz, $^4J = 1.6$ Hz, H-C(8)), 7.51 (dd, 1H, $^3J = 8.5$, 4.1 Hz, H-C(7)), 4.20–4.80 (m, 4H, 4 \times H-CH) 1.74–1.83 (m, 6H, 6 \times H-CH) ppm.

Tetrazole: ^1H NMR (500 MHz, CDCl_3) δ 8.91 (dd, 1H, $^3J = 4.4$ Hz, $^4J = 1.5$ Hz, H-C(7)), 8.75 (dd, 1H, $^3J = 8.4$ Hz, $^4J = 1.5$ Hz, H-C(9)), 7.82 (dd, 1H, $^3J = 8.4$, 4.4 Hz, H-C(8)), 4.20–4.80 (m, 4H, 4 \times H-CH) 1.74–1.83 (m, 6H, 6 \times H-CH) ppm.

4-(Pyrido[2,3-*e*]tetrazolo[1,5-*a*]pyrimidin-5-yl)morpholine (**4d**):

Prepared according to procedure B using diazide **2** (50 mg, 0.235 mmol, 1 eq) and morpholine (61 mg, $d = 1.01$ g/mL, $v = 61$ μL , 0.705 mmol, 1 eq). White amorphous solid (57 mg, 94%). Further crystallization from *n*-PrOH yielded white crystals (m.p. 215 °C). A single crystal for X-ray analysis was obtained by slow evaporation from DCM/Hex.

^1H NMR (500 MHz, DMSO- d_6) δ 8.98 (dd, 1H, $^3J = 4.4$ Hz, $^4J = 1.4$ Hz, H-C(7)), 8.83 (dd, 1H, $^3J = 8.5$ Hz, $^4J = 1.4$ Hz, H-C(9)), 8.06 (dd, 1H, $^3J = 8.5$, 4.4 Hz, H-C(8)), 4.18–4.63 (m, 4H, 4 \times H-C(1')), 3.78–3.84 (m, 4H, 4 \times H-C(2')) ppm. ^{13}C NMR (125 MHz, DMSO- d_6) δ 157.4, 152.6, 148.0, 130.9, 130.6, 128.5, 124.8, 66.2, 48.6 ppm.

IR (KBr): 3045, 3007, 2904, 2858, 1604, 1589, 1550, 1523 cm^{-1} .

HRMS calculated for $[\text{C}_{11}\text{H}_{11}\text{N}_7\text{O} + \text{H}^+] = 258.1098$, found 258.1099.

4-(2-Azidopyrido[3,2-*d*]pyrimidin-4-yl)morpholine (**4dA**) and 4-(pyrido[2,3-*e*]tetrazolo[1,5-*a*]pyrimidin-5-yl)morpholine (**4d**): observed in CDCl_3 solution as a tautomer mixture in 1:4 ratio.

Azide: ^1H NMR (500 MHz, CDCl_3) δ 8.59 (dd, 1H, $^3J = 4.1$ Hz, $^4J = 1.6$ Hz, H-C(7)), 7.96 (dd, 1H, $^3J = 8.5$ Hz, $^4J = 1.6$ Hz, H-C(9)), 7.55 (dd, 1H, $^3J = 8.5$, 4.1 Hz, H-C(8)), 4.34–4.81 (m, 4H, 4 \times H-C(1')), 3.86–3.93 (m, 4H, 4 \times H-C(2')) ppm.

Tetrazole: ^1H NMR (500 MHz, CDCl_3) δ 8.91 (dd, 1H, $^3J = 4.4$ Hz, $^4J = 1.5$ Hz, H-C(7)), 8.79 (dd, 1H, $^3J = 8.5$ Hz, $^4J = 1.5$ Hz, H-C(9)), 7.88 (dd, 1H, $^3J = 8.5$, 4.4 Hz, H-C(8)), 4.34–4.81 (m, 4H, 4 \times H-C(1')), 3.86–3.93 (m, 4H, 4 \times H-C(2')) ppm.

Pyrido[2,3-*e*]tetrazolo[1,5-*a*]pyrimidin-5-amine (**4e**):

Methanolic ammonia (100 μL , $w = 25\%$) was added to a solution of 2,4-diazidopyrido[3,2-*d*]pyrimidine (**2**) (50 mg, 0.235 mmol, 1 eq) dissolved in DCM (1 mL) in a 10 mL glass vial and reaction mixture was stirred overnight. After the reaction completion (HPLC monitoring), crude mixture was evaporated under reduced pressure and crystallized from pyridine to yield brown crystals (27 mg, 61%, m.p. 270 °C).

^1H NMR (500 MHz, DMSO- d_6) δ 8.98 (d, 1H, $^3J = 4.5$ Hz, H-C(7)), 8.77 (d, 1H, $^3J = 8.4$ Hz, H-C(9)), 8.62 (bs, 1H, H-N), 8.47 (bs, 1H, H-N), 8.07 (dd, 1H, $^3J = 8.4$, 4.5 Hz, H-C(8)) ppm. ^{13}C NMR (125 MHz, DMSO- d_6) δ 159.8, 153.7, 149.3, 129.5, 129.2, 128.8, 124.4 ppm.

IR (KBr): 3368, 3303, 3168, 3074, 2480, 1665, 1596, 1545, 1509 cm^{-1} .

HRMS calculated for $[\text{C}_7\text{H}_5\text{N}_7 + \text{H}^+] = 188.0679$, found 188.0684.

5-Hydrazinylpyrido[2,3-*e*]tetrazolo[1,5-*a*]pyrimidine (**4f**):

Hydrazine hydrate (50 mg, 1g/mL, 50 μL , 1.560 mmol, 6.6 eq) was added to a solution of 2,4-diazidopyrido[3,2-*d*]pyrimidine (**2**) (50 mg, 0.235 mmol, 1 eq) dissolved in DCM (1 mL) in a 10 mL glass vial and stirred for 15 min at ambient temperature. After the

reaction completion (HPLC monitoring), the crude mixture was washed with distilled water and MTBE to yield an orange amorphous solid (27 mg, 61%).

^1H NMR (500 MHz, DMSO- d_6) δ 10.49 (bs, 1H, H-N), 8.91 (d, 1H, $^3J = 4.6$ Hz, H-C(7)), 8.71 (d, 1H, $^3J = 8.5$ Hz, H-C(9)), 8.01 (dd, 1H, $^3J = 8.5$, 4.6 Hz, H-C(8)), 5.13 (bs, 2H, H₂-N) ppm. ^{13}C NMR (125 MHz, DMSO- d_6) δ 154.5, 154.0, 149.1, 129.0, 128.8, 128.7, 124.4 ppm.

IR (KBr): 3324, 3234, 3059, 1615, 1596, 1573, 1538, 1517 cm^{-1} .

HRMS calculated for $[\text{C}_7\text{H}_6\text{N}_8 + \text{H}^+] = 203.0788$, found 203.0806.

5-(4-Methylpiperazin-1-yl)pyrido[2,3-*e*]tetrazolo[1,5-*a*]pyrimidine (**4g**):

N-Methylpiperazine (70 mg, 0.90 g/mL, 78 μL , 0.705 mmol, 3 eq) was added to a solution of 2,4-diazidopyrido[3,2-*d*]pyrimidine (**2**) (50 mg, 0.235 mmol, 1 eq) dissolved in DCM (1 mL) in a 10 mL glass vial and stirred for 15 min at ambient temperature. After the reaction completion (HPLC monitoring), the crude mixture was evaporated under reduced pressure and purified by silica gel column chromatography (DCM/MeOH, gradient 0 \rightarrow 2 \rightarrow 5%) to yield pale red crystals (48 mg, 77%, $R_f = 0.15$ in DCM/MeOH 5%, m.p. 185 $^\circ\text{C}$).

^1H NMR (500 MHz, DMSO- d_6) δ 8.98 (dd, 1H, $^3J = 4.4$ Hz, $^4J = 1.5$ Hz, H-C(7)), 8.81 (dd, 1H, $^3J = 8.5$ Hz, $^4J = 1.5$ Hz, H-C(9)), 8.05 (dd, 1H, $^3J = 8.5$, 4.4 Hz, H-C(8)), 4.05–4.75 (m, 4H, 2 \times H₂-C(1')), 2.51–2.56 (m, 4H, 2 \times H₂-C(2')), 2.24 (s, 3H, H₃-C(3')) ppm. ^{13}C NMR (125 MHz, DMSO- d_6) δ 157.4, 152.7, 148.0, 130.8, 130.6, 128.5, 124.8, 54.7, 47.8, 45.5 ppm.

IR (KBr): 3077, 3047, 3012, 2913, 2856, 2804, 2774, 1607, 1591, 1542, 1527 cm^{-1} .

HRMS calculated for $[\text{C}_{12}\text{H}_{14}\text{N}_8 + \text{H}^+] = 271.1414$, found 271.1436.

2-Azido-4-(4-methylpiperazin-1-yl)pyrido[3,2-*d*]pyrimidine (**4gA**) and 5-(4-methylpiperazin-1-yl)pyrido[2,3-*e*]tetrazolo[1,5-*a*]pyrimidine (**4g**): observed in CDCl_3 solution as a tautomer mixture in a 21:79 ratio.

Azide: ^1H NMR (500 MHz, CDCl_3) δ 8.59 (dd, 1H, $^3J = 4.1$ Hz, $^4J = 1.7$ Hz, H-C(6)), 7.94 (dd, 1H, $^3J = 8.5$ Hz, $^4J = 1.7$ Hz, H-C(8)), 7.54 (dd, 1H, $^3J = 8.5$, 4.1 Hz, H-C(7)), 4.15–4.95 (m, 4H, 2 \times H₂-C(1')), 2.57–2.61 (m, 4H, 2 \times H₂-C(2')), 2.36 (s, 3H, H₃-C(3')) ppm.

Tetrazole: ^1H NMR (500 MHz, CDCl_3) δ 8.92 (dd, 1H, $^3J = 4.4$ Hz, $^4J = 1.6$ Hz, H-C(7)), 8.78 (dd, 1H, $^3J = 8.4$ Hz, $^4J = 1.6$ Hz, H-C(9)), 7.85 (dd, 1H, $^3J = 8.4$, 4.4 Hz, H-C(8)), 4.15–4.95 (m, 4H, 2 \times H₂-C(1')), 2.61–2.65 (m, 4H, 2 \times H₂-C(2')), 2.37 (s, 3H, H₃-C(3')) ppm.

5-(Cyclopentylloxy)pyrido[2,3-*e*]tetrazolo[1,5-*a*]pyrimidine (**5a**):

Cyclopentanol (24 mg, 0.28 mmol, 1.2 eq) was added to 2,4-diazidopyrido[3,2-*d*]pyrimidine (**2**) (50 mg, 0.23 mmol, 1 eq) and K_2CO_3 (39 mg, 0.28 mmol, 1.2 eq) solution in MeCN (1 mL) under a N_2 atmosphere and the resulting reaction mixture was stirred at 80 $^\circ\text{C}$ for 3 days. Water (10 mL) was added to the reaction mixture and extracted with DCM (3 \times 5 mL). The combined organic phase was washed with saturated aqueous NaCl solution (2 \times 10 mL), dried over anhydrous Na_2SO_4 , filtered, and evaporated under reduced pressure. The crude product was purified by silica gel column chromatography (DCM/MeOH, gradient 0 \rightarrow 1%) to yield a white amorphous solid (19 mg, 32%, $R_f = 0.50$ in 5% DCM/MeOH).

^1H NMR (500 MHz, DMSO- d_6) δ 9.09 (dd, 1H, $^3J = 4.5$ Hz, $^4J = 1.5$ Hz, H-C(7)), 8.91 (dd, 1H, $^3J = 8.5$ Hz, $^4J = 1.5$ Hz, H-C(9)), 8.14 (dd, 1H, $^3J = 8.5$, 4.5 Hz, H-C(8)), 5.78 (tt, 1H, $^3J = 6.1$, 3.0 Hz, H-C(1')), 2.08–2.17 (m, 2H, 2 \times H-CH), 1.94–2.02 (m, 2H, 2 \times H-CH), 1.76–1.85 (m, 2H, 2 \times H-CH), 1.65–1.74 (m, 2H, 2 \times H-CH) ppm. ^{13}C NMR (125 MHz, DMSO- d_6) δ 163.5, 152.3, 150.5, 130.9, 129.7, 129.6, 124.4, 81.7, 32.2, 23.6 ppm.

IR (KBr): 3065, 3041, 2975, 2945, 2874, 1605, 1542 cm^{-1} .

HRMS calculated for $[\text{C}_{12}\text{H}_{12}\text{N}_6\text{O} + \text{H}^+] = 257.1145$, found 257.1167.

2-Azido-4-(cyclopentylloxy)pyrido[3,2-*d*]pyrimidine (**5aA**) and 5-(cyclopentylloxy)pyrido[2,3-*e*]tetrazolo[1,5-*a*]pyrimidine (**5a**): observed in CDCl_3 solution as a tautomer mixture in 7:93 ratio.

Azide: ^1H NMR (500 MHz, CDCl_3) δ 8.87 (dd, 1H, $^3J = 4.1$ Hz, $^4J = 1.5$ Hz, H-C(6)), 8.08 (dd, 1H, $^3J = 8.5$ Hz, $^4J = 1.5$ Hz, H-C(8)), 7.69 (dd, 1H, $^3J = 8.5$, 4.1 Hz, H-C(7)), 5.76 (tt, 1H, $^3J = 6.6$, 3.6 Hz, H-C(1')), 2.19–2.28 (m, 2H, 2 \times H-CH), 2.04–2.13 (m, 2H, 2 \times H-CH), 1.88–1.98 (m, 2H, 2 \times H-CH), 1.68–1.77 (m, 2H, 2 \times H-CH) ppm.

Tetrazole: ^1H NMR (500 MHz, CDCl_3) δ 9.13 (dd, 1H, $^3J = 4.6$ Hz, $^4J = 1.5$ Hz, H-C(7)), 8.85 (dd, 1H, $^3J = 8.4$ Hz, $^4J = 1.5$ Hz, H-C(9)), 7.97 (dd, 1H, $^3J = 8.4$, 4.6 Hz, H-C(8)), 5.95 (tt, 1H, $^3J = 6.5$, 3.6 Hz, H-C(1')), 2.19–2.28 (m, 2H, 2 \times H-CH), 2.04–2.13 (m, 2H, 2 \times H-CH), 1.88–1.98 (m, 2H, 2 \times H-CH), 1.68–1.77 (m, 2H, 2 \times H-CH) ppm.

5-Propoxyppyridol[2,3-*e*]tetrazolol[1,5-*a*]pyrimidine (5b):

n-Propanol (17 mg, 0.28 mmol, 1.2 eq) was added to 2,4-diazidopyrido[3,2-*d*]pyrimidine (2) (50 mg, 0.23 mmol, 1 eq) and K_2CO_3 (39 mg, 0.28 mmol, 1.2 eq) solution in MeCN (1 mL) under a N_2 atmosphere and the resulting reaction mixture was stirred at 80 °C for 3 days. Water (10 mL) was added to the reaction mixture and extracted with DCM (3 \times 5 mL). The combined organic phase was washed with a saturated aqueous NaCl solution (2 \times 10 mL), dried over anhydrous Na_2SO_4 , filtered, and evaporated under reduced pressure. The crude product was purified by silica gel column chromatography (DCM/MeOH, gradient 0–1%) to yield a white amorphous solid (11 mg, 20%, $R_f = 0.65$ in 5% DCM/MeOH).

^1H NMR (500 MHz, $\text{DMSO-}d_6$) δ 9.09 (dd, 1H, $^3J = 4.5$ Hz, $^4J = 1.5$ Hz, H-C(7)), 8.91 (dd, 1H, $^3J = 8.5$ Hz, $^4J = 1.5$ Hz, H-C(9)), 8.15 (dd, 1H, $^3J = 8.5$, 4.5 Hz, H-C(8)), 4.63 (t, 2H, $^3J = 6.7$ Hz, H-C(1')), 1.93 (qt, 2H, $^3J = 7.4$, 6.7 Hz, H-C(2')), 1.07 (t, 3H, $^3J = 7.4$ Hz, H-C(3')) ppm. ^{13}C NMR (125 MHz, $\text{DMSO-}d_6$) δ 164.0, 152.3, 150.6, 131.0, 129.7, 129.5, 124.4, 70.3, 21.4, 10.4 ppm.

IR (KBr): 3062, 2974, 2942, 2884, 1607, 1543 cm^{-1} .

HRMS calculated for $[\text{C}_{10}\text{H}_{10}\text{N}_6\text{O} + \text{H}^+]$ = 231.0989, found 231.0991.

2-Azido-4-propoxyppyridol[3,2-*d*]pyrimidine (5bA) and 5-propoxyppyridol[2,3-*e*]tetrazolol[1,5-*a*]pyrimidine (5b): observed in CDCl_3 solution as a tautomer mixture in a 2:23 ratio.

Azide: ^1H NMR (500 MHz, CDCl_3) δ 8.87 (dd, 1H, $^3J = 4.2$ Hz, $^4J = 1.5$ Hz, H-C(6)), 8.08 (dd, 1H, $^3J = 8.6$ Hz, $^4J = 1.5$ Hz, H-C(8)), 7.70 (dd, 1H, $^3J = 8.6$, 4.2 Hz, H-C(7)), 4.63 (t, 2H, $^3J = 7.0$ Hz, H-C(1')), 2.01 (sextet, 2H, $^3J = 7.2$ Hz, H-C(2')), 1.08 (t, 3H, $^3J = 7.5$ Hz, H-C(3')) ppm.

Tetrazole: ^1H NMR (500 MHz, CDCl_3) δ 9.13 (dd, 1H, $^3J = 4.5$ Hz, $^4J = 1.5$ Hz, H-C(7)), 8.86 (dd, 1H, $^3J = 8.5$ Hz, $^4J = 1.5$ Hz, H-C(9)), 8.00 (dd, 1H, $^3J = 8.5$, 4.5 Hz, H-C(8)), 4.80 (t, 2H, $^3J = 7.0$ Hz, H-C(1')), 2.06 (sextet, 2H, $^3J = 7.2$ Hz, H-C(2')), 1.11 (t, 3H, $^3J = 7.2$ Hz, H-C(3')) ppm.

***N*-(4-Methoxybenzyl)-2-(4-phenyl-1H-1,2,3-triazol-1-yl)pyrido[3,2-*d*]pyrimidin-4-amine (6a):**

Prepared according to procedure C using *N*-(4-methoxybenzyl)pyrido[2,3-*e*]tetrazolol[1,5-*a*]pyrimidin-5-amine (4a) (42 mg, 0.137 mmol, 1 eq), phenylacetylene (21 mg, $d = 0.93$ g/mL, $v = 23$ μL , 0.205 mmol, 1.5 eq), $\text{CuSO}_4 \cdot 5\text{H}_2\text{O}$ (7 mg, 0.027 mmol, 0.2 eq), sodium ascorbate (11 mg, 0.055 mmol, 0.4 eq), and triethylamine (28 mg, $d = 0.73$ g/mL, $v = 38$ μL , 0.273 mmol, 2 eq). Purified by silica gel column chromatography (DCM/MeOH, gradient 0–1%) to yield white amorphous solid (46 mg, 82%, $R_f = 0.55$ in 5% DCM/MeOH).

^1H NMR (500 MHz, $\text{DMSO-}d_6$) δ 9.64 (t, 1H, $^3J = 6.4$ Hz, H-N), 9.36 (s, 1H, H-C(1'')), 8.84 (dd, 1H, $^3J = 4.3$ Hz, $^4J = 1.5$ Hz, H-C(6)), 8.22 (dd, 1H, $^3J = 8.5$ Hz, $^4J = 1.5$ Hz, H-C(8)), 8.07 (d, 2H, $^3J = 7.7$ Hz, 2 \times H-C(2'')), 7.90 (dd, 1H, $^3J = 8.5$, 4.3 Hz, H-C(7)), 7.51 (t, 2H, $^3J = 7.7$ Hz, 2 \times H-C(3'')), 7.49 (d, 2H, $^3J = 8.7$ Hz, 2 \times H-C(2')), 7.40 (t, 1H, $^3J = 7.7$ Hz, H-C(4'')), 6.88 (d, 2H, $^3J = 8.7$ Hz, 2 \times H-C(3')), 4.85 (d, 2H, $^3J = 6.4$ Hz, $\text{H}_2\text{-C}(1')$), 3.69 (s, 3H, $\text{H}_3\text{-CO}$) ppm. ^{13}C NMR (125 MHz, $\text{DMSO-}d_6$) δ 160.6, 158.4, 150.8, 148.6, 146.5, 144.8, 135.4, 131.2, 130.8, 130.1, 129.5, 129.1, 129.0, 128.3, 125.6, 120.0, 113.7, 55.0, 43.3 ppm.

^1H NMR (500 MHz, CDCl_3) δ 8.84 (s, 1H, H-C(1'')), 8.69 (dd, 1H, $^3J = 4.2$ Hz, $^4J = 1.4$ Hz, H-C(6)), 8.27 (dd, 1H, $^3J = 8.5$ Hz, $^4J = 1.4$ Hz, H-C(8)), 7.99 (d, 2H, $^3J = 7.8$ Hz, 2 \times H-C(2'')), 7.72 (dd, 1H, $^3J = 8.5$, 4.2 Hz, H-C(7)), 7.72 (s, 1H, H-N), 7.47 (t, 2H, $^3J = 7.8$ Hz, 2 \times H-C(3'')), 7.42 (d, 2H, $^3J = 8.7$ Hz, 2 \times H-C(2')), 7.38 (t, 1H, $^3J = 7.8$ Hz, H-C(4'')), 6.93 (d, 2H, $^3J = 8.7$ Hz, 2 \times H-C(3')), 4.91 (d, 2H, $^3J = 5.8$ Hz, $\text{H}_2\text{-C}(1')$), 3.81 (s, 3H, $\text{H}_3\text{-CO}$) ppm. ^{13}C NMR (125 MHz, CDCl_3) δ 161.1, 159.6, 151.4, 148.5, 147.7, 145.3, 136.2, 131.5, 130.5, 129.7, 129.3, 129.0, 128.7, 128.5, 126.2, 119.0, 114.5, 55.5, 45.0 ppm.

IR (KBr): 2930, 1609, 1593, 1513 cm^{-1} .

HRMS calculated for $[\text{C}_{23}\text{H}_{19}\text{N}_7\text{O} + \text{H}^+]$ = 410.1724, found 410.1730.

N-(4-Methoxybenzyl)-2-(4-(*p*-tolyl)-1*H*-1,2,3-triazol-1-yl)pyrido[3,2-*d*]pyrimidin-4-amine (**6b**):

Prepared according to procedure C using *N*-(4-methoxybenzyl)pyrido[2,3-*e*]tetrazolo[1,5-*a*]pyrimidin-5-amine (**4a**) (71 mg, 0.231 mmol, 1 eq), tolylacetylene (40 mg, *d* = 0.92 g/mL, *v* = 44 μ L, 0.347 mmol, 1.5 eq), CuSO₄·5H₂O (12 mg, 0.046 mmol, 0.2 eq), sodium ascorbate (18 mg, 0.092 mmol, 0.4 eq), and triethylamine (47 mg, *d* = 0.73 g/mL, *v* = 64 μ L, 0.462 mmol, 2 eq). Purified by silica gel column chromatography (DCM/MeOH, gradient 0→1%) to yield a white amorphous solid (70 mg, 71%, *R*_f = 0.60 in 5% DCM/MeOH).

¹H NMR (500 MHz, DMSO-*d*₆) δ 9.63 (t, 1H, ³*J* = 6.3 Hz, H-N), 9.29 (s, 1H, H-C(1'')), 8.84 (dd, 1H, ³*J* = 4.3 Hz, ⁴*J* = 1.5 Hz, H-C(6)), 8.22 (dd, 1H, ³*J* = 8.4 Hz, ⁴*J* = 1.5 Hz, H-C(8)), 7.95 (d, 2H, ³*J* = 8.1 Hz, 2 \times H-C(2'')), 7.90 (dd, 1H, ³*J* = 8.4, 4.3 Hz, H-C(7)), 7.49 (d, 2H, ³*J* = 8.7 Hz, 2 \times H-C(2')), 7.31 (d, 2H, ³*J* = 8.1 Hz, 2 \times H-C(3'')), 6.88 (d, 2H, ³*J* = 8.7 Hz, 2 \times H-C(3')), 4.84 (d, 2H, ³*J* = 6.3 Hz, H₂-C(1')), 3.69 (s, 3H, H₃-CO), 2.36 (s, 3H, H₃-C(4'')) ppm. ¹³C NMR (125 MHz, DMSO-*d*₆) δ 160.6, 158.4, 150.8, 148.6, 146.5, 144.8, 137.7, 135.3, 131.2, 130.8, 129.5 (2 \times C), 129.1, 127.3, 125.5, 119.5, 113.7, 55.0, 43.3, 20.9 ppm.

¹H NMR (500 MHz, CDCl₃) δ 8.80 (s, 1H, H-C(1'')), 8.68 (dd, 1H, ³*J* = 4.3 Hz, ⁴*J* = 1.5 Hz, H-C(6)), 8.26 (dd, 1H, ³*J* = 8.4 Hz, ⁴*J* = 1.5 Hz, H-C(8)), 7.87 (d, 2H, ³*J* = 8.0 Hz, 2 \times H-C(2'')), 7.71 (dd, 1H, ³*J* = 8.4, 4.3 Hz, H-C(7)), 7.71 (s, 1H, H-N), 7.41 (d, 2H, ³*J* = 8.7 Hz, 2 \times H-C(2')), 7.28 (d, 2H, ³*J* = 8.0 Hz, 2 \times H-C(3'')), 6.92 (d, 2H, ³*J* = 8.7 Hz, 2 \times H-C(3')), 4.91 (d, 2H, ³*J* = 5.8 Hz, H₂-C(1')), 3.81 (s, 3H, H₃-CO), 2.41 (s, 3H, H₃-C(4'')) ppm. ¹³C NMR (125 MHz, CDCl₃) δ 161.1, 159.6, 151.4, 148.4, 147.8, 145.3, 138.4, 136.2, 131.5, 129.7 (2 \times C), 129.4, 128.7, 127.6, 126.1, 118.6, 114.5, 55.5, 44.9, 21.5 ppm.

IR (KBr): 3163, 3058, 2921, 2834, 1609, 1594, 1563, 1511 cm⁻¹.

HRMS calculated for [C₂₄H₂₁N₇O + H⁺] = 424.1880, found 424.1897.

4-(1-(4-(4-Methoxybenzyl)amino)pyrido[3,2-*d*]pyrimidin-2-yl)-1*H*-1,2,3-triazol-4-yl)benzonitrile (**6c**):

Prepared according to procedure C using *N*-(4-methoxybenzyl)pyrido[2,3-*e*]tetrazolo[1,5-*a*]pyrimidin-5-amine (**4a**) (50 mg, 0.162 mmol, 1 eq), *p*-cyanophenylacetylene (31 mg, 0.243 mmol, 1.5 eq), CuSO₄·5H₂O (8 mg, 0.032 mmol, 0.2 eq), sodium ascorbate (13 mg, 0.065 mmol, 0.4 eq), and triethylamine (33 mg, *d* = 0.73 g/mL, *v* = 45 μ L, 0.324 mmol, 2 eq). Purified by silica gel column chromatography (DCM/MeOH, gradient 0→1%) to yield a white amorphous solid (49 mg, 69%, *R*_f = 0.70 in 5% DCM/MeOH). A single crystal for X-ray analysis was obtained by slow evaporation from CHCl₃/MeOH.

¹H NMR (500 MHz, DMSO-*d*₆) δ 9.67 (t, 1H, ³*J* = 6.3 Hz, H-N), 9.61 (s, 1H, H-C(1'')), 8.85 (dd, 1H, ³*J* = 4.3 Hz, ⁴*J* = 1.5 Hz, H-C(6)), 8.28 (d, 2H, ³*J* = 8.2 Hz, 2 \times H-C(2'')), 8.23 (dd, 1H, ³*J* = 8.5 Hz, ⁴*J* = 1.5 Hz, H-C(8)), 7.98 (d, 2H, ³*J* = 8.2 Hz, 2 \times H-C(3'')), 7.91 (dd, 1H, ³*J* = 8.5, 4.3 Hz, H-C(7)), 7.49 (d, 2H, ³*J* = 8.7 Hz, 2 \times H-C(2')), 6.88 (d, 2H, ³*J* = 8.7 Hz, 2 \times H-C(3')), 4.86 (d, 2H, ³*J* = 6.3 Hz, H₂-C(1')), 3.69 (s, 3H, H₃-CO) ppm. ¹³C NMR (125 MHz, DMSO-*d*₆) δ 160.6, 158.4, 150.6, 148.8, 144.9, 144.7, 135.4, 134.6, 133.0, 131.3, 130.7, 129.6, 129.1, 126.2, 121.8, 118.8, 113.7, 110.6, 55.0, 43.3 ppm.

¹H NMR (500 MHz, CDCl₃) δ 8.93 (s, 1H, H-C(1'')), 8.71 (dd, 1H, ³*J* = 4.3 Hz, ⁴*J* = 1.5 Hz, H-C(6)), 8.26 (dd, 1H, ³*J* = 8.5 Hz, ⁴*J* = 1.5 Hz, H-C(8)), 8.10 (d, 2H, ³*J* = 8.4 Hz, 2 \times H-C(2'')), 7.76 (d, 2H, ³*J* = 8.4 Hz, 2 \times H-C(3'')), 7.75 (t, 1H, ³*J* = 5.8 Hz, H-N), 7.73 (dd, 1H, ³*J* = 8.5, 4.3 Hz, H-C(7)), 7.41 (d, 2H, ³*J* = 8.7 Hz, 2 \times H-C(2')), 6.93 (d, 2H, ³*J* = 8.7 Hz, 2 \times H-C(3')), 4.91 (d, 2H, ³*J* = 5.8 Hz, H₂-C(1')), 3.82 (s, 3H, H₃-CO) ppm. ¹³C NMR (125 MHz, CDCl₃) δ 161.1, 159.6, 151.2, 148.7, 145.9, 145.2, 136.2, 134.9, 132.9, 131.5, 129.6, 129.1, 128.8, 126.6, 120.2, 118.9, 114.5, 111.9, 55.5, 45.0 ppm.

IR (KBr): 3414, 2223, 1610, 1586, 1556, 1510 cm⁻¹.

HRMS calculated for [C₂₄H₁₈N₈O + H⁺] = 435.1676, found 435.1694.

2-(4-Hexyl-1*H*-1,2,3-triazol-1-yl)-*N*-(4-methoxybenzyl)pyrido[3,2-*d*]pyrimidin-4-amine (**6d**):

Prepared according to procedure C using *N*-(4-methoxybenzyl)pyrido[2,3-*e*]tetrazolo[1,5-*a*]pyrimidin-5-amine (**4a**) (71 mg, 0.231 mmol, 1 eq), 1-octyne (38 mg, *d* = 0.72 g/mL, *v* = 53 μ L, 0.347 mmol, 1.5 eq), CuSO₄·5H₂O (12 mg, 0.046 mmol, 0.2 eq), sodium ascorbate (18 mg, 0.092 mmol, 0.4 eq), and triethylamine (47 mg, *d* = 0.73 g/mL, *v* = 64 μ L, 0.462 mmol,

2 eq). Purified by silica gel column chromatography (DCM/MeOH, gradient 0→1%) to yield aa white amorphous solid (80 mg, 83%, $R_f = 0.55$ in 5% DCM/MeOH).

^1H NMR (500 MHz, DMSO- d_6) δ 9.61 (t, 1H, $^3J = 6.3$ Hz, H-N), 8.82 (dd, 1H, $^3J = 4.3$ Hz, $^4J = 1.5$ Hz, H-C(6)), 8.60 (s, 1H, H-C(1'')), 8.18 (dd, 1H, $^3J = 8.4$, $^4J = 1.5$ Hz, H-C(8)), 7.88 (dd, 1H, $^3J = 8.4$, 4.3 Hz, H-C(7)), 7.45 (d, 2H, $^3J = 8.7$ Hz, 2 \times H-C(2'')), 6.86 (d, 2H, $^3J = 8.7$ Hz, 2 \times H-C(3')), 4.77 (d, 2H, $^3J = 6.3$ Hz, H₂-C(1')), 3.70 (s, 3H, H₃-CO), 2.73 (t, 2H, $^3J = 7.4$ Hz, H-C(2'')), 1.68 (quintet, 2H, $^3J = 7.4$ Hz), 1.25–1.40 (m, 6H, H₂-C(4''), H₂-C(5''), H₂-C(6'')), 0.87 (t, 3H, $^3J = 7.0$ Hz, H-C(7'')) ppm. ^{13}C NMR (125 MHz, DMSO- d_6) δ 160.6, 158.4, 150.8, 148.5, 147.4, 144.8, 135.3, 131.1, 130.7, 129.4, 129.0, 120.7, 113.7, 55.0, 43.3, 31.0, 28.7, 28.2, 24.8, 22.0, 13.9 ppm.

^1H NMR (500 MHz, CDCl₃) δ 8.67 (dd, 1H, $^3J = 4.3$ Hz, $^4J = 1.5$ Hz, H-C(6)), 8.36 (s, 1H, H-C(1'')), 8.25 (dd, 1H, $^3J = 8.5$ Hz, $^4J = 1.5$ Hz, H-C(8)), 7.69 (dd, 1H, $^3J = 8.5$, 4.3 Hz, H-C(7)), 7.67 (t, 1H, $^3J = 5.8$ Hz, H-N), 7.39 (d, 2H, $^3J = 8.7$ Hz, 2 \times H-C(2'')), 6.92 (d, 2H, $^3J = 8.7$ Hz, 2 \times H-C(3')), 4.88 (d, 2H, $^3J = 5.8$ Hz, H₂-C(1')), 3.81 (s, 3H, H₃-CO), 2.83 (t, 2H, $^3J = 7.6$ Hz, H-C(2'')), 1.76 (quintet, 2H, $^3J = 7.6$ Hz, H-C(3'')), 1.30–1.45 (m, 6H, H₂-C(4''), H₂-C(5''), H₂-C(6'')), 0.89 (t, 3H, $^3J = 7.0$ Hz, H-C(7'')) ppm. ^{13}C NMR (125 MHz, CDCl₃) δ 161.0, 159.5, 151.5, 148.6, 148.3, 145.3, 136.2, 131.4, 129.6, 129.4, 128.6, 120.2, 114.5, 55.5, 44.9, 31.8, 29.5, 29.1, 25.9, 22.7, 14.2 ppm.

IR (KBr): 3431, 3351, 3057, 2928, 2856, 1651, 1609, 1591, 1568, 1557, 1511 cm^{-1} .

HRMS calculated for [C₂₃H₂₇N₇O + H⁺] = 418.2350, found 418.2362.

Methyl 1-(4-(4-methoxybenzyl)amino)pyrido[3,2-d]pyrimidin-2-yl)-1H-1,2,3-triazole-4-carboxylate (6e):

Prepared according to procedure C using *N*-(4-methoxybenzyl)pyrido[2,3-*e*]tetrazolo[1,5-*a*]pyrimidin-5-amine (4a) (52 mg, 0.169 mmol, 1 eq), methylpropionate (21 mg, $d = 0.95$ g/mL, $v = 23$ μL , 0.254 mmol, 1.5 eq), CuSO₄·5H₂O (8 mg, 0.034 mmol, 0.2 eq), sodium ascorbate (13 mg, 0.068 mmol, 0.4 eq), and triethylamine (34 mg, $d = 0.73$ g/mL, $v = 47$ μL , 0.338 mmol, 2 eq). Purified by silica gel column chromatography (DCM/MeOH, gradient 0→1%) and crystallization from *n*-PrOH to yield white crystals (13 mg, 20%, $R_f = 0.50$ in 5% DCM/MeOH, m.p. 154 °C).

^1H NMR (500 MHz, CDCl₃) δ 9.17 (s, 1H, H-C(1'')), 8.71 (dd, 1H, $^3J = 4.3$ Hz, $^4J = 1.5$ Hz, H-C(6)), 8.28 (dd, 1H, $^3J = 8.5$ Hz, $^4J = 1.5$ Hz, H-C(8)), 7.76 (t, 1H, $^3J = 5.8$ Hz, H-N), 7.73 (dd, 1H, $^3J = 8.5$, 4.3 Hz, H-C(7)), 7.38 (d, 2H, $^3J = 8.6$ Hz, 2 \times H-C(2'')), 6.92 (d, 2H, $^3J = 8.6$ Hz, 2 \times H-C(3')), 4.88 (d, 2H, $^3J = 5.8$ Hz, H₂-C(1')), 4.02 (s, 3H, H₃-C(2'')), 3.81 (s, 3H, H₃-C(4')) ppm. ^{13}C NMR (125 MHz, CDCl₃) δ 161.3, 161.1, 159.6, 150.9, 148.9, 145.1, 139.9, 136.3, 131.6, 129.6, 129.0, 128.9, 127.4, 114.5, 55.5, 52.5, 45.0 ppm.

IR (KBr): 3326, 3179, 3056, 2949, 1736, 1608, 1592, 1573, 1558, 1513 cm^{-1} .

HRMS calculated for [C₁₉H₁₇N₇O₃ + H⁺] = 392.1466, found 392.1472.

2-(4-Phenyl-1H-1,2,3-triazol-1-yl)pyrido[3,2-d]pyrimidin-4-amine (7):

2,4-Diazidopyrido[3,2-*d*]pyrimidine (50 mg, 0.235 mmol, 1 eq), phenylacetylene (120 mg, 1.175 mmol, 5 eq), sodium ascorbate (19 mg, 0.094 mmol, 0.4 eq), CuSO₄·5H₂O (12 mg, 0.047 mmol, 0.2 eq), and NEt₃ (47 mg, $d = 0.73$ g/mL, 65 μL , 0.469 mmol, 2 eq) were dissolved in THF (1 mL), H₂O (0.1 mL) in a 10 mL glass vial and stirred at 70 °C overnight. After the reaction completion (HPLC monitoring), the resulting mixture was filtered through the silica gel/Na₂SO₄ plug and evaporated under reduced pressure. The crude product was purified by silica gel column chromatography (DCM/MeOH, gradient 0→5→10%) to yield a white amorphous solid (10 mg, 15%, $R_f = 0.20$ in 5% DCM/MeOH).

^1H NMR (500 MHz, DMSO- d_6) δ 9.24 (s, 1H, H-C(1'')), 8.85 (dd, 1H, $^3J = 4.3$ Hz, $^4J = 1.5$ Hz, H-C(7)), 8.71 (s, 1H, H-N), 8.60 (s, 1H, H-N), 8.21 (dd, 1H, $^3J = 8.5$ Hz, $^4J = 1.5$ Hz, H-C(9)), 8.04 (d, 2H, $^3J = 7.7$ Hz, 2 \times H-C(2'')), 7.91 (dd, 1H, $^3J = 8.5$, 1.5 Hz, H-C(8)), 7.50 (t, 2H, $^3J = 7.7$ Hz, 2 \times H-C(3')), 7.39 (t, 1H, $^3J = 7.7$ Hz, H-C(4')) ppm. ^{13}C NMR (125 MHz, DMSO- d_6) δ 163.7, 151.2, 148.7, 146.4, 145.1, 135.2, 130.9, 130.0, 129.3, 129.0, 128.3, 125.6, 119.7 ppm.

IR (KBr): 3461, 3282, 3164, 1647, 1578, 1556, 1513 cm^{-1} .

HRMS calculated for [C₁₅H₁₁N₇ + H⁺] = 290.1149, found 290.1177.

N-Hexyl-2-((triphenylphosphorylidene)amino)pyrido[3,2-*d*]pyrimidin-4-amine (8):

Triphenylphosphine (116 mg, 0.442 mmol, 1.5 eq) and *N*-hexylpyrido[2,3-*e*]tetrazolo[1,5-*a*]pyrimidin-5-amine (4b) (80 mg, 0.295 mmol, 1 eq) were dissolved in DCM (1 mL) and stirred for 3 days at room temperature. The reaction mixture was evaporated under reduced pressure and the crude product was purified by silica gel column chromatography (DCM/MeOH, gradient 0→1→2%) and precipitation from DCM/MTBE as a white amorphous solid (48 mg, 32%, $R_f = 0.20$ in 5% DCM/MeOH). A crystalline sample of the product was obtained for its HCl salt, ((4-(hexylamino)pyrido[3,2-*d*]pyrimidin-2-(1*H*)-ylidene)amino)triphenylphosphonium chloride (8'), which was obtained by precipitation from HCl containing the DCM/MTBE system. A single crystal for X-ray analysis was obtained by slow evaporation from CHCl_3 .

^1H NMR (500 MHz, $\text{DMSO-}d_6$) δ 12.60 (s, 1H, H-N), 9.39 (t, 1H, $^3J = 6.2$ Hz, H-N), 8.57 (dd, 1H, $^3J = 4.3$ Hz, $^4J = 1.5$ Hz, H-C(6)), 7.85 (dd, 1H, $^3J = 8.6$ Hz, $^4J = 1.5$ Hz, H-C(8)), 7.82 (ddd, 6H, $^3J_{\text{H-P}} = 12.6$ Hz, $^3J = 7.6$ Hz, $^4J = 1.4$ Hz, $6 \times \text{H-C}(1'')$), 7.80 (dd, 1H, $^3J = 8.6$, 4.3 Hz, H-C(7)), 7.74 (tdt, 3H, $^3J = 7.6$ Hz, $^5J_{\text{H-P}} = 1.7$ Hz, $^4J = 1.4$ Hz, $3 \times \text{H-C}(3'')$), 7.64 (td, 6H, $^3J = 7.6$ Hz, $^4J_{\text{H-P}} = 3.4$ Hz, $6 \times \text{H-C}(2'')$), 2.81 (td, 2H, $^3J = 7.5$, 6.2 Hz, $\text{H}_2\text{-C}(1')$), 0.86–1.19 (m, 8H, $\text{H}_2\text{-C}(2')$, $\text{H}_2\text{-C}(3')$, $\text{H}_2\text{-C}(4')$, $\text{H}_2\text{-C}(5')$), 0.82 (t, 3H, $^3J = 7.4$ Hz, H-C(6')) ppm.

^1H NMR (500 MHz, CDCl_3) δ 14.08 (s, 1H, H-N), 8.89 (dd, 1H, $^3J = 8.5$ Hz, $^4J = 1.4$ Hz, H-C(6)), 8.36 (dd, 1H, $^3J = 4.4$ Hz, $^4J = 1.4$ Hz, H-C(8)), 7.80–7.86 (m, 6H, $6 \times \text{H-C}(1'')$), 7.57–7.63 (m, 3H, $3 \times \text{H-C}(3'')$), 7.53 (dd, 1H, $^3J = 8.5$, 4.4 Hz, H-C(7)), 7.48–7.54 (m, 6H, $6 \times \text{H-C}(2'')$), 7.37 (t, 1H, $^3J = 6.1$ Hz, H-N), 2.93 (td, 2H, $^3J = 7.2$, 6.1 Hz, $\text{H}_2\text{-C}(1')$), 1.11–1.37 (m, 8H, $\text{H}_2\text{-C}(2')$, $\text{H}_2\text{-C}(3')$, $\text{H}_2\text{-C}(4')$, $\text{H}_2\text{-C}(5')$), 0.89 (t, 3H, $^3J = 7.2$ Hz, H-C(6')) ppm. ^{13}C NMR (125 MHz, CDCl_3) δ 159.2, 156.9, 145.3, 137.8 (d, $^2J_{\text{C-P}} = 4.4$ Hz), 133.3 (d, $^3J_{\text{C-P}} = 10.3$ Hz), 132.9 (d, $^4J_{\text{C-P}} = 2.8$ Hz), 129.1, 129.1 (d, $^2J_{\text{C-P}} = 12.8$ Hz), 127.3, 127.2 (d, $^1J_{\text{C-P}} = 103.3$ Hz), 126.3, 41.0, 31.5, 29.0, 26.7, 22.7, 14.2 ppm. ^{31}P NMR (202 MHz, CDCl_3) δ 19.6 ppm.

IR (KBr): 3255, 3048, 2952, 2927, 2855, 2694, 1624, 1609, 1586, 1547, 1516 cm^{-1} .

HRMS calculated for $[\text{C}_{31}\text{H}_{32}\text{N}_5\text{P} + \text{H}^+]$ = 506.2468, found 506.2468.

2-Chloro-*N*-hexylpyrido[3,2-*d*]pyrimidin-4-amine (9):

n-Hexylamine (75 mg, 97 μL , 0.75 mmol, 3 eq) was added to 2,4-dichloropyrido[3,2-*d*]pyrimidine (1) (50 mg, 0.25 mmol, 1 eq) solution in DCM (1 mL) and stirred for 15 min. After the reaction completion (HPLC monitoring), an additional DCM (5 mL) was added and the mixture was washed with 0.5 M $\text{HCl}_{(\text{aq})}$ solution (2×5 mL), followed by a saturated $\text{NaCl}_{(\text{aq})}$ wash (2×5 mL). The organic phase was dried over anhydrous Na_2SO_4 , filtered, and evaporated under reduced pressure. The crude product was purified by silica gel column chromatography (DCM/MeOH, gradient 0→1%) to yield a colorless oil (59 mg, 89%, $R_f = 0.70$ in 5% DCM/MeOH).

^1H NMR (500 MHz, CDCl_3) δ 8.66 (d, 1H, $^3J = 4.5$ Hz, H-C(6)), 8.01 (d, 1H, $^3J = 8.4$ Hz, H-C(8)), 7.64 (dd, 1H, $^3J = 8.4$, 4.5 Hz, H-C(7)), 7.33 (bs, 1H, H-N), 3.66 (q, 2H, $^3J = 6.8$ Hz, $\text{H}_2\text{-C}(1')$), 1.69–1.77 (m, 2H, $\text{H}_2\text{-C}(2')$), 1.45 (m, 2H, $\text{H}_2\text{-C}(3')$), 1.29–1.39 (m, 4H, $\text{H}_2\text{-C}(4')$, $\text{H}_2\text{-C}(5')$), 0.90 (t, 3H, $^3J = 6.8$ Hz, $\text{H}_3\text{-C}(6')$) ppm. ^{13}C NMR (125 MHz, CDCl_3) δ 161.0, 158.7, 148.3, 145.6, 135.2, 130.9, 128.4, 41.2, 31.6, 29.3, 26.7, 22.7, 14.2 ppm.

HRMS calculated for $[\text{C}_{13}\text{H}_{17}\text{ClN}_4 + \text{H}^+]$ = 265.1215, found 265.1194.

4. Conclusions

In conclusion, we found simple and effective reaction conditions for $\text{S}_{\text{N}}\text{Ar}$ reactions of 2,4-diazidopyrido[3,2-*d*]pyrimidine with *N*-, *O*-, *S*- nucleophiles and obtained 5-substituted tetrazolo[1,5-*a*]pyrido[2,3-*e*]pyrimidines in high yields. The developed synthesis route via diazide is more rapid and convenient than the conventional route by stepwise substitution of the corresponding 2,4-dichloropyrido[3,2-*d*]pyrimidine. 2,4-Diazidopyrido[3,2-*d*]pyrimidine and the obtained tetrazolo[1,5-*a*]pyrido[2,3-*e*]pyrimidines exist in azide-tetrazole equilibrium in solutions favoring the tetrazole tautomer. The equilibrium is susceptible to solvent polarity, temperature, and substituents in the fused ring system. The calculated thermodynamic values of tautomerization ($\Delta G_{298} = -3.33$ to -7.52 kJ/mol) assert a higher tetrazole stability compared to azido tautomers. Substituents with stronger

electron-donating properties direct equilibrium toward the tetrazole tautomer. The obtained tetrazolo[1,5-*a*]pyrido[2,3-*e*]pyrimidines can be transformed into 1,2,3-triazoles via the CuAAC reaction using the CuSO₄/ascorbate catalytic system. Finally, the single crystal X-ray analysis of tetrazolo[1,5-*a*]pyrido[2,3-*e*]pyrimidines depicts the tetrazole tautomer as the most stable form in the solid phase.

Supplementary Materials: The following supporting information can be downloaded at: <https://www.mdpi.com/article/10.3390/molecules27227675/s1>, Gibbs and Van't plots, complete table of thermodynamic values calculated and ¹H, ¹³C and ³¹P NMR spectra are available in the supporting information.

Author Contributions: Conceptualization, I.N. and M.T.; Methodology, M.T.; Investigation, K.L.; Writing—original draft preparation, K.L. and A.M.; Writing—review and editing, I.N. and M.T.; Visualization, K.L.; Supervision, I.N. and M.T.; Project administration, I.N. and M.T.; Funding acquisition, K.L. and I.N. All authors have read and agreed to the published version of the manuscript.

Funding: This research was funded by the Latvian Council of Science grant LZP-2020/1-0348 and the European Social Fund within Project No. 8.2.2.0/20/1/008 “Strengthening of PhD students and academic personnel of Riga Technical University and BA School of Business and Finance in the strategic fields of specialization” of the Specific Objective 8.2.2 “To Strengthen Academic Staff of Higher Education Institutions in Strategic Specialization Areas” of the Operational Program “Growth and Employment”.

Informed Consent Statement: Not applicable.

Conflicts of Interest: The authors declare no conflict of interest.

Sample Availability: Samples of the compounds are not available.

References

1. Wang, S.; Yuan, X.-H.; Wang, S.-Q.; Zhao, W.; Chen, X.-B.; Yu, B. FDA-Approved Pyrimidine-Fused Bicyclic Heterocycles for Cancer Therapy: Synthesis and Clinical Application. *Eur. J. Med. Chem.* **2021**, *214*, 113218. [[CrossRef](#)] [[PubMed](#)]
2. Xing, K.; Zhang, J.; Han, Y.; Tong, T.; Liu, D.; Zhao, L. Design, Synthesis and Bioactivity Evaluation of 4,6-Disubstituted Pyrido[3,2-*d*]pyrimidine Derivatives as Mnk and HDAC Inhibitors. *Molecules* **2020**, *25*, 4318. [[CrossRef](#)] [[PubMed](#)]
3. Wang, Z.; Gao, Y.; He, L.; Sun, S.; Xia, T.; Hu, L.; Yao, L.; Wang, L.; Li, D.; Shi, H.; et al. Structure-Based Design of Highly Potent Toll-like Receptor 7/8 Dual Agonists for Cancer Immunotherapy. *J. Med. Chem.* **2021**, *64*, 7507–7532. [[CrossRef](#)] [[PubMed](#)]
4. Wang, M.; Tian, C.; Xue, L.; Li, H.; Cong, J.; Fang, F.; Yang, J.; Yuan, M.; Chen, Y.; Guo, Y.; et al. Design, Synthesis and Biological Activity of N5-Substituted Tetrahydropteroate Analogs as Non-Classical Antifolates against Cobalamin-Dependent Methionine Synthase and Potential Anticancer Agents. *Eur. J. Med. Chem.* **2020**, *190*, 112113. [[CrossRef](#)]
5. Shah, K.; Queener, S.; Cody, V.; Pace, J.; Gangjee, A. Development of Substituted Pyrido[3,2-*d*]pyrimidines as Potent and Selective Dihydrofolate Reductase Inhibitors for Pneumocystis Pneumonia Infection. *Bioorg. Med. Chem. Lett.* **2019**, *29*, 1874–1880. [[CrossRef](#)]
6. Degorce, S.L.; Aagaard, A.; Anjum, R.; Cumming, I.A.; Diène, C.R.; Fallan, C.; Johnson, T.; Leuchowius, K.J.; Orton, A.L.; Pearson, S.; et al. Improving Metabolic Stability and Removing Aldehyde Oxidase Liability in a 5-Azaquinazoline Series of IRAK4 Inhibitors. *Bioorg. Med. Chem.* **2020**, *28*, 115815. [[CrossRef](#)]
7. Mackman, R.L.; Mish, M.; Chin, G.; Perry, J.K.; Appleby, T.; Aktoudianakis, V.; Metobo, S.; Pyun, P.; Niu, C.; Daffis, S.; et al. Discovery of GS-9688 (Selgantolimod) as a Potent and Selective Oral Toll-Like Receptor 8 Agonist for the Treatment of Chronic Hepatitis B. *J. Med. Chem.* **2020**, *63*, 10188–10203. [[CrossRef](#)]
8. Sebris, A.; Turks, M. Recent Investigations and Applications of Azidoazomethine-Tetrazole Tautomeric Equilibrium. *Chem. Heterocycl. Compd.* **2019**, *55*, 1041–1043. [[CrossRef](#)]
9. Tišler, M. Some Aspects of Azido-Tetrazolo Isomerization. *Synthesis* **1973**, *1973*, 123–136. [[CrossRef](#)]
10. Ostrovskii, V.A.; Popova, E.A.; Trifonov, R.E. Developments in Tetrazole Chemistry (2009–2016). In *Advances in Heterocyclic Chemistry*; Scriven, E.F.V., Ramsden, C.A., Eds.; Academic Press: Cambridge, MA, USA, 2017; Volume 123, pp. 1–62. ISBN 9780128120927.
11. Sirakanyan, S.N.; Spinelli, D.; Geronikaki, A.; Hovakimyan, A.A.; Noravyan, A.S. New Heterocyclic Systems Derived from Pyridine: New Substrates for the Investigation of the Azide/Tetrazole Equilibrium. *Tetrahedron* **2014**, *70*, 8648–8656. [[CrossRef](#)]
12. Scapin, E.; Zimmer, G.C.; Vieira, J.C.B.; Rodrigues, C.A.B.; Afonso, C.A.M.; Zanatta, N.; Bonacorso, H.G.; Frizzo, C.P.; Martins, M.A.P. Reactivity of Trifluoromethyl-tetrazolo[1,5-*a*]pyrimidines in Click Chemistry and Hydrogenation. *J. Fluor. Chem.* **2022**, *257–258*, 109973. [[CrossRef](#)]

13. Deev, S.L.; Shestakova, T.S.; Shenkarev, Z.O.; Paramonov, A.S.; Khalymbadza, I.A.; Eltsov, O.S.; Charushin, V.N.; Chupakhin, O.N. ^{15}N Chemical Shifts and $J_{\text{N-N}}$ -Couplings as Diagnostic Tools for Determination of the Azide-Tetrazole Equilibrium in Tetrazoloazines. *J. Org. Chem.* **2022**, *87*, 211–222. [[CrossRef](#)]
14. Aleksandrova, N.V.; Nikolaenkova, E.B.; Gatilov, Y.V.; Polovyanenko, D.N.; Mamatyuk, V.I.; Krivopalov, V.P. Synthesis and Study of Azide-Tetrazole Tautomerism in 2-Azido-6-phenylpyrimidin-4(3H)-one and 2-Azido-4-chloro-6-phenylpyrimidine. *Rus. Chem. Bull.* **2022**, *71*, 1266–1272. [[CrossRef](#)]
15. Al-Marhabi, A.R.; Abbas, H.A.S.; Ammar, Y.A. Synthesis, Characterization and Biological Evaluation of Some Quinoxaline Derivatives: A Promising and Potent New Class of Antitumor and Antimicrobial Agents. *Molecules* **2015**, *20*, 19805–19822. [[CrossRef](#)]
16. Bräse Stefan, K.B. *Organic Azides: Syntheses and Applications*; Brse, S., Banert, K., Eds.; John Wiley & Sons, Ltd.: Chichester, UK, 2009; ISBN 9780470682517.
17. Guillou, S.; Jacob, G.; Terrier, F.; Goumont, R. An Unexpected Synthesis of 7-Azidofurazano[3,4-*b*]tetrazolopyrazine. *Tetrahedron* **2009**, *65*, 8891–8895. [[CrossRef](#)]
18. Cmoch, P.; Stefaniak, L.; Webb, G.A. NMR Studies of the Equilibria Produced by 6- and 8-Substituted Tetrazolo[1,5-*a*]pyridines. *Magn. Res. Chem.* **1997**, *35*, 237–242. [[CrossRef](#)]
19. Cmoch, P.; Korczak, H.; Stefaniak, L.; Webb, G.A. ^1H , ^{13}C and ^{15}N NMR and IR Studies of Halogen-Substituted Tetrazolo[1,5-*a*]pyridines. *J. Phys. Org. Chem.* **1999**, *12*, 470–478. [[CrossRef](#)]
20. Thomann, A.; Zapp, J.; Hutter, M.; Empting, M.; Hartmann, R.W. Steering the Azido-Tetrazole Equilibrium of 4-Azidopyrimidines via Substituent Variation-Implications for Drug Design and Azide-Alkyne Cycloadditions. *Org. Biomol. Chem.* **2015**, *13*, 10620–10630. [[CrossRef](#)]
21. Novosjolova, I.; Bizdēna, E.; Turks, M. Application of 2,6-Diazidopurine Derivatives in the Synthesis of Thiopurine Nucleosides. *Tetrahedron Lett.* **2013**, *54*, 6557–6561. [[CrossRef](#)]
22. Sebris, A.; Novosjolova, I.; Traskovskis, K.; Kokars, V.; Tetervenoka, N.; Vembris, A.; Turks, M. Photophysical and Electrical Properties of Highly Luminescent 2/6-Triazolyl-Substituted Push-Pull Purines. *ACS Omega* **2022**, *7*, 5242–5253. [[CrossRef](#)]
23. Sebris, A.; Traskovskis, K.; Novosjolova, I.; Turks, M. Synthesis and Photophysical Properties of 2-Azoly-6-piperidinylpurines. *Chem. Heterocycl. Compd.* **2021**, *57*, 560–567. [[CrossRef](#)]
24. Šišulins, A.; Bucevičius, J.; Tseng, Y.T.; Novosjolova, I.; Traskovskis, K.; Bizdēna, Ē.; Chang, H.T.; Tumkevičius, S.; Turks, M. Synthesis and Fluorescent Properties of N(9)-Alkylated 2-Amino-6-triazolylpurines and 7-Deazapurines. *Beilstein J. Org. Chem.* **2019**, *15*, 474–489. [[CrossRef](#)] [[PubMed](#)]
25. Bucevičius, J.; Turks, M.; Tumkevičius, S. Easy Access to Isomeric 7-Deazapurine-1,2,3-Triazole Conjugates via SNAr and CuAAC Reactions of 2,6-Diazido-7-deazapurines. *Synlett* **2018**, *29*, 525–529. [[CrossRef](#)]
26. Jeminejs, A.; Novosjolova, I.; Bizdēna, Ē.; Turks, M. Nucleophile–Nucleofuge Duality of Azide and Arylthiolate Groups in the Synthesis of Quinoxaline and Tetrazoloquinazoline Derivatives. *Org. Biomol. Chem.* **2021**, *19*, 7706–7723. [[CrossRef](#)] [[PubMed](#)]
27. Jeminejs, A.; Goliškina, S.M.; Novosjolova, I.; Stepanovs, D.; Bizdēna, Ē.; Turks, M. Application of Azide-Tetrazole Tautomerism and Arylsulfanyl Group Dance in the Synthesis of Thiosubstituted Tetrazoloquinazolines. *Synthesis* **2021**, *53*, 1443–1456. [[CrossRef](#)]
28. Leškovskis, K.; Mishnev, A.; Novosjolova, I.; Turks, M. Structural Study of Azide-Tetrazole Equilibrium in Pyrido[2,3-*d*]pyrimidines. *J. Mol. Struct.* **2022**, *1269*, 133784. [[CrossRef](#)]
29. Boyomi, S.M.; Ismael, A.-K.M.; Eisa, H.M.; El-Kerdawy, M.M. Some Nucleophilic Substitutions in 2,4- and 2,4,8-Trichloropyrido[3,2-*d*]pyrimidines. *Arch. Pharm. Res.* **1989**, *12*, 8–11. [[CrossRef](#)]
30. Urleb, U.; Stanovnik, B.; Tišler, M. The Synthesis and Transformations of 2-Ethoxycarbonyl-3-isothiocyanatopyridine. Pyrido[3,2-*d*]pyrimidines and Some Azolopyrido[3,2-*d*]pyrimidines. *J. Heterocycl. Chem.* **1990**, *27*, 407–412. [[CrossRef](#)]
31. Ueda, T.; Cheng, Y.C.; Eisa, H.; Broom, A.D. Probing the Thymidylate Synthase Active Site with Bisubstrate Analog Inhibitors. *Nucleosides Nucleosides* **1988**, *7*, 103–115. [[CrossRef](#)]
32. Petrič, A.; Tišler, M.; Stanovnik, B. Syntheses of Some Azolopyridopyrimidines. *Monatsh. Chem.* **1983**, *114*, 615–624. [[CrossRef](#)]
33. Petrič, A.; Tišler, M.; Stanovnik, B. Ring-Opening Reactions of Triazolo- and Tetrazolo-Pyridopyrimidines or Quinoxalines with Some Carbon Nucleophiles. *Monatsh. Chem.* **1985**, *116*, 1309–1319. [[CrossRef](#)]
34. Holzhauser, L.; Liagre, C.; Fuhr, O.; Jung, N.; Bräse, S. Scope of Tetrazolo[1,5-*a*]quinoxalines in CuAAC Reactions for the Synthesis of Triazoloquinoxalines, Imidazoloquinoxalines, and Rhenium Complexes Thereof. *Beilstein J. Org. Chem.* **2022**, *18*, 1088–1099. [[CrossRef](#)]
35. Zhang, L.; Zheng, L.; Guo, B.; Hua, R. One-Pot Synthesis of Multisubstituted 2-Aminoquinolines from Annulation of 1-Aryl Tetrazoles with Internal Alkynes via Double C–H Activation and Denitrogenation. *J. Org. Chem.* **2014**, *79*, 11541–11548. [[CrossRef](#)]
36. Ozols, K.; Cirule, D.; Novosjolova, I.; Stepanovs, D.; Liepinsh, E.; Bizdēna, E.; Turks, M. Development of N^6 -Methyl-2-(1,2,3-triazol-1-yl)-2'-deoxyadenosine as a Novel Fluorophore and Its Application in Nucleotide Synthesis. *Tetrahedron Lett.* **2016**, *57*, 1174–1178. [[CrossRef](#)]
37. Kapilinskis, Z.; Novosjolova, I.; Bizdēna, Ē.; Turks, M. Synthesis of 2-Triazolylpurine Phosphonates. *Chem. Heterocycl. Compd.* **2021**, *57*, 55–62. [[CrossRef](#)]
38. Cīrulis, D.; Novosjolova, I.; Spuris, A.; Mishnev, A.; Bizdēna, Ē.; Turks, M. Toward Unsymmetrical 2,6-Bistriazolylpurine Nucleosides. *Chem. Heterocycl. Compd.* **2021**, *57*, 292–297. [[CrossRef](#)]

39. Erasmus, C.; Aucamp, J.; Smit, F.J.; Seldon, R.; Jordaan, A.; Warner, D.F.; N'Da, D.D. Synthesis and Comparison of in Vitro Dual Anti-Infective Activities of Novel Naphthoquinone Hybrids and Atovaquone. *Bioorg. Chem.* **2021**, *114*, 105118. [[CrossRef](#)]
40. Tikad, A.; Routier, S.; Akssira, M.; Léger, J.-M.; Jarry, C.; Guillaumet, G. Efficient Synthesis of 2-Substituted Pyrido[3,2-*d*]pyrimidines Involving SNAr and Palladium-Catalyzed Cross-Coupling Reactions. *Synthesis* **2009**, *2009*. [[CrossRef](#)]
41. Tikad, A.; Routier, S.; Akssira, M.; Leger, J.-M.; Jarry, C.; Guillaumet, G. Efficient Access to Novel Mono- and Disubstituted Pyrido[3,2-*d*]pyrimidines. *Synlett* **2006**, *2006*, 1938–1942. [[CrossRef](#)]
42. Tikad, A.; Akssira, M.; Massip, S.; Léger, J.-M.; Jarry, C.; Guillaumet, G.; Routier, S. Regiocontrolled SNAr and Palladium Cross-Coupling Reactions of 2,4,7-Trichloropyrido[3,2-*d*]pyrimidine. *Eur. J. Org. Chem.* **2012**, *2012*, 4523–4532. [[CrossRef](#)]
43. Allen, F.H.; Watson, D.G.; Brammer, L.; Orpen, A.G.; Taylor, R. *International Tables for Crystallography*; John Wiley and Sons Limited: New York, NY, USA, 2006; Volume C, pp. 790–811. ISBN 978-0-470-68575-4. [[CrossRef](#)]
44. Gein, V.L.; Prudnikova, A.N.; Kurbatova, A.A.; Dmitriev, M.V. Synthesis of (*E*)-5-Arylviny-7-methyltetrazolo[1,5-*a*]pyrimidines. *Russ. J. Gen. Chem.* **2021**, *91*, 621–625. [[CrossRef](#)]
45. Scapin, E.; Salbego, P.R.S.; Bender, C.R.; Meyer, A.R.; Pagliari, A.B.; Orlando, T.; Zimmer, G.C.; Frizzo, C.P.; Bonacorso, H.G.; Zannatta, N.; et al. Synthesis, Effect of Substituents on the Regiochemistry and Equilibrium Studies of Tetrazolo[1,5-*a*]pyrimidine/2-Azidopyrimidines. *Beilstein J. Org. Chem.* **2017**, *13*, 2396–2407. [[CrossRef](#)] [[PubMed](#)]
46. Manzoor, S.; Yang, J.; Tariq, Q.; Mei, H.; Yang, Z.; Hu, Y.; Cao, W.; Sinditskii, V.P.; Zhang, J. Tetrazole and Azido Derivatives of Pyrimidine: Synthesis, Mechanism, Thermal Behaviour & Steering of Azido–Tetrazole Equilibrium. *Chem. Sel.* **2020**, *5*, 5414–5421. [[CrossRef](#)]
47. Russ, T.; Bats, J.W.; Ried, W.; SOWWIK. CSD Communication. 1992. Available online: <https://www.ccdc.cam.ac.uk/structures/Search?Title=CSD%20Communication&Year=1992&DatabaseToSearch=Published> (accessed on 3 November 2022).
48. Deev, S.L.; Shenkarev, Z.O.; Shestakova, T.S.; Chupakhin, O.N.; Rusinov, V.L.; Arseniev, A.S. Selective ¹⁵N-Labeling and Analysis of ¹³C–¹⁵N J Couplings as an Effective Tool for Studying the Structure and Azido–Tetrazole Equilibrium in a Series of Tetrazolo[1,5-*b*][1,2,4]triazines and Tetrazolo[1,5-*a*]pyrimidines. *J. Org. Chem.* **2010**, *75*, 8487–8497. [[CrossRef](#)] [[PubMed](#)]
49. Krivopalov, V.P.; Denisov, Y.A.; Gatilov, Y.V.; Mamatiuk, V.I.; Mamaev, V.P. Azido-Tetrazole Tautomerism of 2, 4-Diazidopyrimidines and 4, 6-Diazidopyrimidines. *Dokl. Akad. Nauk. SSSR* **1988**, *300*, 115.
50. Sheldrick, G.M. SHELXT—Integrated Space-Group and Crystal-Structure Determination. *Acta Crystallogr. Sect. A Found. Adv.* **2015**, *71*, 3–8. [[CrossRef](#)]
51. Sheldrick, G.M. A Short History of SHELX. *Acta Crystallogr. A* **2008**, *64*, 112–122. [[CrossRef](#)]
52. Farrugia, L.J. WinGX and ORTEP for Windows: An Update. *J. Appl. Crystallogr.* **2012**, *45*, 849–854. [[CrossRef](#)]
53. Bruno, I.J.; Cole, J.C.; Edgington, P.R.; Kessler, M.; Macrae, C.F.; McCabe, P.; Pearson, J.; Taylor, R. New Software for Searching the Cambridge Structural Database and Visualizing Crystal Structures. *Acta Crystallogr. B* **2002**, *58*, 389–397. [[CrossRef](#)]
54. Spek, A.L. Single-Crystal Structure Validation with the Program PLATON. *J. Appl. Crystallogr.* **2003**, *36*, 7–13. [[CrossRef](#)]

Leškovskis, K.; Mišņovs, A.; Novosjolova, I.; Krumm, B.; Klapötke, T.;
Turks, M.

**2,4,6,8-Tetraazidopyrimido[5,4-*d*]pyrimidine:
a Novel Energetic Binary Compound**

Cryst. Eng. Comm. **2023**, *25*, 3866-3869

doi:10.1039/D3CE00563A

Publikācijas pielikums pieejams bez maksas
[Royal Society of Chemistry mājaslapā](#)

The Supporting Information is available free of charge on the
[Royal Society of Chemistry website](#)

Pārpublicēts ar *Royal Society of Chemistry* atļauju.
Copyright © Royal Society of Chemistry 2023

Reprinted with the permission from Royal Society of Chemistry.
Copyright © Royal Society of Chemistry 2023


 Cite this: *CrystEngComm*, 2023, 25, 3866

 Received 5th June 2023,
Accepted 11th June 2023

DOI: 10.1039/d3ce00563a

rsc.li/crystengcomm

Quadruple azidation of 2,4,6,8-tetrachloropyrimido[5,4-d]pyrimidine gave tetraazidopyrimido[5,4-d]pyrimidine (C₆N₁₆) with 86% yield. The title compound undergoes azide–tetrazole tautomerism in neutral organic solvents, but exists as a protonated C₂-symmetric tetraazide dication in trifluoroacetic acid. On the other hand, in the solid state it occurs as a monotetrazole tautomer as revealed by its single crystal X-ray analysis. The newly obtained binary compound C₆N₁₆ is very sensitive towards both impact (<1 J) and friction (1 N). A detonation velocity of 7477 m s⁻¹ with a 20.8 GPa detonation pressure was calculated using the EXPLO5 code (version V7.01.01).

In the last few decades, heterocycles have marched in the field of energetic materials as promising building blocks for designing novel explosives.^{1,2} Nitrogen-rich frameworks, such as polyazido-tetrazoles, triazoles, furazans, triazines, and tetrazines, yield highly energetic materials with high heats of formation due to their intrinsic high energy N–N and C–N bonds.³ Moreover, the main combustion product of such nitrogen-rich compounds is non-toxic nitrogen gas. Hence, nitrogen-rich compounds are currently the most promising candidates for next-generation “green” explosives.⁴ The environmental concerns justify the replacement of conventionally used toxic heavy metal salt primary explosives (lead azide, lead styphnate) with eco-friendly substitutes.^{5,6}

Binary C_xN_y organic compounds are of great interest in materials science for synthesizing carbon nitride nanotubes for semiconductor, optoelectronic, and energy harvesting applications.^{7,8} Common starting materials are

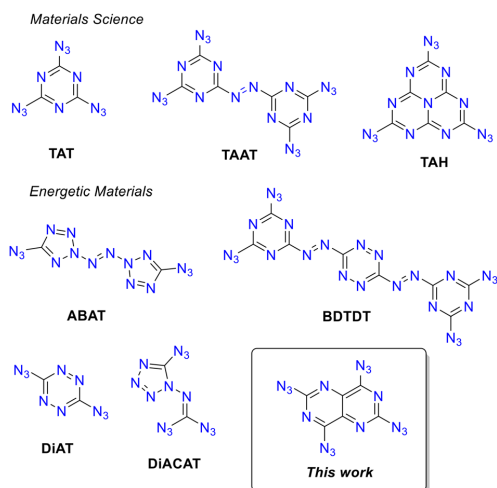
2,4,6,8-Tetraazidopyrimido[5,4-d]pyrimidine: a novel energetic binary compound†

 Kristaps Leškovskis,^a Anatoly Mishnev,^b Irina Novosjolova,^a Burkhard Krumm,^c Thomas M. Klapötke^c and Māris Turks^{a*}

binary polyazidoazines: 1,3,5-triazidotriazine (TAT),^{9,10} 4,4',6,6'-tetraazido(azo)-1,3,5-triazine (TAAT)¹¹ and triazidoheptazine (TAH)¹² (Fig. 1). As a result of their high nitrogen content, these materials are also impact sensitive and with explosive properties.

With the extension of the nitrogen content even up to 90%: 2,5-diazidotetrazine (DiAT),¹³ 3,6-bis-(2-(4,6-diazido-1,3,5-triazin-2-yl)-diazenyl)-1,2,4,5-tetrazine (BDTDT),¹⁴ 1-diazidocarbamoyl-5-azidotetrazole (DiACAT)¹⁵ and 2,2'-azobis(5-azidotetrazole) (ABAT),¹⁶ are demonstrating the sheer extreme of impact and friction sensitivities.

Recently, our group has developed several novel synthetic methodologies for functionalization of fused pyrimidines, exploring the synthetic utility of azide as a functional group and azide–tetrazole tautomeric equilibrium thereof.^{17–23} While studying diazidopyridopyrimidines,^{24,25} we ought to design a similar heterocyclic azide with explosive properties.


 Fig. 1 Energetic binary C_xN_y compounds.

^a Institute of Technology of Organic Chemistry, Faculty of Materials Science and Applied Chemistry, Riga Technical University, P. Valdena str. 3, Riga, Latvia. E-mail: maris.turks@rtu.lv

^b Latvian Institute of Organic Synthesis, Aizkraukles str. 21, Riga, Latvia

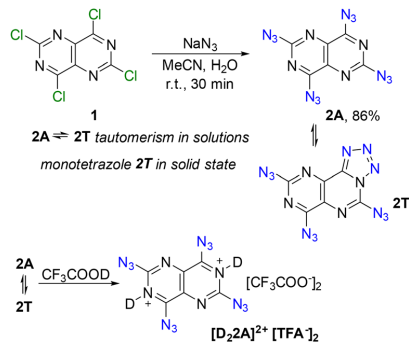
^c Department of Chemistry, Ludwig-Maximilian University of Munich, Butenandtstr. 5-13(D), 81377 Munich, Germany

† Electronic supplementary information (ESI) available: Experimental, synthesis procedure and NMR spectra. CCDC 2257695. For ESI and crystallographic data in CIF or other electronic format see DOI: <https://doi.org/10.1039/d3ce00563a>

We realized that the pyrimido[5,4-*d*]pyrimidine backbone, which has been frequently used by medicinal chemists and has produced the marketed drug dipyridamol^{26,27} – an antiplatelet drug for stroke prevention, has never been applied in the synthesis of highly energetic compounds. Yet, it has all the structural features to become an energetic C₆N₁₆ binary compound, if all four carbon atoms are substituted with azido groups.

Herein, we present here the synthesis of a novel, highly energetic, and very sensitive binary organic compound – 2,4,6,8-tetraazidopyrimido[5,4-*d*]pyrimidine (C₆N₁₆, abbreviated as **TAPP**) and its physical properties. The abbreviation **TAPP** comprises both azide and tetrazole tautomers of compound **2**, as the ratio/distribution of the latter are dependent on aggregate state and solvent properties. The target compound **TAPP** was obtained in 86% yield from the commercially available perchloropyrimido[5,4-*d*]pyrimidine (**1**) by the addition of sodium azide in aqueous MeCN at ambient temperature (Scheme 1).[‡] The quadruple nucleophilic aromatic substitution reaction with the azide nucleophile is very efficient likewise to substitutions in other fused pyrimidine series, for which the first substitution can provide the tetrazole tautomer at equilibrium concentration. The electron withdrawing properties of the intermediate fused tetrazolo–heterocycle accelerate the S_NAr reactions with the remaining incoming azide nucleophiles.²²

Due to both poor solubility in conventional (neutral) organic solvents and the presence of the azide–tetrazole equilibrium (2A ↔ 2T, Scheme 1), the NMR spectral data of **TAPP** were obtained in TFA-*d*₁. The latter provides dication [D₂2A]²⁺ *in situ* and thus shifts the tautomeric equilibrium exclusively to the C₂-symmetric tetraazido-form,¹⁸ which reveals only three ¹³C signals in the ¹³C-NMR spectrum (Scheme 1). ¹⁵N NMR spectrum of dication [D₂2A]²⁺ reveals two sets of azido groups for which nitrogen atoms N_α, N_β and N_γ appear at –253/–260 ppm, –151/–152 ppm and –125/–131 ppm, respectively (Fig. 2). Additionally, reaction of **1** + 4 Na¹⁵NN₂ provided a mixture of partially ¹⁵N-labeled analog of **TAPP**, which was sufficient to determine the chemical shifts of N_α and N_γ of the azido groups



Scheme 1 Synthesis of tetraazidopyrimido[5,4-*d*]pyrimidine (**2**, abbreviated as **TAPP**).

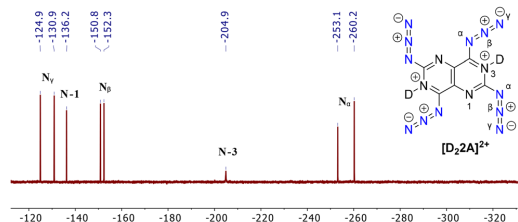


Fig. 2 ¹⁵N NMR (51 MHz) spectrum of **TAPP** in its di-deuterated [D₂2A]²⁺[TFA]₂ form in TFA-*d*₁.

(ESI[†]). Nitrogen atoms of the heterocyclic backbone N-1 and N-3 reveal the chemical shifts of –136 ppm and –205 ppm, respectively. The latter is characteristic for protonated/deuterated N-3 nitrogen, which in its unprotonated form would provide a signal by approximately 70 ppm downfield.²⁸

The X-ray quality single crystals of compound **TAPP** were obtained by slow evaporation of MeCN solution. The ORTEP representation of **TAPP** in its 2T form is shown in Fig. 3, and the crystal data are depicted in Table 1. A search of the Cambridge Structural Database (CSD, version 5.43, November, 2021) for a previously obtained fused tricyclic pyrimido–tetrazolo–pyrimidine heterocyclic system did not reveal any hits, giving us the opportunity to describe the solid state structure of such an annulated tricyclic binary compound for the first time. The molecules of tautomer **2T** in the crystal are essentially planar. Atomic deviations from the least squares mean plane of the heterocyclic system do not exceed 0.036(2) Å. The largest deviation from the mean plane is 0.205(2) Å for the N22 atom. The azide groups are not strictly linear; the valence angles N14–N15–N16, N17–N18–N19 and N20–N21–N22 are equal to 171.4(3)°, 173.1(4)°, 170.7(3)°, respectively. Bond lengths in the tautomer **2T** are in good agreement with their standard values as has been observed for other azido-pyrimidines and tetrazolo-pyrimidines.²⁹ In the crystal, the molecules are assembled in the layers stabilized by π···π stacking interactions and spaced by 3.019(3) Å. The calculated packing index, or percent filled space, is 70.3.

Physical and energetic properties of **TAPP** are tested for the solid material, which represents the 2T tautomer (Table 2); compound **TAPP** is extremely sensitive towards both impact and friction. The impact sensitivity was measured to be below 1 J, and the friction sensitivity was 1 N. Differential thermal

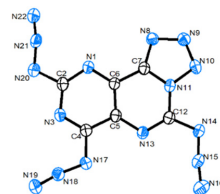


Fig. 3 ORTEP view (50% probability ellipsoids) of **TAPP** in its 2T form; CCDC deposition number 2257695.

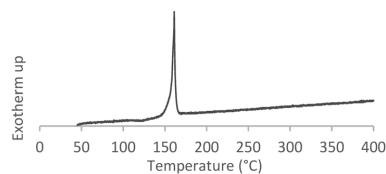
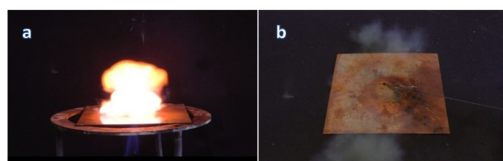
Table 1 Crystal data for TAPP in its 2T form^a

Chemical formula	C ₆ N ₁₆
<i>M_r</i> (g mol ⁻¹)	296.22
Crystal system, space group	Orthorhombic, <i>Pca</i> 2 ₁
Crystal size (mm)	0.40 × 0.06 × 0.03
Temperature (K)	150
<i>a</i> (Å)	12.0754(3)
<i>b</i> (Å)	10.5591(3)
<i>c</i> (Å)	8.8651(3)
<i>V</i> (Å ³)	1130.35(6)
<i>Z</i>	4
<i>μ</i> (mm ⁻¹)	1.17
Calculated density (mg mm ⁻³)	1.74

^a For refinement details see Table S1 (ESI[†]); details of crystal packing are depicted in Fig. S1 (ESI[†]).

analysis did not show a melting point, but only a sharp exothermic decomposition at 155 °C (Fig. 4). The compound is light-sensitive and turns yellow after exposure to daylight or a UV lamp (254 nm). The density of the compound TAPP was calculated to be 1.703 g cm⁻³ using low temperature density data from single crystal X-ray diffraction of tetrazolo-tautomer 2T. The density is very close to that of TAT (1.707 g cm⁻³).

Next, other tests typical for characterization of energetic materials were carried out. Thus, compound TAPP deflagrated upon subjecting to a hot plate test, and a clear detonation was observed in the hot needle test (Fig. 5). A heat of formation of 5095 kJ kg⁻¹ was calculated using the atomization method based on CBS-4M electronic enthalpies (ESI[†]). The detonation pressure and velocity of TAPP were calculated to be 20.8 GPa and 7477 m s⁻¹, respectively. The detonation velocity of TAPP is comparable to other binary explosives and greater than that of lead azide. On the other hand, the calculated detonation pressure for the TAPP is comparable to that of TAT and is around two thirds to that of BDDTD and lead azide. The detonation energy parameters of TAPP were found to be slightly larger than those of TNT as

**Fig. 4** DTA analysis of solid TAPP in its 2T form.**Fig. 5** a) Hot plate test: the moment of deflagration; b) hot needle test: the moment of detonation.

the heat of detonation (Q_{det}) for TAPP is 1.04 TNT equivalents and E° is 1.12 TNT equivalents. Finally, even if two runs of pentaerythritol tetranitrate (PETN) initiation tests with the newly obtained TAPP were negative, this molecular scaffold opens possibilities for structural design of novel fused azido-pyrimidine energetic materials.

In summary, 2,4,6,8-tetraazidopyrimido[5,4-*d*]pyrimidine was obtained by simple azidation of the commercially available 2,4,6,8-tetrachloropyrimido[5,4-*d*]pyrimidine derivative under mild and user friendly conditions. Compound TAPP exhibits azide-tetrazole tautomerism in solutions of neutral organic solvents and crystallizes in the solid state as a monotetrazole tautomer. This new energetic binary compound C₆N₁₆ is sensitive towards impact and friction and reveals other physical parameters that uncovers the pyridopyrimidine scaffold as a useful structural entity for design of other energetic materials in the future.

Table 2 Physical and energetic properties of solid TAPP in its 2T form and their comparison with other energetic compounds

Measured values	TAPP (2T)	TAT ^d	BDDTD ^e	Pb(N ₃) ₂ ^f
Impact sensitivity (J)	<1	1.5	5	2.5–4
Friction sensitivity (N)	1	<5	29	0.1–1
Electrostatic discharge (mJ)	13	360	174	<5
ρ (g cm ⁻³)	1.703 ^a	1.707	1.763	4.8
N balance (%)	75.7	82.4	79.13	28.9
Ω^b (%)	-64.8	-47.0	-55.7	-11.0
$T_{melting}$ (°C)	Decomp.	94	Decomp.	190
$T_{decomposition}$ (°C)	155	187	189	315
Calculated values				
$\Delta H_{formation}$ (kJ kg ⁻¹)	5095	5159	6130	1546
$T_{detonation}$ (K)	3787	3536 ^g	4740	3401
P_{CJ} ^c (GPa)	20.8	22.6 ^g	29.4	33.8
V_{det} (m s ⁻¹)	7477	7866 ^g (TMD)	8602	5920

^a From X-ray diffraction analysis recalculated to 298 K using $\rho_{298} = \rho_{T/(1 + \alpha_v(298 - T))}$ equation, where $\alpha_v = 0.00015$ and T = crystal analysis temperature. ^b Oxygen balance with respect to CO₂ ($\Omega_{CO_2} = (nO - 2xC - yH/2)/(1600/FW)$). ^c Detonation pressure at the Chapman-Jouguet point. ^d Ref. 11. ^e Ref. 14. ^f Ref. 30. ^g Ref. 31.

Conflicts of interest

There are no conflicts to declare.

Acknowledgements

K. L. and M. T. thank the Baltic-German University Liaison Office project supported by the German Academic Exchange Service (DAAD) with funds from the Foreign Office of the Federal Republic Germany. I. N. thanks the Latvian Council of Science grant LZP-2020/1-0348. K. L. thanks the European Social Fund within Project No. 8.2.2.0/20/1/008 “Strengthening of PhD students and academic personnel of Riga Technical University and BA School of Business and Finance in the strategic fields of specialization”.

Notes and references

‡ Caution! The title compound is a powerful energetic material with high sensitivities towards shock and friction. Therefore, proper security precautions (safety glass, face shield, earthed equipment and shoes, Kevlar gloves and ear plugs) must be applied while synthesizing and handling the described compound. Synthesis procedure: 2,4,6,8-tetrachloropyrimido[5,4-*d*]pyrimidine (1) (200 mg, 0.741 mmol, 1 equiv.) was suspended in MeCN (3 mL) in a round bottom flask (10 mL) and a solution of NaN₃ (289 mg, 4.446 mmol, 6 equiv.) in water (1 mL) was added. The resulting suspension was stirred at ambient temperature for 30 min. After reaction completion (monitored by HPLC), water (10 mL) was added to the reaction mixture. The formed precipitate was filtered and washed with additional amount of distilled water (5 mL) and cold ethanol (5 mL). **TAPP** was obtained as slightly yellow amorphous solid, *R_f* = 0.85 (50% Hex/EtOAc). Yield: 188 mg, 86%. ¹³C NMR (101 MHz, CDCl₃), data for the major C₂-symmetric tetra-azido tautomer: δ 163.1 (C₂, C₆), 157.3 (C₄, C₈), 135.7 (C₅, C₇) ppm. ¹³C NMR (126 MHz, CF₃COOD) δ 165.3 (C₂, C₆), 160.1 (C₄, C₈), 131.2 (C₅, C₇). ¹⁵N NMR (51 MHz, CF₃COOD) δ -124.9, -130.9 (2 × N₁), -136.2 (N₁), -150.8, -152.3 (2 × N_β), -204.9 (N₃), -253.1, -260.3 (2 × N_α) ppm. HRMS calculated for [C₆N₁₆ + H]⁺ = 297.0565, found 297.0556. IR (Nujol) 2214, 2161, 2111, 1617, 1583, 1538, 1506, 1456, 1313, 1275, 1223, 1168, 968, 775, 756, 722, 665 cm⁻¹.

- 1 H. Gao and J. M. Shreeve, *Chem. Rev.*, 2011, **111**, 7377–7436.
- 2 P. F. Pagoria, G. S. Lee, A. R. Mitchell and R. D. Schmidt, *Thermochim. Acta*, 2002, **384**, 187–204.
- 3 H. Xue, Y. Gao, B. Twamley and J. M. Shreeve, *Chem. Mater.*, 2005, **17**, 191–198.
- 4 D. Herweyer, J. L. Brusso and M. Murugesu, *New J. Chem.*, 2021, **45**, 10150–10159.
- 5 M. H. V. Huynh, M. A. Hiskey, T. J. Meyer and M. Wetzler, *Proc. Natl. Acad. Sci.*, 2006, **103**, 5409–5412.
- 6 Q. N. Tariq, S. Manzoor, M. N. Tariq, W. L. Cao, W. S. Dong, F. Arshad and J. G. Zhang, *ChemistrySelect*, 2022, **7**, e202200017.
- 7 P. Kumar, E. Vahidzadeh, U. K. Thakur, P. Kar, K. M. Alam, A. Goswami, N. Mahdi, K. Cui, G. M. Bernard, V. K. Michaelis and K. Shankar, *J. Am. Chem. Soc.*, 2019, **141**, 5415–5436.

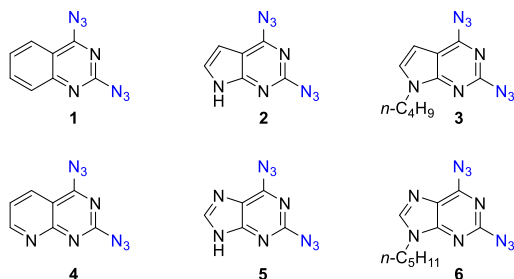
- 8 Y. Zhu, Y. Feng, S. Chen, M. Ding and J. Yao, *J. Mater. Chem. A*, 2020, **8**, 25626–25648.
- 9 E. Ott and E. Ohse, *Ber. Dtsch. Chem. Ges.*, 1921, **54**, 179–186.
- 10 E. Keßenich, T. M. Klapötke, J. Knizek, H. Nöth and A. Schulz, *Eur. J. Inorg. Chem.*, 1998, 2013–2016.
- 11 M. H. V. Huynh, M. A. Hiskey, E. L. Hartline, D. P. Montoya and R. Gilardi, *Angew. Chem., Int. Ed.*, 2004, **43**, 4924–4928.
- 12 D. R. Miller, D. C. Swenson and E. G. Gillan, *J. Am. Chem. Soc.*, 2004, **126**, 5372–5373.
- 13 M. H. V. Huynh, M. A. Hiskey, D. E. Chavez, D. L. Naud and R. D. Gilardi, *J. Am. Chem. Soc.*, 2005, **127**, 12537–12543.
- 14 D. Chen, H. Yang, Z. Yi, H. Xiong, L. Zhang, S. Zhu and G. Cheng, *Angew. Chem., Int. Ed.*, 2018, **57**, 2081–2084.
- 15 T. M. Klapötke, F. A. Martin and J. Stierstorfer, *Angew. Chem., Int. Ed.*, 2011, **50**, 4227–4229.
- 16 M. Benz, T. M. Klapötke, J. Stierstorfer and M. Voggenreiter, *J. Am. Chem. Soc.*, 2022, **144**, 6143–6147.
- 17 A. Sebris, I. Novosjolova, K. Traskovskis, V. Kokars, N. Tetervenoka, A. Vembris and M. Turks, *ACS Omega*, 2022, **7**, 5242–5253.
- 18 A. Sebris, K. Traskovskis, I. Novosjolova and M. Turks, *Chem. Heterocycl. Compd.*, 2021, **57**, 560–567.
- 19 A. Jeminejs, I. Novosjolova, Ē. Bizdēna and M. Turks, *Org. Biomol. Chem.*, 2021, **19**, 7706–7723.
- 20 A. Jeminejs, S. Goliškina, I. Novosjolova, D. Stepanovs, Ē. Bizdēna and M. Turks, *Synthesis*, 2021, **53**, 1543–1556.
- 21 D. Cīrule, I. Novosjolova, A. Spuris, A. Mishnev, Ē. Bizdēna and M. Turks, *Chem. Heterocycl. Compd.*, 2021, **57**, 292–297.
- 22 J. M. Zaķis, K. Ozols, I. Novosjolova, R. Vilškersts, A. Mishnev and M. Turks, *J. Org. Chem.*, 2020, **85**, 4753–4771.
- 23 A. Šišuljins, J. Bučevičius, Y.-T. Tseng, I. Novosjolova, K. Traskovskis, Ē. Bizdēna, H.-T. Chang, S. Tumkevičius and M. Turks, *Beilstein J. Org. Chem.*, 2019, **15**, 474–489.
- 24 K. Leškovskis, A. Mishnev, I. Novosjolova and M. Turks, *J. Mol. Struct.*, 2022, **1269**, 133784.
- 25 K. Leškovskis, A. Mishnev, I. Novosjolova and M. Turks, *Molecules*, 2022, **27**, 7675.
- 26 D. Royston, in *Pharmacology and Physiology for Anesthesia*, Elsevier, 2019, pp. 870–894.
- 27 R. C. Harmon, in *xPharm: The Comprehensive Pharmacology Reference*, Elsevier, 2007, pp. 1–7.
- 28 D. T. Major, A. Laxer and B. Fischer, *J. Org. Chem.*, 2002, **67**, 790–802.
- 29 F. H. Allen, D. G. Watson, L. Brammer, A. G. Orpen and R. Taylor, in *International Tables for Crystallography*, International Union of Crystallography, Chester, England, 2006, pp. 790–811.
- 30 D. Fischer, T. M. Klapötke and J. Stierstorfer, *Angew. Chem., Int. Ed.*, 2014, **53**, 8172–8175.
- 31 *Energetic Materials Encyclopedia*, ed. T. M. Klapötke and D. Gruyter, Berlin/Boston, 2nd edn, 2021, vol. 1–3.

Leškovskis, K.; Klapötke, T. M.; Novosjolova, I.; Turks M.

Annelētu diazidopirimidīnu drošības profils
Safety Profile of Fused Diazidopyrimidines

Nepublicētie rezultāti / Unpublished results

Organiskie azīdi ar augstu slāpekļa saturu ir ārēja triecienu un termiski jutīgi potenciāli sprāgstošī savienojumi. Slāpekļa saturoši heterocikli ar azīda funkcionālajām grupām α -pozīcijā cikla slāpeklim dod azidoazometīna struktūras fragmentu, kam raksturīgs azīda-tetrazola tautomērais līdzsvars un augstāka triecienu un termiskā stabilitāte salīdzinot ar vienkāršiem aromātiskiem azīdiem. Tomēr savienojumi, kuru slāpekļa saturs pārsniedz 50% robežu kā anelētie diazidopirimidīni **1-6**, pēc vispārīgām drošas laboratorijas praksēm uzskatāmi par potenciāli bīstamiem (1. attēls).



1. attēls. Anelētie diazidopirimidīni

Mūsu pētniecības grupā bieži lietotajiem azidoheterocikliem noteicām to enerģētisko profilu sadarbībā ar profesora Tomasa Klapetkes (Thomas M. Klapötke) grupu no Mīnhenes Ludviga Maksimiliāna universitātes, lai gūtu pārliecību par drošuma līmeni darbā ar tiem (1. tabula).

1. tabula

Anelēto diazidopirimidīnu noteiktie fizikālie parametri

Savienojums	N (%) ^a	BJ ^b (N)	TJ ^c (J)	EI (mJ) ^d	k.p. (°C)	T _{sad.} ^e
1	53	288	2	>480	126	172
2	63	80	<1	>480	sadalās	168
3	49	>360	20	>480	85	155
4	59	40	2	>480	171	175
5	69	120	<1	>480	sadalās	166
6	51	>360	20	>480	58	159

a – Slāpekļa balance; b – berzes jutība; c – triecienu jutība; d – elektrostātiskās izlādes jutība; e – sadalīšanās sākuma temperatūra.

Eksperimentālā daļa

Savienojumi **1**¹, **2**², **3**³, **4**⁴, **5**⁵ and **6**⁶ sintezēti pēc literatūras metodēm. Diferenciālā termālā analīze sadalīšanās temperatūras noteikšanai veikta ar *OZM Research DTA 552-Ex* instrumentu ar sildīšanas ātrumu 5 °C min⁻¹. Triecienujutības testi veikti saskaņā ar STANAG 44897 standartu lietojot *BAM* āmuru pielietojot 1 no 6 metodi. Berzes jutības testi veikti saskaņā ar STANAG 448710 standartu lietojot *BAM* berzes instrumentu pielietojot 1 no 6 metodi. Elektrostātiskās izlādes jutība noteikta ar *Electric Spark Tester ESD 2010 EN* no OZM.

Organic azides with high nitrogen content are impact-sensitive and thermally unstable with potentially explosive properties. Nitrogen heterocycles with azide functionality in α -position relative to nitrogen present azidoazomethine structural fragment with its characteristic azide-tetrazole equilibrium and better impact and thermal stability as compared to simple aromatic azides. Nevertheless, compounds exceeding 50% nitrogen content, such as fused diazidopyrimidines **1-6**, are considered potentially explosive in accordance with general laboratory safety guidelines (Figure 1).

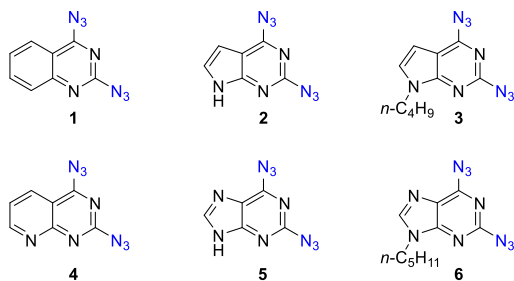


Figure 1. Fused diazidopyrimidines

Hence, in cooperation with Professor Thomas M. Klapötke's group at Ludwig Maximilian University of Munich, we established the safety profile of fused diazidopyrimidines frequently used within our research group to ensure the safety level of work with the aforementioned compounds (Table 1).

Table 1. Physical data and sensitivities of fused diazidopyrimidines

Compound	N (%) ^a	FS ^b (N)	IS ^c (J)	ESD (mJ) ^d	m.p. (°C)	T _{dec.} ^e
1	53	288	2	>480	126	172
2	63	80	<1	>480	decomp.	168
3	49	>360	20	>480	85	155
4	59	40	2	>480	171	175
5	69	120	<1	>480	decomp.	166
6	51	>360	20	>480	58	159

a – Nitrogen content. b - Friction sensitivity. c – Impact sensitivity. d – Electrostatic discharge. e - Temperature of the onset of decomposition.

Experimental

Compounds **1**¹, **2**², **3**³, **4**⁴, **5**⁵ and **6**⁶ were prepared according to literature methods. Differential thermal analysis (DTA) measurements were performed at a heating rate of 5 °C min⁻¹ with an OZM Research DTA 552-Ex instrument to determine the decomposition. The impact sensitivity tests were carried out according to STANAG 44897⁷ using BAM drophammer applying the 1 out of 6 method. The friction sensitivity tests were carried out according to STANAG 448710⁸ using BAM friction tester applying the 1 out of 6 method.

Sensitivity towards electrical discharge using an *Electric Spark Tester ESD 2010 EN* from OZM.

Atsauces / References

- (1) Kalniņa, A.; Bizdēna, Ē.; Kiselovs, G.; Mishnev, A.; Turks, M. *Chem. Heterocycl. Comp.* **2014**, *49*, 1667–1673.
- (2) Bucevičius, J.; Tumkevičius, S. *Chemija* **2015**, *26*, 126–131.
- (3) Bucevicius, J.; Turks, M.; Tumkevicius, S. *Synlett* **2018**, *29*, 525–529.
- (4) Leškovskis, K.; Mishnev, A.; Novosjolova, I.; Turks, M. *J. Mol. Struct.* **2022**, *1269*, 133784.
- (5) Sebris, A.; Traskovskis, K.; Novosjolova, I.; Turks, M. *Chem. Heterocycl. Comp.* **2021**, *57*, 560–567.
- (6) Šišušins, A.; Bucevičius, J.; Tseng, Y.-T.; Novosjolova, I.; Traskovskis, K.; Bizdēna, Ē.; Chang, H.-T.; Tumkevičius, S.; Turks, M. *Beilstein J. Org. Chem.* **2019**, *15*, 474–489.
- (7) NATO Standardization Agreement (STANAG) on Explosives, Impact Sensitivity Tests, No. 4489, 1st Edn., September 17, 1999.
- (8) NATO Standardization Agreement (STANAG) on Explosives, Friction Sensitivity Tests, No. 4487, 1st Edn., August 22, 2002.

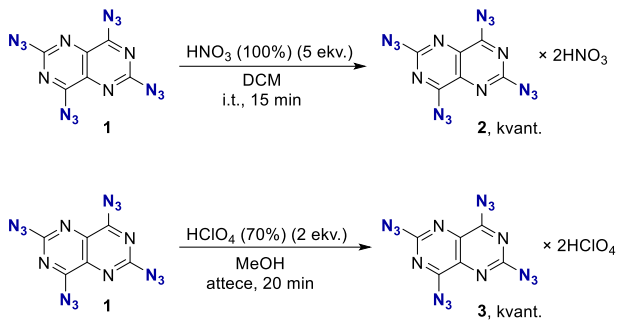
Leškovskis, K.; Novosjolova, I.; Turks M.

2,4,6,8-Tetraazidopirido[5,4-*d*]pirimidīna solvātu sintēze
Synthesis of 2,4,6,8-tetraazidopyrido[5,4-*d*]pyrimidine solvates

Nepublicētie rezultāti / Unpublished results

Balstoties uz tetraazīda augsto šķīdību deitero trifluoretiķskābē, nolēmām izmēģināt tetraazīda sāļu sintēzi ar stipri oksidējošām skābēm. Literatūrā ir zināms, ka heterocikliskiem sāļiem piemīt augstāka izturība pret fizisko ietekmi un labāka termiskā stabilitāte pateicoties starpmolekulārajam ūdeņraža saišu tīklam, zemāks parciālais spiediens un augstāks vielas blīvums nekā vienkāršiem bāzu analogiem. Pie tam oksidējošas skābes anjona klātbūtne palielina skābekļa bilanci, kas uzlabo detonēšanās veiktspēju.^{1,2}

Augstākminētajā nolūkā pārbaudījām tetraazīda **1** bāzes reakcijas ar koncentrētām skābēm, iegūtos maisījumus ietvaicējot gaisa plūsmā (1. shēma). Iegūto produktu stehiometrija noteikta pēc masas bilances pieauguma.



Slāpekļskābes aduktam **2** TFA-*d*₁ šķīdumā ¹⁵N KMR spektrā novērojām signālu pie -37 ppm, kas atrodas nitrāta anjonam raksturīgajā reģionā.

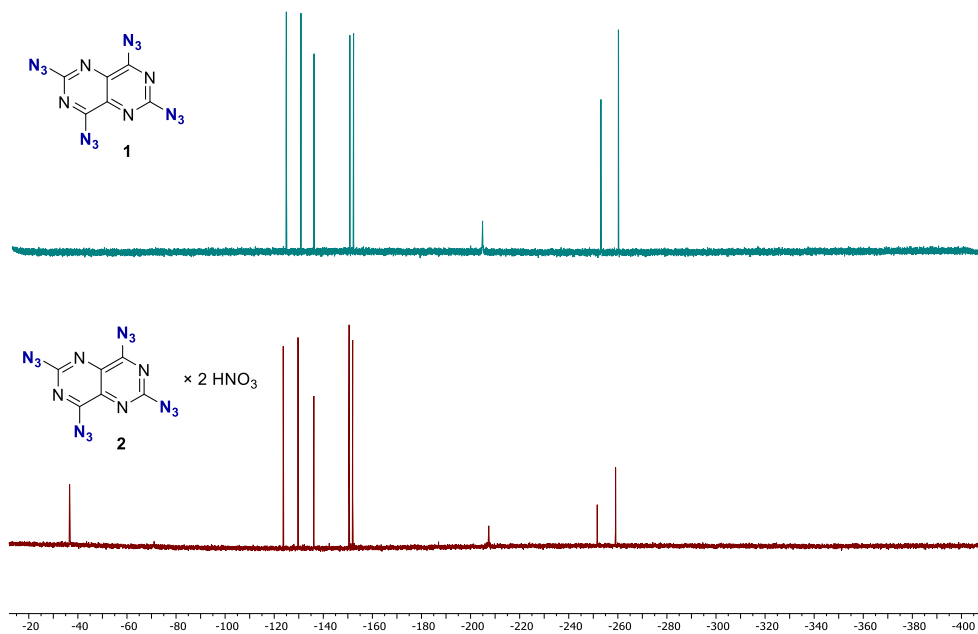
Lai pierādītu produktu struktūras, mēģinājām sagatavot monokristāla paraugu rentgenstruktūranalīzei, tomēr šiem savienojumi izrādījās pārāk sīkkristāliski un iegūti tikai tetraazīda bāzes **1** un trifluoretiķskābes addukta monokristāli.

Ar rentgenstaru difraktometriju (2. attēls) un FT-IR (3. attēls) spektroskopiju noteicām, ka iegūtie produkti strukturāli atšķiras no bāziskās struktūras. FT-IR spektroskopijas aina produktiem ir vienkāršāka salīdzinot ar tetraazīdu, kas apstiprina bāzes **1** pastāvēšanu monotetraazola formā cietā fāzē un skābju adukti kā protonēti sāļi vai solvāti ar ūdeņraža saišu pastāv simetriskā tetraazīda formā.

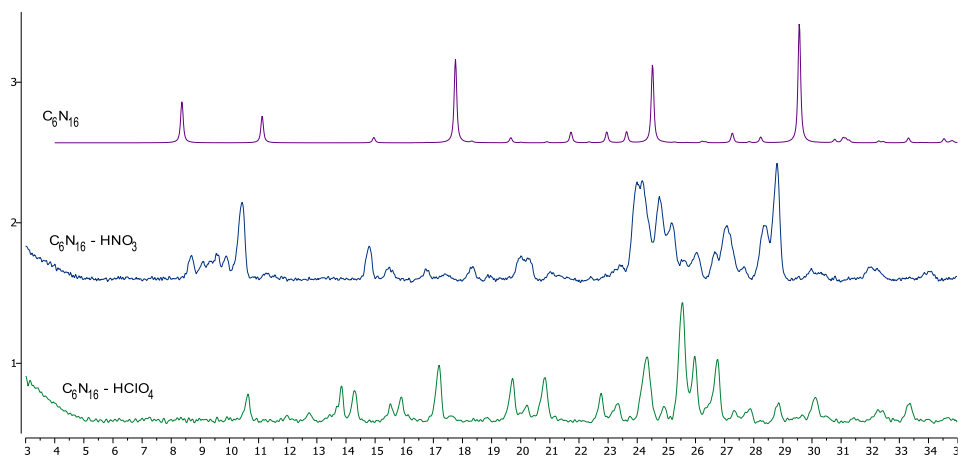
Ar Ramana spektroskopiju vēlējamies novērot nitrāta (1050 cm⁻¹) un perhlorāta (940 cm⁻¹) sāļiem raksturīgos signālus, kuriem parasti ir augsta intensitāte, tomēr produktiem **2** un **3** šādus signālus nenovērojām (4. attēls). Šis rezultāts parāda, ka produkti **2** un **3** visticamāk pastāv solvātu formā, un pilnīga heterocikla protonēšana nav notikusi.

¹ T. M. Klapötke; C. M. Sabaté *Eur. J. Inorg. Chem.* **2008**, 2008, 5350–5366.

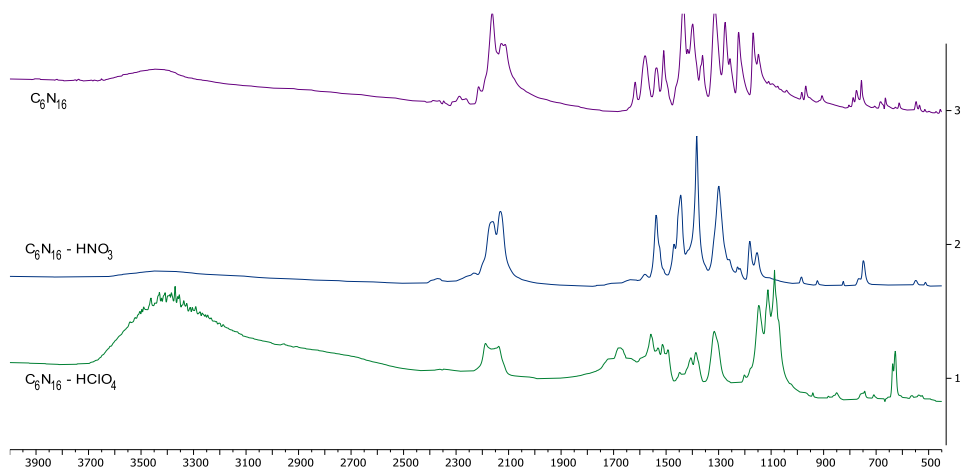
² Y. Gao; H. Gao; C. Piekariski; J. M. Shreeve *Eur. J. Inorg. Chem.* **2007**, 2007, 4965–4972.



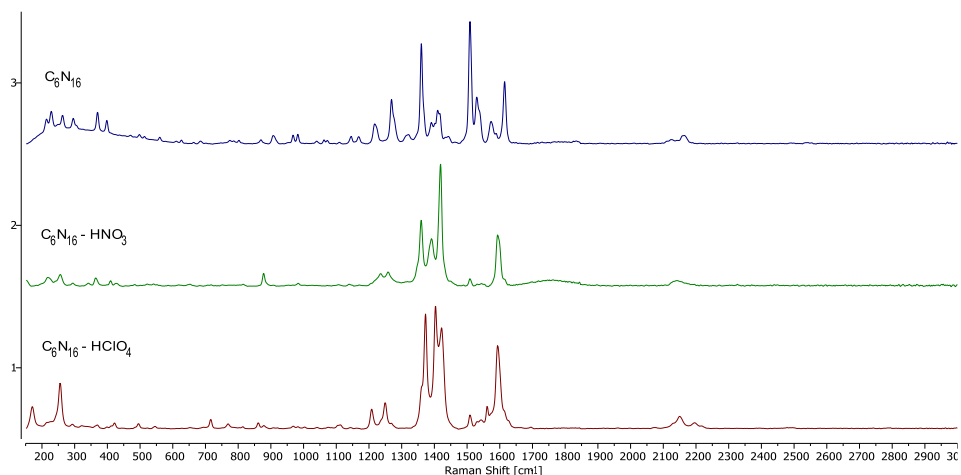
1. attēls. Tetraazīda **1** un tā slāpekļskābes adukta **2** ^{15}N KMR spektri (51 MHz, CF_3COOD)



2. attēls. Tetraazīda bāzes formas **1** un tetraazīda solvātu **2** un **3** pulvera rentgendifrakcijas analīze.



3. attēls. Tetraazīda bāzes formas **1** un tetraazīda solvātu **2** un **3** FT-IR spektri.



4. attēls. Tetraazīda bāzes formas **1** un tetraazīda solvātu **2** un **3** Raman spektri.

Visbeidzot, triecienu un berzes testos iegūtie HNO₃ solvāta **2** (2 J triecienjutība; 40 N berzes jutība) un HClO₄ solvāta **3** (1 J triecienjutība; 40 N berzes jutība) uzrādīja augstāku izturību pret fizisko ietekmi salīdzinot ar tetraazīda bāzi **1** (1 J triecienu jutība; 1 N berzes jutība). Karstās virsmas testā tetraazīda solvāti sadalījās ar uzliesmojumu un karstās adatas testā perhlorāts detonējās. Tomēr veicot sekundārās sprāgstvielas iniciācijas testus, izmantojot tetraazīda perhlorāta (**1**) detonatoru, detonācija pagaidām nenotika.

Eksperimentālā daļa

2.4.6.8-Tetraazidopirimido[5,4-*d*]pirimidīna slāpekļskābes solvāts (2):

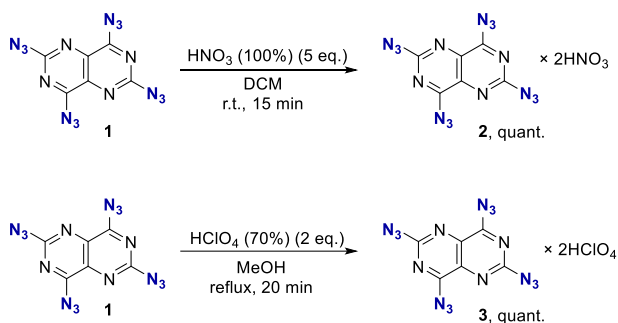
Tetrazīda **1** (100 mg, 0,338 mmol, 1 ekv.) suspensijai metilēnchlorīdā (1 mL) pievieno HNO₃ (100%) (70 μL, *d* = 1,52 mg/mL, 106 mg, 1,688 mmol, 5 ekv.). Reakciju maisa 20 min. istabas temperatūrā. Reakcijas maisījumu ietvaicē ar gaisa plūsmu un žāvē pazeminātā spiedienā. Iegūst dzeltenu cietu vielu 142 mg (kvant.). ¹³C KMR (126 MHz, CF₃COOD) δ 165,4, 160,2, 130,9. ¹⁵N KMR (51 MHz, CF₃COOD) δ -36,6, -123,7, -129,7, -136,1, -150,5, -152,0, -207,4, -251,6, -259,1.

2.4.6.8-Tetraazidopirimido[5,4-*d*]pirimidīna perhlorskābes solvāts (3):

Tetrazīda **1** (80 mg, 0,270 mmol, 1 ekv.) suspensijai metanolā (1 mL) pievieno HClO₄ (70%) ūdens šķīdumu (46 μL, *d* = 1,67 mg/mL, 54 mg, 0,540 mmol, 2 ekv.). Reakciju silda 20 min. šķīdinātāja viršanas temperatūrā. Reakcijas maisījumu ietvaicē ar gaisa plūsmu un žāvē pazeminātā spiedienā. Iegūst dzeltenu cietu vielu 134 mg (kvant.).

Noting the high solubility of tetraazide in CF_3COOD , we envisioned the synthesis of tetraazide salts or solvates with strongly oxidizing acids. It is well known that heterocycle salts are more durable to physical impact and more thermally stable due to the formed intermolecular hydrogen bonding network; their vapor pressure is lower, and density is higher than neutral heterocycle precursors. Furthermore, improved oxygen balance due to the presence of oxidizing acid anions increases detonation performance.^{1,2}

The syntheses of acid adducts **2** and **3** were performed by the addition of concentrated acids to the tetraazide **1** base, followed by solvent evaporation under airflow (Scheme 1). The stoichiometry of the solvates were calculated based on the increment of the obtained product mass.



Scheme 1. Synthesis of tetraazide solvates **2** and **3**

In the ^{15}N NMR spectrum of nitric acid adduct **2** in $\text{TFA}-d_1$ solution we observed an additional signal at -37 ppm corresponding to nitrate anion (Figure 1).

Numerous attempts of sample preparation for single crystal X-ray analysis of adducts **2** and **3** were made. However, these samples appeared to be as crystalline powder. So far we were able to obtain suitable monocrystals only for the tetraazide base **1** and for CF_3COOH adduct.

Nevertheless, we performed powder XRD (Figure 2) and FT-IR (Figure 3) analysis to confirm the structures and observed distinct spectra for each compound. The FT-IR spectra of adducts **2** and **3** were simpler in comparison with the tetraazide base **1**. This can be attributed to the fact that tetraazide base **1** exists as a monotetrazole tautomer in the solid phase. In contrast, the acid adducts are either protonated or coordinated with hydrogen bond network and exist as a symmetric tetraazide tautomer.

Further, with the help of Raman spectroscopy, we searched to observe high-intensity signals at 1050-^1 and 940 cm^{-1} characteristic for nitrate and perchlorate anions, respectively. Intriguingly, such signals were observed in the Raman spectra of adducts **2** and **3**. This result shows that products **2** and **3** most likely exist as solvates and complete protonation of the heterocycle has not occurred.

¹ T. M. Klapötke; C. M. Sabaté *Eur. J. Inorg. Chem.* **2008**, 2008, 5350–5366.

² Y. Gao; H. Gao; C. Piekarski; J. M. Shreeve *Eur. J. Inorg. Chem.* **2007**, 2007, 4965–4972.

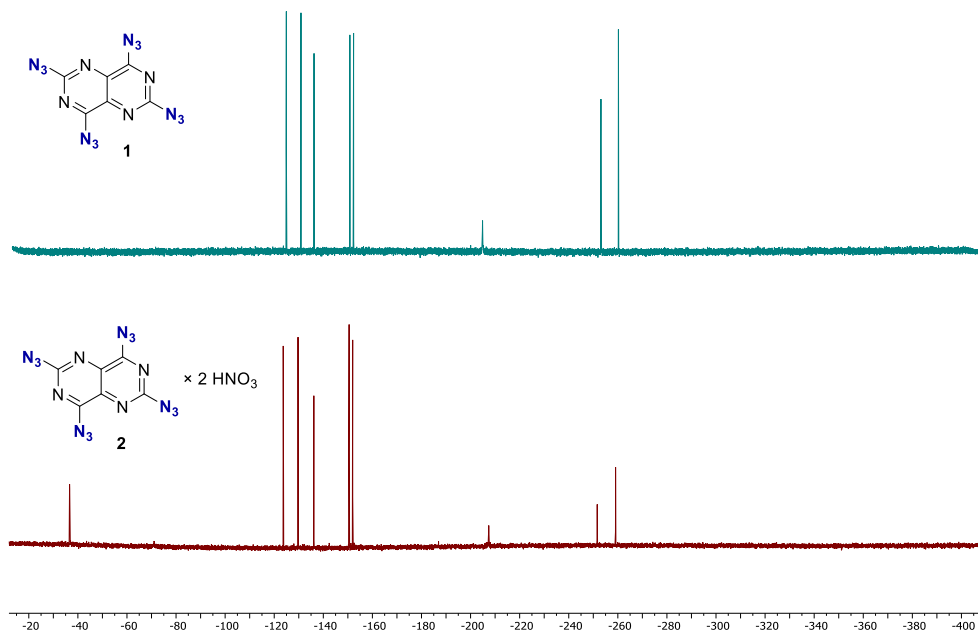


Figure 1. ^{15}N NMR spectra of tetraazide **1** and nitric acid adduct **2** (51 MHz, CF_3COOD)

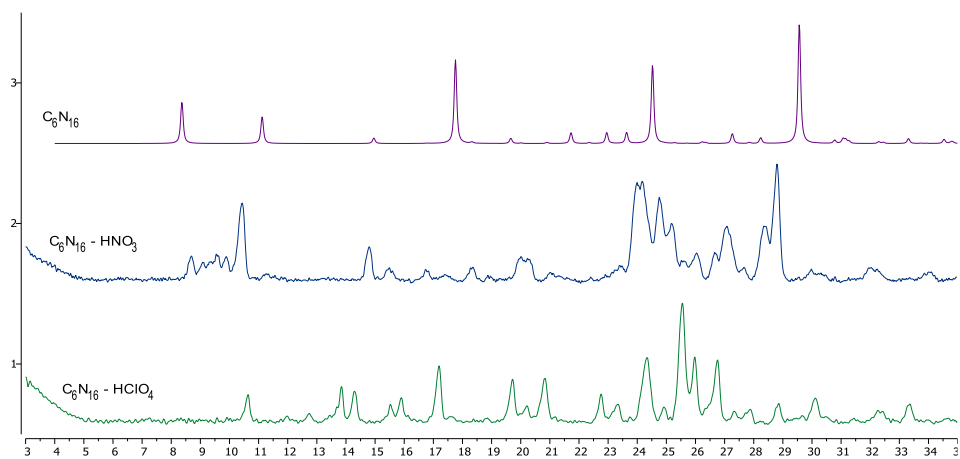


Figure 2. XRD of tetraazide **1** and tetraazide adducts **2** and **3**

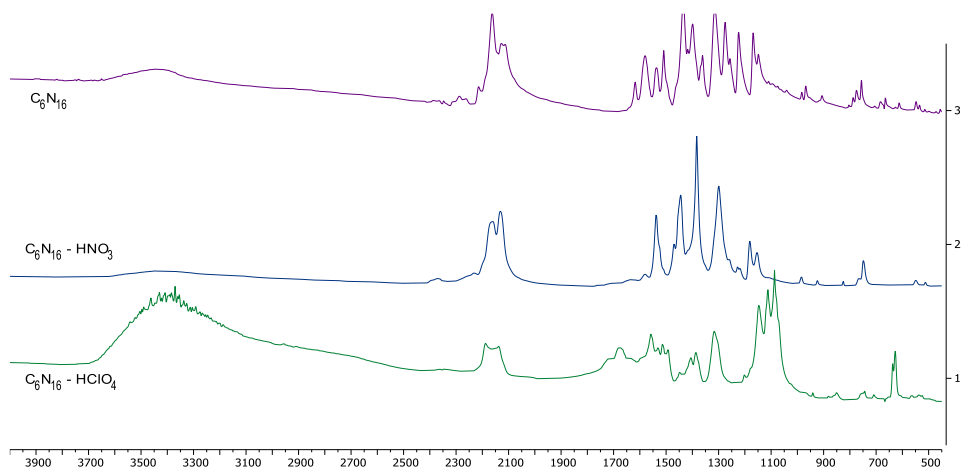


Figure 3. FT-IR spectra of tetraazide **1** and tetraazide adducts **2** and **3**

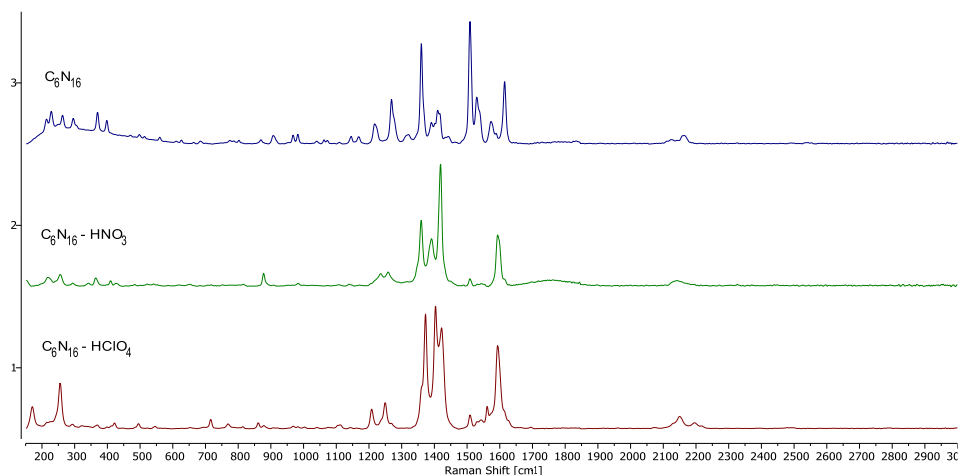


Figure 4. Raman spectra of tetraazide **1** and tetraazide adducts **2** and **3**

Finally, the acid adducts showed impact sensitivity of 2 J for nitric acid adduct **2** and 1 J for the perchloric acid adduct **3** and friction sensitivities of 40 N, thus outperforming the tetraazide base **1** in terms of safety (1 J impact sensitivity and 1 N friction sensitivity for **1**). The salts deflagrated in a hot plate test, and the perchloric acid adduct **3** successfully detonated in a hot needle test. Despite the detonation, an explosion was not achieved when a secondary explosive (PETN) initiation test with the perchloric acid adduct **3** detonator was performed.

Synthesis procedure

2,4,6,8-Tetraazidopyrimido[5,4-*d*]pyrimidine nitric acid adduct (2):

To a suspension of tetrazide **1** (100 mg, 0.338 mmol, 1 eq.) in DCM (1 mL) was added HNO₃ (100%) (70 μL, *d* = 1.52 mg/mL, 106 mg, 1.688 mmol, 5 eq.). After 20 minutes, the reaction mixture was evaporated under airflow and further dried under reduced pressure. Product **2** was obtained as a yellow solid 142 mg (quant.). ¹³C NMR (126 MHz, CF₃COOD) δ 165.4, 160.2, 130.9. ¹⁵N NMR (51 MHz, CF₃COOD) δ -36.6, -123.7, -129.7, -136.1, -150.5, -152.0, -207.4, -251.6, -259.1.

2,4,6,8-Tetraazidopyrimido[5,4-*d*]pyrimidine perchloric acid adduct (3):

To a suspension of tetrazide **1** (80 mg, 0.270 mmol, 1 eq.) in methanol (1 mL) was added aqueous solution of HClO₄ (70%) (46 μL, *d* = 1.67 mg/mL, 54 mg, 0.540 mmol, 2 eq.). The reaction was refluxed for 20 minutes, and the solvent evaporated under airflow and dried under reduced pressure. Product **3** was obtained as a yellowish solid 134 mg (quant.).



Kristaps Leškovskis dzimis 1995. gadā Rīgā. Rīgas Tehniskajā universitātē ieguvis bakalaura (2018) un maģistra grādu (2020) inženierķīmijā. Patlaban ir RTU Dabaszinātņu un tehnoloģiju fakultātes Ķīmijas un ķīmijas tehnoloģijas institūta pētnieks. Zinātniskās intereses saistītas ar heterociklu ķīmiju, azīda funkcionālās grupas pārvērtībām un augsti enerģētiskiem savienojumiem.

Kristaps Leškovskis was born in 1995 in Riga. He obtained a Bachelor's in 2018 and a Master's degree in 2020 in Chemical Engineering from Riga Technical University. Currently, he is a researcher at the Institute of Chemistry and Chemical Technology at the Faculty of Natural Sciences and Technologies of RTU. His research interests are related to the chemistry of heterocycles, azide functional group transformations and high-energy compounds.